

NATURAL RESOURCES CANADA - INVENTIVE BY NATURE

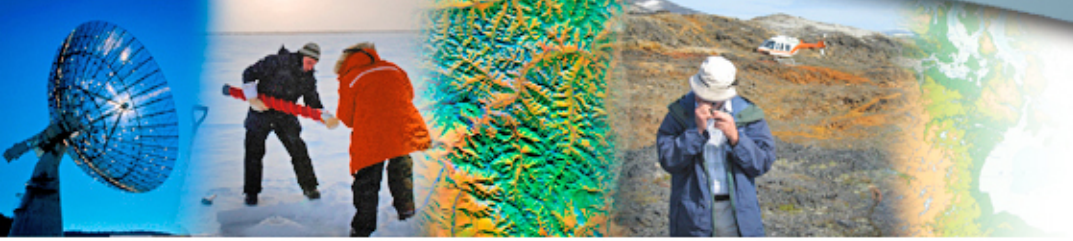
Geological Survey of Canada
Scientific Presentation 34

Presentations of the 2014 TGI-4 unconformity-related uranium workshop

E.G. Potter[1] (ed.)

[1] Geological Survey of Canada, 601 Booth Street, Ottawa, Ontario

2015



NATURAL RESOURCES CANADA - INVENTIVE BY NATURE

Presented at: 2014 Targeted Geoscience Initiative 4 unconformity-related uranium deposits workshop, Saskatoon, Saskatchewan

Date presented: December 2014

© Her Majesty the Queen in Right of Canada, as represented by the Minister of Natural Resources Canada, 2015

doi:10.4095/296519

This publication is available for free download through GEOSCAN (http://geoscan.nrcan.gc.ca/).

Recommended citation

Potter, E.G. (ed.), 2015. Presentations of the 2014 TGI-4 unconformity-related uranium workshop; Geological Survey of Canada, Scientific Presentation 34, 363 p. doi:10.4095/296519

Publications in this series have not been edited; they are released as submitted by the author.

Table of Contents

Welcome and brief introduction
Eric Potter **1**

Graphite-bearing and graphite-depleted basement rocks in the Dufferin Lake zone, south-central Athabasca Basin, Saskatchewan
Marjolaine Pascal, Kevin M. Ansdell, Irvine R. Annesley **8**

Mineralogy of a fertile fluid conduit related to unconformity-type uranium deposits in the Athabasca Basin
Erin E. Adlakha, Keiko Hattori, Gerard Zaluski, Tom G. Kotzer, and Eric G. Potter **41**

Geometric and hydrodynamic modelling and fluid-structural relationships in the southeastern Athabasca Basin and significance for uranium mineralization
Zenghua Li, Guoxiang Chi, Kathryn M. Bethune, Sean A. Bosman, and Colin D. Card **68**

Preliminary studies of fluid composition, thermal conditions, fluid-structural relationships and graphite alteration of the Phoenix uranium deposit, Athabasca Basin, Saskatchewan
Kewen Wang, Guoxiang Chi, Kathryn M. Bethune, and Colin D. Card **103**

Fe and Mg Signatures of the Bong Uranium Deposit, Thelon Basin, Nunavut
Eric G. Potter, Ryan Sharpe, Isabelle Girard, Mostafa Fayek, Paul Gammon, David Quirt, and John Robbins **151**

Fe isotopic composition of alteration minerals from McArthur River zone 4 deposit, Athabasca Basin, Saskatchewan
Andrés Acevedo and T. Kurt Kyser **171**

Basin development and multi-element lithogeochemistry of Athabasca Basin samples
Paul Ramaekers **188**

Application of regional geochemical datasets to uranium exploration in the Athabasca Basin, Saskatchewan
Donald M. Wright and Eric G. Potter **229**

Geomathematical and mineralogical study of sandstones overlying the Phoenix uranium deposits and the REE-rich Maw Zone, Athabasca Basin, Canada
Shishi (Chris) Chen, Keiko Hattori, Eric C. Grunsky, and Yongxing Liu **241**

Summary of surficial geochemical surveys over concealed uranium ore of the Phoenix and Millennium deposits, Athabasca Basin
Keiko Hattori, Michael J. Power, Shishi (Chris) Chen, Jack Dann, Austin Krahenbil, Nickolas Dudek, Chad Sorba, Tom G. Kotzer, and Eric G. Potter **258**

Ground truthing of the 'Eastern Athabasca Basin' regional airborne gamma-ray survey: Context for exploration of deeply buried unconformity-related uranium deposits
Richard Fortin, Janet E. Campbell, Brad J.A. Harvey, Martin W. McCurdy, Laurel E. Sinclair, Michelle A. Hanson, Eric G. Potter, and Charles W. Jefferson **282**

Camie River deposit and evolution of the Otish Basin
Dejan Milidragovic, Marion Lesbros-Piat-Desvial, Julia J. King, Georges Beaudoin, Mike A. Hamilton, and Robert A. Creaser..... **333**



CANADA 1842 GEOLOGICAL SURVEY - COMMISSION GÉOLOGIQUE

TGI 4 Ore Systems

TGI-4 unconformity-related U workshop

Cameco

University of Regina

Peridot Geoscience Ltd.

uOttawa

DENISON MINES

University of Manitoba

Queen's University

Université Laval

AREVA

University of Saskatchewan

Saskatchewan Ministry of the Economy



Targeted Geoscience Initiative 4 (TGI-4)

TGI-4 is a ***collaborative*** federal geoscience program that provides industry with the ***next generation of geoscience knowledge and innovative techniques***, which will result in more effective targeting of buried mineral deposits.



TGI-4 Uranium Collaborations

TGI 4 Ore Systems

Cameco Corp.:

Alexandre Aubin
Eric Bort
Aaron Brown
Tom Kotzer
Tyler Mathieson
Brian McGill
Scott Rogers
Vlad Sopuck
Gary Witt
Garnet Wood
Gerard Zaluski

AREVA:

David Quirt
John Robbins

Denison Mines Corp.:

Chad Sorba
Yongxing Liu

D.E. Jiricka Enterprises:

Dan Jiricka

Peridot Geoscience Ltd.:

Donald Wright

Provincial/Territorial:

Sean Bosman (SGS)
Jason Berenyi (SGS)
Colin Card (SGS)
Gary Delaney (SGS)
Claude Dion (MRN-QC)
Michelle Hanson (SGS)
Bill Slimmon (SGS)
Luke Ootes (NTGO)



TGI-4 Uranium

TGI 4 Ore Systems

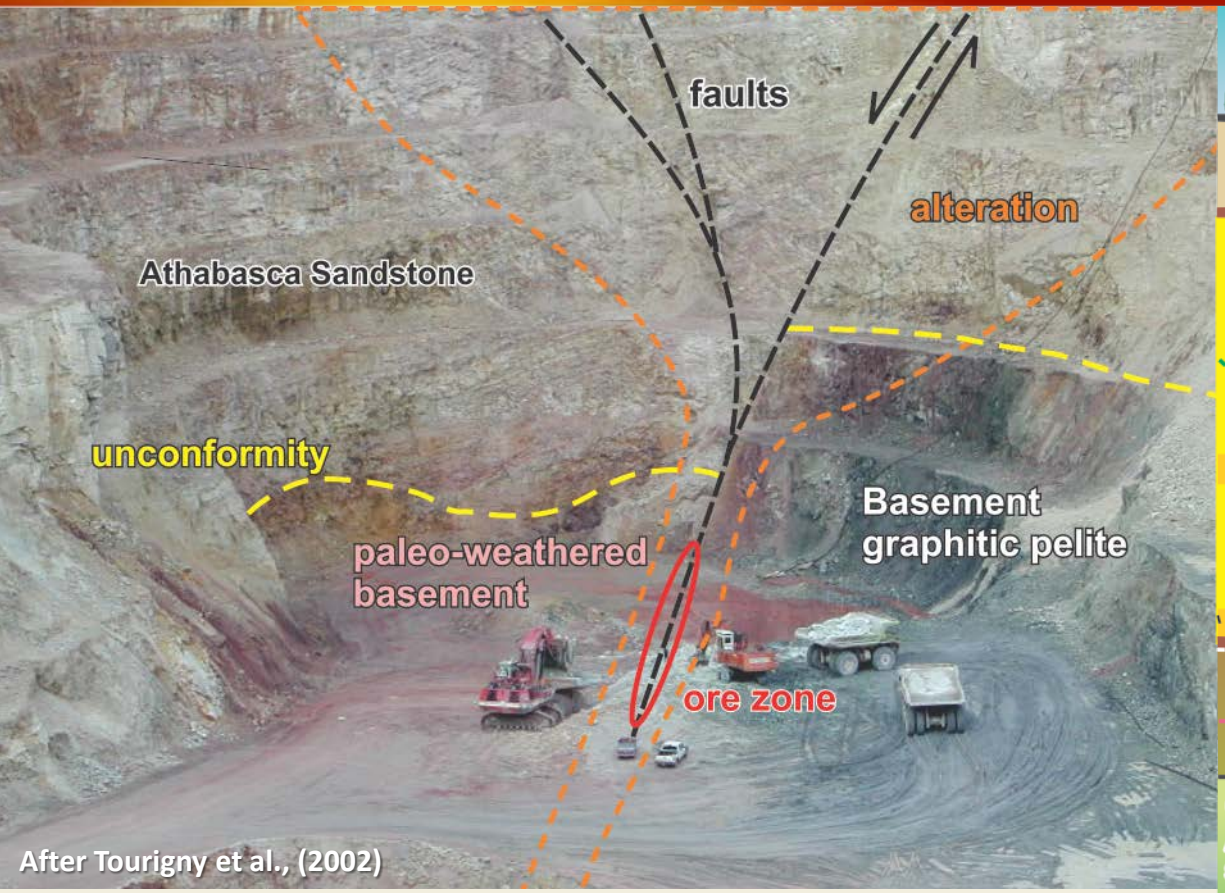
Two subprojects:

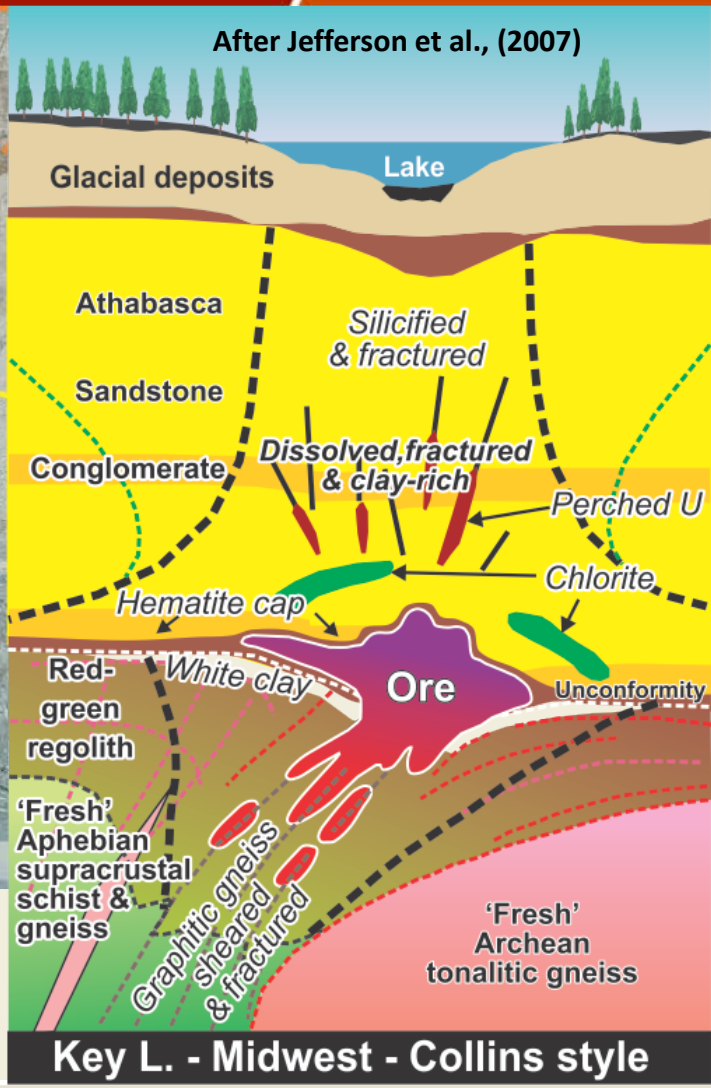
1) **Basement-to-surface expressions of deep mineralization and refinement of critical factors leading to the genesis of <u>unconformity-related</u> uranium deposits; and**

2) **Recognition of uranium ore system alteration signatures in complex terranes: IOCG vs albite-hosted uranium vs. volcanic-hosted uranium.**

TGI-4 Unconformity-related systems: basement to surface expressions & genetic controls

TGI 4 Ore Systems





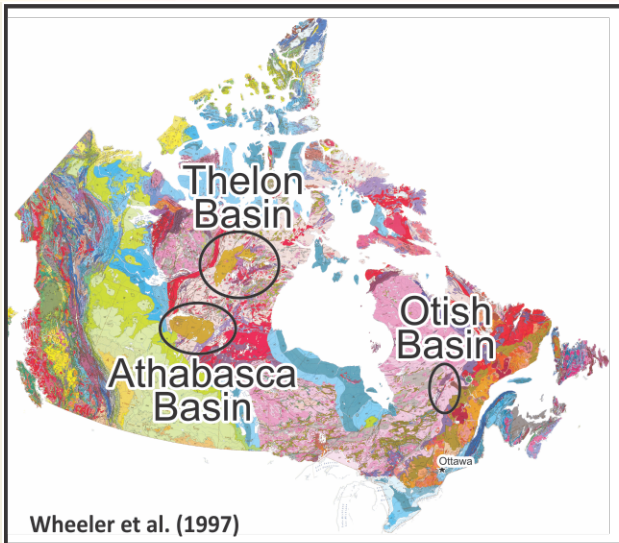
System-wide approach: basement to surface expressions of mineralization and refinement of critical factors leading to the genesis of the deposits.

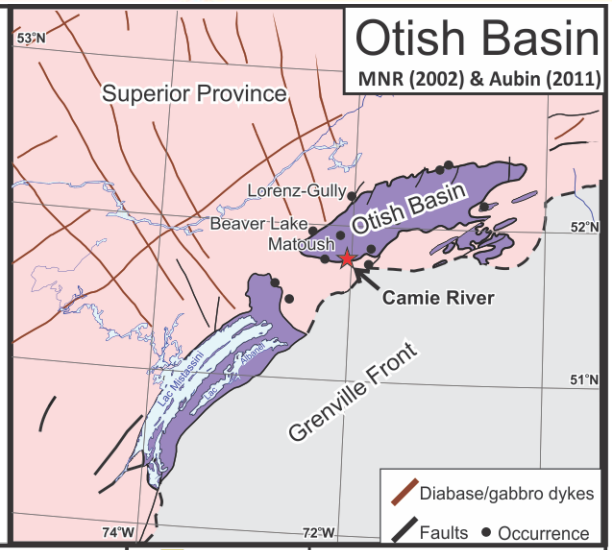
TGI-4 Uranium

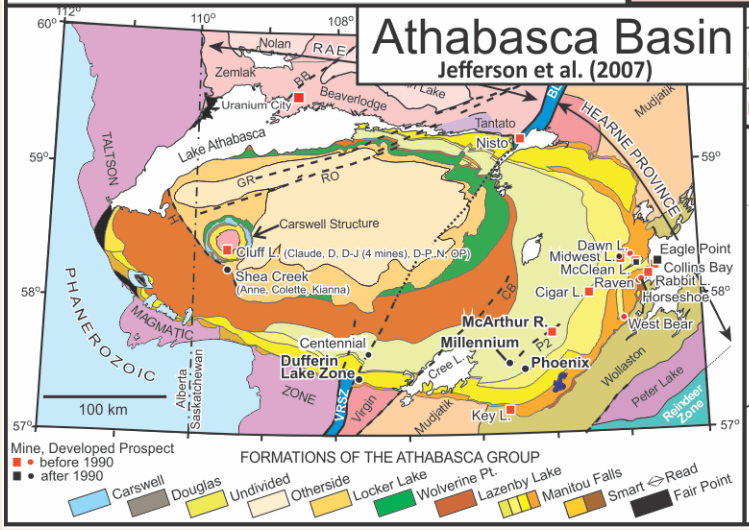
TGI-4 Ore Systems

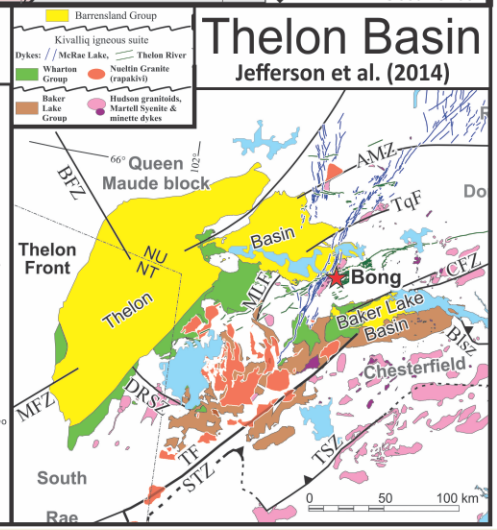
Project areas:

1) Athabasca Basin (Phoenix, Millennium, McArthur River deposits and the Dufferin Lake and Maw zones)
2) Thelon Basin (Bong deposit)
3) Otish Basin (Camie River deposit).











Basement to surface expressions

Time	Authors (* - speaker)	Topic
9:00 - 9:15	Eric Potter	Welcome / introductions
9:15 - 9:45	Marjolaine Pascal, Kevin Ansdell*, Irvine Annesley	Graphite-bearing and graphite-depleted basement rocks in the Dufferin Lake zone, south-central Athabasca Basin
9:45 - 10:15	Erin Adlakha*, Keiko Hattori, Gerard Zaluski, Tom Kotzer, Bill Davis, Eric Potter	The nature and chemistry of ore fluids associated with the McArthur River uranium deposit: new insights from alteration minerals found along the P2 fault
10:15-10:30	BREAK	
10:30 - 11:00	Zenghua Li*, Guoxiang Chi, Kathryn Bethune, Sean Bosman, Colin Card	Geometric and hydrodynamic modelling and fluid-structural relationships in the southeast Athabasca Basin and significance for uranium mineralization
11:00 - 11:30	Kewen Wang*, Guoxiang Chi, Kathryn Bethune, Zenghua Li, Colin Card	Fluid composition, thermal conditions, fluid-structural relationships and graphite alteration of the Phoenix uranium deposit, Athabasca Basin
11:30 - 12:00	Eric Potter*, Ryan Sharpe, Isabelle Girard, Mostafa Fayek, Paul Gammon, David Quirt, John Robbins	Fe and Mg signatures of the Bong deposit, Thelon Basin
12:00 - 1:00	LUNCH	Discussion: summary open file report(s)
1:00 - 1:30	Andrés Acevedo, Kurt Kyser*	Fe isotopic composition of alteration minerals from McArthur River zone 4 deposit, Athabasca Basin
1:30 - 2:00	Paul Ramaekers* et al.	Basin development, lithogeochemistrty and mineralization of the Athabasca Basin
2:00 - 2:30	Donald Wright*, Eric Potter	Application of regional geochemical datasets to uranium exploration in the Athabasca Basin, Saskatchewan
2:30 - 3:00	Shishi (Chris) Chen*, Keiko Hattori, Eric Grunsky, Yongxing Liu	Geomathematical and Mineralogical Study of Sandstones Overlying Phoenix Uranium Deposits and the REE-rich Maw Zone, Athabasca Basin
3:00 - 3:15	BREAK	
3:15 - 3:45	Keiko Hattori*, Michael Power, Shishi Chen, Austin Krahenbil, Nickolas Dudek, Chad Sorba, Tom Kotzer, Eric Potter	Summary of surficial geochemical surveys over concealed uranium ore of the Phoenix and Millennium deposits, Athabasca Basin
3:45 - 4:15	Richard Fortin*, Janet Campbell, Brad Harvey, Laurel Sinclair, Martin McCurdy, Michelle Hanson, Eric Potter, Charlie Jefferson	Ground truthing of the 'Eastern Athabasca Basin' regional airborne gamma-ray survey: Context for exploration of deeply buried unconformity type uranium deposits.
4:15 - 4:45	Dejan Milidragovic*, Marion Lesbro-Piat-Desvial, Julia King, Georges Beaudoin, Mike Hamilton, Robert Creaser	Camie River deposit and evolution of the Otish Basin
4:45 - 5:15	All	Discussion and TGI-4 synthesis volume manuscript

Graphite-bearing and graphite-depleted basement rocks in the Dufferin Lake Zone, south-central Athabasca Basin

Marjolaine Pascal

Supervisors: Kevin Ansdell and Irvine Annesley



Collaborators and sponsors

Dan Jiricka, Tom Kotzer
Michel Cuney, Marie-Christine Boiron



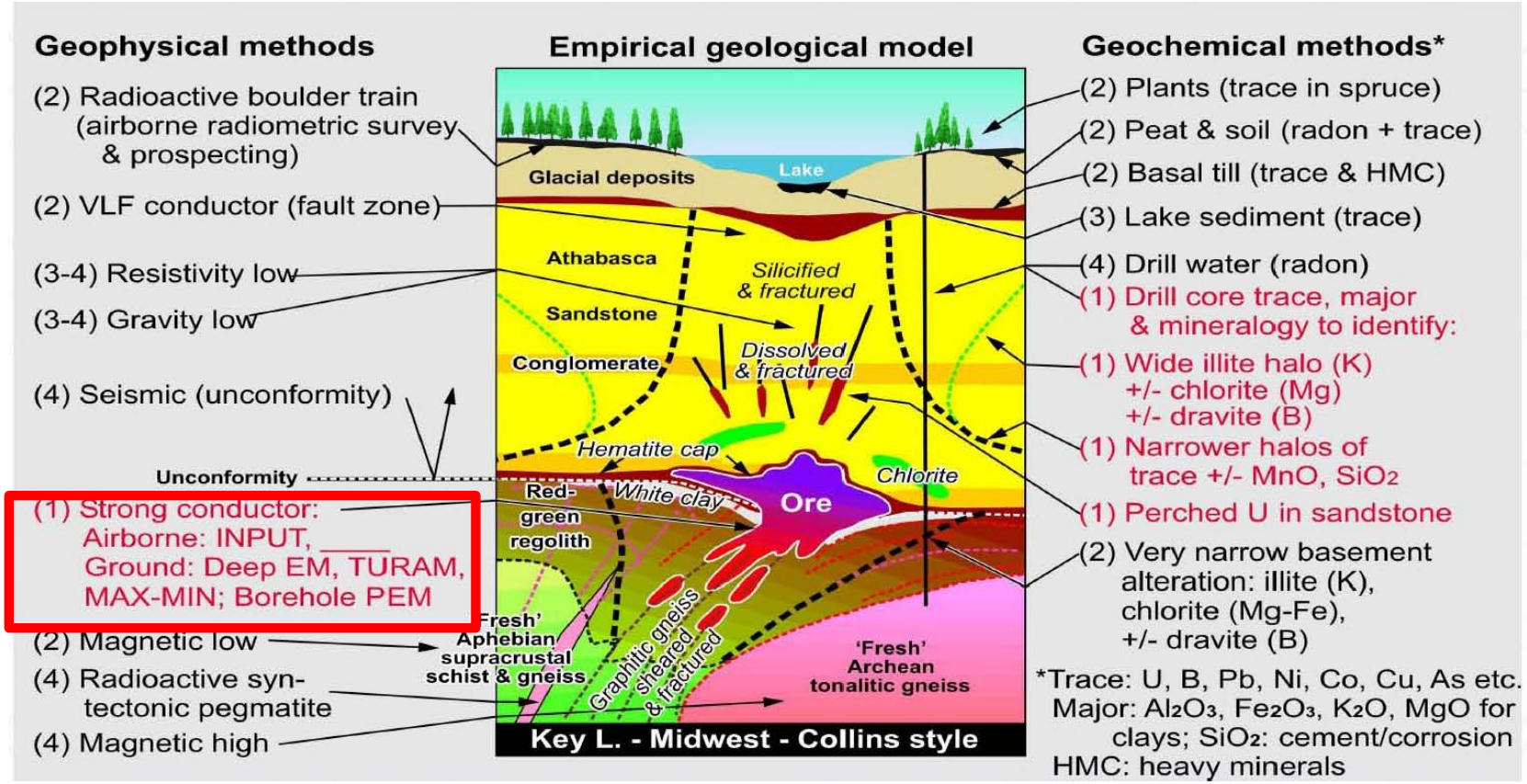






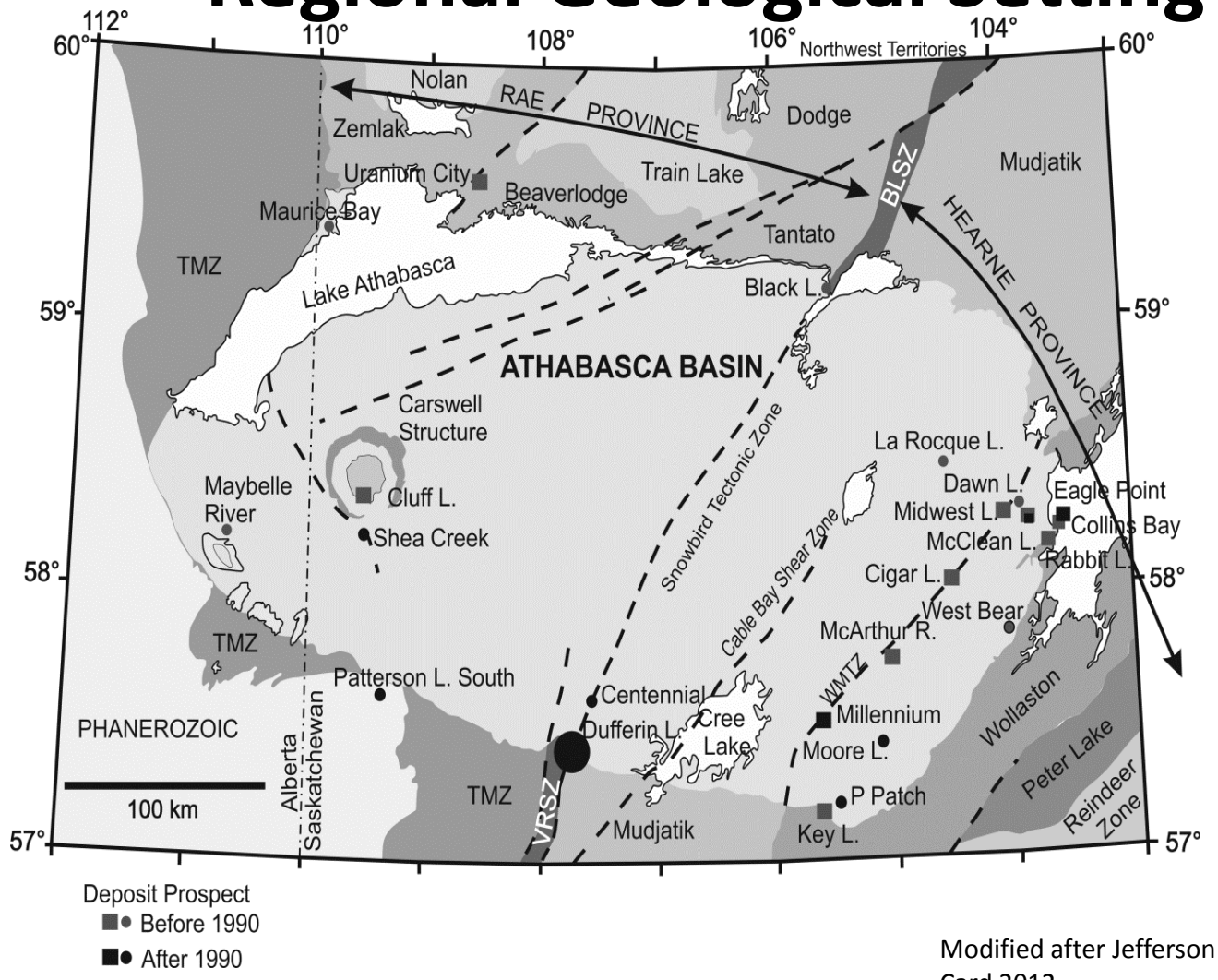


Uranium exploration



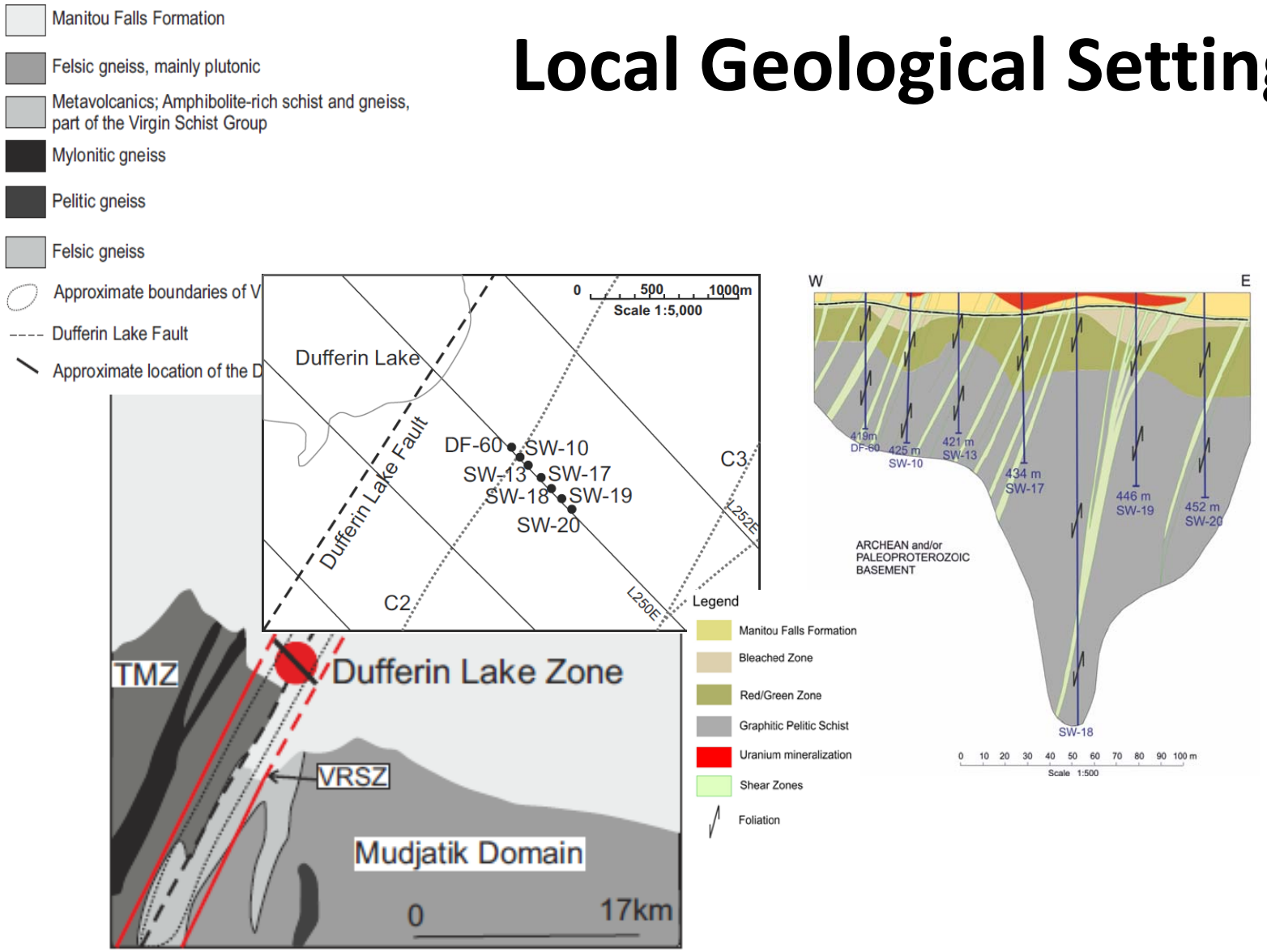
Jefferson et al. 2007

Regional Geological Setting



Modified after Jefferson et al. 2007, Card 2012

Local Geological Setting

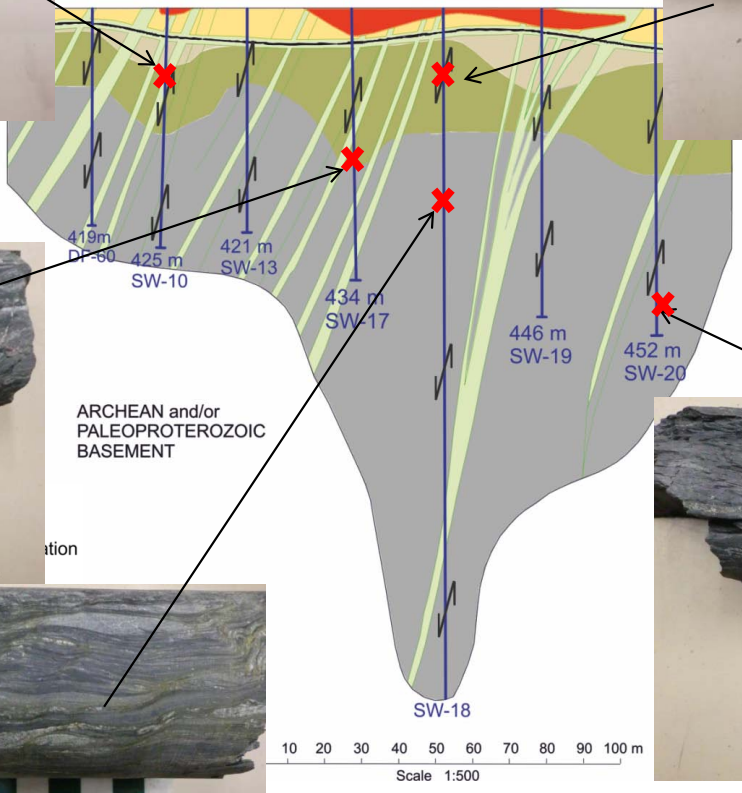


Dufferin Lake Zone – cross-section



Red/Green Zone (RGZ): hematitic and chloritic Pelitic Schist







Variably graphitic (+sulfides) Pelitic Schist (VGPS)





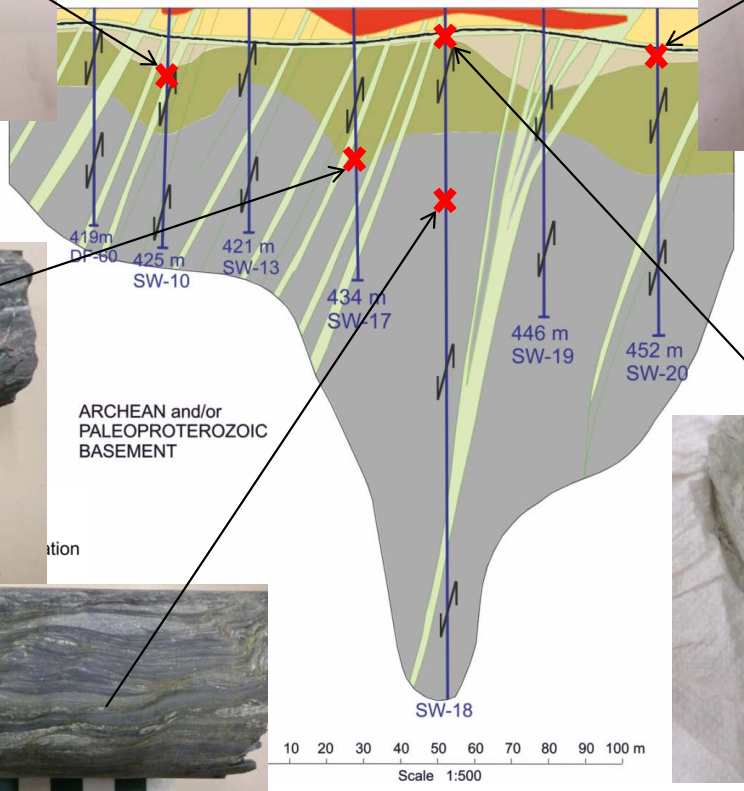
Dufferin Lake Zone – cross-section



Red/Green Zone (RGZ): hematitic and chloritic Pelitic Schist



Bleached Zone: foliated, clay alteration





Variably graphitic (+sulfides) Pelitic Schist (VGPS)





Unconformity: friable, bleached and clay alteration

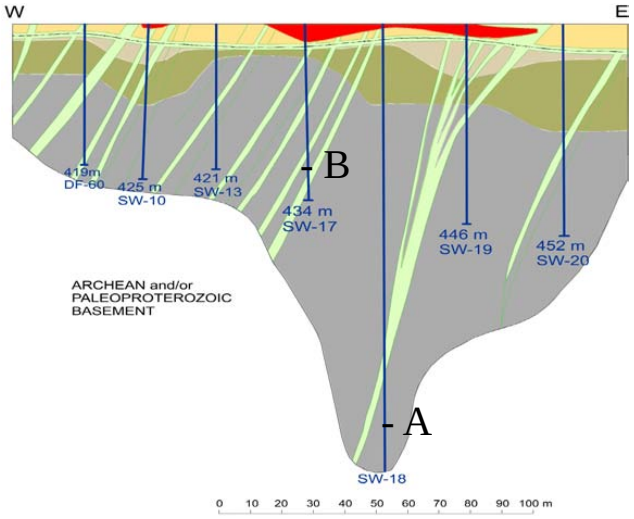
Objective

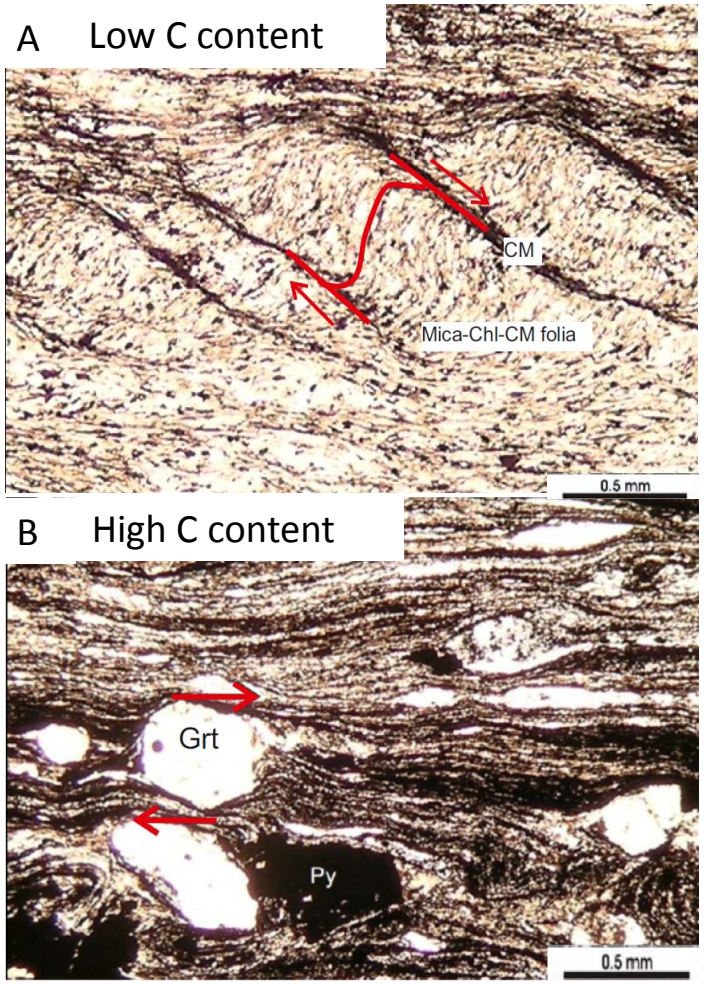
The goal of the project was thus to provide possible constraints on the processes that might have been operating to consume graphite

- Approach:
  - Mineralogy and composition of the variably graphitic pelitic schists, and graphite-depleted rocks
  - Characterize the different types of carbon species present in the graphitic and graphite-depleted rocks
  - Providing information on the fluid(s) that have interacted with these rocks
- When and how did consumption of graphite (and sulfides) in the basement rocks occur?

Variably Graphitic (Sulfidic) Pelitic Schist

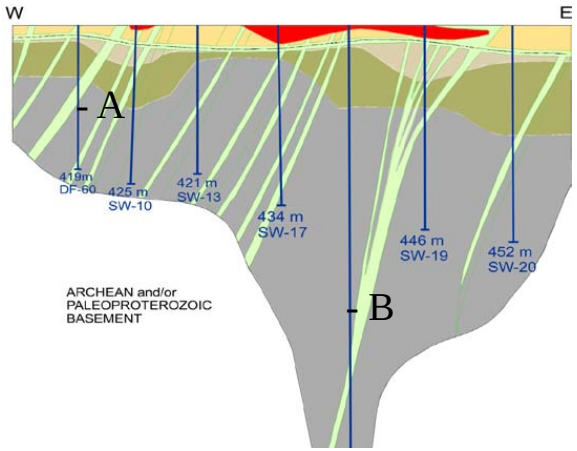
- Porphyroblastic, variably mylonitic
- Strong ductile deformation
  - quartz, chlorite, muscovite, CM/graphite define foliation
  - relict garnet and staurolite porphyroblasts

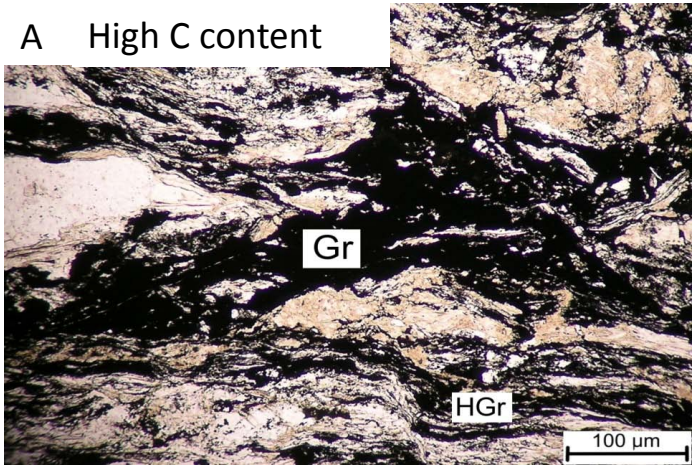


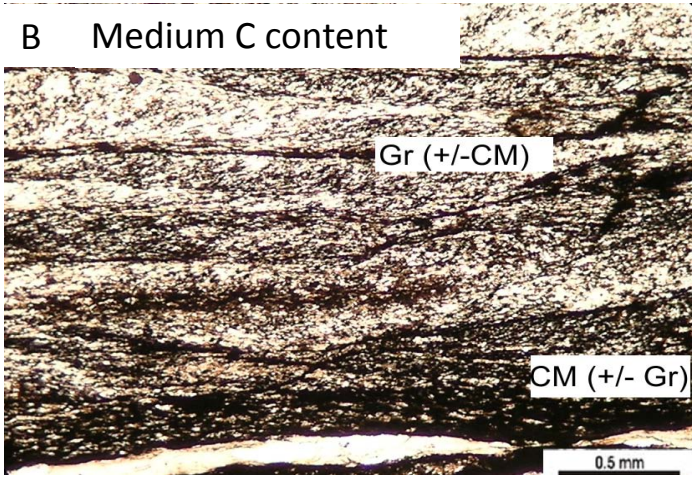


Variably Graphitic (Sulfidic) Pelitic Schist

- Three carbon species:
  - highly crystalline carbon (Gr)
  - semi-graphite (or hydrothermal graphite) (HGr)
  - carbonaceous matter (CM)
- Concentrated along foliation, within shear zones and along younger brittle fault zones

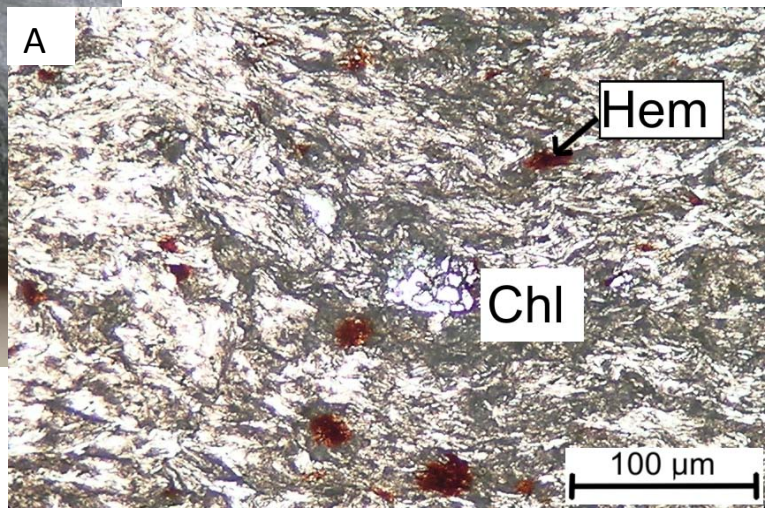


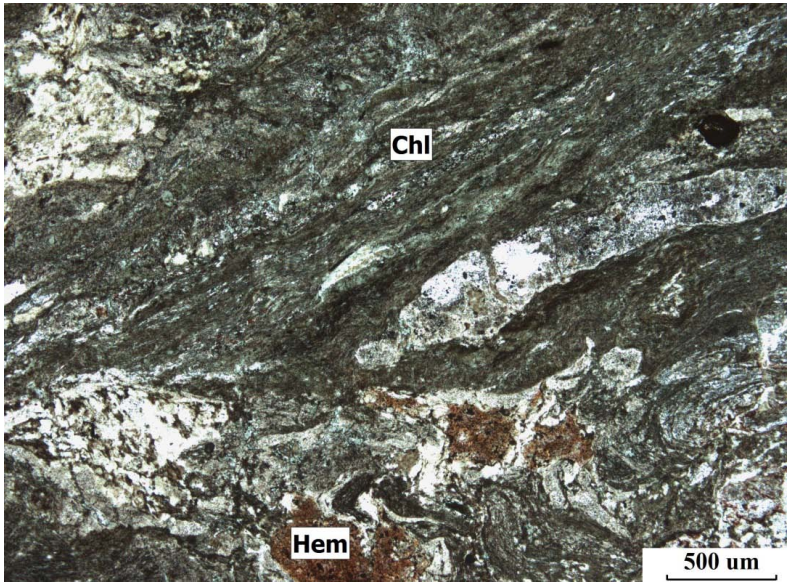


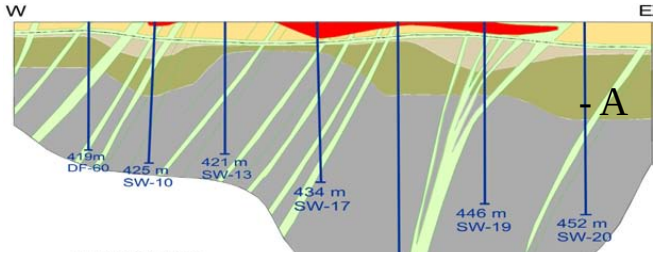


Green Zone

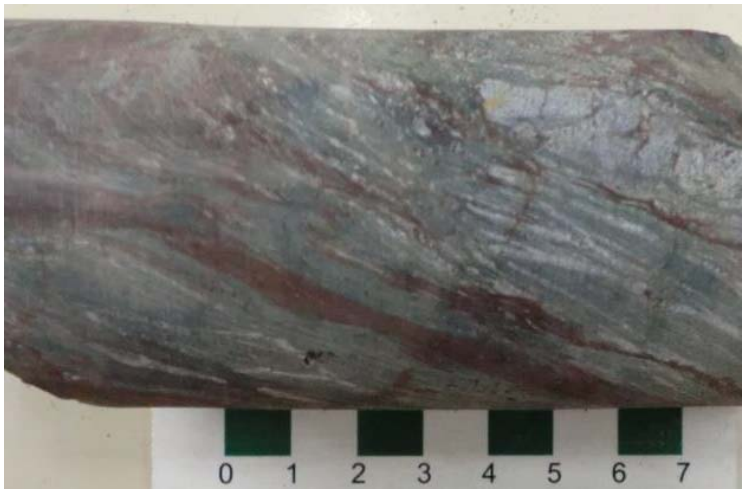

0 1 2 3 4 5 6 7

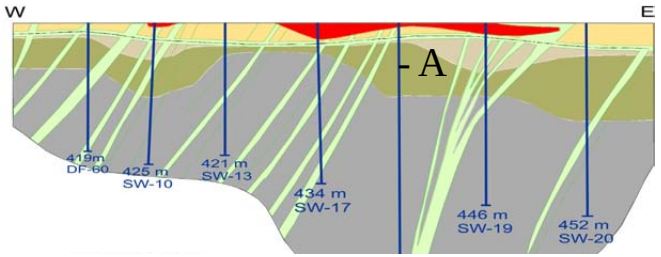

A
Hem
Chl
100 µm

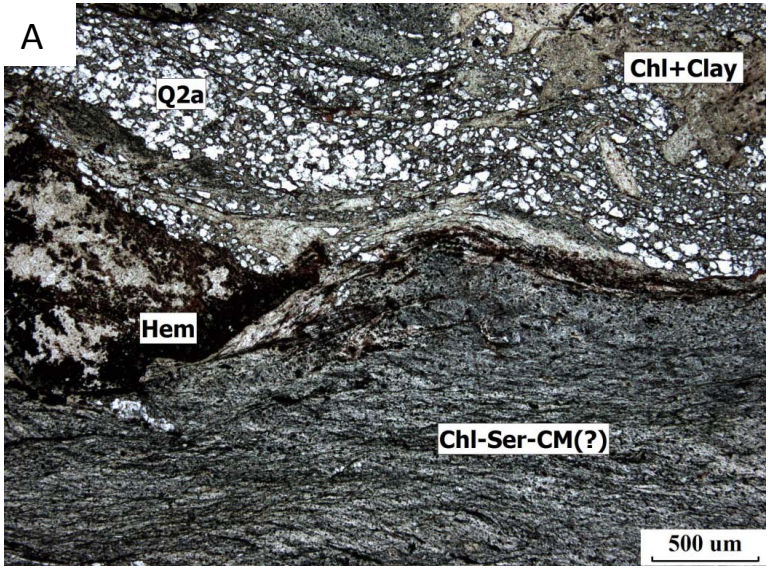

Chl
Hem
500 um

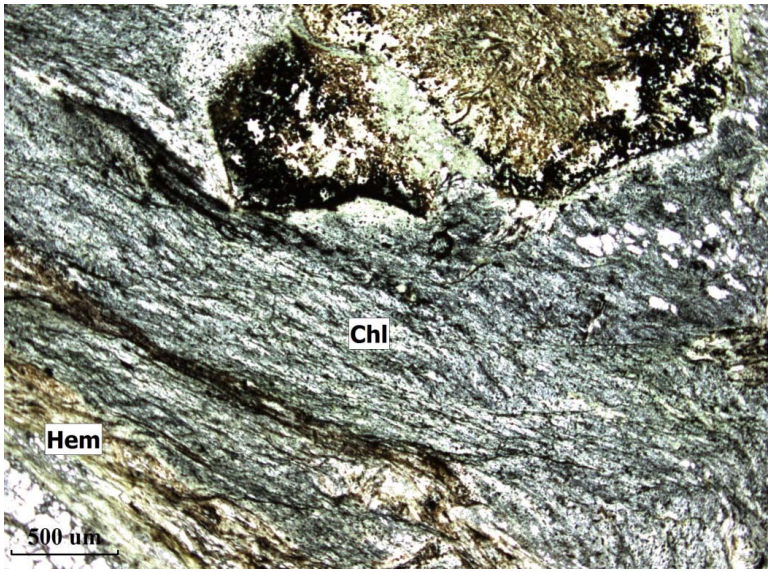

W
E
A
419m
DF-60
425 m
SW-10
421 m
SW-13
434 m
SW-17
446 m
SW-19
452 m
SW-20

Transition Green Zone to Red Zone



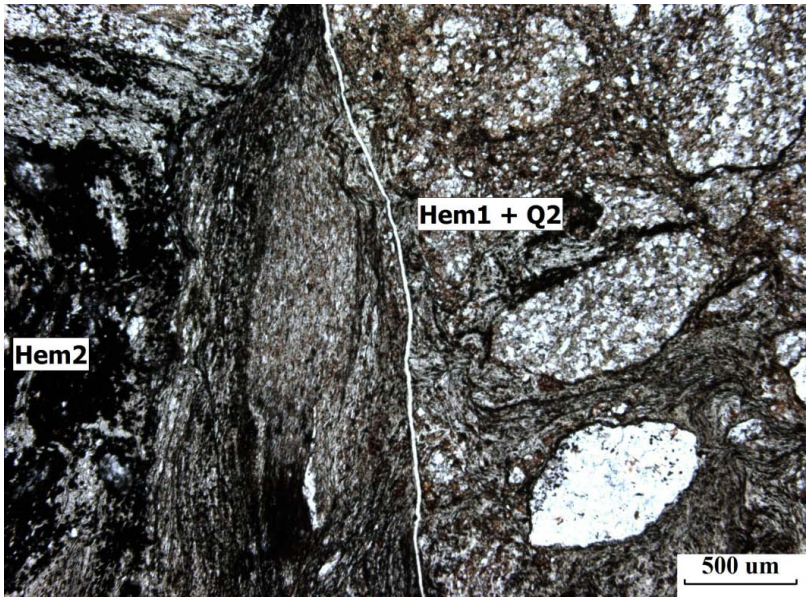






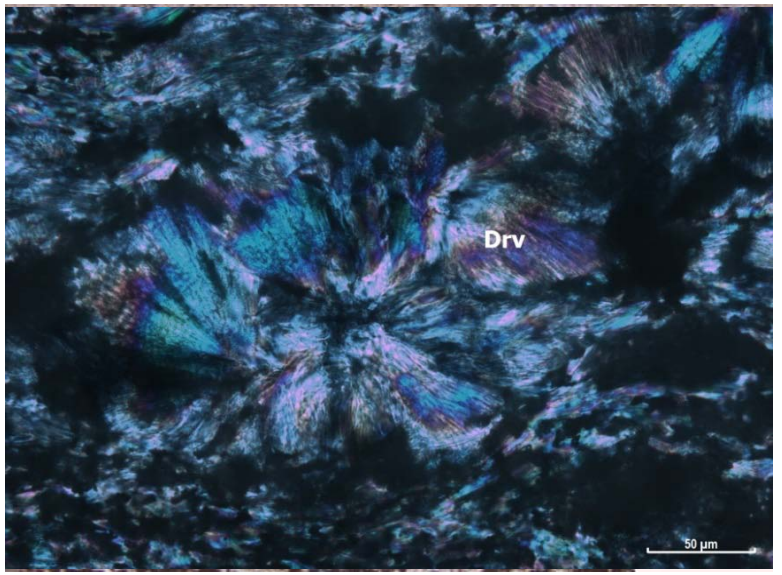
Red Zone





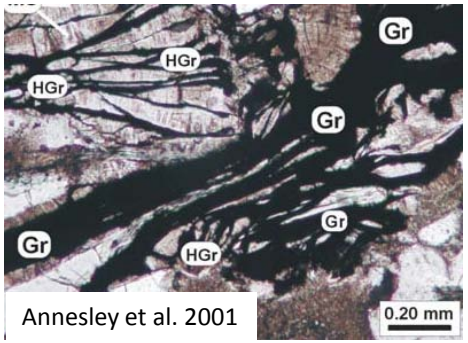
Bleached Zone





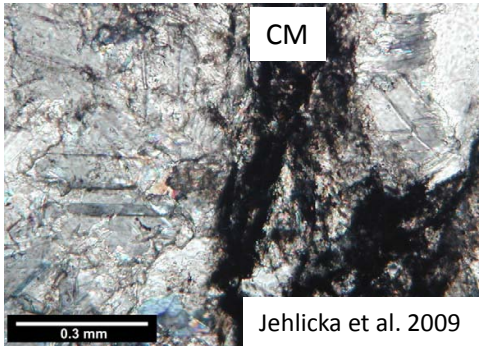
Raman Spectra and Carbon Species

Well-crystallised carbon = Gr



Annesley et al. 2001

Semi-graphite - HGr



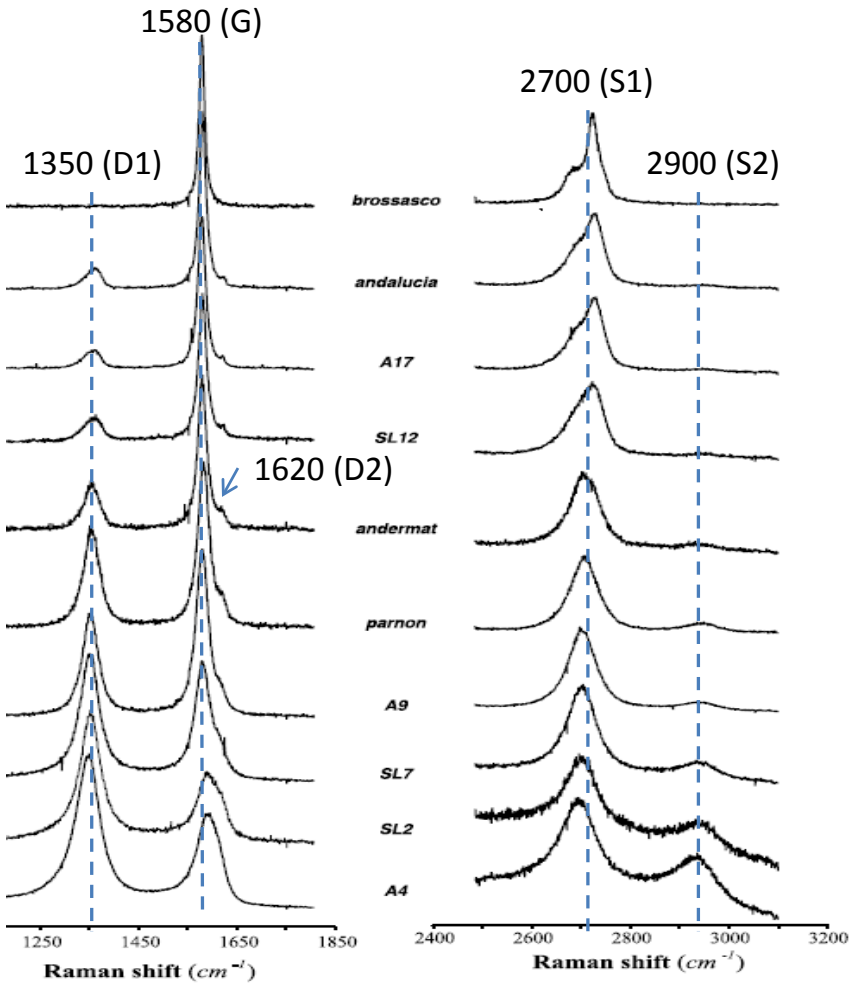
Jehlicka et al. 2009

Poorly-crystallised carbon = CM

(Beyssac et al., 2002)

First-order region

Second-order region

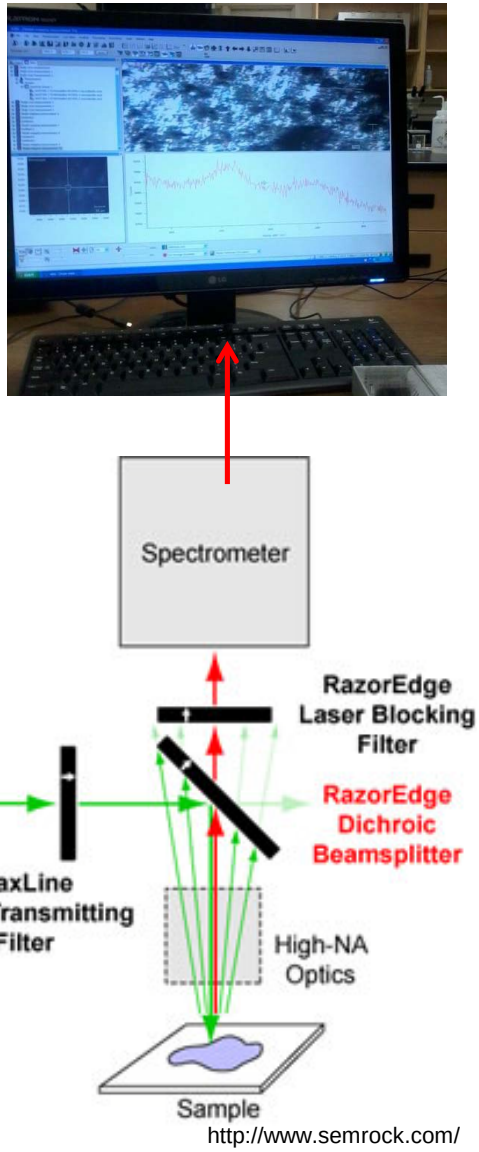


Raman spectroscopy (SSSC)



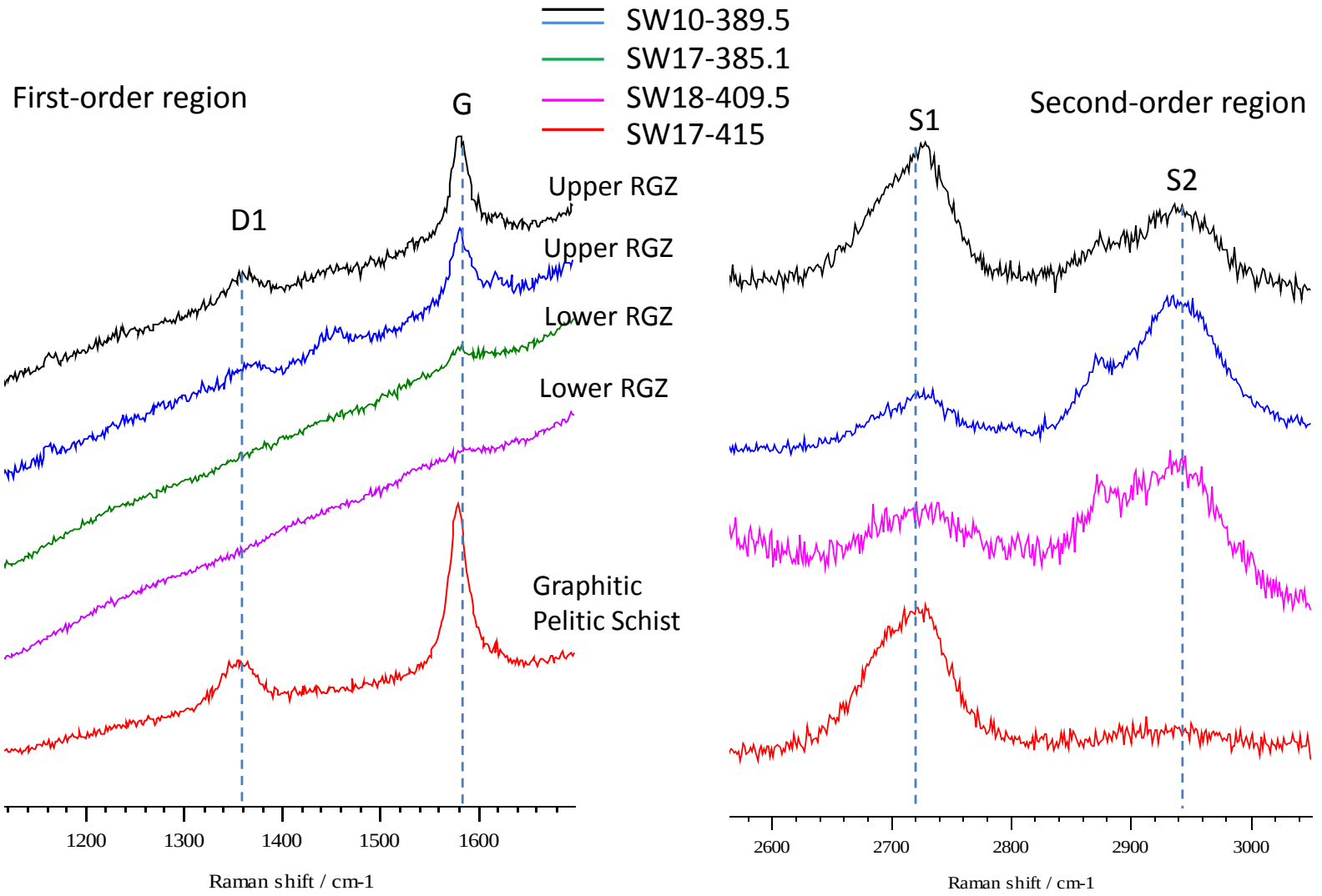


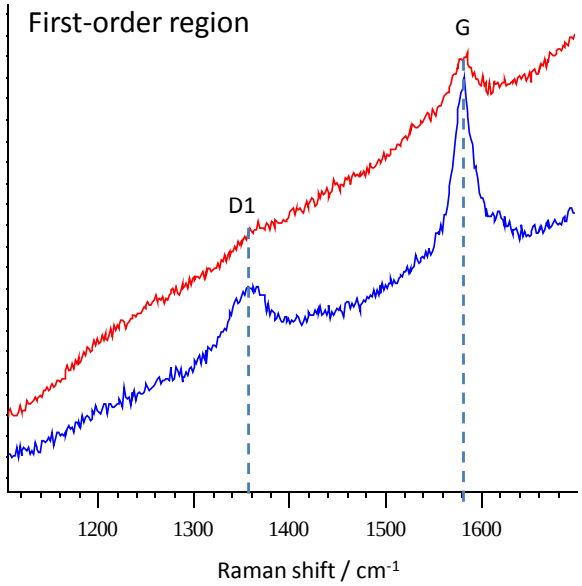
514 nm laser beam
point focused

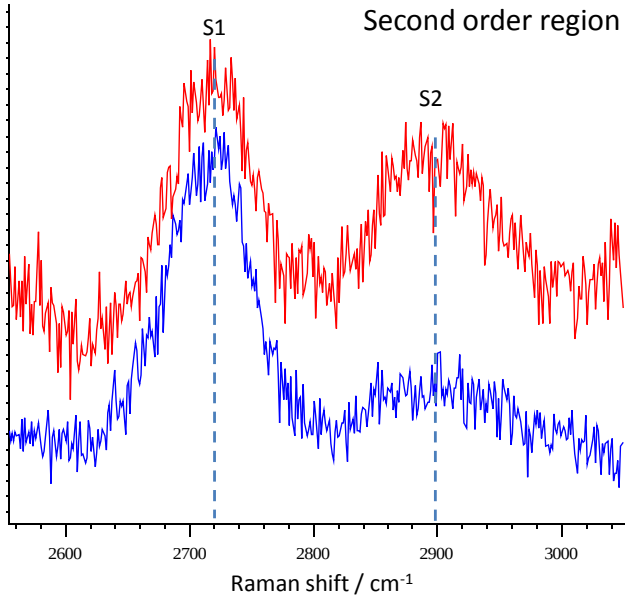


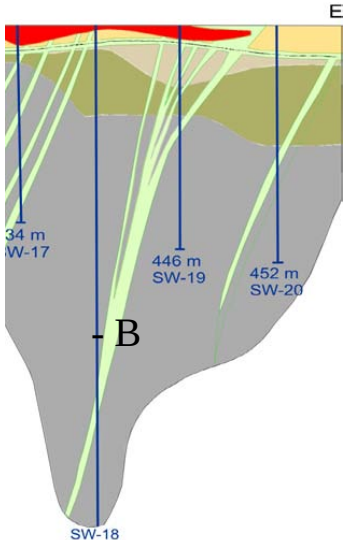
http://www.semrock.com/

Different Raman spectra of carbon species in the different zones



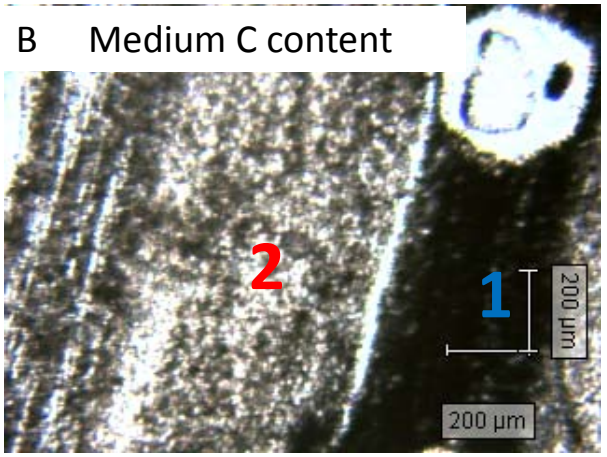




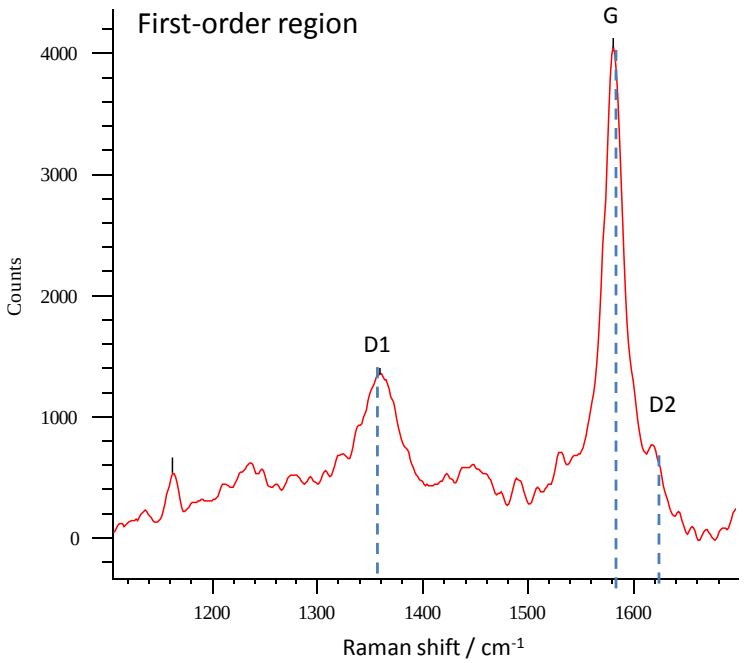


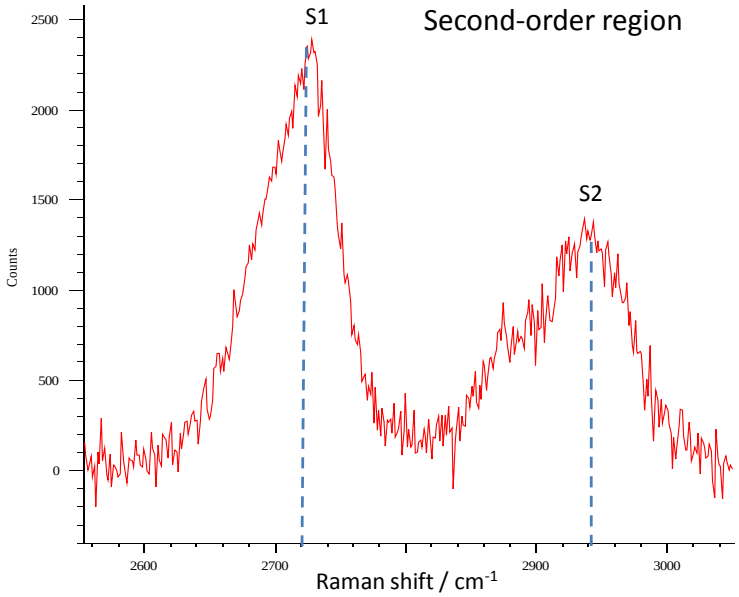
Region 1: HGr-Gr

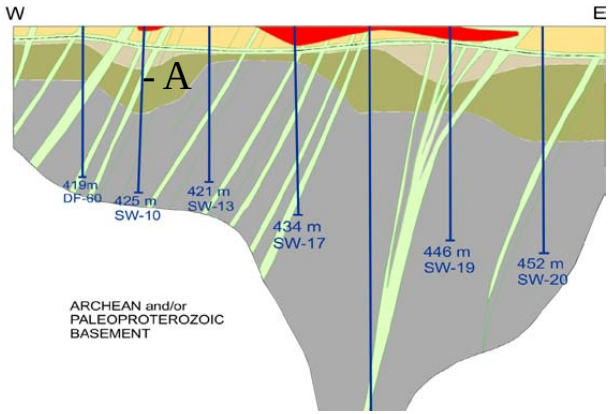
Region 2: HGr-CM




X
Sample from the upper RGZ


First-order region
G
D1
D2
Counts
4000
3000
2000
1000
0
1200
1300
1400
1500
1600
Raman shift / cm-1


Second-order region
S1
S2
Counts
2500
2000
1500
1000
500
0
2600
2700
2900
3000
Raman shift / cm-1


W
E
- A
419m
DF-60
425 m
SW-10
421 m
SW-13
434 m
SW-17
446 m
SW-19
452 m
SW-20
ARCHEAN and/or
PALEOPROTEROZOIC
BASEMENT

Raman parameters

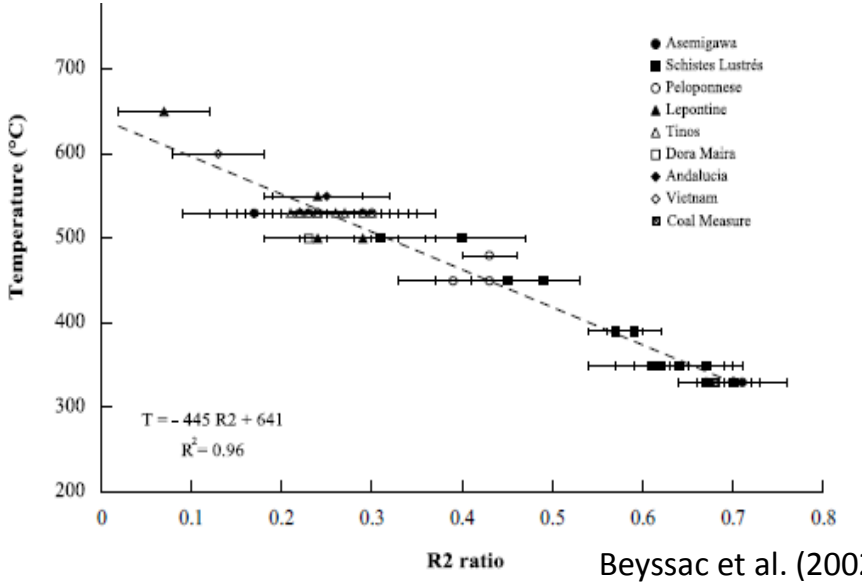
R1	R2	T(°C)
0.34	0.38	470
0.30	0.39	468
0.44	0.48	426
0.48	0.56	390
0.48	0.51	415
0.48	0.42	456
0.39	0.28	518
0.39	0.48	430
0.58	0.26	525
0.53	0.28	514
0.33	0.40	463
0.29	0.21	547
0.35	0.43	449
0.36	0.33	495
0.27	0.53	405
0.35	0.45	439
0.29	0.36	479
0.46	0.45	440
0.46	0.47	434
0.43	0.49	421
0.40	0.44	444

- Intensity ratio: **R1= D/G**
- Peak area ratio: **R2 = D1/(G+D1+D2)**

- *Peak metamorphic temperature (Beyssac et al. 2002):*

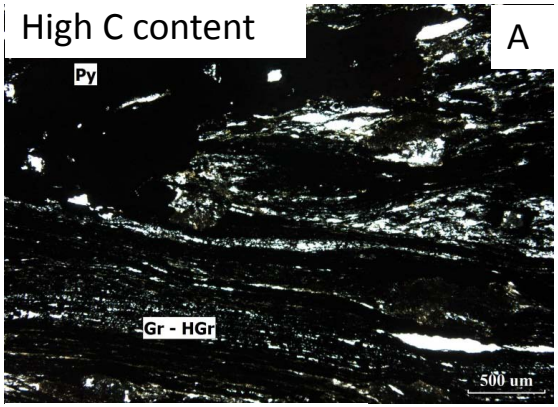
T(°C)= -445R2+641

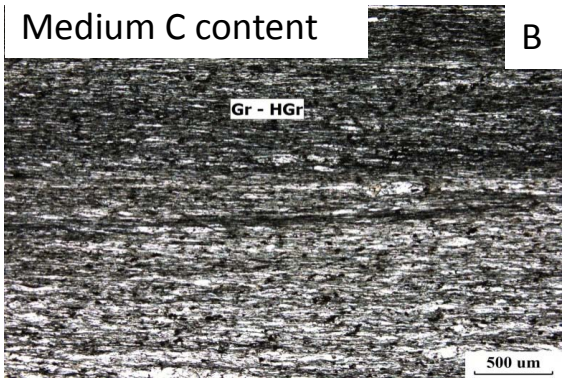
390 < T(°C) <547 (For the graphitic pelitic schist)

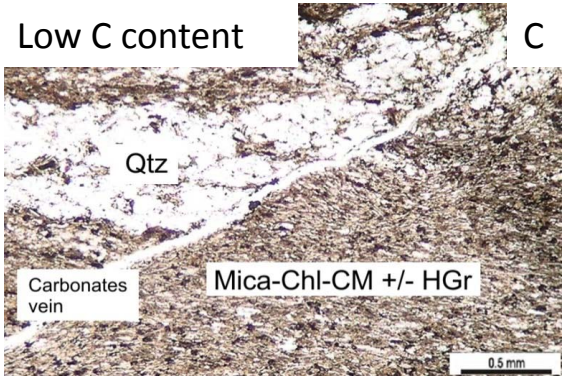


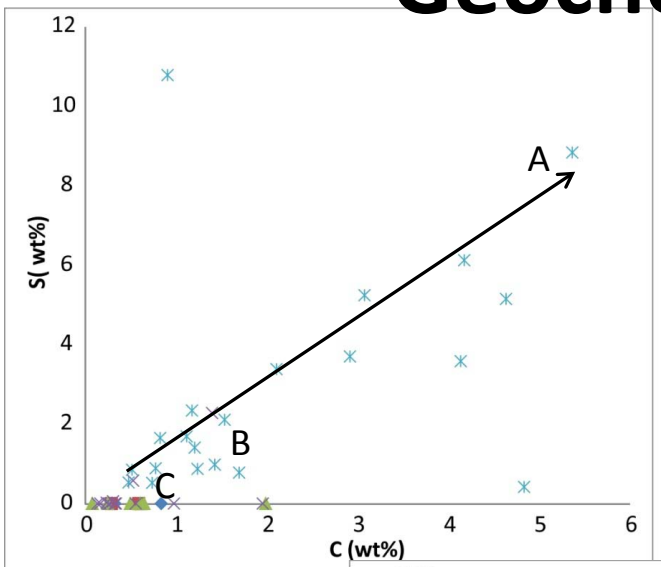
Beyssac et al. (2002)

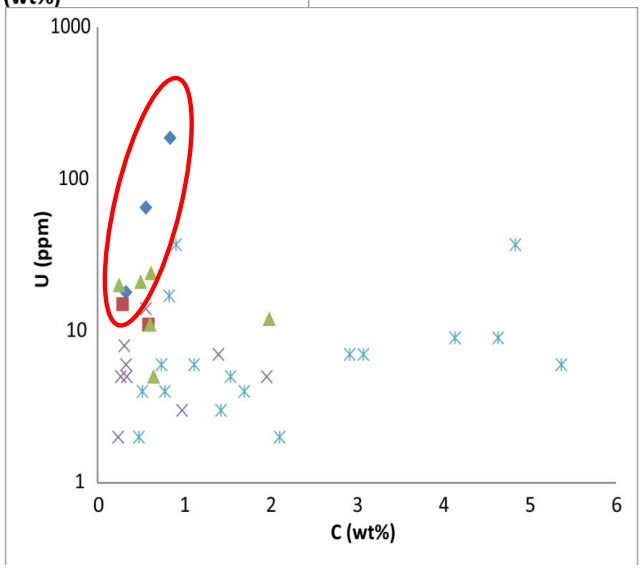
Geochemistry



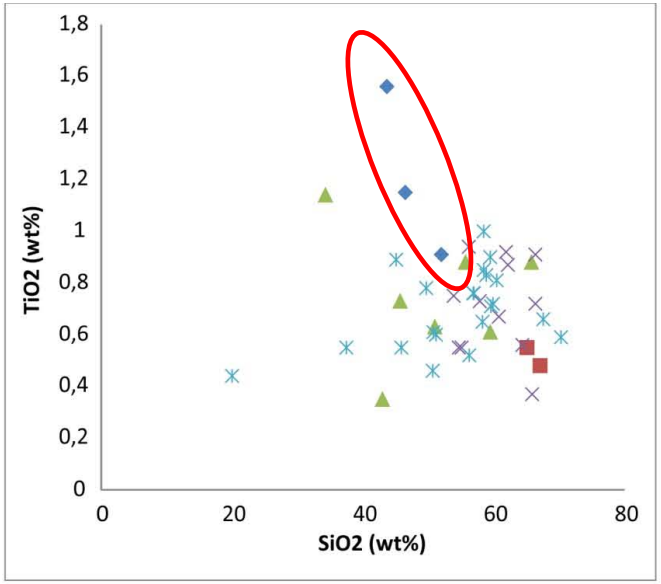


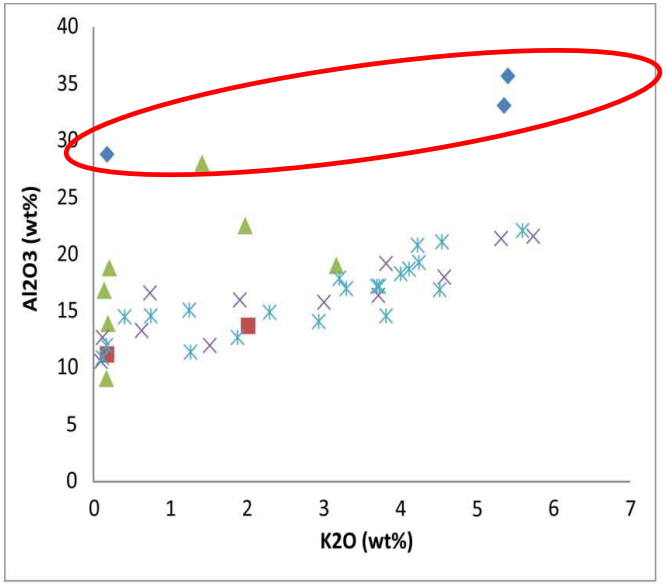


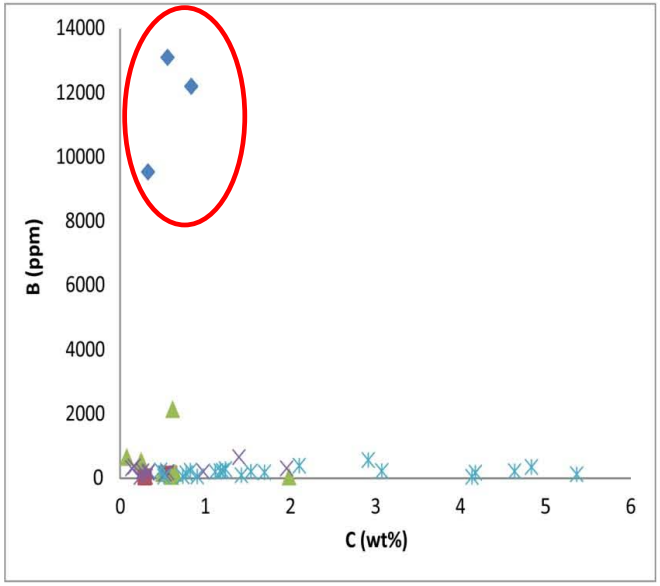


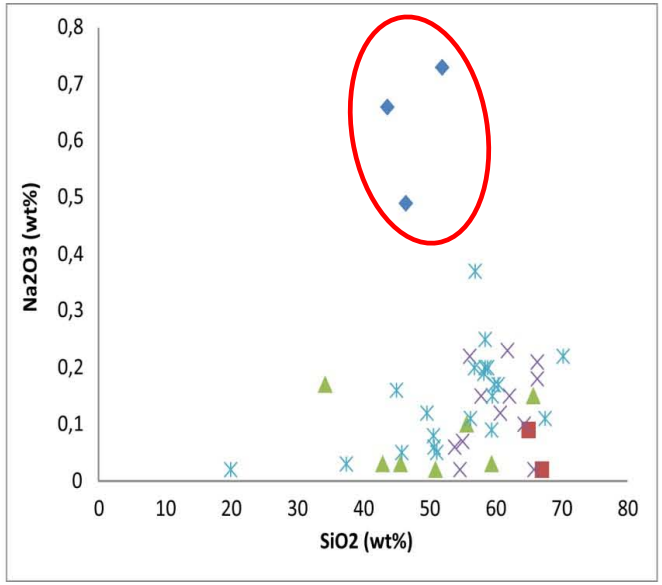




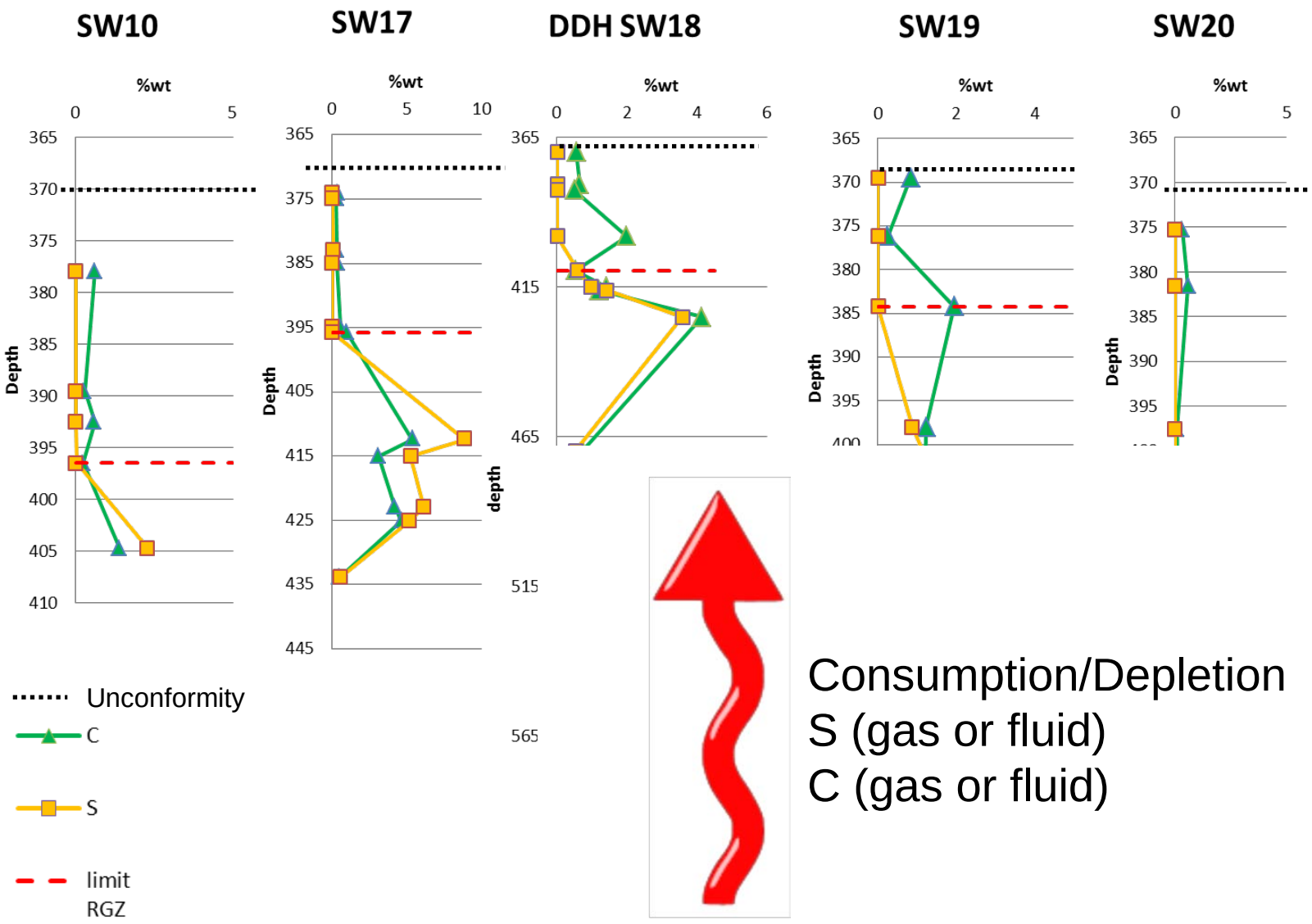






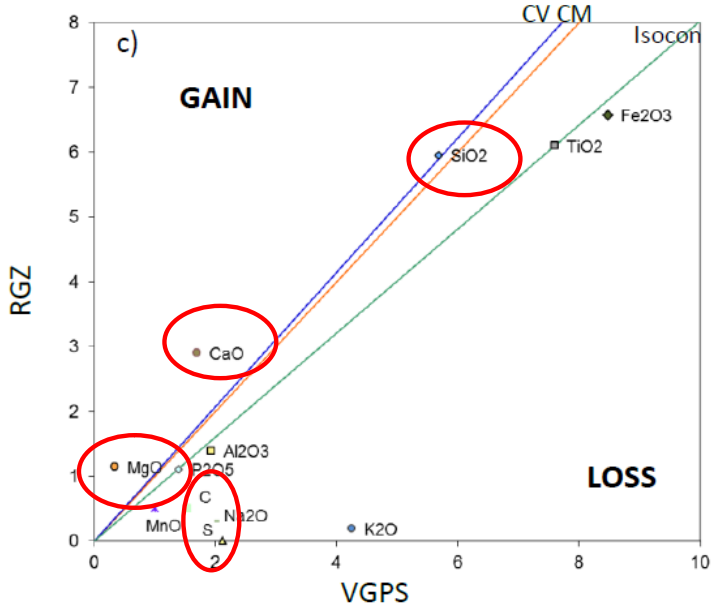


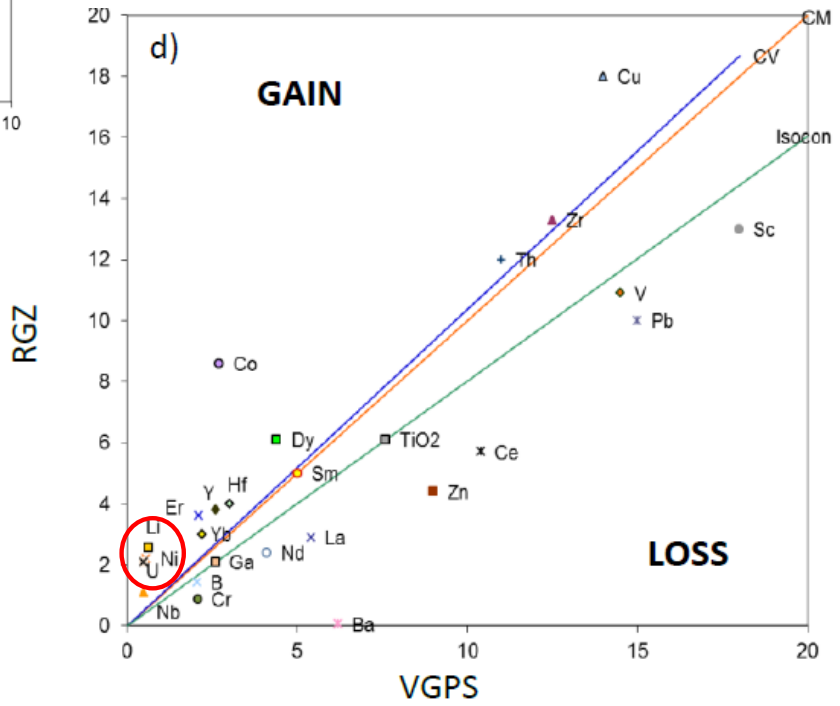
- Bleached Zone
- Red Zone
- RGZ
- Green zone
- Graphitic pelitic schist


SW10
SW17
DDH SW18
SW19
SW20
%wt
Depth
depth
Unconformity
C
S
limit
RGZ
Consumption/Depletion
S (gas or fluid)
C (gas or fluid)

Mass-balance

VGPS *vs.* RGZ





- Loss in C, S, LREE
- Gain in U, metals, HREE
- Gain in mass and volume
- Quartz formation
- Crystallization of late carbonates
- Formation of Mg-bearing chlorite

Fluid inclusion study: Quartz Generations

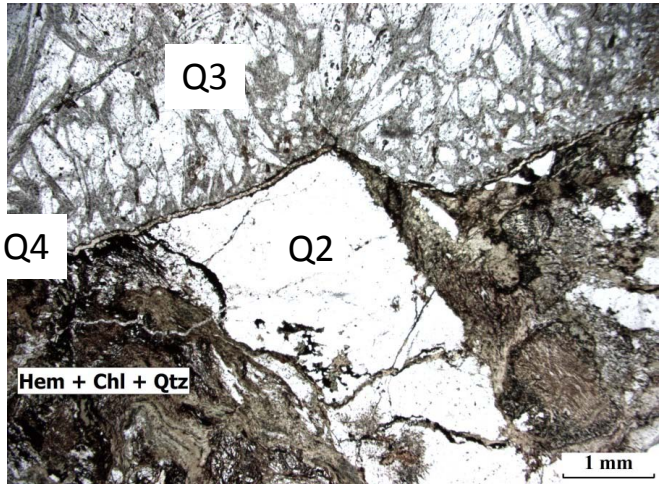
Q1: metamorphic quartz

Q2: quartz vein subparallel to the fabric, pre- to syn-ductile deformation

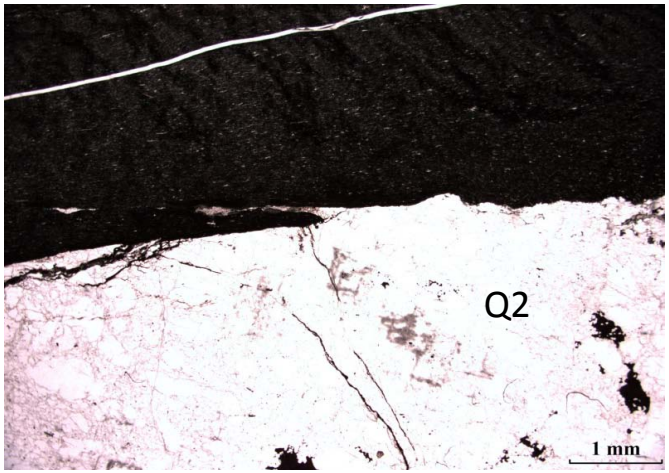
Q3: brittle quartz vein consisting of druzy quartz, and carbonates

Q4: late narrow quartz veinlets with carbonate, hematite and pyrite

•Only Q3 and/or Q4 could potentially be related to uranium mineralization

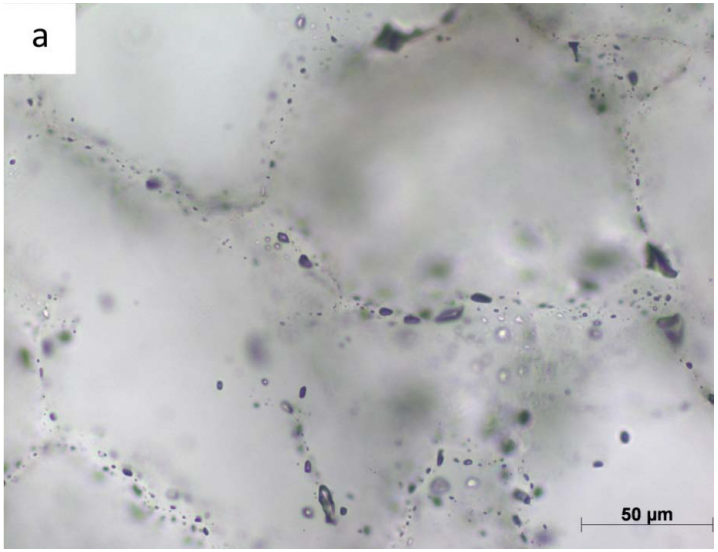


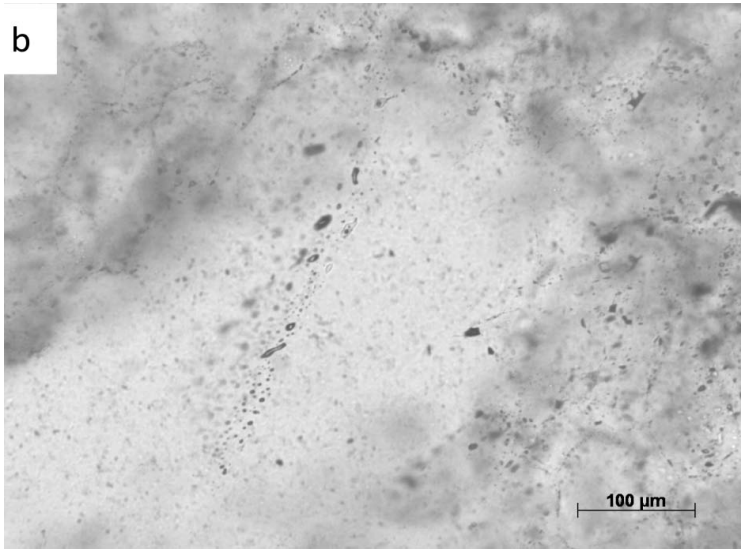
Sample SW18-382.5 from the RGZ

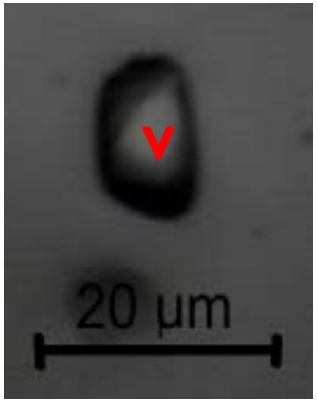


Sample SW42-484.0 from the variably graphitic pelitic schist

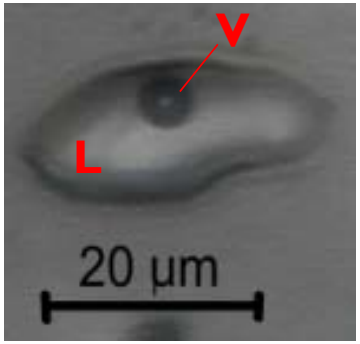
Fluid Inclusion Types







monophase vapor

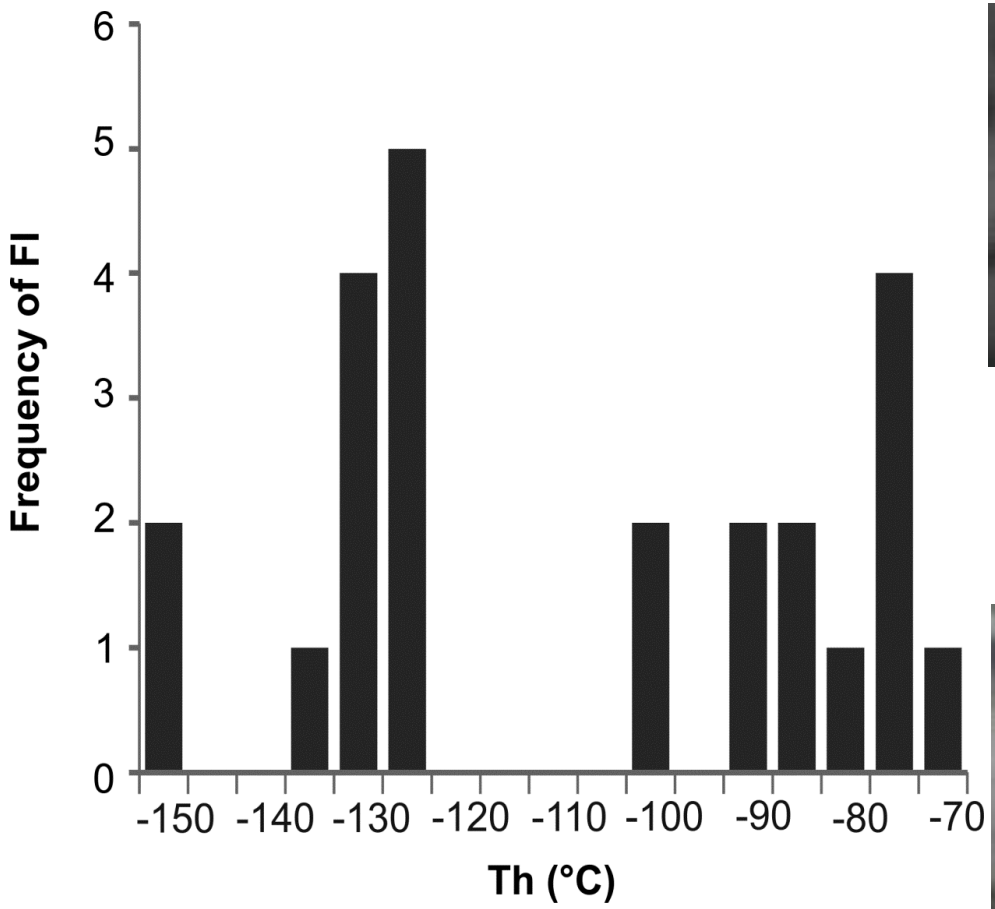


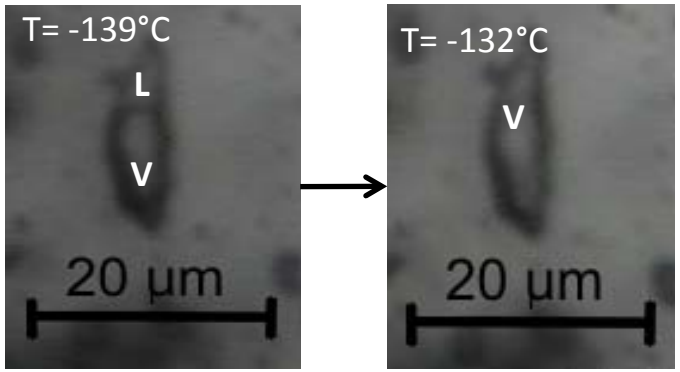
two-phase

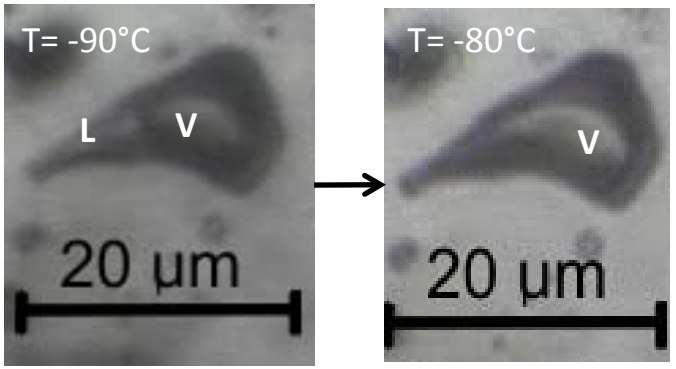


three-phase

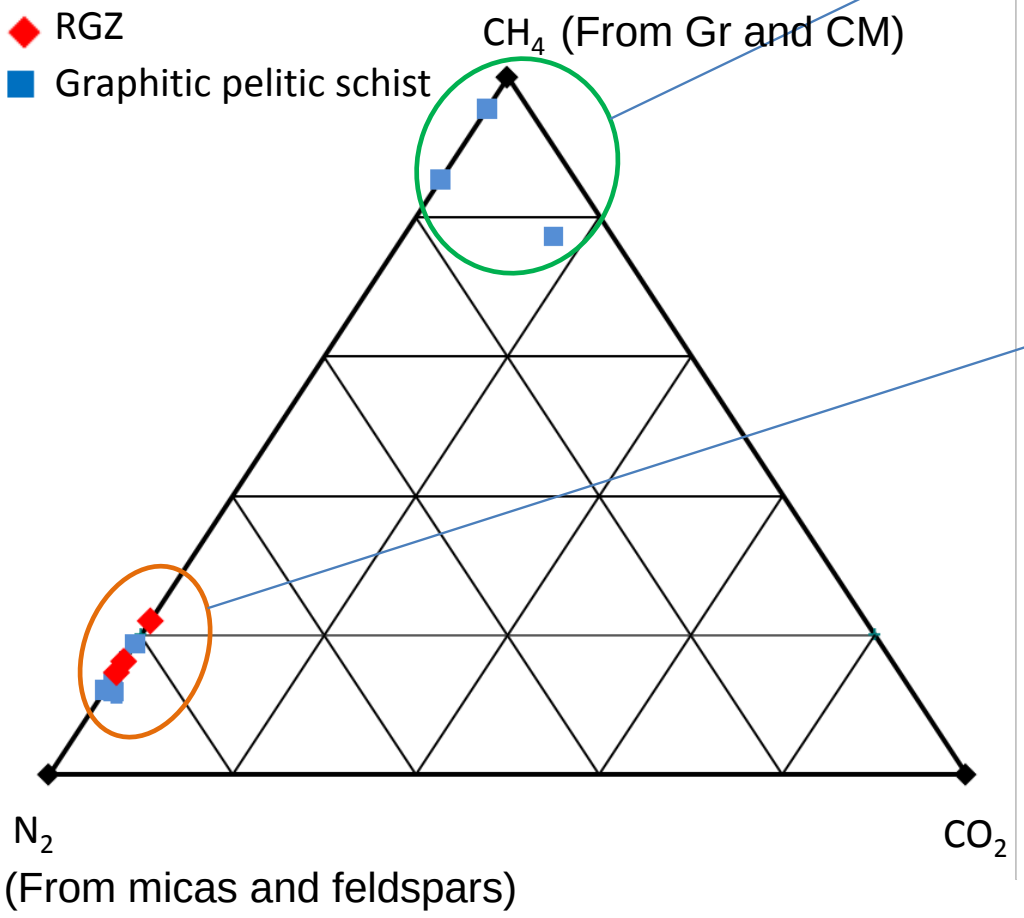
Results: Graphitic Pelitic Schist







Raman Analysis: Results



- In graphitic pelitic schist

0 <CO2 (%wt)< 16.4
77.2 <CH4 (%wt)< 95.5
4.5 <N2 (%wt)< 14.7
-81 <Th (°C)< -74.1

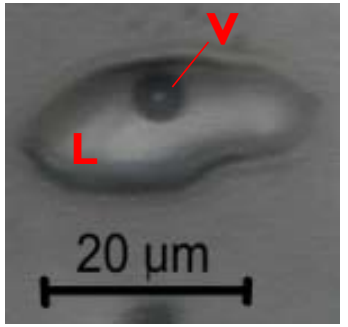
- In graphitic pelitic schist

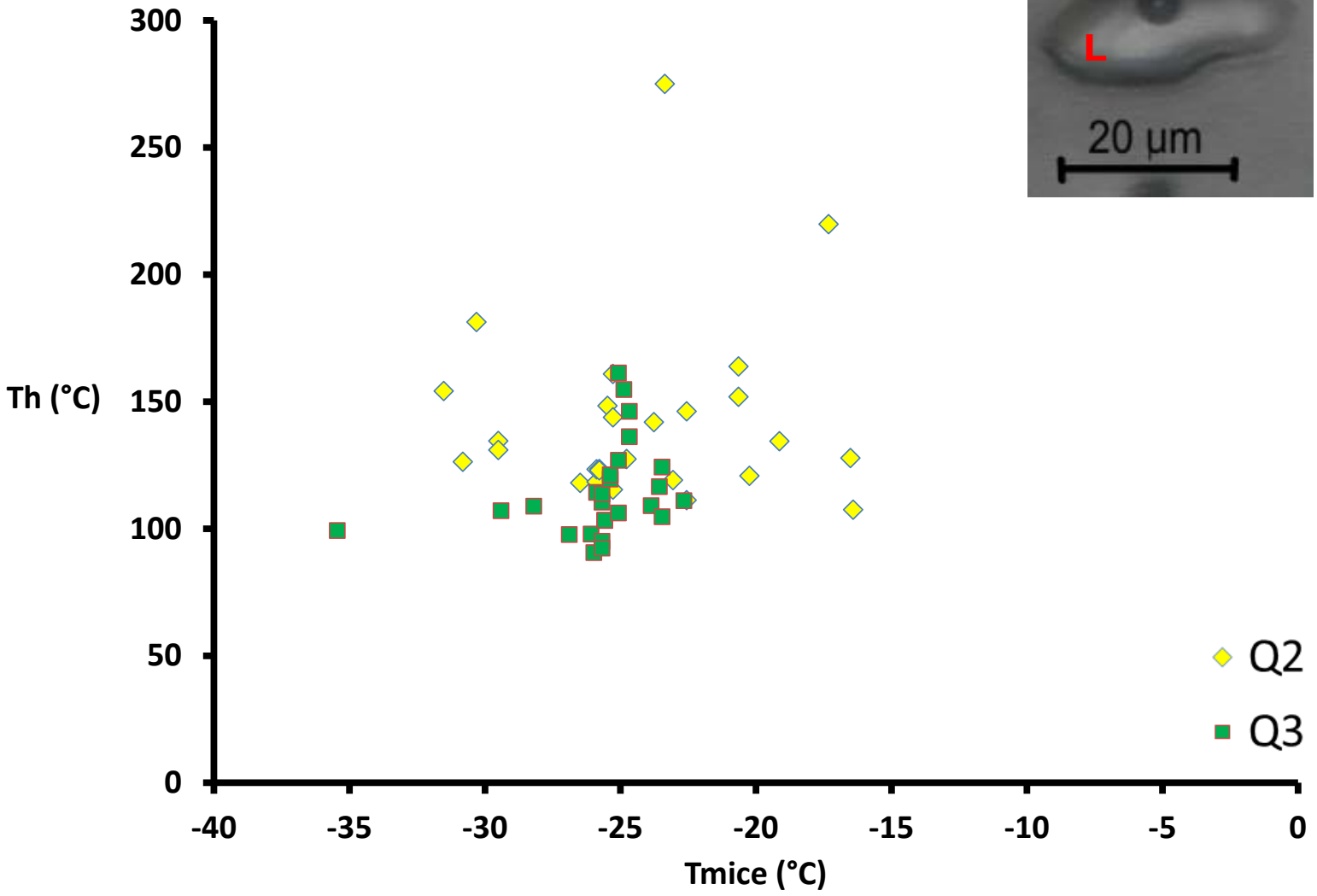
0 <CO2 (%wt)< 1.9
11.0 <CH4 (%wt)< 18.8
81.2 <N2 (%wt)< 87.8
-152.1 <Th (°C)< -100.8

- In RGZ

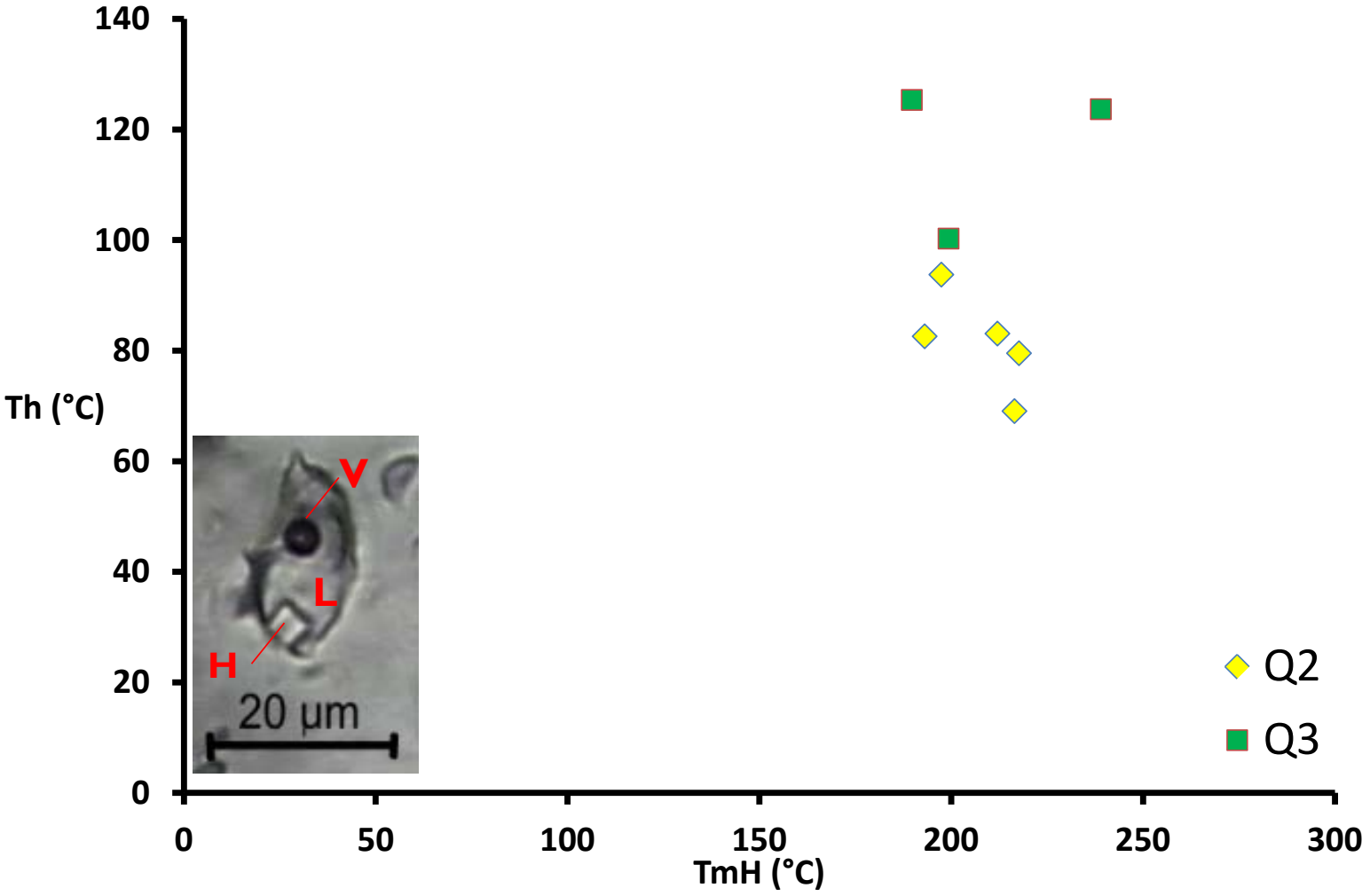
CO2 (%wt) = 0
14.7 <CH4 (%wt)< 22.1
77.9 <N2 (%wt)< 85.3
Th (°C) = -137.3

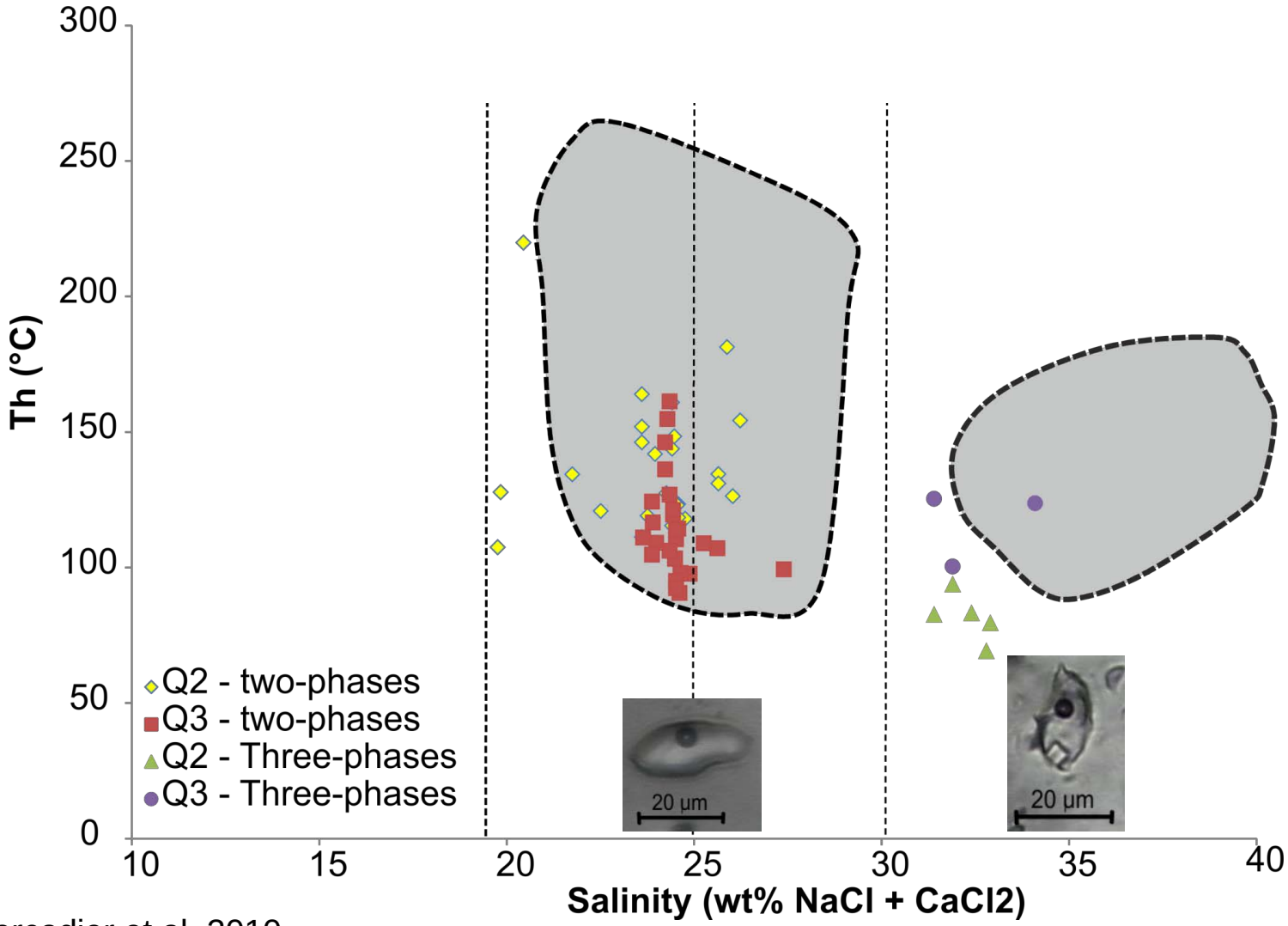
Results: Red/Green Zone





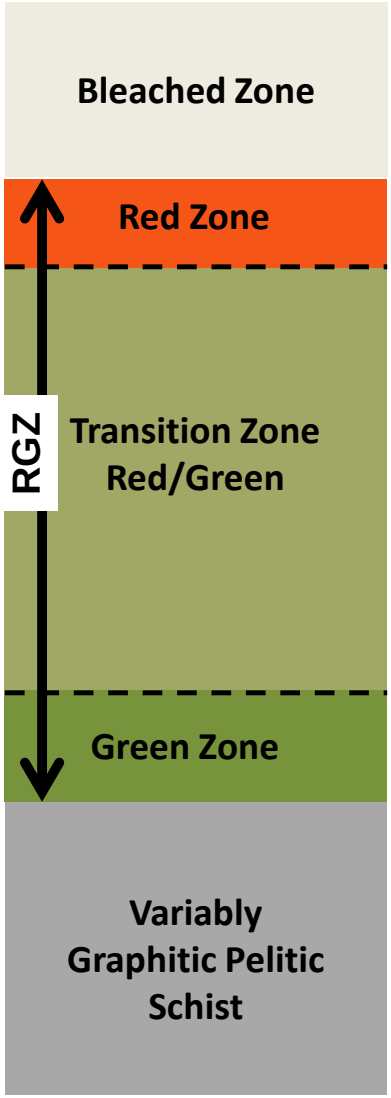
Results: Red/Green Zone





Mercadier et al. 2010

Summary



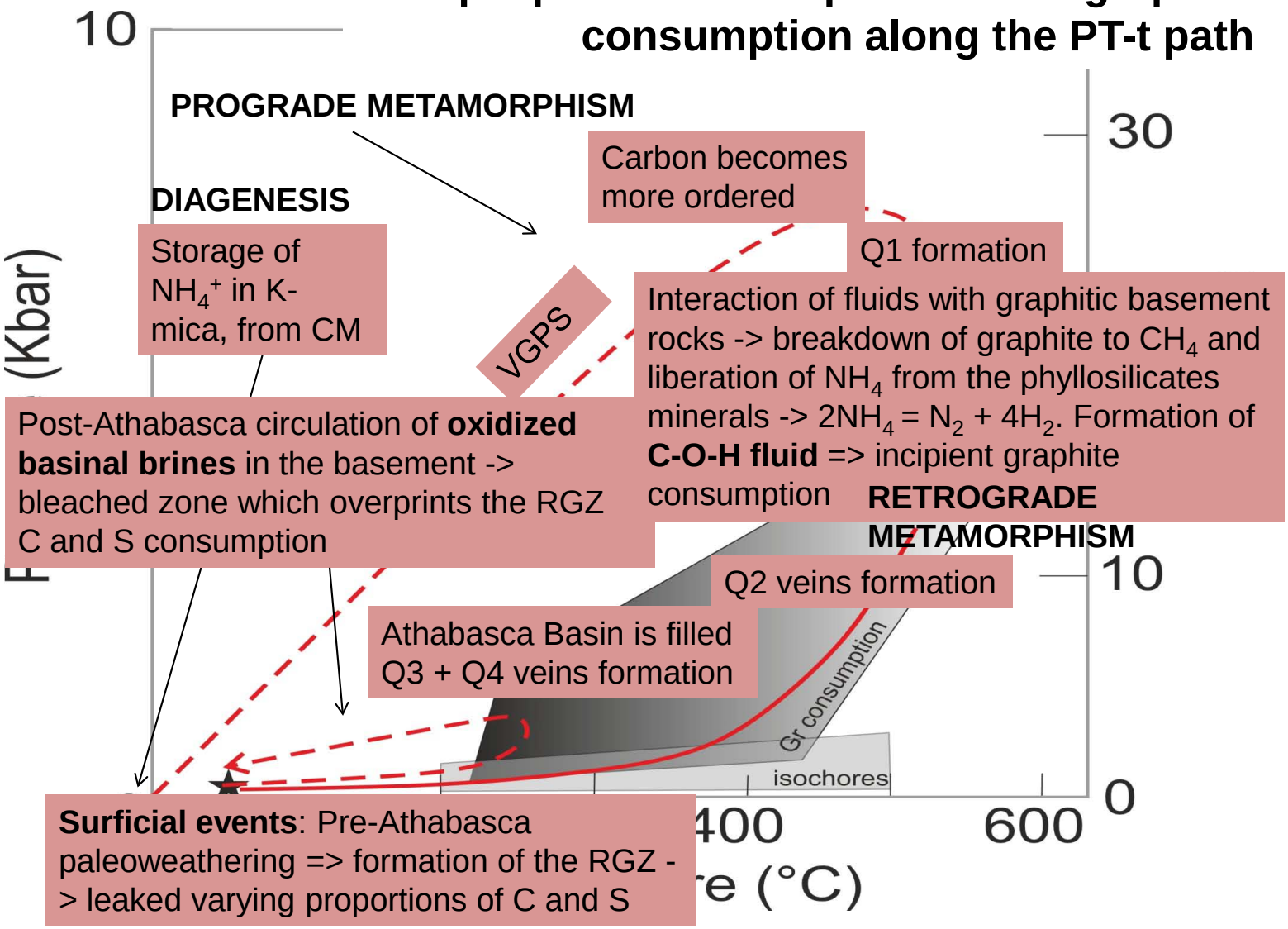
- No recognized carbon species
- Most highly altered with enrichments in Al, Na, K, B, and U
- Quartz and hematite dissolution, dravite and kaolinite formation

---

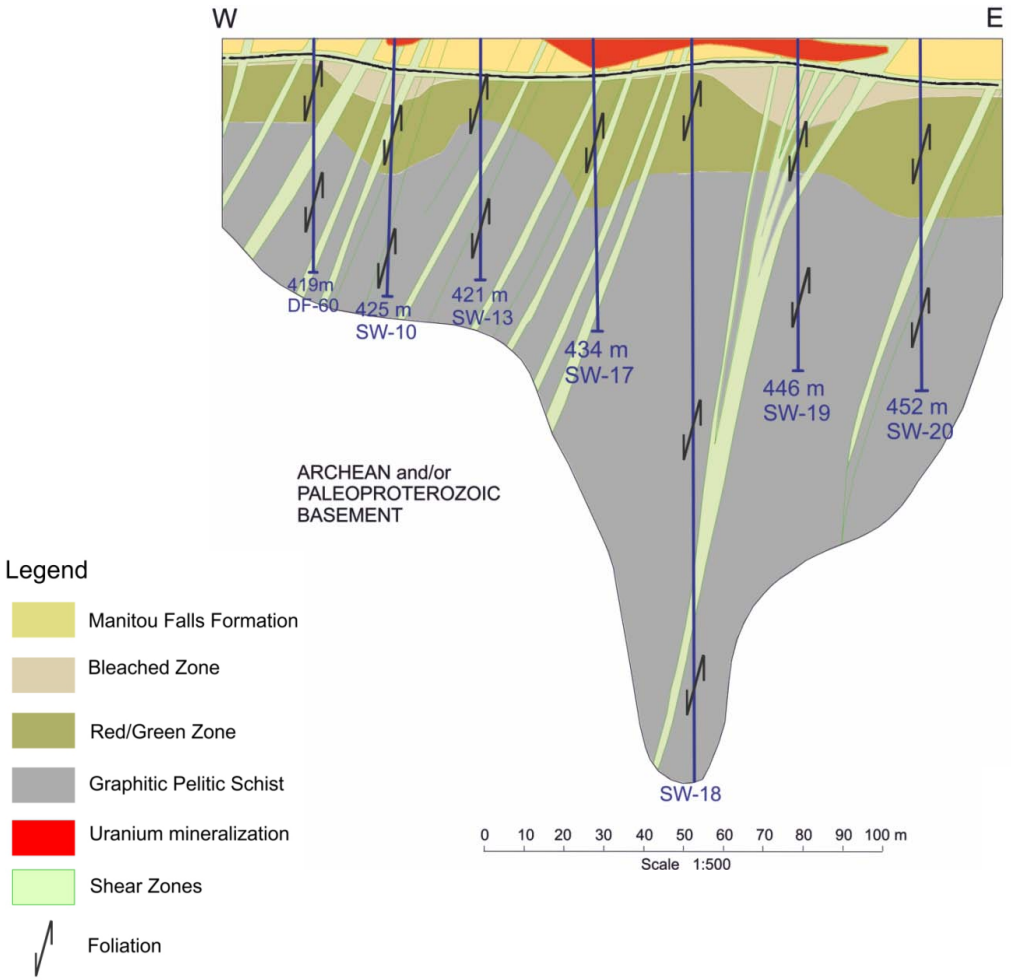
- Variable loss of carbon (+ sulfide) confirmed macroscopically, petrographically, and geochemically
- Carbon species present, but in very low to low quantity
- Mainly amorphous carbon
- Similar major element composition with the graphitic pelitic schist
- Quartz +/- hematite overprint the original fabric, and may be linked to the loss of graphite (exact timing unknown)
- Evidence for 2 brines:
  - The regional basinal fluid (Na-Ca-Mg brine)
  - An evolved brine possibly related to U mineralization (Na-Ca-Mg-Li brine)

- No fresh rocks (variably retrograded)
- Different kinds of mainly well-ordered carbon species
- Monophase vapor FI
  - Could be generated by the breakdown of graphite to **CH_4** and associated feldspars/micas to NH_4 and **N_2/H_2**
- ***<u>Three possible reductants for uranium mineralization</u>***

Multiple processes responsible for graphite consumption along the PT-t path



Last slide – link to mineralization???



Timing of graphite destruction still unknown

Possible that migration of C (and S) species which could have interacted with the U-bearing oxidized basinal brine above the unconformity to produce the mineralization in the sandstone



S (gas or fluid)
C (gas or fluid)

Mineralogy of a fertile fluid conduit related to unconformity-type uranium deposits in the Athabasca Basin.

TGI4 Workshop 2014

E. E. Adlakha[1], K. Hattori[1], G. Zaluski[2], T. Kotzer[2] and E.G. Potter[3]

[1]Department of Earth Science, University of Ottawa, Ottawa, Ontario, Canada, K1N 6N5 (*correspondence: eadla028@uottawa.ca)

[2]Cameco Corporation, Exploration Office, Saskatoon, SK. Canada, S7M 1J3 [3]Geological Survey of Canada, Ottawa, Ontario, Canada, K1A 0E8

Introduction

- P2 reverse fault (045/45-60SW)
  - along graphitic pelite in basement
- hosts the McArthur River U deposit
    - world's largest high-grade deposit
- evidence for extensive fluid/rock interaction
    - potential fluid pathway

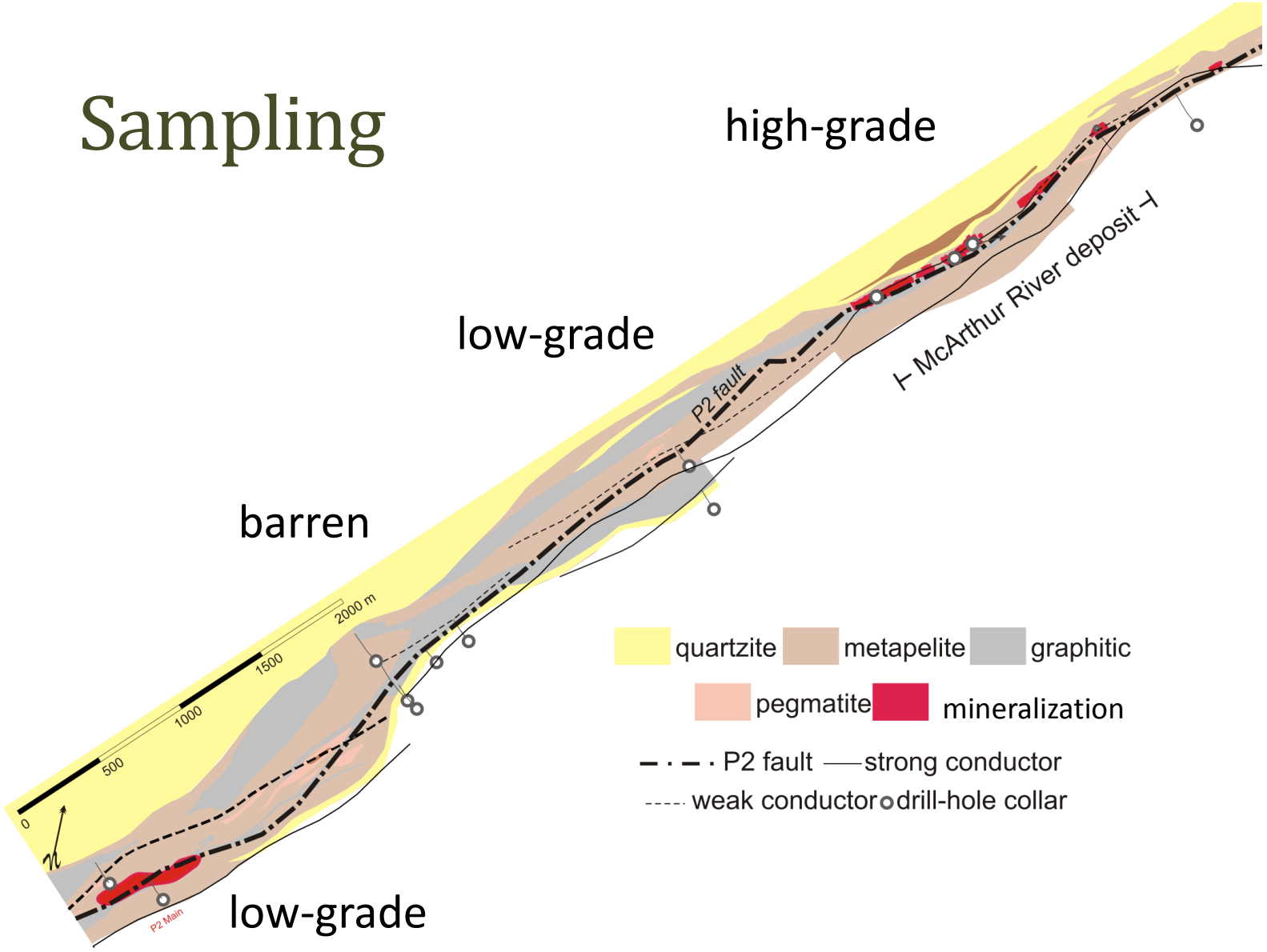
Study Objective

- evaluate role of P2 fault for uranium mineralization
- identify alteration associated with mineralization
- improve exploration criteria for unconformity-type uranium deposits

Outline

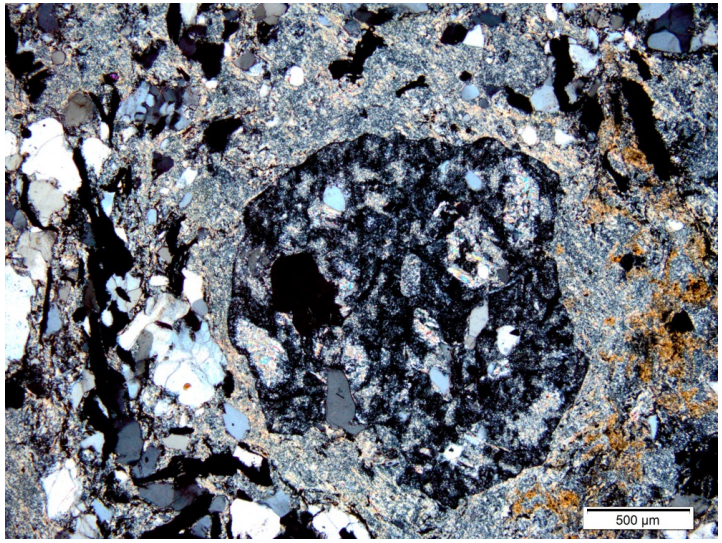
- Sampling
- Observations:
  - Distribution
  - Petrographic
  - Chemical
- Interpretation
- Implications
  - U models
  - Exploration

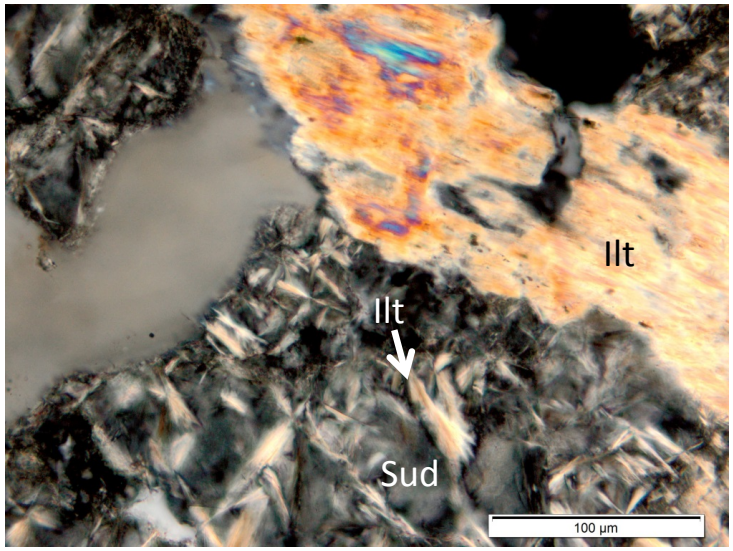
Sampling


high-grade
low-grade
barren
low-grade
McArthur River deposit
P2 fault
P2 Main
0
500
1000
1500
2000 m
quartzite
metapelite
graphitic
pegmatite
mineralization
P2 fault
strong conductor
weak conductor
drill-hole collar

Distribution

- Sudoite and Illite are common in the basements rocks of and outside the P2 fault



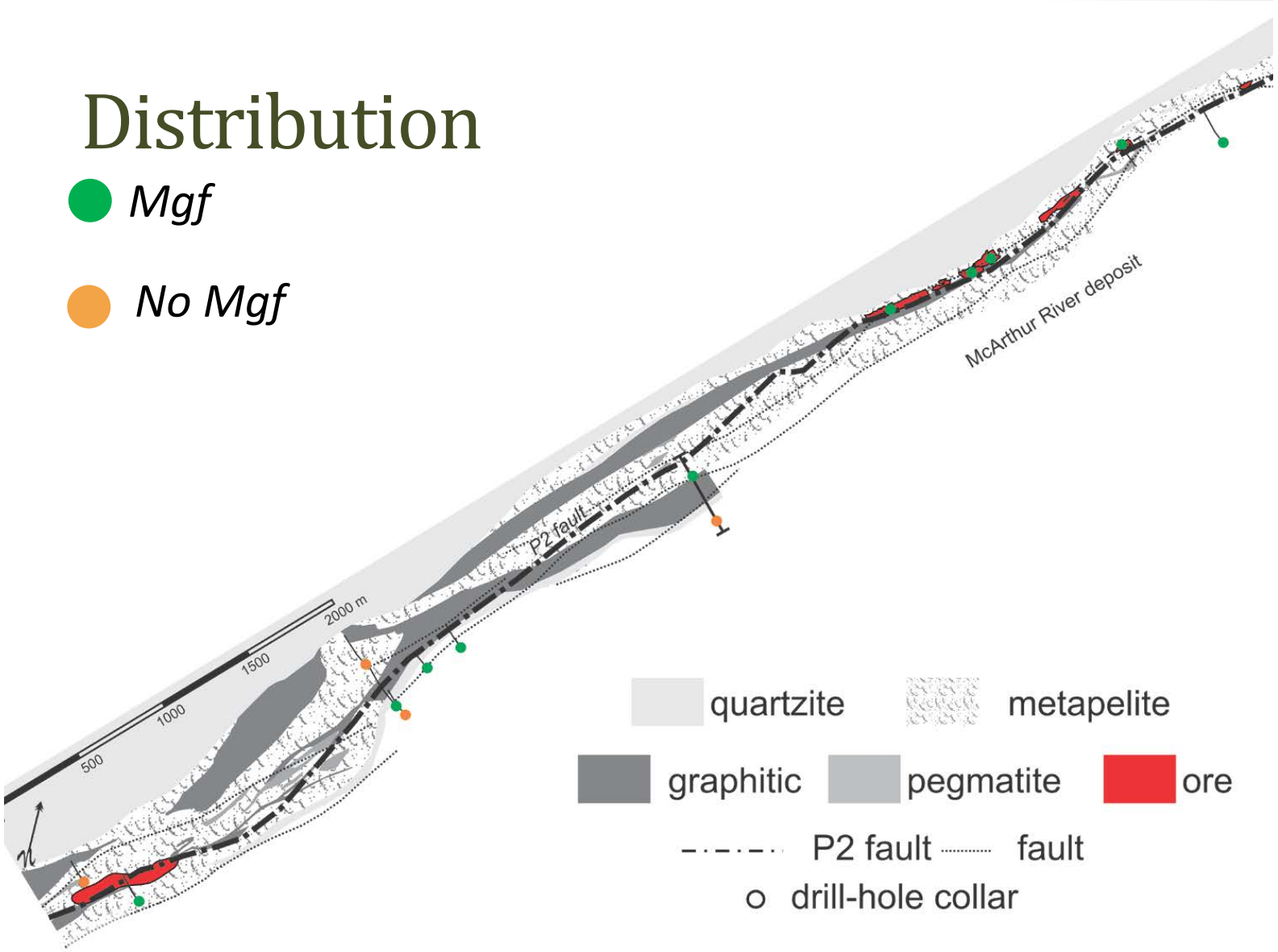


Distribution

- Sudoite and illite are common in the basements rocks of and outside the P2 fault
- Magnesio-foitite (Mgf) and APS minerals occur in basement rocks along the P2 fault and are abundant near the mineralization.
  - Mgf is constrained to the P2 fault in the basement
  - APS minerals occur outside the P2 fault, but are chemically distinct.. More on that later.

Distribution

- *Mgf*
- *No Mgf*

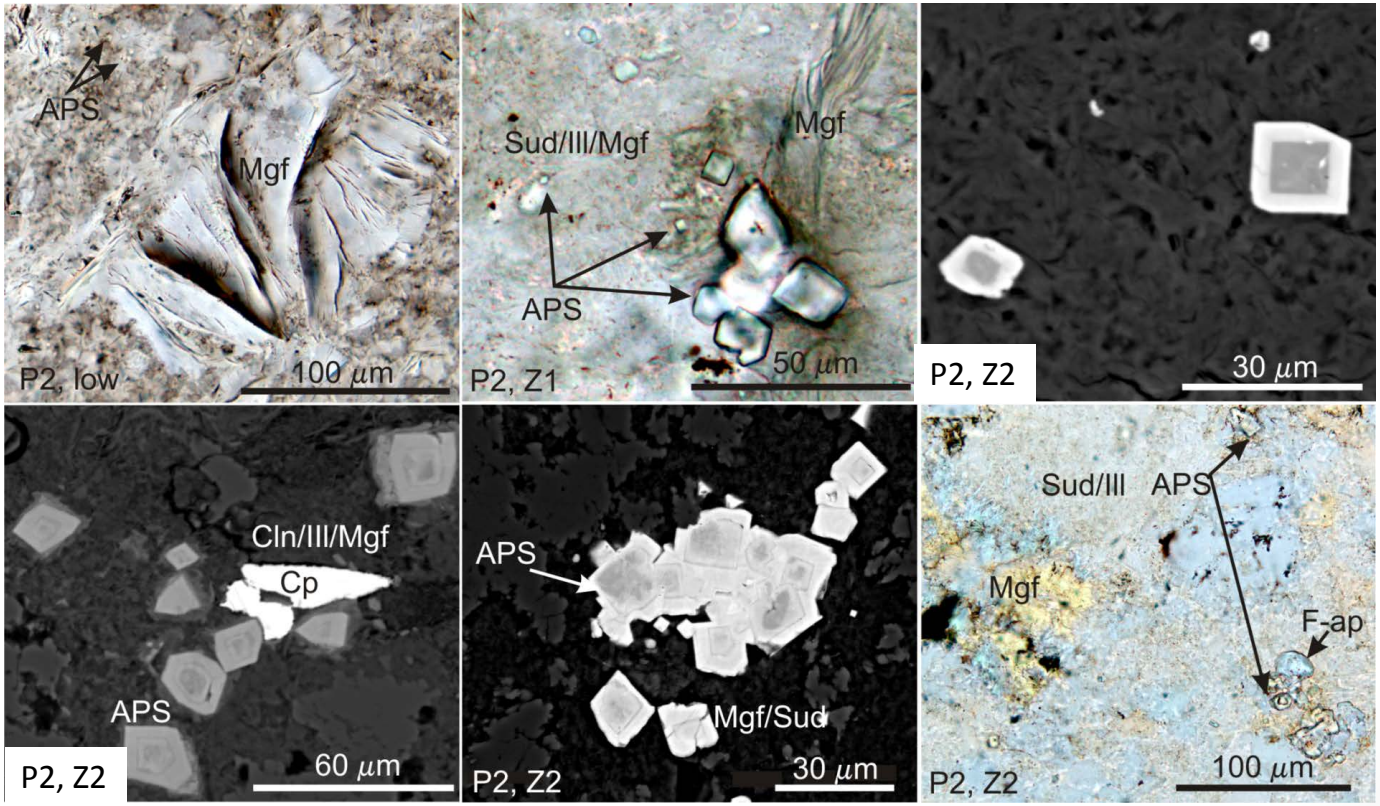


Petrographic Observations

- Mgf and APS are in equilibrium with sudoite and/or illite (similar to ore zone alteration)

Petrographic Observations

- Mgf and APS are in equilibrium with sudoite and/or illite

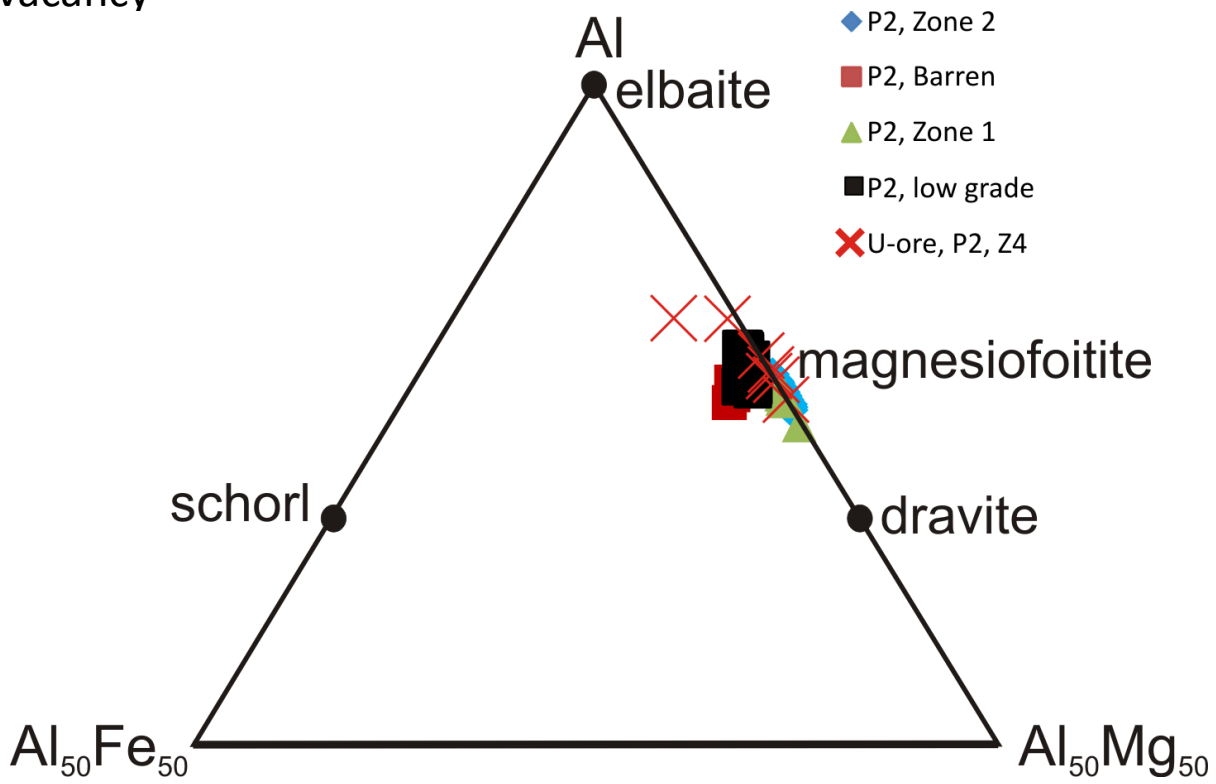


Chemical Observations

- Mgf and APS show consistent chemistry along P2
  - Mgf has large x-site vacancy

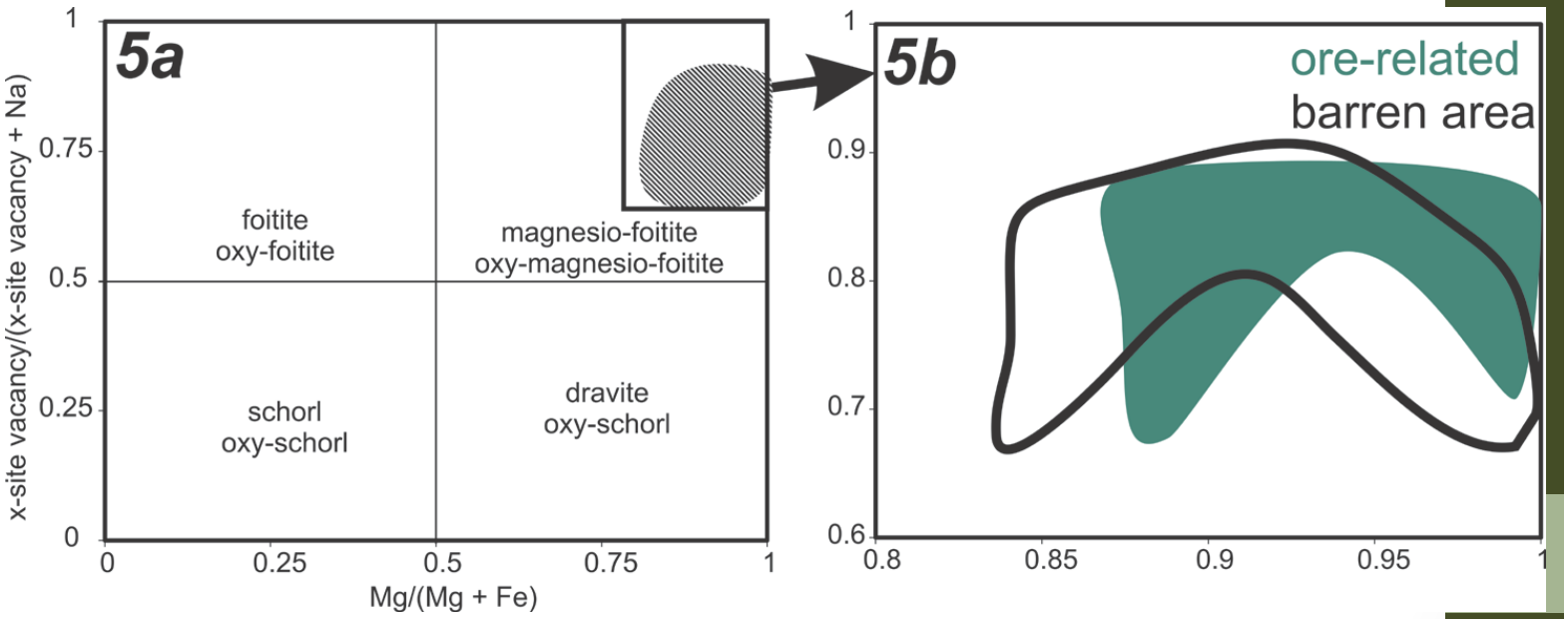
Chemical Observations

- Mgf shows consistent chemistry along P2 & has high x-site vacancy



Chemical Observations

- Mgf shows consistent chemistry along P2 & has high x-site vacancy

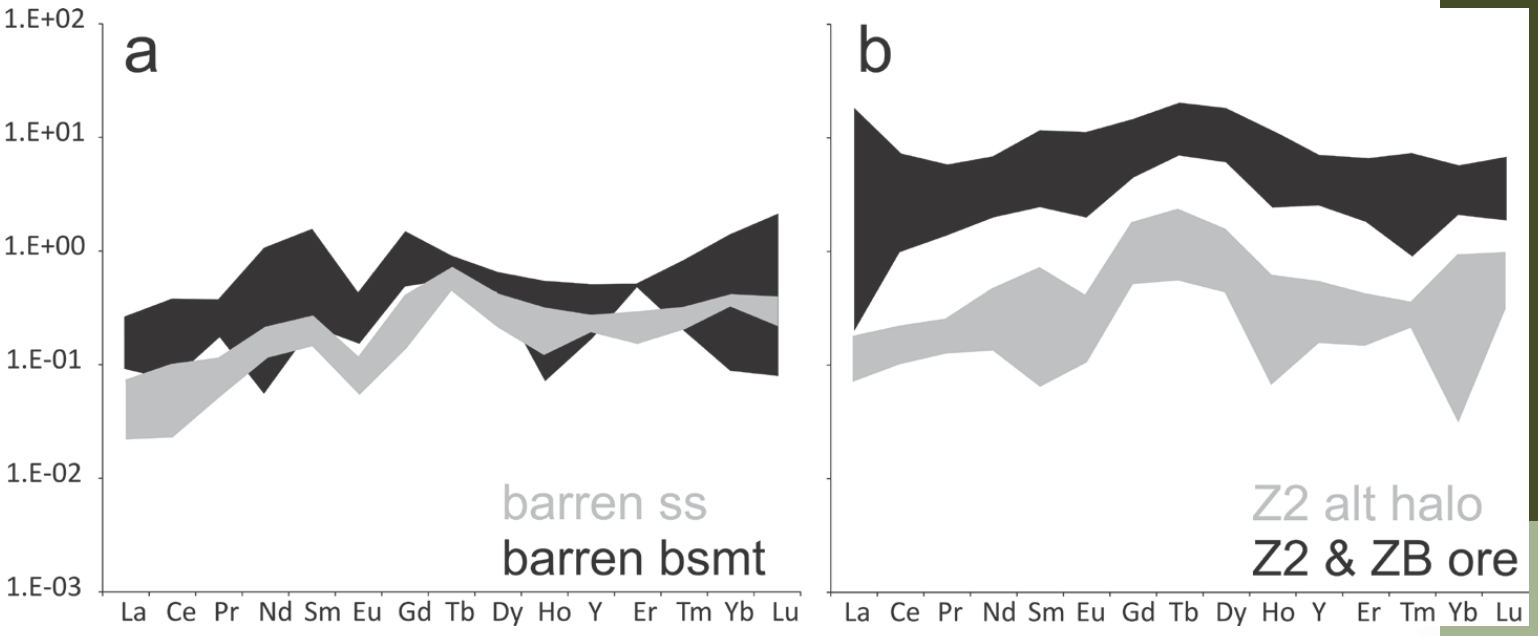


Chemical Observations

- Mgf and APS show consistent chemistry along P2
  - Mgf has large x-site vacancy
  - Mgf contains $[LREE]_N/[HREE]_N$ <0.7

Chemical Observations

- Mgf contains $[LREE]_N/[HREE]_N$ <0.7

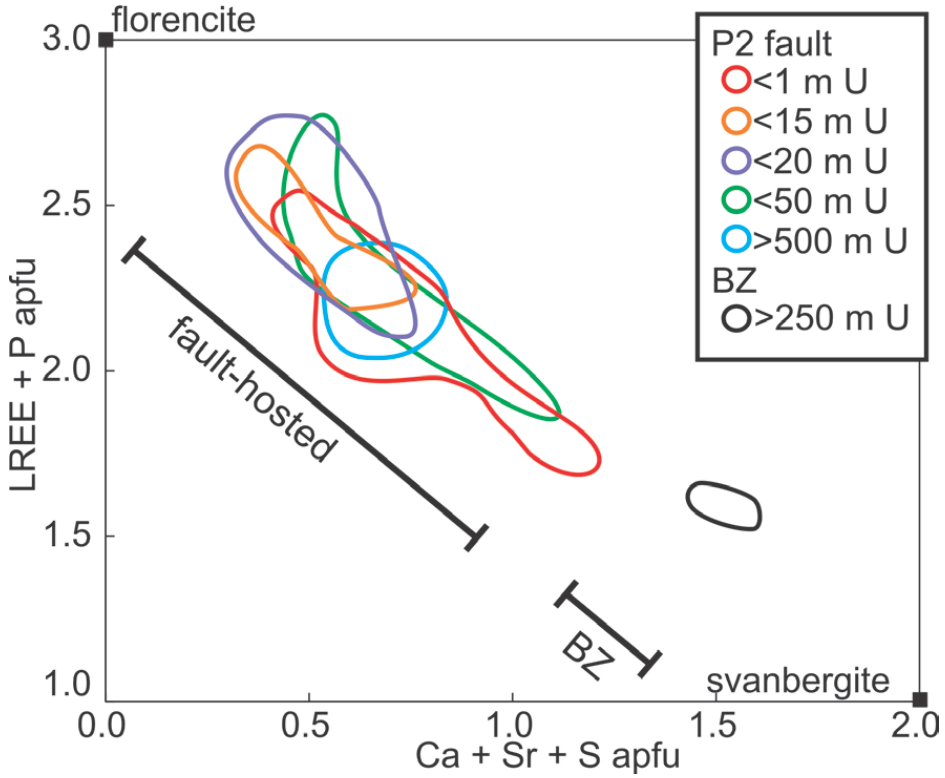


Chemical Observations

- Mgf and APS show consistent chemistry along P2
  - Mgf has large x-site vacancy
  - Mgf contains $[LREE]_N/[HREE]_N$ <0.7
  - APS along P2 are LREE- and P-rich relative to APS outside the fault

Chemical Observations

- APS along P2 are LREE- and P-rich relative to APS outside the fault

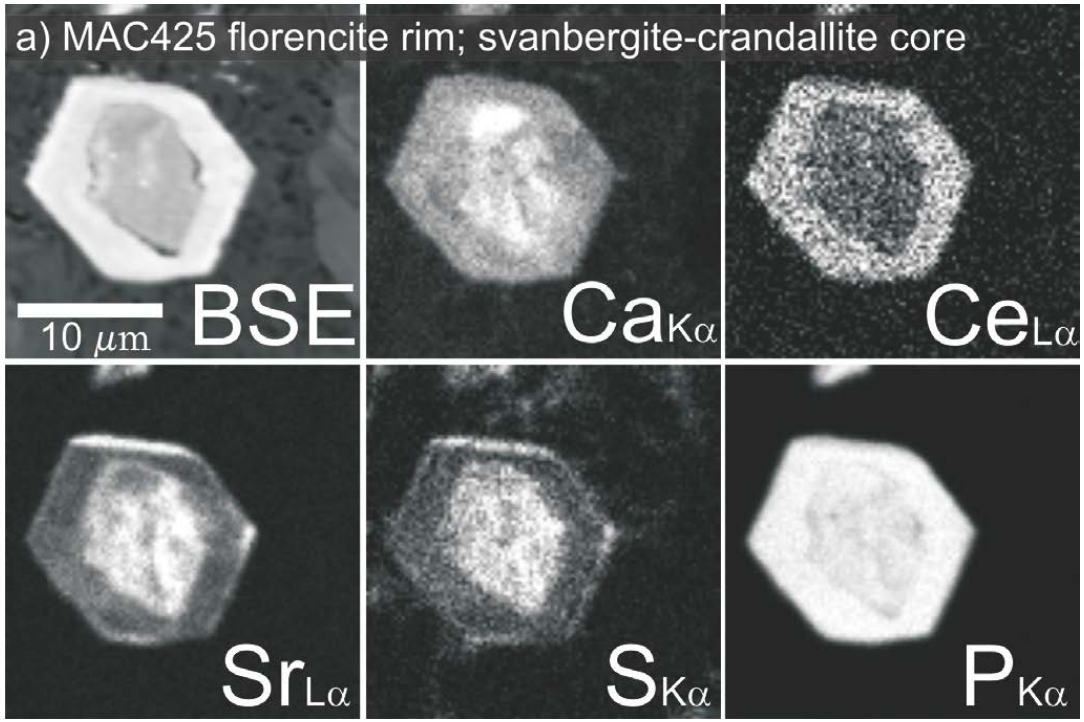


Chemical Observations

- Mgf and APS show consistent chemistry along P2
  - Mgf has large x-site vacancy
  - Mgf contains $[LREE]_N/[HREE]_N$ <0.7
  - APS along P2 are LREE- and P-rich relative to APS outside the fault
  - APS along P2 are zoned with LREE- and P-rich rims and Sr-Ca-SO_4^{2-} rich cores

Chemical Observations

- APS along P2 are zoned with LREE- and P-rich rims and Sr-Ca-SO_4^{2-} rich cores

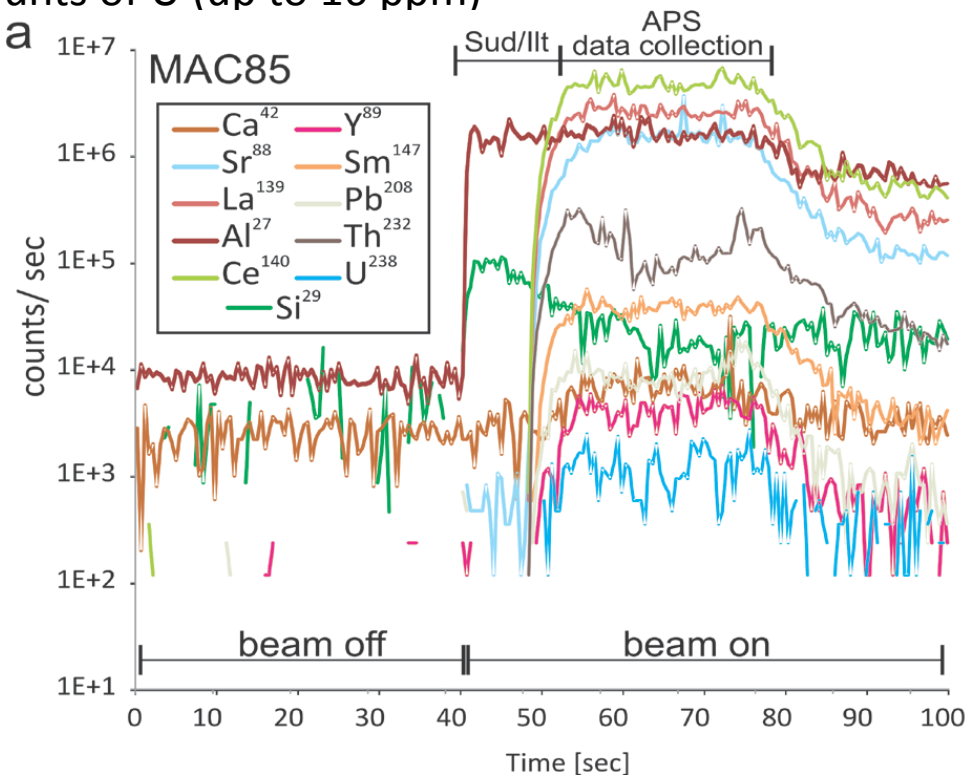


Chemical Observations

- Mgf and APS show consistent chemistry along P2
  - Mgf has large x-site vacancy
  - Mgf contains $[LREE]_N/[HREE]_N$ <0.7
  - APS along P2 are LREE- and P-rich relative to APS outside the fault
  - APS along P2 are zoned with LREE- and P-rich rims and Sr-Ca-SO_4^{2-} rich cores
  - APS along P2 and proximal to mineralization contain trace amounts of U (up to 16 ppm)

Chemical Observations

- APS along P2 and proximal to mineralization contain trace amounts of U (up to 16 ppm)



Summary of Observations

Distribution:

- Mgf occurs in basement rocks only along the P2 fault and is abundant near the mineralization.

Petrographic Observations:

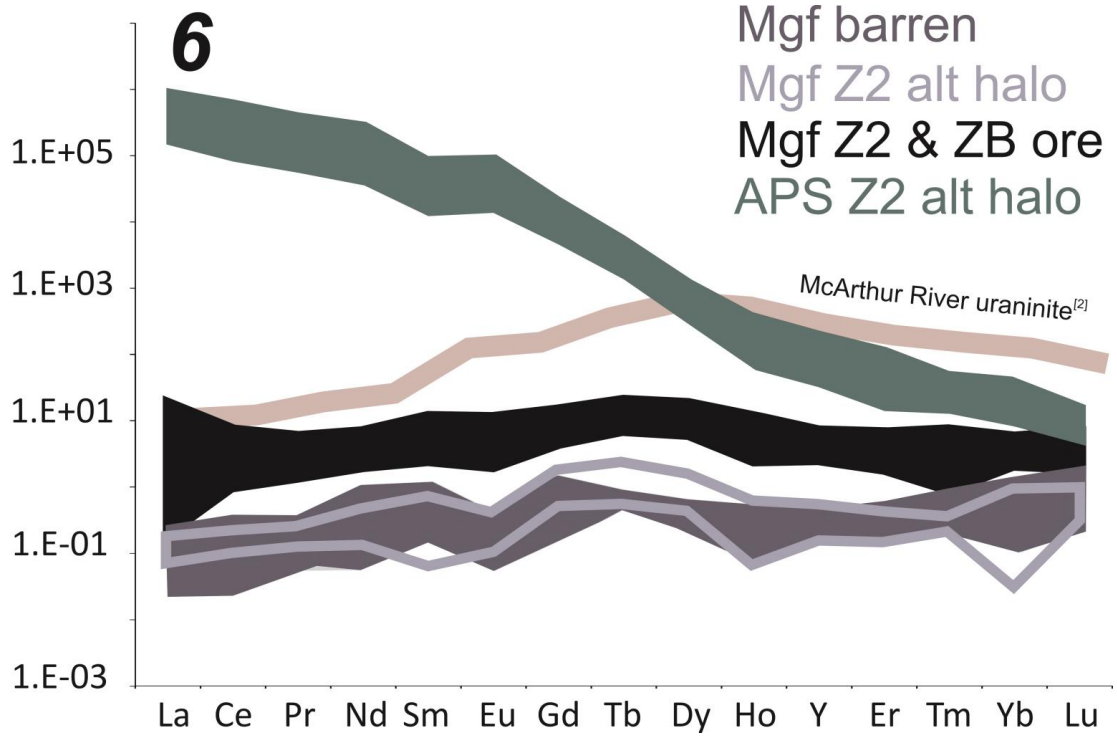
- Mgf and APS occur with alteration similar as in ore zone

Chemical Observations:

- Mgf contains $[LREE]_N/[HREE]_N$ <0.7
- APS are LREE- and P-rich relative to APS outside the fault
- APS are zoned: LREE+P rims & Sr-Ca-SO_4^{2-} cores
- APS contains U

Interpretation

- Spatial association and chemistry suggest LREE-APS and Mgf are contemporaneous



Interpretation

- Fluid chemistry:
  - Uraniferous based on U in APS minerals
  - low Na^+/H^+ ratios based on low alkali contents in Mgf
  - Changed from SO_4^{2-} -bearing and oxidizing to P+LREE rich and reducing, based on APS chemistry and compositional zoning

Implication for deposit model

- P2 fault was a conduit for uraniferous fluids, yet the fluids did not form uranium deposits all along the P2… the McArthur River deposit likely formed where a significant volume of oxidizing fluid became reduced by the basement.

Implication for exploration

- The data suggests that APS minerals and Mgf can be useful when targeting fertile basement structures as they do not occur in the basement outside the P2 structure.

Acknowledgements

- Glenn Poirier of the Museum of Nature for his help with SEM & EMPA analysis;
- Cameco Geologists Aaron Brown, Doug Adams, Remi Labelle, and Brian McGill for all of their assistance during field work at McArthur River;
- Zhoaping Yang from the GSC for assistance with LA ICP-MS work;
- We acknowledge the RAP bursary to EEA and a grant to KH from NRCan through the TGI-4 uranium ore systems project.

Geometric and hydrodynamic modelling and fluid-structural relationships in the southeastern Athabasca Basin and significance for uranium mineralization

Zenghua Li[1], Guoxiang Chi[1], Kathryn Bethune[1],
and
Sean Bosman[2], Colin Card[2]

[1] University of Regina

[2] Saskatchewan Geological Survey

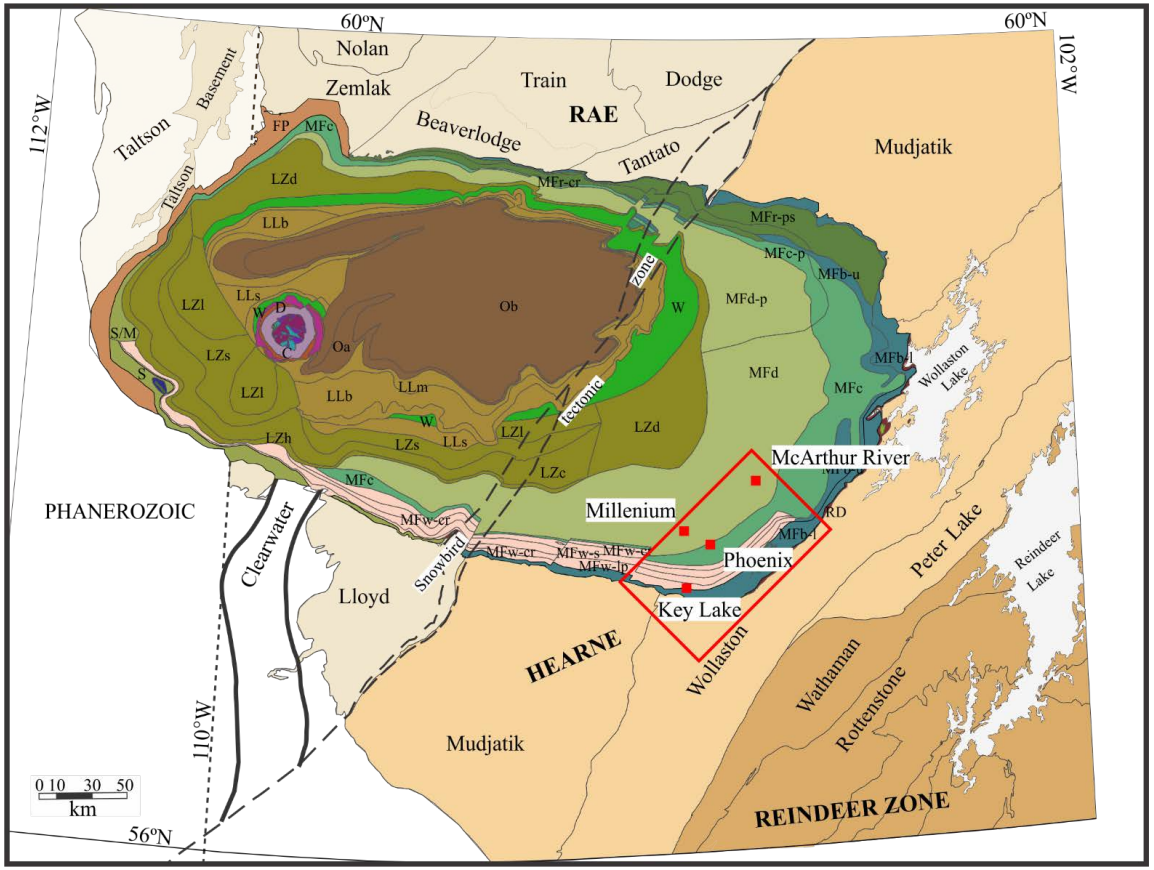
4 December, 2014

Outline

- Introduction
- Previous studies and unsolved problems
- Objectives & research methods
- Results
  1) 3D modelling of the unconformity surface of the southeastern Athabasca Basin
  2) Hydrodynamic background of the Athabasca Basin
  3) Fluid convection due to geothermal gradients
  4) Effects of spacing of basement faults on fluid convection
  5) Effects of networks of basement faults on fluid convection
  6) Coupled interaction between fluid flow and mechanical compression
- Summary



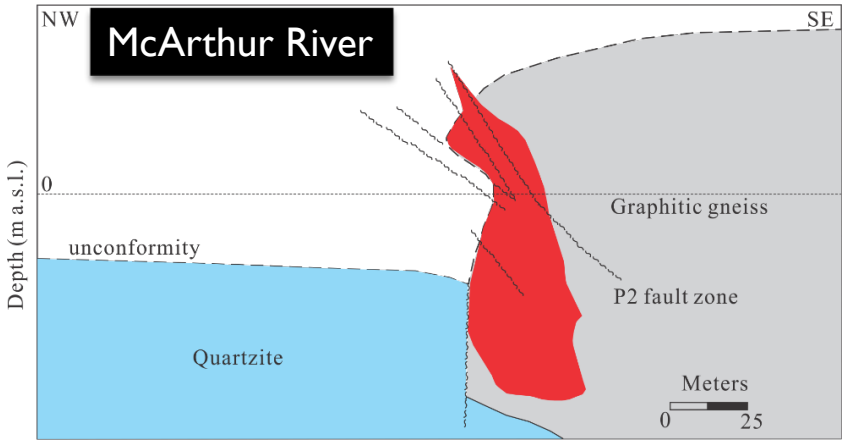
Introduction

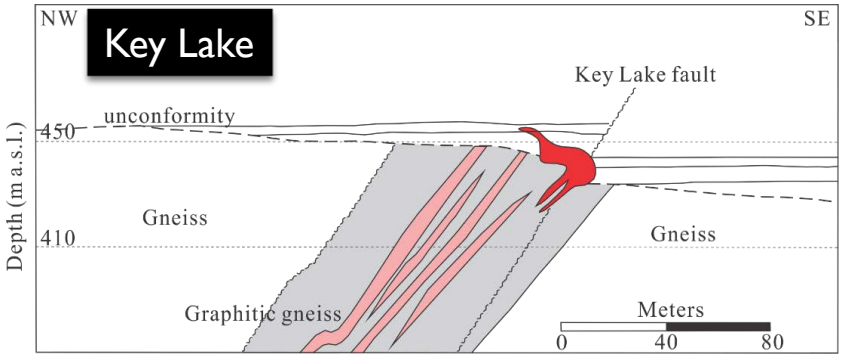


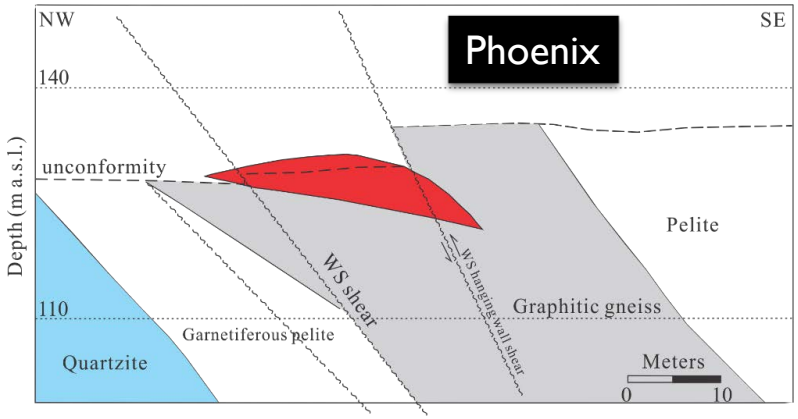
Geological map of northern Saskatchewan (modified from Card et al., 2014; Ramaekers et al., 2007 and Geological Atlas of Saskatchewan).

Introduction

Structural controls on mineralization







Previous studies and unsolved problems

- What special factors focused fluid flow at specific sites within the basin, especially along fault zones and within wider structural zones, and why some faults are more prospective than others?

- While recent studies advocate that fluid flow was either downward into basement fault zones ("ingress" deposits), or upward and outward from such zones ("egress" deposits), and that these systems were potentially linked (Jefferson et al. 2007), the dynamics involved remain poorly understood.

- Fluid flow related to uranium mineralization in the Athabasca Basin may has been driven by thermally induced fluid convection (Raffensperger and Garven, 1995), but little is known regarding how basement faults influence fluid convection and in turn how these factors may affect the localization of mineralization.



Objectives & research methods

- 3D geomodelling

  To evaluate the spatial configuration of basement structures, the unconformity surface, alteration patterns, and uranium mineralization.

- Numerical modelling

  To test the effects of various combinations of lithologies, orientations of structures, stress fields and thermal conditions on fluid flow.

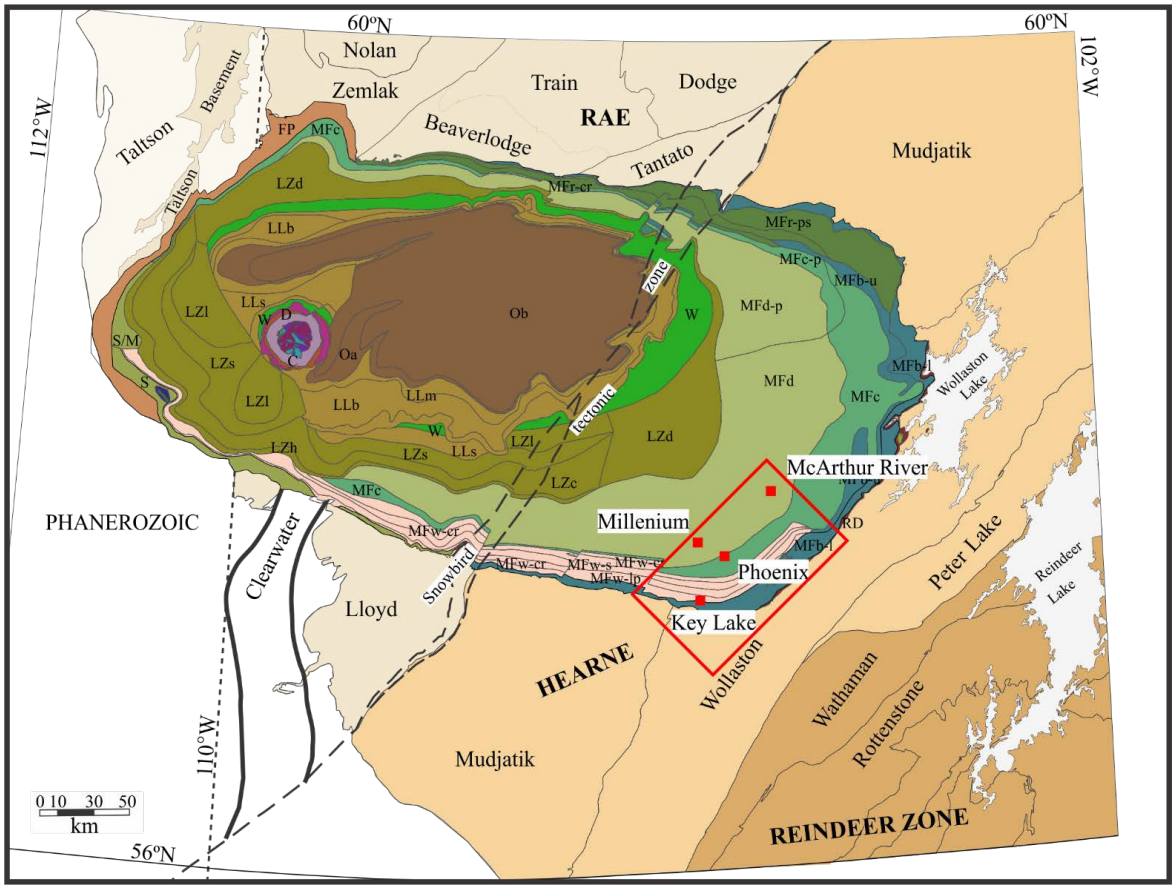


Results

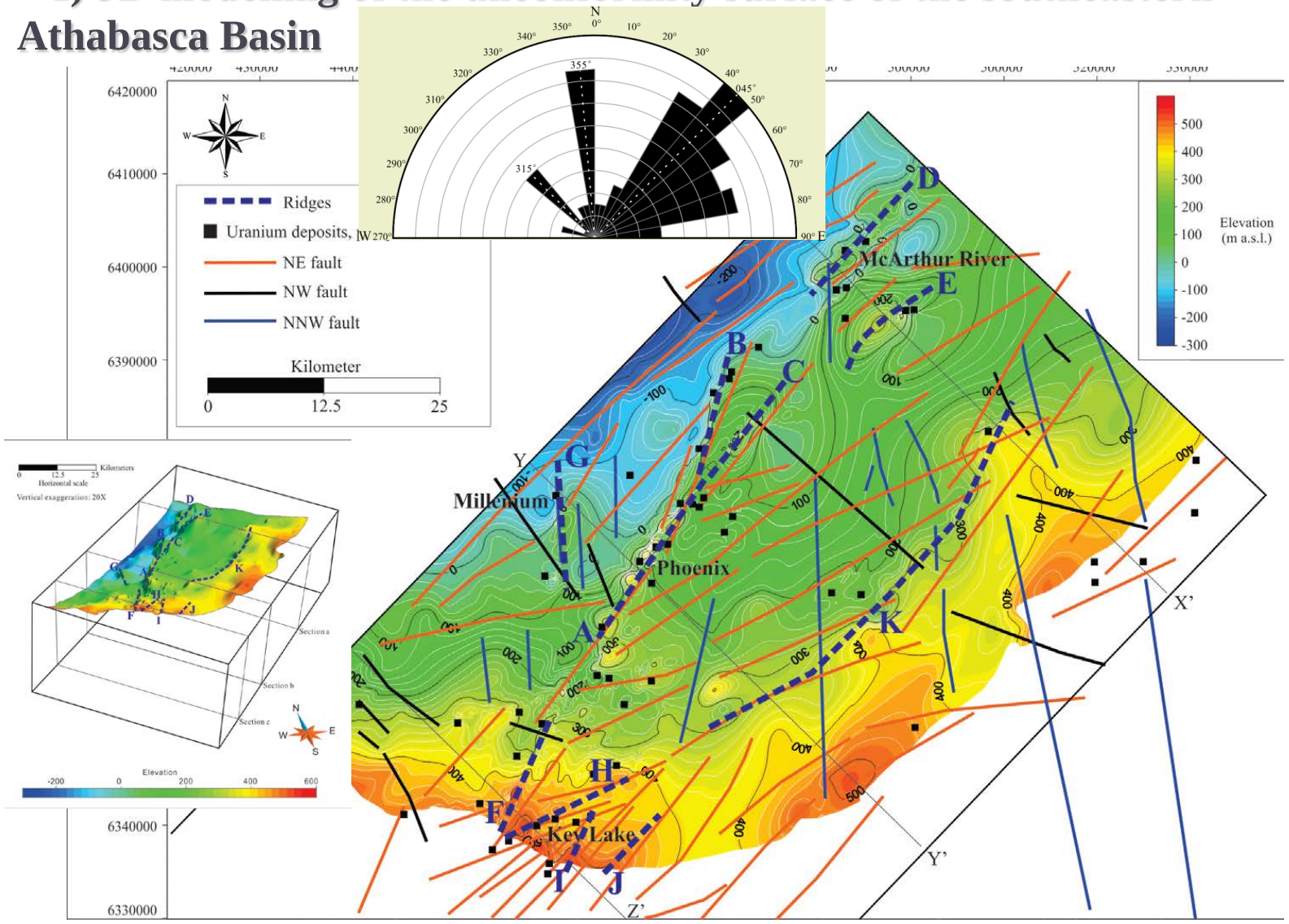
1) 3D modelling of the unconformity surface of the south-eastern Athabasca Basin
2) Hydrodynamic background of the Athabasca Basin
3) Fluid convection due to geothermal gradients
4) Effects of spacing of basement faults on fluid convection
5) Effects of networks of basement faults on fluid convection
6) Coupled interaction between fluid flow and mechanical compression



1) 3D modelling of the unconformity surface of the southeastern Athabasca Basin

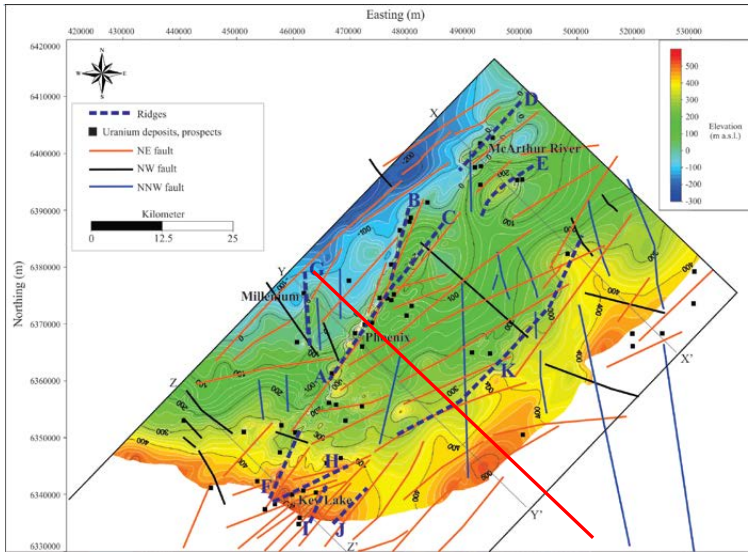


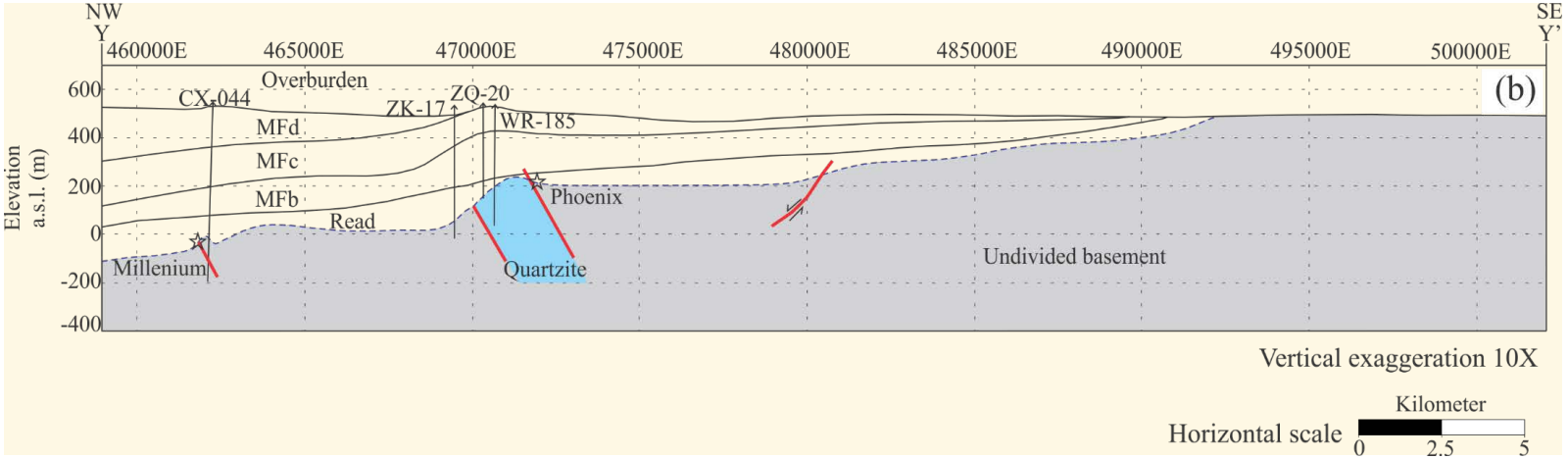
1) 3D modelling of the unconformity surface of the southeastern Athabasca Basin



1) 3D modelling of the unconformity surface of the southeastern Athabasca Basin

- Product of combined action of three main factors:
  - 1) pre-Athabasca group ductile faulting;
  - 2) differential weathering/erosion of stronger versus weaker units;
  - 3) post-Athabasca fault reactivation, localized in pre-existing, weak graphite rich ductile shear zones.



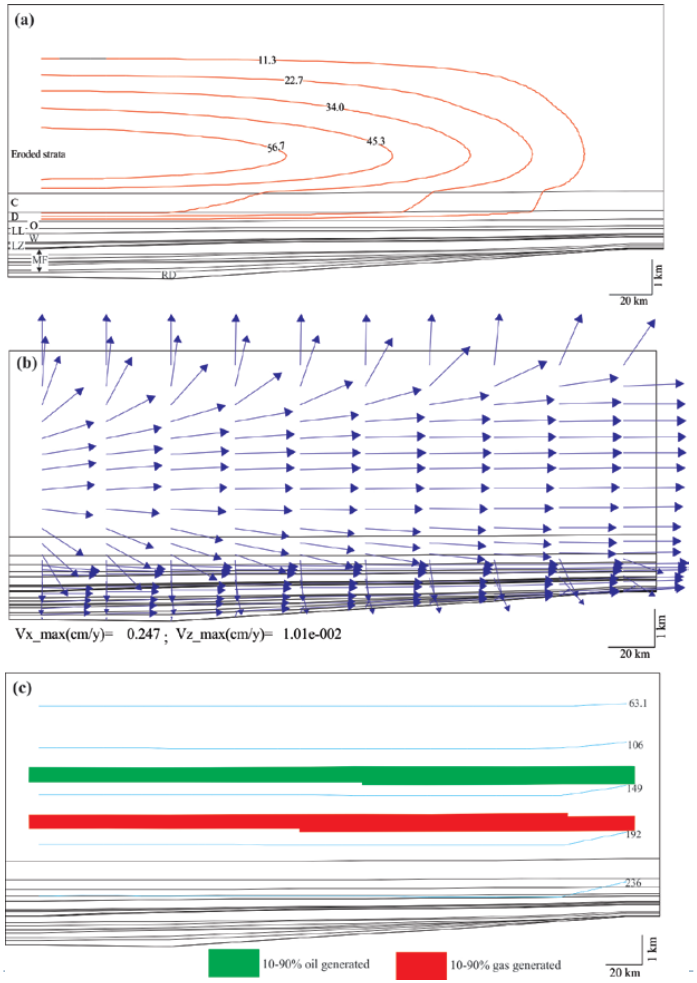


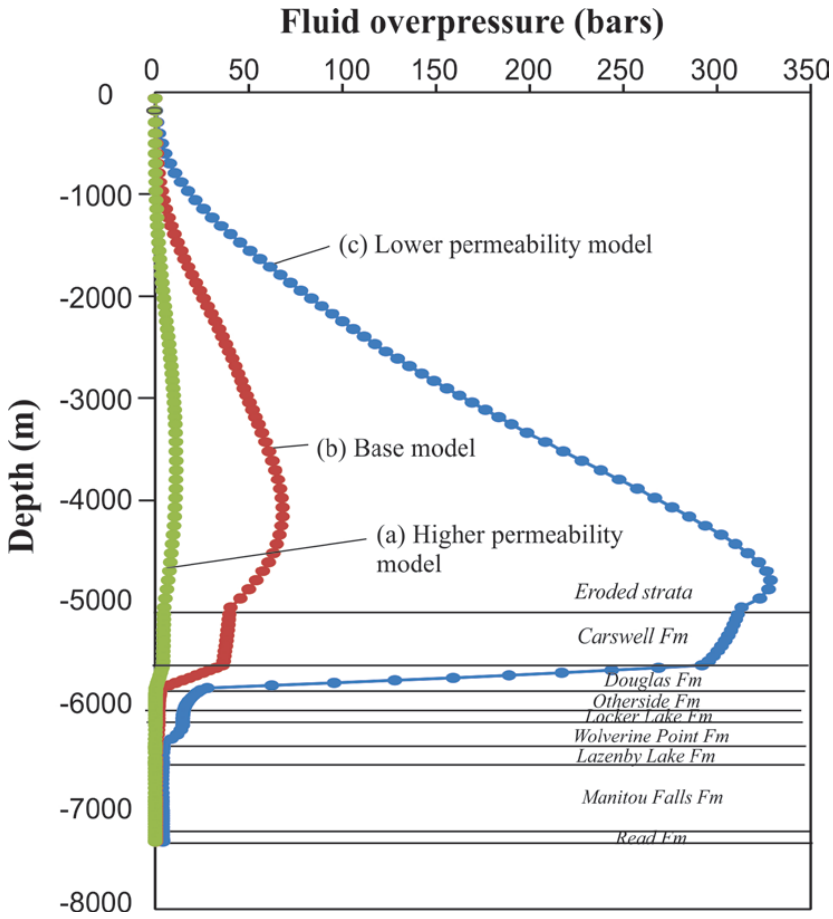
2) Hydrodynamic background of the Athabasca Basin

- Recent numerical study by Chi, Bosman and Card (2013) confirmed that no significant fluid overpressure was developed due to disequilibrium sediment compaction in the basin during sedimentation from ca. 1740 to 1541 Ma (Rainbird et al., 2007);
- A complementary study was undertaken to evaluate how hydrocarbon generation processes in the Douglas Formation, which contains total organic carbon (TOC) of up to 3.56 wt.%, may have affected fluid overpressure development in the basin (Chi, Li and Bethune, 2014).



2) Hydrodynamic background of the Athabasca Basin





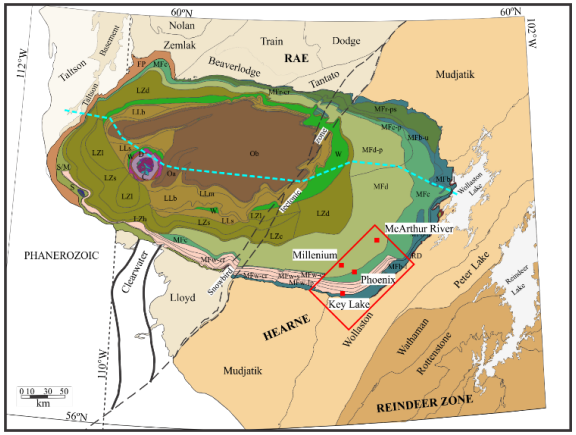
Chi, Li and Bethune, 2014

2) Hydrodynamic background of the Athabasca Basin

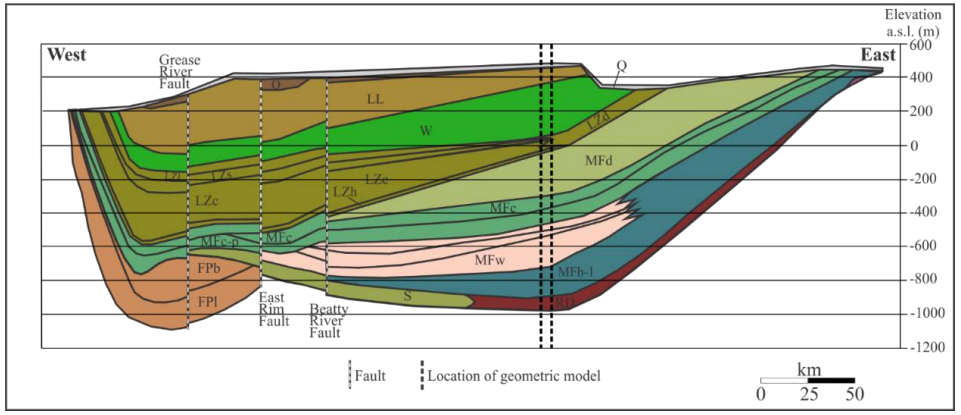
- The numerical modelling results presented above indicate that fluid pressures in the Athabasca basin were close to hydrostatic values throughout its history (Chi et al., 2013; 2014).
- This suggests that fluid flow driven by topographic relief (e.g., Alexandre and Kyser, 2012) or convection related to fluid density variation due to thermal gradients (e.g., Raffensperger and Garven, 1995) are both theoretically plausible.



3) Fluid convection due to geothermal gradients

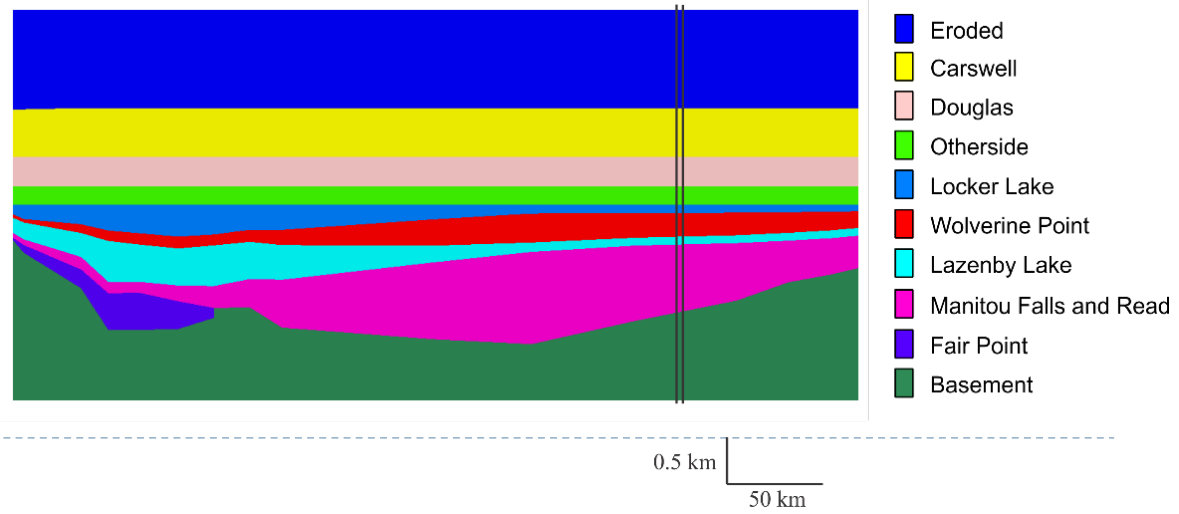


modified from Card et al., 2014 and Ramaekers et al., 2007

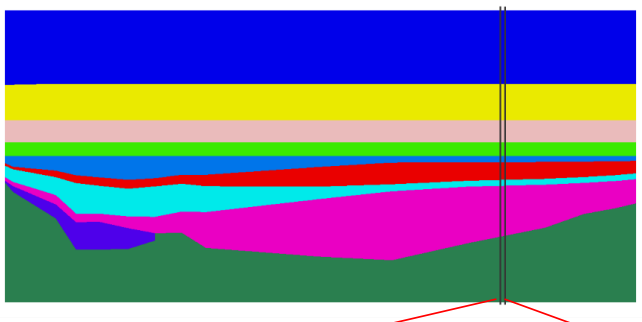


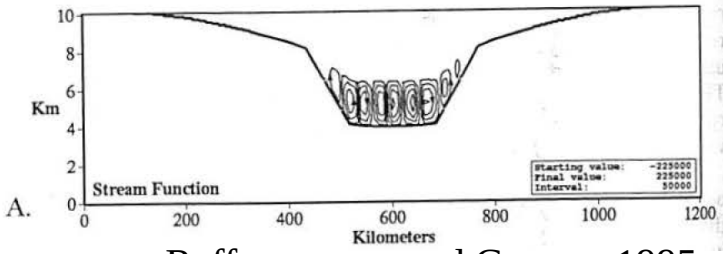
modified from Ramaekers et al., 2007

The physical model is similar to that used by Chi et al. (2013), where the basin is divided into several layers with <u>different permeabilities</u>.



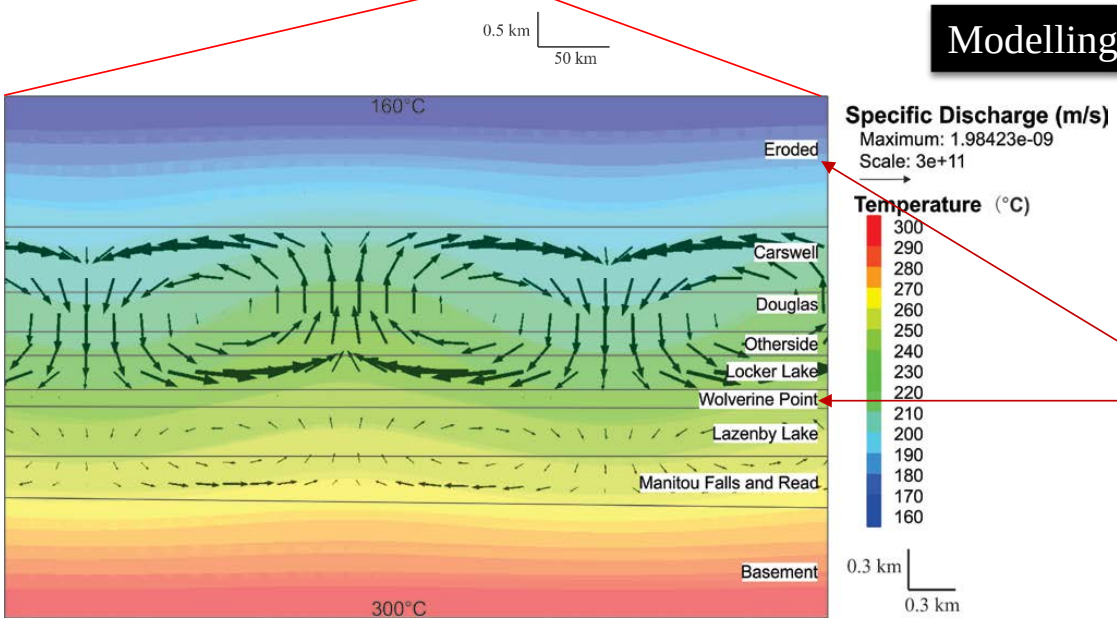
3) Fluid convection due to geothermal gradients





Raffensperger and Garven, 1995

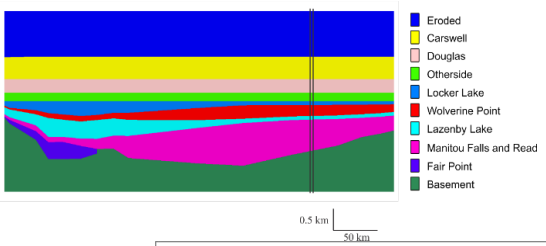
Modelling without vertical exaggeration



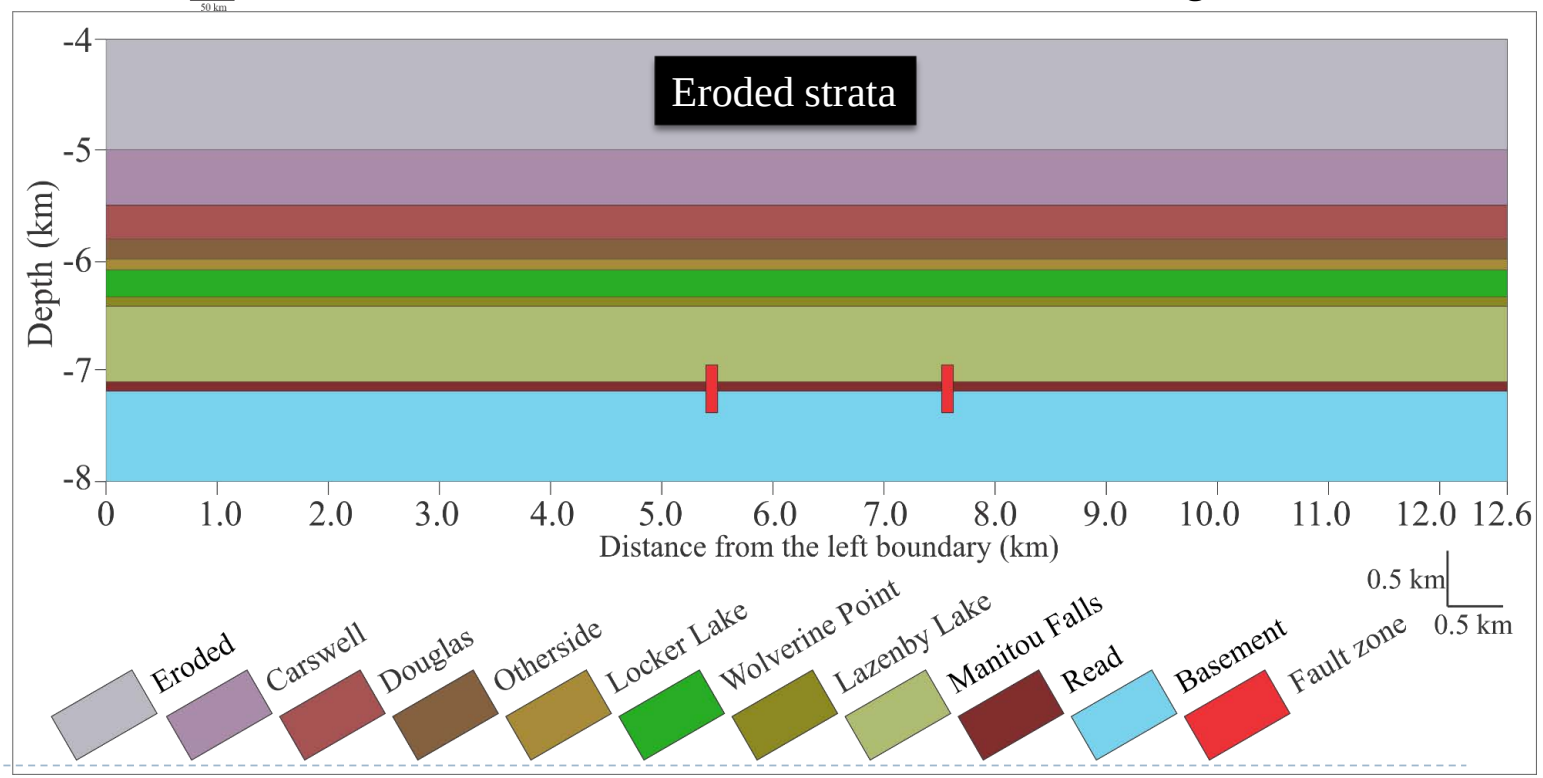
low permeability

35 °C/km

4) Effects of spacing of basement faults on fluid convection



Thermal gradient 35 °C/km



4) Effects of spacing of basement faults on fluid convection

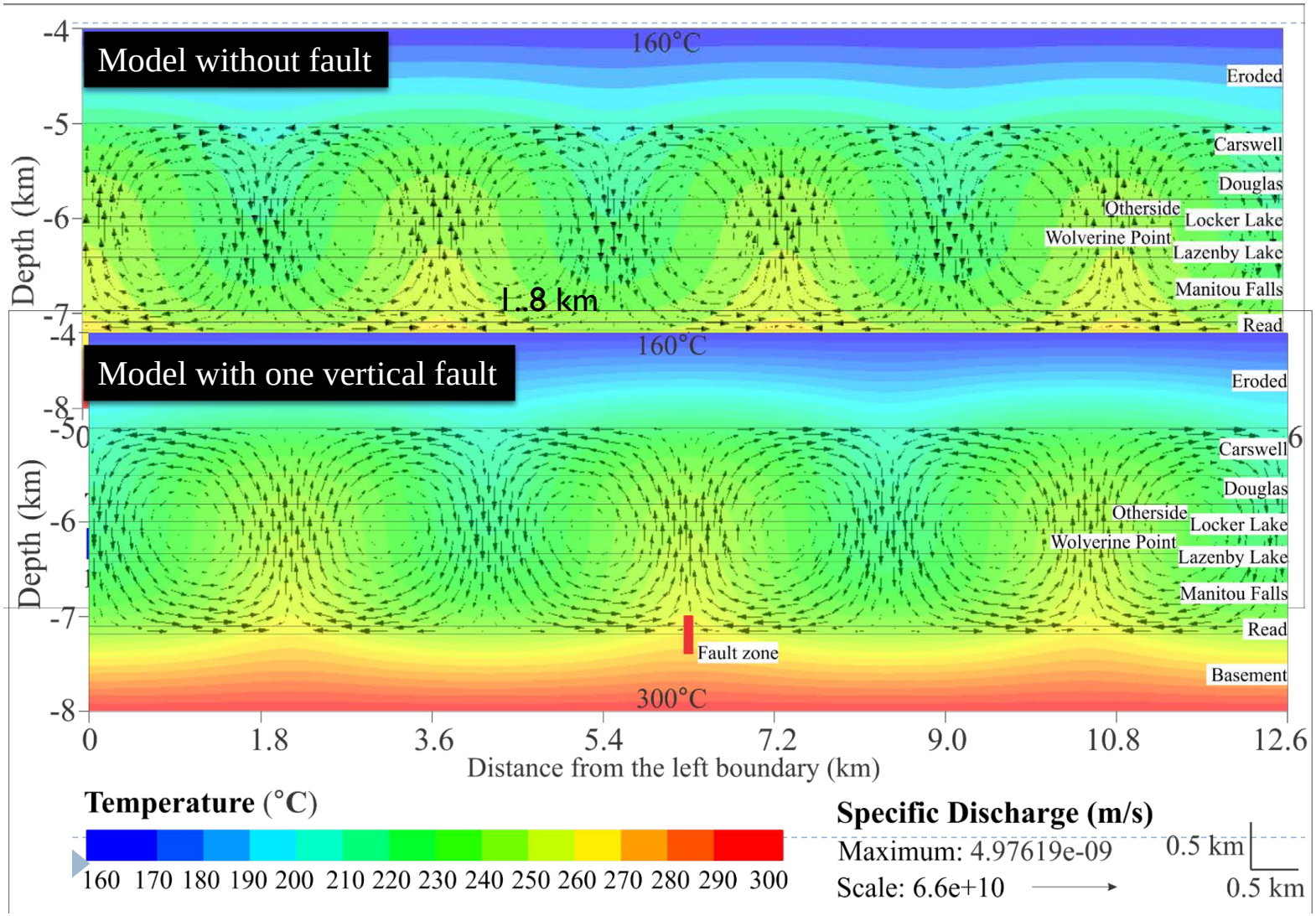
- Physical properties

	Density (kg/m^3)	Porosity	Permeability (m^2)	Thermal conductivity ($W/(m \cdot °C)$)	Thermal expansivity ($°C^{-1}$)	Specific heat capacity ($J/(kg \cdot °C)$)
Eroded strata	2,400	0.15	1.0×10^{-15}	2.5	8.0×10^{-6}	803.0
Athabasca Group	2,500	0.2	3.0×10^{-13}	3.5	10.0×10^{-6}	803.0
Basement	2,650	0.1	3.0×10^{-16}	2.5	8.0×10^{-6}	803.0
Fault zone	2,400	0.2	1.0×10^{-12}	4.0	10.0×10^{-6}	803.0
Water	1,000			0.6	1.85×10^{-3}	4,185.0

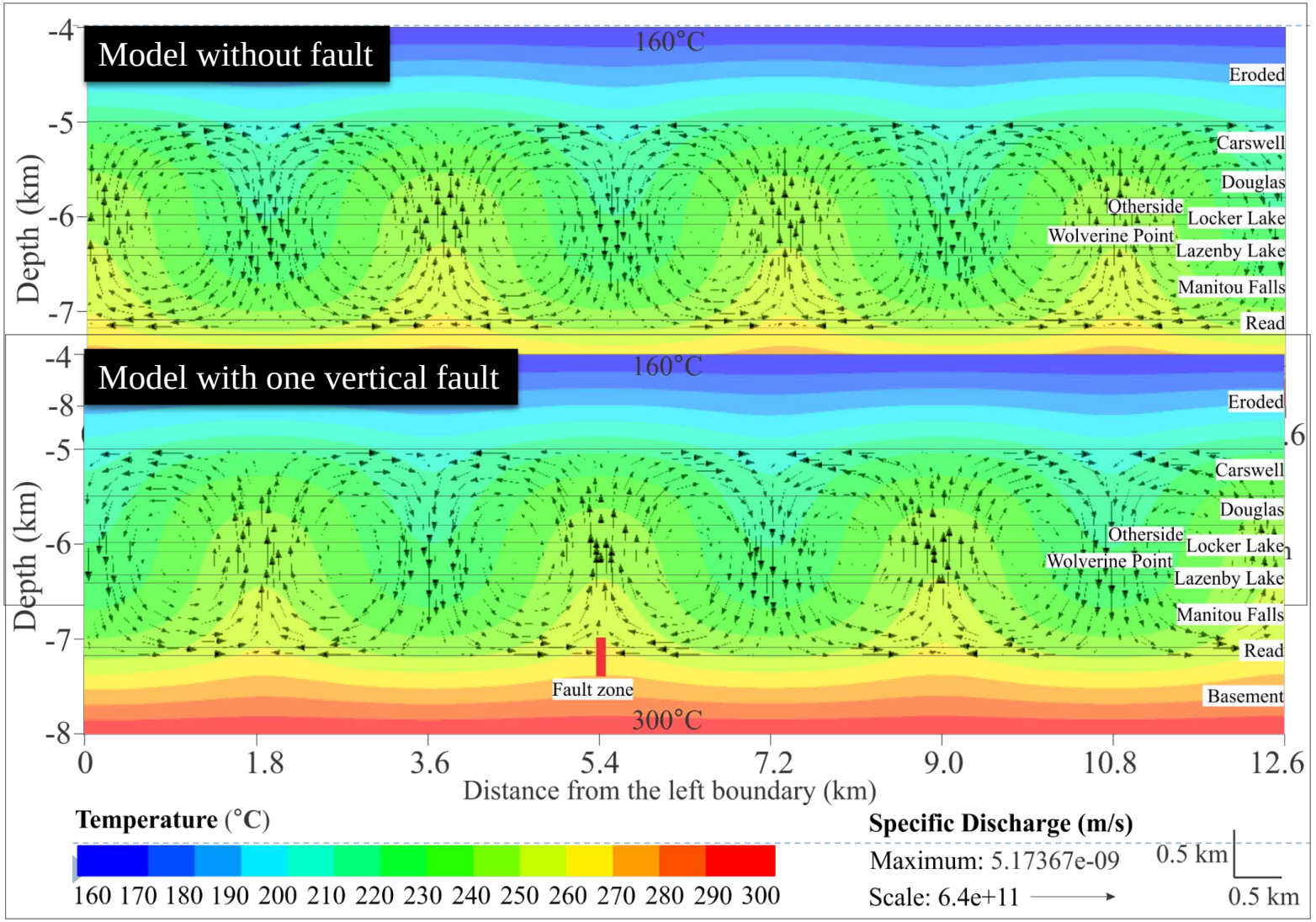
Raffensperger and Garven (1995)
Cui and others (2012)
FLAC3D manual (2012)

Geothermal gradient: 35 °C/km

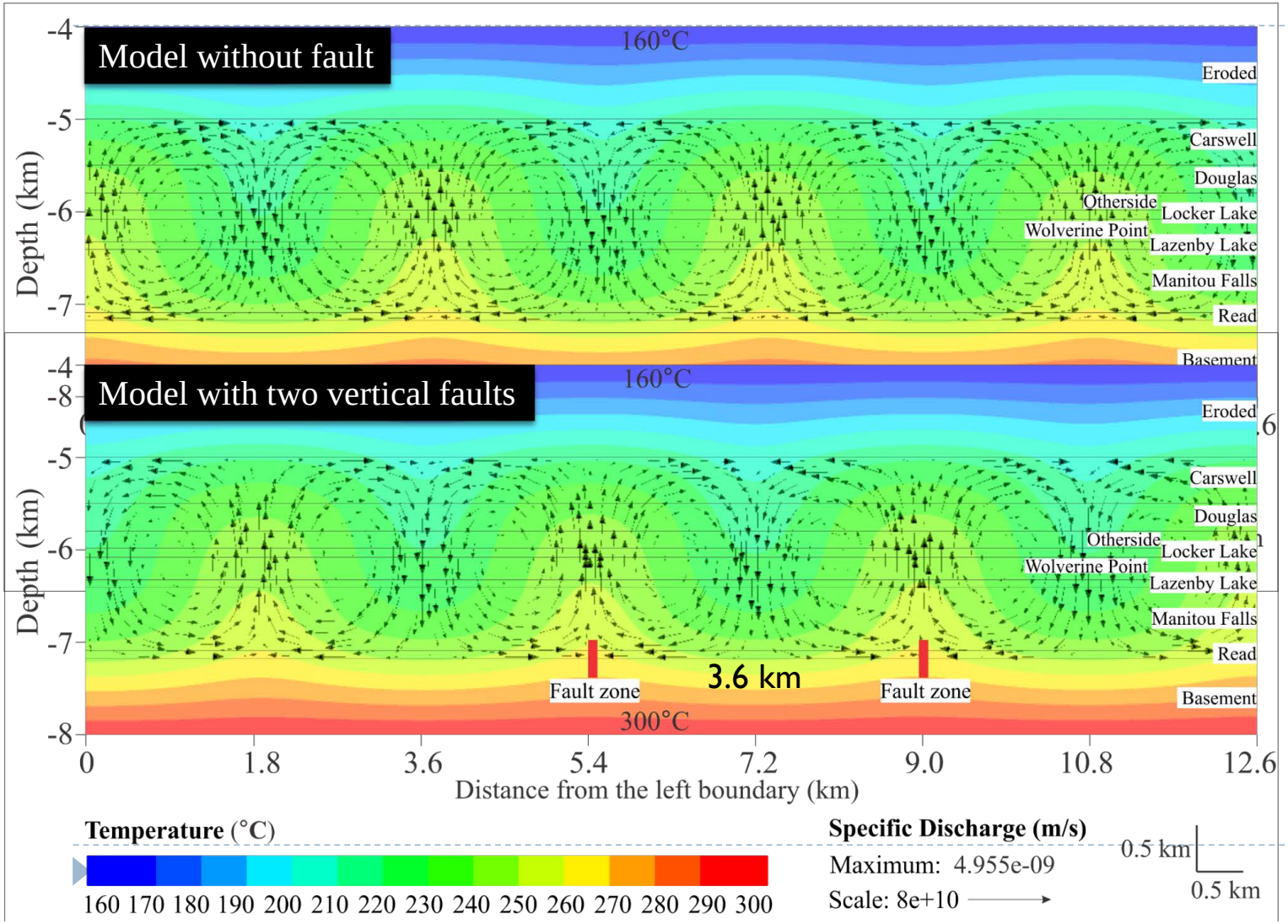
4) Effects of spacing of basement faults on fluid convection



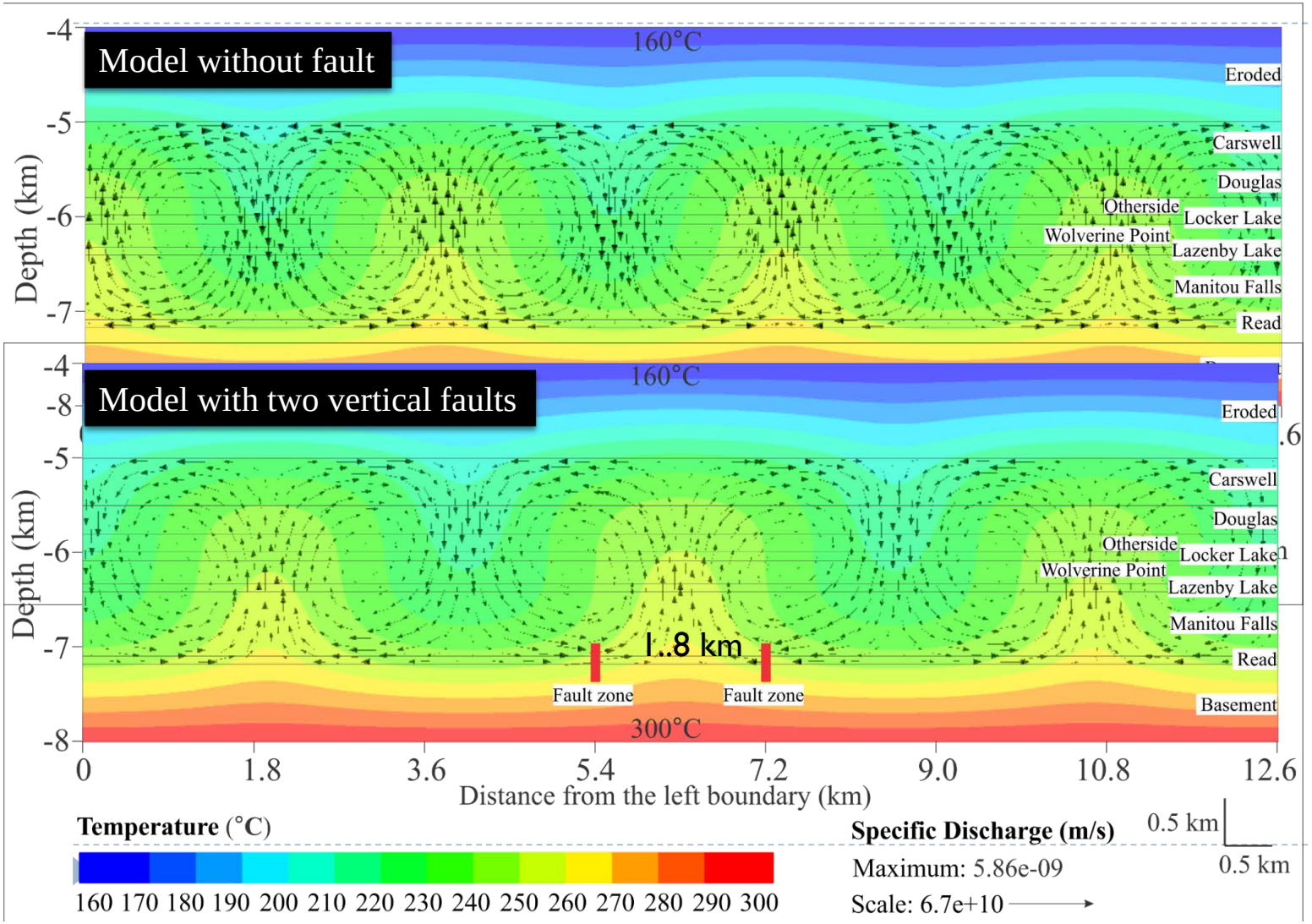
4) Effects of spacing of basement faults on fluid convection

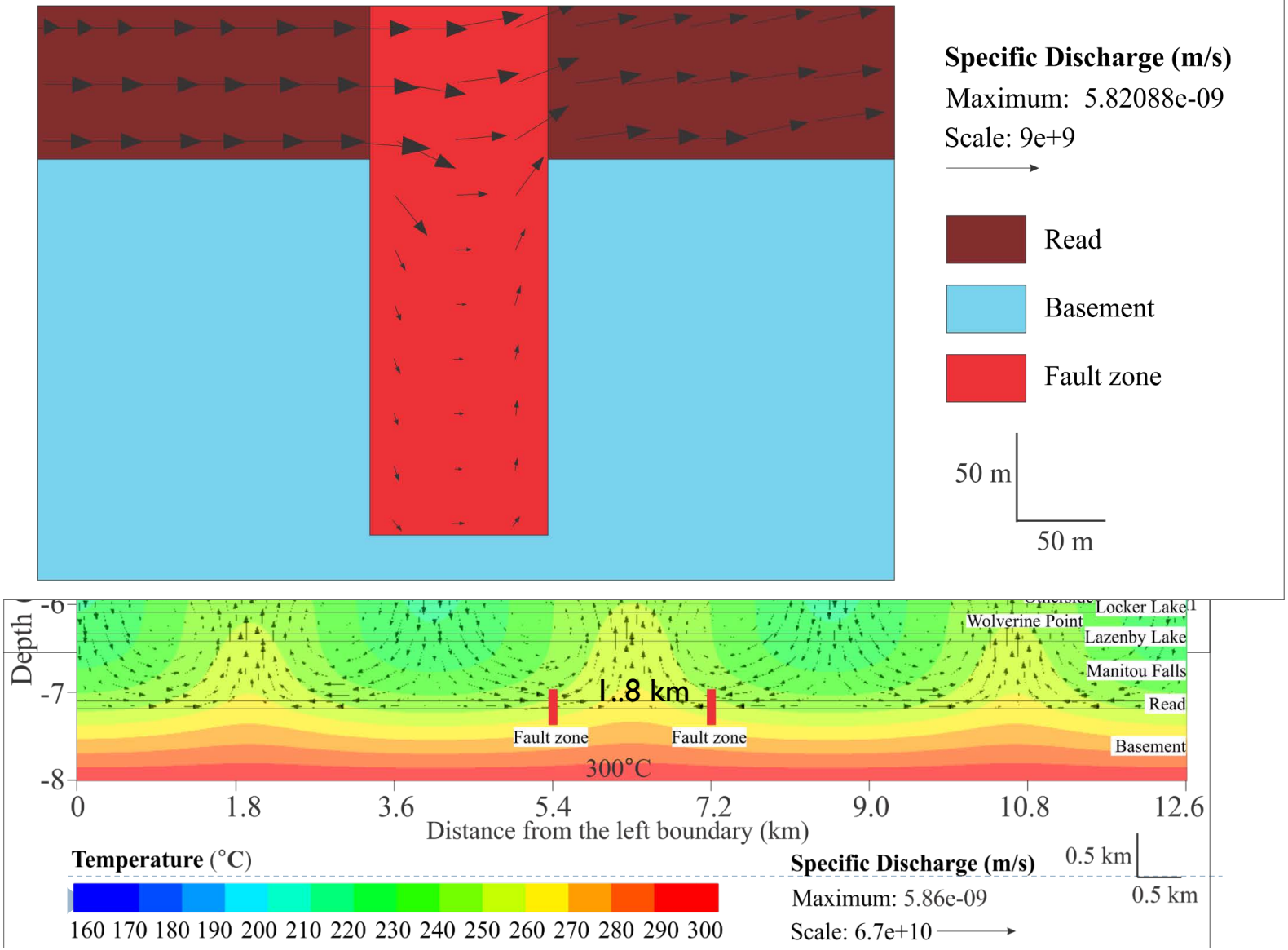


4) Effects of spacing of basement faults on fluid convection



4) Effects of spacing of basement faults on fluid convection




Specific Discharge (m/s)
Maximum: 5.82088e-09
Scale: 9e+9
Read
Basement
Fault zone
50 m
50 m
Depth
-6
-7
-8
1..8 km
Fault zone
Fault zone
300°C
Locker Lake
Wolverine Point
Lazenby Lake
Manitou Falls
Read
Basement
0
1.8
3.6
5.4
7.2
9.0
10.8
12.6
Distance from the left boundary (km)
Temperature (°C)
160 170 180 190 200 210 220 230 240 250 260 270 280 290 300
Specific Discharge (m/s)
Maximum: 5.86e-09
Scale: 6.7e+10
0.5 km
0.5 km

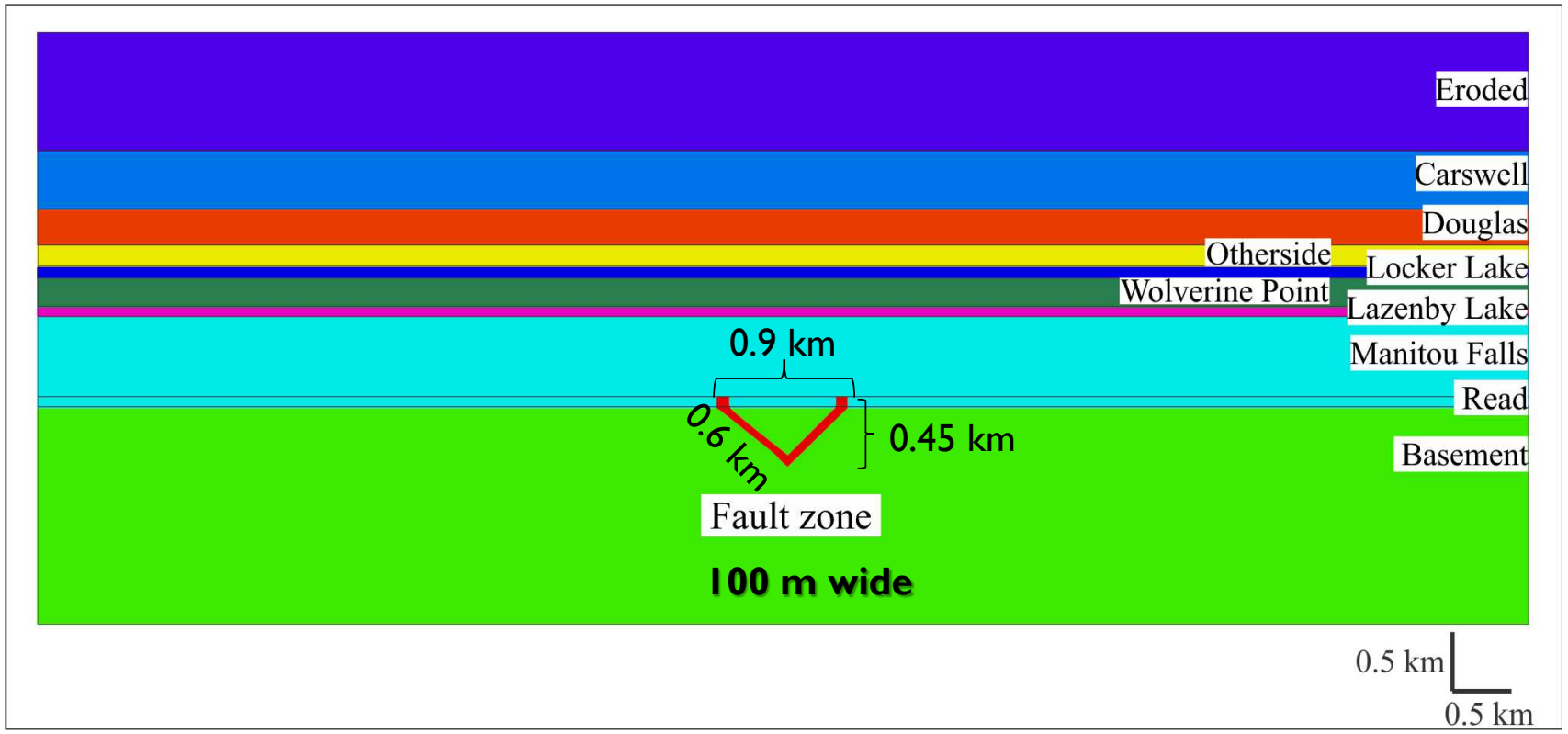
4) Effects of spacing of basement faults on fluid convection

- Initial numerical modelling results indicate that the location and spacing of basement faults influences thermally driven fluid convection.
- Isolated faults generally coincide with upwelling flow or are within a convection cell. In the latter case, fluid may flow into and out of the same fault zone.
- However, fluid can not go down along fault zone, or only very limited component.



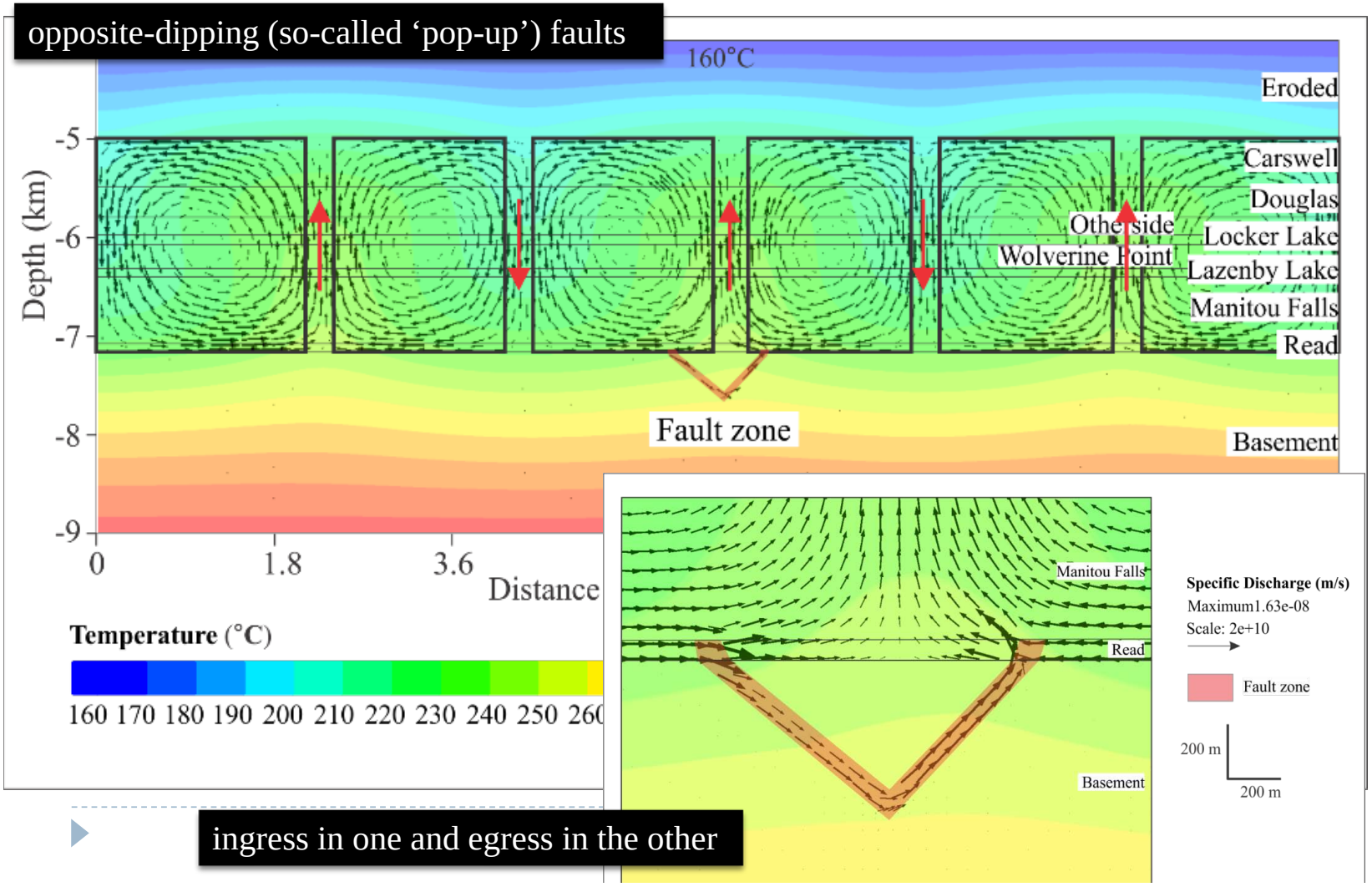
5) Effects of networks of basement faults on fluid convection

opposite-dipping (so-called ‘pop-up’) faults



5) Effects of networks of basement faults on fluid convection

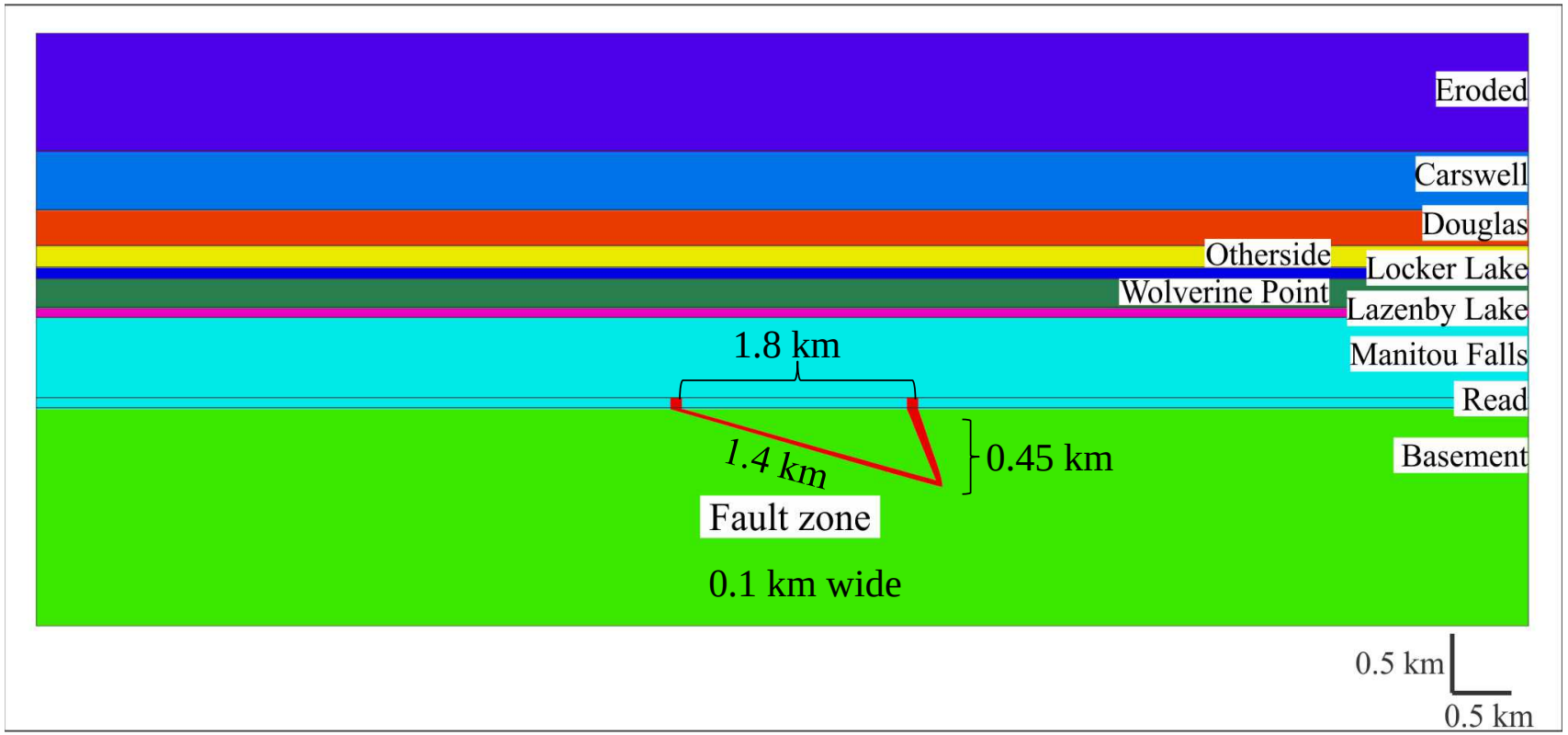
opposite-dipping (so-called ‘pop-up’) faults



ingress in one and egress in the other

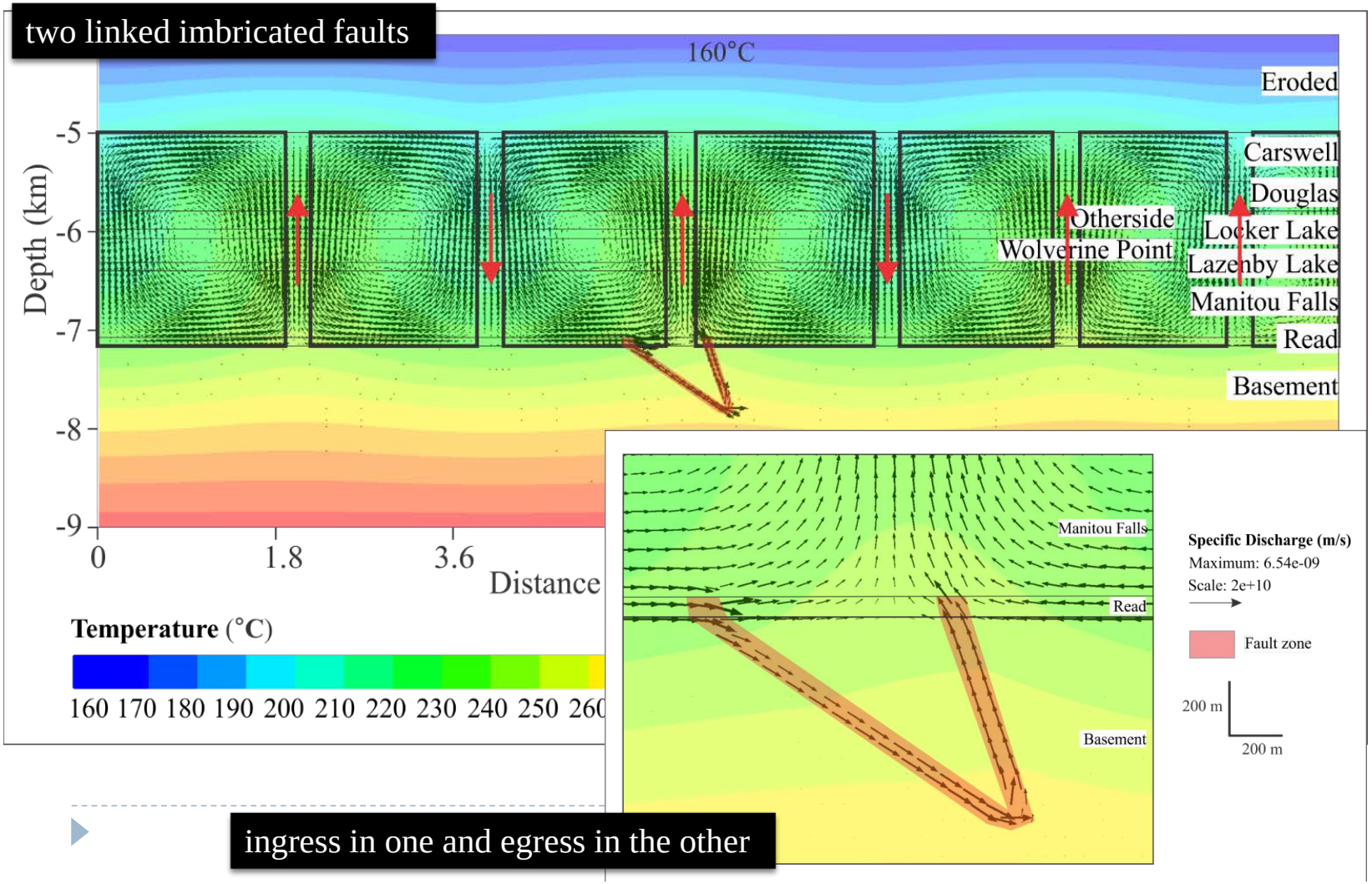
5) Effects of networks of basement faults on fluid convection

two linked imbricated faults



5) Effects of networks of basement faults on fluid convection

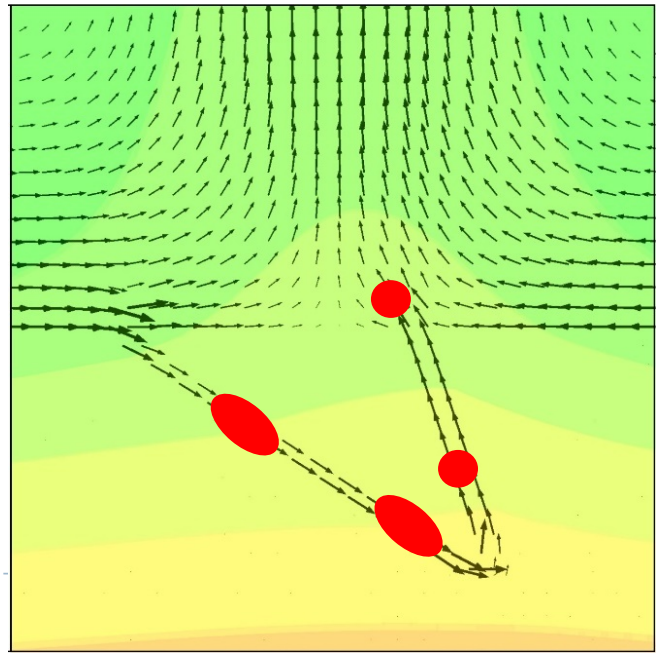
two linked imbricated faults



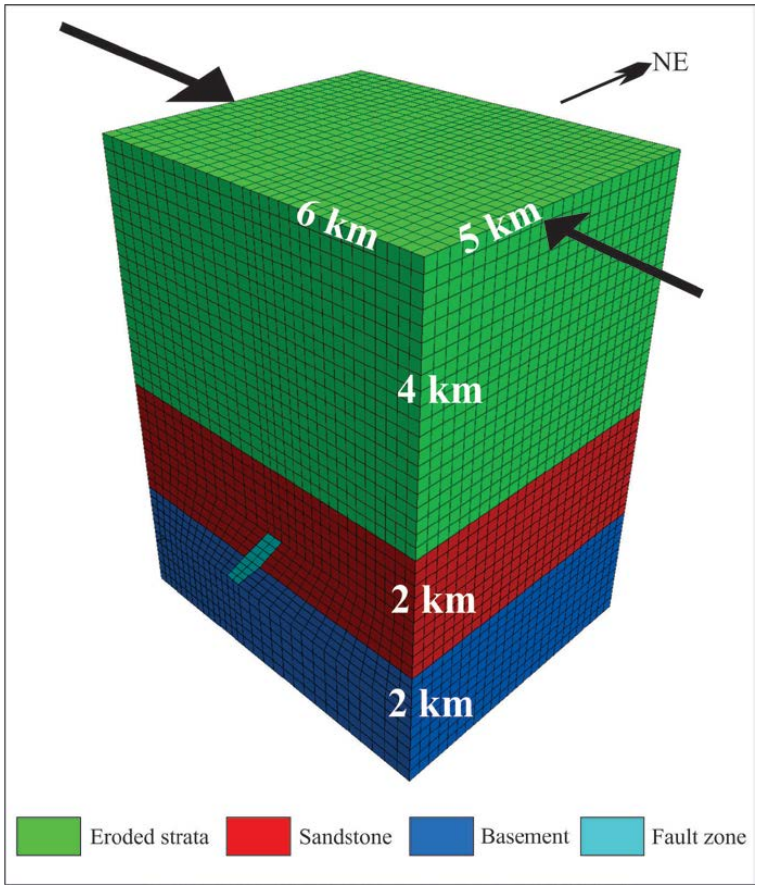
ingress in one and egress in the other

5) Effects of networks of basement faults on fluid convection

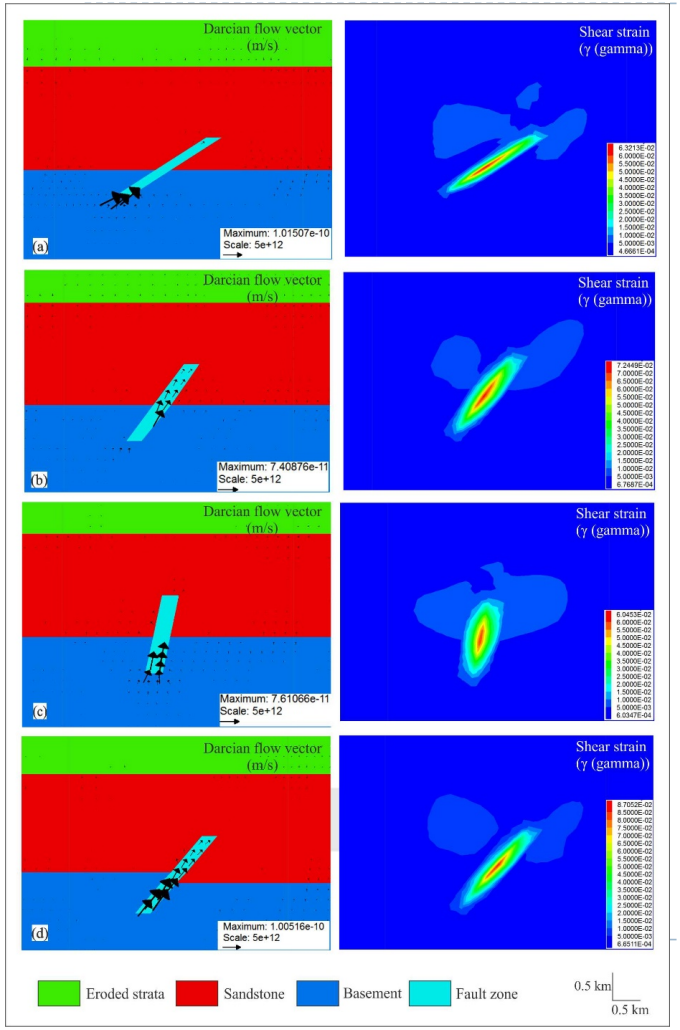
- For connected faults, either in pop-up or imbricated pattern, fluid may flow into one fault zone (ingress) and out of the other (egress), the results maybe explain the egress and ingress styles of the deposits.



6) Coupled interaction between fluid flow and mechanical compression



6) Coupled interaction between fluid flow and mechanical compression



- The modelling run shows that during compressive deformation, fluids migrate up the fault, which is consistent with the results of Cui and others (2012). The results of different models incorporating faults with different dip angles show that flow patterns are generally the same among the models.
- However, the model with the most shallowly dipping fault shows slightly greater flow rates than the other models.
- The model with offset on the fault also shows a slightly greater flow rate.
- The fault zones represent the most significant loci of shear strain in all models; as might be expected, the dip of the fault also strongly controls the orientation of the high strain zone which propagates into the sandstone.

Summary

- A **3D model of the sub-Athabasca unconformity** has been constructed using publicly available geological and drill-hole data. Faults have been identified primarily using the basement geophysical signature.

- These features are the product of the **combined action of three main factors**: 1) pre-Athabasca group ductile faulting; 2) differential weathering/erosion of stronger versus weaker units; and 3) post-Athabasca fault reactivation, localized in pre-existing, weak graphite rich ductile shear zones.



Summary (Con't)

- The numerical modeling results indicate that fluid pressures in the Athabasca basin were **close to hydrostatic values** throughout its development, and that thermal convection cells may have been well developed in the lower part of the basin, particularly below the Wolverine Point Formation.

- Numerical modelling results indicate that the **location, spacing and networks of basement faults influence thermally driven fluid convection**. Faults control the initial position of the convection and fluid flow can penetrate into the basement along fault zones under specific conditions. These results further support the empirical relationship that faults crosscutting the unconformity play an important role in localizing fluid flow and uranium mineralization.



Summary (Con't)

- The results have shed light on the spacing of mineralization centers as well as the **coexistence of fertile versus barren structures**. If it is assumed that individual convection cells controlled potential mineralization centers, the spacing between these mineralization centers may be just a few kilometers.

- The various relationships between convection cells and faults (position and spacing) may **explain why some faults are more favorable for fluid flow than others**, in addition to other constraints such as fault kinetics and orientations. All these factors are potentially important in determining whether a given structure may host mineralization.



Ongoing work

- Supplementary numerical modelling for already finished models
- Modelling of coupled thermal transport, deformation and fluid flow



Acknowledgements

- This project is supported by TGI-4 (Targeted Geoscience Initiative 4), a collaborative federal geoscience program led by Natural Resources Canada.
- Access to the GoCAD license is provided by the Saskatchewan Geological Survey.

University of Regina

TGI 4 Ore Systems

Saskatchewan Ministry of the Economy

Thanks!

Preliminary Studies of Fluid Composition, Thermal Condition, Fluid-structural Relationships and Graphite Alteration of the Phoenix Uranium Deposit, Athabasca Basin, Saskatchewan

Kewen Wang[1], Guoxiang Chi[1], Kathryn Bethune[1] and Colin Card[2]

[1] University of Regina
[2] Saskatchewan Geological Survey
December 4th, 2014

Outline

- Introduction
- Previous studies and unsolved problems
- Objectives
- Research methods
- Sampling and core description
- Petrographic study
- Fluid inclusion (FI) study
- Microstructrual study of fluid inclusion planes (FIP)
- Raman spectroscopic study of graphite
- Summary

Introduction

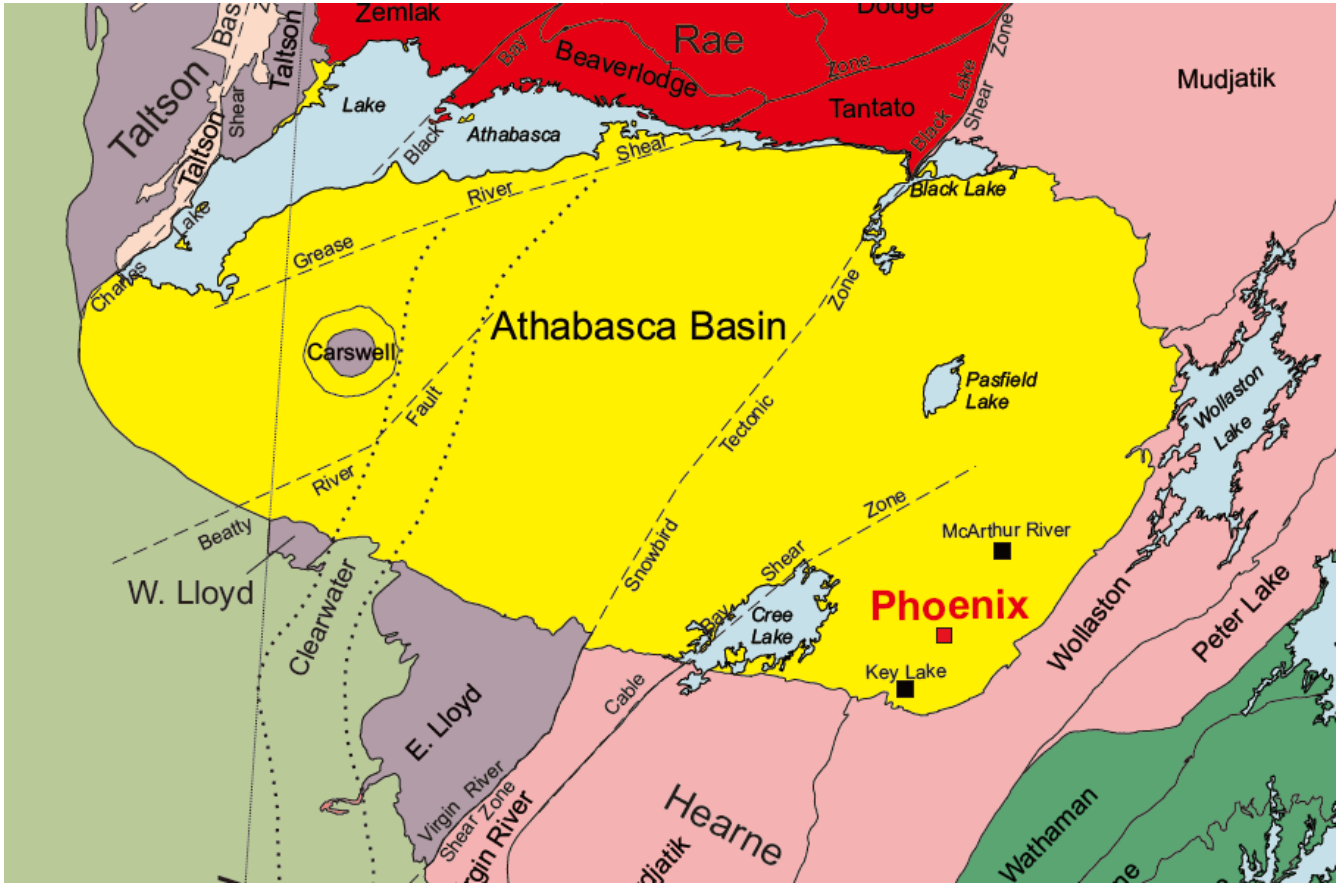


Fig. 1. Geological location of Phoenix uranium deposit (Modified from Card et al., 2007)

Introduction

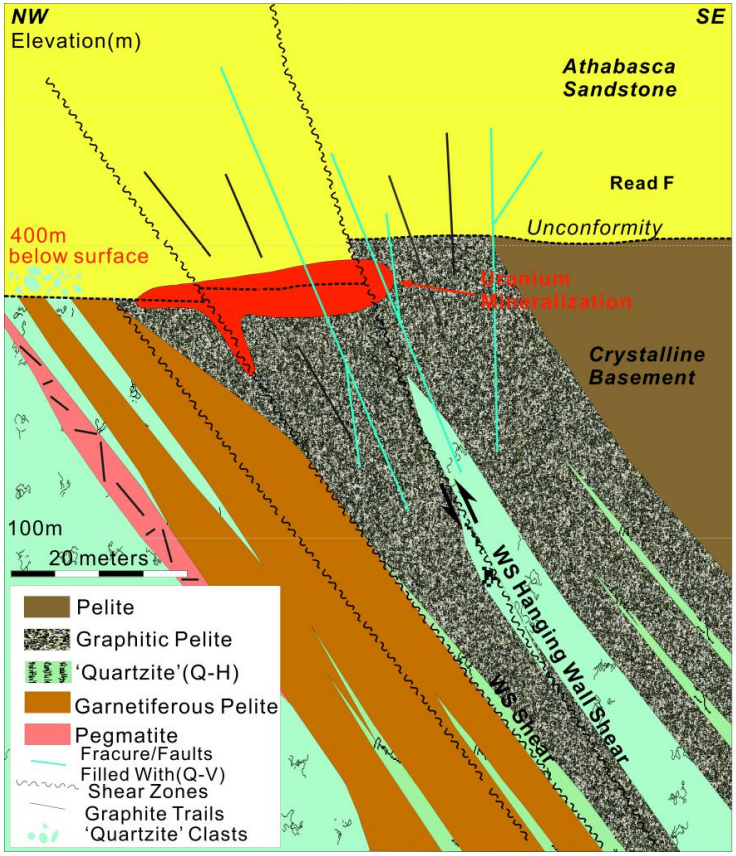


Fig. 2. Schematic cross section of the Phoenix deposit (modified from Gamelin et al., 2010)

Previous studies and unsolved problems

- Similar features as other unconformity-related uranium deposits (e.g. Kerr, 2010; Power et al., 2012; Dann et al., 2014); but X, T and P?
- The structural controls on mineralization- the hydrodynamic relationship between structures and fluid pressure?
- Degradation of graphite near U concentration (Wang et al., 1989)?

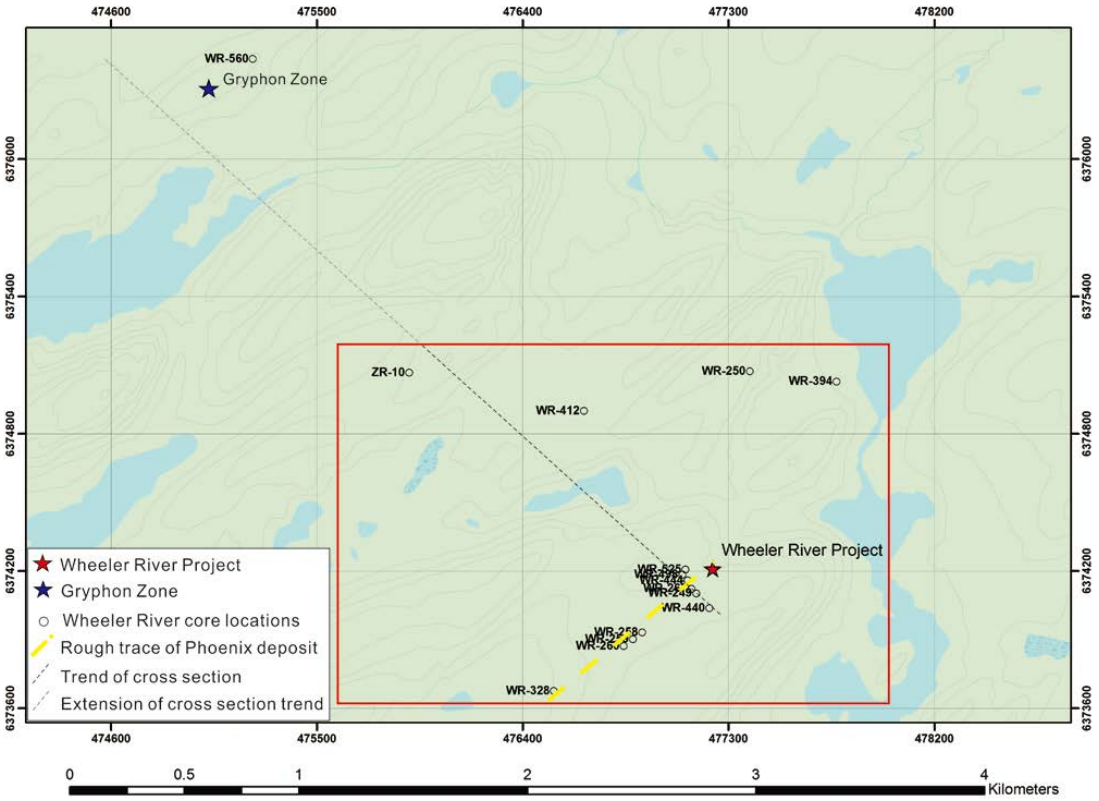
Objectives

- Fluid composition
- Thermal conditions
- Fluid-structural relationships
- The role of graphite

Research methods

- Field (drill core) investigation
- Petrographic study
- Petrographic and microthermometric studies of FI
- Microstructural study of FIP
- Petrographic and Raman spectroscopic studies of graphite

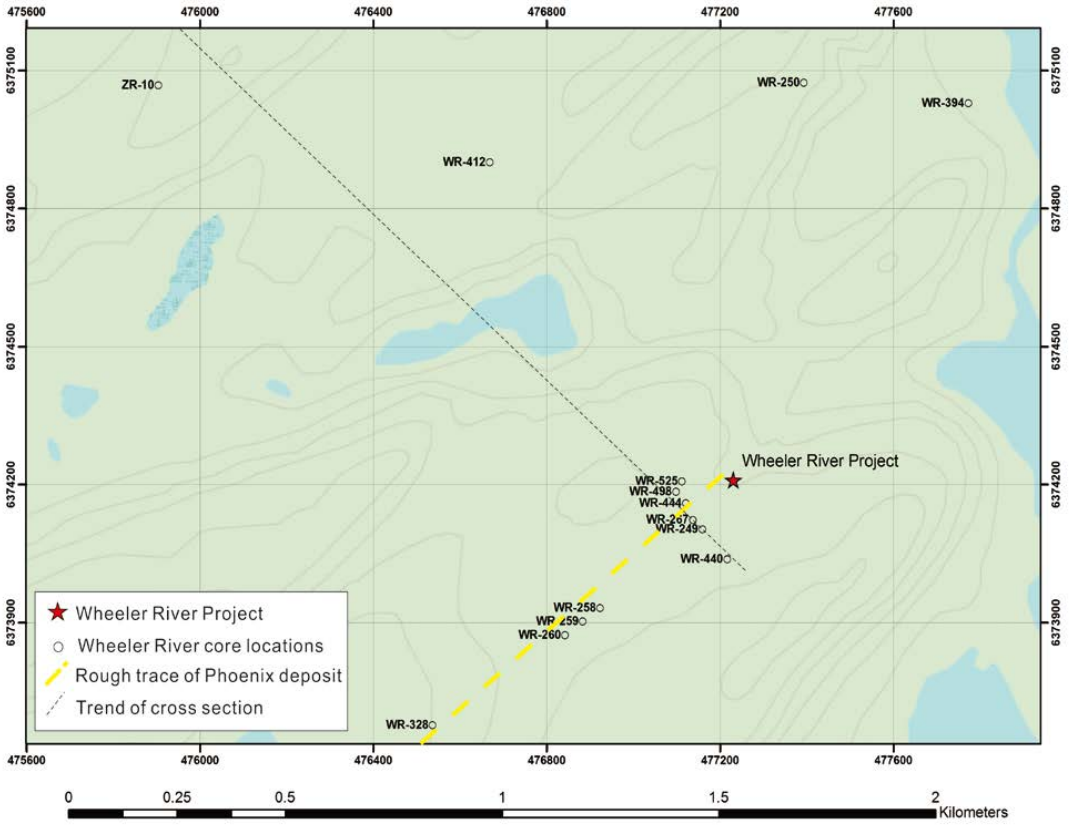
Sampling & core description



- 120 samples
- 15 drill cores

Fig. 3A. Map showing locations of studied drill cores in the Wheeler River area and the location of the cross-section

Sampling & core description



- 120 samples
- 15 drill cores

Fig. 3B. Insert map of Figure 3A

Sampling & core description

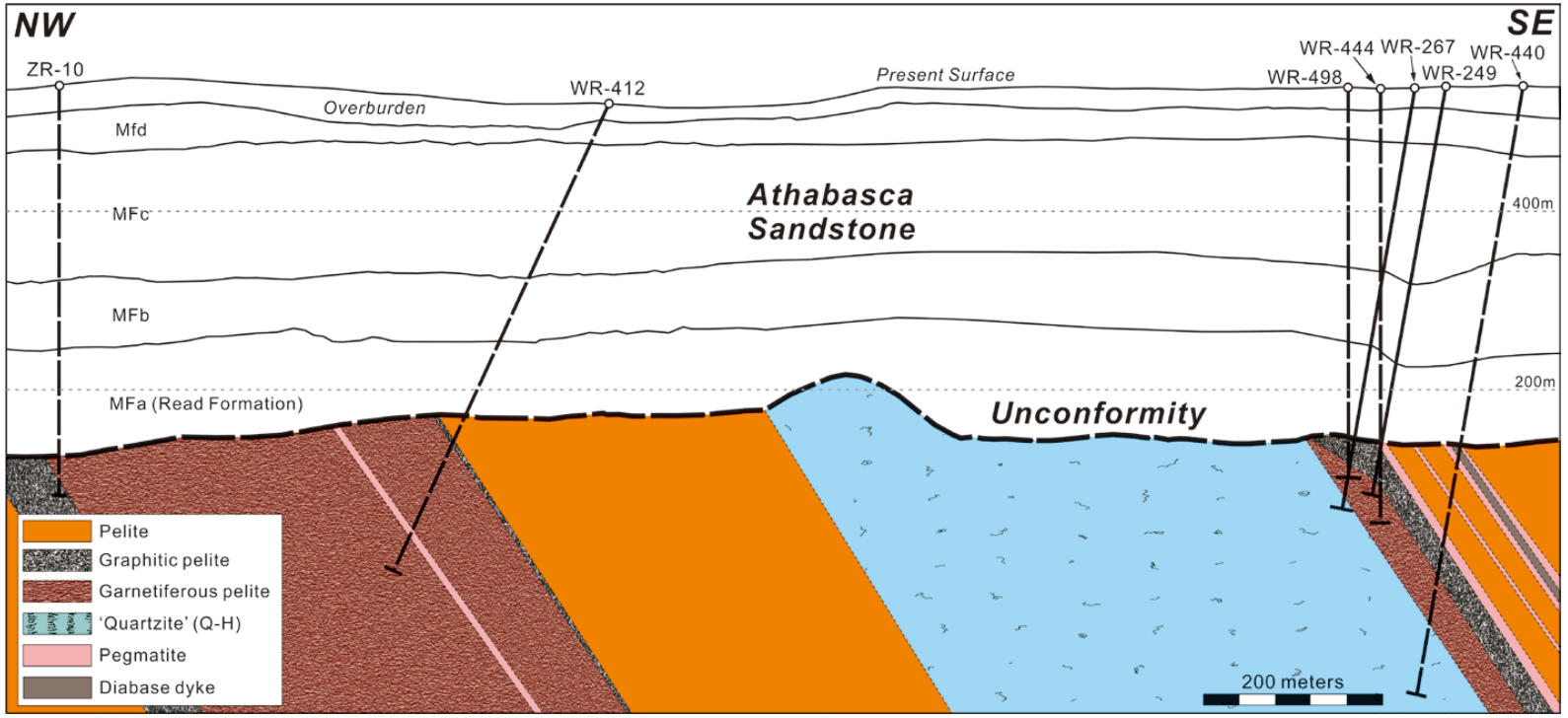


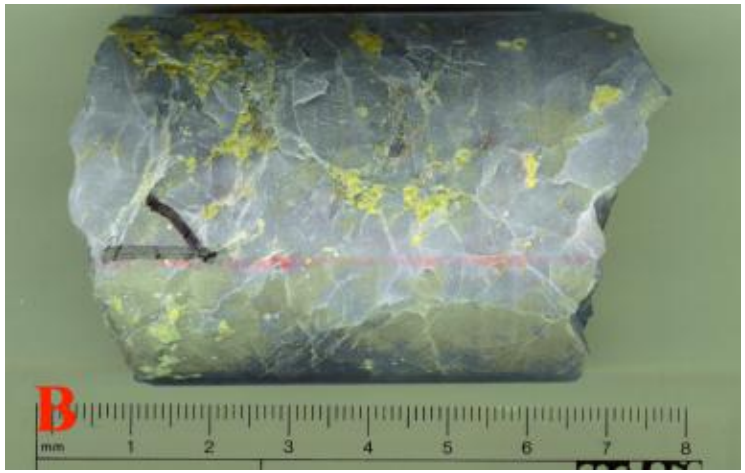
Fig. 4. Schematic NW-SE cross-section of the Phoenix deposit and neighboring area; note only drill cores examined in this study are shown (modified from Arseneau and Revering, 2010)

Sampling & core description



Fig. 5A. Garnetiferous pelite with interstitial graphite ((WR-440, 618.8m);

Sampling & core description



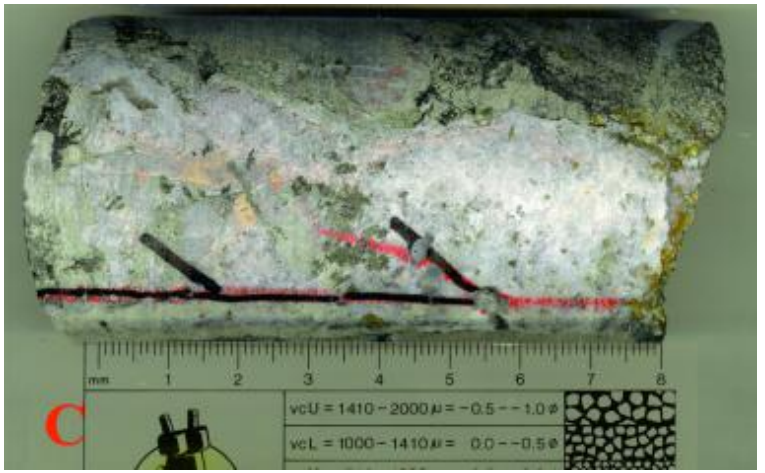


Fig. 5B. Oriented sample of massive quartz (WR-440, 674m); 5C. Pegmatite intrusion cut by a calcite vein with minor quartz (WR-440, 479.6m);

Sampling & core description

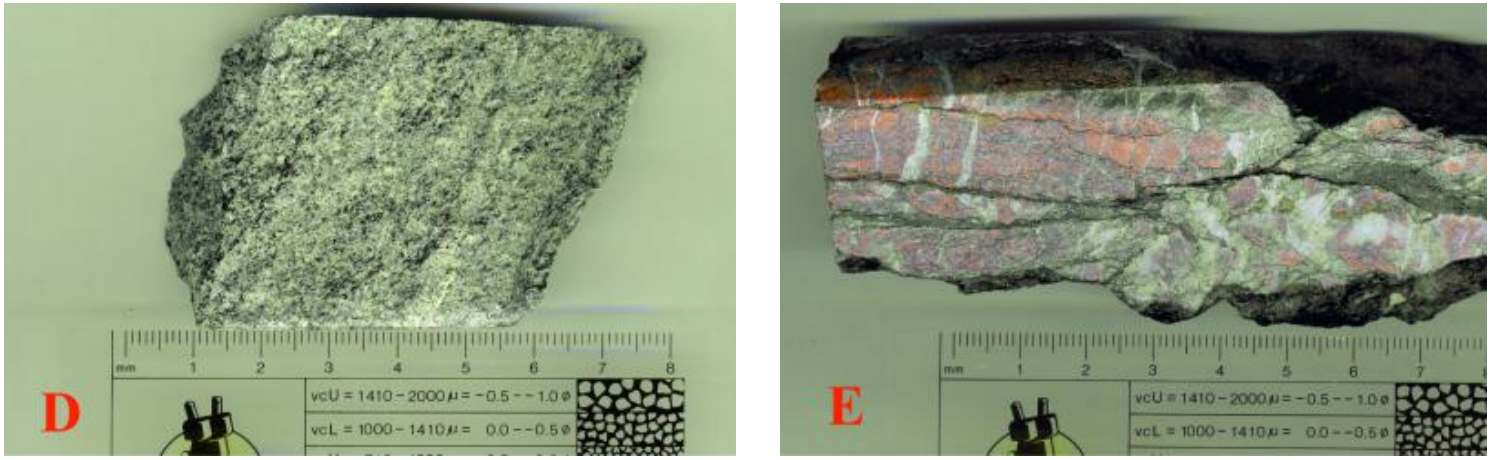


Fig. 5D. Weakly mineralized graphitic pelite (WR-328, 394.2m); 5E. Pegmatite cut by graphite-filled fractures (WR-440, 603m);

Sampling & core description



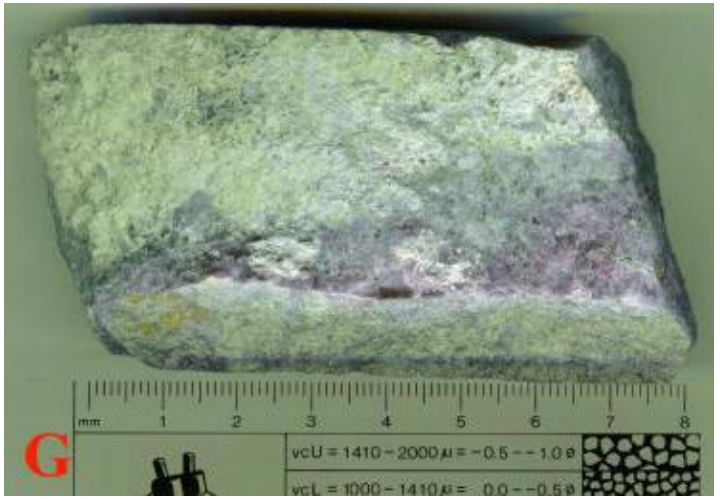


Fig. 5F. Druzy quartz cutting strongly bleached sandstone (WR-267, 348.9m); 5G. Vuggy quartz cutting silicified sandstone (WR-328, 318.1m);

Sampling & core description



Fig. 5H. Drusy quartz vein cutting bleached sandstone (WR-525; 355.3m);
5I. Drusy quartz vein cutting strongly altered granite (WR-560, 736m);

Sampling & core description



Fig. 5J. Drusy quartz cutting silicified sandstone (WR-328, 304.1m)

Petrographic study

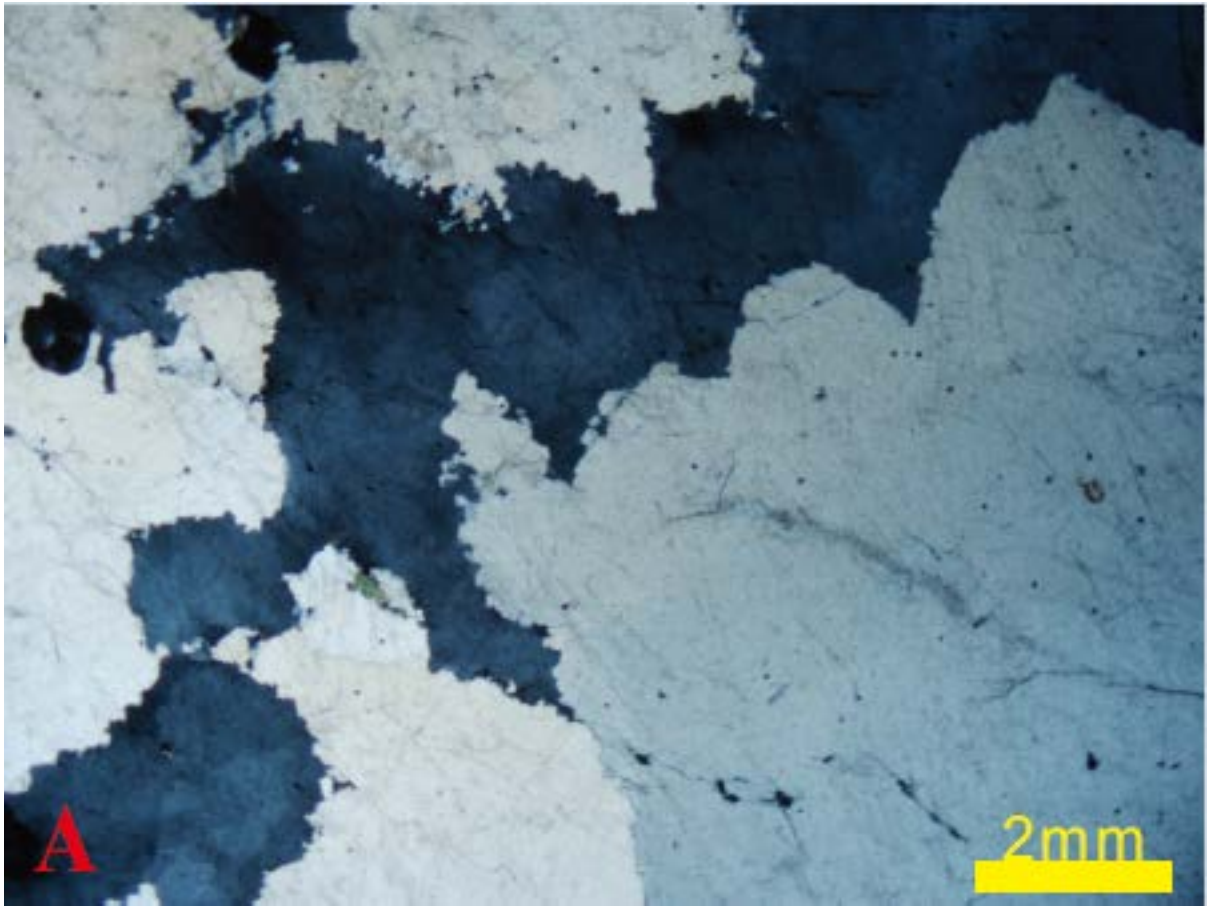


Fig. 6A. Photomicrograph showing massive quartz with grain size up to 28mm from the basement (WR-440, 674m);

Petrographic study

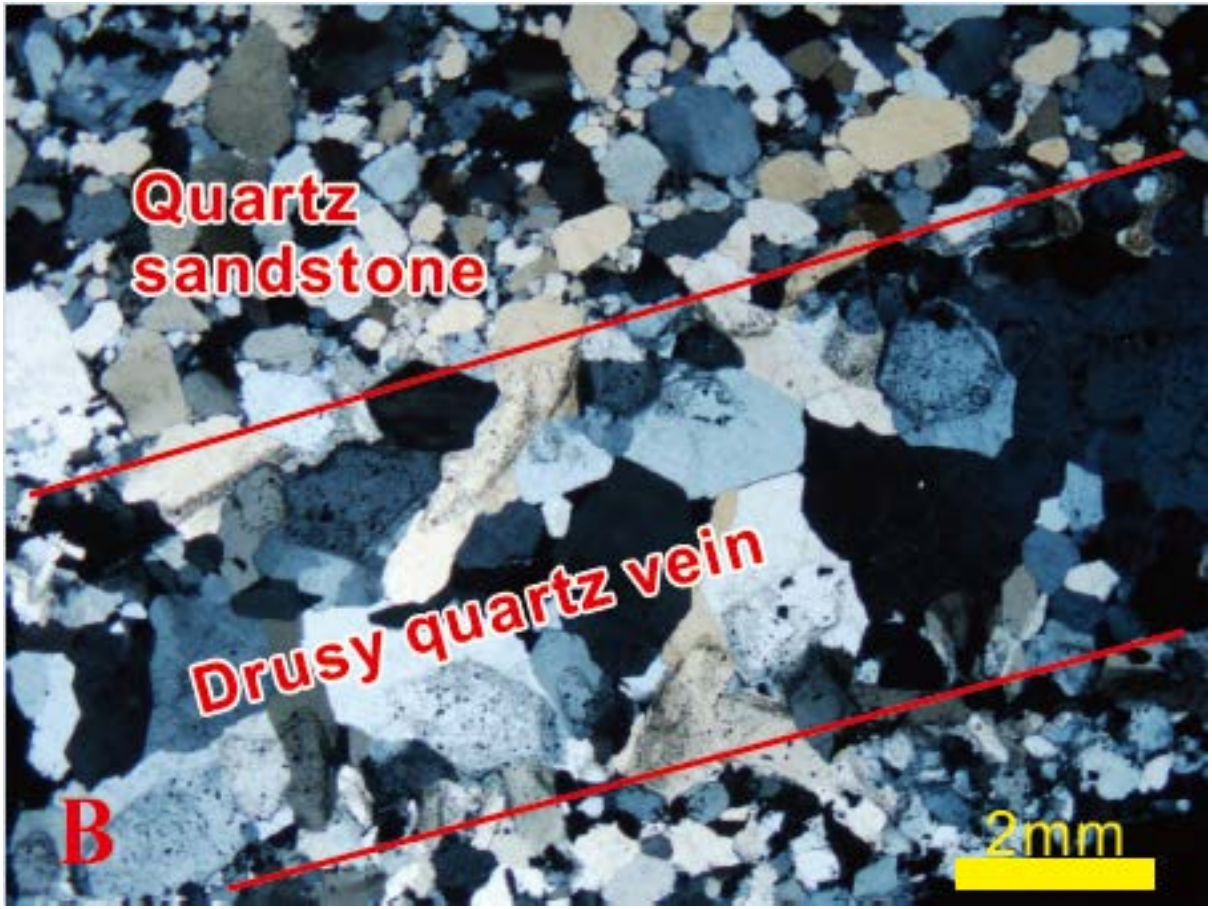


Fig. 6B. Photomicrograph showing drusy quartz cutting quartz sandstone (WR-250, 341.8m);

Petrographic study

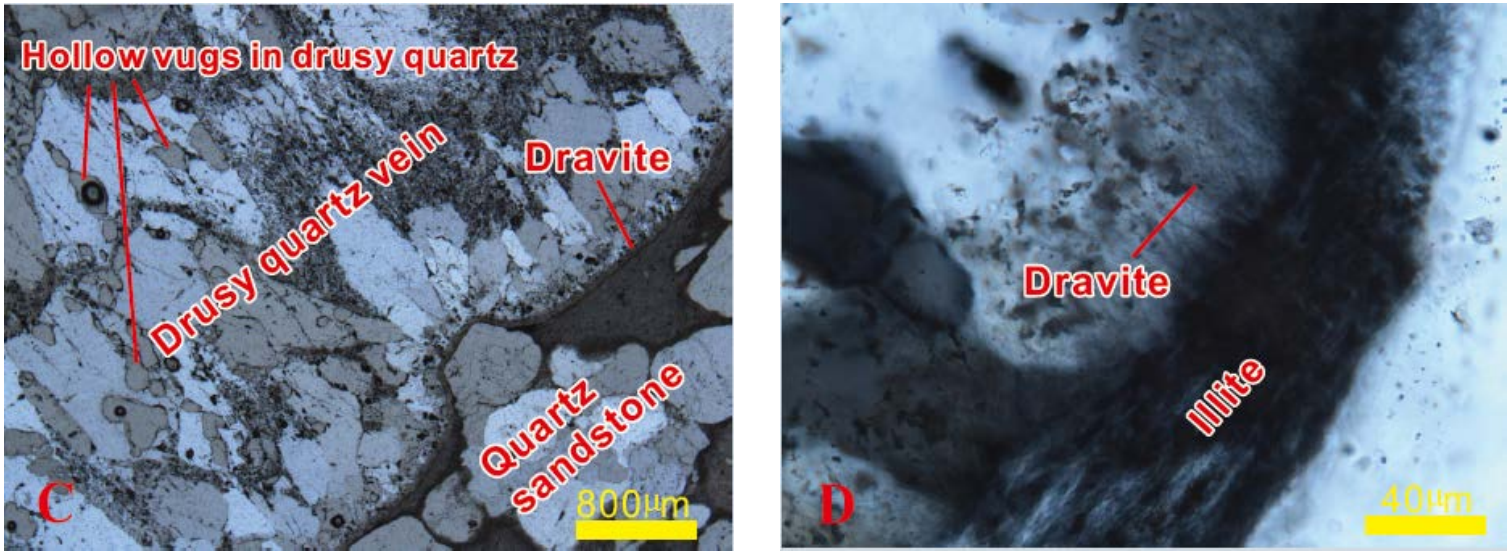


Fig. 6C. Drusy quartz vein with dissolved hollows cutting quartz sandstone; note dravite occurring in between (WR-328, 304.1m); 6D. Illite and dravite alteration along the boundary between sandstone and drusy quartz (WR-328, 304.1m);

Petrographic study

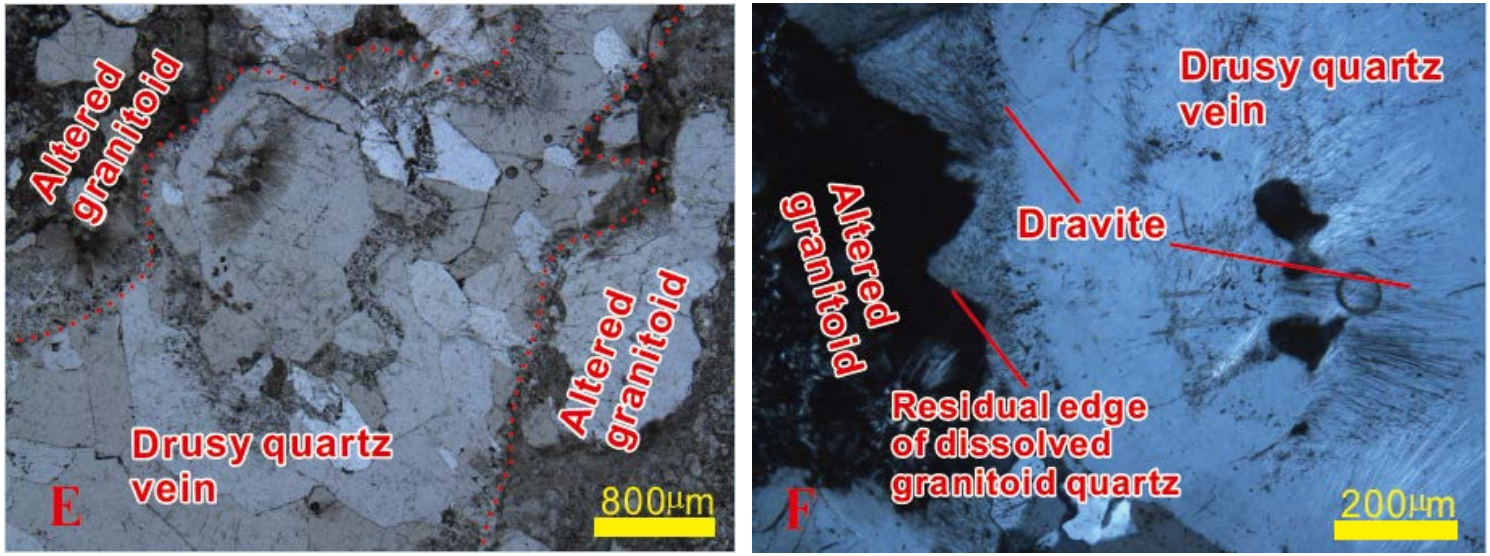


Fig. 6E. Drusy quartz vein cutting altered granitoid (WR-560, 736m, **Gryphon zone**); 6F. Dravite developed along the edge of dissoved granitoid quartz, as well as within drusy quartz (WR-560, 736m, **Gryphon zone**);

Petrographic study

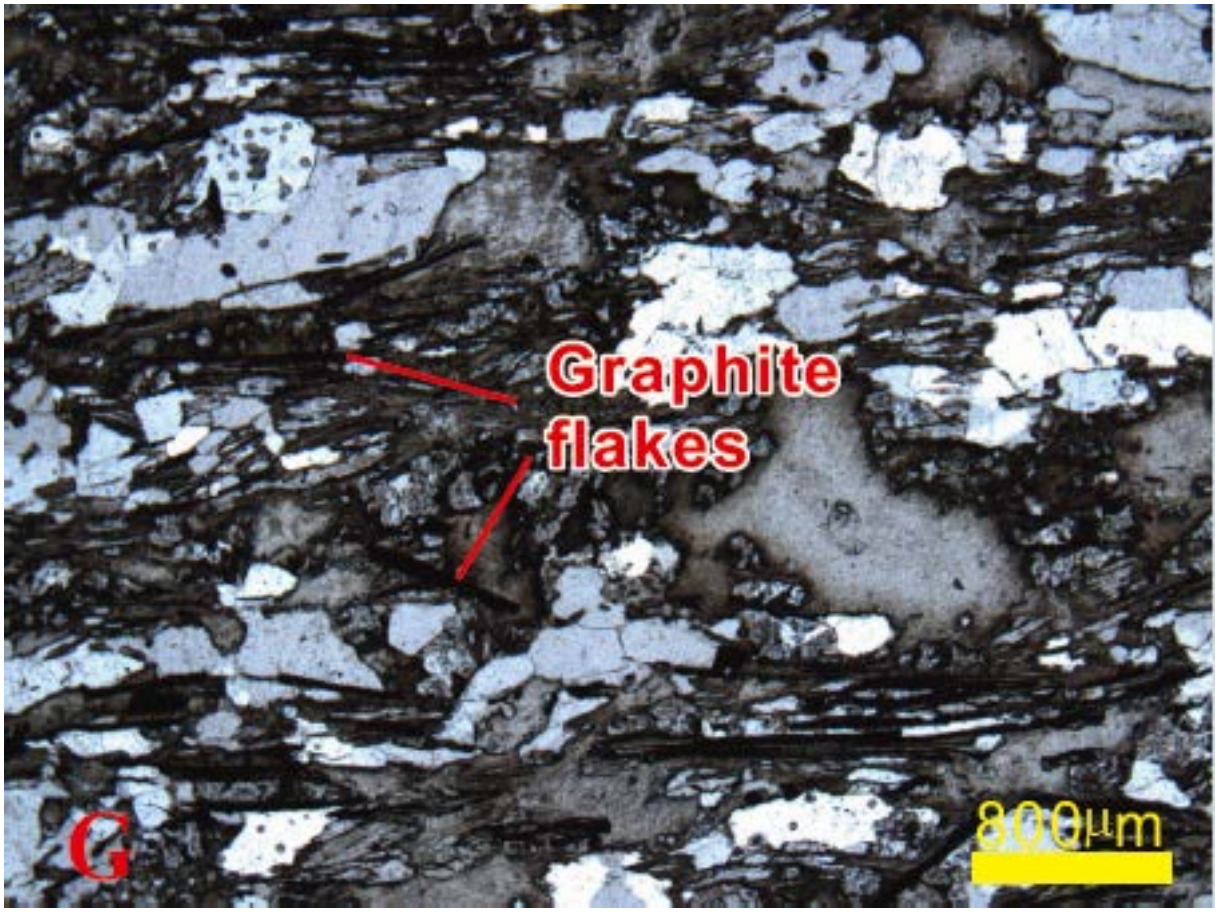


Fig. 6G. Photomicrograph showing graphitic pelite (WR-267, 423.8m);

Petrographic study

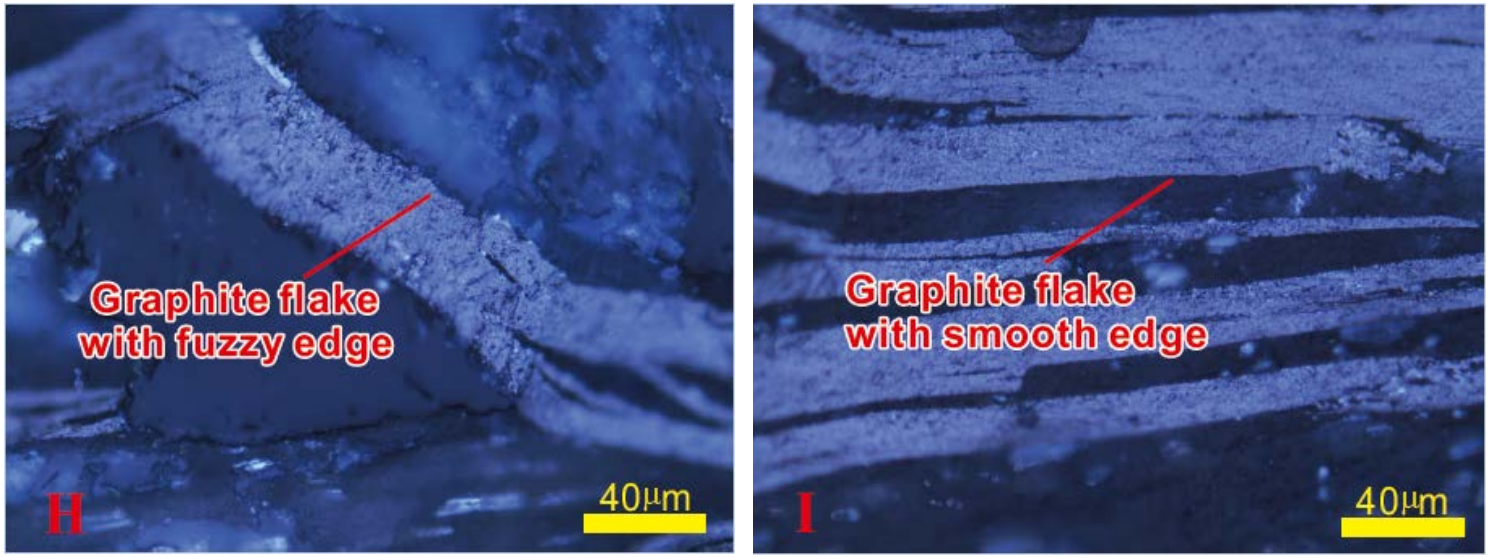


Fig. 6H. Photomicrograph showing gaphite (RFL) in pelite 5m from ore-body (WR-267, 414.1m); 6I. Photomicrograph showing gaphite (RFL) in pelite 25m from ore-body (WR-267, 433m)

Fluid inclusion (FI) study

- Petrographic and microthermometric studies
- Aqueous fluid inclusions (aq-FI)
- CO_2-dominated fluid inclusions (CO_2-FI)

FI study - Aqueous FI

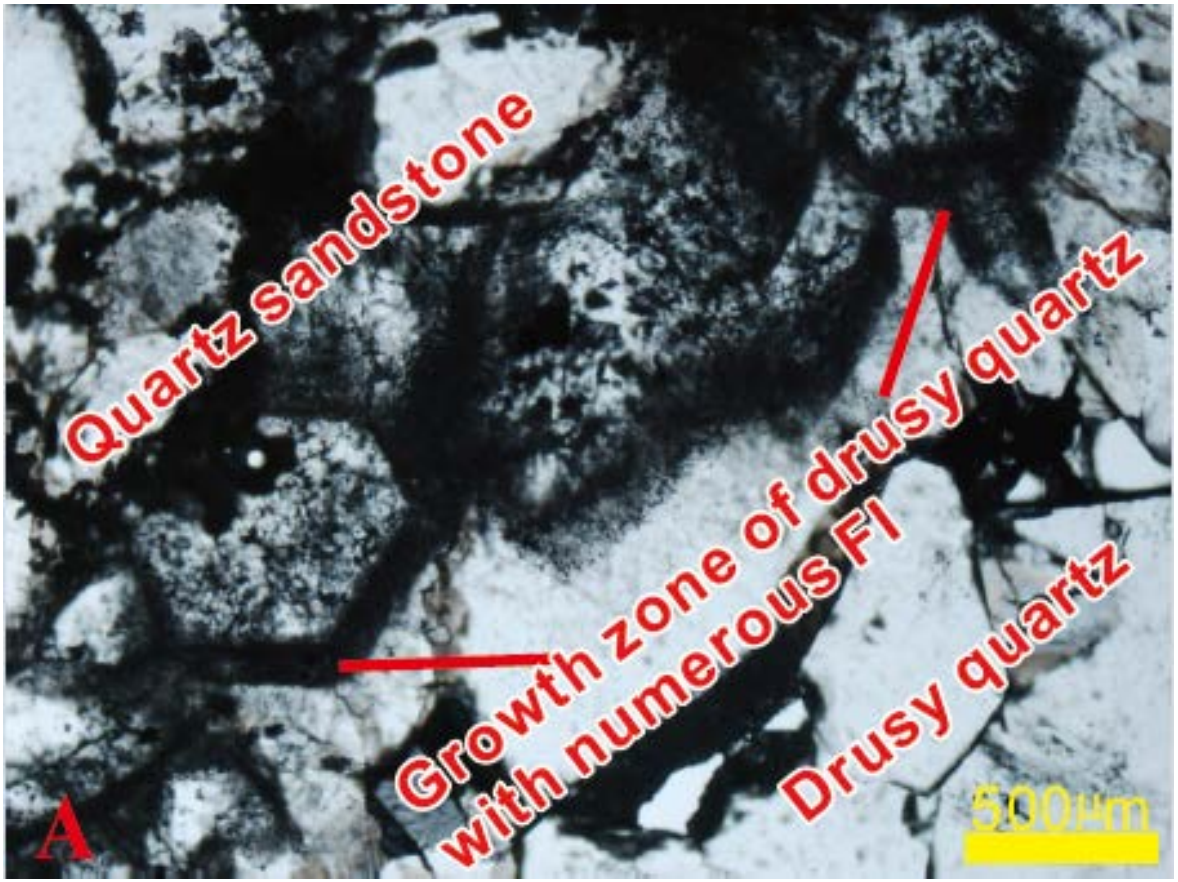


Fig. 7A. Aqueous inclusions distributed along the growth zone of the drusy quartz veins near the unconformity and in the overlying Manitou Falls Formation;

FI study - Aqueous FI

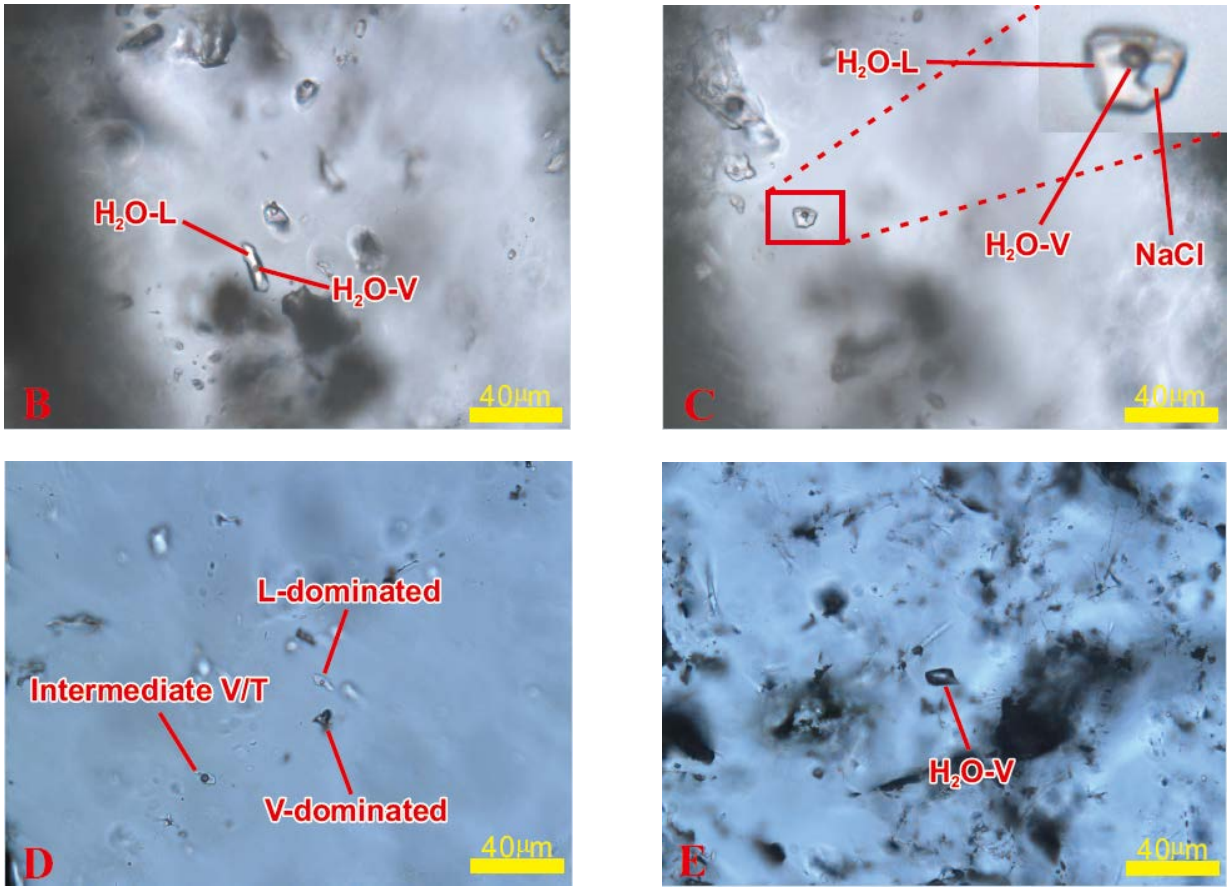
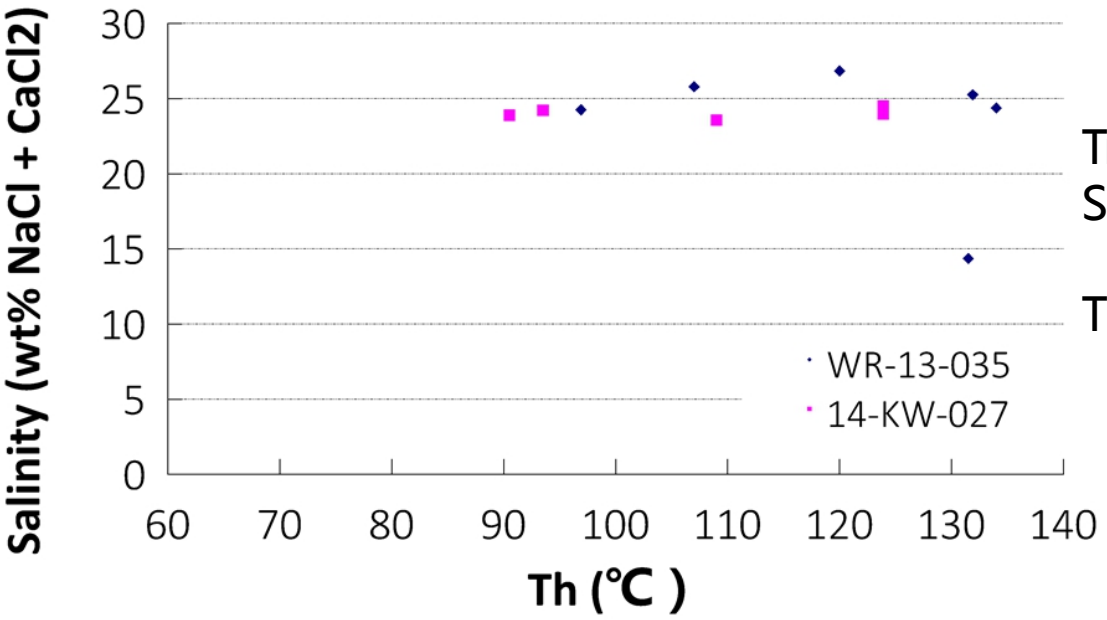


Fig. 7B, C, D &E. Abundant biphase with variable V/T ratios and vapour-only aqueous inclusions found in the euhedral crystals of the secondary vuggy quartz veins and cements;

FI study - Aqueous FI



Tm-ice: -33.6- -23.6°C
S: 23.6-26.8 wt%

Th: 80-135 °C

Fig. 7F. Homogenization temperature (Th) versus salinity diagram for the studied aqueous inclusions;

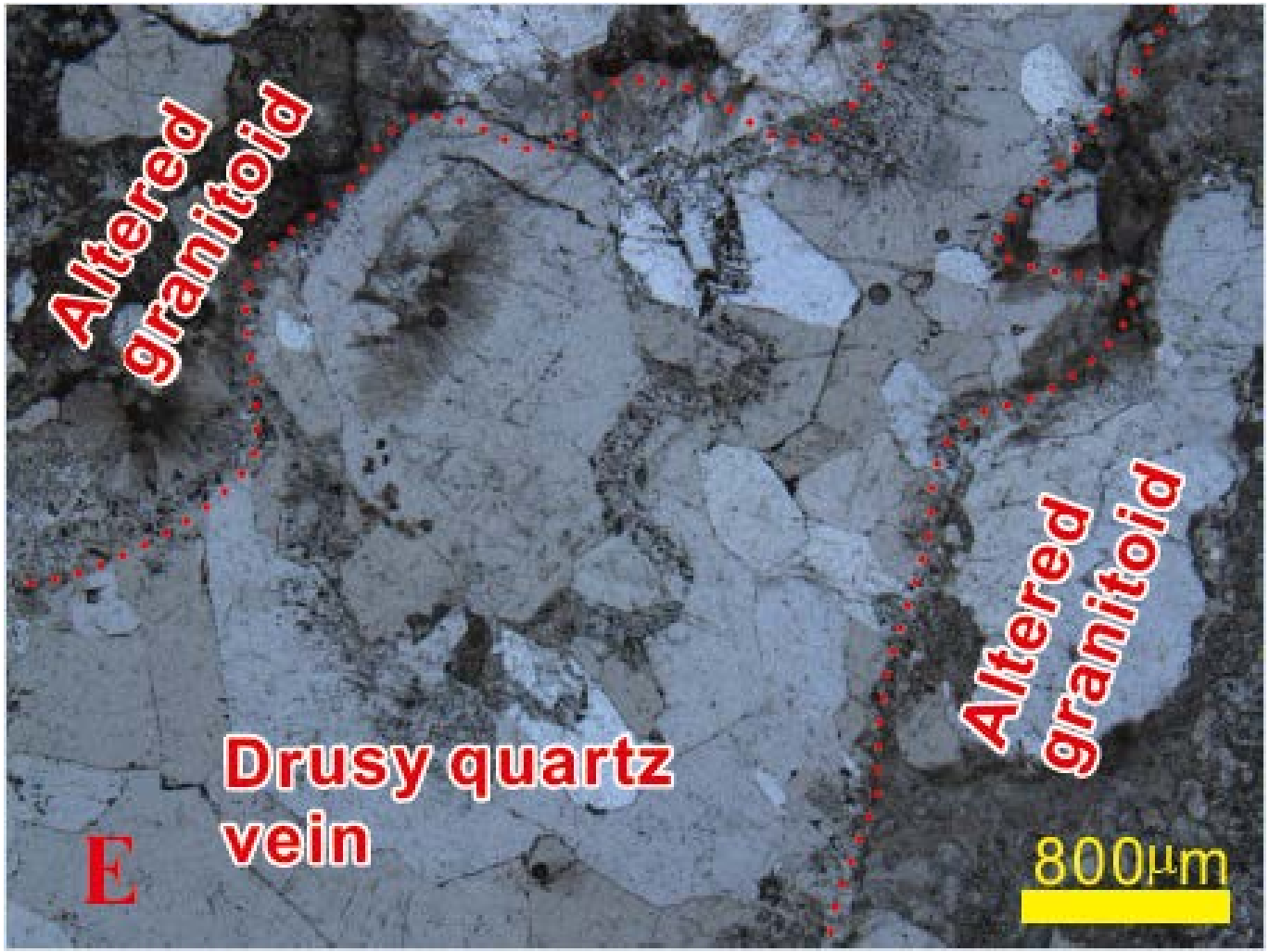


Fig. 6E. Drusy quartz vein cutting altered granitoid (WR-560, 736m, **Gryphon zone**)

FI study - Aqueous FI

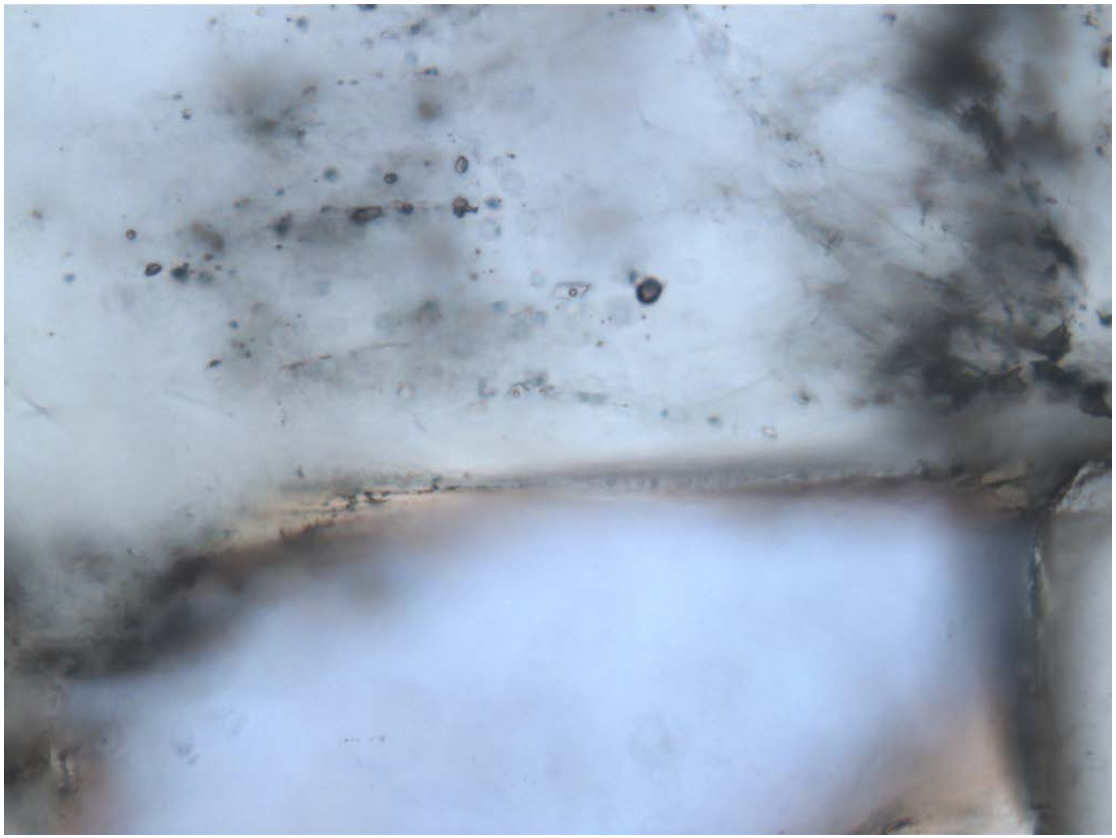


Fig. 7G. Fluid inclusions with various V/T ratios in the growth zone of drusy qtz cutting altered granitoid in the basement (WR-560, 736m, **Gryphon zone**);

FI study - Aqueous FI

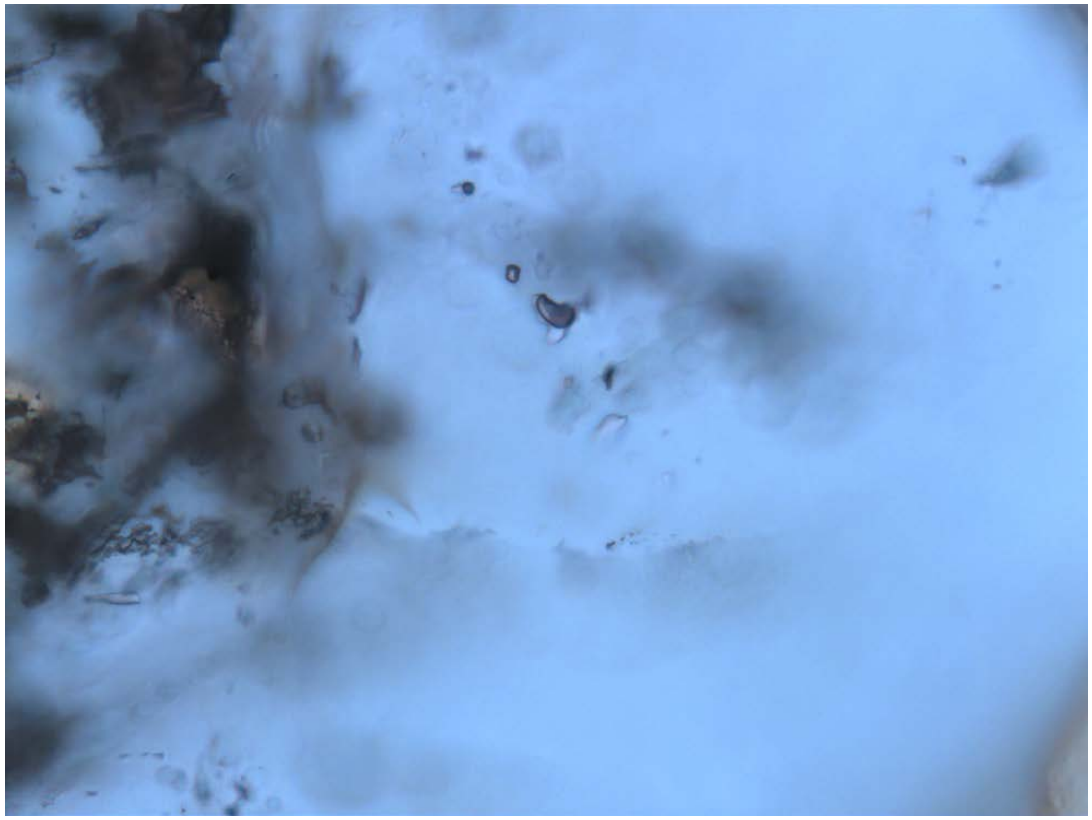


Fig. 7H. Abundant vapour dominant-FI in the growth zone of drusy qtz cutting altered granitoid in the basement (WR-560, 736m, **Gryphon zone**)

FI study - CO_2 FI

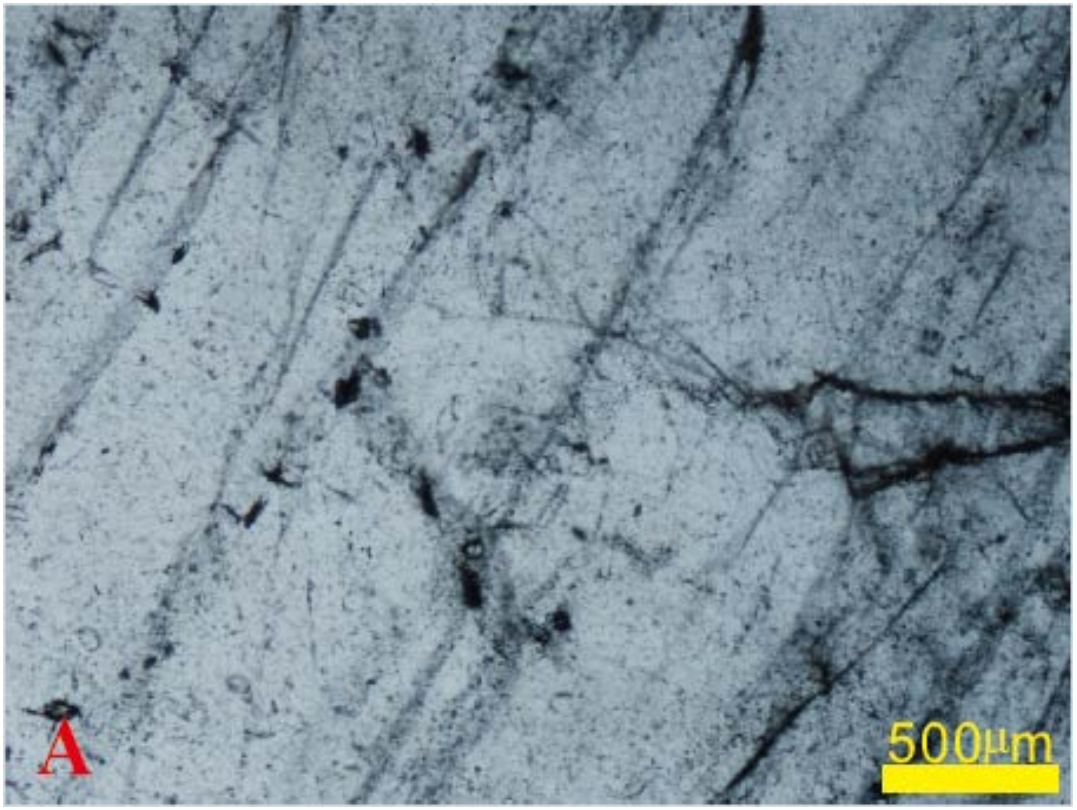


Fig. 8A. Fluid inclusions distributed along parallel microfractures in massive quartz (WR-440, 674m);

FI study - CO_2 FI

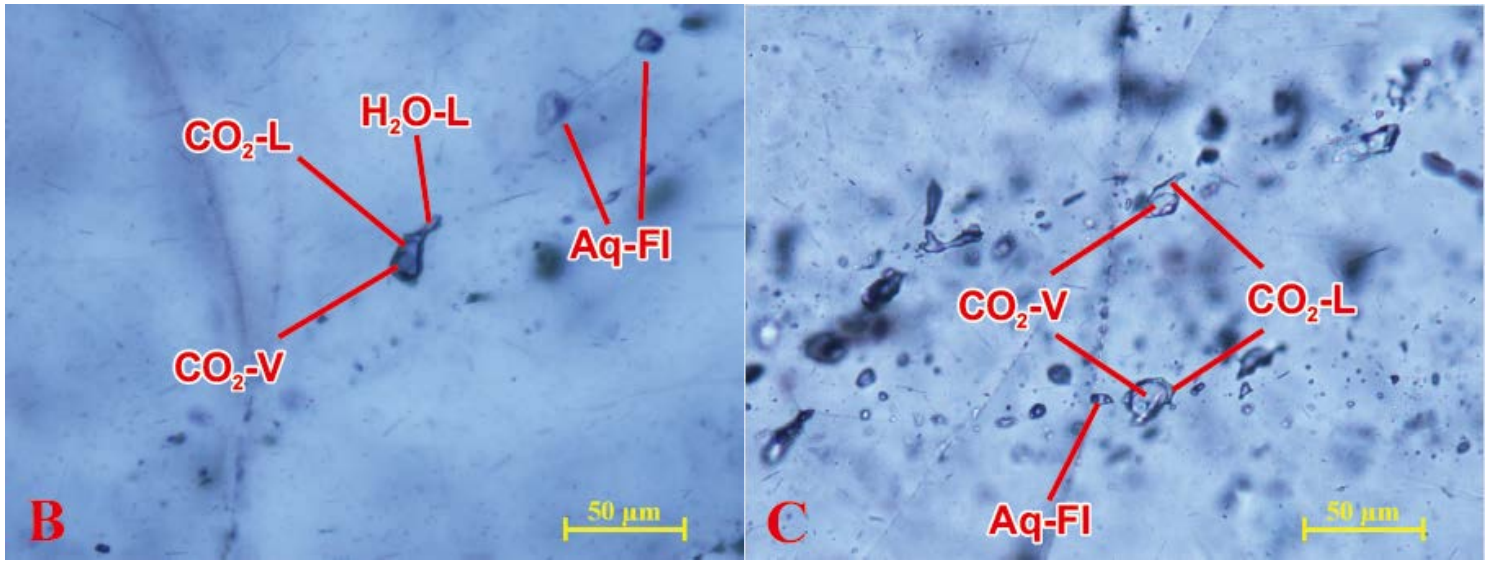


Fig. 8B. CO_2-dominated inclusions with three phases (WR-440, 479.6m); 8C. CO_2-dominated inclusions with two phases (WR-440, 479.6m)

FI study- Preliminary conclusions

- Th and salinity values- within the lower T ranges reported for the McArthur River deposit (Derome et al., 2005);
- Vapour-only **aq-FI** + biphase **aq-FI** - boiling during the formation of drusy quartz;
- Low Th (80 to 135 °C) of biphase aq-FI - waning stage of U mineralization system, at lower T and P than the main phase.

FI study- Preliminary conclusions (Cont'd)

- **CO_2-FI** in the basement- before the Athabasca basin and U mineralization, probably in the late retrograde metamorphic stage of Trans-Hudson orogeny;
- Microfractures formed in this stage may have been re-opened during the formation of the Athabasca basin- basinal brines into the basement (Mercadier et al., 2010).

Microstructrual study of FIP



Fig. 9A. Picture of an oriented core showing a dolomite – quartz vein cutting graphic pelite (WR-440, 604.1m);

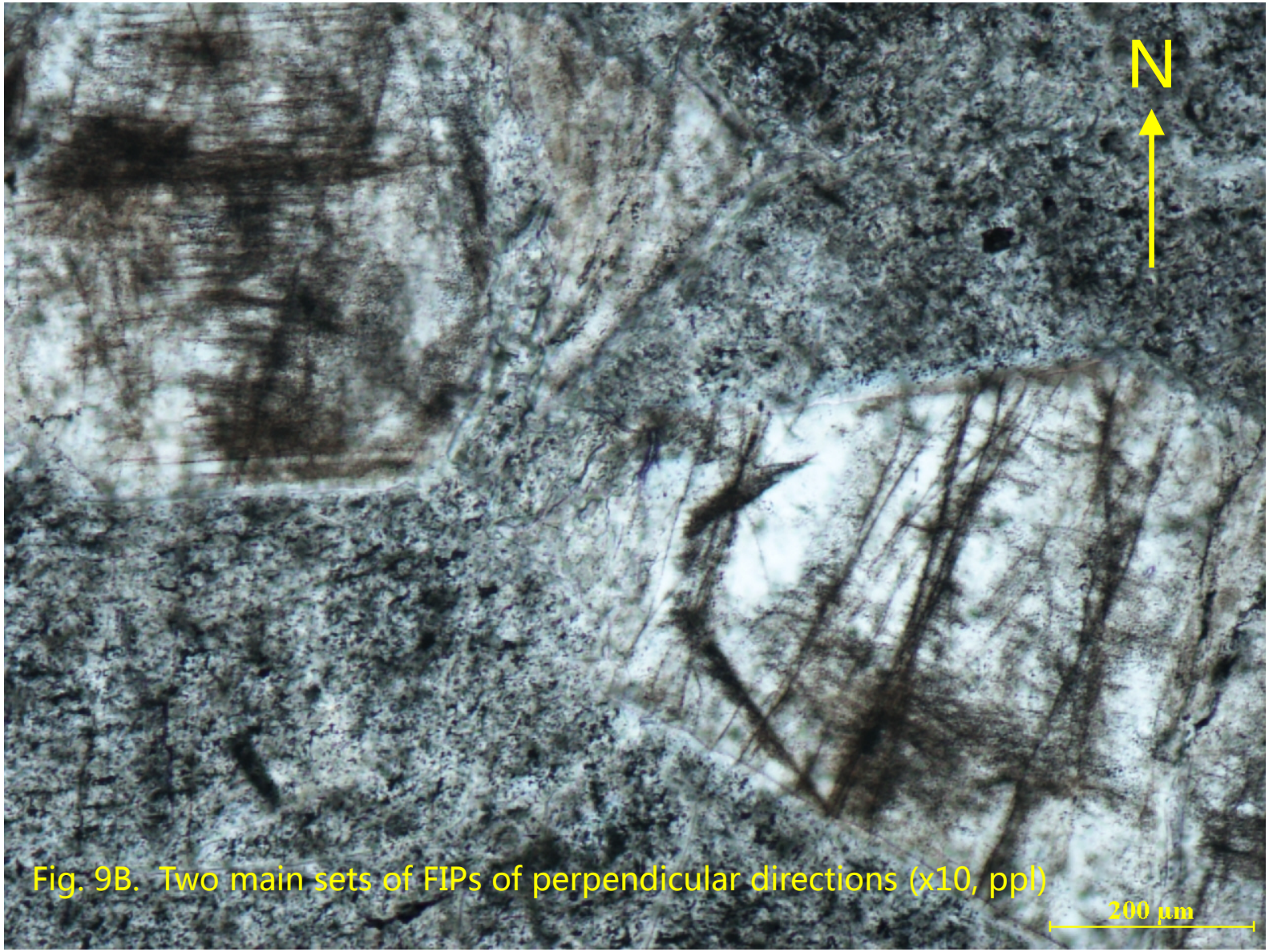


Fig. 9B. Two main sets of FIPs of perpendicular directions (x10, ppl)

Microstructrual study of FIP

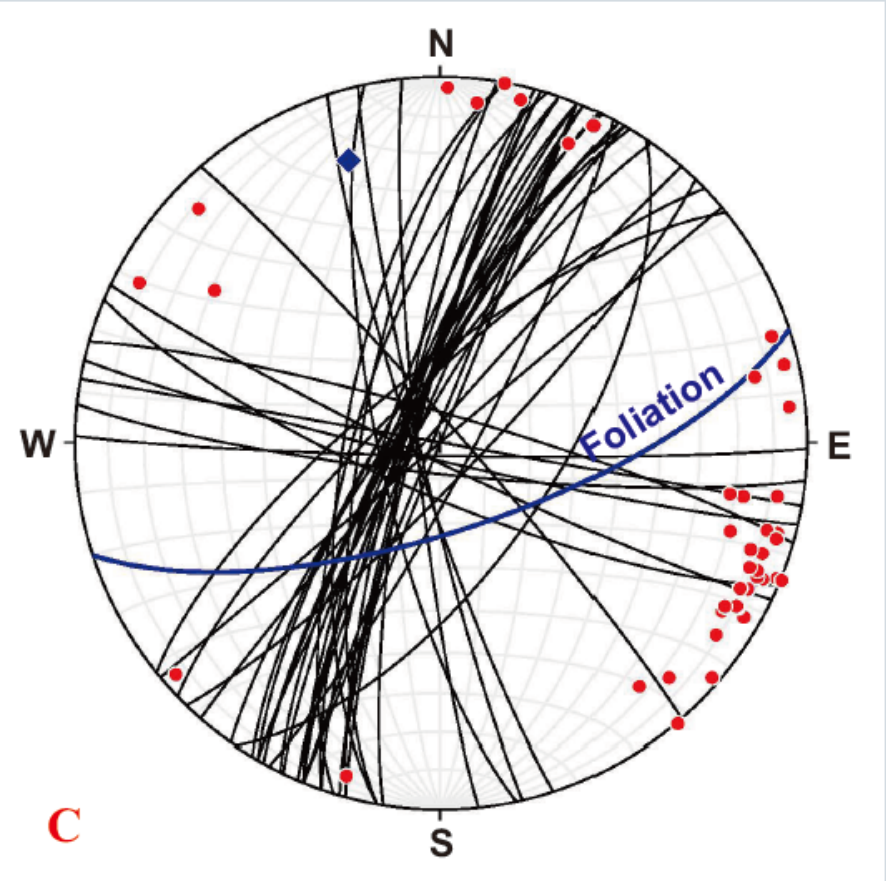


Fig. 10. Stereonet projection (n = 43) of the FIPs

- Red dots- poles to the FIPs (subhorizontal)

- Trending:
- 190-210° (longer)
- 90-110° (shorter)

- Dipping: subvertical
- Average 80°

Microstructrual study of FIP

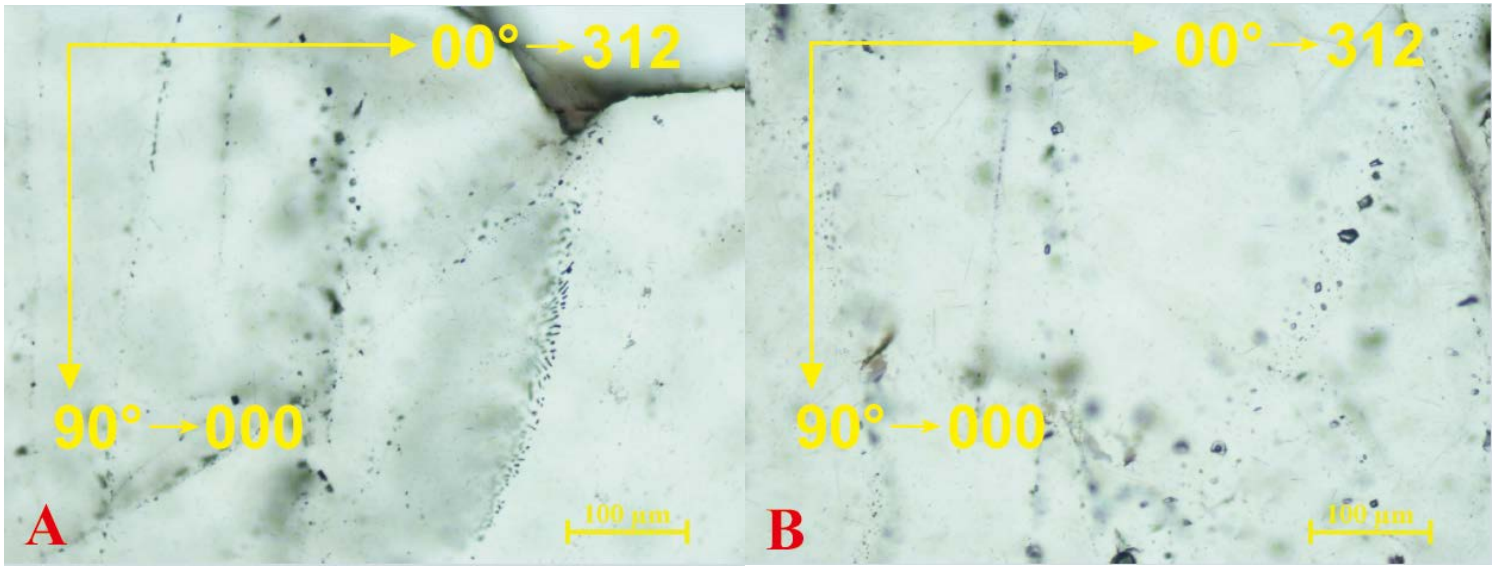


Fig. 11A. Crosscutting FIPs in pegmatoid quatz (WR-440, 479.6m); 11B. Crosscutting FIPs hosting aqueous fluid inclusions and carbonic fluid inclusions (WR-440, 479.6m)

FIP study- Preliminary conclusions

- The two main directions of FIP (horizontally cut)-two different stress field
- WNW- ESE σ3 (long)
- NNE- SSW σ3 (short)
- Both σ3- subhorizontal (poles to FIP)

- FI in horizontal section- too small
- FI in vertical section- CO_2-FI and aq-FI- ongoing
- More work on FIPs is underway with other oriented samples.

Raman spectroscopic study of graphite

- WR-267, U_3O_8 (19.98%) starts at 405m (over 3.5m)

Sample No.	Depth.	Distance from LB of U mzn
14-KW-048	414.1m	5m
14-KW-051	423.8m	15m
14-KW-053	433m	25m

Table. 1. Sample number, depth and relative distance from mineralization zone of studied samples

Raman spectroscopic study of graphite

- To avoid mechanical damage- graphite beneath transparent mineral (Beyssac et al., 2003);
- 30s, 4-6 spectra;
- 1st order: 1000-2000 cm^{-1}; 2nd order: 2000-3500 cm^{-1}.

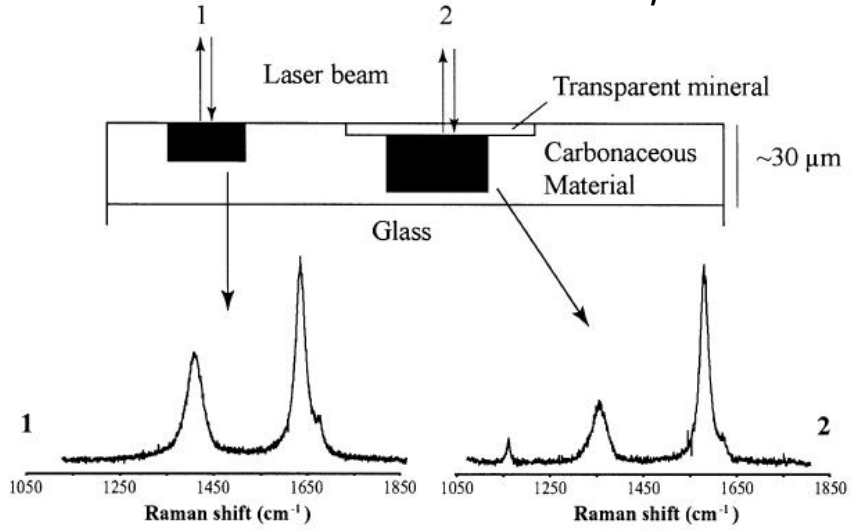


Fig. 12. Comparison between the Raman spectra of CM measured (1) at the surface of the thin section and (2) beneath a transparent mineral (Beyssac et al., 2003)

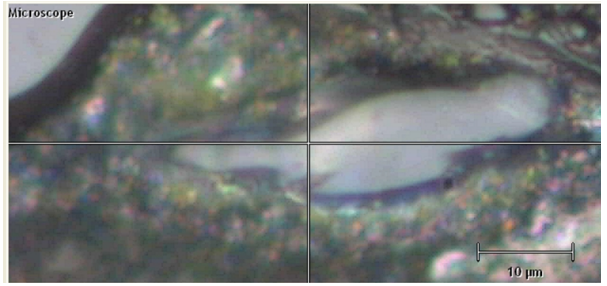


Fig. 13. 14-KW-051, point 4, graphite below qtz

Raman spectroscopic study of graphite

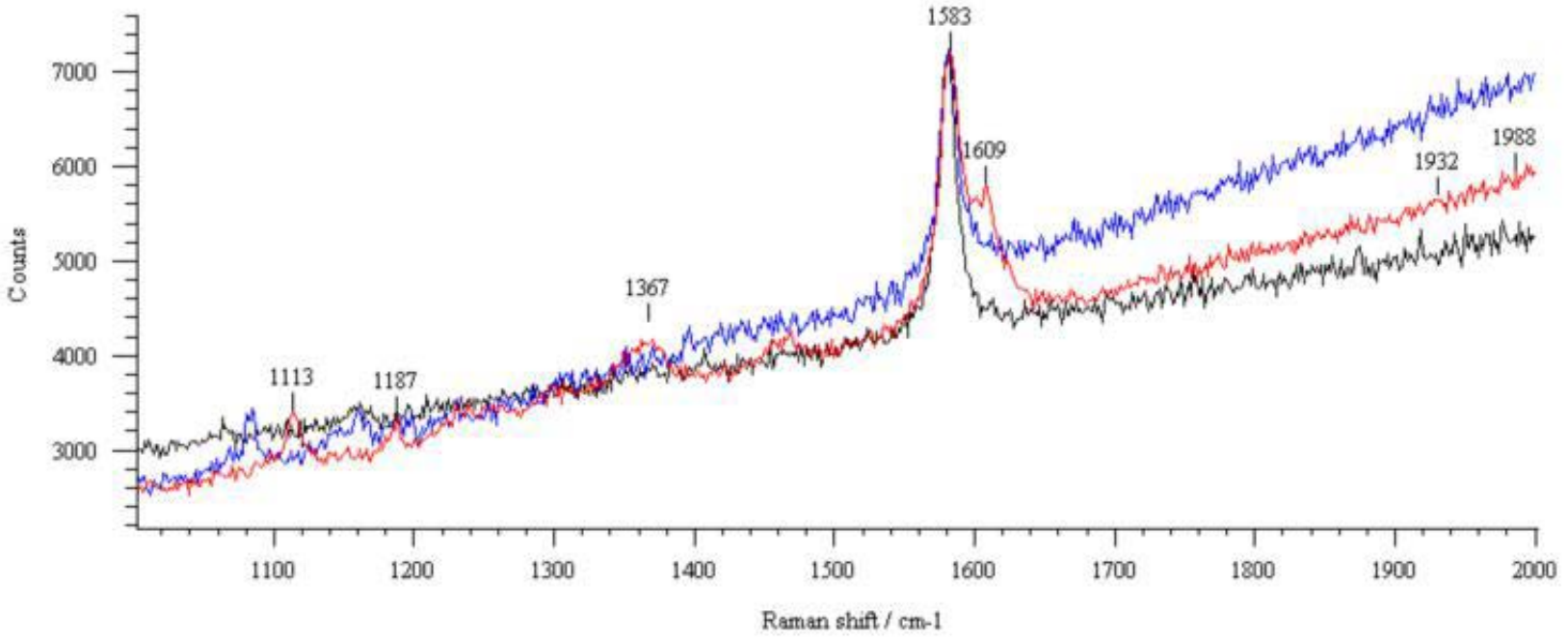


Fig. 14. Representative Raman spectra of graphite in the first-order region of three samples with different distances from the ore zone; Red: 14-KW-048, 5m from ore zone; Blue: 14-KW-051, 15m from the ore zone; Black: 14-KW-053, 25m from the ore zone

Raman spectroscopic study of graphite

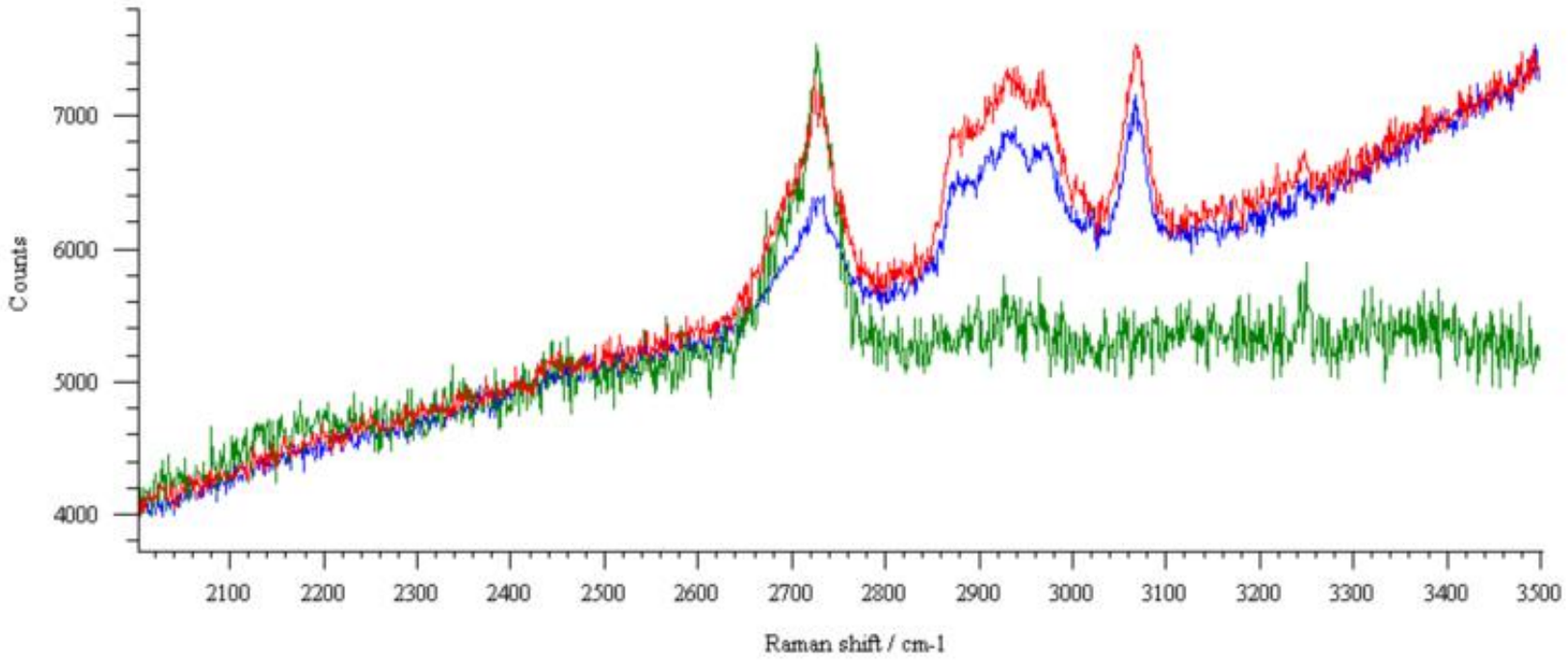


Fig. 15. Representative Raman spectrum of the second-order region of two samples; Blue: 14-KW-048, 5m from ore zone (focus close to thin section surface); Red: 14-KW-048, 5m from ore zone (focus further from thin section surface); Green: 14-KW-051, 15m from the ore zone

Graphite study- Preliminary conclusions

- Graphite in all there samples is generally well crystallized;
- Highest D1 and S2 intensities of the sample closest to the mineralization zone (14-KW-048)- graphite near the mineralization is relatively disordered.

Summary

- **Field, petrography & FI-** different structural regimes and fluid systems were developed in the **pre-Athabasca stage** vs. the **syn- to post-Athabasca, uranium mineralization stage;**
- **Pre-Athabasca stage:**
  - **ductile deformation** (foliations)
  - pegmatization and massive silicification
  - circulation of metamorphic fluids, in a relatively **high P-T** environment (CO_2-FI);

Summary (Cont'd)

- **Syn- to post-Athabasca stage:**
  - brittle deformation (fractures filled by drusy quartz) in the basal Athabasca group and the uppermost part of the basement
  - circulation of basinal brines in a relatively low P-T environment (aq-FI)
  - fluid may have experienced boiling (vapour-only and biphase aq-FI);

Summary (Cont'd)

- **Preliminary FIP-orientation studies:**

  - subvertical microfractures are developed in the basement rocks- after the ductile deformation stage

  - oriented NNE-SSW and WNW-ESE- sub-horizontal σ3 was once trending WNW-ESE and NNE-SSW respectively

  - timing of these regimes?

  - σ1 and σ2?

Summary (Cont'd)

- **Preliminary Raman spectroscopic study of graphite:**

  - graphite- **increasingly disordered** toward the ore zone

  - if confirmed by further studies (SEM? FI?- ongoing)- maybe used to investigate the role of graphite in U mineralization and as an **indicator** of mineralization

Acknowledgements

This project is supported by TGI-4 (Targeted Geoscience Initiative 4), a collaborative federal geoscience program led by Natural Resources Canada.

University of Regina

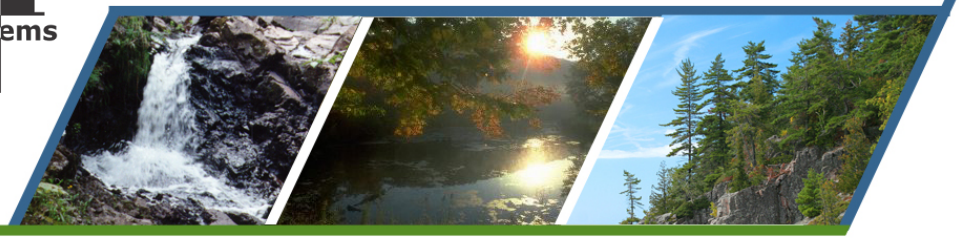
TGI 4 Ore Systems

Saskatchewan Ministry of the Economy

Thank you!



TGI 4 Ore Systems



Fe and Mg Signatures of the Bong Uranium Deposit, Thelon Basin, Nunavut.

Eric Potter[1], Ryan Sharpe[2], Isabelle Girard[1], Mostafa Fayek[2], Paul Gammon[1], David Quirt[3], John Robbins[3]



1 - Geological Survey of Canada;
2 - University of Manitoba;
3 - AREVA Resources Canada Inc.

Natural Resources Canada | Ressources naturelles Canada

Introduction



Hydrothermal Fe- and Mg-bearing minerals are often associated with basement- and sandstone-hosted, unconformity-related U systems (cf. Hoeve & Sibbald, 1978; Quirt & Wasyliuk, 1997; Jefferson et al., 2007)

Fe and Mg-minerals often cited as a product of U precipitation mechanisms:

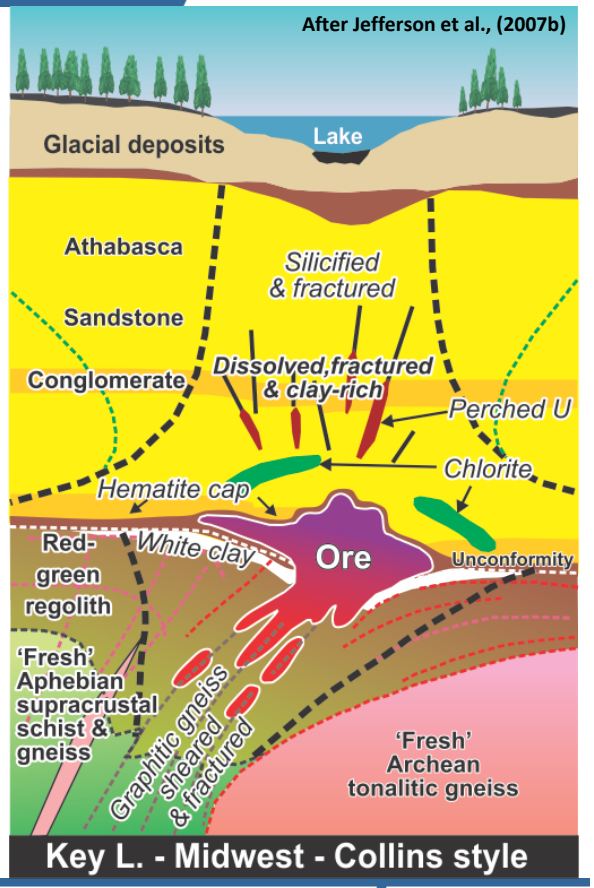
[Biotite - amphibole - Fe-rich chlorite + oxidizing & acidic fluids] → sudoite

(e.g. Wallis et al., 1985; Alexandre et al., 2005)

Fe oxidation coupled with U reduction

[$Fe^{2+} \rightarrow Fe^{3+} \nearrow é$] [$U^{6+} + 2é \rightarrow U^{4+}$]

to form uraninite and Fe^{3+}-bearing Fe-oxide/hydroxides and Mg-rich minerals.



Magnesium & Iron Isotope Systematics



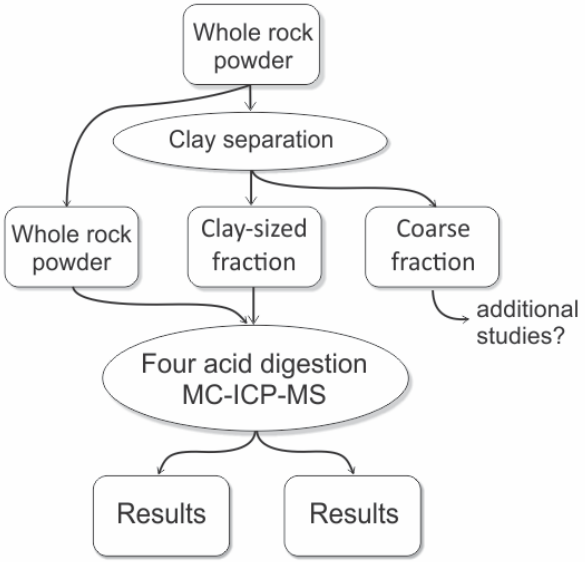
- **δ^{56}Fe of crust & sedimentary rocks = 0.00 ± 0.08 ‰,** incl. alteration and weathering products - although large Fe fractionations occur during redox reactions or changes in bonding states (Heimann et al., 2008; Johnson et al., 2008; Craddock and Dauphas, 2010).

- **δ^{26}Mg of upper cont. crust & mantle derived minerals = - 0.1 and - 0.3 ‰,** with a strong mineralogical control on fractionation between carbonates, clays and waters during low-temperatures processes such as weathering (Young and Galy, 2004; Pogge von Strandmann et al., 2008; Handler et al., 2009; Bourdon et al., 2010; Li et al., 2010; Wimpenny et al., 2014).

- Using mineralogical (primary minerals and alteration assemblages), textural (crystal size), Fe-speciation (Fe^{2+}, Fe^{3+} molecular concentrations) and isotopic data (Mg and Fe isotopic signatures) in concert, there is **potential to discriminate weathering from diagenetic and hydrothermal signatures, particularly in terms of barren (no redox reactions) from fertile alteration (redox reactions evident).**

Sample Preparation

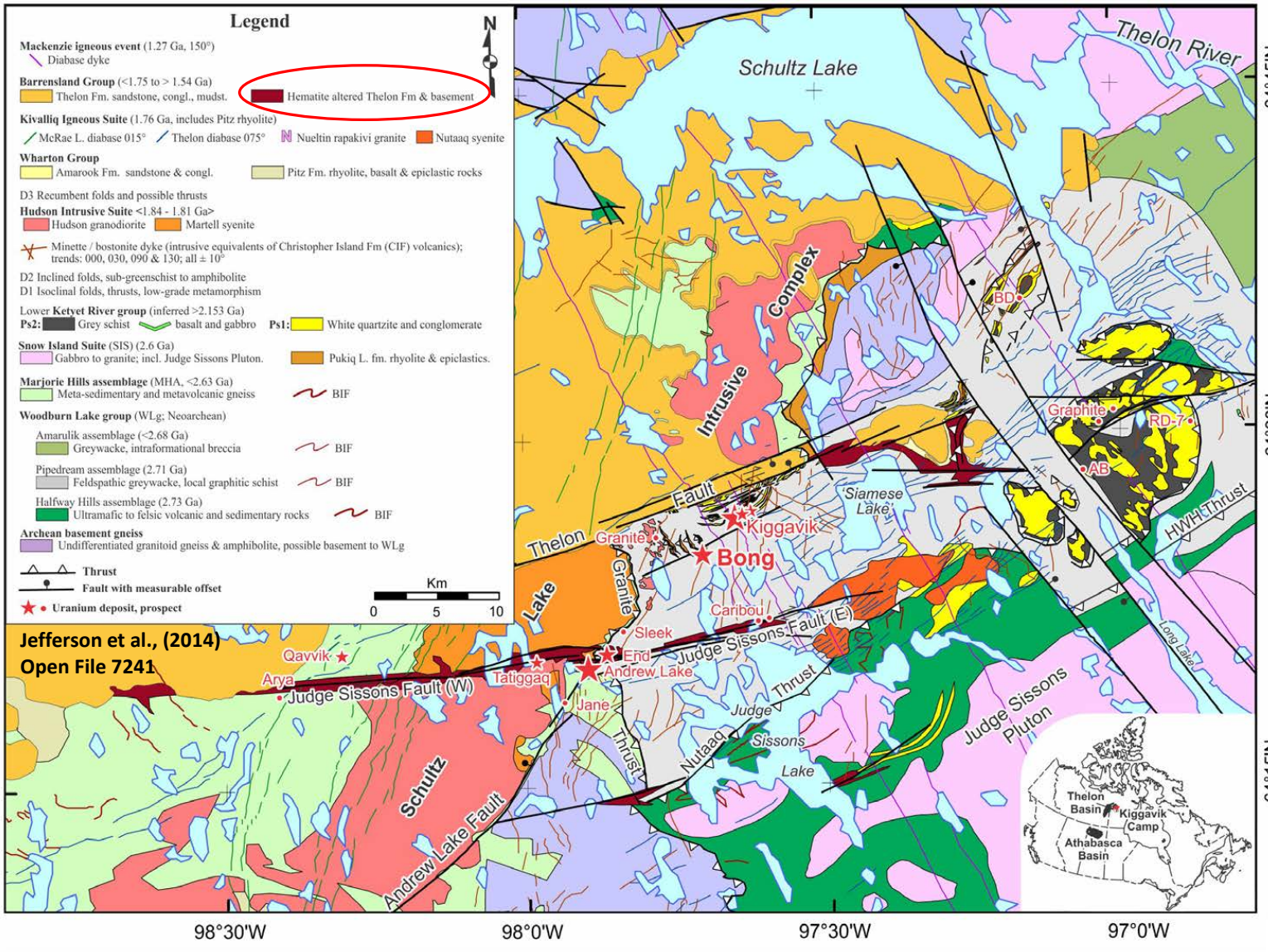
- Near-total four acid decomposition (HNO_3, HF, HCl, $HClO_4$)
- Mg was separated and purified on a cation exchange resin (adapted from Wombacher et al., 2008)
- Fe was separated and purified by anion exchange (adapted from Chapman et al., 2005).
- Isotope ratios determined on a Nu Plasma double-focusing multi-collector ICP-MS at GSC Ottawa





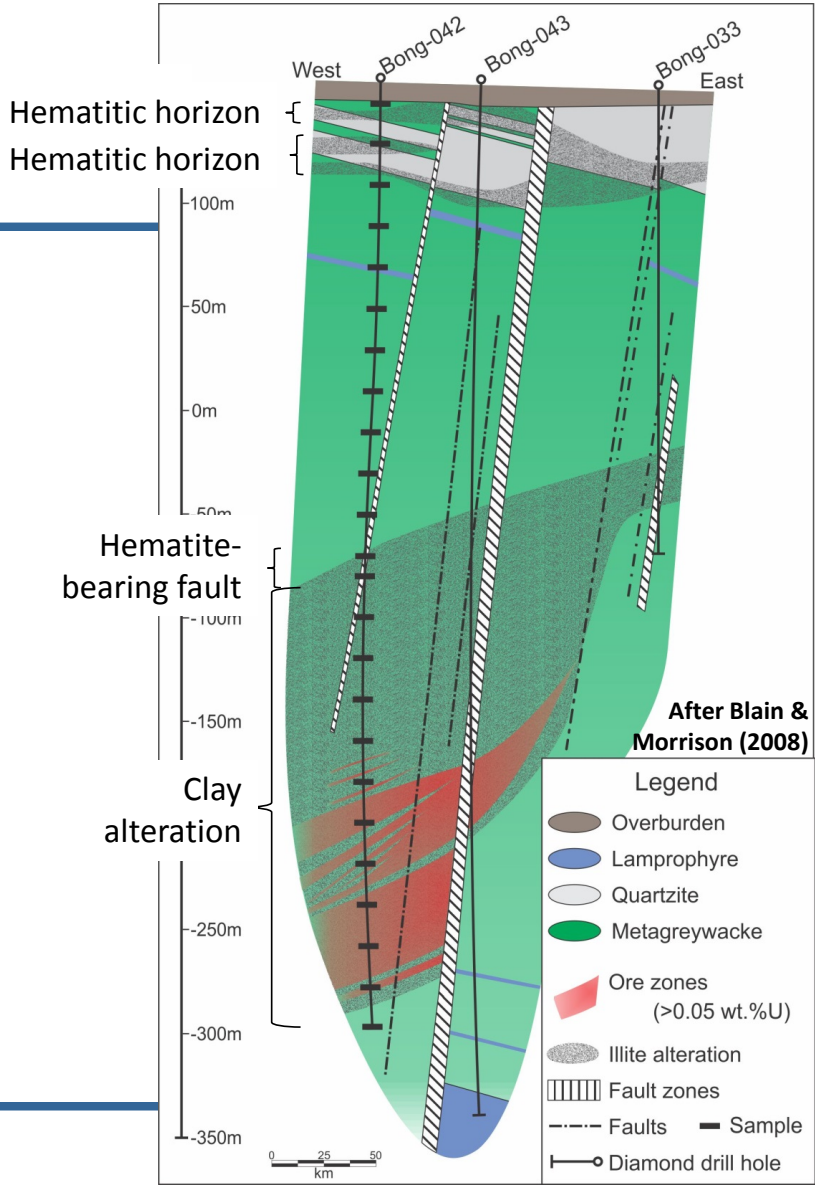
$$\delta^{xx}Mg = \left\{ \frac{(^{xx}Mg / {}^{24}Mg)_{sample}}{(^{xx}Mg / {}^{24}Mg)_{DSM3}} - 1 \right\} \times 10^3$$

$$\delta^{xx}Fe = \left\{ \frac{(^{xx}Fe / {}^{54}Fe)_{sample}}{(^{xx}Fe / {}^{54}Fe)_{IRMM014}} - 1 \right\} \times 10^3$$


Legend
N
Mackenzie igneous event (1.27 Ga, 150°)
Diabase dyke
Barrensland Group (<1.75 to > 1.54 Ga)
Thelon Fm. sandstone, congl., mudst.
Hematite altered Thelon Fm & basement
Kivalliq Igneous Suite (1.76 Ga, includes Pitz rhyolite)
McRae L. diabase 015°
Thelon diabase 075°
Nueltin rapakivi granite
Nutaaq syenite
Wharton Group
Amarook Fm. sandstone & congl.
Pitz Fm. rhyolite, basalt & epiclastic rocks
D3 Recumbent folds and possible thrusts
Hudson Intrusive Suite <1.84 - 1.81 Ga>
Hudson granodiorite
Martell syenite
Minette / bostonite dyke (intrusive equivalents of Christopher Island Fm (CIF) volcanics); trends: 000, 030, 090 & 130; all ± 10°
D2 Inclined folds, sub-greenschist to amphibolite
D1 Isoclinal folds, thrusts, low-grade metamorphism
Lower Ketyet River group (inferred >2.153 Ga)
Ps2: Grey schist
basalt and gabbro
Ps1: White quartzite and conglomerate
Snow Island Suite (SIS) (2.6 Ga)
Gabbro to granite; incl. Judge Sissons Pluton.
Pukiq L. fm. rhyolite & epiclastics.
Marjorie Hills assemblage (MHA, <2.63 Ga)
Meta-sedimentary and metavolcanic gneiss
BIF
Woodburn Lake group (WLg; Neoarchean)
Amarulik assemblage (<2.68 Ga)
Greywacke, intraformational breccia
BIF
Pipedream assemblage (2.71 Ga)
Feldspathic greywacke, local graphitic schist
BIF
Halfway Hills assemblage (2.73 Ga)
Ultramafic to felsic volcanic and sedimentary rocks
BIF
Archean basement gneiss
Undifferentiated granitoid gneiss & amphibolite, possible basement to WLg
Thrust
Fault with measurable offset
Uranium deposit, prospect
Km
0 5 10
Jefferson et al., (2014)
Open File 7241
Schultz Lake
Thelon River
Intrusive Complex
BD
Graphite
RD-7
AB
HWH Thrust
Siamese Lake
Fault
Kiggavik
Bong
Thelon Granite
Granite
Lake
Caribou
Sleek
End
Andrew Lake
Judge Sissons Fault (E)
Judge Sissons Thrust
Judge Sissons Pluton
Long Lake
Qavvik
Arya
Judge Sissons Fault (W)
Tatiggaq
Jane
Thrust
Nutaaq
Judge Sissons Lake
Schultz
Andrew Lake Fault
Thelon Basin
Kiggavik Camp
Athabasca Basin
64°45'N
64°30'N
64°15'N
98°30'W
98°0'W
97°30'W
97°0'W

Bong Deposit

- Host: Woodburn Lake Group metagreywacke
- Uranium enrichment is associated with a broad alteration halo characterized by intense illitization ± chloritization
- Clay alteration: 236 – 315m
- uranium enrichment plus clay alteration: 315 – 414m.
- Hematitic horizons: 0 – 9m, 26 – 43m and fault zone (220-240m)



Bong Deposit: alteration

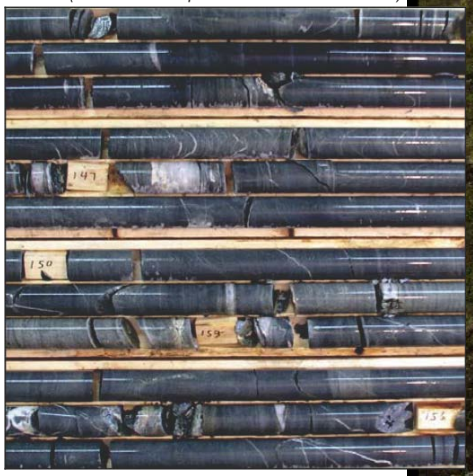




Blain & Morrison (2008)

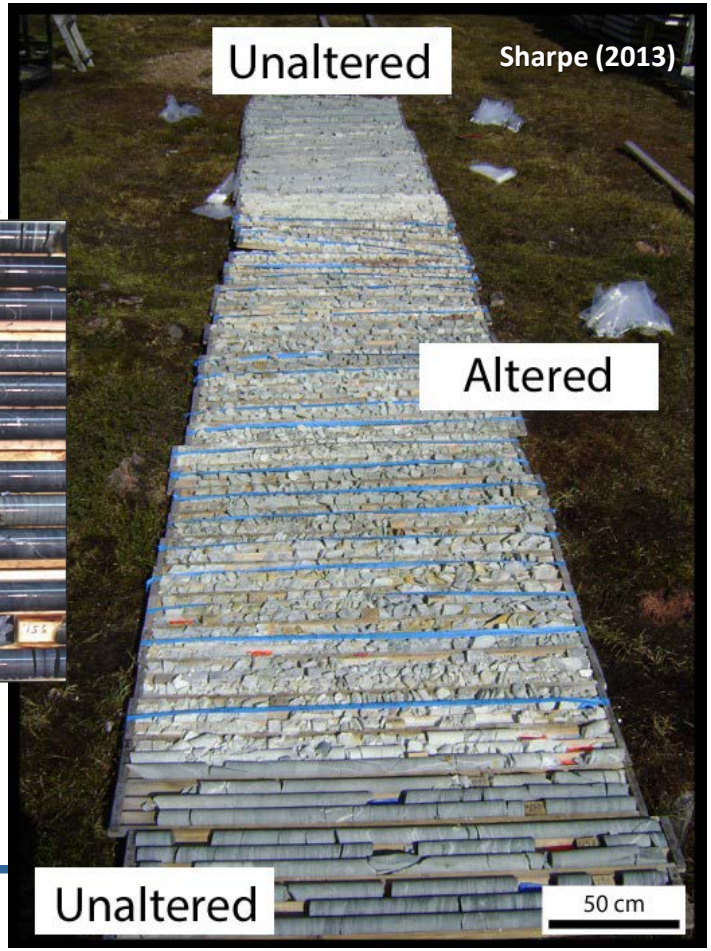
Upper hematitic horizon in quartzite & metagreywacke

Least-altered metagreywacke





Clay-altered host (bleached zone) with minor hematite

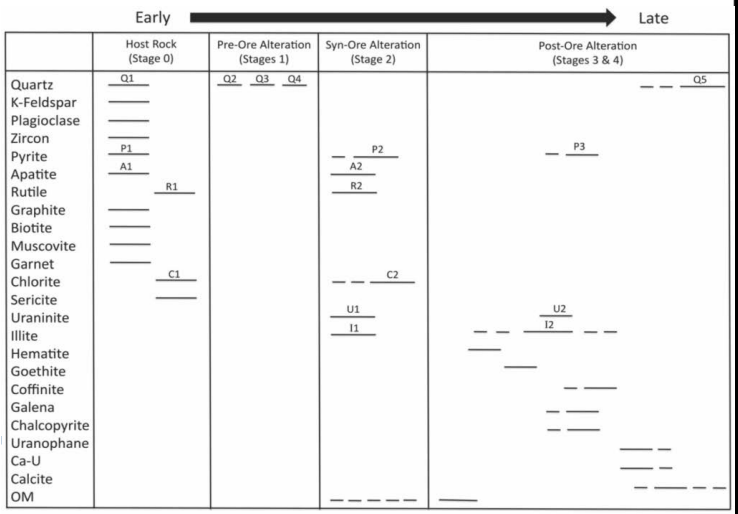


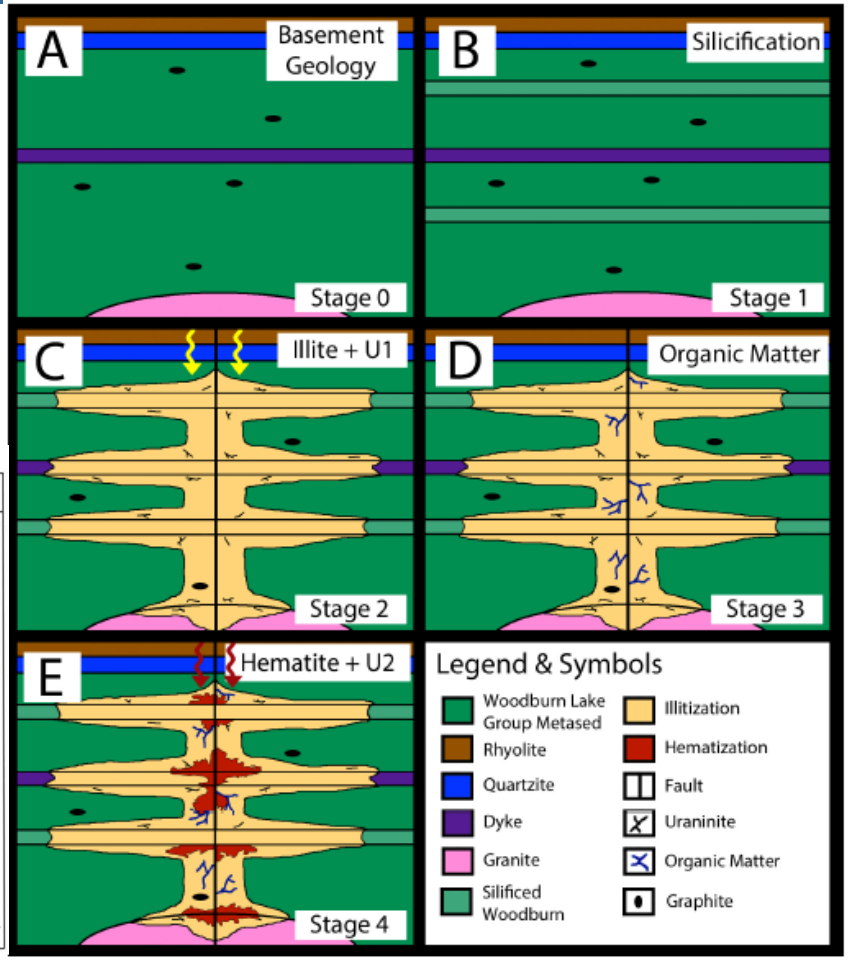
Bong Deposit: Sharpe (2013) model



Uranium precipitated in two stages:

1) illite + chlorite alteration and U1 in veins and associated with organic matter
2) U2 in miniature roll-fronts (Sharpe, 2013).





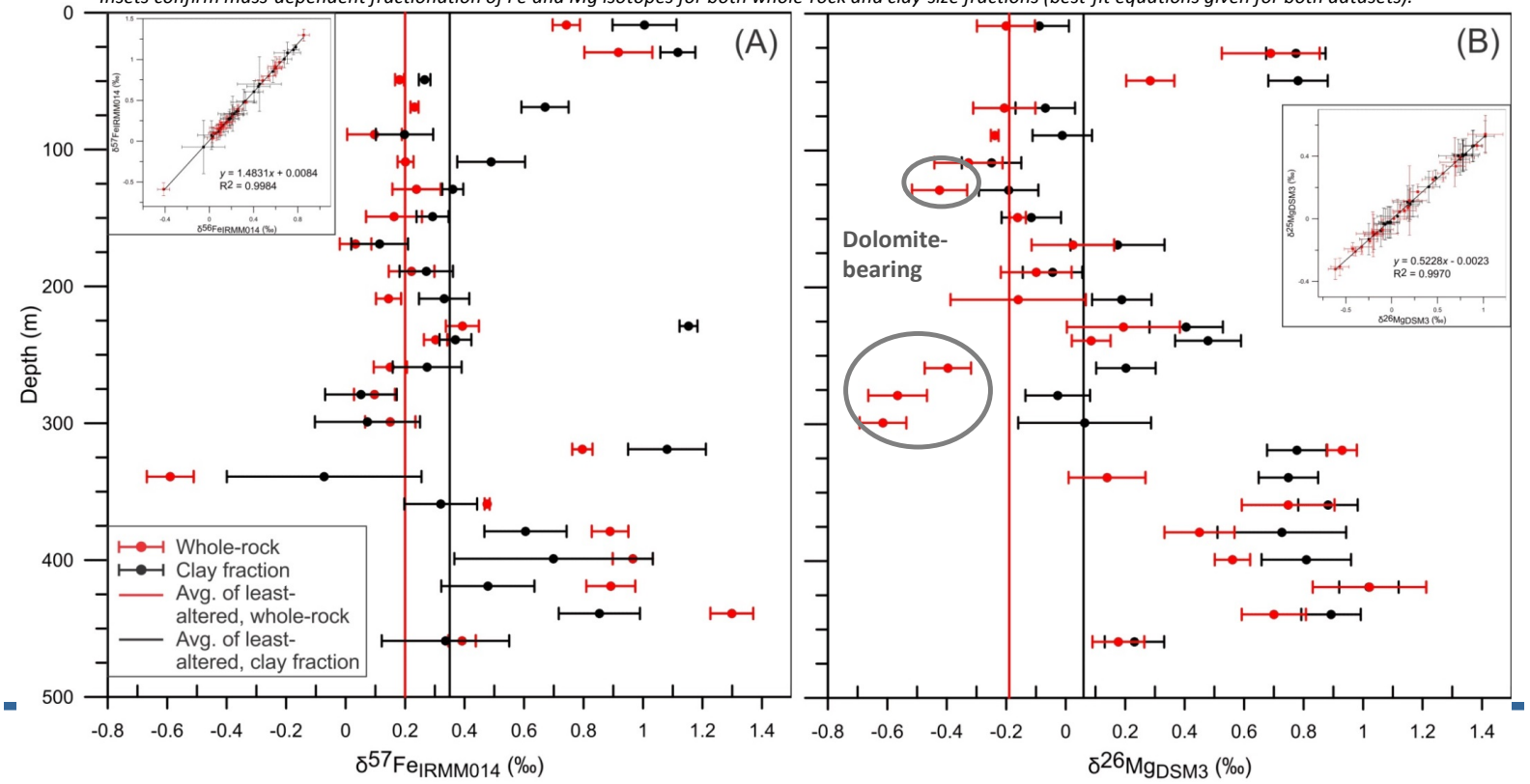
Isotope results



Relatively high δ values recorded in two zones (shifts of ca. +0.7 ‰ $\delta^{57}Fe$ & +0.8 ‰ $\delta^{26}Mg$)

clay-fraction is more variable and includes additional zone of elevated values (Fe)

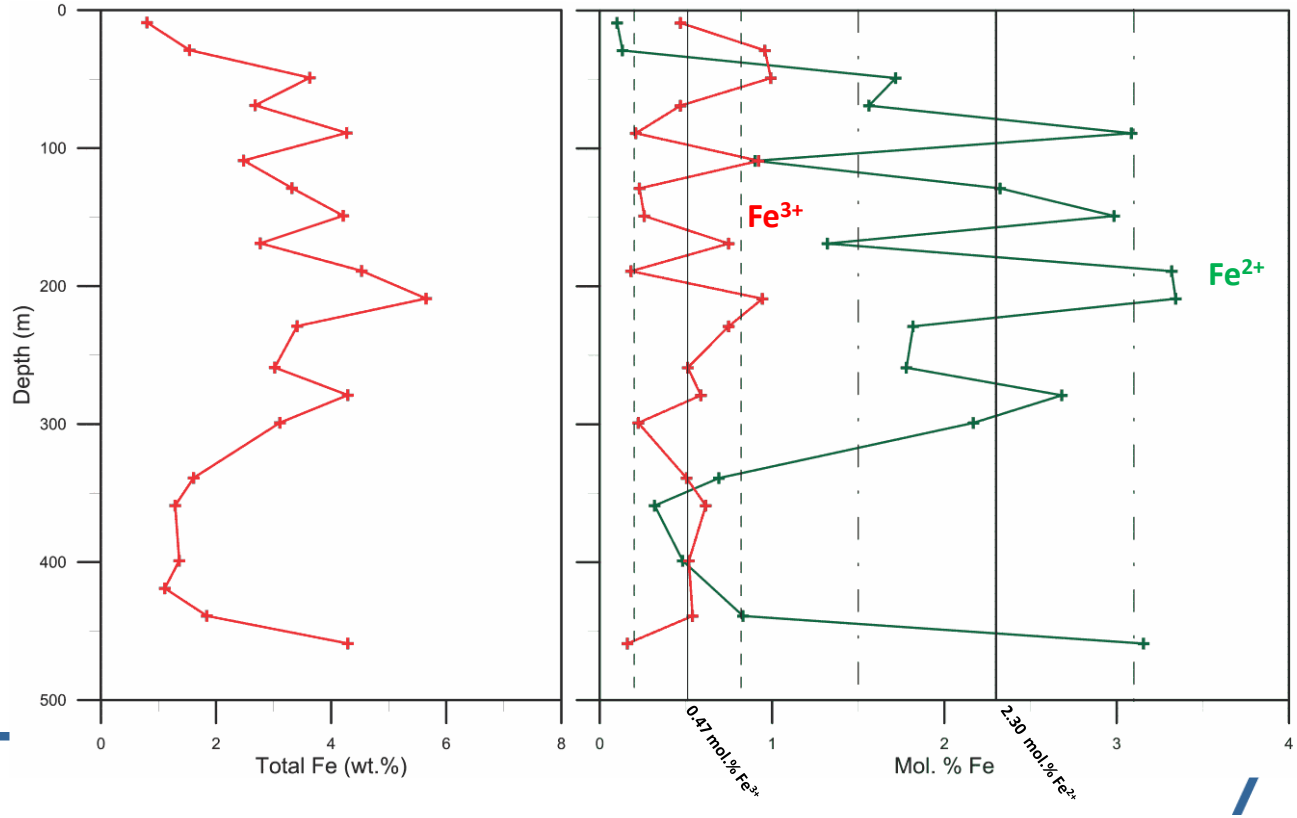
Insets confirm mass-dependent fractionation of Fe and Mg isotopes for both whole-rock and clay-size fractions (best-fit equations given for both datasets).



Fe speciation results (Sharpe, 2013)



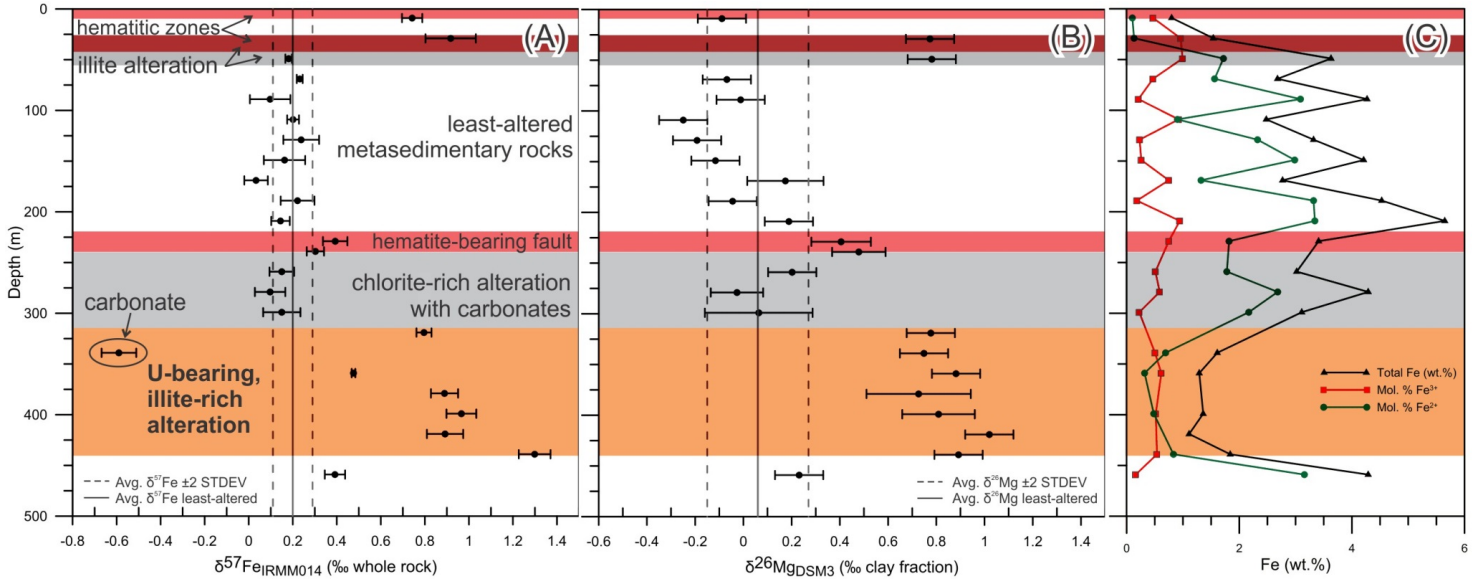
Mirror of Fe and Mg isotopic results: drop in total Fe (wt. %) reflects significant reductions in Fe^{2+} concentrations (0.47 vs 2.30 mol.% Fe^{2+})



Preliminary Observations



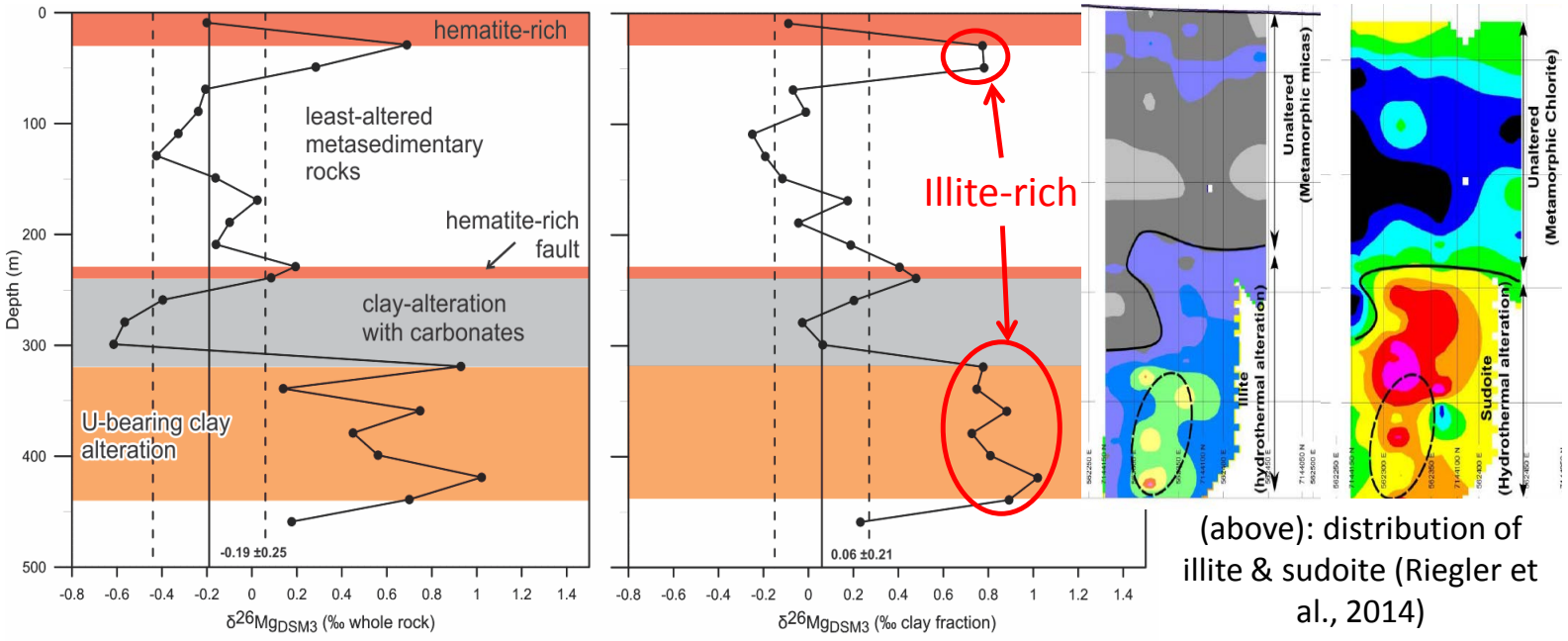
- Zones with high $\delta^{57}Fe$ and $\delta^{26}Mg$ values are associated with the U-bearing clay alteration of the Bong deposit and hematitic horizons
- These zones correlate with relative losses of Fe^{2+} whereas the molar concentrations of Fe^{3+} remain relatively constant.
- The association of similar elevated isotopic values between hematitic and clay-altered zones, lack of enrichment in generally insoluble Fe^{3+} -bearing minerals and presence of K-feldspar in the upper hematitic zone suggests that the hematite-rich horizons are unlikely to have formed through paleoweathering processes, as historically cited



Discussion – Mg isotopes



- Zones with high $\delta^{26}Mg$ values are associated with the U-bearing clay alteration of the Bong deposit and the lower unit of the upper hematite-bearing horizons - reflecting presence of clay alteration (e.g. Tipper et al., 2006; 2012; Opfergelt et al. , 2012; Wimpenny et al., 2014).
- However, analyses of clay-altered zone above the U-bearing clay alteration yielded low δ values, which may reflect presence of carbonate minerals or relative sudoite-illite abundances (cf. Riegler et al., 2014)



(above): distribution of illite & sudoite (Riegler et al., 2014)

Preliminary conclusions……



- Mg isotopic results appear to reflect clay formation under acidic conditions, whereby illite preferentially incorporated the heavier Mg isotopes (e.g. Wimpenny et al., 2014) in both the U-bearing zone and upper hematitic horizon

- Fe isotopic data appear to reflect redox reactions in the U-bearing clay-altered zone and in the upper hematite-rich zones

- Clay alteration above U-bearing zone not characterized by high $\delta^{57}Fe$ or $\delta^{26}Mg$ values may reflect: lack of redox signature, the presence of carbonate minerals, or changes in sudoite vs. illite abundance

- **Therefore, U-bearing zones are best characterized by high whole rock δFe and clay-sized δMg isotopic values but with moderate clay-sized δFe values.**

Next…..



Can the distal enrichment in Fe^{3+}-bearing minerals coupled with lighter Mg / Fe isotope compositions be used as a vector to ore zones?

e.g. Hydrothermal alteration of MORB indicated by heavier Fe isotopes and associated mineral products plus Si-Fe deposits enriched in lighter Fe isotopes (Rouxel et al., 2003)

On going:

Weak acid leaches and non-mineralized drill holes (Bong deposit)

Whole rock and clay-fraction analyses of samples from the McArthur River deposit with linkages to study by Andrés Acevedo & Kurt Kyser

Acknowledgments



- AREVA Resources Canada Inc., for access to samples and permission to publish results
- University of Manitoba
- Discussions with Charlie Jefferson, Sally Pehrsson, Simon Jackson and Shauna Madore (GSC)

Magnesium Systematics



Three naturally occurring stable isotopes:

- ^{24}Mg = 78.99%
- ^{25}Mg = 10 %
- ^{26}Mg =11.01 %

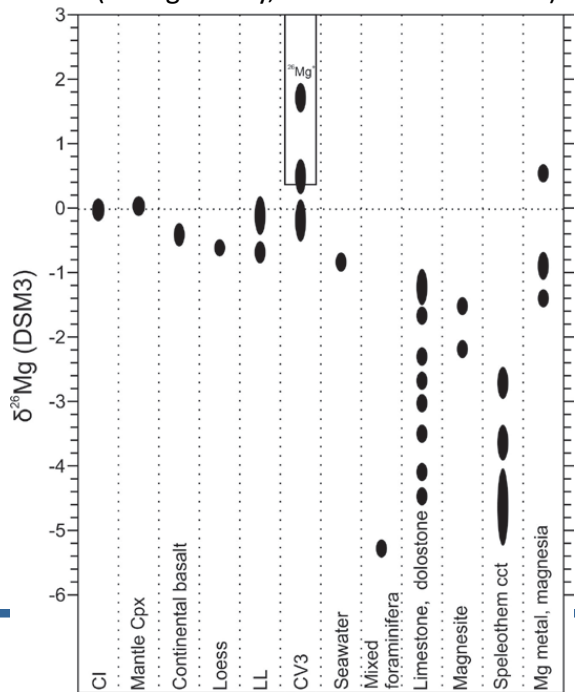
Data reported in δ notation as per mil (‰) deviation from Dead Sea magnesium (DSM3)

Upper continental crust and mantle derivatives $\delta^{26}Mg$ values between: - 0.1 and - 0.3

(Pogge von Strandmann et al., 2008; Handler et al., 2009; Bourdon et al., 2010; Li et al., 2010; Wimpenny et al., 2014).

Strong fractionation in carbonate minerals

Representative $\delta^{26}Mg$ compositions (Young & Galy, 2004 and refs therein)



Iron Systematics



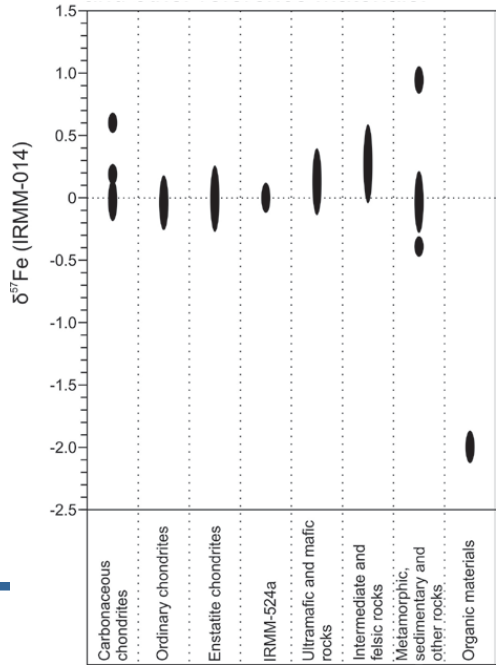
- Four naturally occurring stable isotopes:
  - ^{54}Fe = 5.845%
  - ^{56}Fe = 91.754%,
  - ^{57}Fe = 2.119%
  - ^{58}Fe = 0.282%

Data reported in δ notation as per mil (‰) deviation from Isotopic Reference Material (IRMM014)

Significant fractionations generally restricted to natural low-temp processes in which redox or bonding changes occur (Johnson et al., 2008).

Crust avg. $\delta^{56}Fe = 0.00 \pm 0.08$ ‰, which extends to most siliclastic sedimentary rocks (Heimann et al., 2008).

Representative $\delta^{57}Fe$ compositions
(Craddock & Dauphas, 2010 and refs therein)



References (1/3)



Alexandre, P., Kyser, K., Polito, P., and Thomas, D., 2005. Alteration mineralogy and stable isotope geochemistry of Paleoproterozoic basement-hosted unconformity-type uranium deposits in the Athabasca Basin, Canada; Economic Geology, v. 100, p. 1547–1563.

Beard B.L., Johnson C.M., Skulan J.L., Nealson K.H., Cox L. and Sun H., 2003. Application of Fe isotopes to tracing the geochemical and biological cycling of Fe; Chemical Geology, v. 195, p. 87–117.

Blain, M. and Morrison, D., 2008. Kiggavik Project, Annual Report, 2010, volume 1; AREVA Resources Canada Inc., Internal Report, 31 p.

Bourdon B., Tipper E. T., Fitoussi C. and Stracke A. 2010. Chondritic Mg isotope composition of the Earth; Geochimica et Cosmochimica Acta, v. 74, p. 5069–5083.

Chapman, J.B., Mason T.F.D., Weiss D. J., Coles B.J. and Wilkinson J. J., 2005. Chemical Separation and Isotopic Variations of Cu and Zn From Five Geological Reference Materials; Geostandards and Geoanalytical Research, v. 30, p. 5–16.

Craddock, P. R. and Dauphas, N., 2011. Iron isotopic compositions of geological reference materials and chondrites; Geostandards and Geoanalytical Research, v. 35, p. 101–123.

Dideriksen, K., Christiansen, B. C., Frandsen, C., Balic-Zunic, T., Mørup, S. and Stipp, S. L. S., 2010. Paleo-redox boundaries in fractured granite; Geochimica et Cosmochimica Acta, v. 74, p. 2866–2880.

Eriksson, K.A. and Soegaard, K., 1985. The petrography and geochemistry of Archean and early Proterozoic sediments: implication of crustal compositional and surfaces processes; Geological Survey of Finland, Bulletin 331, p 8–32.

Gall, Q., 1994. Proterozoic Paleoweathering and Diagenesis, Thelon Basin, Northwest Territories, Canada; Ph.D. thesis, Carleton University, 369 p.

Handler M., Baker J., Schiller M., Bennett V. and Yaxley G., 2009. Magnesium stable isotope composition of Earth's upper mantle; Earth and Planetary Science Letters, v. 282, p. 306–313.

References (2/3)



Heimann, A., Beard, B.L., Johnson, C.M., 2008. The role of volatile exsolution and sub-solidus fluid/rock interactions in producing high $^{56}Fe/^{54}Fe$ ratios in siliceous igneous rocks, Geochimica et Cosmochimica Acta 72, p. 4379–4396

Hoeve, J., and Sibbald, T. I., 1978. On the genesis of Rabbit Lake and other unconformity-type uranium deposits in northern Saskatchewan, Canada; Economic Geology, v. 73, p. 1450–1473.

Jefferson, C.W., Thomas, D.J., Gandhi, S.S., Ramaekers, P., Delaney, G., Brisbin, D., Cutts, C., Portella, P. and Olson, R.A., 2007a. Unconformity-associated uranium deposits of the Athabasca basin, Saskatchewan and Alberta; *in* EXTECH IV: Geology and Uranium EXploration TECHnology of the Proterozoic Athabasca Basin, Saskatchewan and Alberta, C.W. Jefferson and G. Delaney (eds.); Geological Survey of Canada Bulletin 588, p. 23-67.

Jefferson, C. W., Thomas, D., Quirt, D., Mwenifumbo, C. J. and Brisbin, D., 2007b. Empirical models for Canadian unconformity-associated uranium deposits, *in* Proceedings of Exploration 07, B. Milkereit (ed.); Fifth Decennial International Conference on Mineral Exploration, p. 741-769.

Jefferson, C.W., Pehrsson, S., Peterson, T., Tschirhart, V., Anand, A., Wollenberg, P., Riegler, T., Bethune, K., Chorlton, L.B., McEwan, B., LeCheminant, A.N., Tschirhart, P., Scott, J.M.J., Davis, W., McNicoll, V., Riemer, W., White, J.C., Patterson, J., Morris, W.A., Keating, P. and Stieber, C., 2014. Bedrock geology of the western Marjorie-Tehek supracrustal belt and Aberdeen Sub-basin margin in parts of NTS 66A and 66B, Nunavut — context of the Kiggavik uranium camp; Geological Survey of Canada, Open File 7241.

Johnson, C. M., Beard, B. L. and Roden, E. E., 2008. The iron isotope fingerprints of redox and biogeochemical cycling in modern and ancient Earth; Annual Review of Earth and Planetary Sciences, v. 36, p. 457–493.

Li W.-Y., Teng F.-Z., Ke S., Rudnick R. L., Gao S., Wu F.-Y. and Chappell B. W., 2010. Heterogeneous magnesium isotopic composition of the upper continental crust; Geochimica et Cosmochimica Acta, v. 74, p. 6867–6884.

Matthews, P.E. and Scharrer, R.H., 1968. A graded unconformity at the base of the early Precambrian Pongola System; Transactions of the Royal Society of South Africa, v. 71, p. 257–271.

References (3/3)



Pogge von Strandmann P. A. E., Burton K. W., James R. H., van Calsteren P., Gislason S. R. and Sigfússon B., 2008. The influence of weathering processes on riverine magnesium isotopes in a basaltic terrain; Earth and Planetary Science Letters, v. 276, p. 187–197.

Quirt, D.H. and Wasyliuk, K., 1997. Kaolinite, dickite and other clay minerals in the Athabasca Group, Canada and the Kombolgie Formation, Australia; *in* Clays for Our Future — Proceedings of the 11th International Clay Conference, A.R. Mermut and J.K. Torrance (eds.), Ottawa, June 15 to 21, Conference CD-ROM, p. A61

Riegler, T., Lescuyer, J-L., Wollenberg, P., Quirt, D. and Beaufort, D., 2014. Alteration related to uranium deposits in the Kiggavik-Andrew Lake structural trend, Nunavut Canada: new insights from petrography and clay mineralogy; The Canadian Mineralogist, v. 52, p. 27–45.

Rouxel, O., Dobbek, N., Ludden, J. and Fouquet, Y., 2003. Iron isotope fractionation during oceanic crust alteration; Chemical Geology, v. 202, p. 155–182.

Sharpe, R., 2013. The geochemistry and geochronology of the Bong uranium deposit, Thelon basin, Nunavut, Canada; unpublished M.Sc. thesis, University of Manitoba, 213 p.

Wallis, R. H., Saracoglu, N., Golightly, J. P. and Brummer, J. J., 1984. Geology of the McClean uranium deposits, northern Saskatchewan, *in* Geology of Uranium Deposits, T. I. I. Sibbald, and W. Petruk (eds.); Canadian Institute of Mining, Metallurgy and Petroleum, Special Volume 32, p. 101–131.

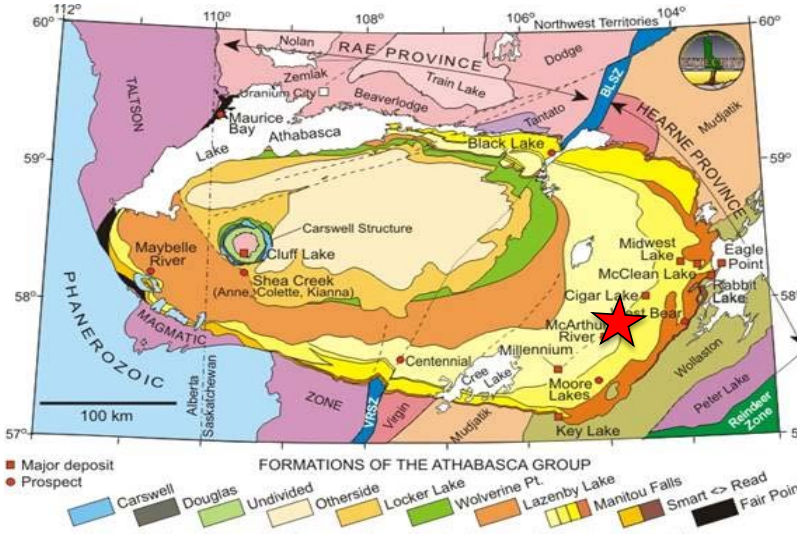
Wimpenny, J., Colla, C. A., Yin, Q. Z., Rustad, J. R. and Casey, W. H., 2014. Investigating the behaviour of Mg isotopes during the formation of clay minerals; Geochimica et Cosmochimica Acta, v. 128, p. 178–194.

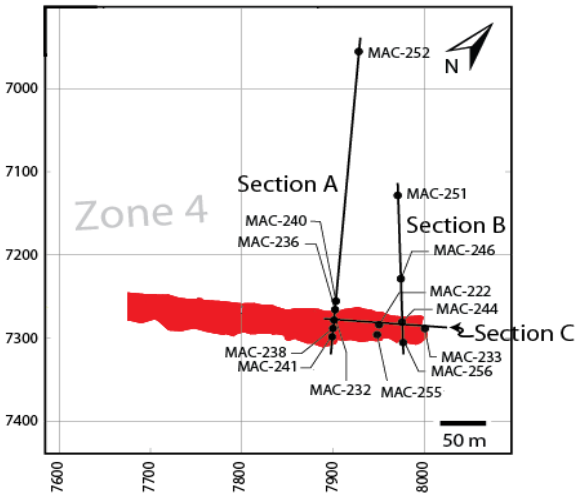
Wombacher, F., Eisenhauer, A., Heuserac, A. and Weyer, S., 2009. Separation of Mg, Ca and Fe from geological reference materials for stable isotope ratio analyses by MC-ICP-MS and double-spike TIMS; Journal of Analytical Atomic Spectrometry, v. 24, p. 627–636.

Young, E. D. and Galy, A., 2004. The isotope geochemistry and cosmochemistry of magnesium; Reviews in Mineralogy and Geochemistry, v. 55, p. 197–230.

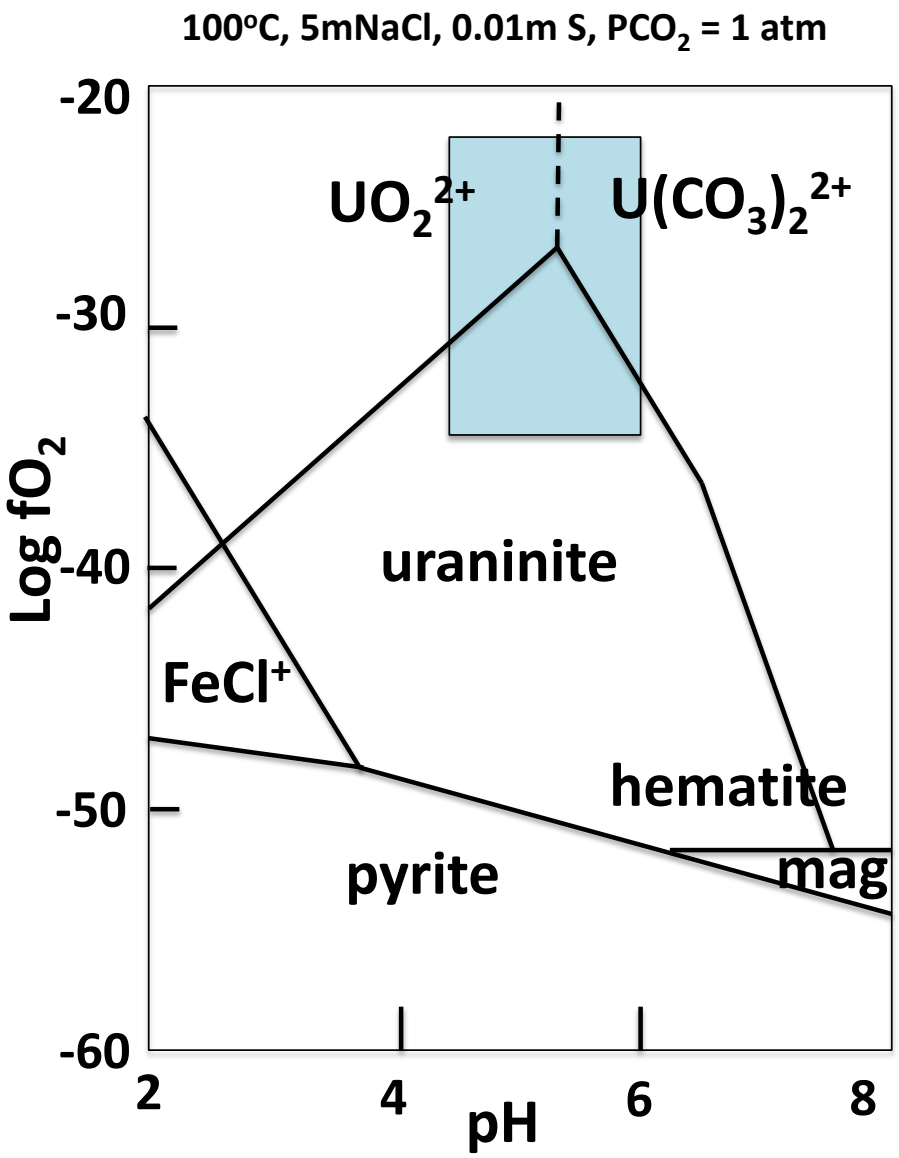
Fe isotopic composition of alteration minerals from McArthur River zone 4 deposit, Athabasca Basin

Andrés Acevedo & Kurt Kyser
Department of Geol Sci & Geol Eng
Queen's University





Department of Geological Sciences, Queen's University
Queen's Facility for Isotope Research



Why Fe?

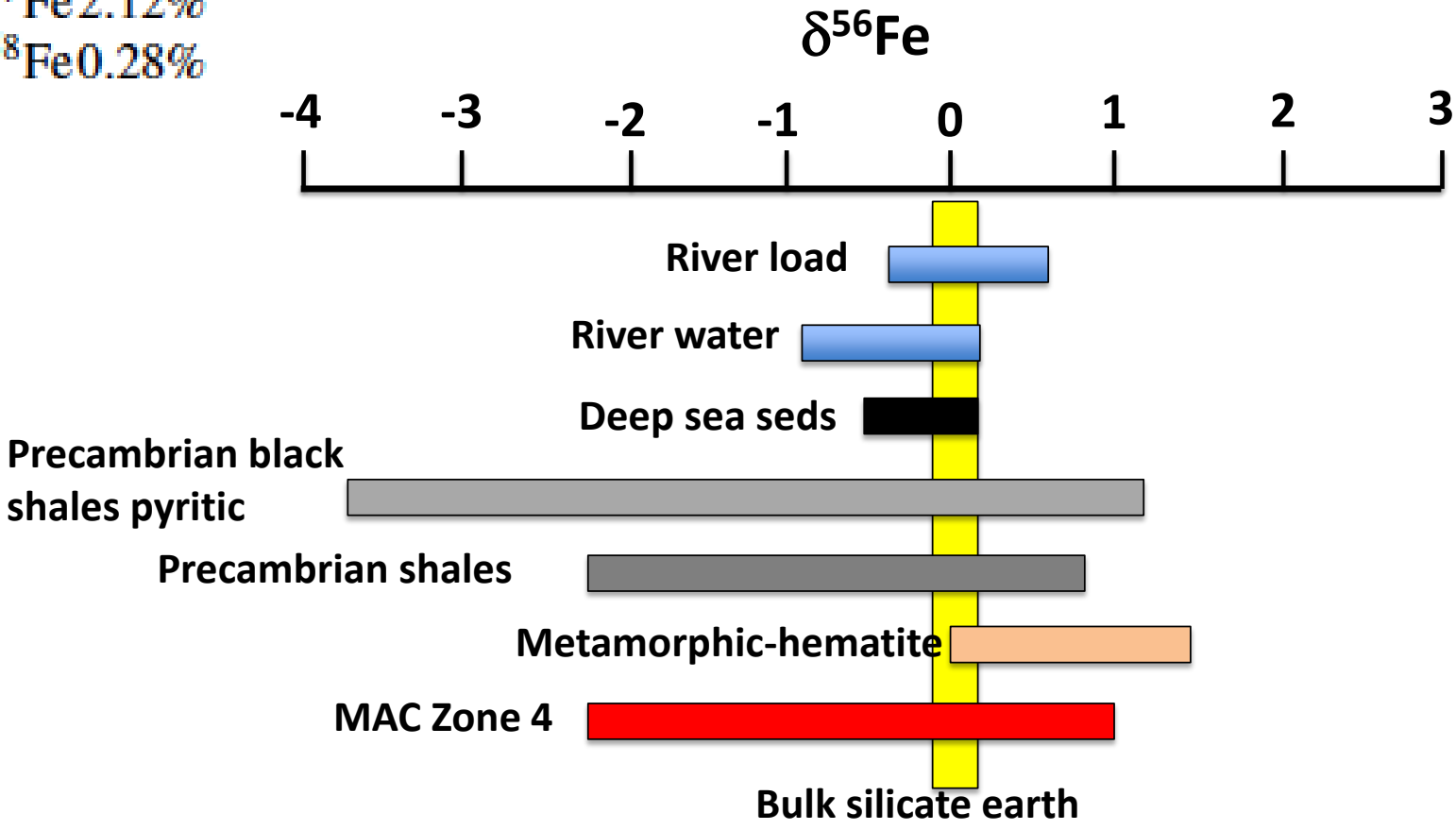
$U^{6+}_{(aq)} + 2Fe^{2+}_{(aq)} + 2H_2O \leftrightarrow U^{4+}O_{2(uraninite)} + 2Fe^{3+}_{(chlorite\ or\ hematite)} + 4H^{+}_{(aq)}$

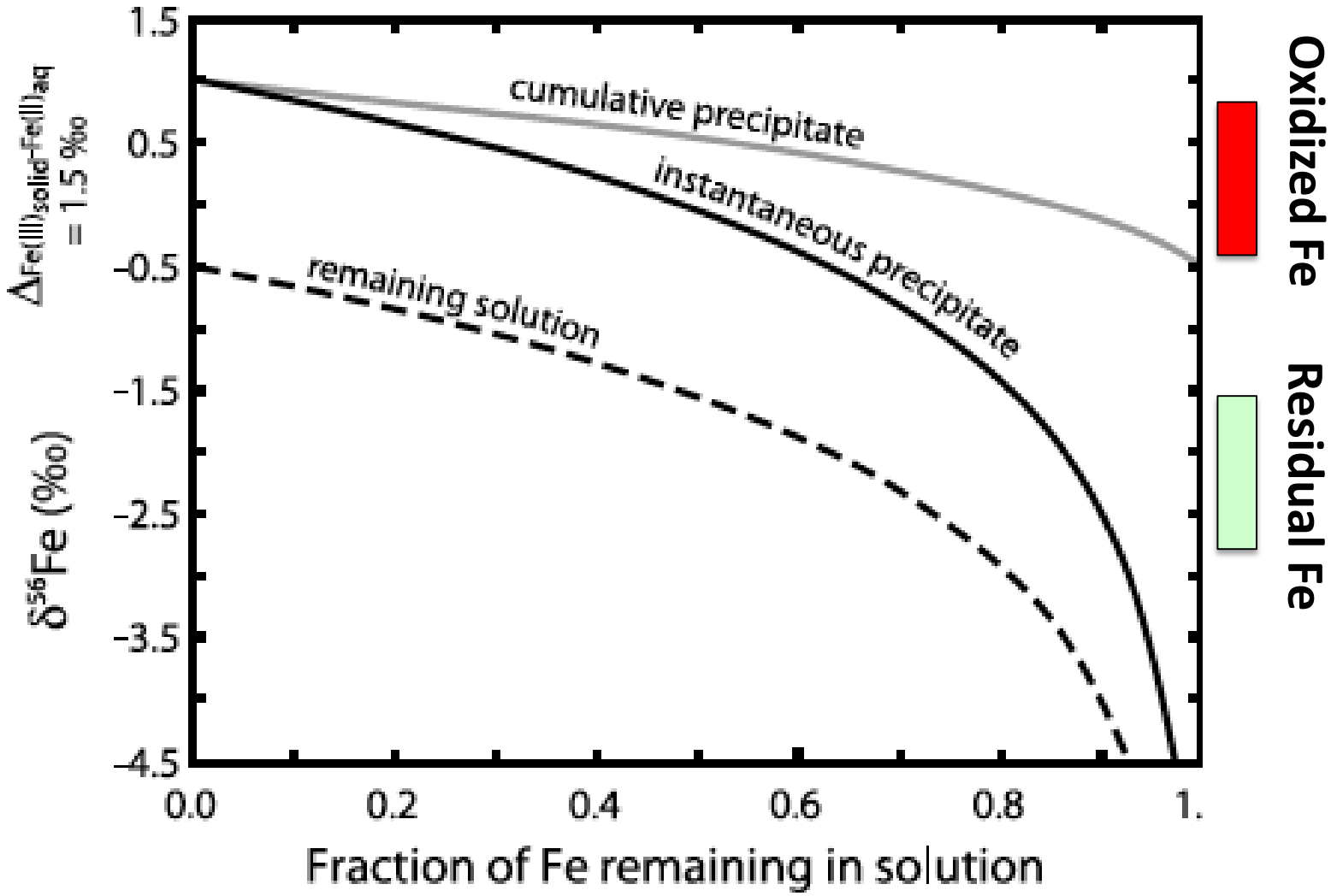
For, Fe isotopes, the heavy isotope of Fe goes into oxidized phases



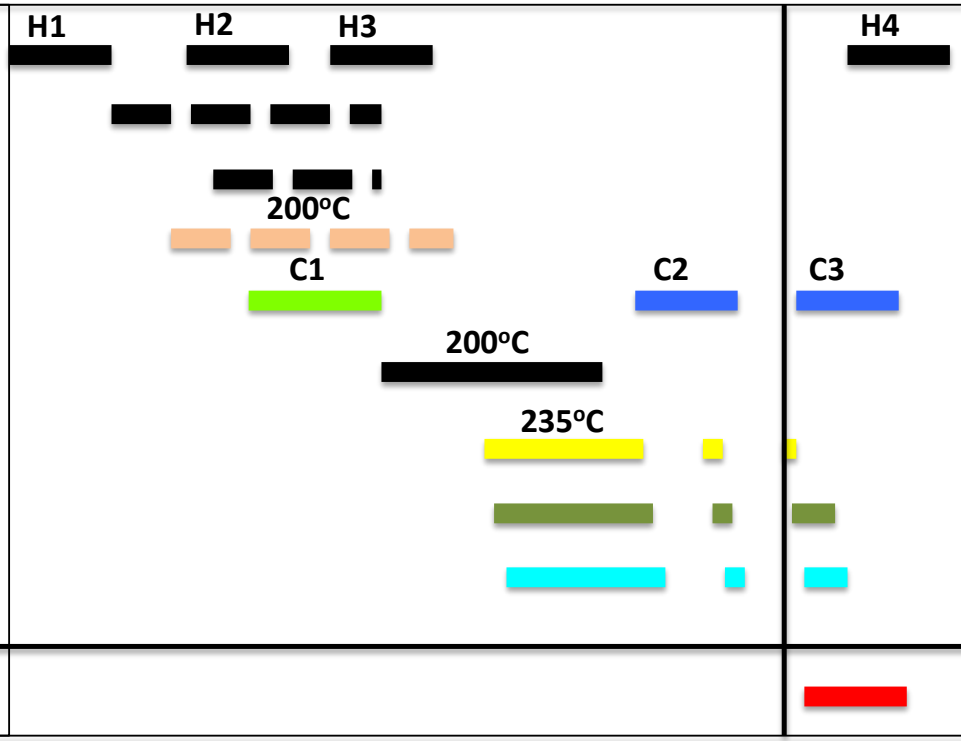
$$\delta^{56}Fe = \{(^{56}Fe/^{54}Fe)_{sample}/(^{56}Fe/^{54}Fe)_{IRMM\text{-}014} - 1\} \times 10^3$$

^{54}Fe 5.84%
^{56}Fe 91.76%
^{57}Fe 2.12%
^{58}Fe 0.28%




1.5
0.5
−0.5
−1.5
−2.5
−3.5
−4.5
0.0
0.2
0.4
0.6
0.8
1.
cumulative precipitate
instantaneous precipitate
remaining solution
$\Delta_{Fe(III)_{solid}-Fe(III)_{aq}}$ = 1.5 ‰
δ^{56}Fe (‰)
Fraction of Fe remaining in solution
Oxidized Fe
Residual Fe

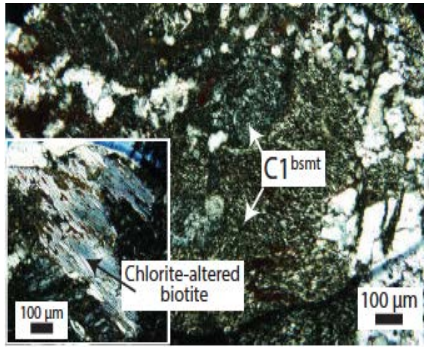
Mineral paragenesis McArthur River Zone 4

Hematite	H	
APS	APS	
Dolomite	D	
Kaolin+Illite	I1+Dkt	
Chlorite		
Magnesiofoitite	T1	
Illite	I1	
Illite + Chlorite	I1b+C2b	
Illite-Chlorite Mixed Layer	ICML	
Uranium	U	

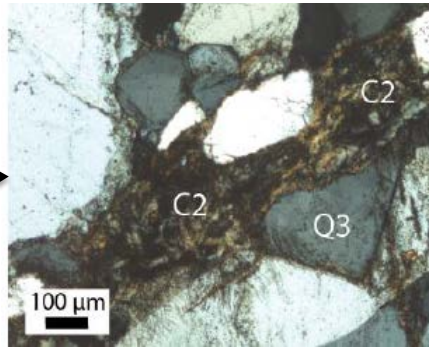
We examined clay fractions reflecting these various events



Pre-ore alt bsmt



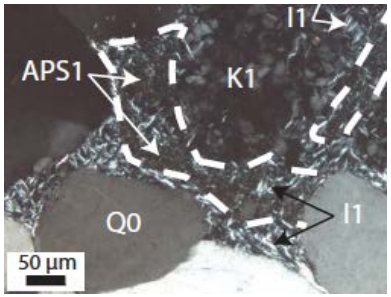
Pre-ore alt bsmt



Fe^{2+} in basement—$\delta^{56}Fe$ near 0‰

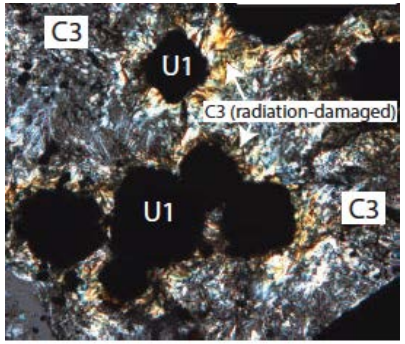
Fe^{2+} in C1bsmt—$\delta^{56}Fe$ > 0‰

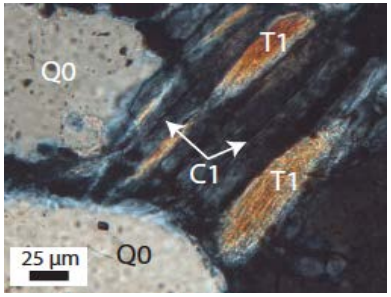
Fe^{3+} in C2bsmt—$\delta^{56}Fe$ >> 0‰



Fe^{3+} in diagenetic C1, I1 & ICML —$\delta^{56}Fe$ near 0 ‰

Syn-ore alt bsmt

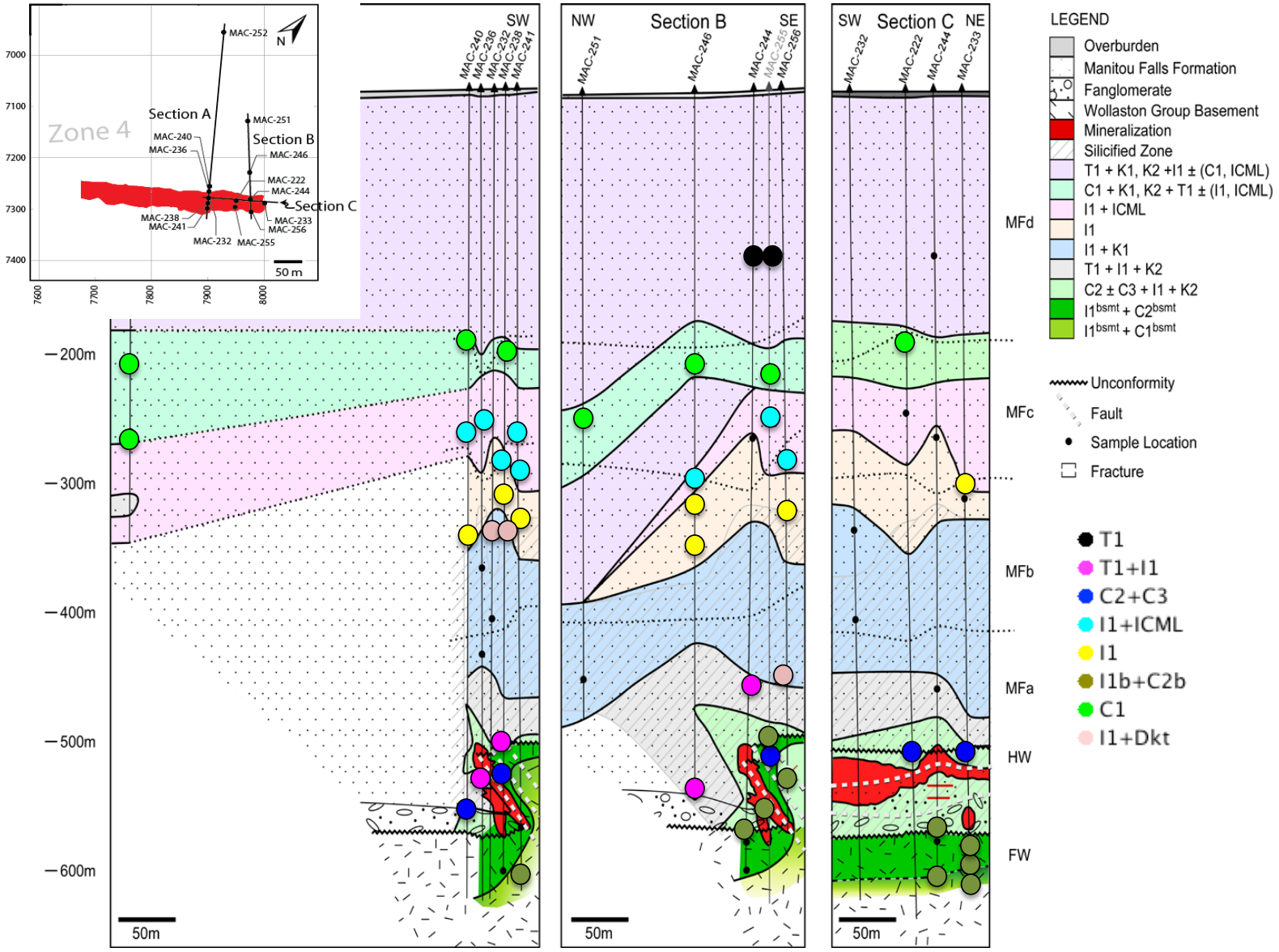




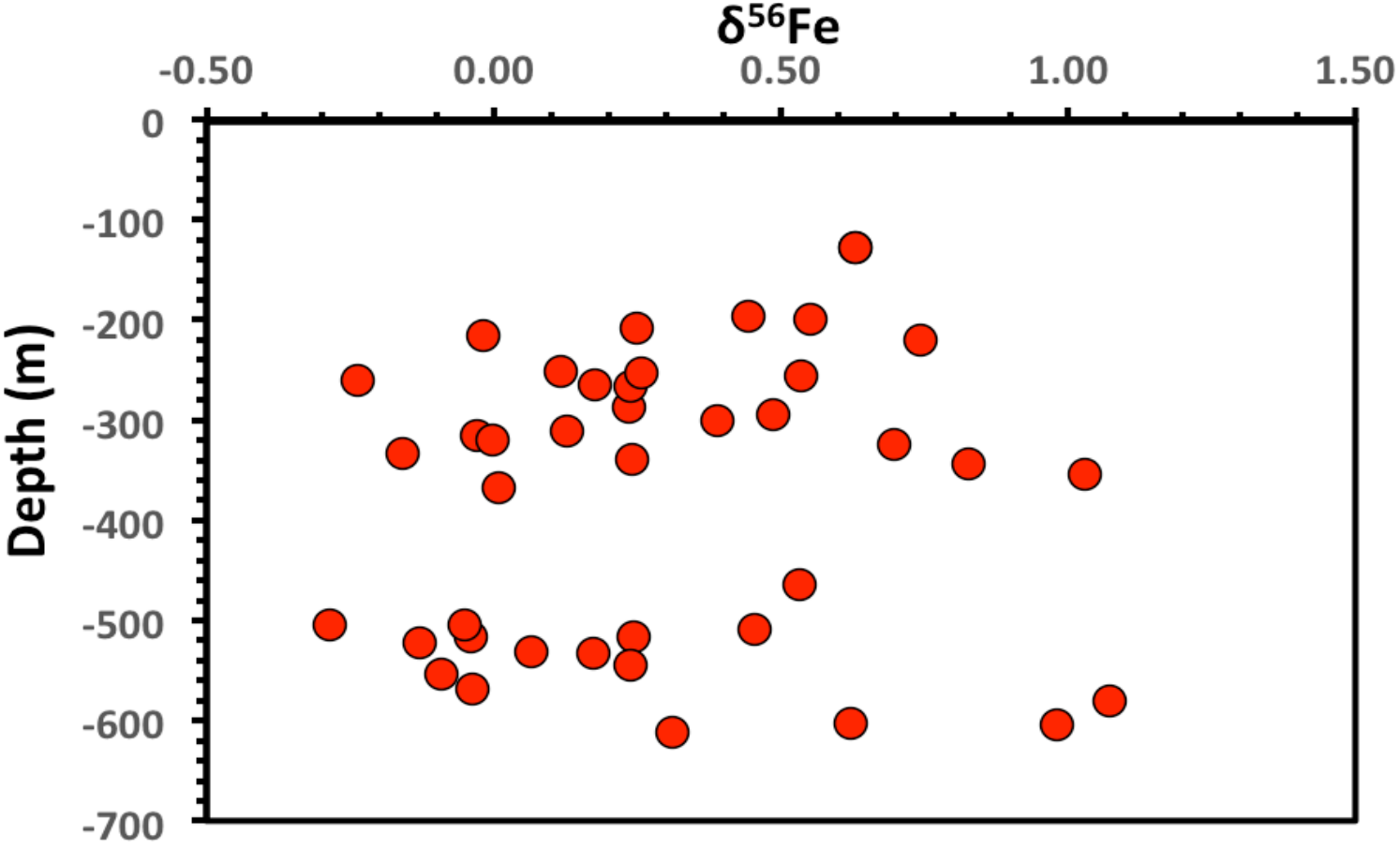
Fe^{2+} remaining will have high $^{56}Fe/^{54}Fe$ and affect minerals in sandstone T1 & I1 ($\delta^{56}Fe$ >0‰)

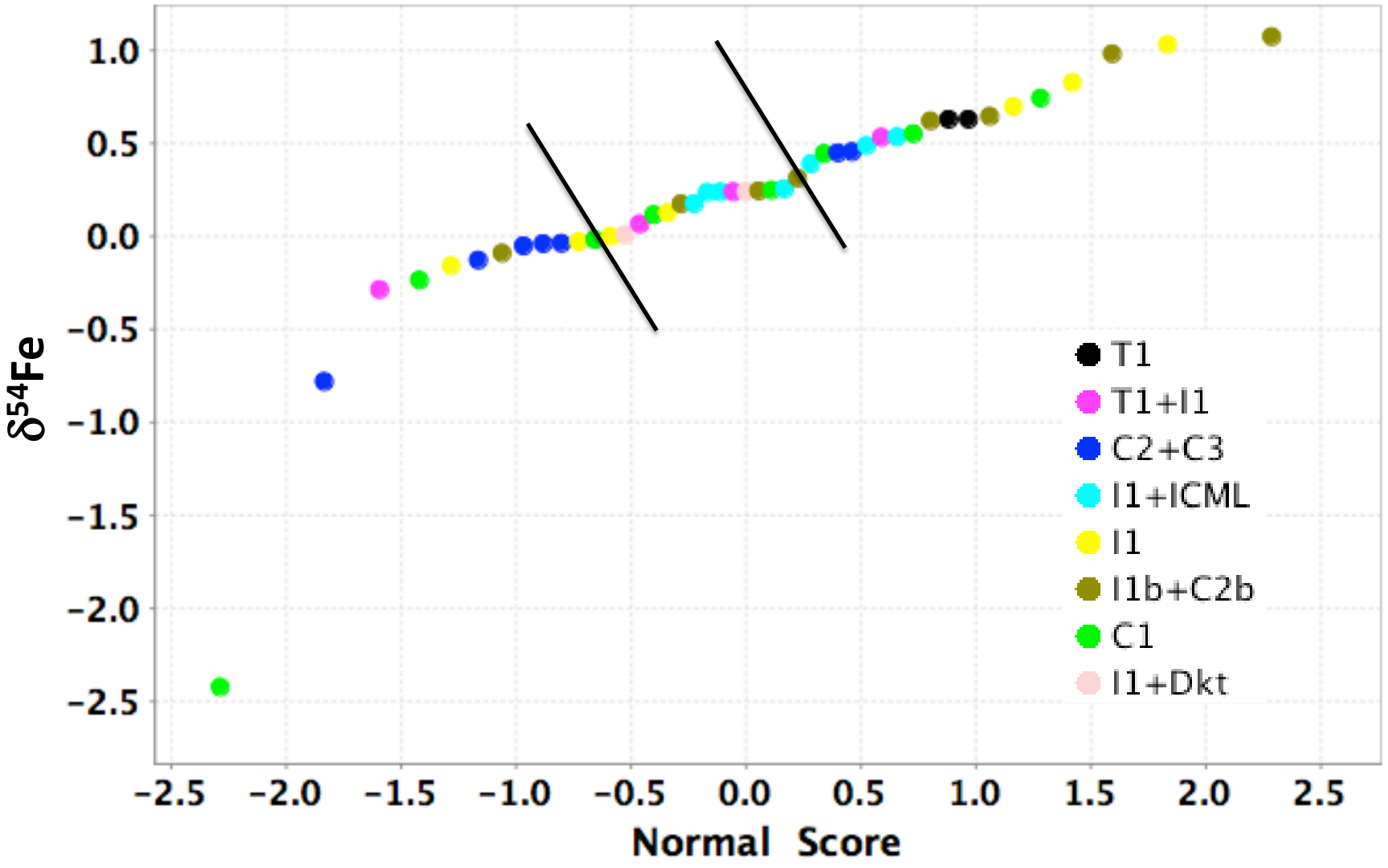
Later fluids leach ^{56}Fe or bring in Fe^{2+} resulting in $\delta^{56}Fe$ << 0‰

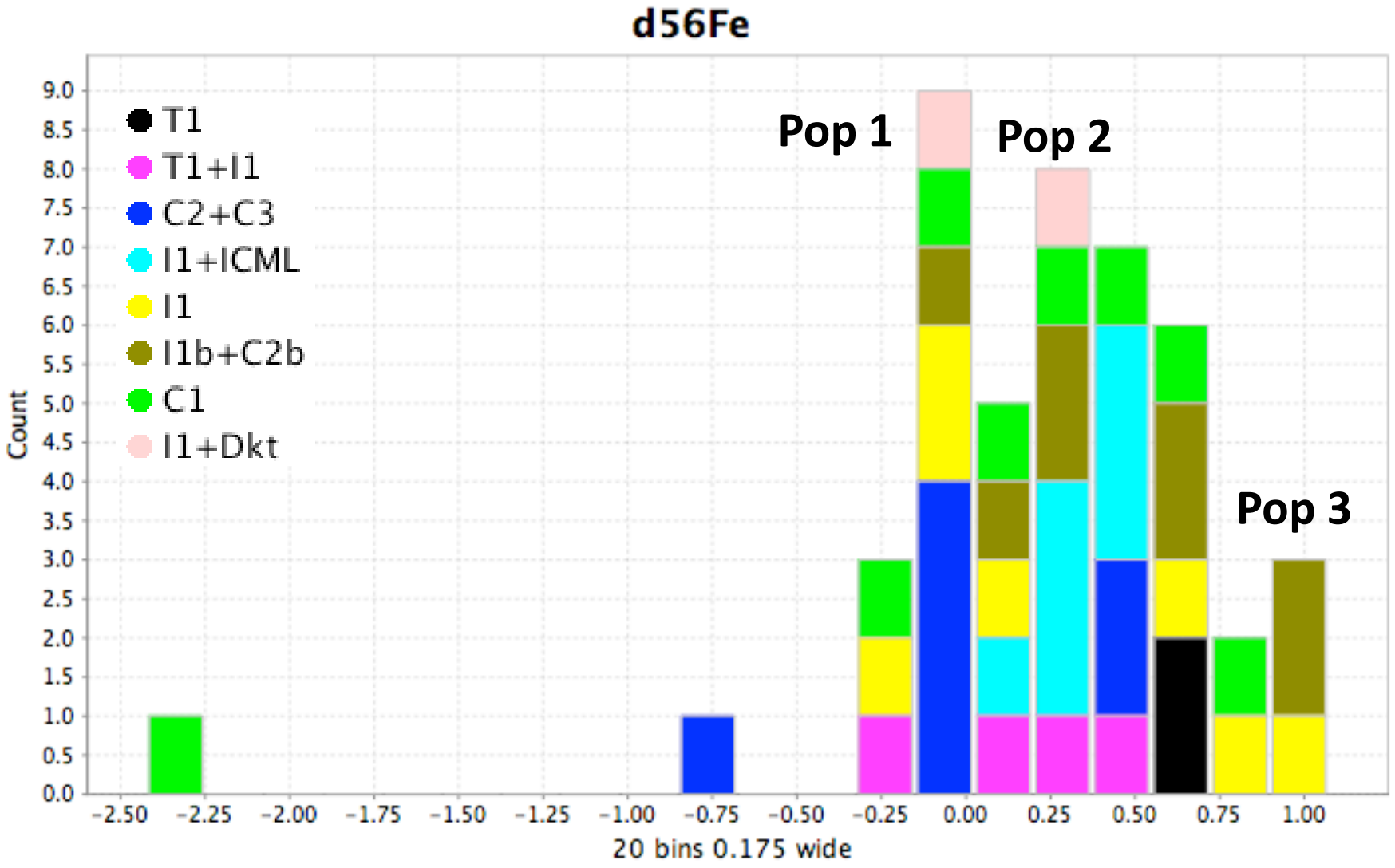
Fe^{3+} in C3—$\delta^{56}Fe$ >> 0‰

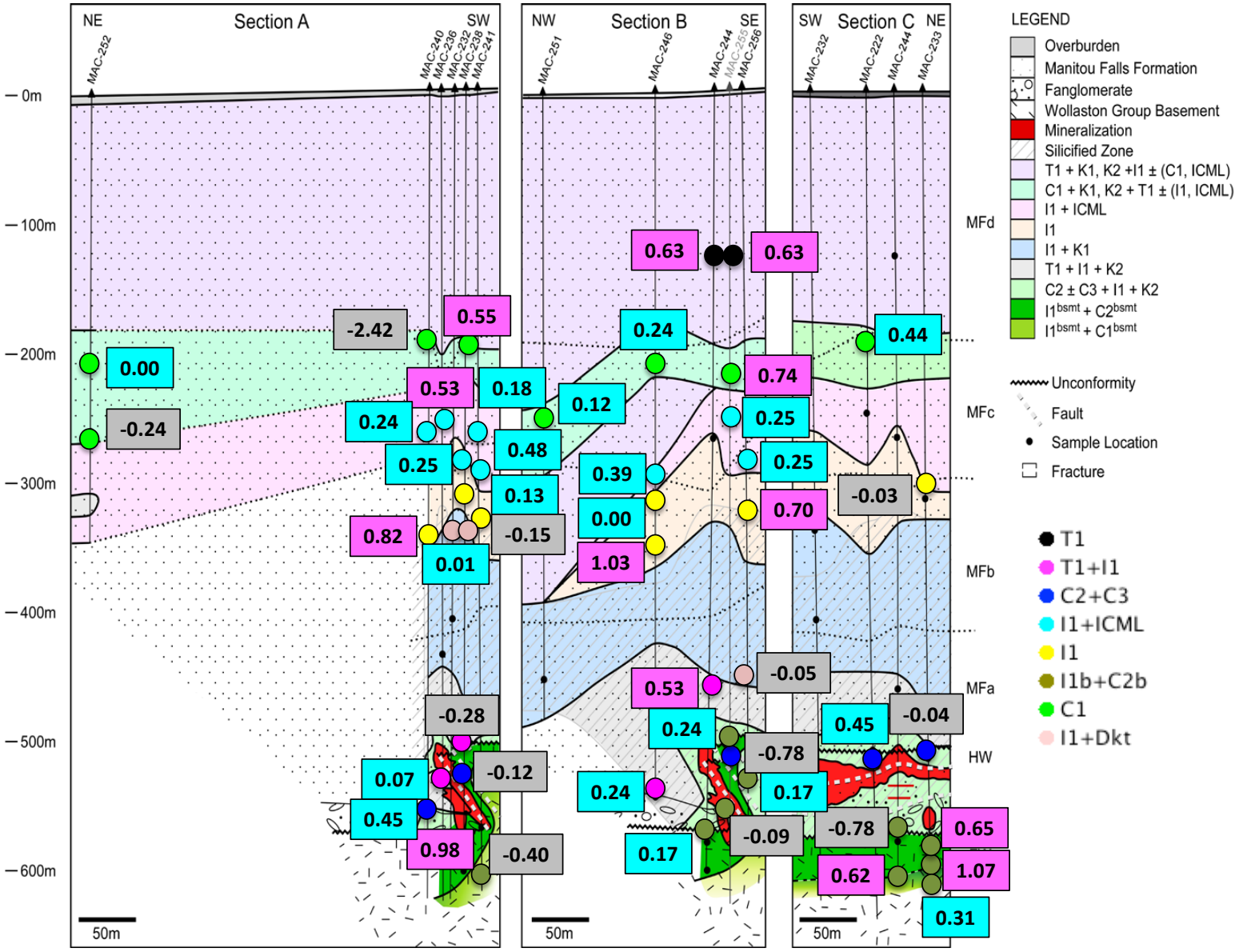

Zone 4
Section A
Section B
Section C
MAC-252
MAC-251
MAC-240
MAC-236
MAC-246
MAC-222
MAC-244
MAC-233
MAC-256
MAC-238
MAC-241
MAC-232
MAC-255
N
50 m
7000
7100
7200
7300
7400
7600
7700
7800
7900
8000
SW
NW
Section B
SE
SW
Section C
NE
MAC-240
MAC-236
MAC-232
MAC-238
MAC-241
MAC-251
MAC-246
MAC-244
MAC-255
MAC-256
MAC-232
MAC-222
MAC-244
MAC-233
−200m
−300m
−400m
−500m
−600m
50m
50m
50m
MFd
MFc
MFb
MFa
HW
FW
LEGEND
Overburden
Manitou Falls Formation
Fanglomerate
Wollaston Group Basement
Mineralization
Silicified Zone
T1 + K1, K2 +I1 ± (C1, ICML)
C1 + K1, K2 + T1 ± (I1, ICML)
I1 + ICML
I1
I1 + K1
T1 + I1 + K2
C2 ± C3 + I1 + K2
I1bsmt + C2bsmt
I1bsmt + C1bsmt
Unconformity
Fault
Sample Location
Fracture
T1
T1+I1
C2+C3
I1+ICML
I1
I1b+C2b
C1
I1+Dkt

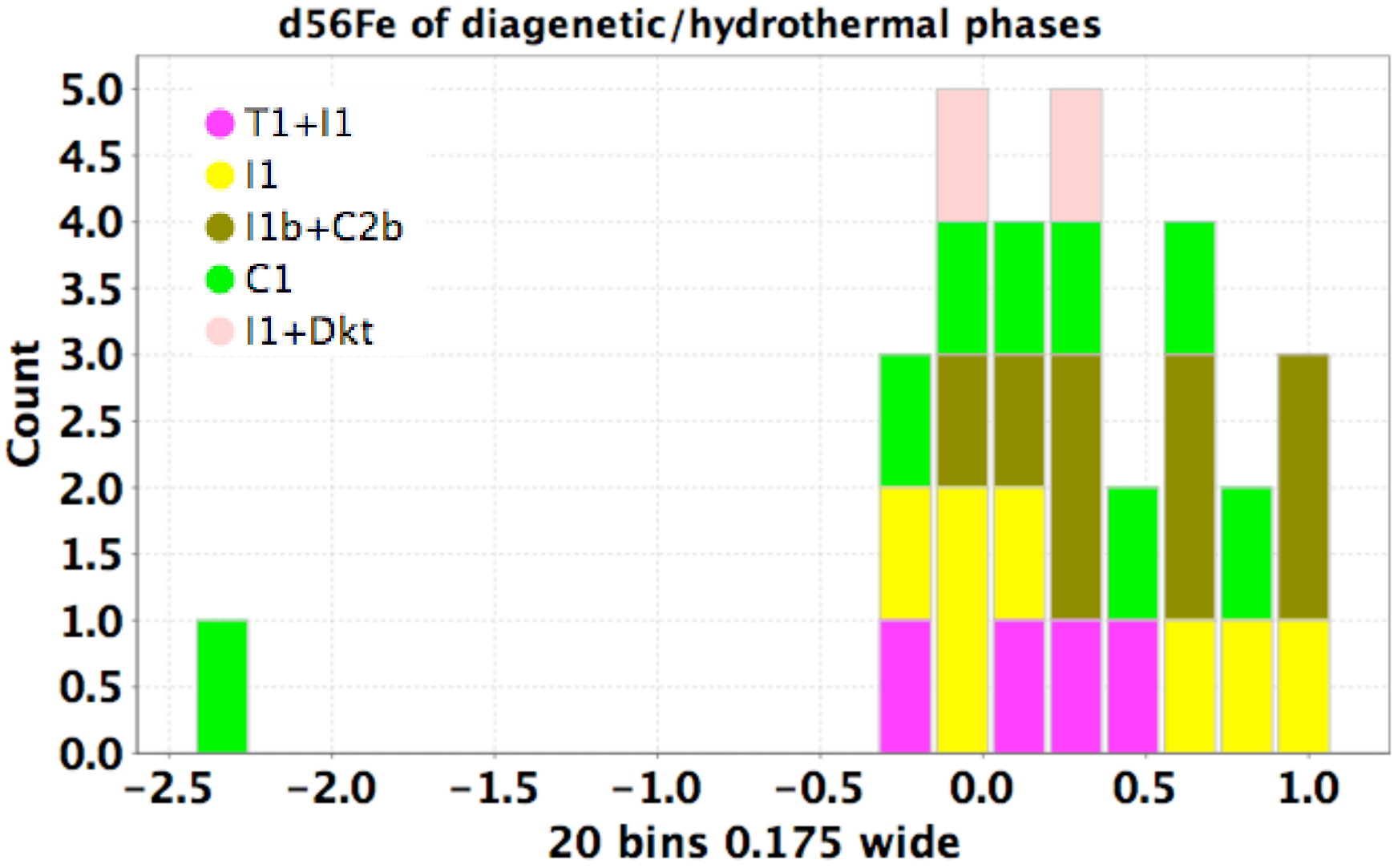
Fe isotopic compositions are variable—do not correlate with depth, distance from ore zone, $Fe^{3+}/Fe_{T,}$ or crystal chemistry indicating that Fe isotopes record more than one process

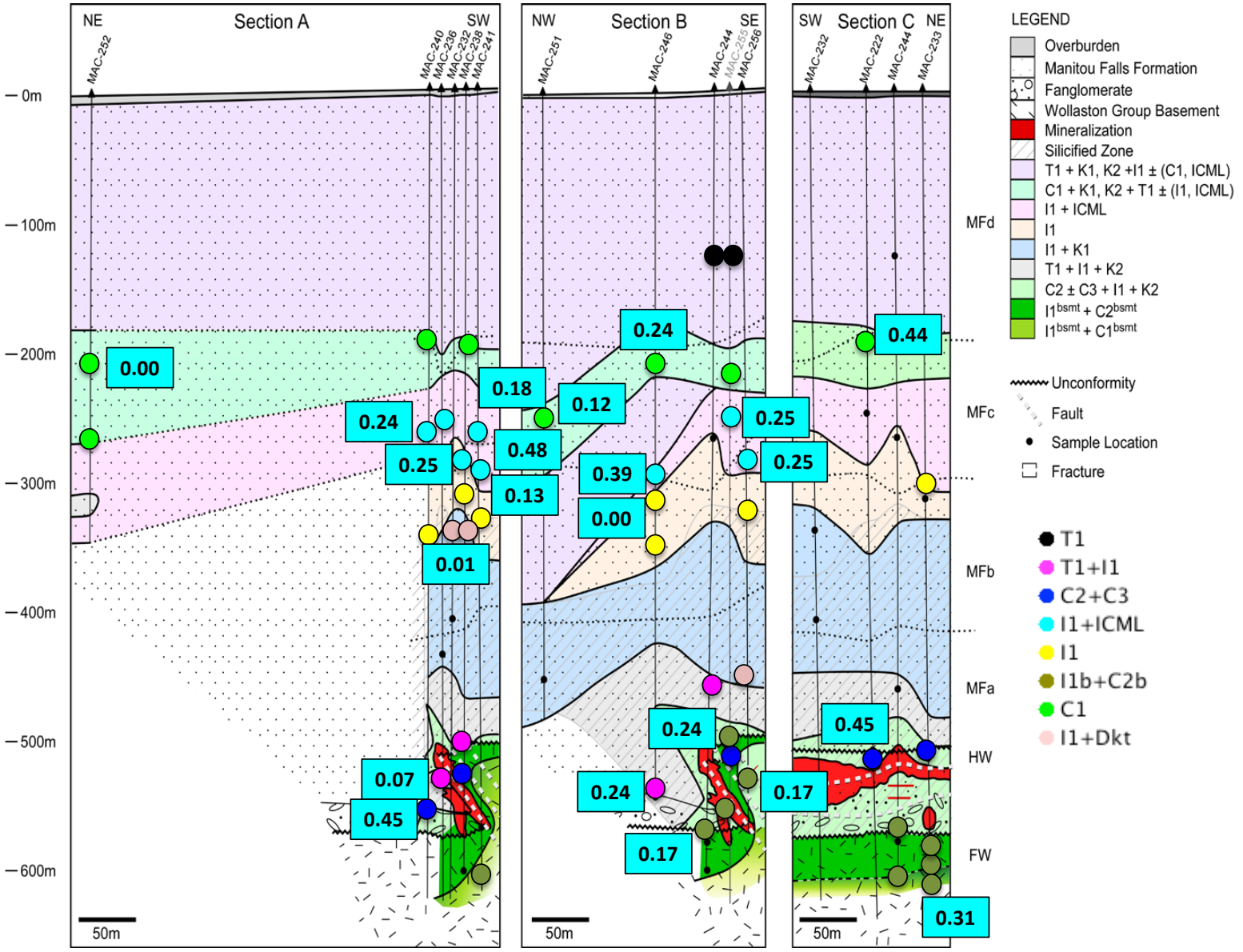


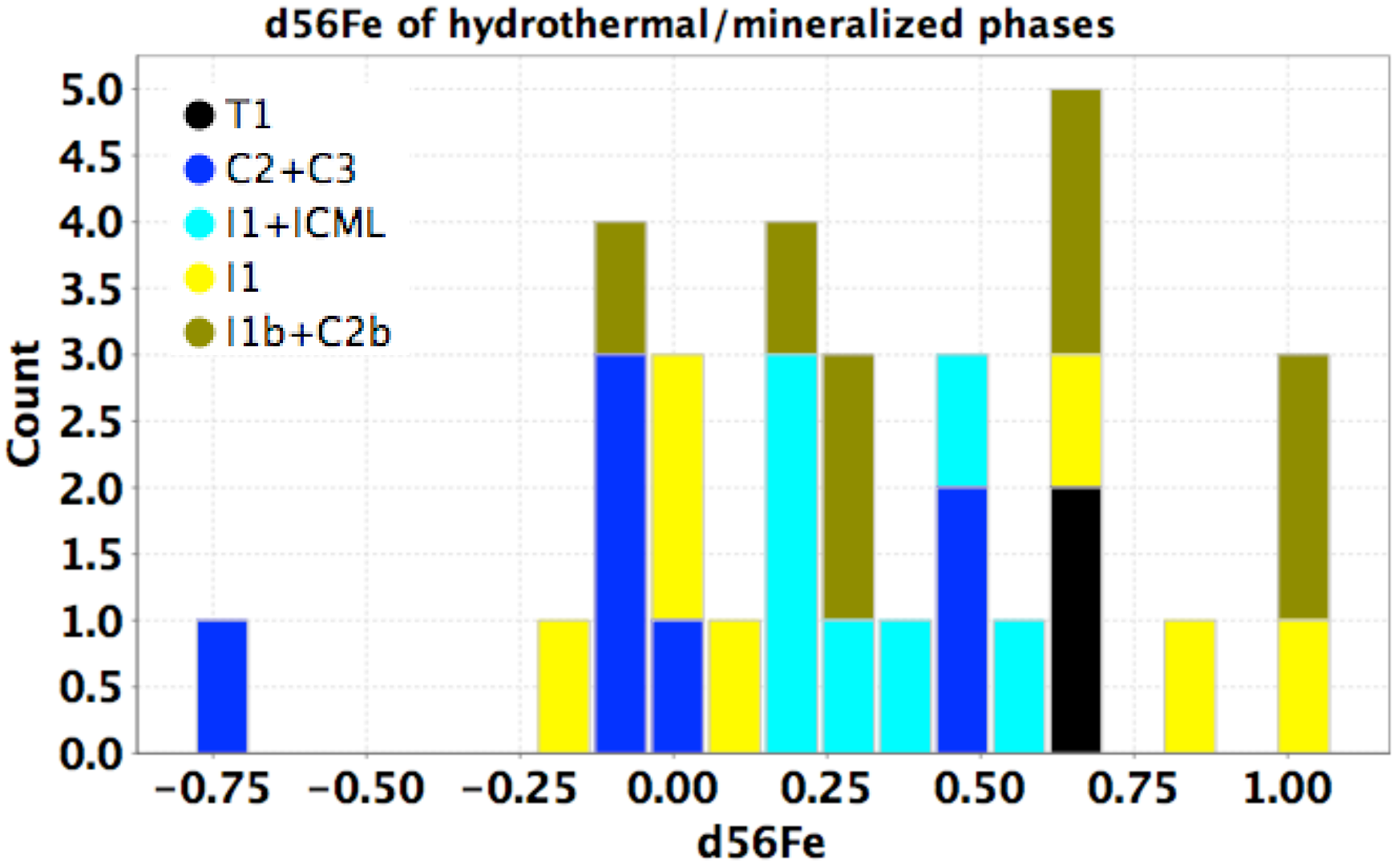

δ54Fe
1.0
0.5
0.0
-0.5
-1.0
-1.5
-2.0
-2.5
-2.5
-2.0
-1.5
-1.0
-0.5
0.0
0.5
1.0
1.5
2.0
2.5
Normal Score
T1
T1+I1
C2+C3
I1+ICML
I1
I1b+C2b
C1
I1+Dkt

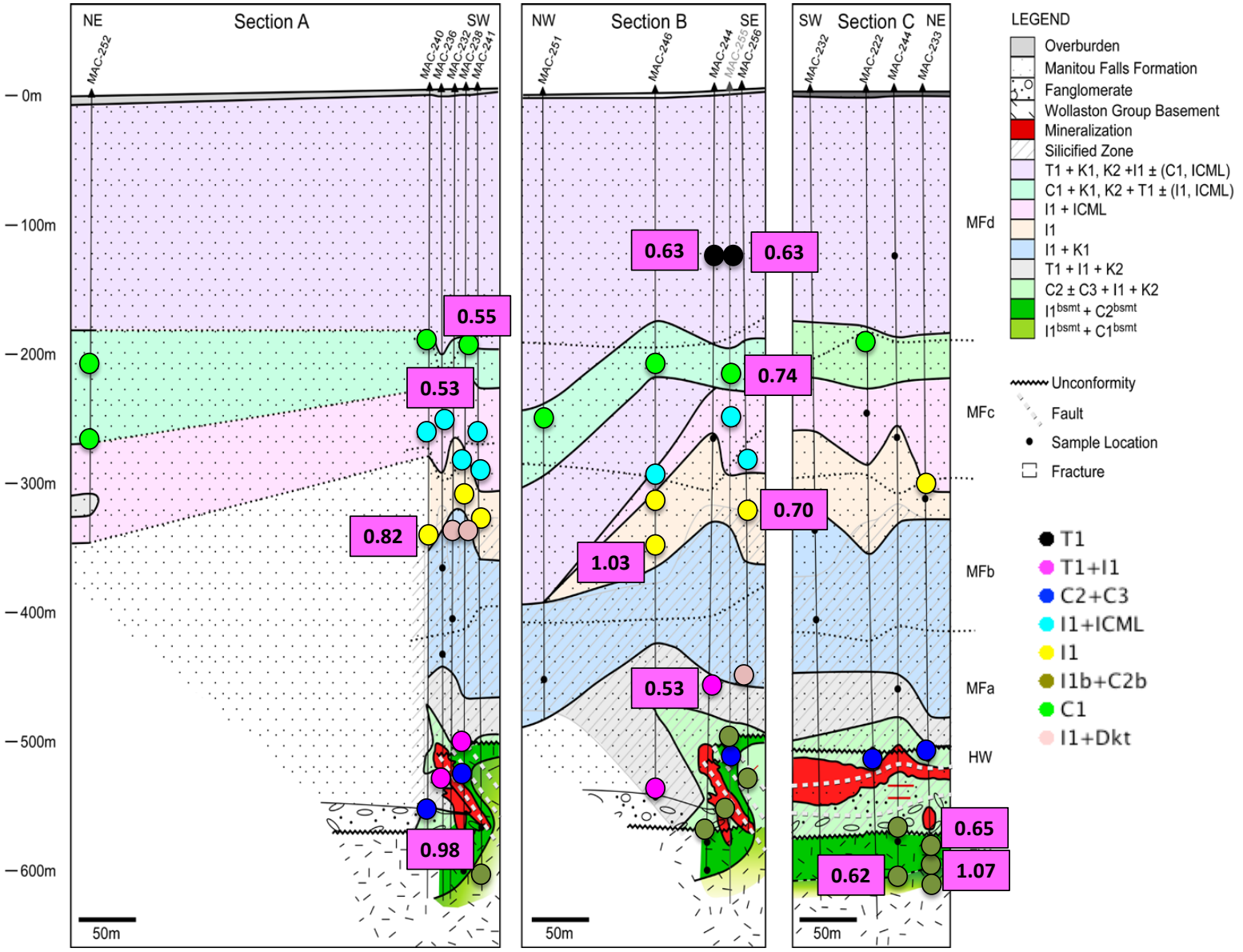

d56Fe
T1
T1+I1
C2+C3
I1+ICML
I1
I1b+C2b
C1
I1+Dkt
Pop 1
Pop 2
Pop 3
Count
9.0
8.5
8.0
7.5
7.0
6.5
6.0
5.5
5.0
4.5
4.0
3.5
3.0
2.5
2.0
1.5
1.0
0.5
0.0
-2.50
-2.25
-2.00
-1.75
-1.50
-1.25
-1.00
-0.75
-0.50
-0.25
0.00
0.25
0.50
0.75
1.00
20 bins 0.175 wide

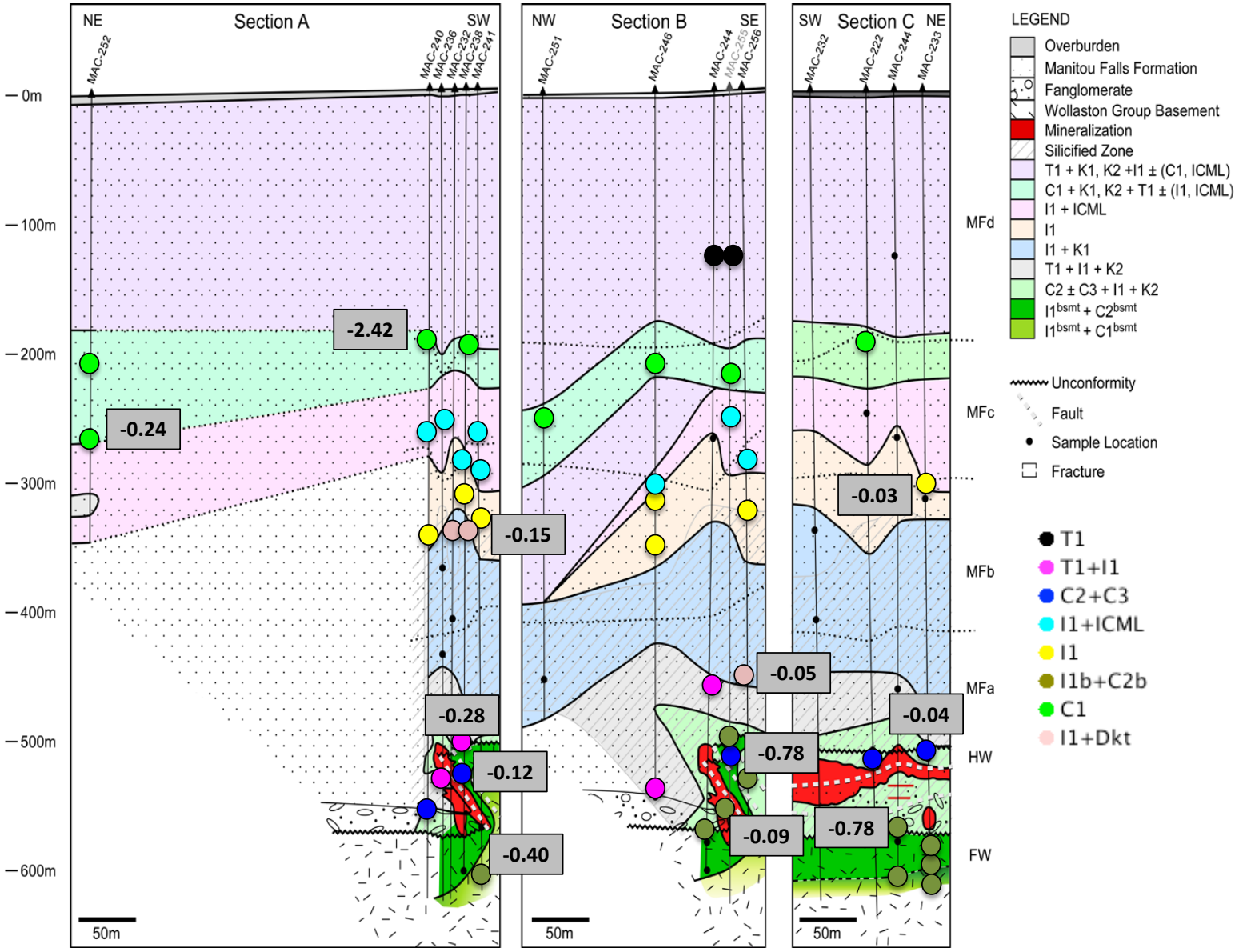

NE
Section A
SW
MAC-252
MAC-240
MAC-236
MAC-232
MAC-238
MAC-241
NW
Section B
SE
MAC-251
MAC-246
MAC-244
MAC-255
MAC-256
SW
Section C
NE
MAC-232
MAC-222
MAC-244
MAC-233
0m
100m
200m
300m
400m
500m
600m
MFd
MFc
MFb
MFa
HW
50m
50m
50m
0.00
-0.24
-2.42
0.55
0.53
0.18
0.24
0.48
0.25
0.13
0.82
-0.15
0.01
-0.28
-0.12
0.07
0.45
0.98
-0.40
0.63
0.63
0.24
0.12
0.39
0.00
1.03
0.53
0.24
0.24
0.17
-0.09
0.17
0.74
0.25
0.25
0.70
-0.05
-0.78
0.44
-0.03
0.45
-0.04
-0.78
0.65
0.62
1.07
0.31
LEGEND
Overburden
Manitou Falls Formation
Fanglomerate
Wollaston Group Basement
Mineralization
Silicified Zone
T1 + K1, K2 +I1 ± (C1, ICML)
C1 + K1, K2 + T1 ± (I1, ICML)
I1 + ICML
I1
I1 + K1
T1 + I1 + K2
C2 ± C3 + I1 + K2
I1bsmt + C2bsmt
I1bsmt + C1bsmt
Unconformity
Fault
Sample Location
Fracture
T1
T1+I1
C2+C3
I1+ICML
I1
I1b+C2b
C1
I1+Dkt


d56Fe of diagenetic/hydrothermal phases
T1+I1
I1
I1b+C2b
C1
I1+Dkt
Count
5.0
4.5
4.0
3.5
3.0
2.5
2.0
1.5
1.0
0.5
0.0
−2.5
−2.0
−1.5
−1.0
−0.5
0.0
0.5
1.0
20 bins 0.175 wide


NE
Section A
SW
MAC-252
MAC-240
MAC-236
MAC-232
MAC-238
MAC-241
NW
Section B
SE
MAC-251
MAC-246
MAC-244
MAC-255
MAC-256
SW
Section C
NE
MAC-232
MAC-222
MAC-244
MAC-233
0m
100m
200m
300m
400m
500m
600m
MFd
MFc
MFb
MFa
HW
FW
50m
50m
50m
0.00
0.24
0.25
0.18
0.48
0.13
0.01
0.07
0.45
0.24
0.12
0.39
0.00
0.24
0.24
0.17
0.17
0.25
0.25
0.44
0.45
0.31
LEGEND
Overburden
Manitou Falls Formation
Fanglomerate
Wollaston Group Basement
Mineralization
Silicified Zone
T1 + K1, K2 +I1 ± (C1, ICML)
C1 + K1, K2 + T1 ± (I1, ICML)
I1 + ICML
I1
I1 + K1
T1 + I1 + K2
C2 ± C3 + I1 + K2
I1bsmt + C2bsmt
I1bsmt + C1bsmt
Unconformity
Fault
Sample Location
Fracture
T1
T1+I1
C2+C3
I1+ICML
I1
I1b+C2b
C1
I1+Dkt


d56Fe of hydrothermal/mineralized phases
T1
C2+C3
I1+ICML
I1
I1b+C2b
Count
5.0
4.5
4.0
3.5
3.0
2.5
2.0
1.5
1.0
0.5
0.0
−0.75
−0.50
−0.25
0.00
0.25
0.50
0.75
1.00
d56Fe


NE
Section A
SW
MAC-252
MAC-240
MAC-236
MAC-232
MAC-238
MAC-241
NW
Section B
SE
MAC-251
MAC-246
MAC-244
MAC-255
MAC-256
SW
Section C
NE
MAC-232
MAC-222
MAC-244
MAC-233
0m
100m
200m
300m
400m
500m
600m
50m
50m
50m
0.55
0.53
0.82
0.98
0.63
0.63
0.74
0.70
1.03
0.53
0.65
0.62
1.07
MFd
MFc
MFb
MFa
HW
LEGEND
Overburden
Manitou Falls Formation
Fanglomerate
Wollaston Group Basement
Mineralization
Silicified Zone
T1 + K1, K2 +I1 ± (C1, ICML)
C1 + K1, K2 + T1 ± (I1, ICML)
I1 + ICML
I1
I1 + K1
T1 + I1 + K2
C2 ± C3 + I1 + K2
I1bsmt + C2bsmt
I1bsmt + C1bsmt
Unconformity
Fault
Sample Location
Fracture
T1
T1+I1
C2+C3
I1+ICML
I1
I1b+C2b
C1
I1+Dkt


NE
Section A
SW
MAC-252
MAC-240
MAC-236
MAC-232
MAC-238
MAC-241
NW
Section B
SE
MAC-251
MAC-246
MAC-244
MAC-255
MAC-256
SW
Section C
NE
MAC-232
MAC-222
MAC-244
MAC-233
0m
100m
200m
300m
400m
500m
600m
-2.42
-0.24
-0.15
-0.28
-0.12
-0.40
-0.05
-0.78
-0.09
-0.03
-0.04
-0.78
MFd
MFc
MFb
MFa
HW
FW
50m
50m
50m
LEGEND
Overburden
Manitou Falls Formation
Fanglomerate
Wollaston Group Basement
Mineralization
Silicified Zone
T1 + K1, K2 +I1 ± (C1, ICML)
C1 + K1, K2 + T1 ± (I1, ICML)
I1 + ICML
I1
I1 + K1
T1 + I1 + K2
C2 ± C3 + I1 + K2
I1bsmt + C2bsmt
I1bsmt + C1bsmt
Unconformity
Fault
Sample Location
Fracture
T1
T1+I1
C2+C3
I1+ICML
I1
I1b+C2b
C1
I1+Dkt

Summary

$\delta^{56}Fe$ values indicate 3 populations of data that reflect 3 processes:

(1) most have $\delta^{56}Fe$ 0 to 0.5‰—the initial values of the system (bkgr)
(2) $\delta^{56}Fe$ > 0.5‰—near the ore zone or in sandstone directly above the extension of the P2 fault system—related to oxidation of Fe during ore formation
(3) $\delta^{56}Fe$ < 0‰ along boundaries, unc, faults within ore zone—later fluids

Most mineral types have values within all three populations.

Fe isotopes record processes associated with redox reactions in ore deposits, which have not been revealed before, only surmised

Fe isotopes at McArthur support the role of Fe as one reductant for U

Basin Development and Multi-element lithogeochemistry of Athabasca Basin samples



Recognizing geothermal signatures

Let’s discuss:

Basin development is the key to Athabasca Basin U deposits because:

- U ages roughly coincide with tectonic events
- Each major tectonic change sets up a new basin hydrology
- Changing tectonics change the nature of old faults and change the chemistry along the faults

-These changes leave a lithogeochemical record

-Multivariate lithogeochemical studies help to identify facies: sedimentary, diagenetic, and within deposits
-Combined with geochronological a.o. work perhaps they may identify specific events, and map the history of the faults hosting the lithogeochemical facies

Principal Component Analysis -is the simplest form of factor analysis

PCA replaces the original variables with fewer 'factors' accounting for much of the same information

The factor loading table shows how the variables contribute to the factor, and from that it may be possible to interpret it, in this study, as a lithofacies or a diagenetic facies.

Factor scores are calculated for each sample. They show the relative importance of each factor in each sample.

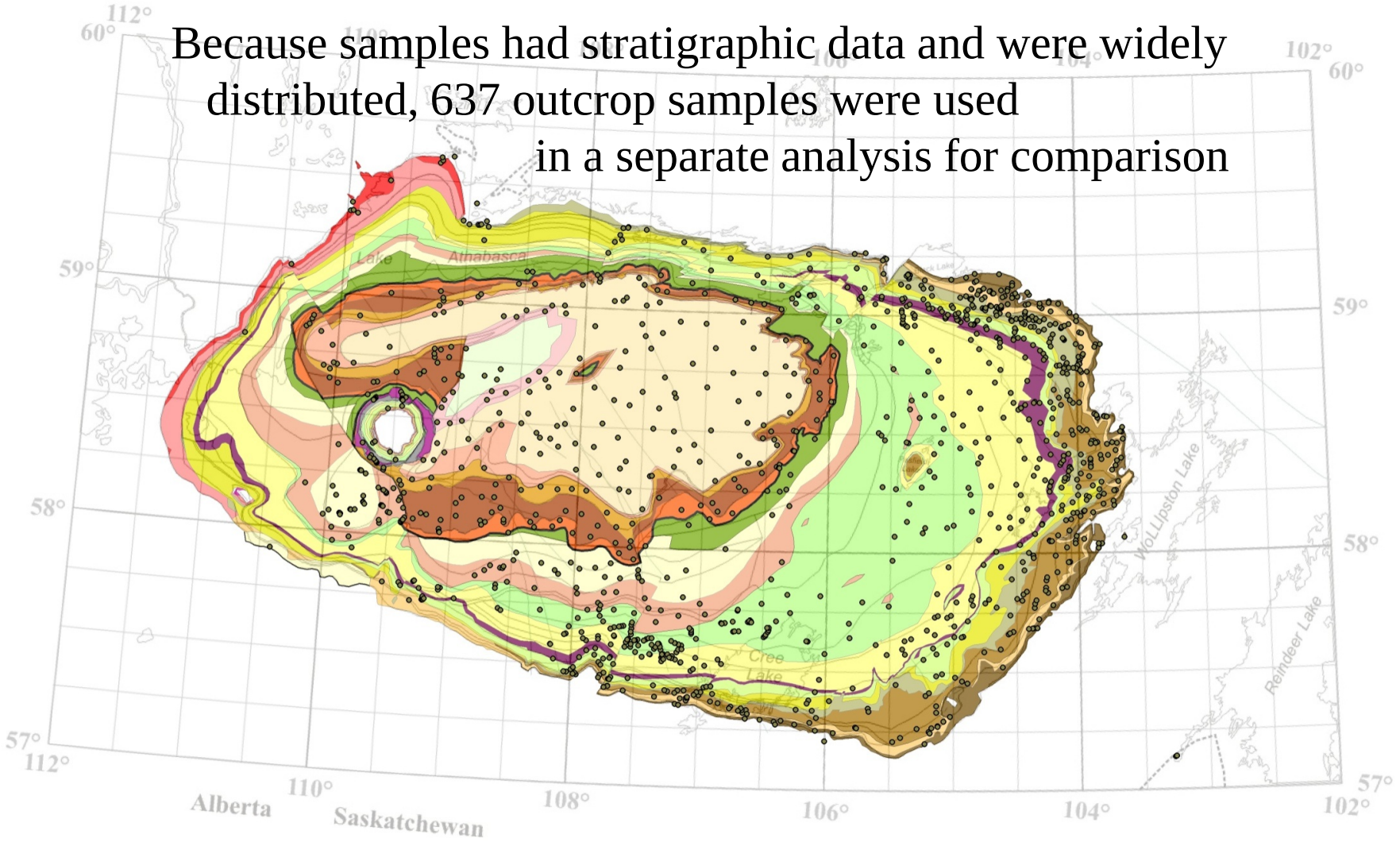
Anomalously high factor scores for a particular factor – i.e. a litho- or alteration facies, for the samples are what is shown on the maps.

The main GSC and SGS data compilation used has data on over 40,000 samples.

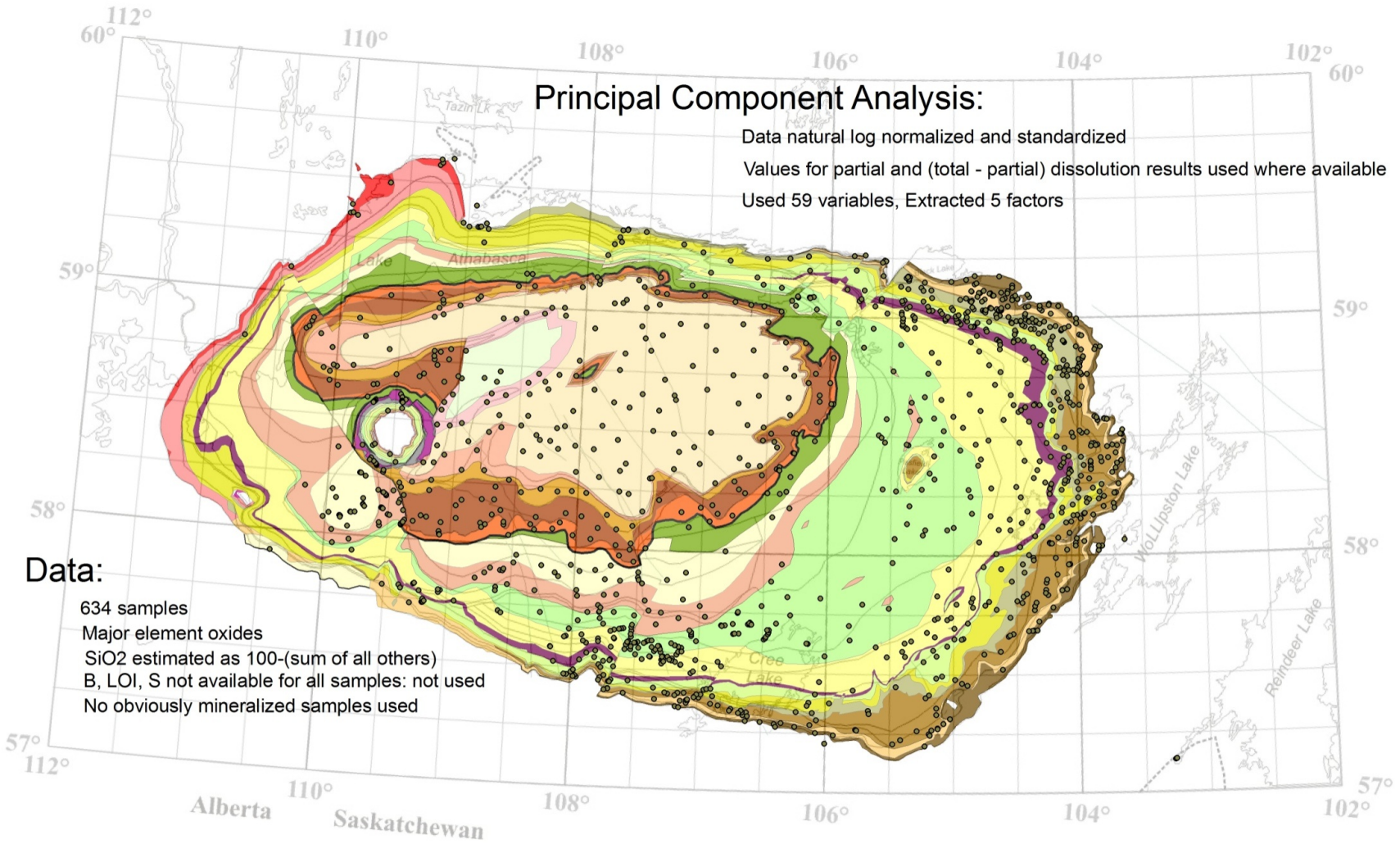
To get the broadest first regional overview the study used as many elements as possible; as factor analysis does not permit missing values only 11162 were available.
For these samples the elements used were:

Major elements
trace elements, including As and B
partial and total dissolution data for Co Cu Mo Ni Pb U V Zn

Because samples had stratigraphic data and were widely distributed, 637 outcrop samples were used in a separate analysis for comparison



Athabasca Basin: outcrops used in lithogeochemistry study



The 5 factor extraction is used to speed up presentation
Nine factors were found to be interpretable

F1
-detrital HV
-most of U
-immobile metals

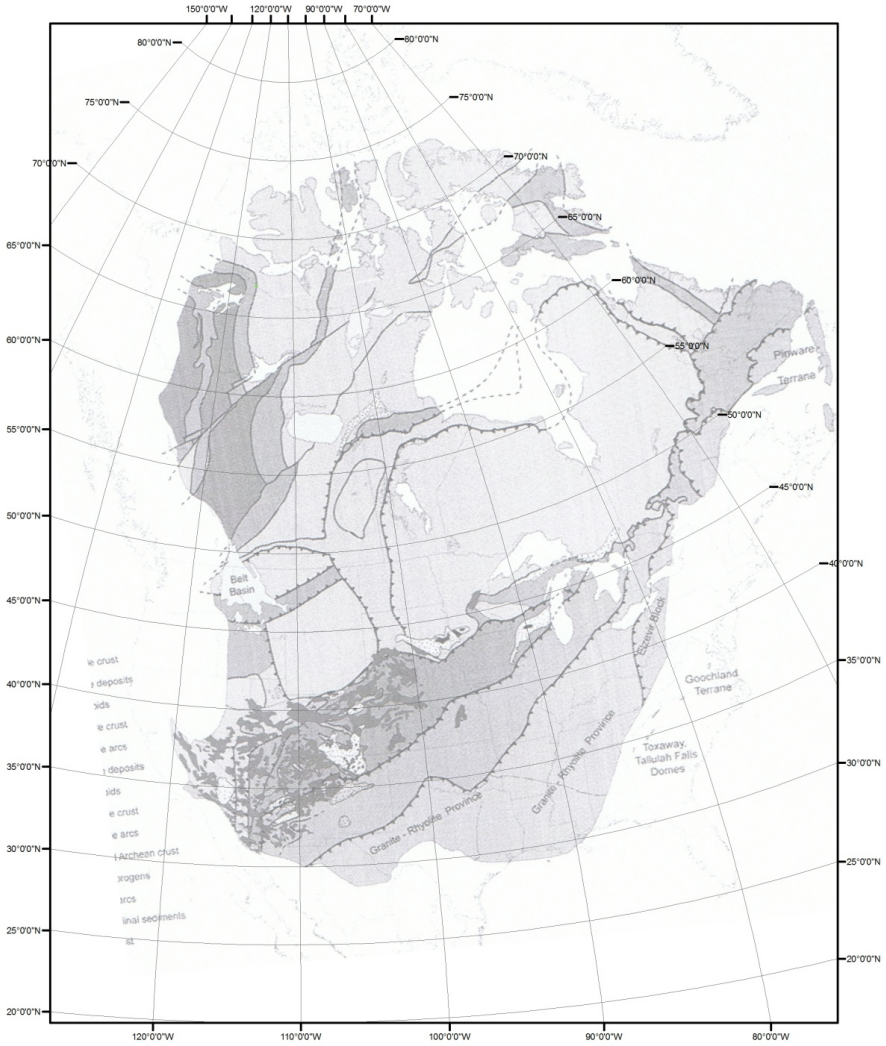
F2
-detrital, diagenetic
LREE, P, Th
monazite to APS

F3
-lithofacies
-illite, kaol.
-vs clean
- sandstone

F4
-alteration
-soluble metals to limonite

F5
detrital and hydrothermal
-oxydized HREE Y U mineralization?

Factor	1		2		3		4			
positive	Resistate HV includes U		LREE Sr Pb P Ba		Clays Mg Rb K Ga Ni-d Al Na (Li Ca Ni)		Mobile Co Ni Sb V Mo Fe Mn (U-pd)			
negative	(Si Cu)		(Si)		Si					
HF	0.887	CE	0.872	MGO	0.735	CO_PD	0.717	Y	0.857
TA	0.879	LA	0.859	RB	0.712	NI_PD	0.645	HO	0.852
ZR_D	0.873	PR	0.841	K2O	0.660	SB_PD	0.645	ER	0.838
TH_D	0.854	ND	0.829	GA	0.635	V_PD	0.635	DY	0.832
NB	0.834	SR	0.801	NI_D	0.614	FE2O3	0.623	TB	0.786
ZR_PD	0.815	SM	0.772	AL2O3	0.606	CU_PD	0.615	YB	0.784
TH_PD	0.810	PB_D	0.753	NA2O	0.558	MO_PD	0.591	GD	0.628
TIO2	0.810	P2O5	0.726	LI	0.497	CR	0.568	EU	0.618
U_D	0.802	BA	0.693	CAO	0.496	CO_D	0.560	SM	0.505
W	0.664	EU	0.685	NI_PD	0.457	SN	0.453	ND	0.388
AS_PD	0.633	GD	0.676	BE	0.432	MNO	0.433	SC	0.359
U_PD	0.620	PB_PD	0.491	CR	0.430	V_D	0.411	**U_D**	0.359
SC	0.604	TB	0.460	SC	0.424	**U_PD**	0.334	PR	0.328
MO_D	0.574	AG	0.448	CO_D	0.420	W	0.313	ZR_D	0.316
V_D	0.563	AS_PD	0.385	V_D	0.400	ZN_PD	0.278	HF	0.313
BE	0.505	BE	0.385	BA	0.340	NI_D	0.261	BE	0.292
AL2O3	0.502	DY	0.376	AG	0.283	CAO	0.260	P2O5	0.290
SN	0.497	TH_D	0.375	TIO2	0.279	MGO	0.249	CE	0.266
GA	0.479	GA	0.349	FE2O3	0.263	TH_PD	0.216	ZR_PD	0.256
YB	0.466	NB	0.319	NB	0.259	BE	0.210	LA	0.240
PB_PD	0.408	HO	0.306	YB	0.241	AG	0.186	CU_PD	0.237
MO_PD	0.406	ER	0.296	EU	0.237	EU	0.184	MGO	0.227
P2O5	0.398	K2O	0.295	ZN_PD	0.231	P2O5	0.179	TIO2	0.226
FE2O3	0.364	SN	0.292	PR	0.225	AS_PD	0.170	W	0.201
ER	0.354	RB	0.286	ND	0.218	GD	0.169	**U_PD**	0.193



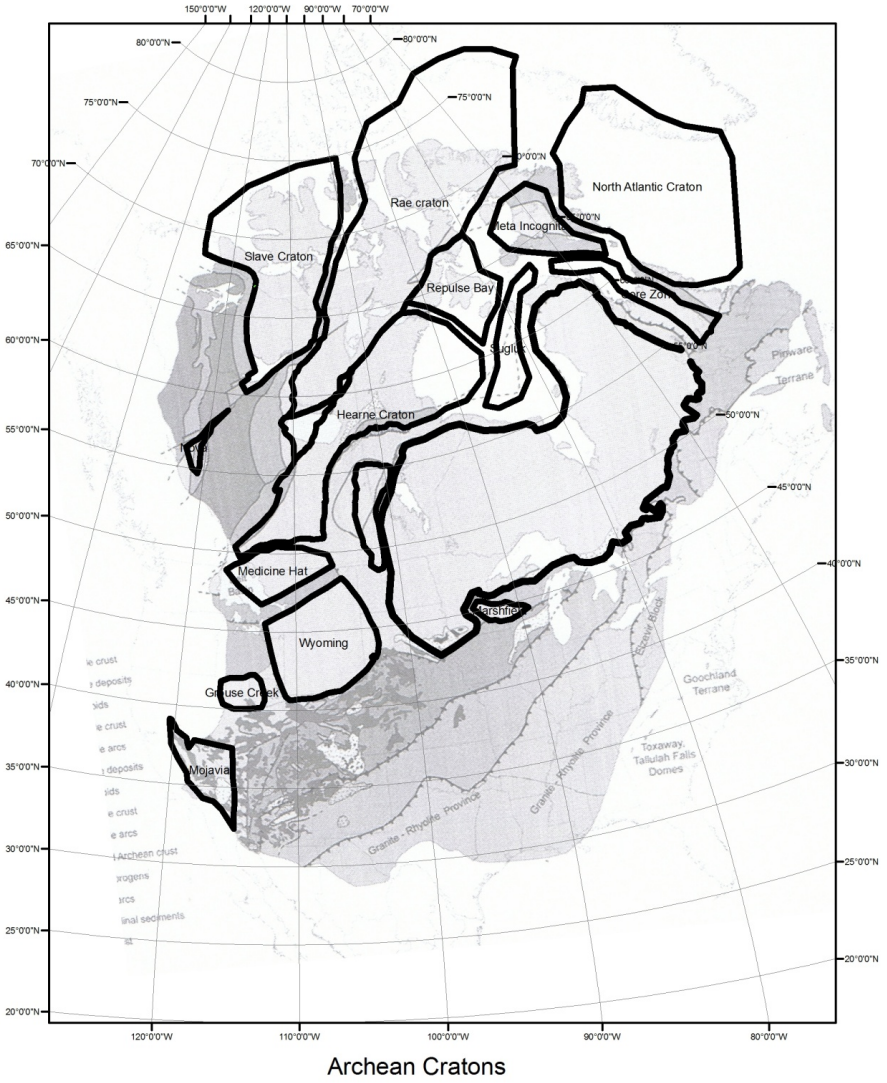
Background map: Whitmeyer and Karlstrom 2011

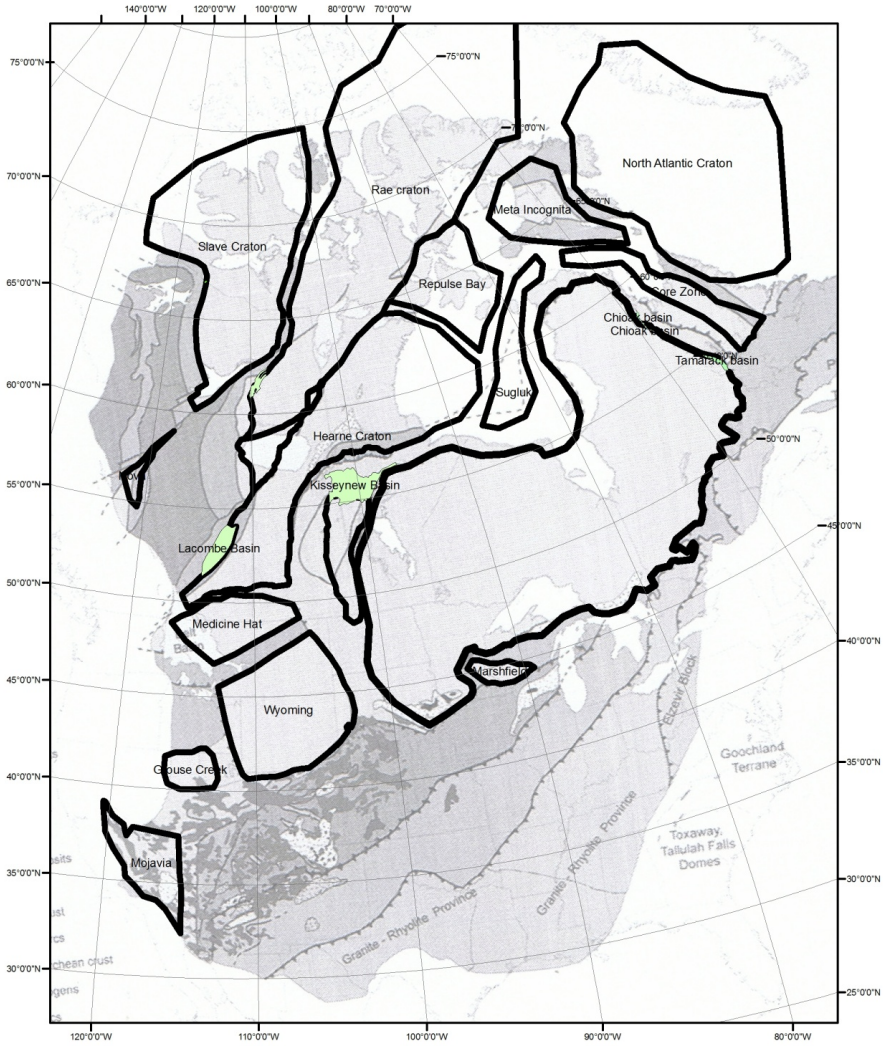
Craton junctions

-weak – host basins

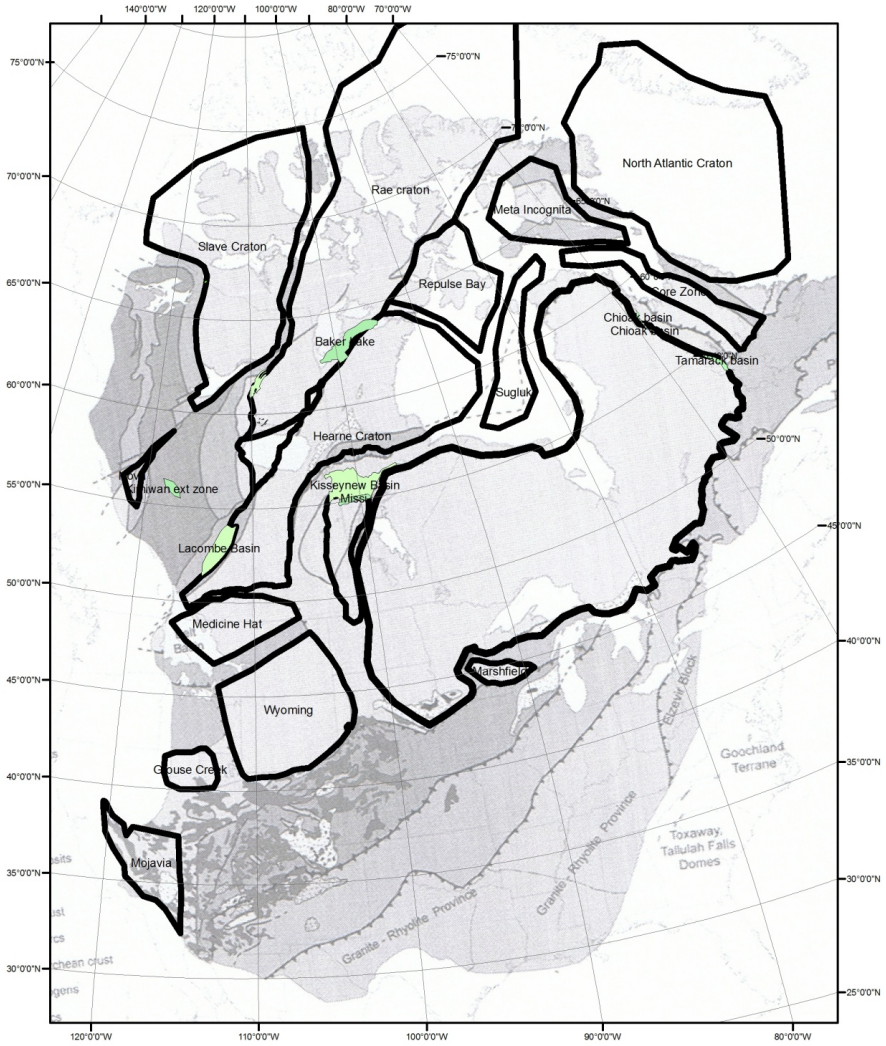
-recent work shows they are often anomalously hot

-i.e focussing zones for hydrothermal systems

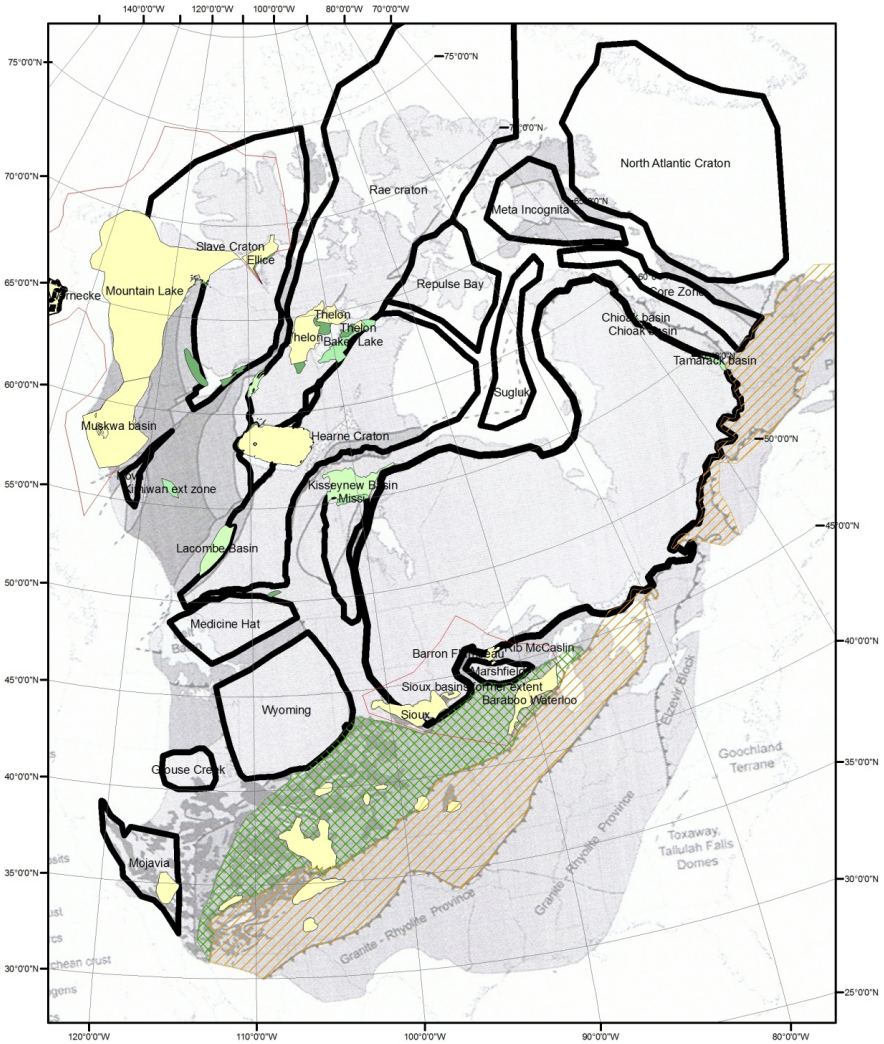




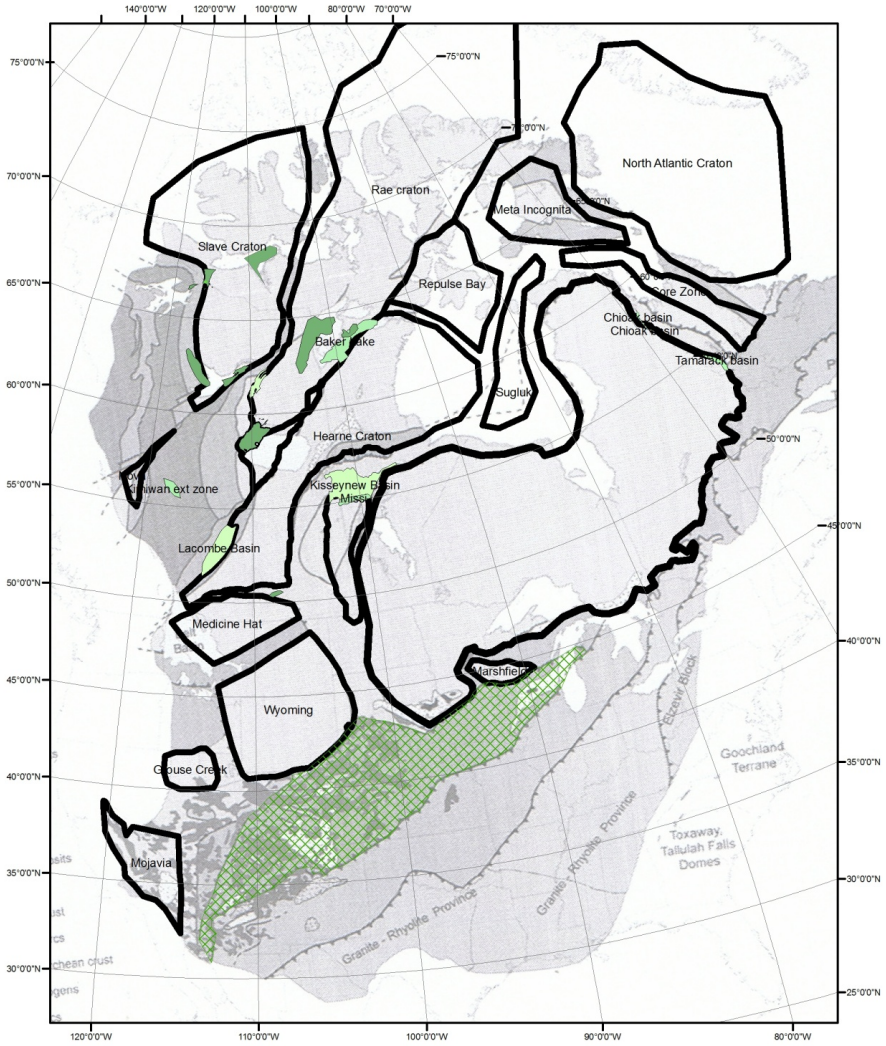
1.88-1.85 Ga THO Rae Nonacho basins



1.86-1.80 Ga THO Churchill Superior basins



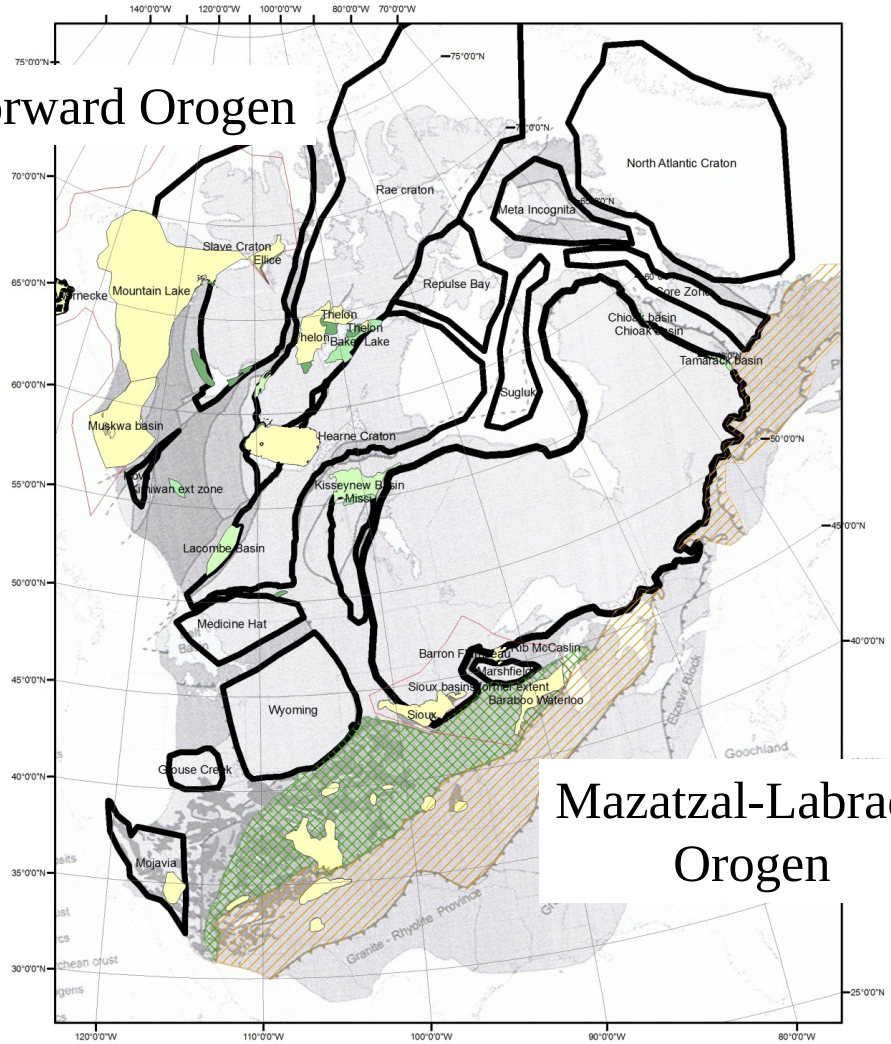
1.73-1.63 Ga LateTHO, Forward, Penokean basins;Yavapai basins



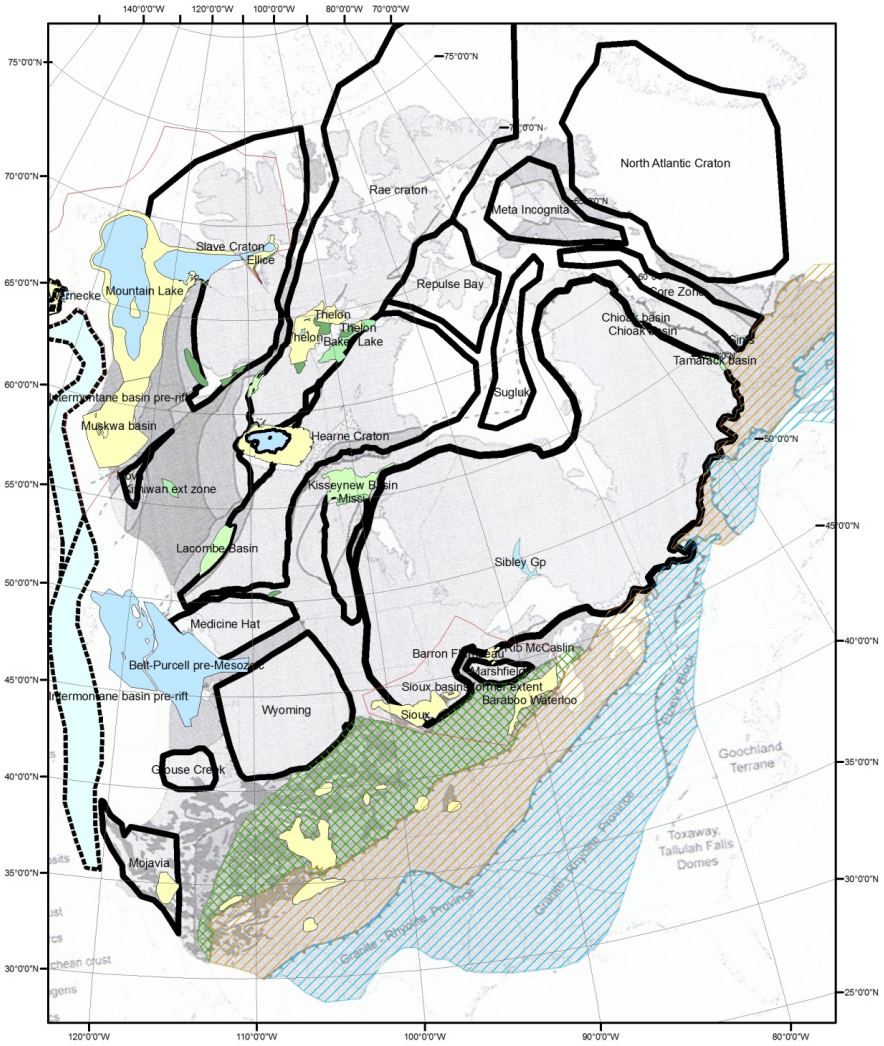
1.76-1.72 Ga THO basins Yavapai crust docking

The Forward-Mazatzal squeeze:

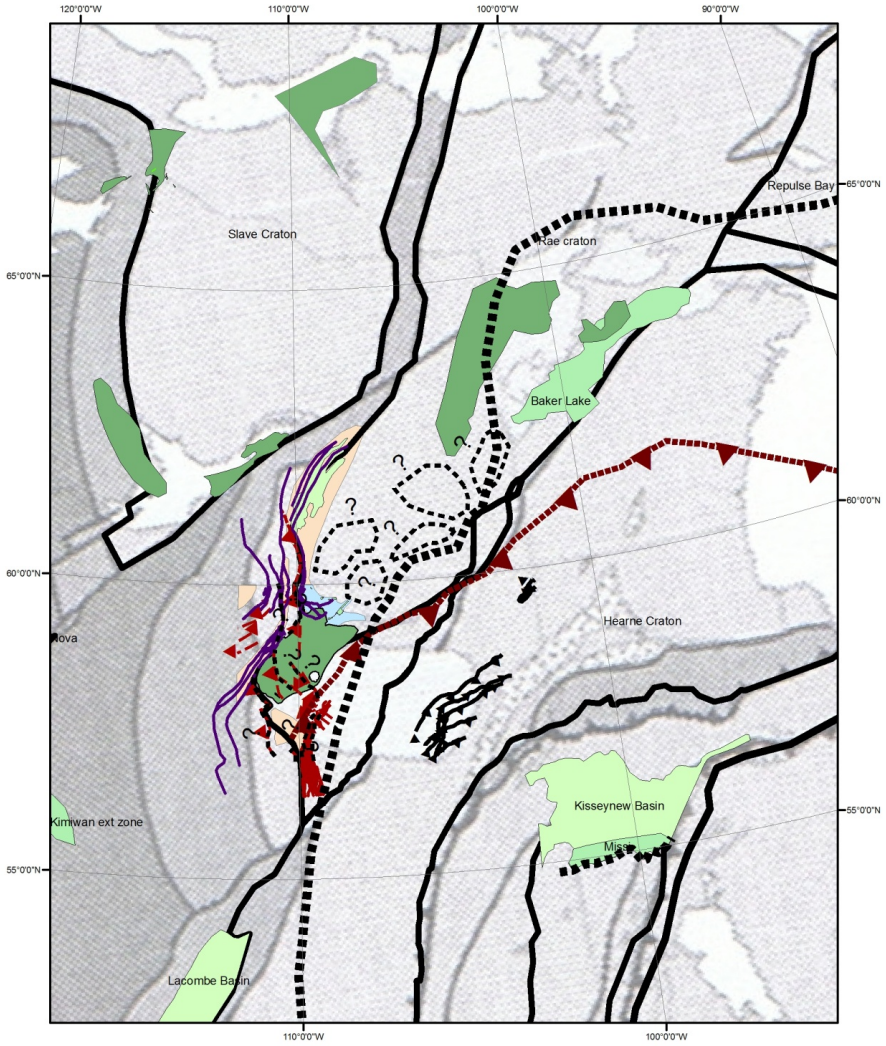
Orogens on opposing sides of Laurentia with opposing directions of movement



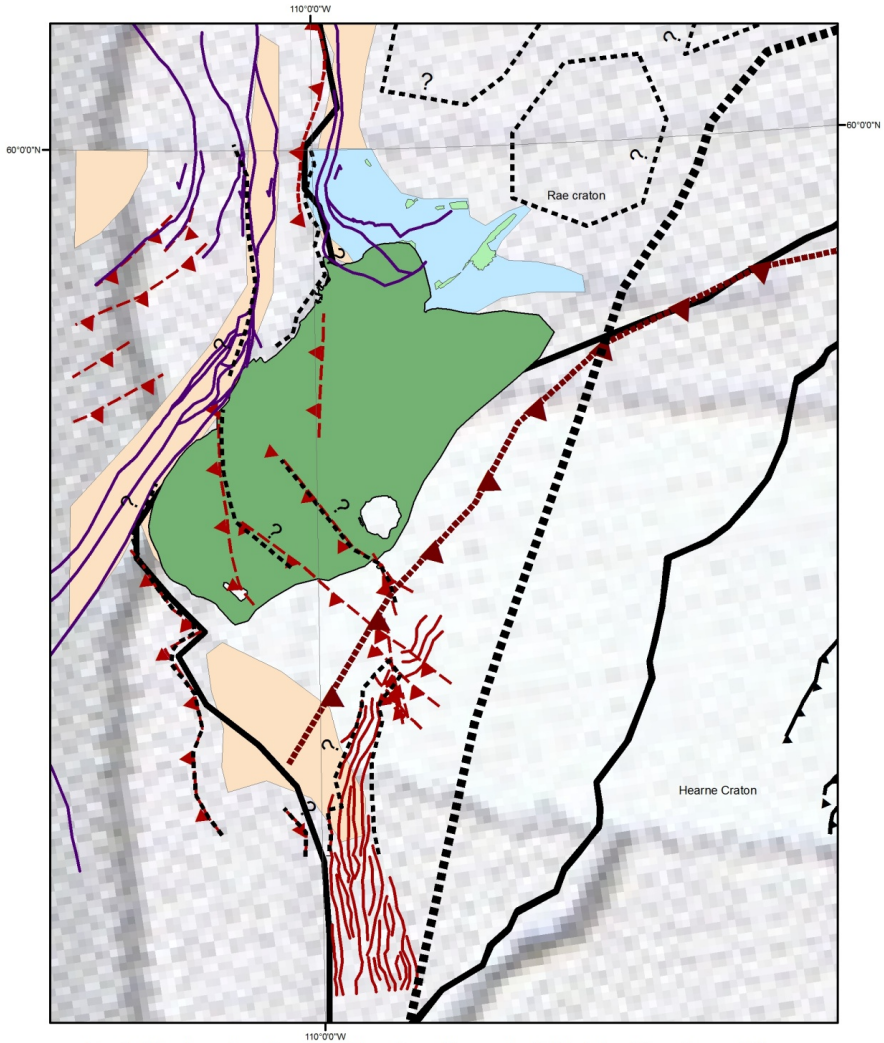
1.73-1.63 Ga LateTHO, Forward-Racklan, Penokean basins;Yavapai basins
Mazatzal, Labrador docking 1.69-1.65 Ga



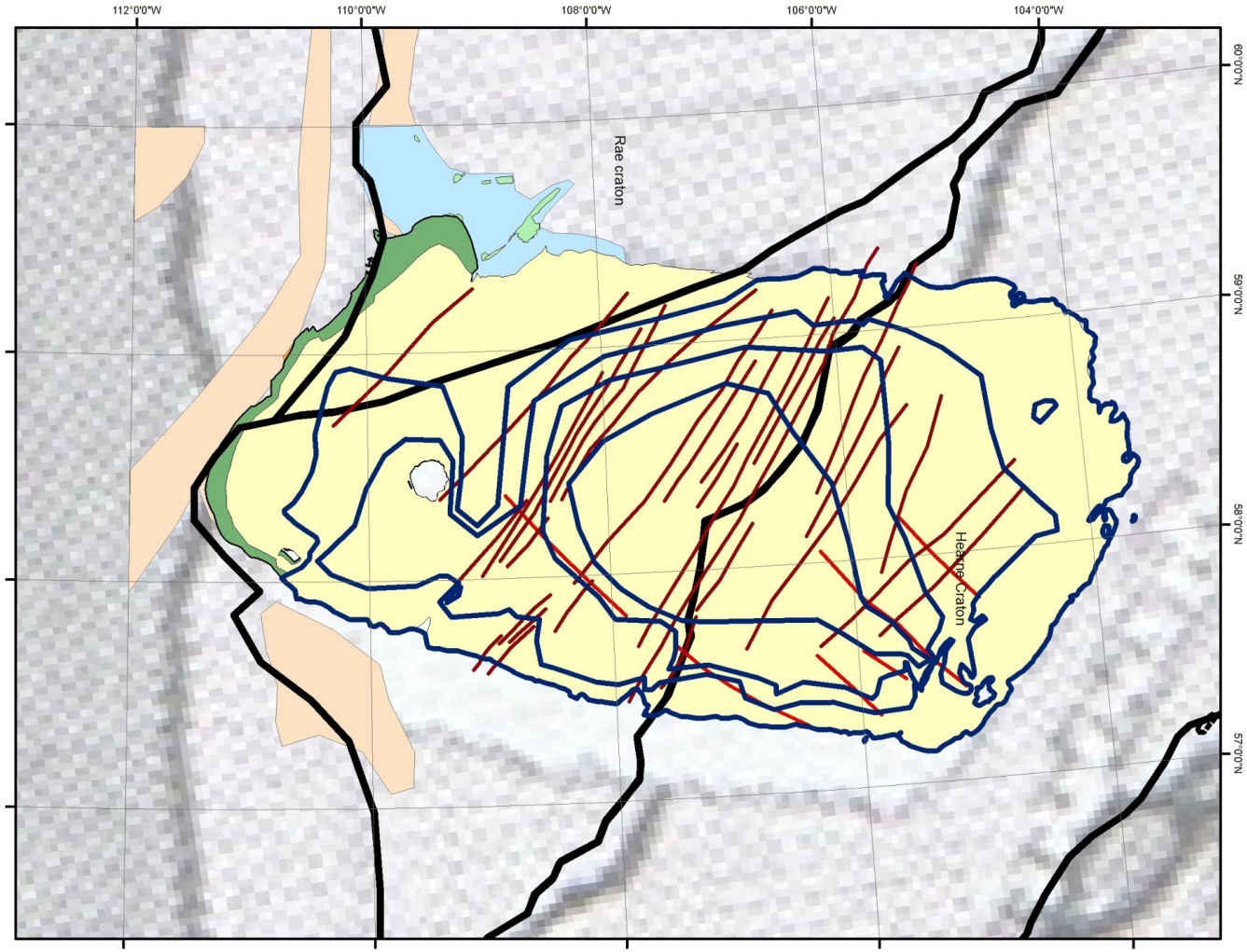
1.55-1.35 Ga Dismal Lk McFarlane etc. Aborted continent breakup basins
Granite-Rhyolite, Pinware crust formation
Main U emplacement Athbasca Basin



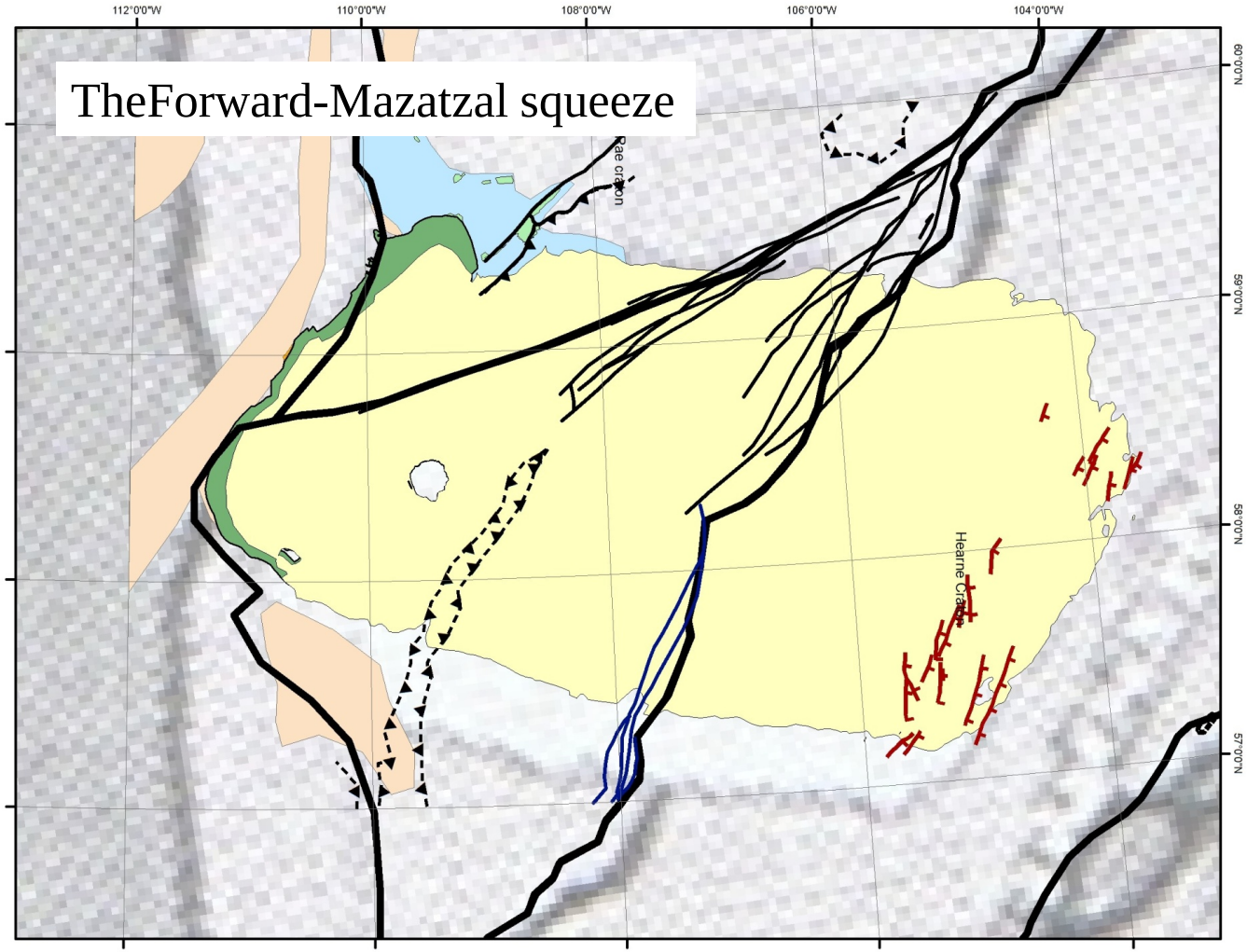
Early Hudsonian foreland basins: Nonacho?
1820 Ma "Laramide" collisional stage Hudsonian basins: Martin, Baker
Waning stage THO "Laramide" basin: Jackfish, Nueltin, Pitz, Swift Current



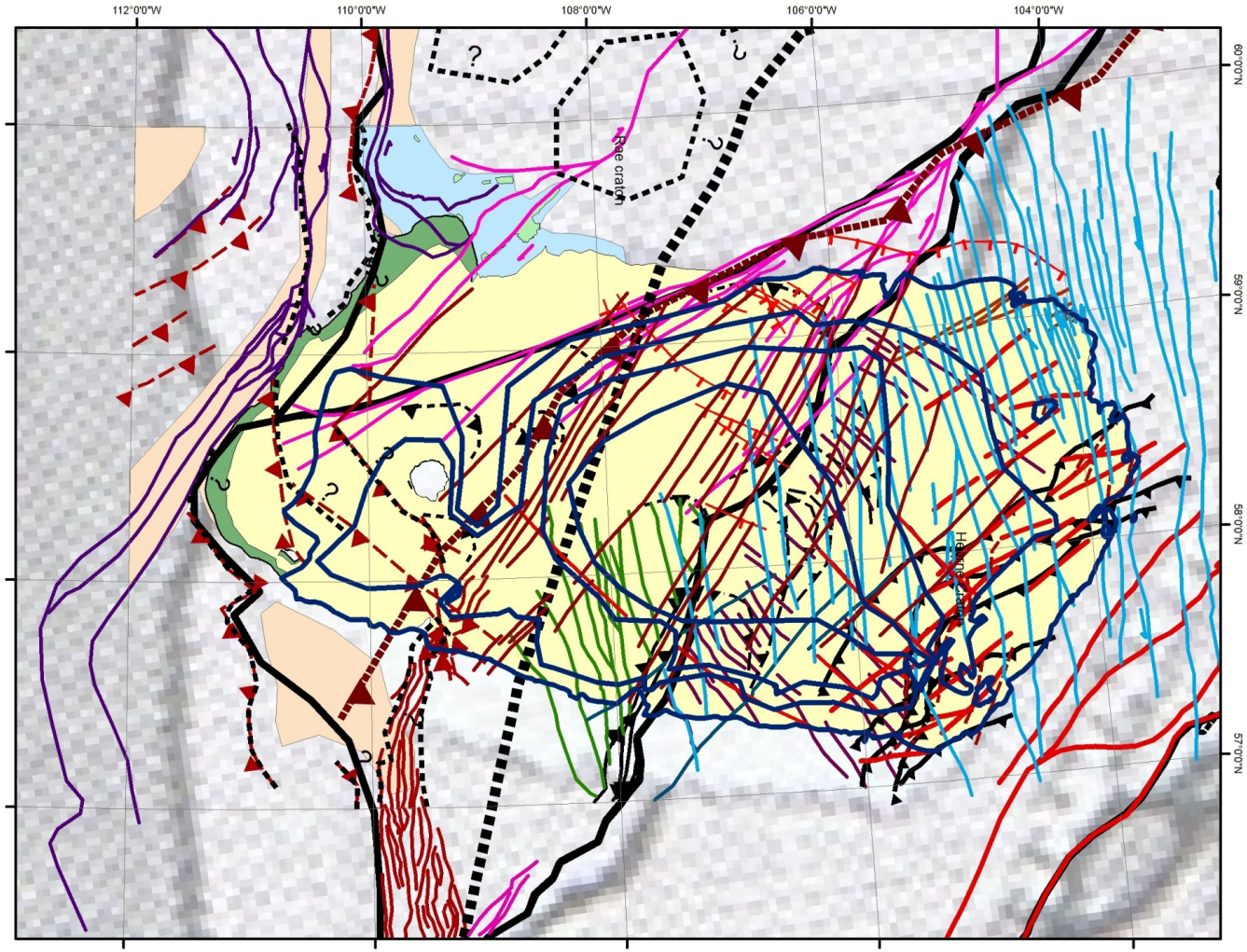
Early Hudsonian foreland basins: NonachoThluicho Burntwood ?
1820 Ma "Laramide" collisional stage Hudsonian basins: Martin
Waning stage THO "Laramide" basin:
Jackfish, Swift Current Nueltin-type granites, rhyolites



Athabasca Seq 2: Read to Wolverine Point 1.73-1.63 Ga
Seq 2 basin development faults
50 m isopach of Read Fm, showing NW basin rift axis



Athabasca Seq 2: Faults prone to reactivation during the Forward - Mazatzal squeeze
NW-SE contraction 1.69-1.65 Ga
i.e. during Wolverine Point time deposition and the hiatus between it and Locker Lake deposition



Athabasca Seq 2: Read to Wolverine Point 1.73-1.63 Ga
Seq 2 basin development faults and Taltson Snowbird and THO faults
50 m isopach of Read Fm, showing NW basin rift axis

Faults identified from:

-large linear mag lows

-surface lineaments

-offsets between ddh

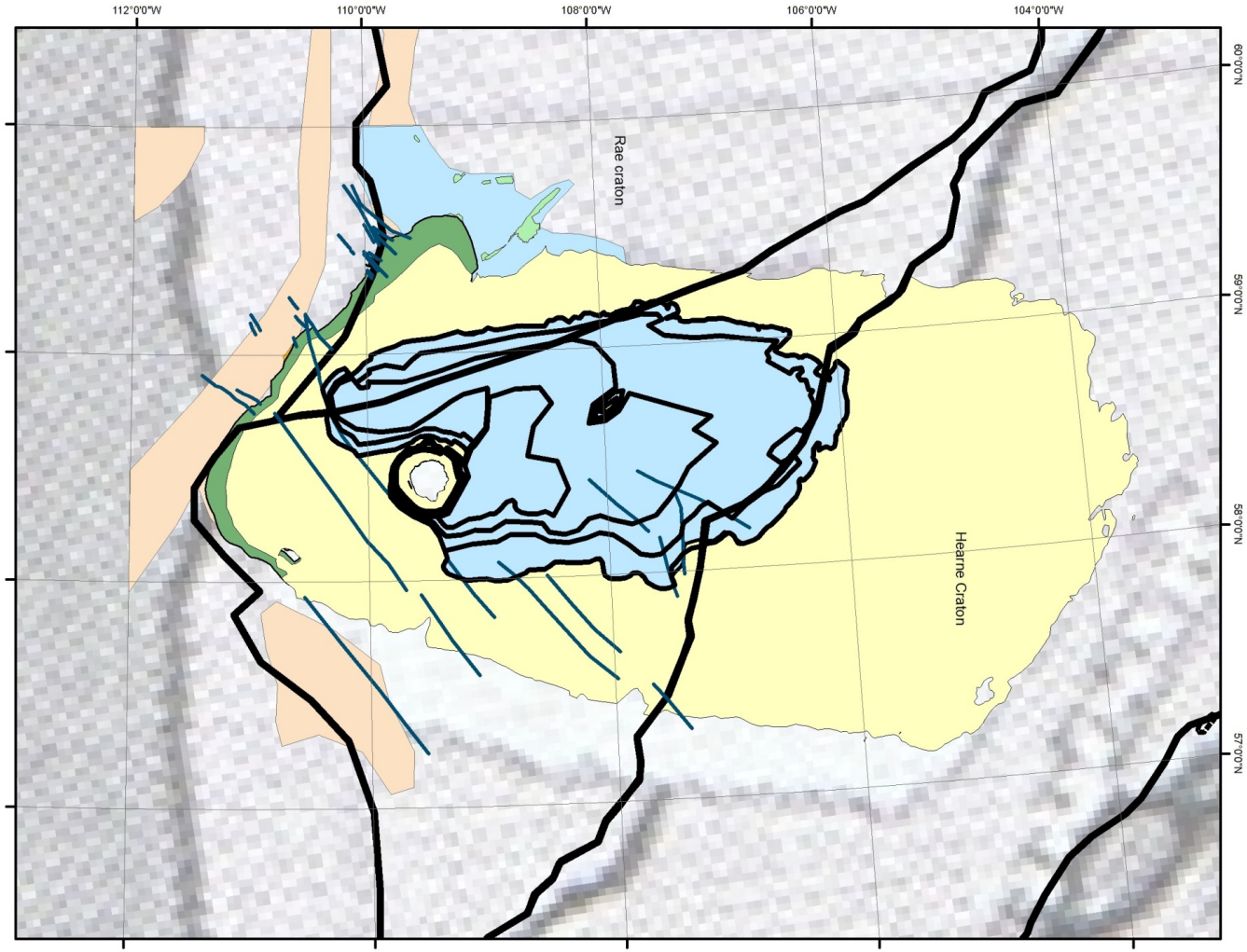
-study and geochronology where the faults extent beyond present basin limits, i.e. the literature

-Fault type and age(s) of movement determined from:

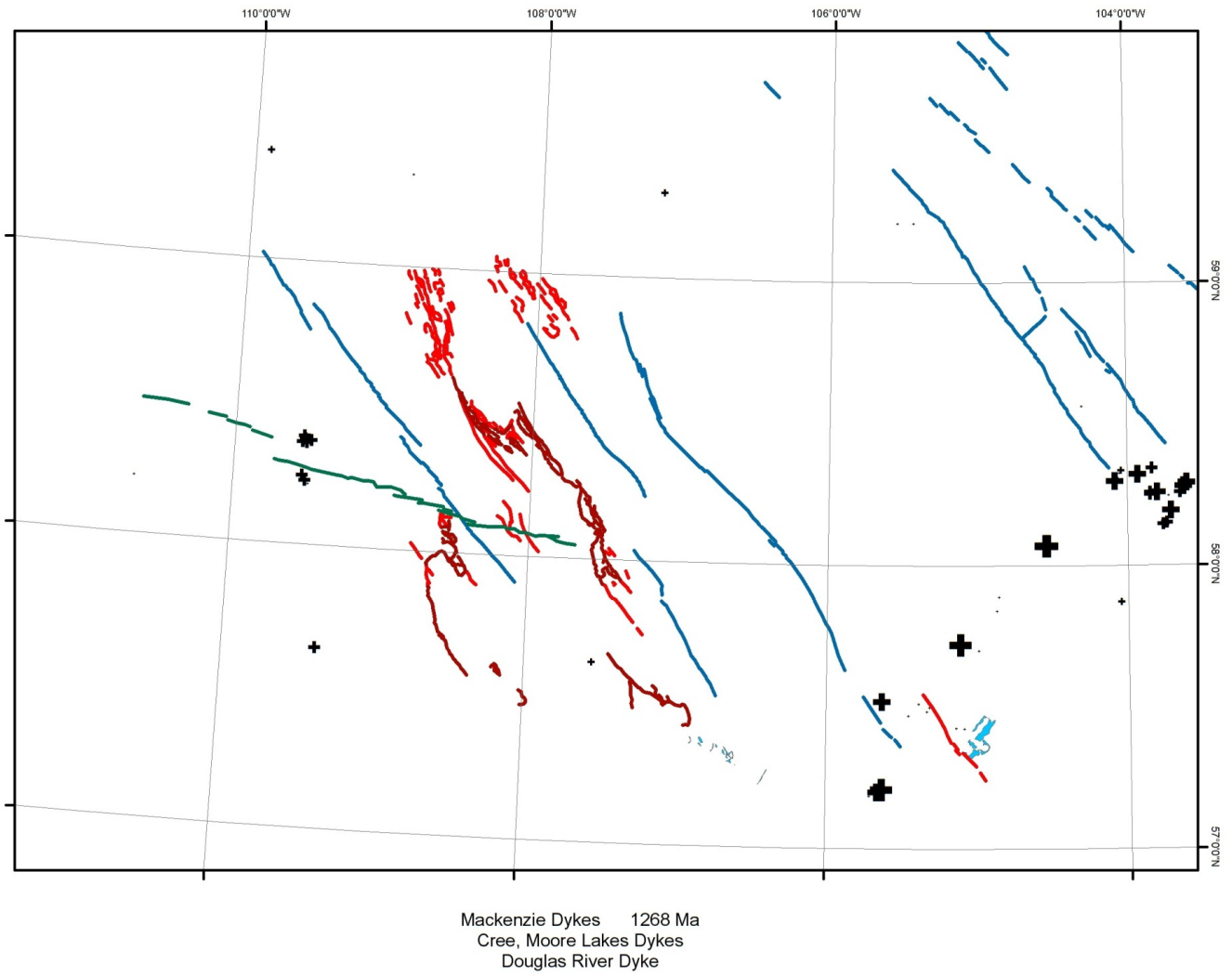
-displacements of specific strat units

-geochronology from literature

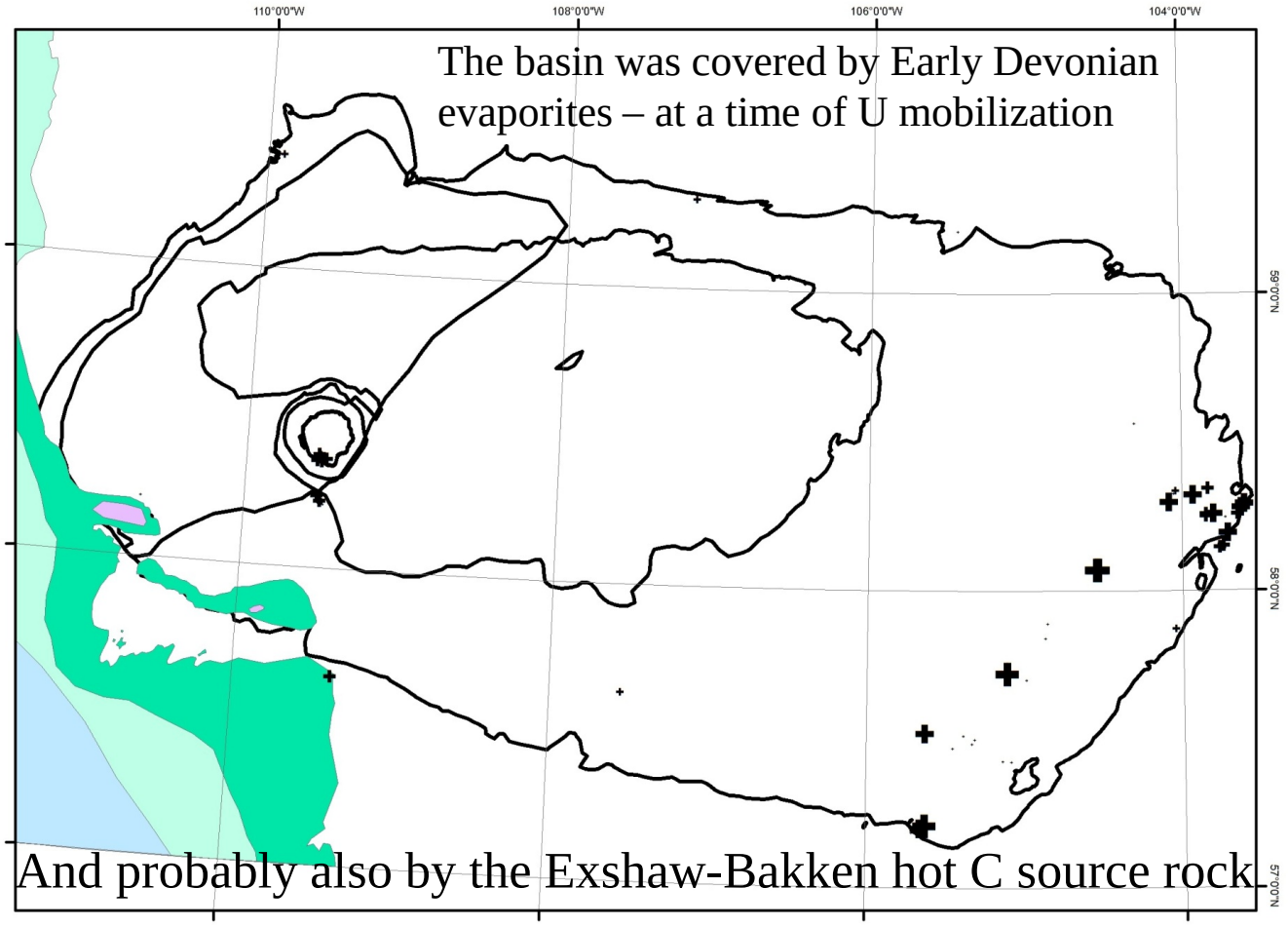
-comparison of isopach and lineaments



1.55-1.35 Ga Athabasca Seq 3: Locker Lake to Carswell
Basin forming faults
100 m isopachs of Locker Lake Fm show SW sediment source
and suggest a NW trending half-graben



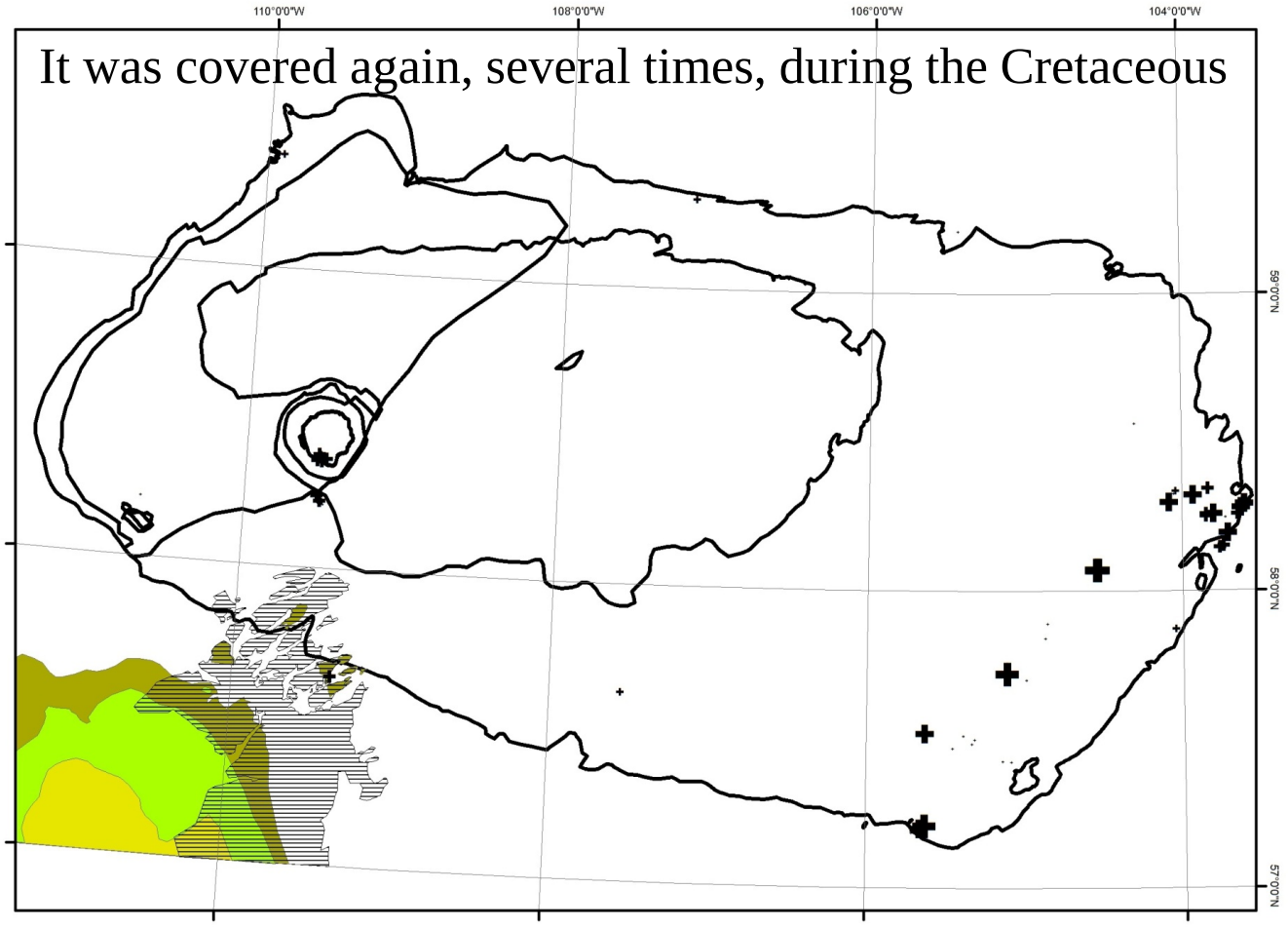
There were at least 3 generations of Post-Athabasca Intrusives



Devonian - at base Elk Point Group evaporites - likely covered all of the Athabasca Basin

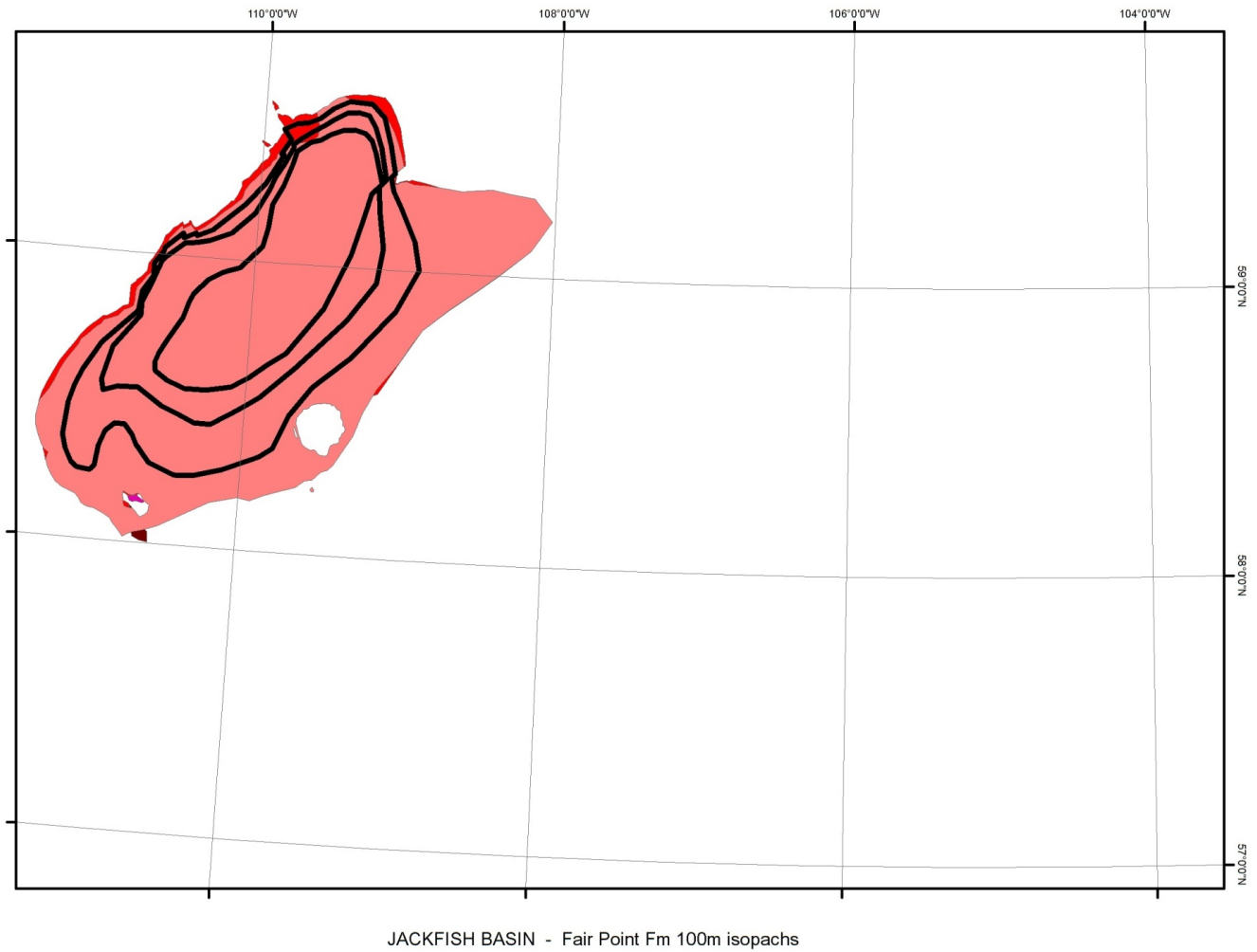
Carboniferous - hydrocarbon rich shales may have covered the basin (Exshaw - Bakken) and left pyrobitumen

Time of U mobilization



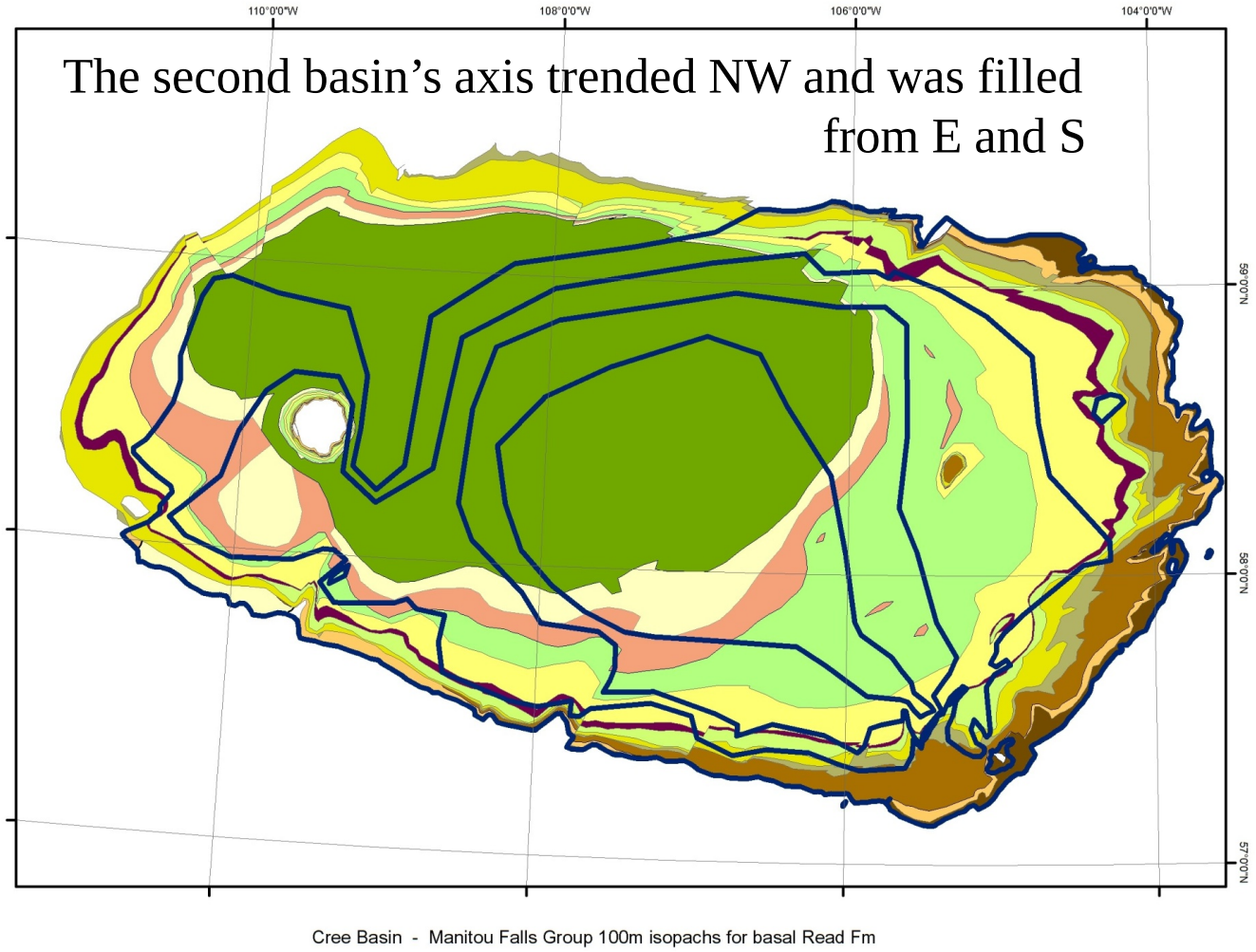
Cretaceous - Mannville Group coals were buried over 1000 m in the McMurray area

Summary of basin development



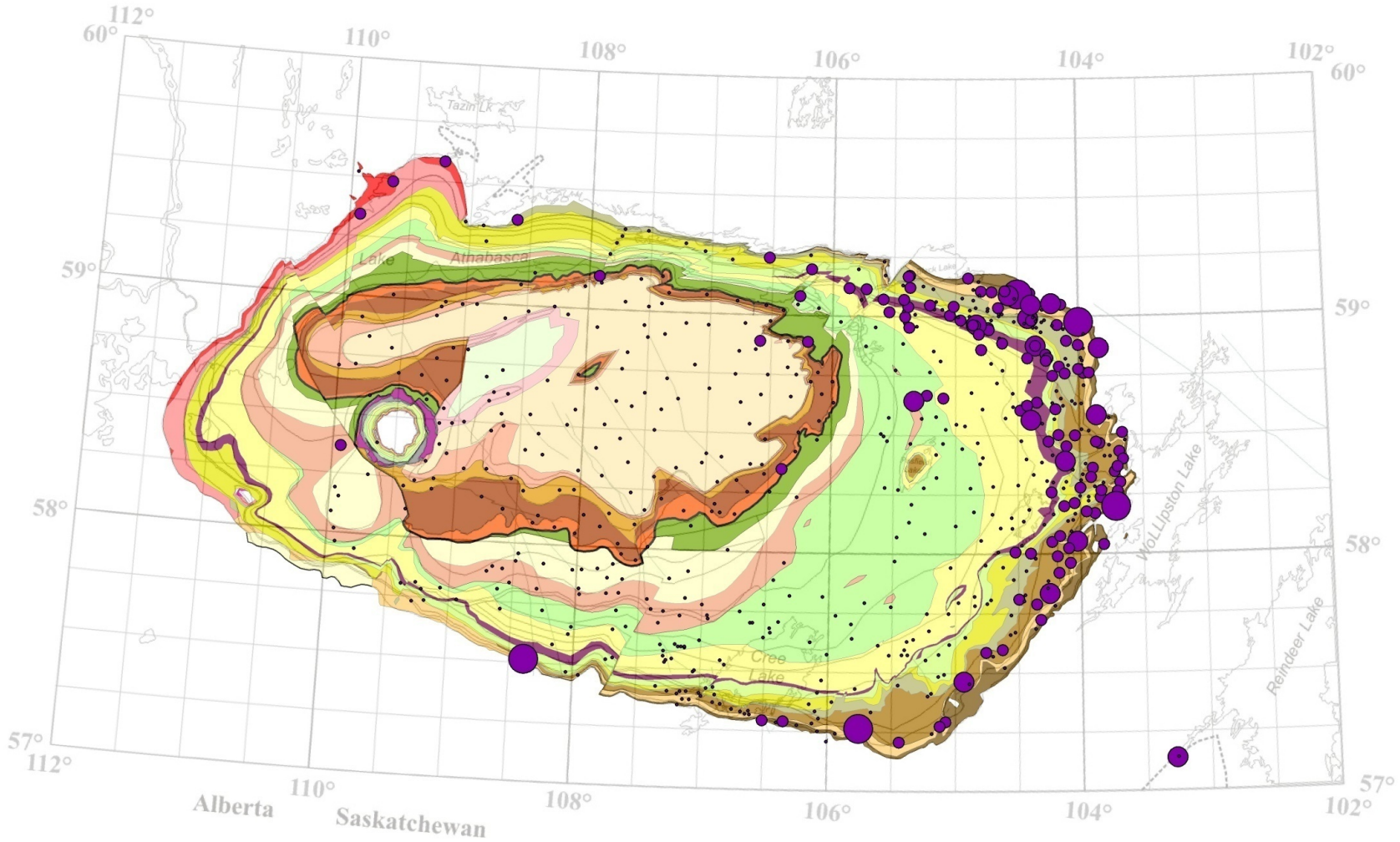
JACKFISH BASIN - Fair Point Fm 100m isopachs

The Athabasca Basin developed in stages over at least 200 Ma
The first basin trended NE, and drained to the NW



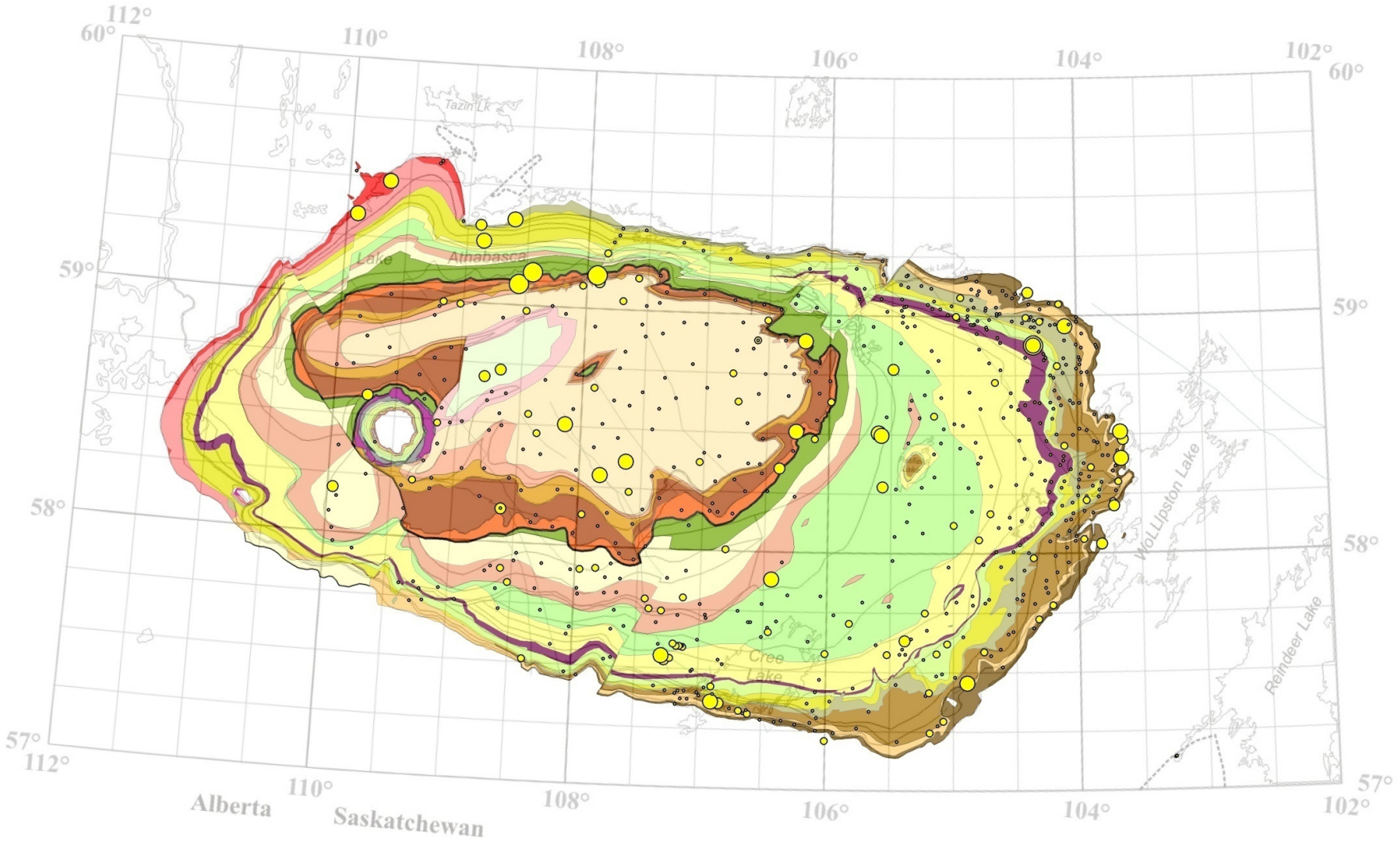
Cree Basin - Manitou Falls Group 100m isopachs for basal Read Fm

Regional NW-SE compression may have terminated deposition

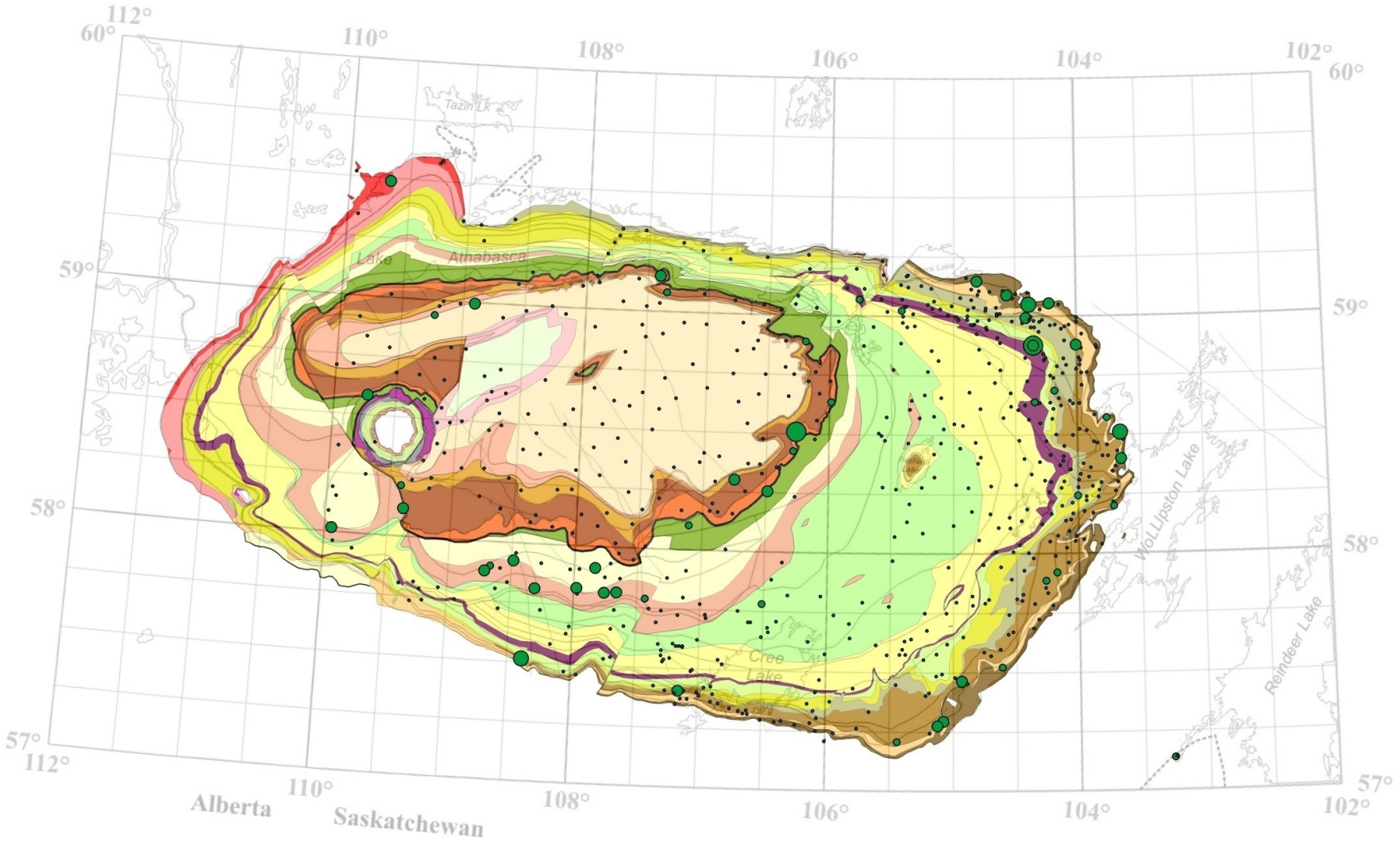


PCA Factor Scores: F1pos (large): Manitou Falls cgl are the least mature

Heavy detrital minerals

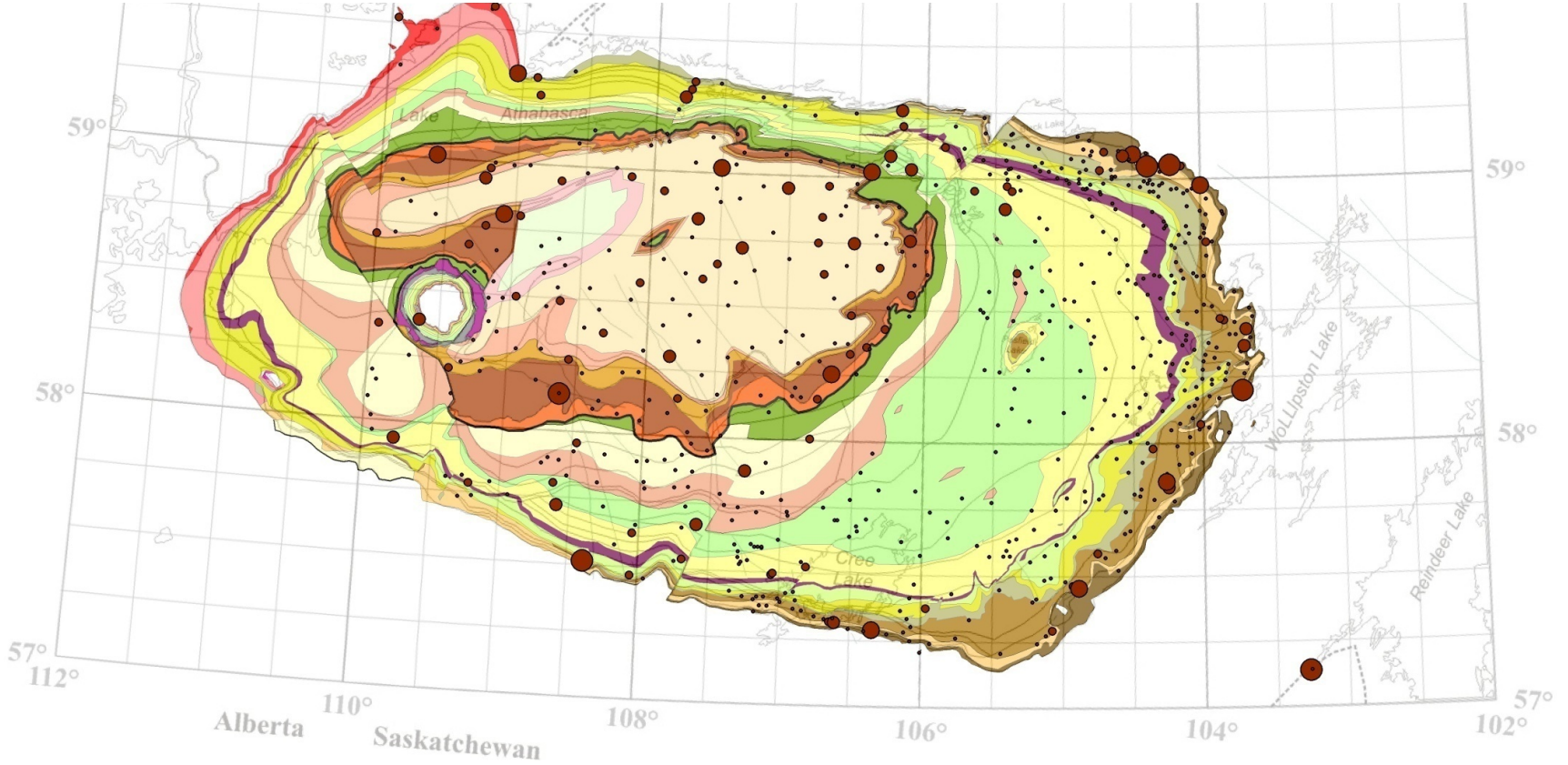


PCA Factor Scores: F3: Clays vs Silica



PCA Factor Scores: F2pos: LREE Sr Pb P Ba, weak Al : alumino phosphates?

Limonite is a metal trap an is very mobile: more work is needed on this factor to determine whether samples reflect detrital Fe or mobilized Fe, and for the latter, at what time the Fe moved



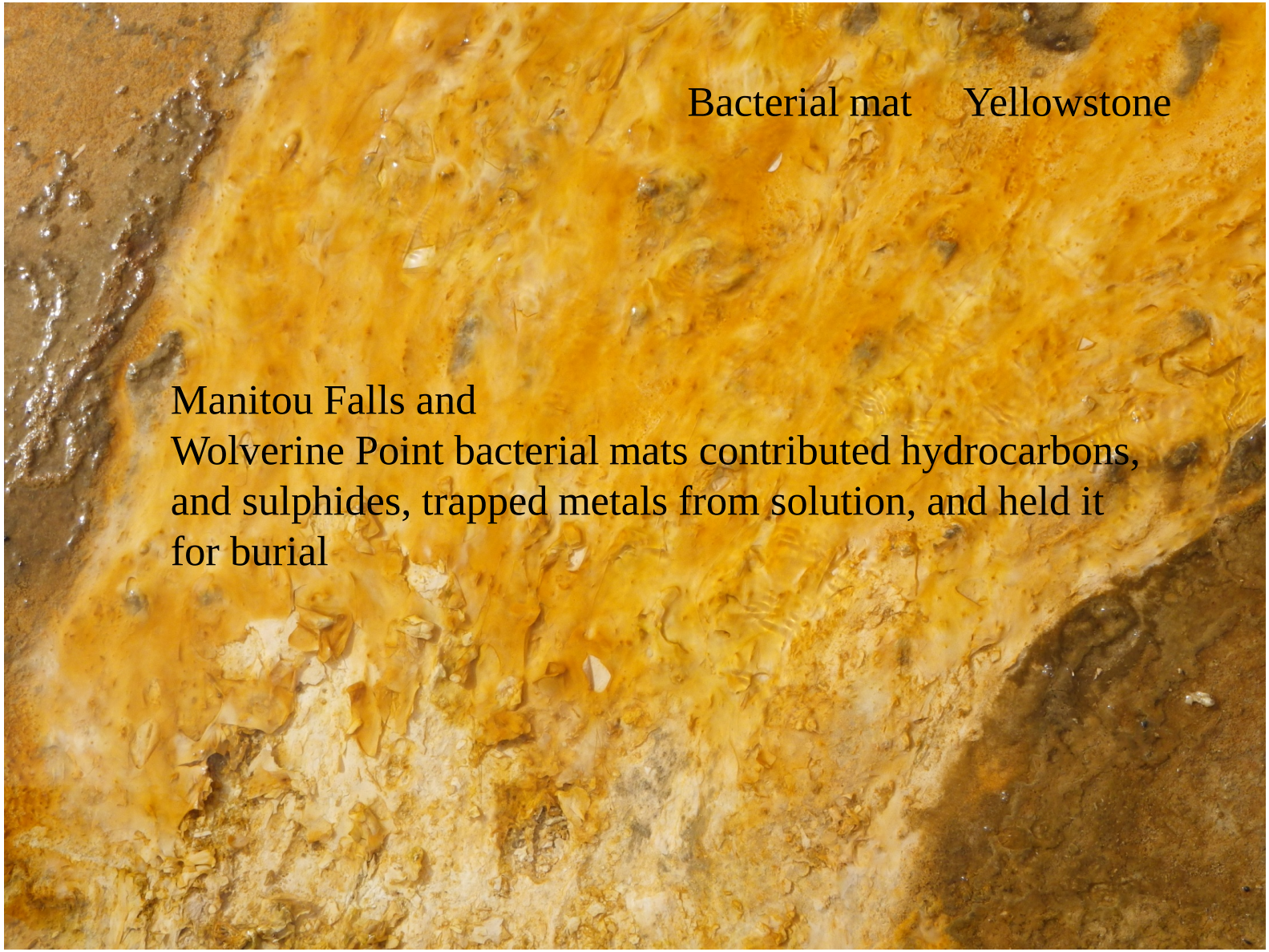
PCA Factor Scores: F4: Mobile Co Ni Sb V Mo Fe Mn U: enriched Fe Mn oxides, hydroxides

The second basin terminated with an evaporitic unit
(Wolverine Point) that may have been as organic-rich
as the Douglas Fm -
but, unlike the Douglas, was oxydized and lost its hydrocarbons.

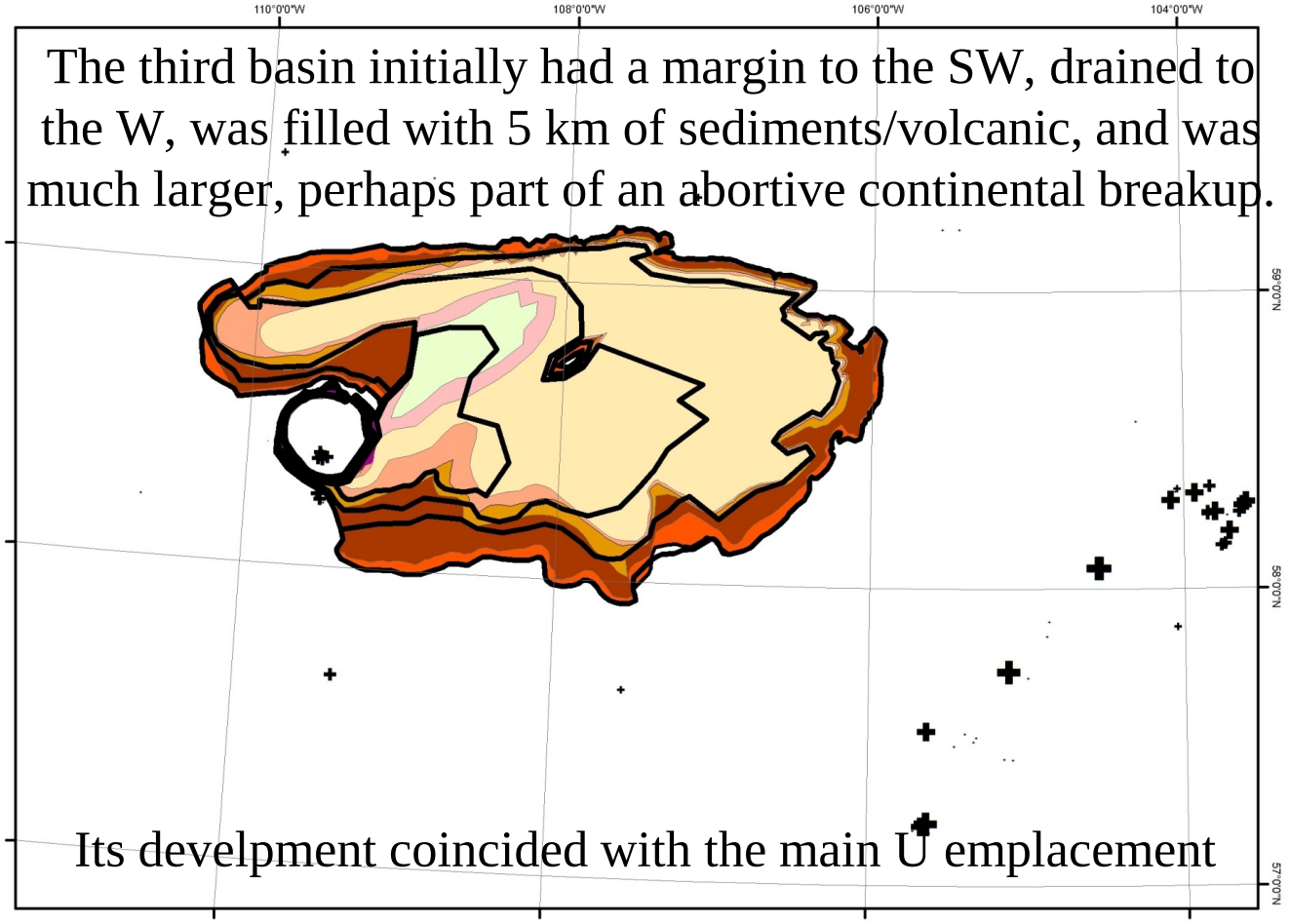
It contributed salts as well as reductants.

Depleted hydrocarbon sources, like depleted U source areas, are evidence of metallogenetic activity, not U-rich and C-rich units.

B accumulates in the margins of salars. They also produce much the world's Li


Bacterial mat Yellowstone
Manitou Falls and
Wolverine Point bacterial mats contributed hydrocarbons,
and sulphides, trapped metals from solution, and held it
for burial

The third basin initially had a margin to the SW, drained to the W, was filled with 5 km of sediments/volcanic, and was much larger, perhaps part of an abortive continental breakup.

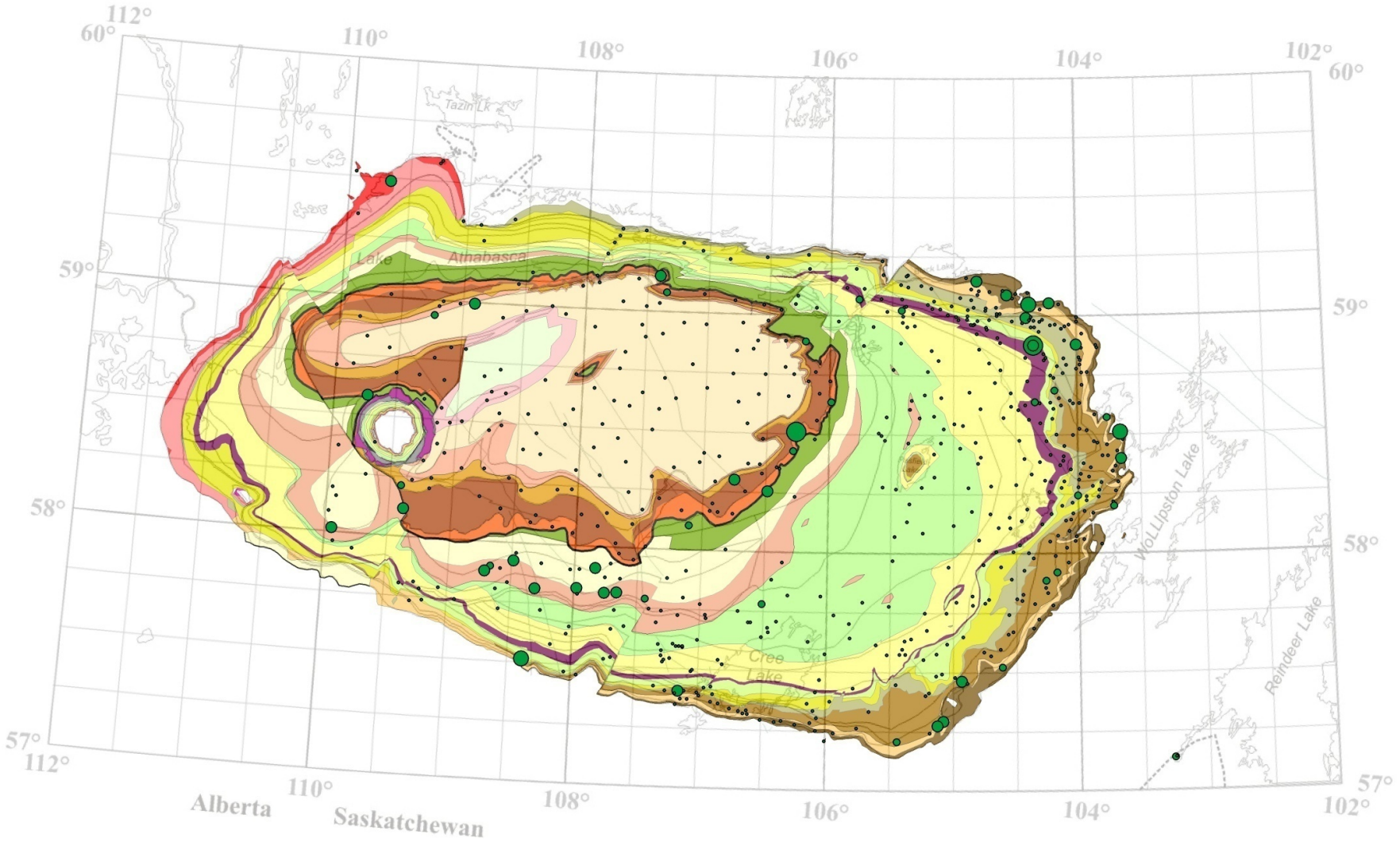


Its develpment coincided with the main U emplacement

Mirror Basin - McFarlane Group 100m isopachs for basal Locker Lake Fm

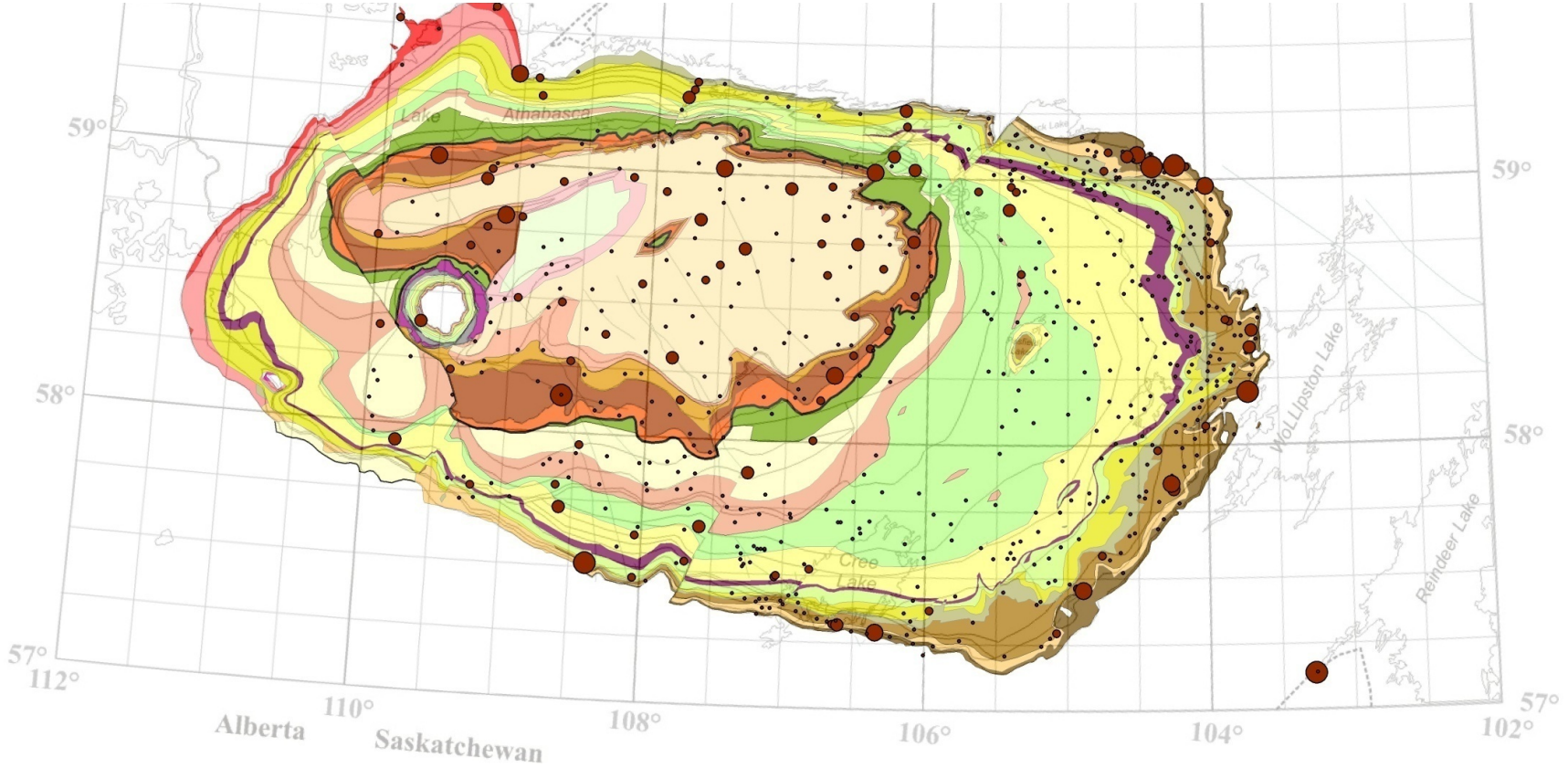
Basin formed at the time of main U ore deposition - Douglas Fm ca. 1540 Ma U deposits marked by + signs.

Subsidence estimated at ca. 5000 m
Topography driven circulation to North. Highlands to south

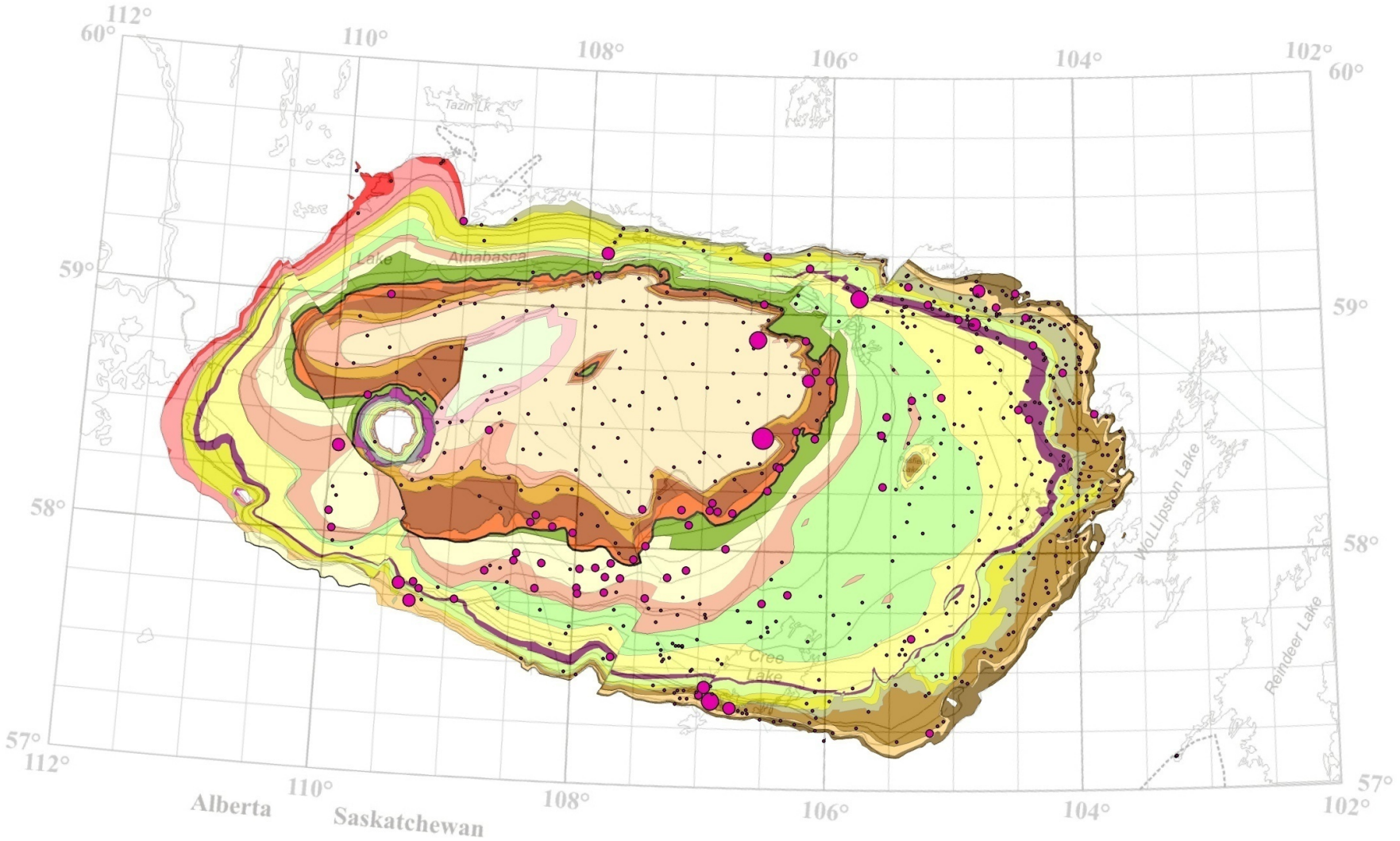


PCA Factor Scores: F2pos: LREE Sr Pb P Ba, weak Al : alumino phosphates?

Limonite is a metal trap an is very mobile: more work is needed on this factor to determine whether samples reflect detrital Fe or mobilized Fe, and for the latter, at what time the Fe moved

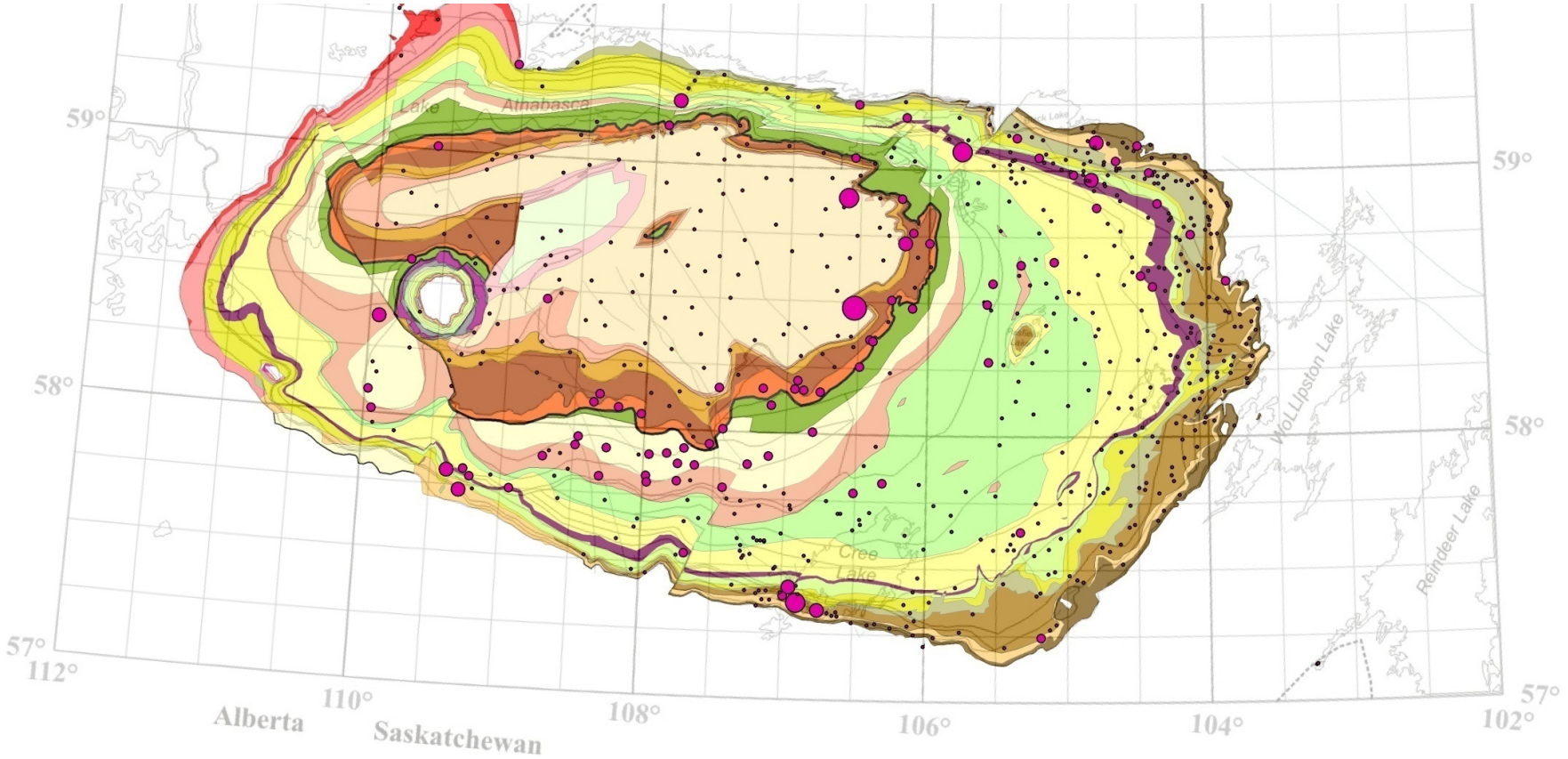


PCA Factor Scores: F4: Mobile Co Ni Sb V Mo Fe Mn U: enriched Fe Mn oxides, hydroxides



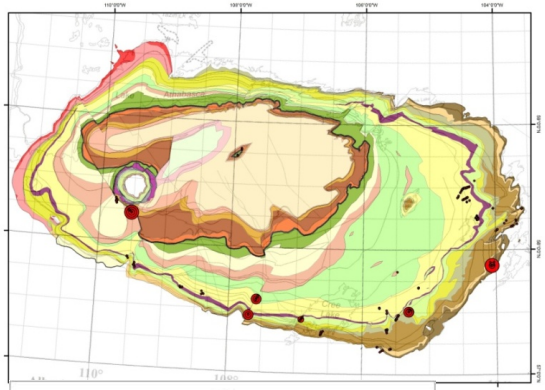
PCA Factor Scores: F5: Y HREE: Oxydized hydrothermal alteration signature?

Note that at least some of greatest anomalies occured during or after the time of main U emplacement



PCA Factor Scores: F5: Y HREE: Oxydized hydrothermal alteration signature?

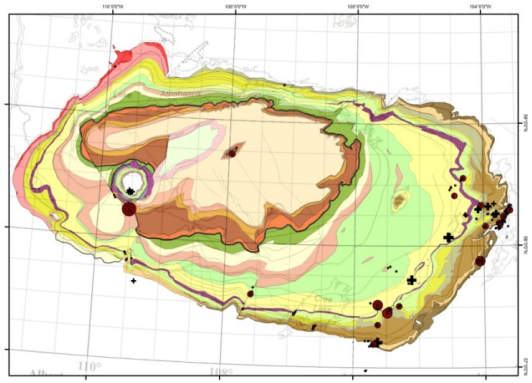
Sandstone F2 HREE U1

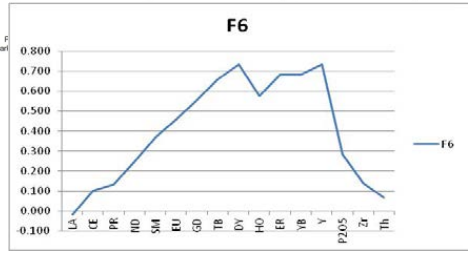




in Mineralized areas

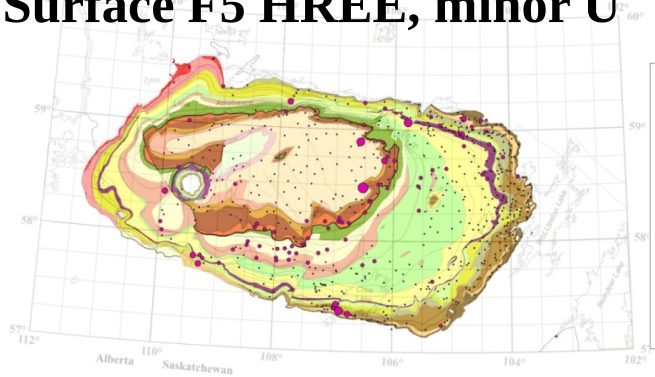
Bsmt F6 HREE U2

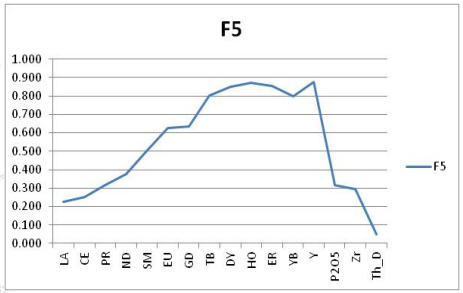




REE loadings of the factors

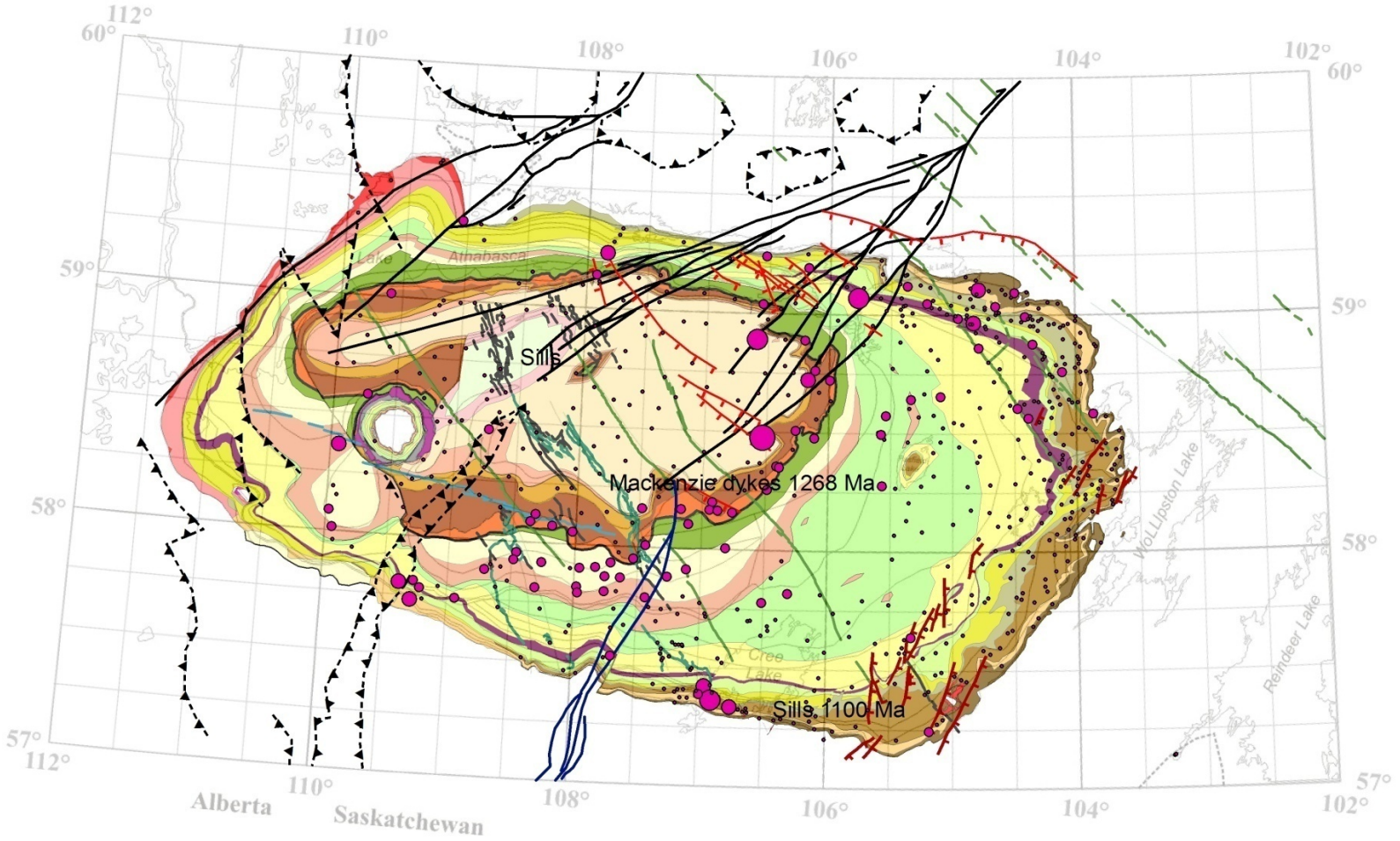
Surface F5 HREE, minor U





PCA Factor Scores: F5: Y HREE: Oxydized hydrothermal alteration signature?

PCA Factor Scores F5: Y HREE - Oxydized hydrothermal alteration signature?
Faults with activity during time of Forward Orogeny and U mineralization
Dykes and sills



Conclusions

-Multivariate analysis of multielement geochemical data from barren and mineralized drill core can define element suites that reflect sedimentary, diagenetic and alteration processes.

-The distribution of some factors helps to identify and map structural or sedimentary zones important **in focussing hydrothermal systems**, sediment source areas, and diagenetic facies.

-Related factors in mineralized and barren rock may permit the interpretation of barren rock as a past pathway for hydrothermal fluids.

-These results should be intergrated with geochronological and structural studies

Peridot Geoscience Ltd.

Application of Regional Geochemical Datasets to Uranium Exploration in the Athabasca Basin, Saskatchewan

D.M. Wright[1] and E.G. Potter[2]

[1] - Peridot Geosciences Ltd., Kanata, ON, don@peridotgeo.com

[2] - Geological Survey of Canada, Ottawa, ON, epotter@NRCan-RNCan.gc.ca

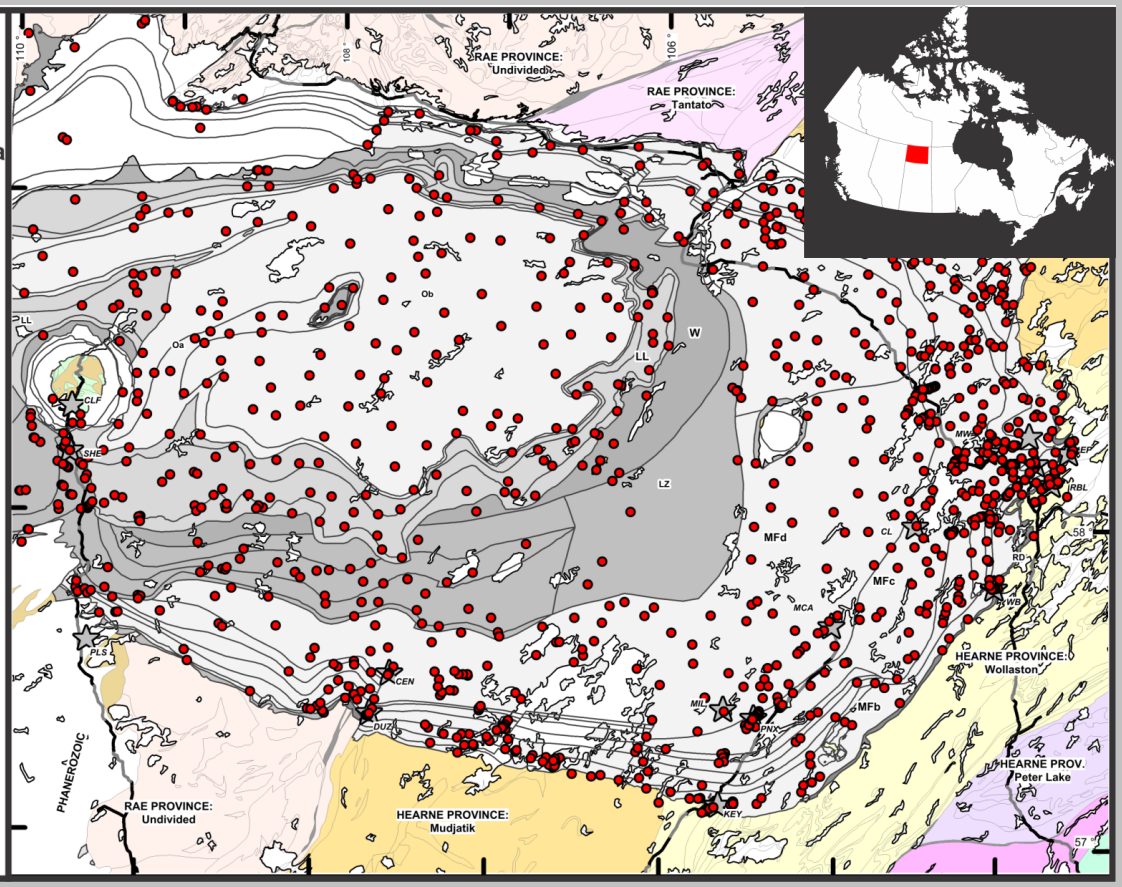
Regional Geochemical Data Patterns
Approach

GSC Open File 7495[1]

- Compilation of:
  - SGS Data Files
  - Mineral Assessment Data
  - Other GSC Open Files
- ~20,000 Athabasca Group Samples (ver. 2014.2, in press)
- Athabasca Group Samples within 50 m of surface

GSC Open File 7614[2]

- Interrogation of Athabasca Group Multielement Data
- Definition of four (4) inter-element processes:
  - Uranium - Thorium
  - Yttrium - Phosphorous
  - Magnesium - Lithium
  - Copper - Cobalt

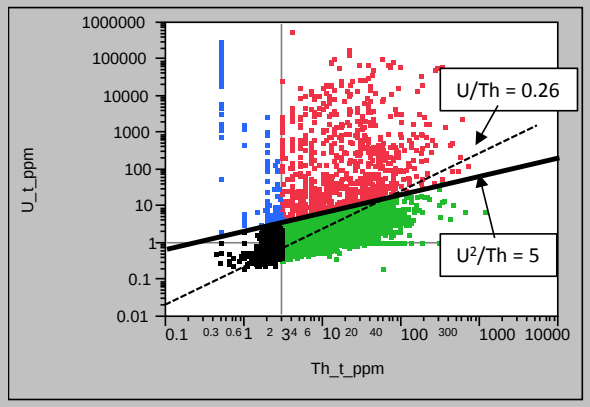


1: Wright et al., 2014 **2**: Wright and Potter., 2014 **Background Lithology**: SK Geological Atlas, 2014

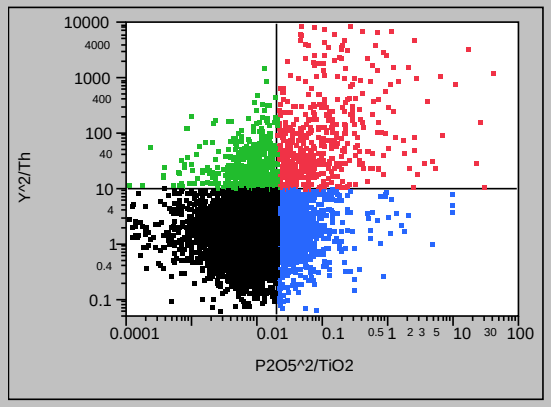
Regional Geochemical Data Patterns

Geochemical Processes

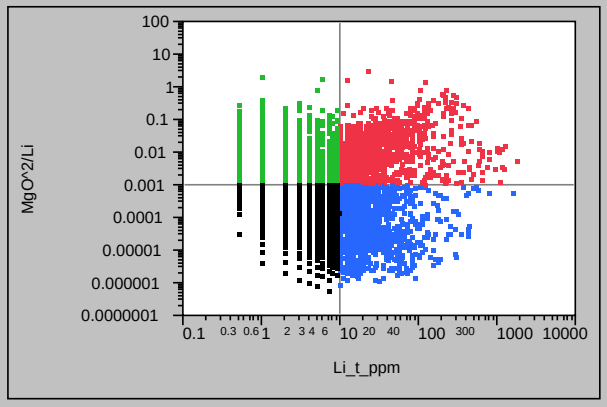
Process 1 - Uranium Enrichment



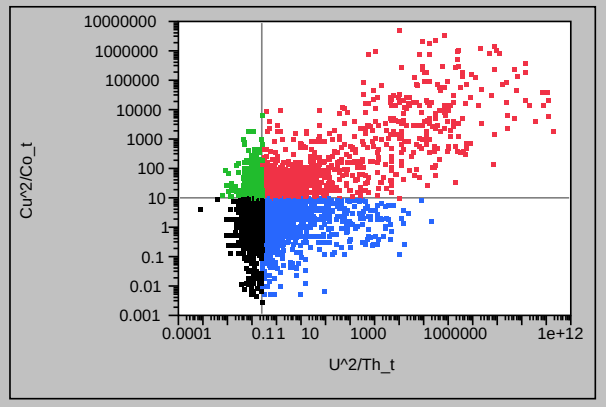
Process 2 - Y^2/Th vs. $P_2O_5{}^2/TiO_2$



Process 3 - MgO^2/Li vs. Li



Process 4 - Cu^2/Co vs. U^2/Th

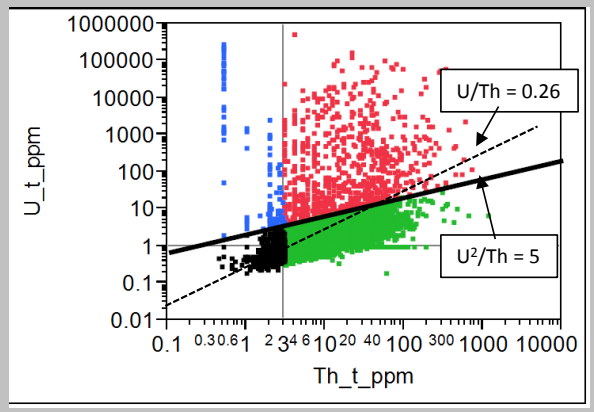


Wright and Potter., 2014

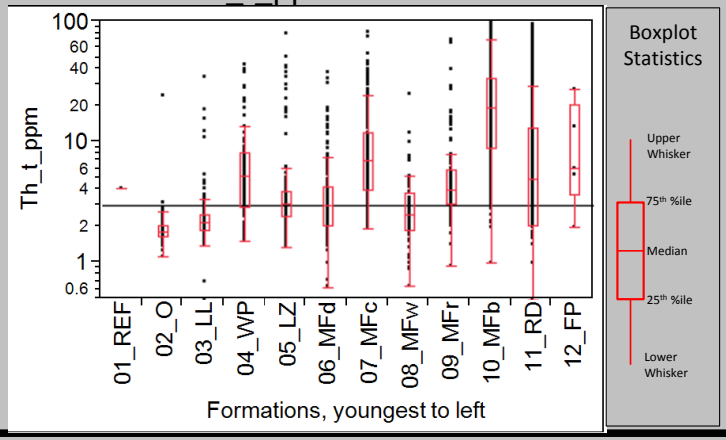
Regional Geochemical Data Patterns
Uranium vs. Thorium

- Uranium mineralization = enrichment of uranium relative to thorium
- Best modeled using the ratio U^2/Th = U x U/Th to isolate mobilized U from background U-Th patterns
- *Note: U/Th = 0.26 (Upper Continental Crust Average, Cuney 2010) does not model actual U-Th relationship.*
- Several formations display high average Th contents, requiring the use of the U^2/Th ratio to clearly distinguish uranium enrichment
- The highest average U^2/Th values occur in the Wolverine Point Formation (25^{th} $\%^{ile}$ = 0.25)
  (related to regional stratabound U-rich F-apatite cement)

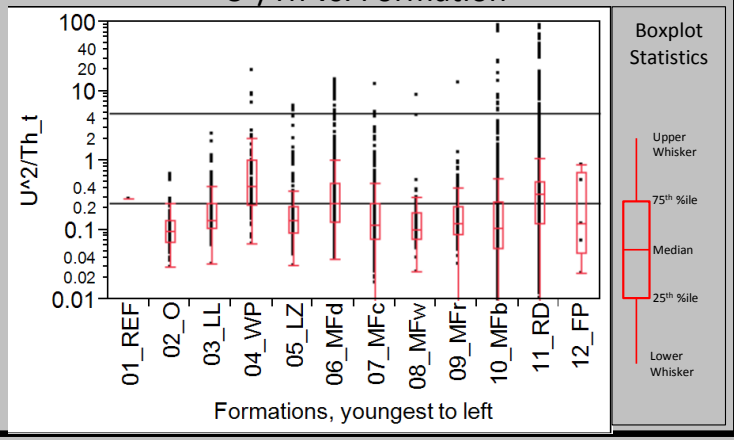
U vs. Th



Th_t_ppm vs. Formation



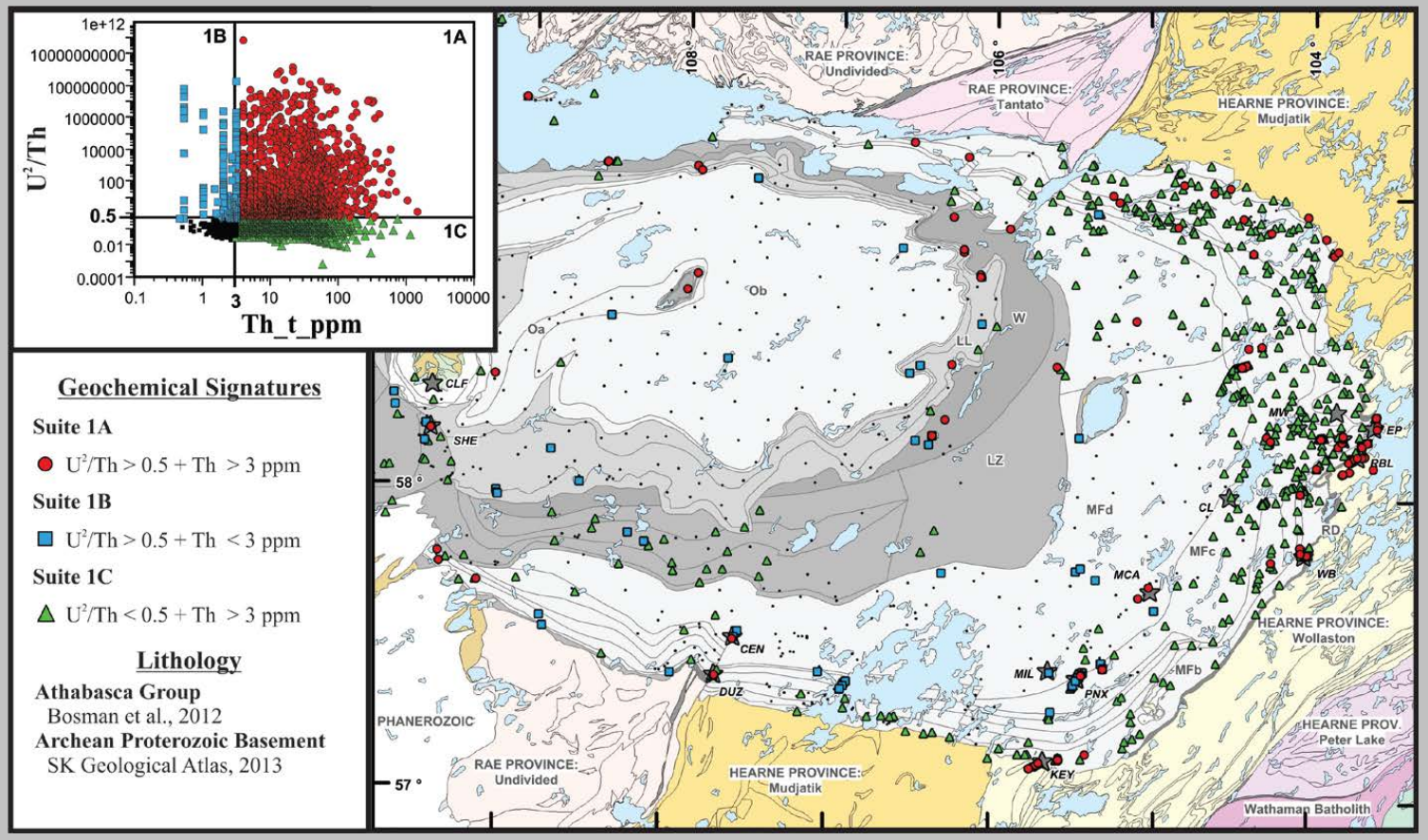
U²/Th vs. Formation



Wright and Potter., 2014

Regional Geochemical Data Patterns

Uranium vs. Thorium



Wright and Potter., 2014

Regional Geochemical Data Patterns

Yttrium vs. Phosphorous

Yttrium – Phosphate Alteration

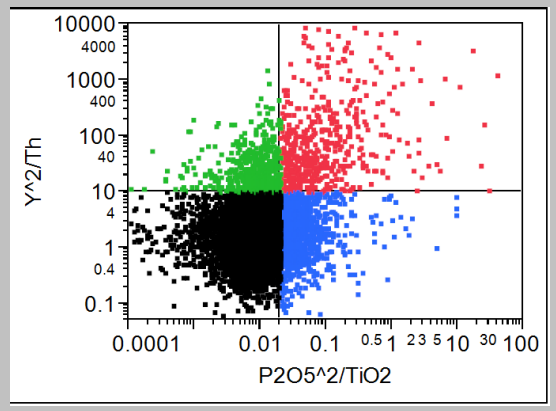
- Fluorapatite, xenotime and aluminum phosphate sulphates record hydrothermal alteration (see notes)

Key Y^2/Th vs. $P_2O_5{}^2/TiO_2$ Groups

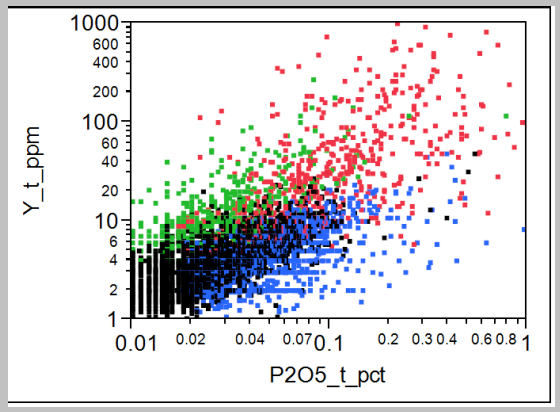
- Red = [$Y^2/Th >= 10$]* + [$P_2O_5{}^2/TiO_2 >= 0.02$]
  - *reflect HFSE enrichment, high P_2O_5*
- Green = [$Y^2/Th > 10$]* + [$P_2O_5{}^2/TiO_2 < 0.02$]
  - *reflect HFSE enrichment, low P_2O_5*
- Blue = [$Y^2/Th < 10$] + [$P_2O_5{}^2/TiO_2 >= 0.02$]
  - *Phosphate alteration in the absence of Y enrichment*

**Highest average Y^2/Th values in Wolverine Point Fm.*

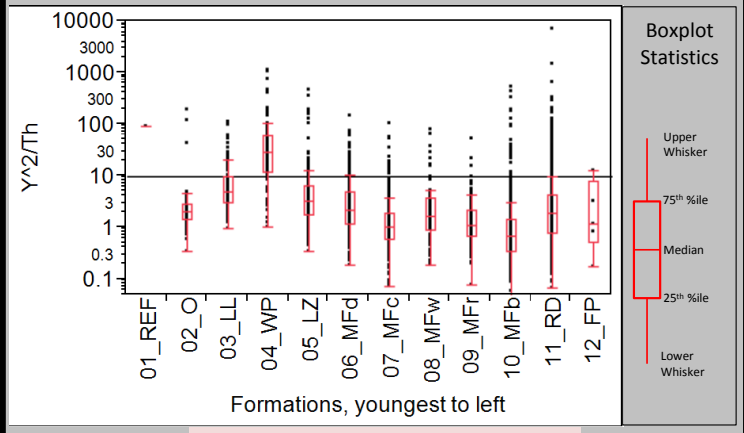
Y^2/Th vs. $P_2O_5{}^2/TiO_2$



Y vs. P_2O_5



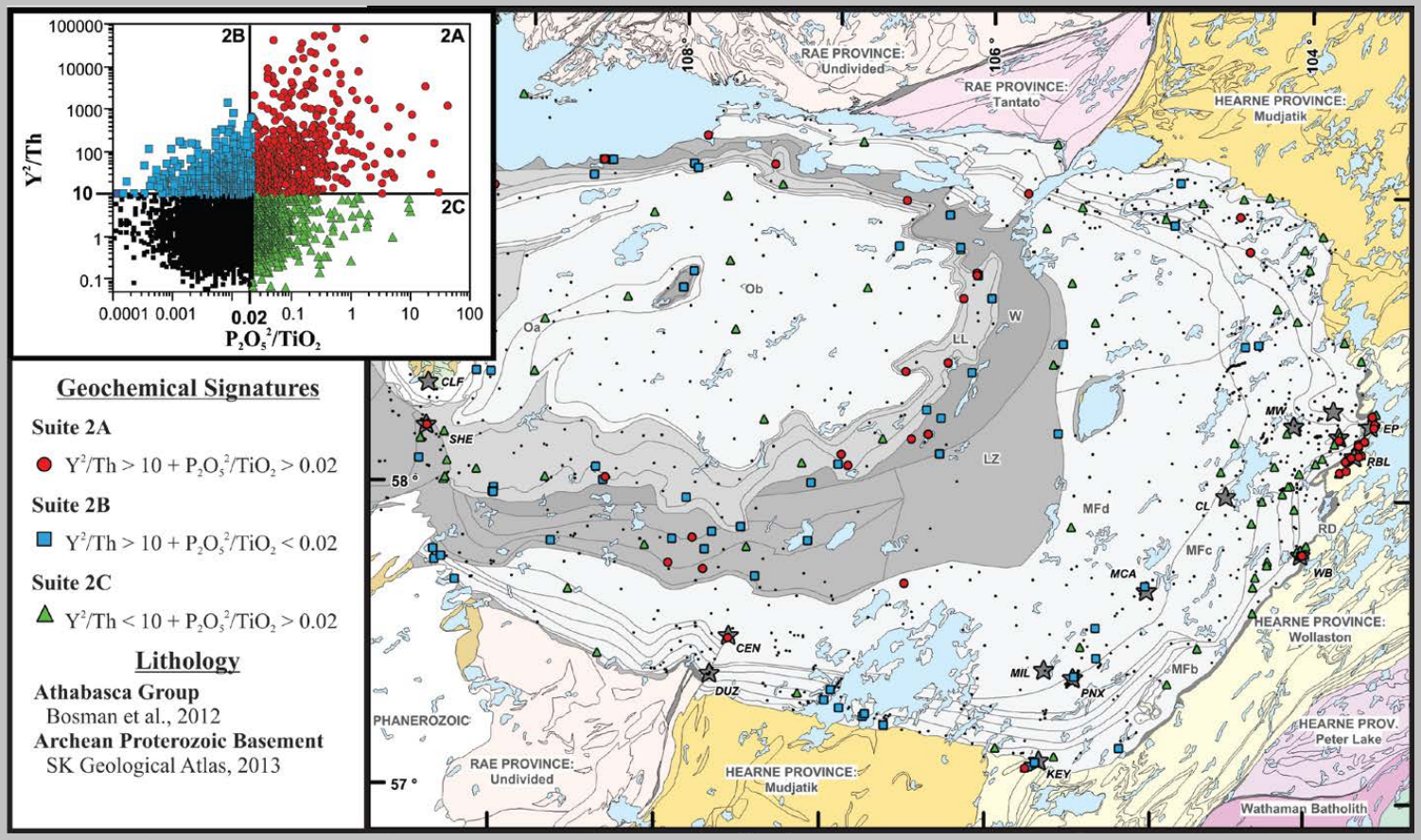
Y^2/Th vs. Formational Unit *



Wright and Potter., 2014

Regional Geochemical Data Patterns

Yttrium vs. Phosphorous



Wright and Potter., 2014

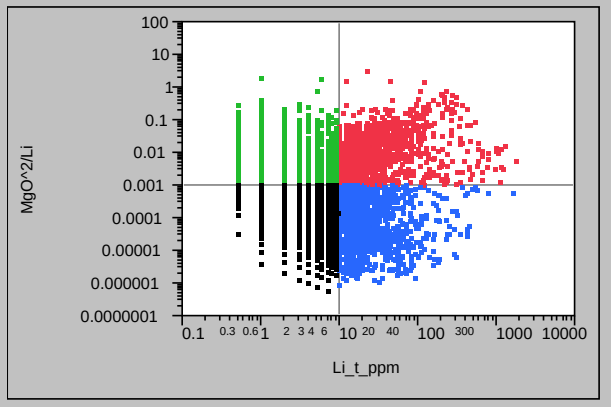
Regional Geochemical Data Patterns
Magnesium vs. Lithium

Magnesium (+/- Boron) vs. Lithium Alteration

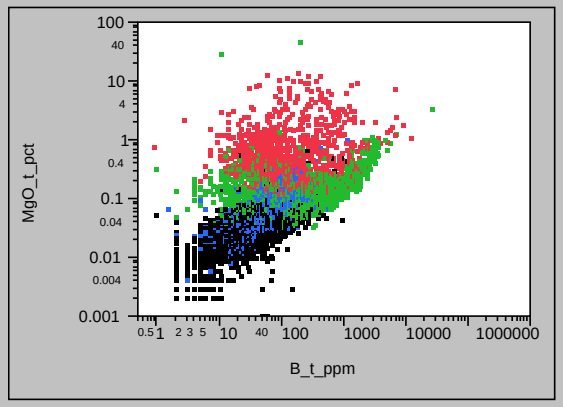
- Dravite is an alteration feature in the Athabasca Basin
- **Key MgO^2/Li vs. Li Groups**
- Red = [$MgO^2/Li > 0.001$] + [$Li > 10$]
  - *Also reflect enrichment of MgO relative to B*.*
  - *Observed stratabound in the Wolverine Point Fm.*
- Green = [$MgO^2/Li > 0.001$] + [$Li < 10$]
  - *Also reflected as $B^2/Li > 1000$**
- Blue = [$MgO^2/Li < 0.001$] + [$Li > 10$]
  - *Lithium alteration.*

* *B analyses are under-represented in AUG dataset*

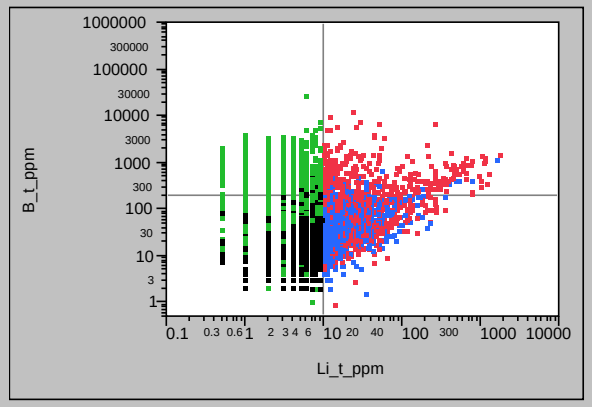
MgO^2/Li vs. Li



MgO vs. B



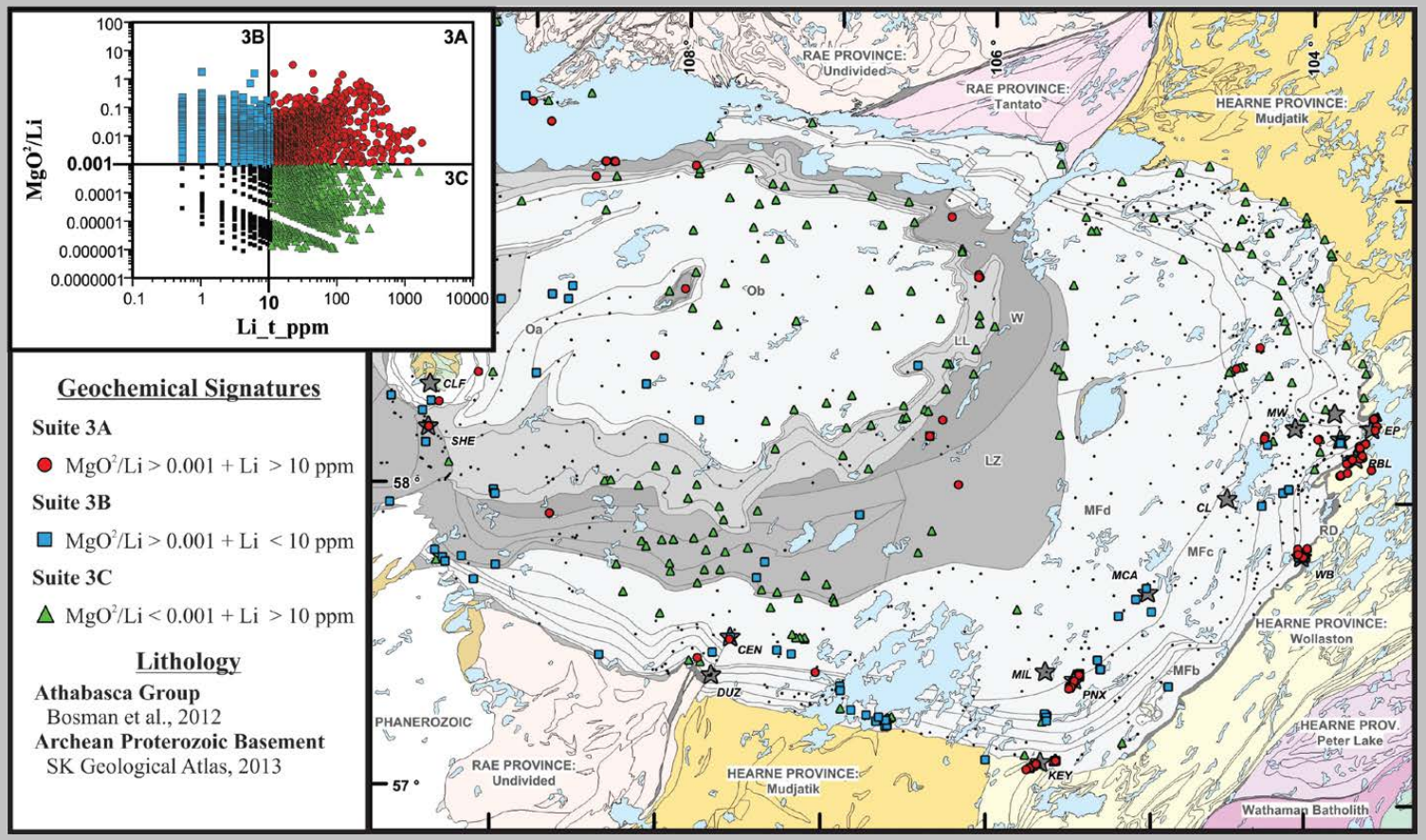
B vs. Li



Wright and Potter., 2014

Regional Geochemical Data Patterns

Magnesium vs. Lithium



Wright and Potter., 2014

Regional Geochemical Data Patterns

Copper vs. Cobalt

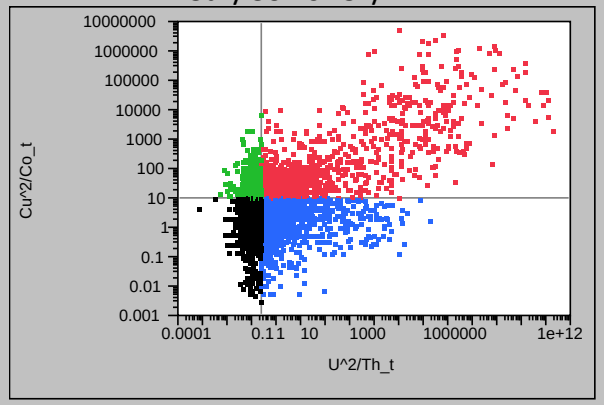
Copper +/- Uranium (re-)mobilization

- Cu^2/Co: mobilization of Cu relative to Co
- U^2/Th: mobilization of U relative to Th

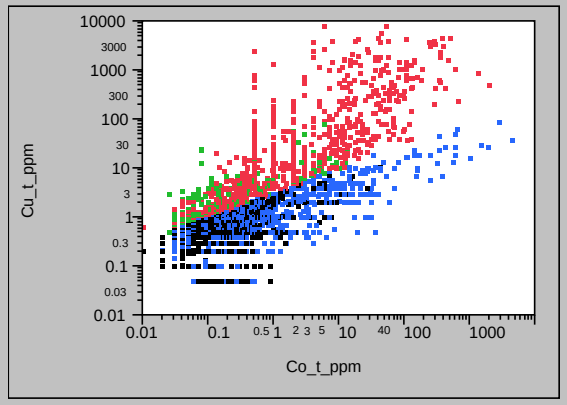
Key Cu^2/Co vs. U^2/Th Groups

- Red = [Cu^2/Co >= 10] +[U^2/Th >= 0.5]
  - *Cu mobilization + U (re-)mobilization*
- Green = [Cu^2/Co >= 10] + [U^2/Th < 0.5]
  - *Copper Alteration – low U*
- Blue = [Cu^2/Co < 10] + [U^2/Th >= 0.5]
  - *U remobilization, low Cu*.

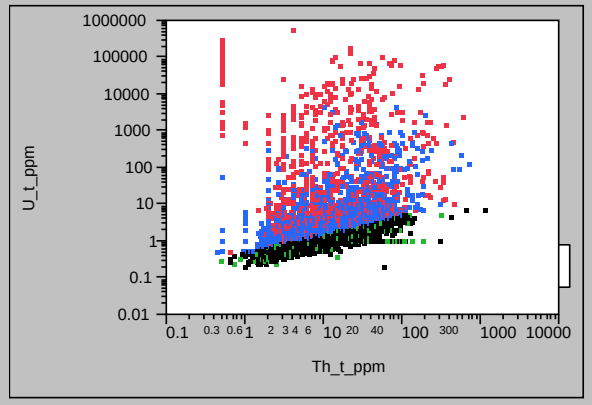
Cu^2/Co vs. U^2/Th



Cu vs. Co



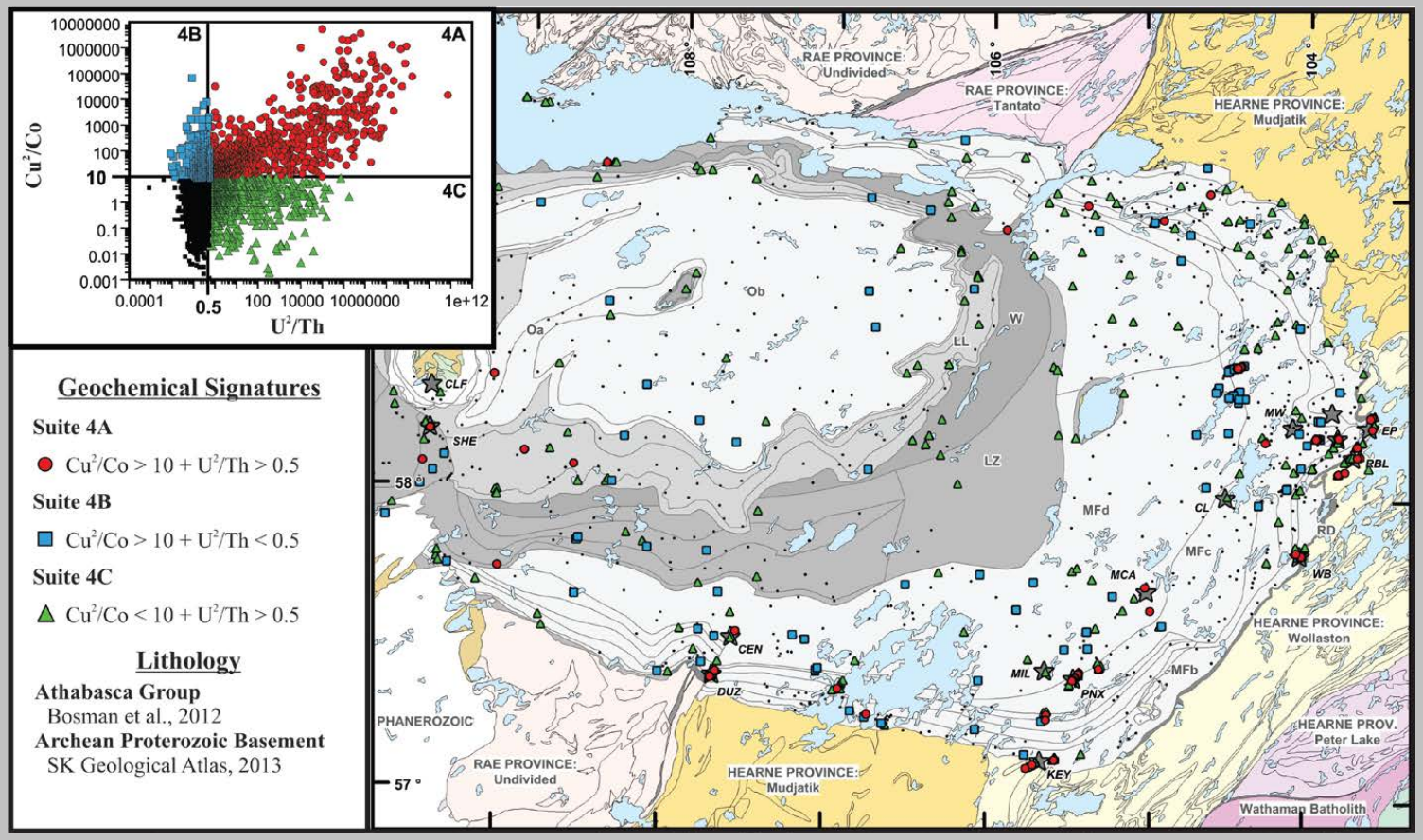
U vs. Th



Wright and Potter., 2014

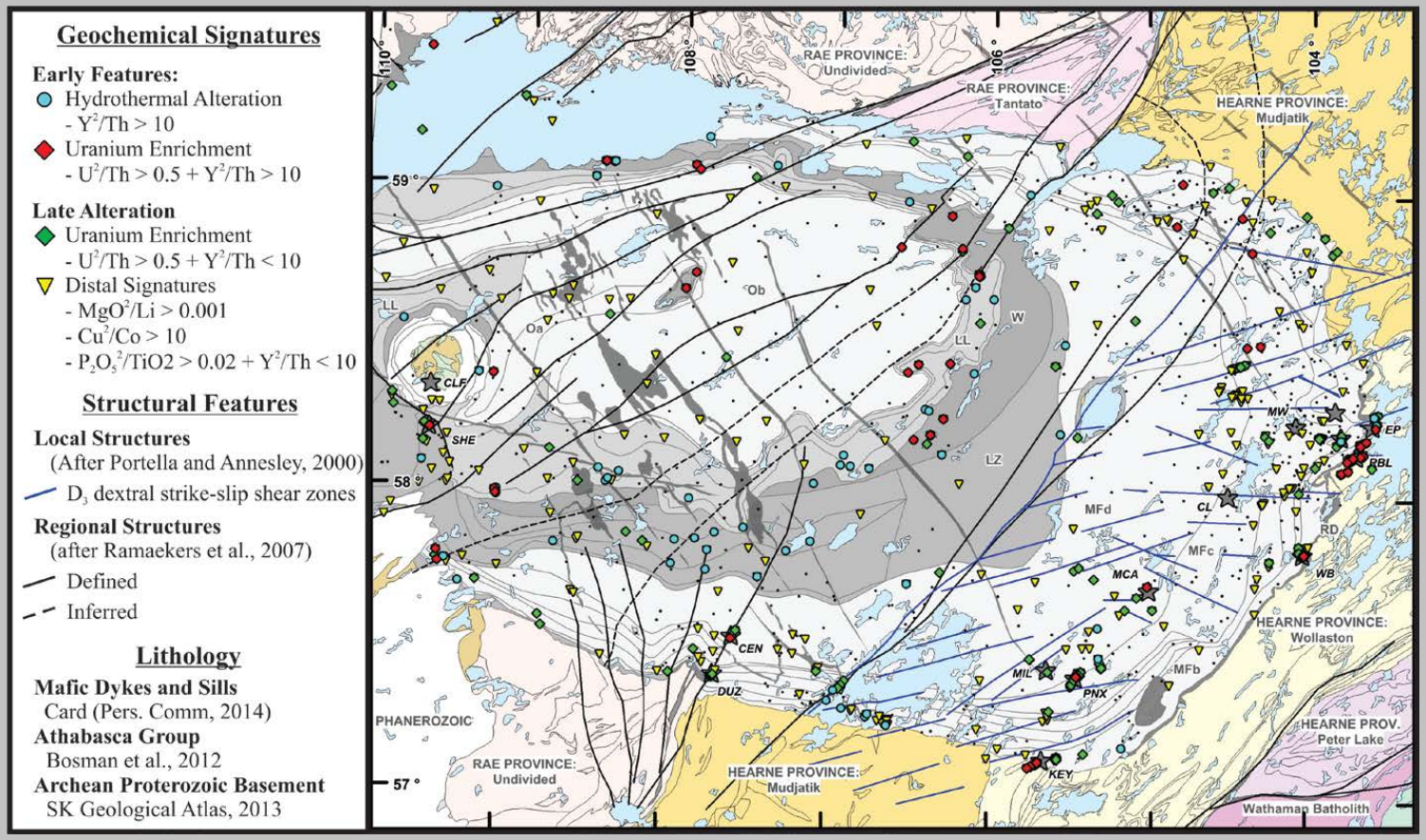
Regional Geochemical Data Patterns

Copper vs. Cobalt



Wright and Potter., 2014

Regional Geochemical Data Patterns
Summary



Wright and Potter., 2014

Geomathematical and Mineralogical Study of Sandstones Overlying Phoenix Uranium Deposits and the REE-rich Maw Zone, Athabasca Basin, Canada

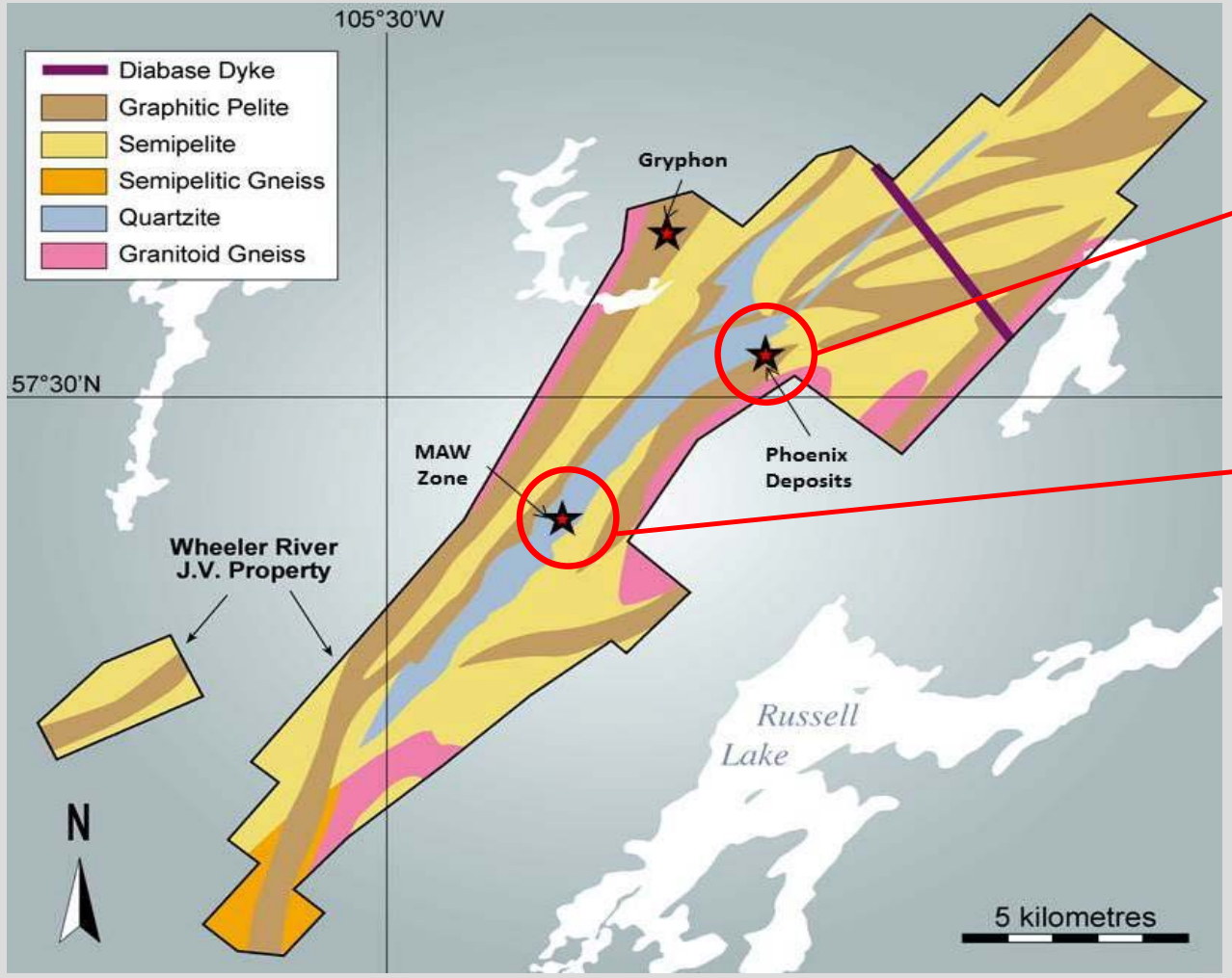
*Shishi (Chris) **Chen**[1], Keiko Hattori[1]*

Eric Grunsky[2]

Yongxing Liu[3]

1 University of Ottawa
Correspondence: schen162@uottawa.ca
2 Geological Survey of Canada
3 Denison Mines Corporation

Introduction



Phoenix Uranium Deposits (indicated resource 70.2 M lbs of U_3O_8)
Low ΣREEs, <150 ppm in sandstones

Maw Zone, high REEs (Σ REE oxides < 8.1 wt%)
Low U, <7.8 ppm

Denison Mines,2014

Objectives

1. To study elemental assemblages associated with U and REE mineralization.
2. To evaluate the relationship between the two styles of mineralization.
3. To provide a geomathematical tool to assess U and REE resource potential.

Dataset

Phoenix: 4630 samples (39 elements each)

Maw Zone: 545 samples (43 elements each)

Methodology

- Data anaysis

  QQ and box-whisker plots, data censoring and imputation

  Centered log-ratio transformation to eliminate “closure problem”

  Simultaneous RQ-mode PCA.

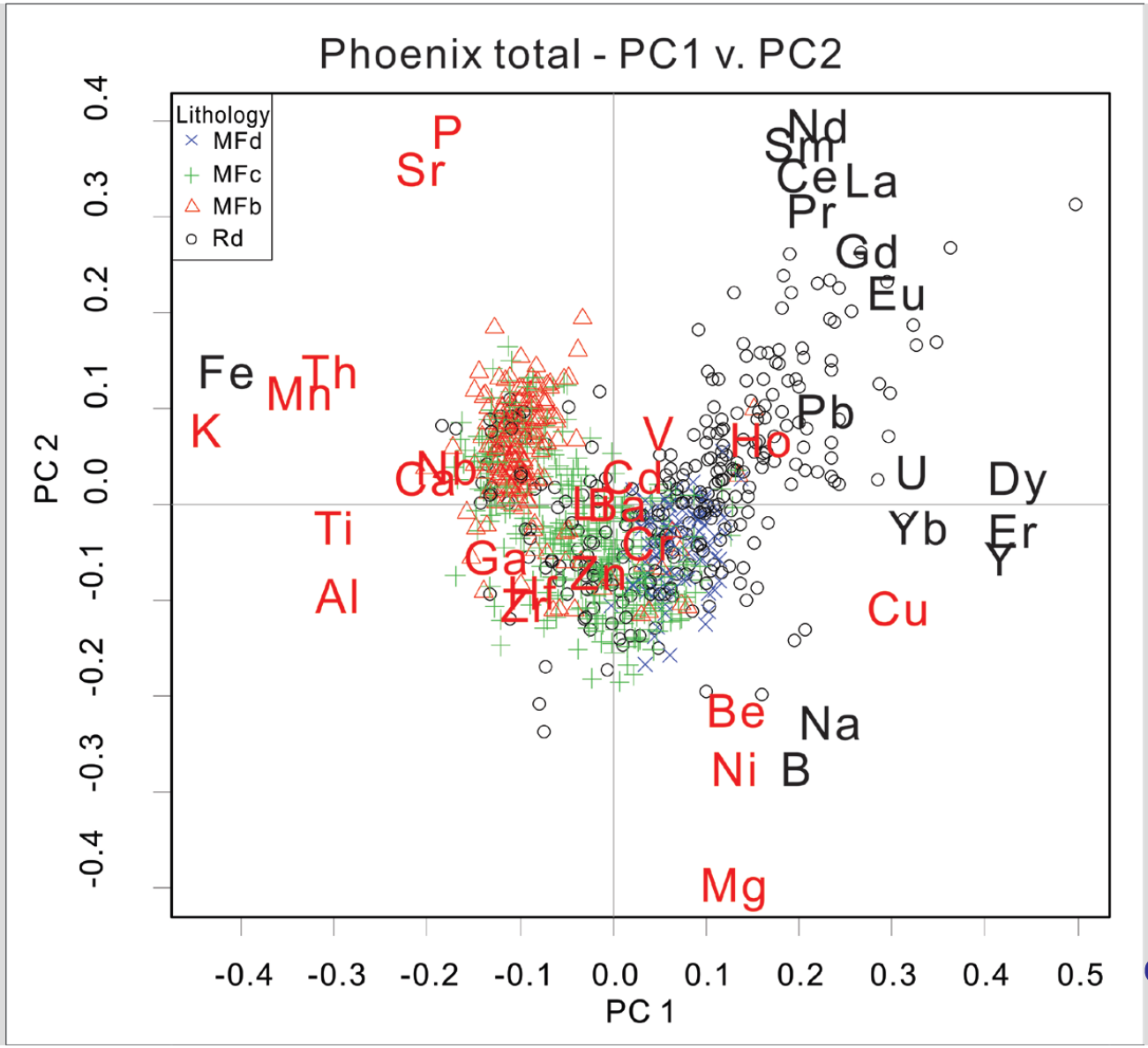
- Mineralogy

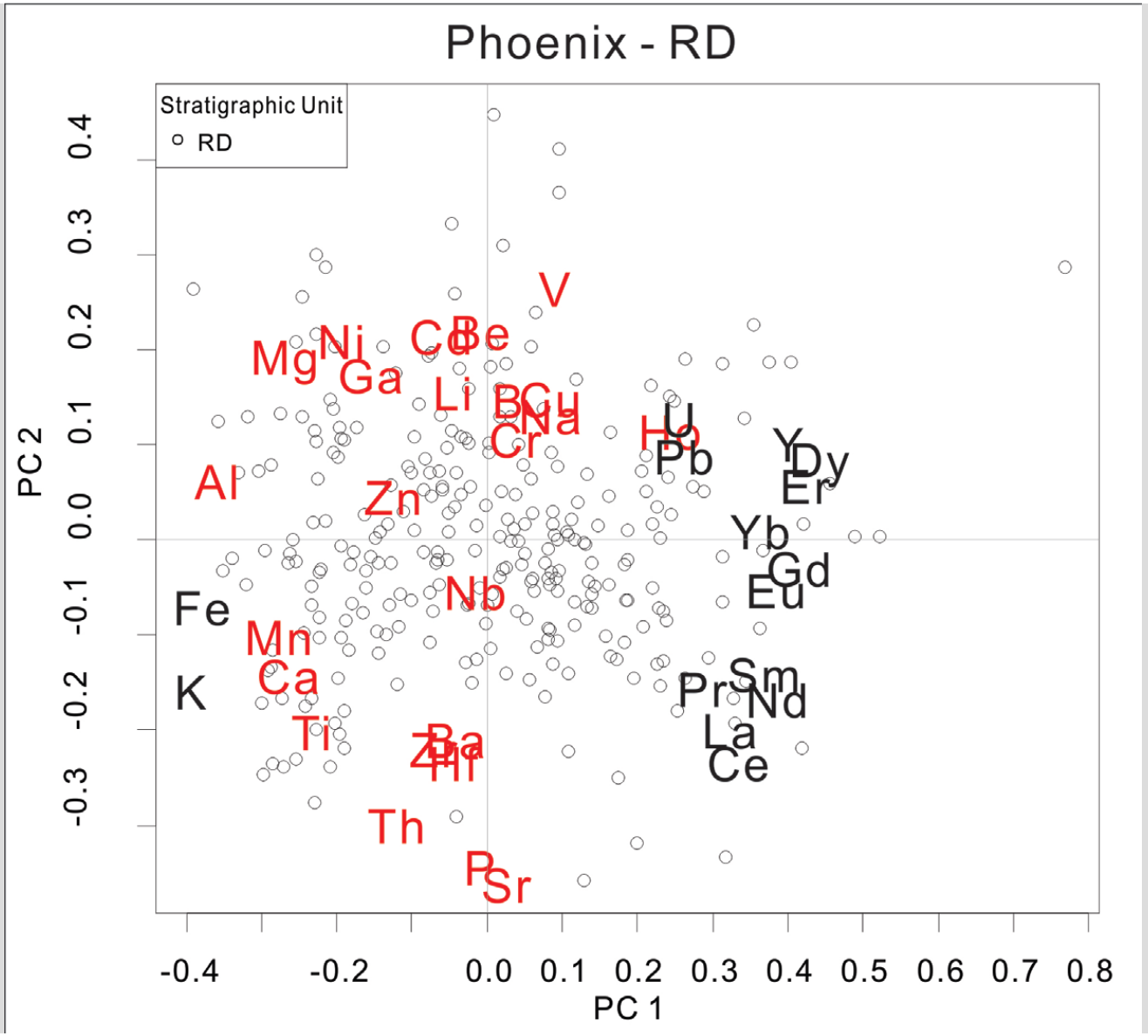
  Petrographic microscopy
  SEM with EDS

Results

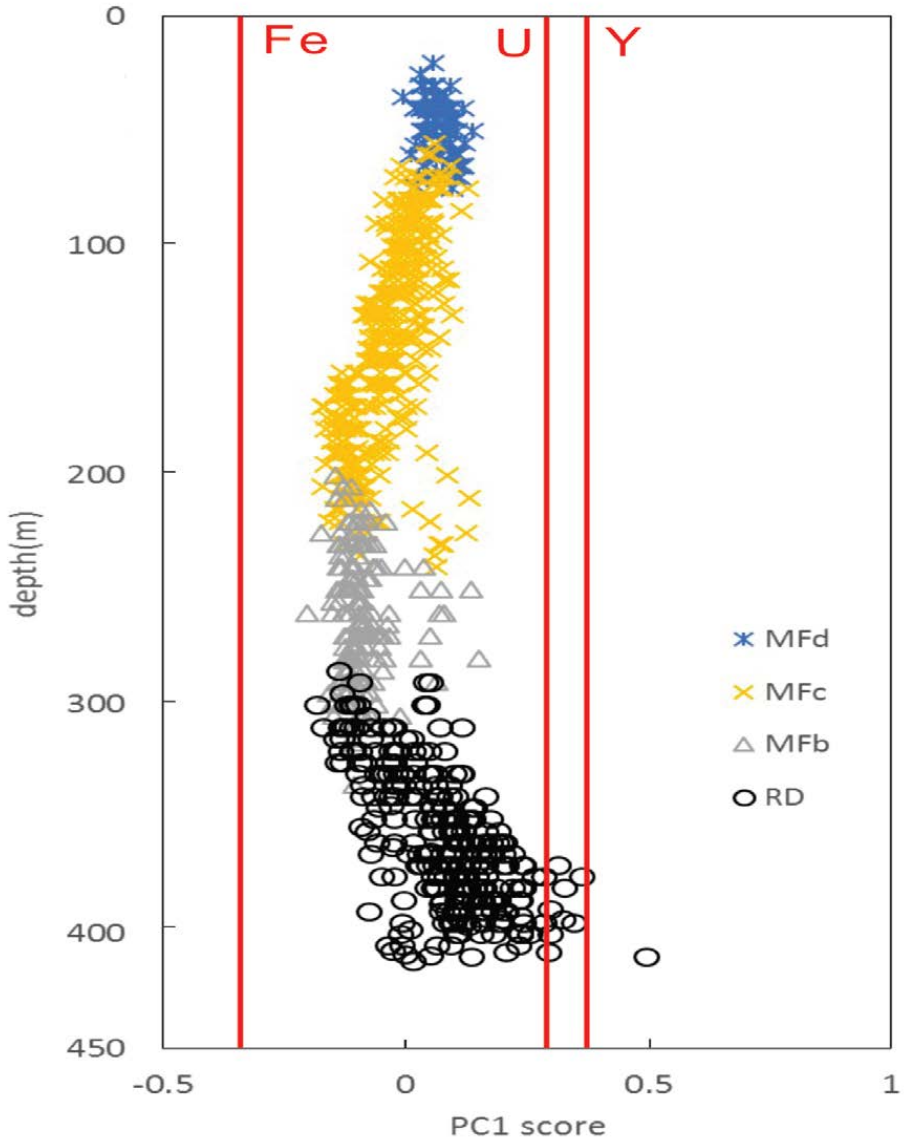
Phoenix dataset

PC1 and PC2 account for 40.2% of total variation of the dataset



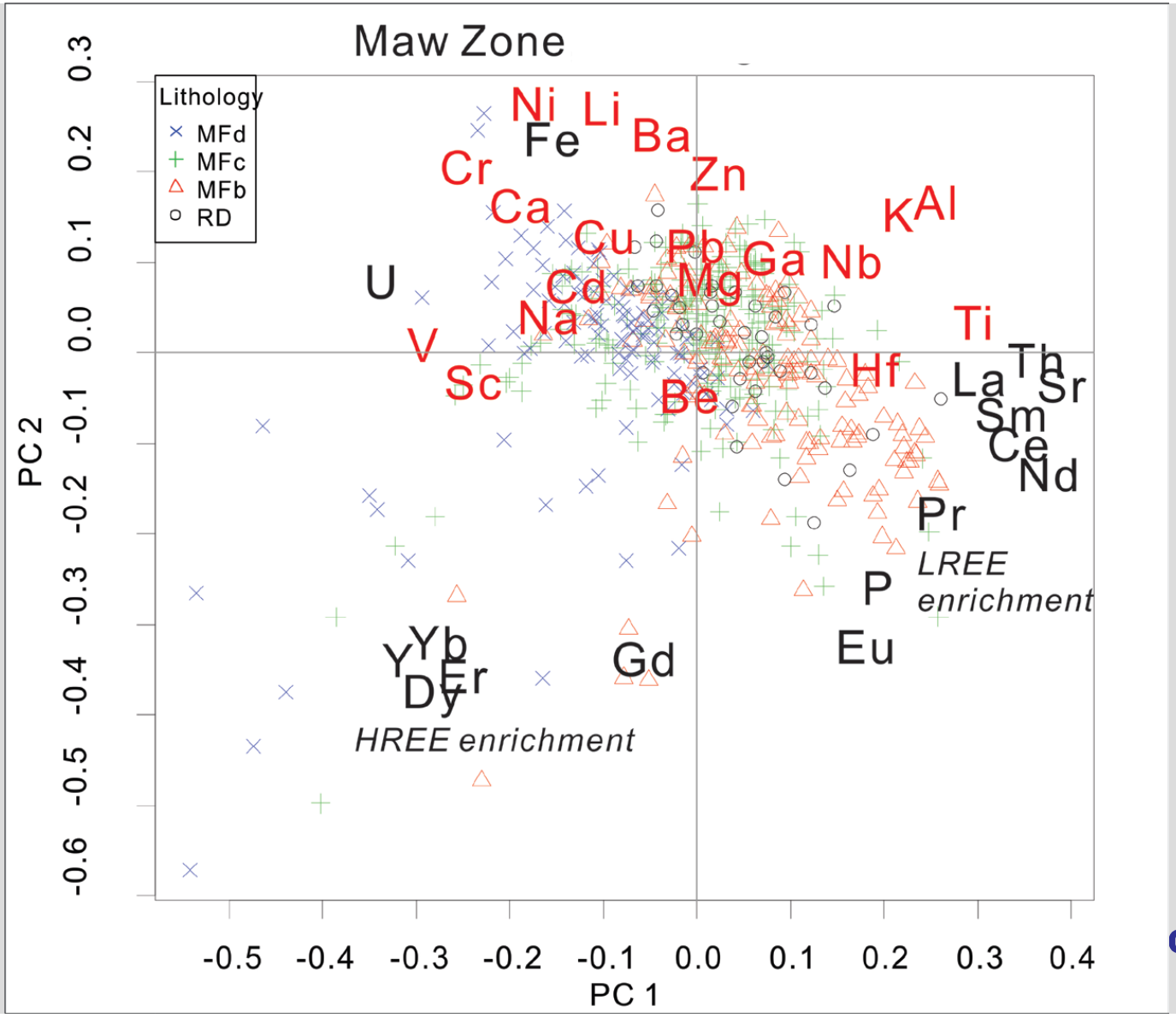

Phoenix - RD
Stratigraphic Unit
RD
PC 2
PC 1
0.4
0.3
0.2
0.1
0.0
-0.1
-0.2
-0.3
-0.4
-0.2
0.0
0.1
0.2
0.3
0.4
0.5
0.6
0.7
0.8
V
Mg
Ni
Ga
Li
Cr
Al
Zn
Nb
Fe
Mn
Ca
K
Ti
Th
Sr
U
Pb
Y
Dy
Er
Yb
Gd
Eu
Sm
Nd
La
Ce

K, Dy, Er, Fe, Y, Mn, Yb, U, Th are top 9 dominant elements in PC1 of Phoenix dataset

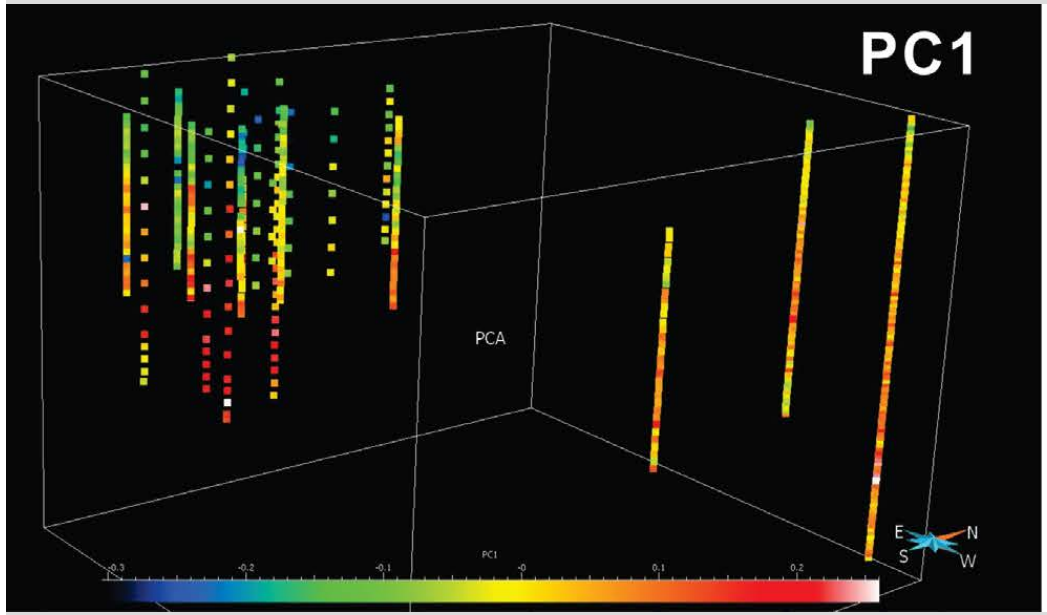


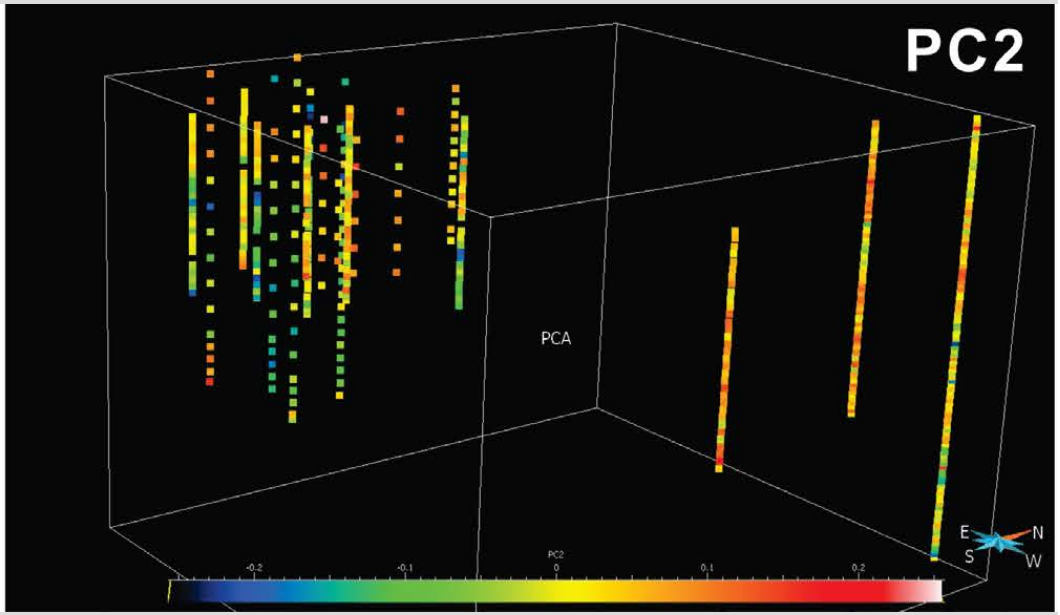
Maw Zone dataset

PC1 and PC2 account for 36.3% of total variation of the dataset



Maw Zone dataset





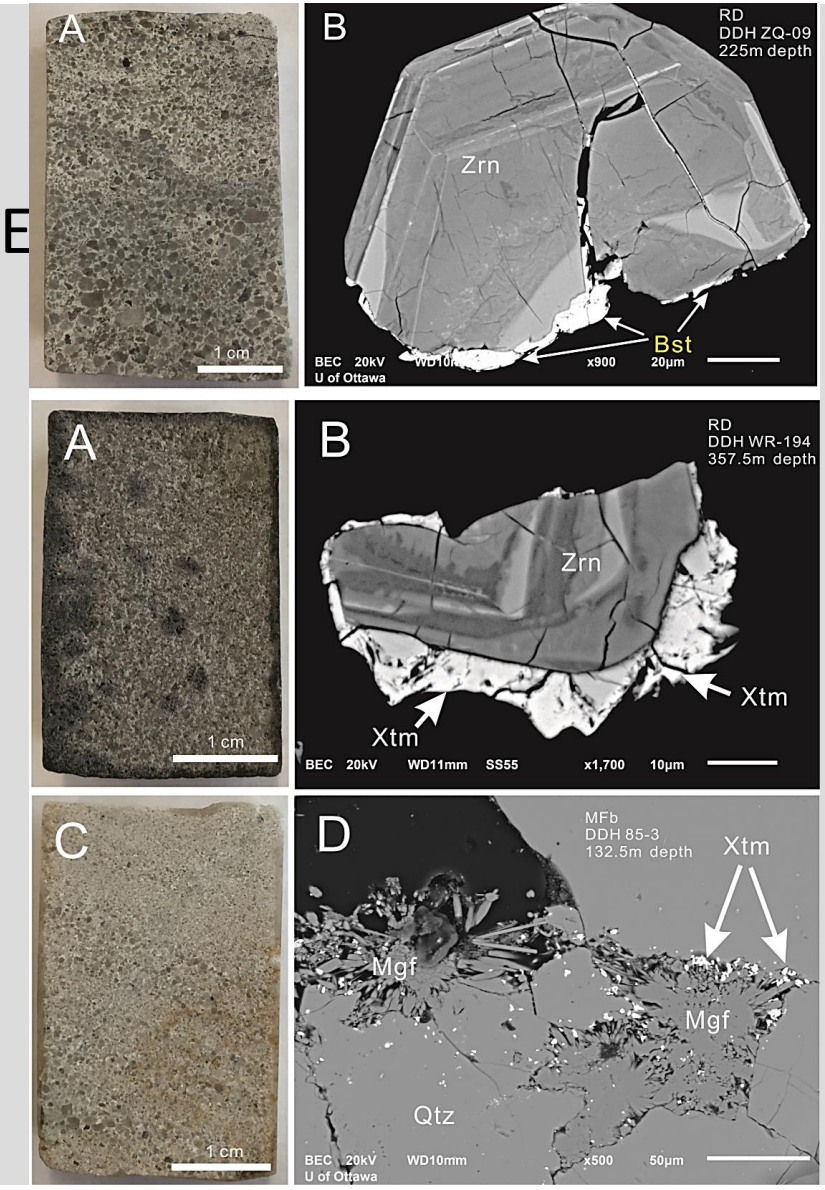
Since HREE show strongly negative scores in PC1 and PC2, this reflects enrichment of xenotime in the upper sandstone unit

TGI 4 Ore Systems

Maw Zone

Minerals hosting HREE

Note buff color
for rocks with high REE



Bst = bastnäsite
Zrn = zircon

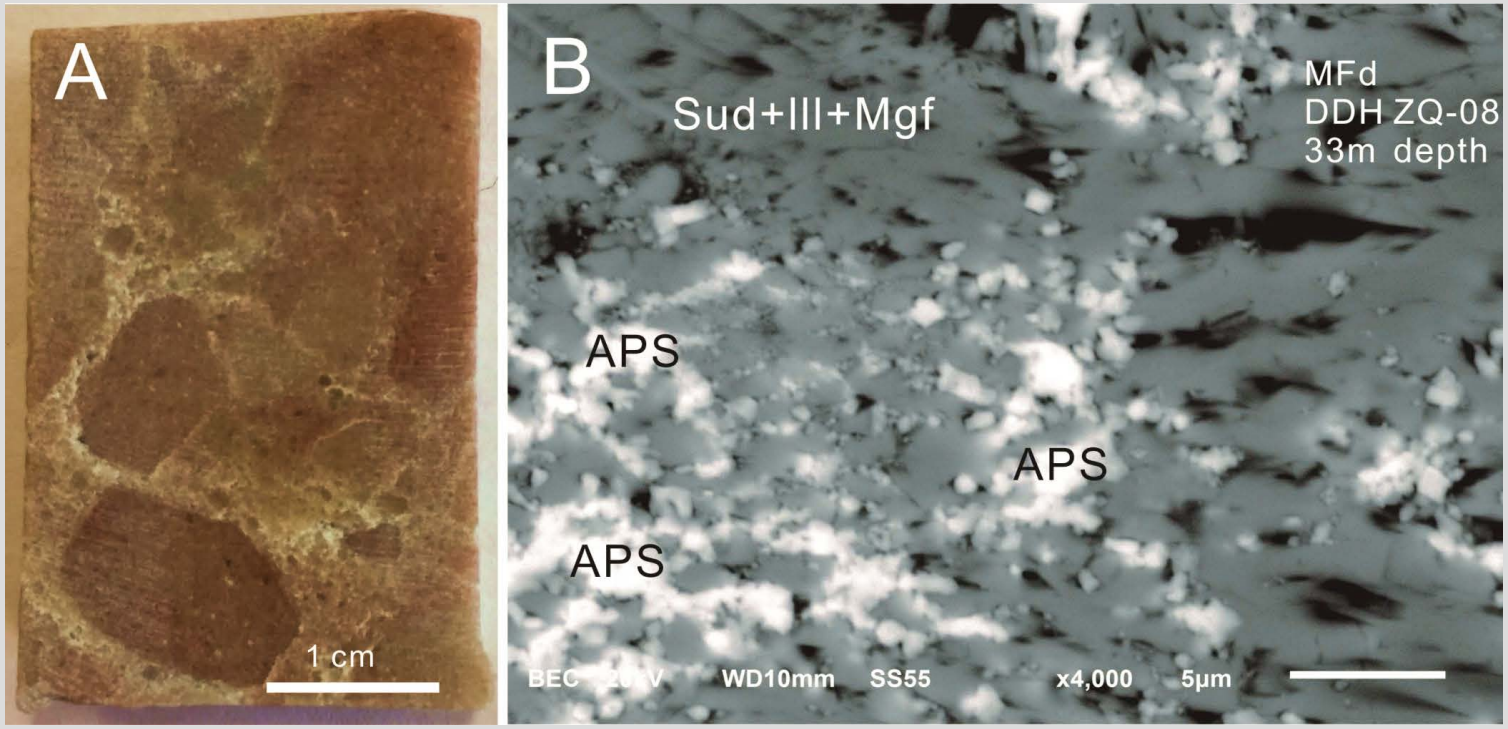
Xtm = Xenotime

Mgf = magnesiofoitite
Qtz = quartz

TGI 4 Ore Systems

Maw Zone

Mineral hosting LREEs



APS = alumino-phosphate-sulfate, Sr-LREE- Al- P-SO_4^{2-} (Svanbergite-florencite)

Summary

- The PCA shows distinct geochemical signatures of sandstone units.

Sandstones above Phoenix deposits

U is associated with HREEs+Y +LREEs + Pb

and inversely correlated with Ti+ Zr+Al+ Th

Maw Zone

relative enrichment of HREEs+Y+P suggesting xenotime

grouping of LREEs+Sr+Th+P suggesting monazite and/or APS minerals.

The mineralogical study confirmed xenotime and APS minerals

Summary

Maw Zone

- REEs inversely correlated with Fe, Cr, and V.
  Late reduced fluids brought REE, and leached Fe oxides

- The absence of U mineralization is explained by
  (i) oxidizing fluids contained low U.
  OR
  (ii) U-bearing fluids did not encounter reduced fluids to precipitate U.
  (timing of the two fluids were different)

Implication

- Mapping PC scores of rocks can assess the potential for U and REE mineralization in the area

Acknowledgements

We thank Denison Mines Ltd for providing us the geochemical data, logistic support, and hospitality during the field work.

The research project is funded by a grant to K.H. from Natural Resources of Canada through the TGI-4 program.

And thanks to Ian O'Connell, Nickolas Dudek and May Devine for help in field work.

Questions?



Maw Zone outcrop

TGI 4 Ore Systems

Preamble

- TGI-4 supported project started in 2011 with two components

1. Identifying fertile structure using alteration minerals
   (Erin Adlakha gave a presentation this AM)

2. Detecting buried deposits using surface media.
   This presentation

Summary

Surficial geochemical Surveys over concealed uranium ore of the Phoenix and Millennium deposits in the Athabasca Basin

Keiko **Hattori**

Michael **Power,** Chris (Shishi) **Chen,** Jack **Dann,**
Austin **Krahenbil,** Nickolas **Dudek**
Chad **Sorba,** Tom **Kotzer,** Eric **Potter**

Outline

- Introduction
  Objectives of the project
- Project areas
- Highlight of results

  Soil (reproducibility, metal sites in humus)
  Sandstones (high metals above ore, “chimney” in ss)
  Gas (radon and helium)
- Summary



Objectives

- Can we detect anomalies in surface media over deeply buried deposits?
- Which media (soil, sandstones, water, gas) is the best ?
- How anomalies are spatially related to deposits, and other features (faults, glacial deposits, swamps)?



Project Sites

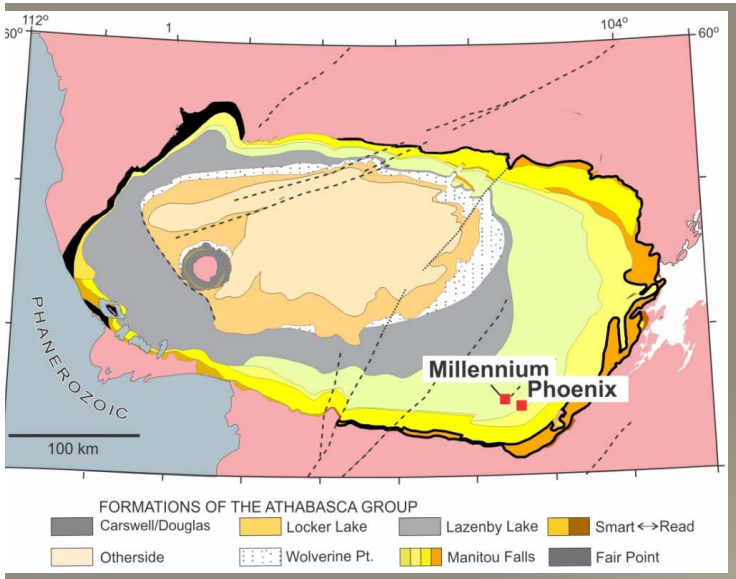
No apparent surface expression.

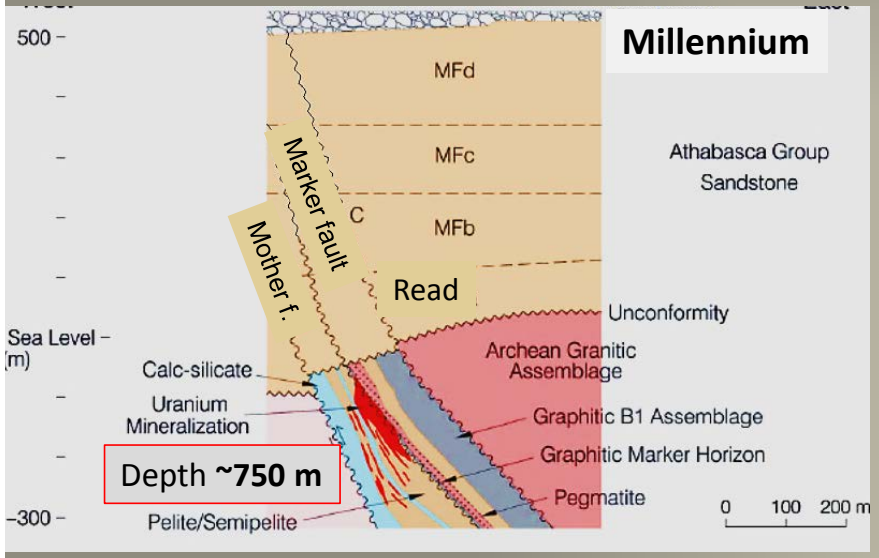
Phoenix (70.2 Mlb U_3O_8)

(Roscoe, 2014)

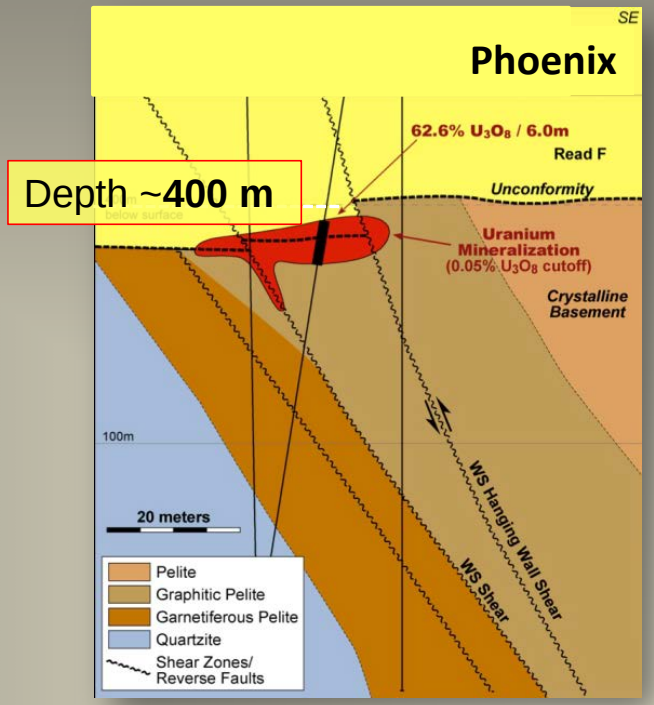
Millennium (75.9 Mlb U_3O_8)

(Cameco Corp, 2014)





Wood et al. 2012



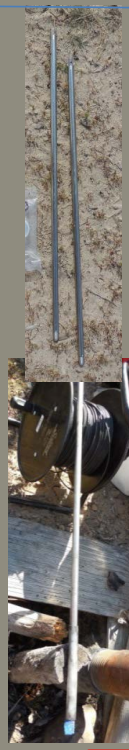
Gamelin et al. 2010

Samples examined

Water Water at a given depth | Radon in water | Helium in water | Rn in pore fluid of soil | Soil



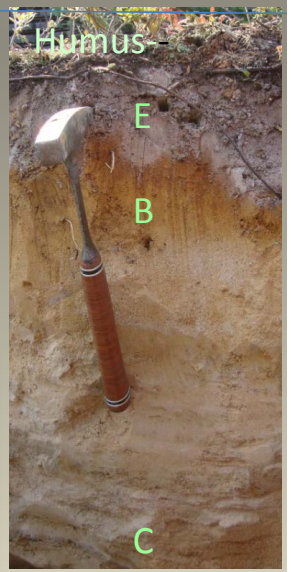
Millennium







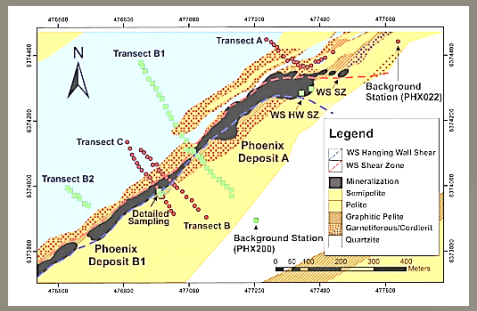


Intro → Area/Sample → soil → sandstone → Rn, He → Summary

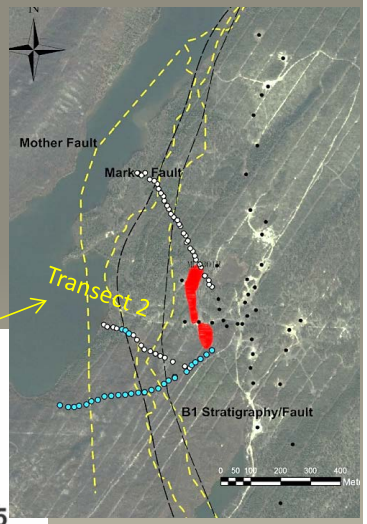
Metals in soil along traverses

Phoenix

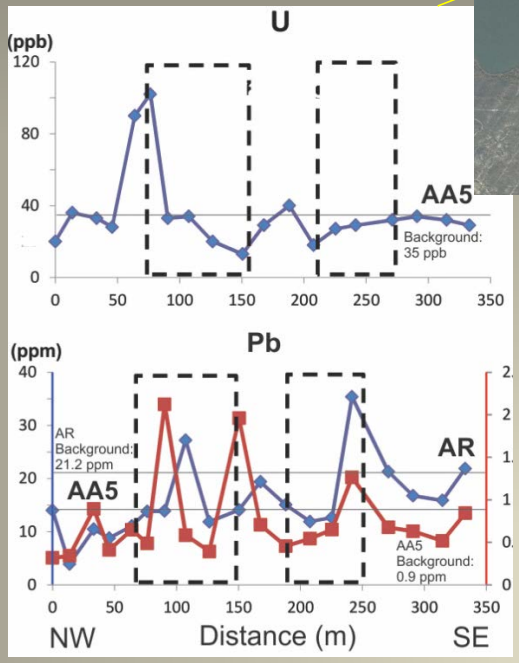
High metals on the surface projection of the deposits and faults



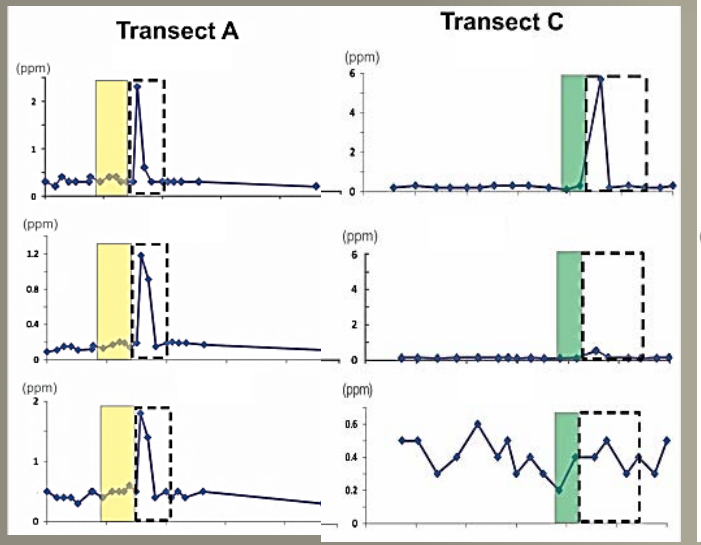
Millennium



B-horizon,, ammonia acetate

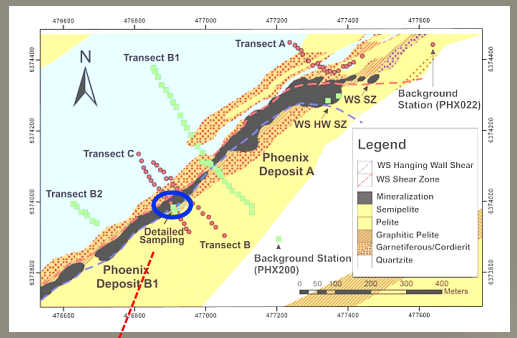


Humus, aqua regia digestion

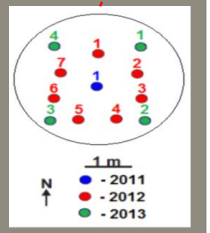


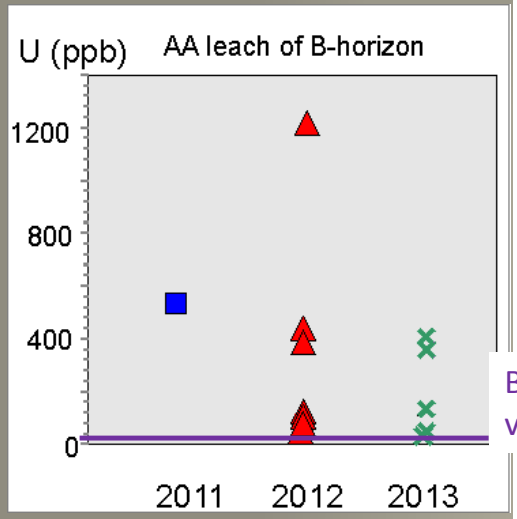
Ore WS Shear

Metal anomalies reproducible?, Phoenix

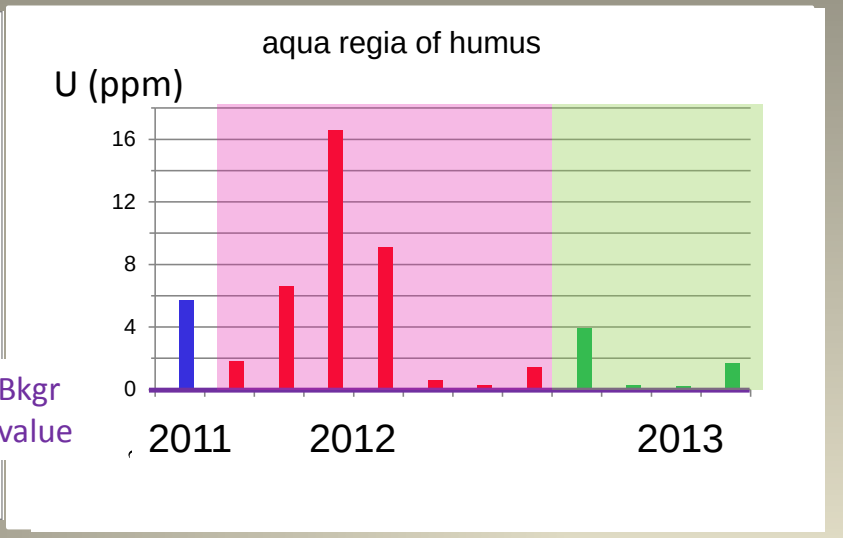


- Values vary, but high
- Sampling in 2012 and 2013, confirming the robustness of anomalies.



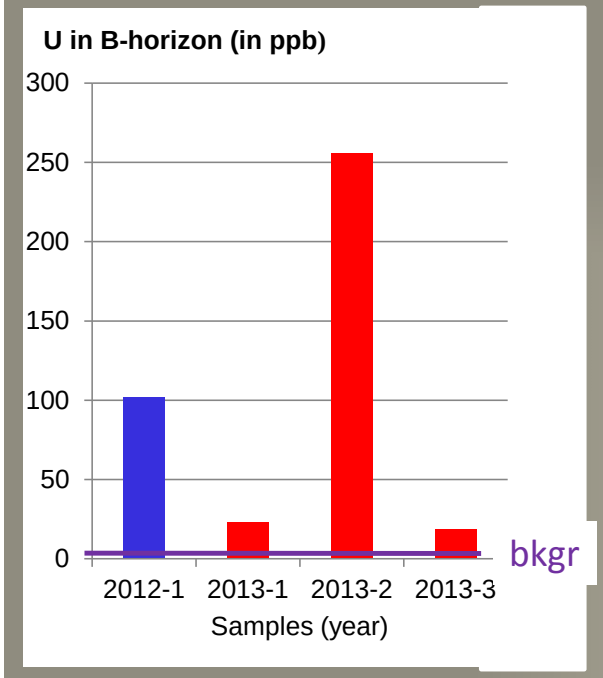


Bkgr value



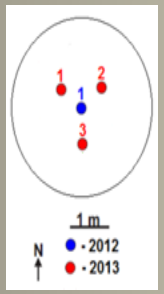
Krahenbil et al., 2014, GSC OFR 7611

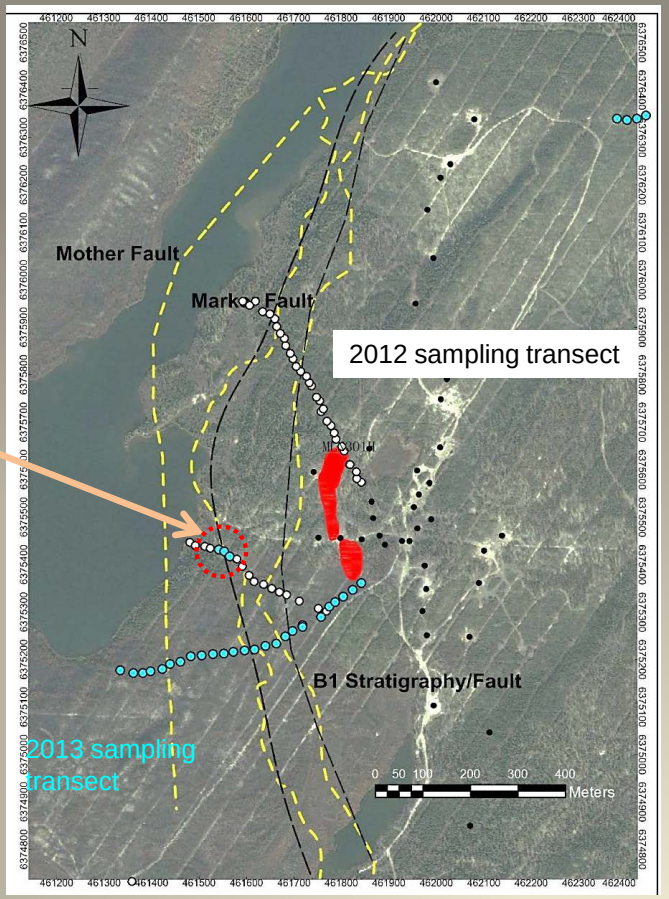
Soil anomalies reproducible?, Millennium



Krahenbil et al., 2014, GSC OFR 7611

Reproducibility test sites in 2013



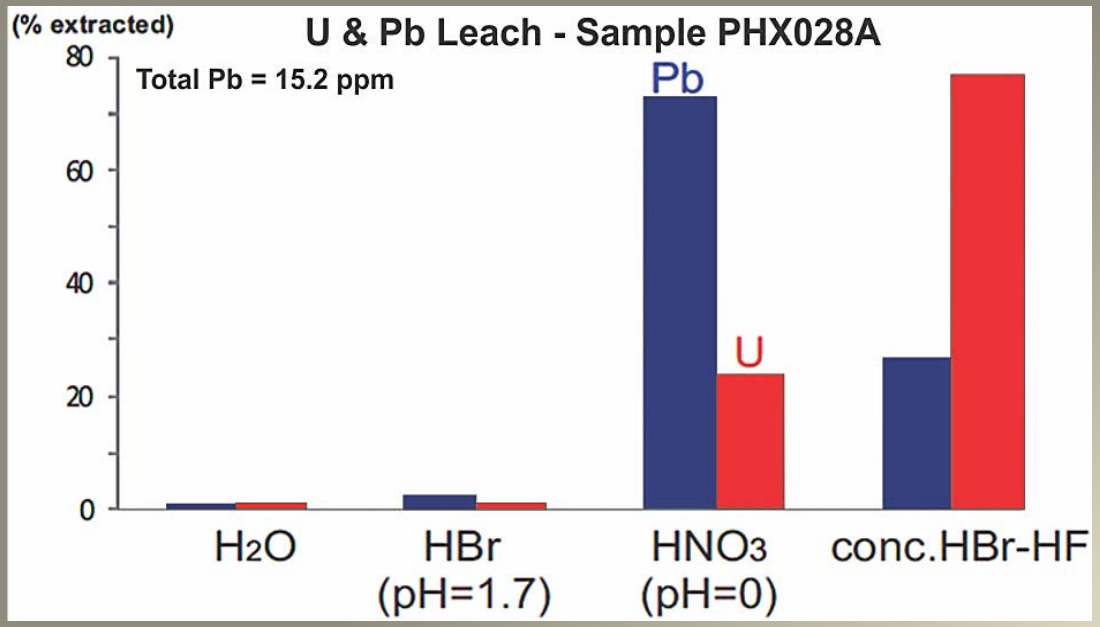


metal in humus, not on the surface

Cu, Ni, Co, As, U, Pb were not extracted in H_2O and weak acid

.

Metals are not adsorbed on the surface, Al-O-OH or Fe-O-OH.
Metals are tightly fixed in organics in humus.

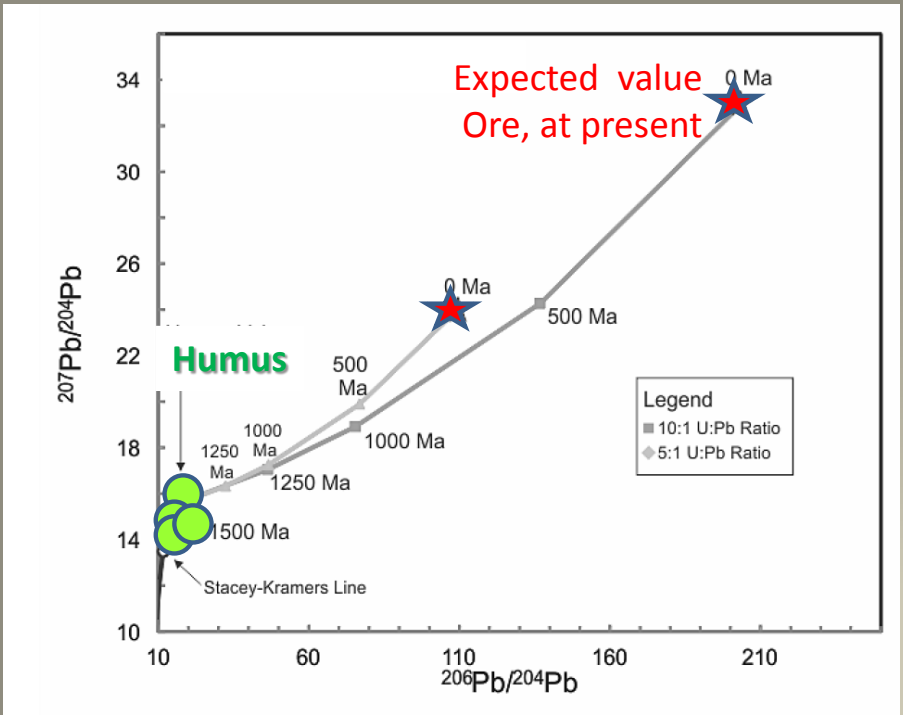


Power et al., 2012, GSC Open File Rep. 7257

Source of metals in humus

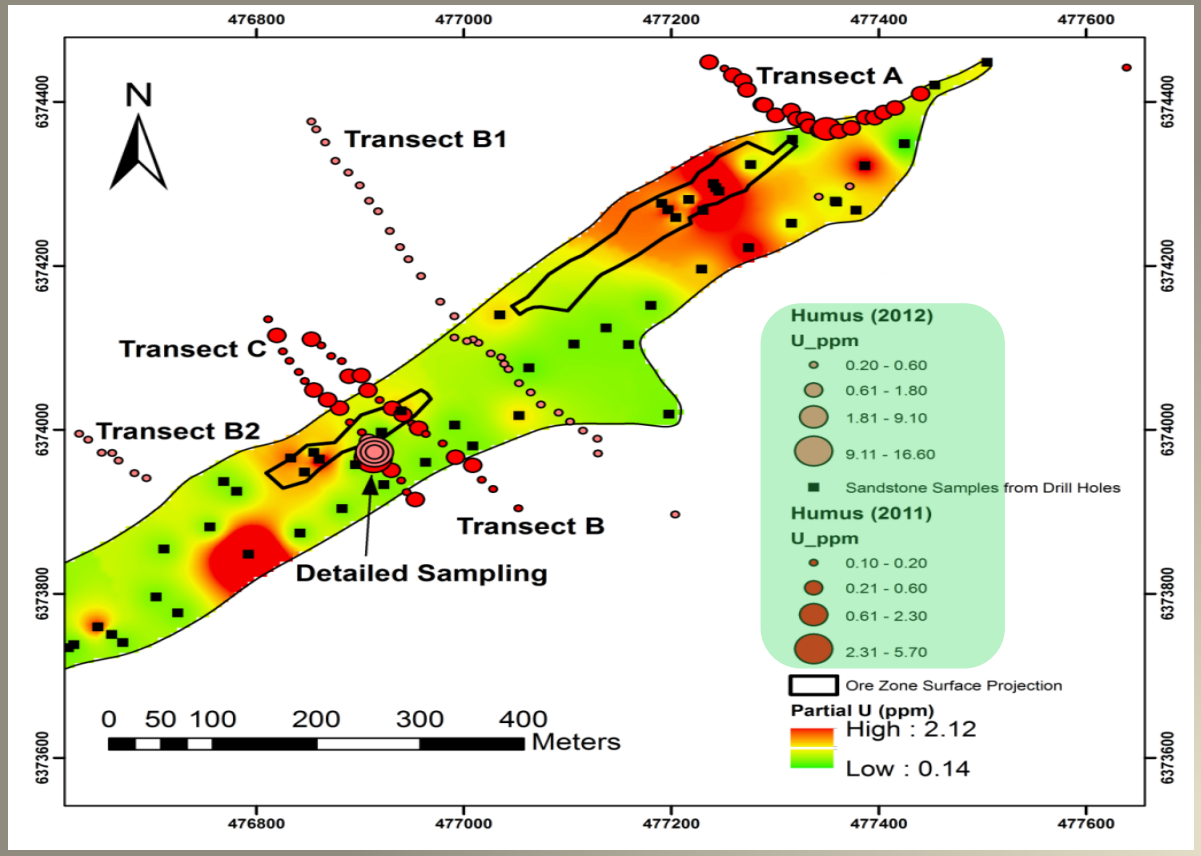
^{206}Pb and ^{207}Pb are decay products of U.

Low ^{206}Pb and ^{207}Pb in humus, not coming from ore



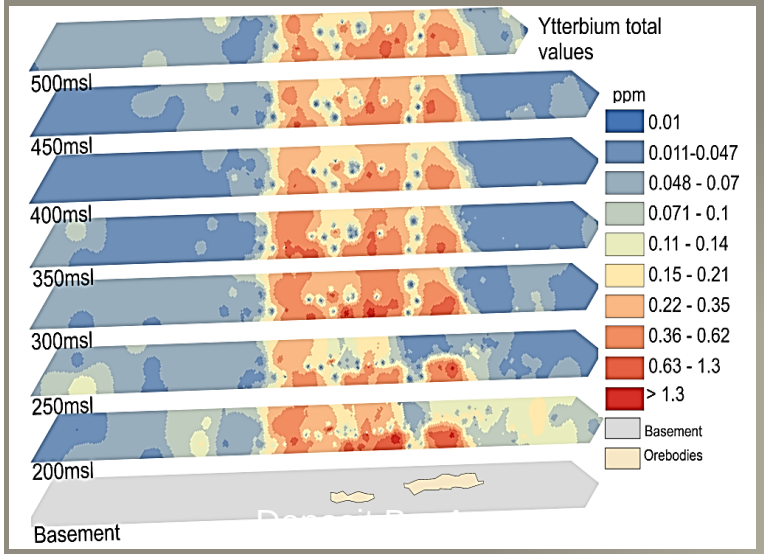
Source of metals in soil
High U in the uppermost sandstone, Phoenix

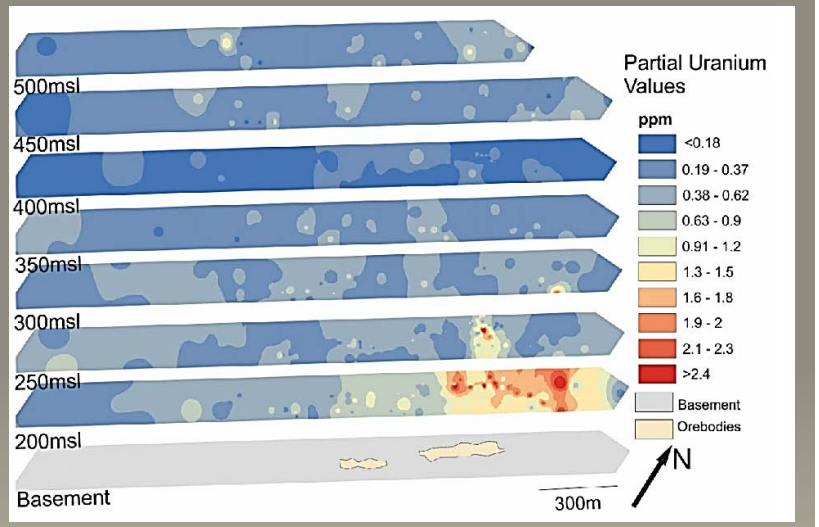
Power et al. GSC OFR, 7235

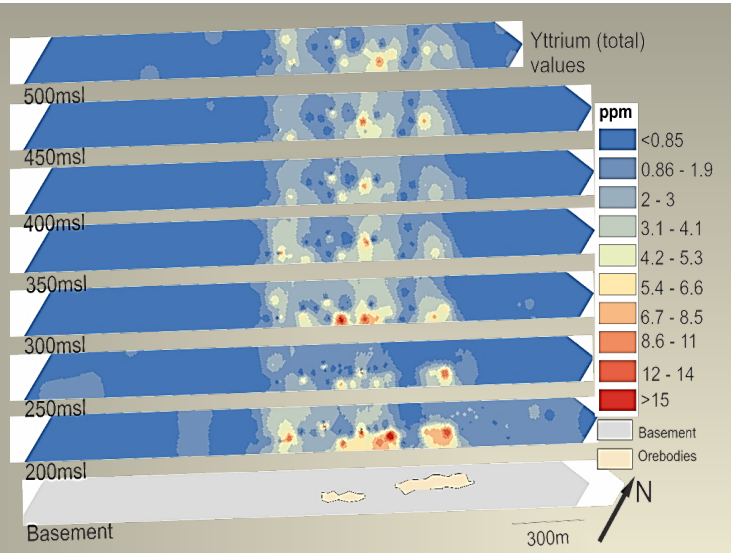


Sandstones

Elements associated with U
Show elevated values above deposits



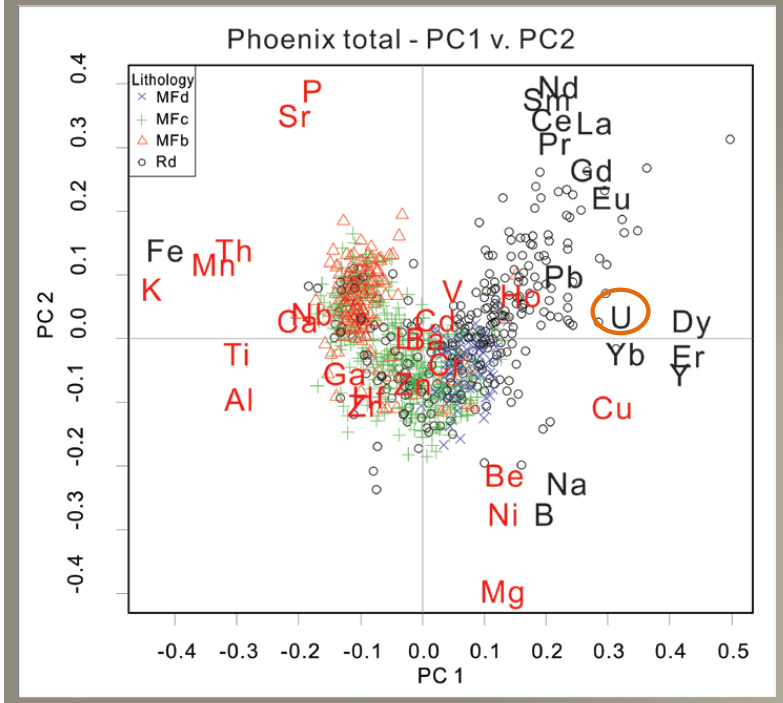




Dann et al., 2014, GSC OFR 7463

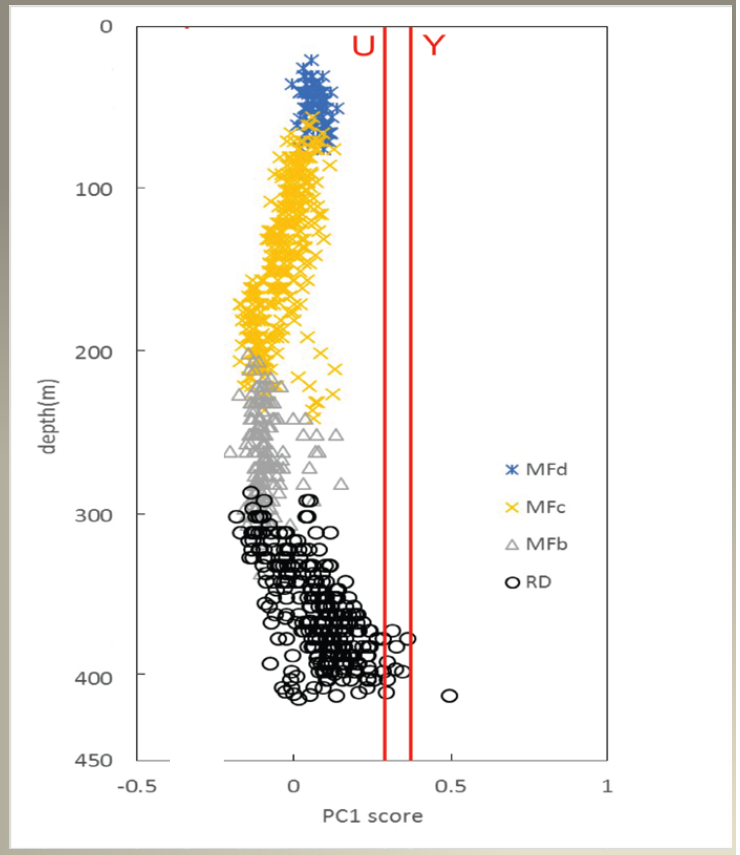
Sandstone PCA, Phoenix

U is correlated with
REE+Y+Pb



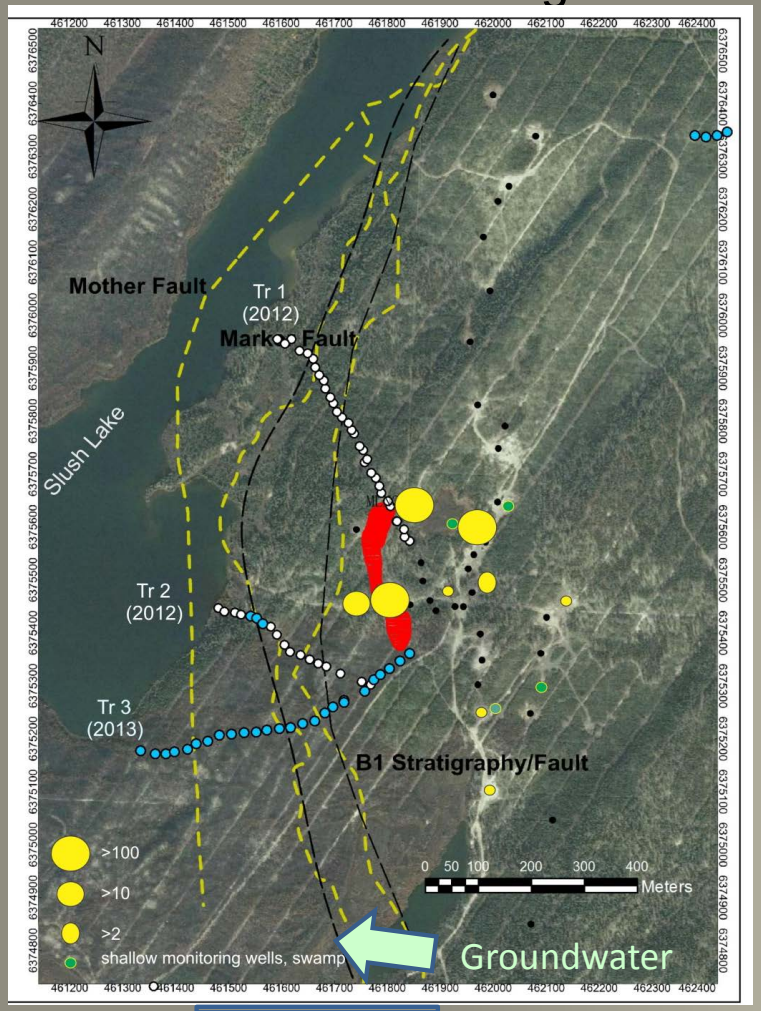
Chen et al., 2014, GSC OFR 7619

The scores of PC1 are high in RD and Mfd.



Helium

High He near the Millennium deposit

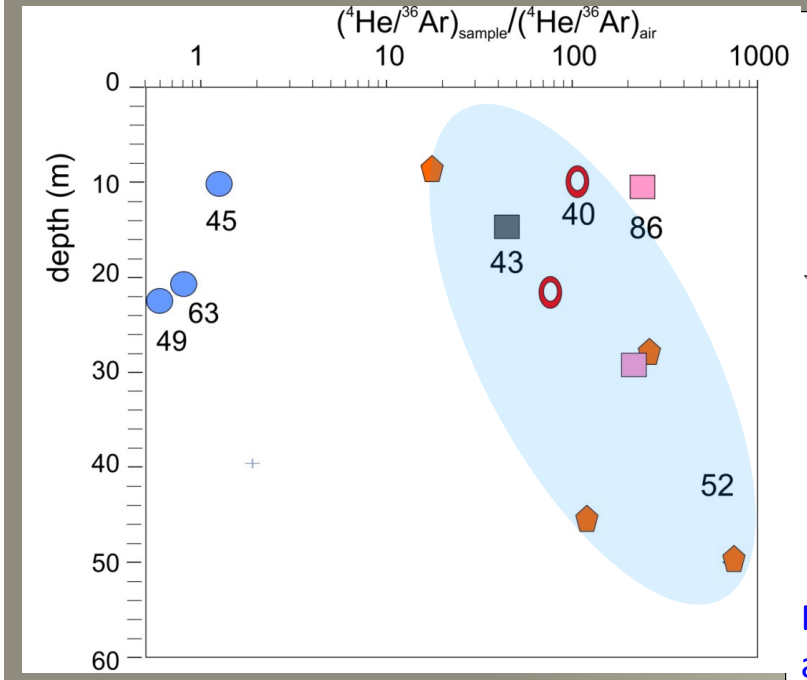


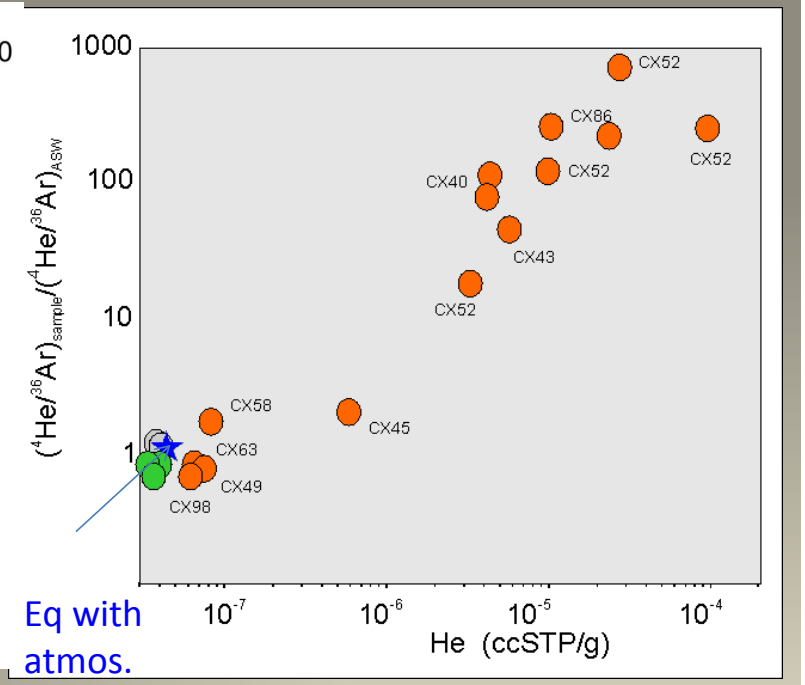
High values above the deposit,
Low values in the eastern part.

Appears to be influenced by water flow

Krahenbil et al., 2014, GSC OFR 7611

Helium above the Millennium deposit





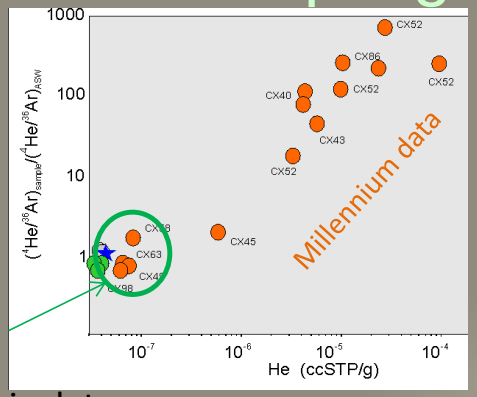
Deeper samples show greater He.

Exploration holes, Monitoring wells

Power et al., 2013; Krahenbil et al., 2014, GSC OFR 7611

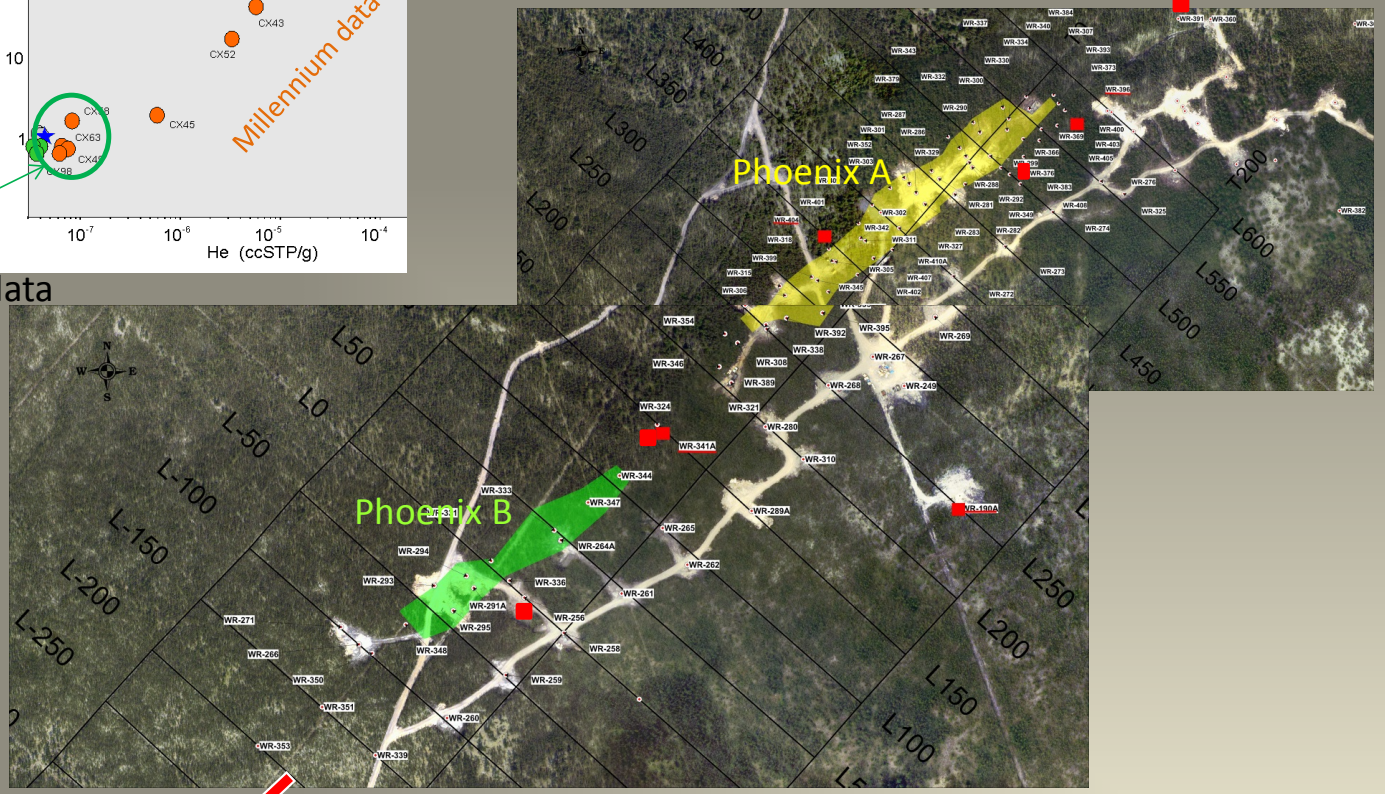
Helium sampling

All samples show low He–
He is not diffused vertically -- move with water flow



Phoenix data

WR 323



WR390, WR252, WR253, WR263

Dudek et al, poster at this conference

Radon

High values, but variations with depth suggest local sources of Rn

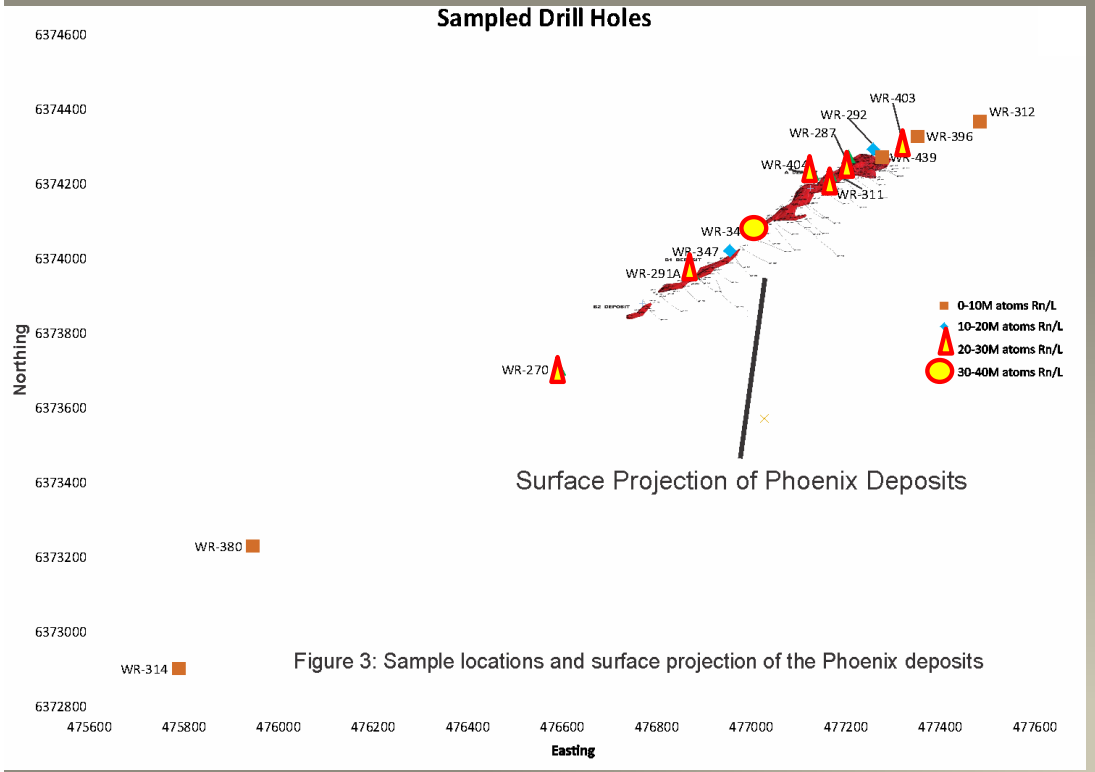
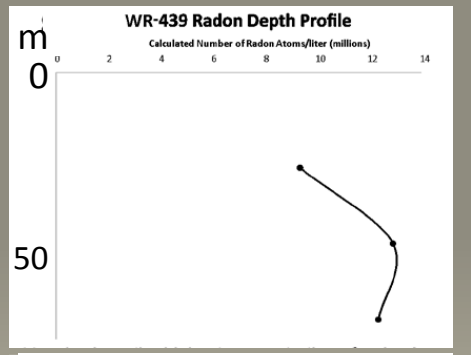
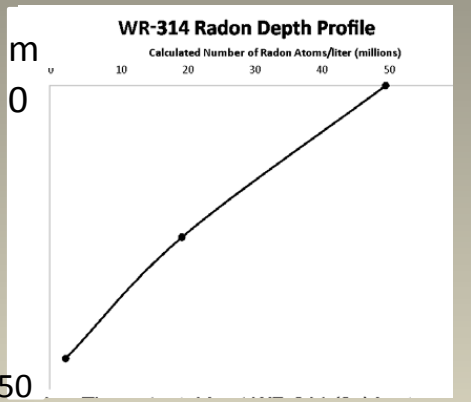


Figure 3: Sample locations and surface projection of the Phoenix deposits





Dudek et al., poster at this conference

The data are comparable to those from the Millennium property by Devine et al. (2014)

Summary

Deeply buried U deposits produce geochemical anomalies in surface media, but the expression may vary in different locations.

Soil

- Metals in humus are in organics (not on the surface).
- Soil anomalies are robust, reproducible.
- Metals likely originated from sandstones.

Sandstones

- High metals values above deposits

  most likely formed during uraniferous hydrothermal activity.

Gases

- Rn are high, coming from shallow sources

  Not drilling action, probably U ± Ra in sandstones
- High He in the Millennium, but low above the Phoenix ore.

  - vertical gas diffusion is not important
  - groundwater flows appear to strongly affect the contents

Publications related to surficial geochemistry

- Chen, S., Hattori, K., Grunsky, E.C. & Liu, Y., **2014**. Principal component analysis of geochemical data from the Phoenix uranium deposits and the REE mineralization in the Maw Zone, Athabasca Basin, Canada. ***GSC OFR, 7689***
- Emberley, J., Hattori, K., Adlakha, E., **2014**. Petrography and chemistry of pyrite from the McArthur River uranium deposit, Saskatchewan***. GSC OFR 7626,*** *doi: 10.4095/294928*
- Krahenbil, A., Hattori, K., Power, M., Kotzer, T., **2014**. Surficial geochemistry associated with the deeply buried Millennium and Phoenix uranium deposits, Athabasca Basin, Northern Saskatchewan. *GSC OFR. 7611.* doi:10.4095/293928*)*
- Chen, S., Hattori, K., Grunsky, E., **2014**. Elemental assemblages in sandstones overlying the Phoenix U deposits and REE-rich Maw Zone, Athabasca Basin, Saskatchewan. ***GSC OFR 7629*** doi:10.4095/295056
- Chen, S., Hattori, K., Grunsky, E., **2014.** Principal component analysis of sandstones overlying the Phoenix uranium deposits, Athabasca Basin. ***GSC OFR 7578.*** doi:10.4095/294920
- Dann, J., Hattori, K., Potter, E., Sorba, C. **2014.** Discrimination of elemental assemblages in the alteration halo of the Phoenix deposit, Saskatchewan, through Applied GIS***. GSC OFR 7463****, doi: 10.4095/293122*.
- Adlakha, E., Hattori, K., Zaluski, G., Kotzer, T., Potter, E.G, **2013.** Alteration within the basement rocks associated with the P2 fault and the McArthur River uranium deposit, Athabasca Basin. GSC OFR 7462, 33 p. doi:10.4095/293364
- Adlakha, E., Hattori, Potter, E., Sopuck, V., **2013.** The paragenesis and chemistry of alteration associated with the P2 fault in metamorphosed basement rocks underlying the Athabasca Basin. GSC OFR 7365, doi:10.4095/292559
- Dann, J., Hattori, K., Sorba, C., Potter, E., **2013**. Elemental assemblages in the alteration halo of the Phoenix deposit, Saskatchewan through applied GIS. GSC OFR 7366. Doi: 10.4095/292564
- Power, M.J., Hattori, K., Sorba, C., Potter, E., **2012**. Geochemical anomalies in the soil and uppermost sandstones overlying the Phoenix uranium deposit, Athabasca Basin, Saskatchewan, Canada. GSC OFR **7257,** 36 p. doi:10.4095/291981
- Power, M.J., Hattori, K., Sorba, C., Potter, E., **2012**. Geochemical anomalies in surface media and uppermost sandstones overlying the concealed Phoenix uranium deposit, Athabasca Basin, SK. GSC OFR. **7235** doi:10.4095/291900

Conference presentations

- Dudek, N., Hattori, K. **2014**. Radon distribution and concentrations above buried uranium ore: Denison Mine's Phoenix deposits, Saskatchewan. Saskatchewan This conference.
- Chen, S., Hattori, K., Grunsky, E., Liu, Y., **2014**.Geomathematic analysis of sandstone compositions overlying the Phoenix U deposits and REE-rich Maw Zone, Athabasca Basin, Saskatchewan. *GAC-MAC, Fredericton, NB.*
- Krahenbil, A., Hattori, K., Power, M., Kotzer, T., **2014**. Surficial geochemistry associated with the deeply buried Millennium and Phoenix uranium deposits, Athabasca Basin, Saskatchewan. *GAC-MAC, Fredericton, NB.*
- Power, M., Hattori, K., Potter, E., **2014.** Geochemical expression above the Phoenix and Millennium uranium deposits, Athabasca Basin. CMIC-PDAC *Minerals Colloquium*, Toronto.
- Chen, S., Hattori, K., Grunsky, E., Liu, Y., 2014. Elemental assemblages in sandstones overlying the Phoenix U depositsand REE-rich Maw Zone, Athabasca Basin, Saskatchewan. CMIC-SEG-PDAC *Minerals Colloquium*, Toronto.
- Krahenbil, A., Hattori, K., Power, M., Power, M., Pinti, D., Kotzer, T., **2014**. Geochemical anomalies in soil and high He above deeply buried Millennium and Phoenix Uranium Deposits, Athabasca Basin, Saskatchewan. CMIC-SEG-PDAC *Minerals Colloquium*, Toronto.
- Power, M., Hattori, K., Pinti, D., Potter, EG, **2013**. Anomalous abundances of He and mobile metals in surface media over the deeply buried Millennium U deposit, Athabasca Basin, Canada. ***2013*** *Goldschmidt Conf. Mineralogical Magazine, vol 77 (5) p.1993.*
- Krahenbil, A., Hattori, K., Kotzer, T., **2013**. Helium dissolved in groundwater in the Millennium uranium property, Athabasca Basin. *Saskatchewan Geological Survey Open House in Saskatoon, December*
- Power, M.J., Hattori, K., Sorba, C., Kotzer, T., Pinti, D.L., Potter, E.G., **2013**, Surface Media Expressions of buried unconformity-related uranium: The Phoenix & Millennium deposits, Athabasca Basin. Special session, Advances in Exploration Techniques, *GAC-MAC, Winnipeg*. Abst. vol. 36, 2013; p. 166
- Dann, J., Hattori, K., Sorba, C., **2012.** Alteration minerals and elemental assemblages around the Phoenix uranium deposit, Athabasca Basin, Saskatchewan. Joint GAC-MAC, St. John's, Nfld
- Power, M., Hattori, K., Sorba, C., **2012**. Geochemical anomalies in surface media and uppermost sandstones overlying the concealed Phoenix uranium deposit, Athabasca Basin, Saskatchewan. GAC-MAC, St. John's, Nfld

Acknowledgements

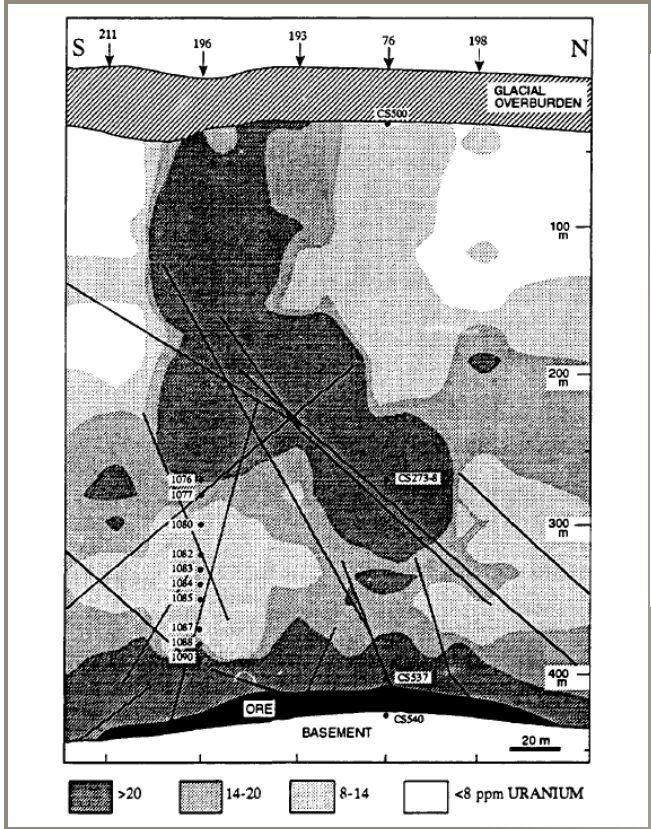






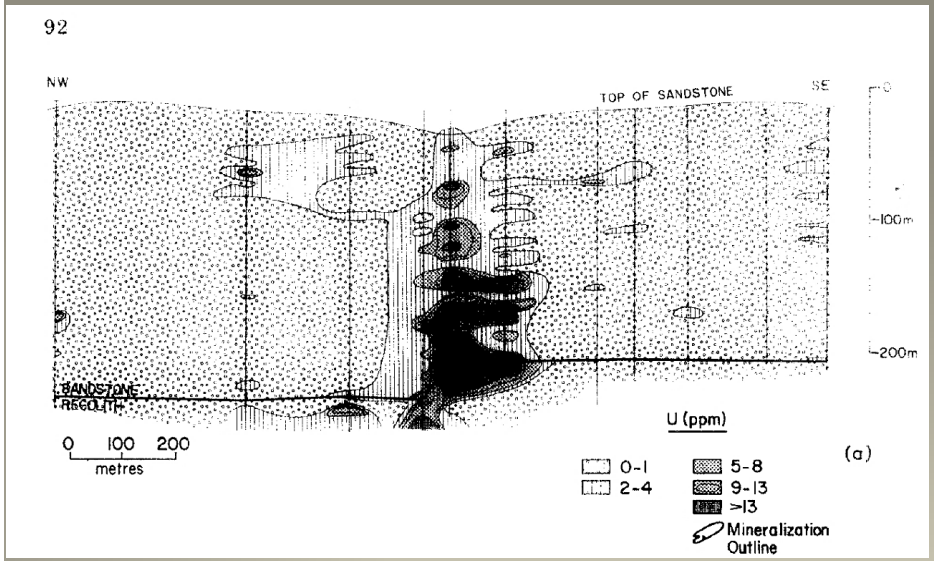


Metal anomalies in sandstones



Cigar Lake

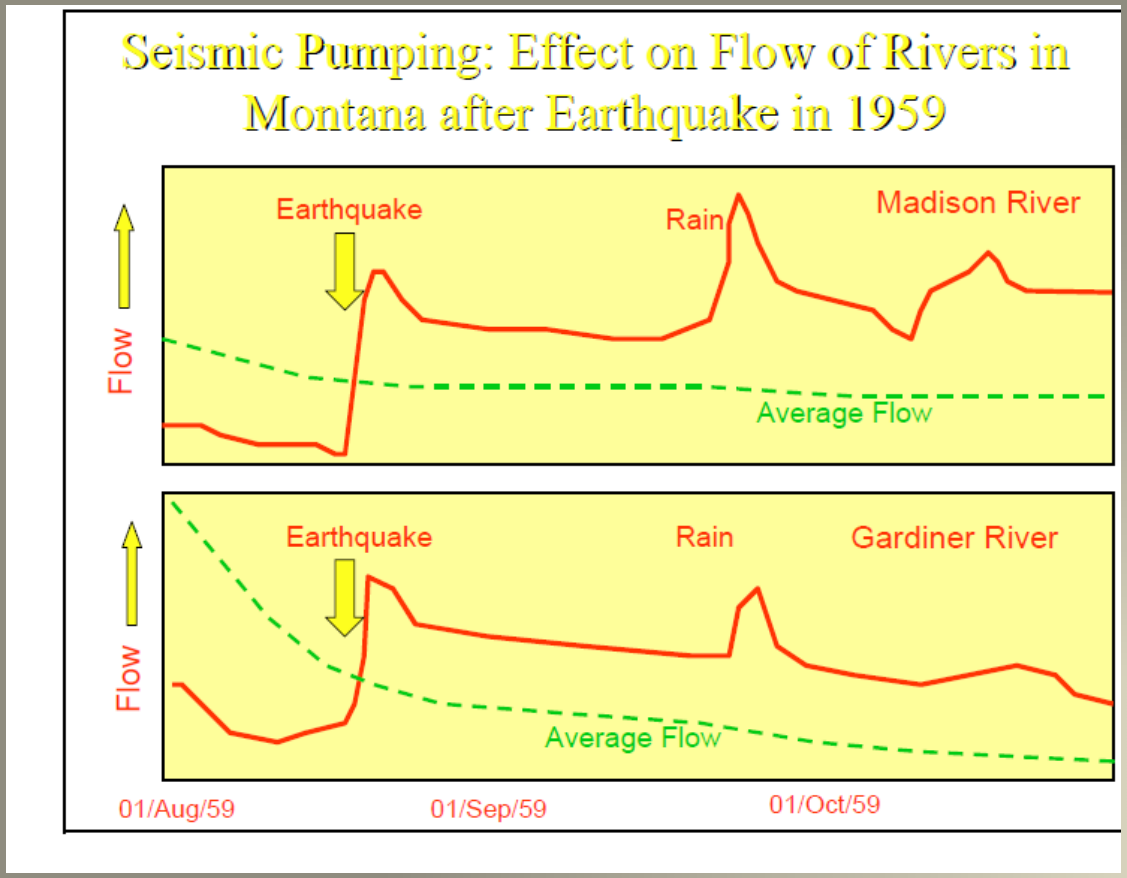
Smellie & Cramer, 1994

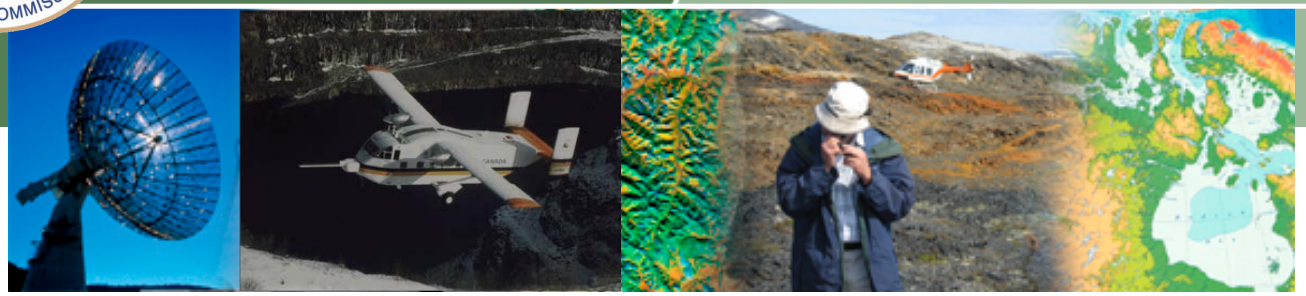


Midwest deposit

Sopuck et al., 1983

Importance of faults for surficial geochem. anomalies





Ground truthing of the 'Eastern Athabasca Basin' regional airborne gamma-ray survey: Context for exploration of deeply buried unconformity-related uranium deposits

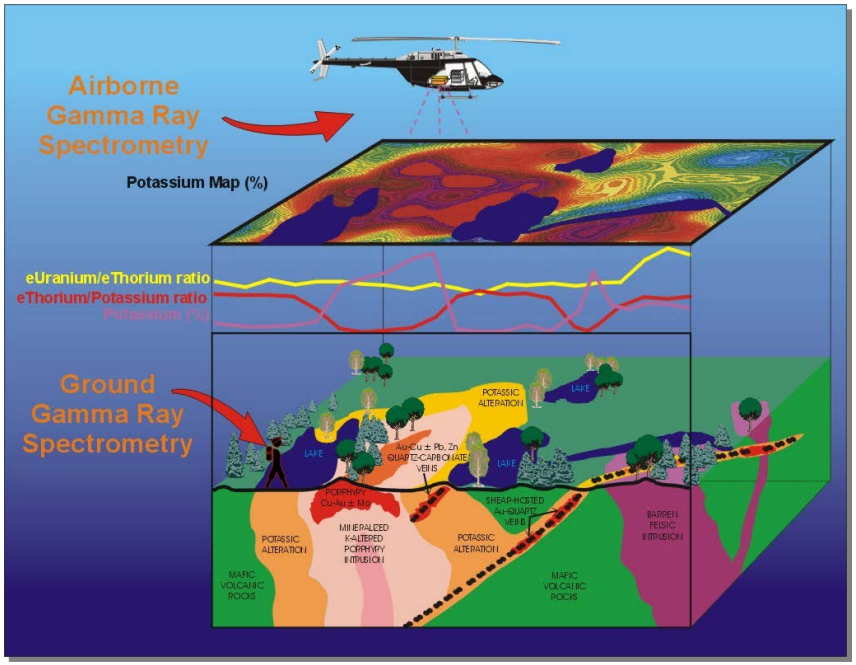
Richard Fortin[1], Campbell, J.E.[1], Harvey, B.J.A.[1], McCurdy, M.W.[1], Hanson, M.A.[2], Sinclair, L.E.[1], Potter, E.G.[1] and Jefferson, C.W.

[1]Geological Survey of Canada, [2]Saskatchewan Geological Survey

Natural Resources Canada | Ressources naturelles Canada

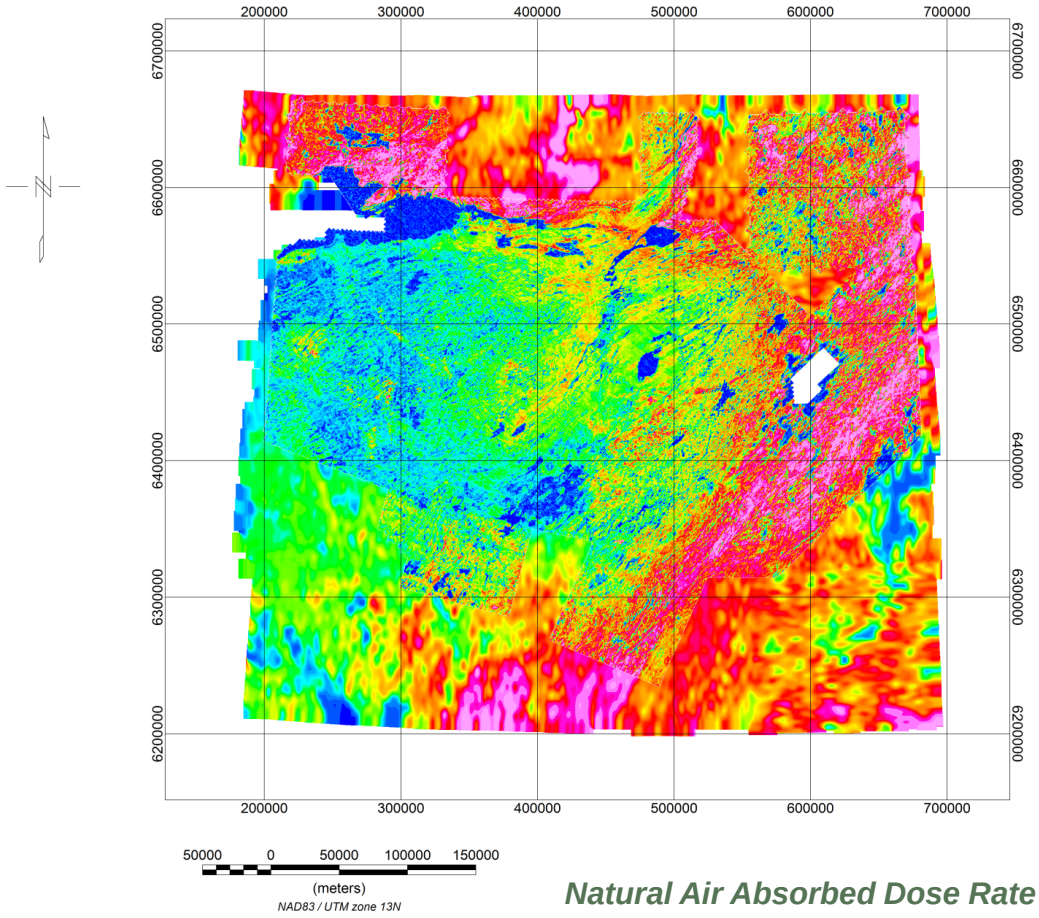
Canada

Gamma-Ray Spectrometry

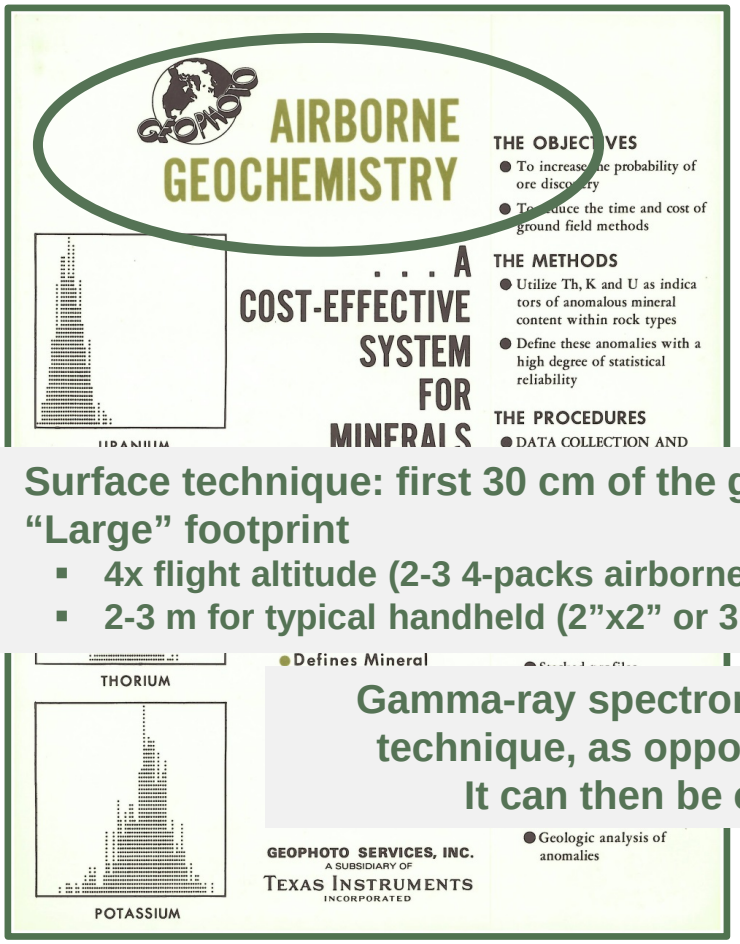








Natural Air Absorbed Dose Rate
Northern Saskatchewan



Brochure for an integrated airborne gamma-ray spectrometry system from Texas Instruments (1970)

- Surface technique: first 30 cm of the ground
- "Large" footprint
  - 4x flight altitude (2-3 4-packs airborne NaI(Tl) detector)
  - 2-3 m for typical handheld (2"x2" or 3"x3" NaI(Tl) detectors)

Gamma-ray spectrometry is a <u>compositional</u> technique, as opposed to a structural one. It can then be considered to be…

Goals

- With uranium exploration shifting toward indirect targets and greater depths better use of existing data is needed to maximize exploration efficiency, and quantify both “hits” and “near-misses”.

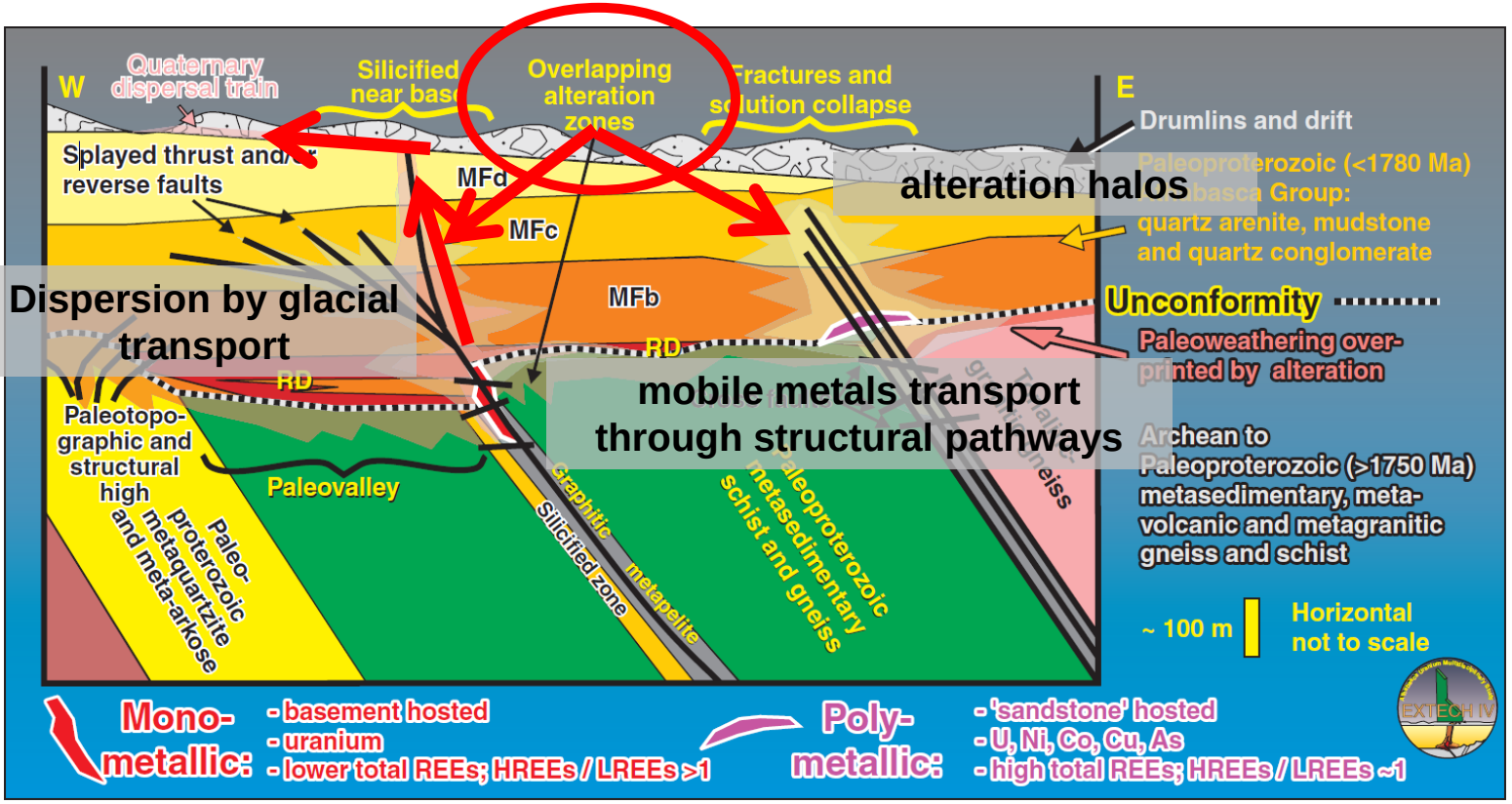
- Recent and historical research has demonstrated that, although deeply buried beneath Athabasca Group sandstones, unconformity type uranium deposits may be targeted by understanding subtle surficial geochemical anomalies.

- Airborne gamma-ray spectrometry provide a mean for efficient mapping of surface geochemical variations, The background in terms of K, U and Th, above which anomalies have to be detected has to be quantified and its genetic linkages understood.

Outline

- Introduction
- Quaternary and radiometric context
- Ground follow-up work in NTS sheet 74H
- Preliminary results from follow-up surveys
- Summary and Conclusion

Geological elements and surface expression of unconformity-related uranium deposits

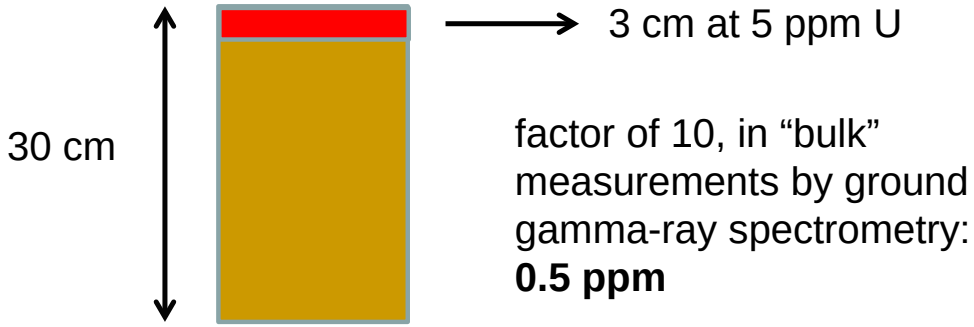


(from Jefferson et al., 2007)

Elements of the unconformity-related uranium deposit exploration model relevant for gamma-ray spectrometry

- K,U enrichment, associated with clay alteration.
  - (Earle et al. 1989, 1990)
  - K enrichment in boulders (Shives et al, 2000)
  - U anomaly in till at Midwest Lake (Simpson and Sopuck, 1983)
- ‘direct detection’ of U mineralization
  - near-surface deposit, mineralized boulder dispersal
  - transport to the surface along structural pathways.
    - exemplified recently at the Phoenix deposit at Wheeler River by (Power et al. 2012)
- glacial dispersal
  - Dispersion of anomalous surface concentrations of K and U
  - increase target size

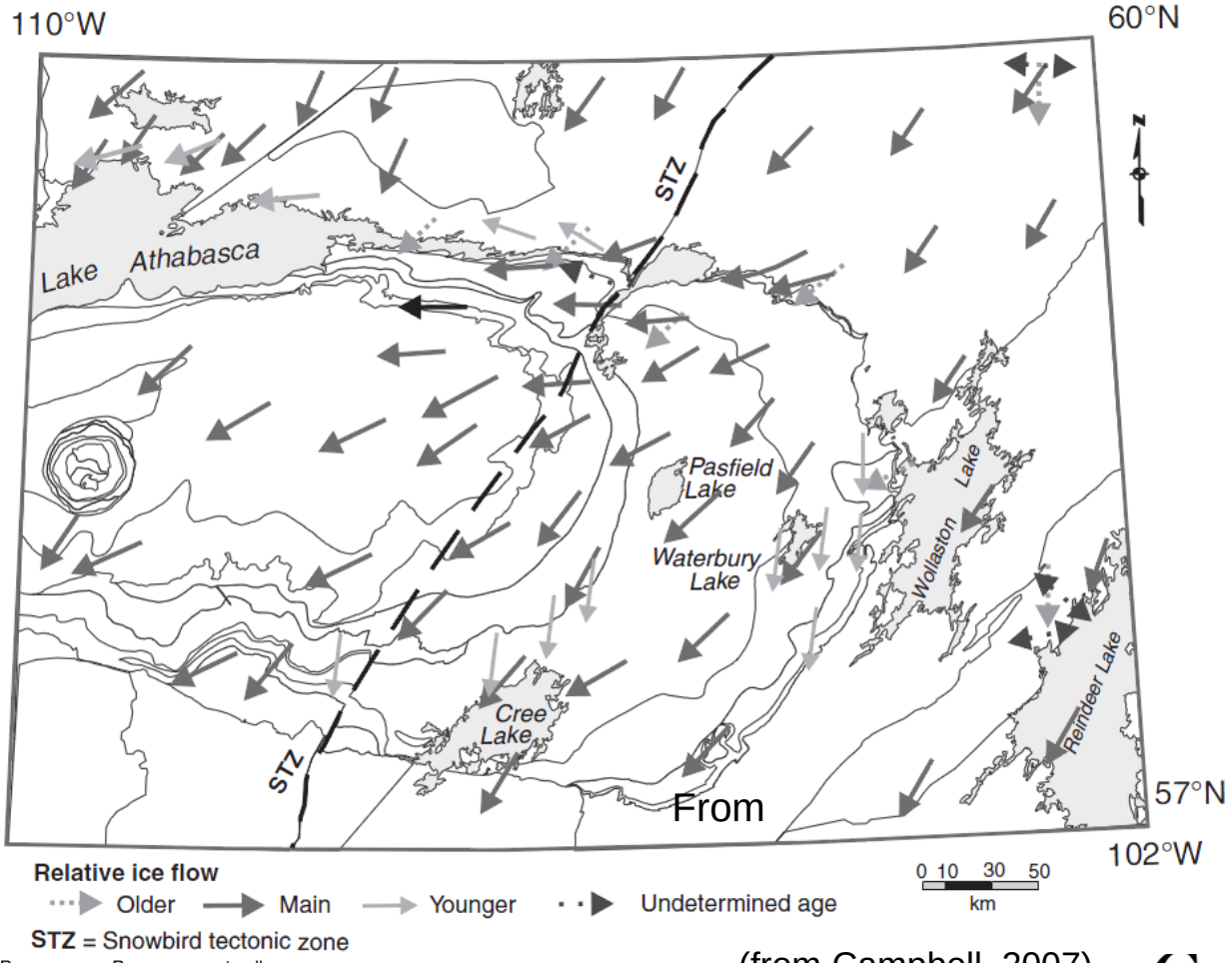
Gamma-ray background of the Eastern Athabasca Basin



	Potassium (%)	Uranium (ppm)	Thorium (ppm)
crustal averages (1)	*2.4*	*3.0*	*12.0*
sedimentary rock (2)	*1.5*	*4.8*	*12.4*
NTS sheet 74H – Basin limit	*0.46*	*0.55*	*4.20*

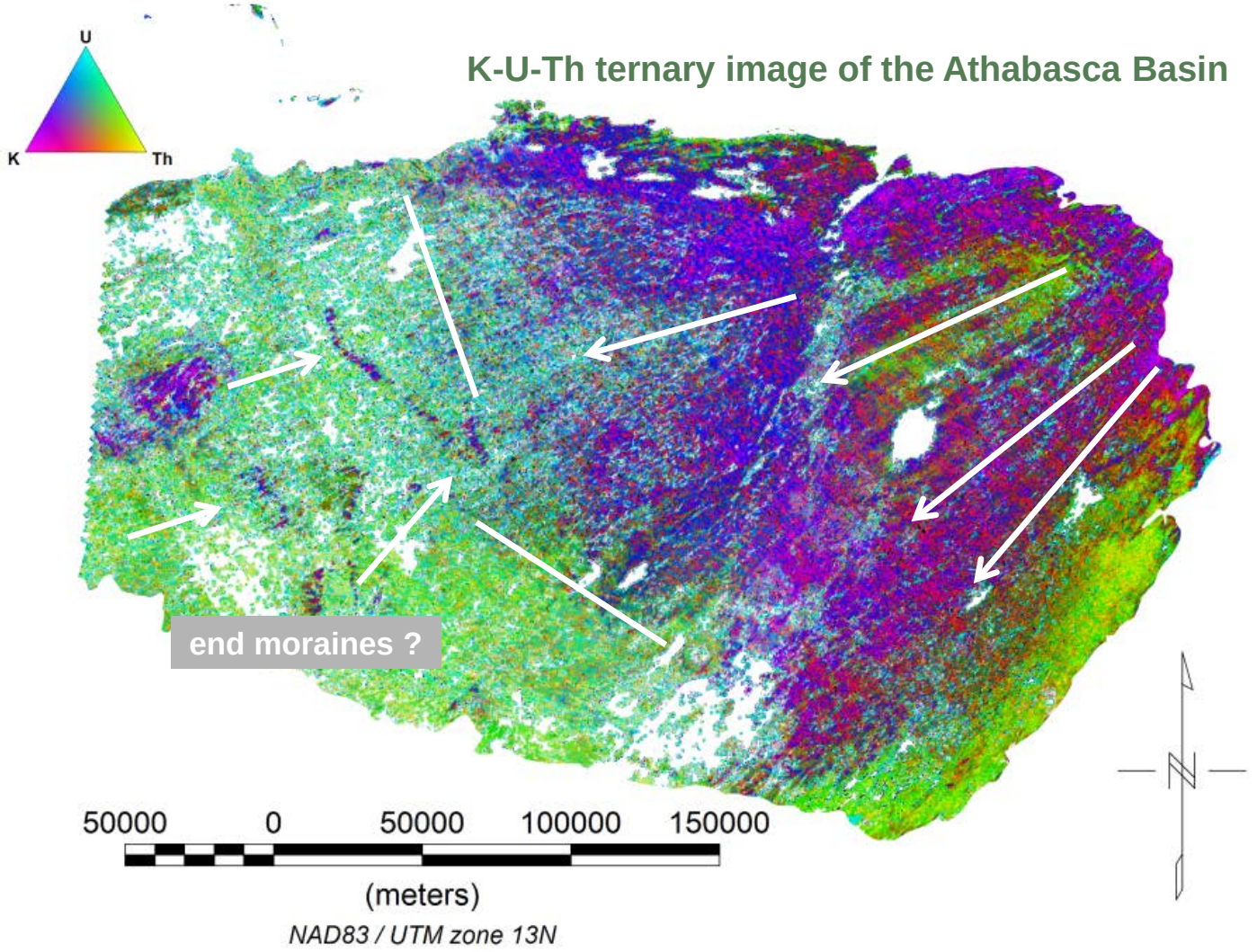
(1) After Killeen, 1979
(2) Dickson and Scott, 1997

Regional ice-flow directions in northern Saskatchewan

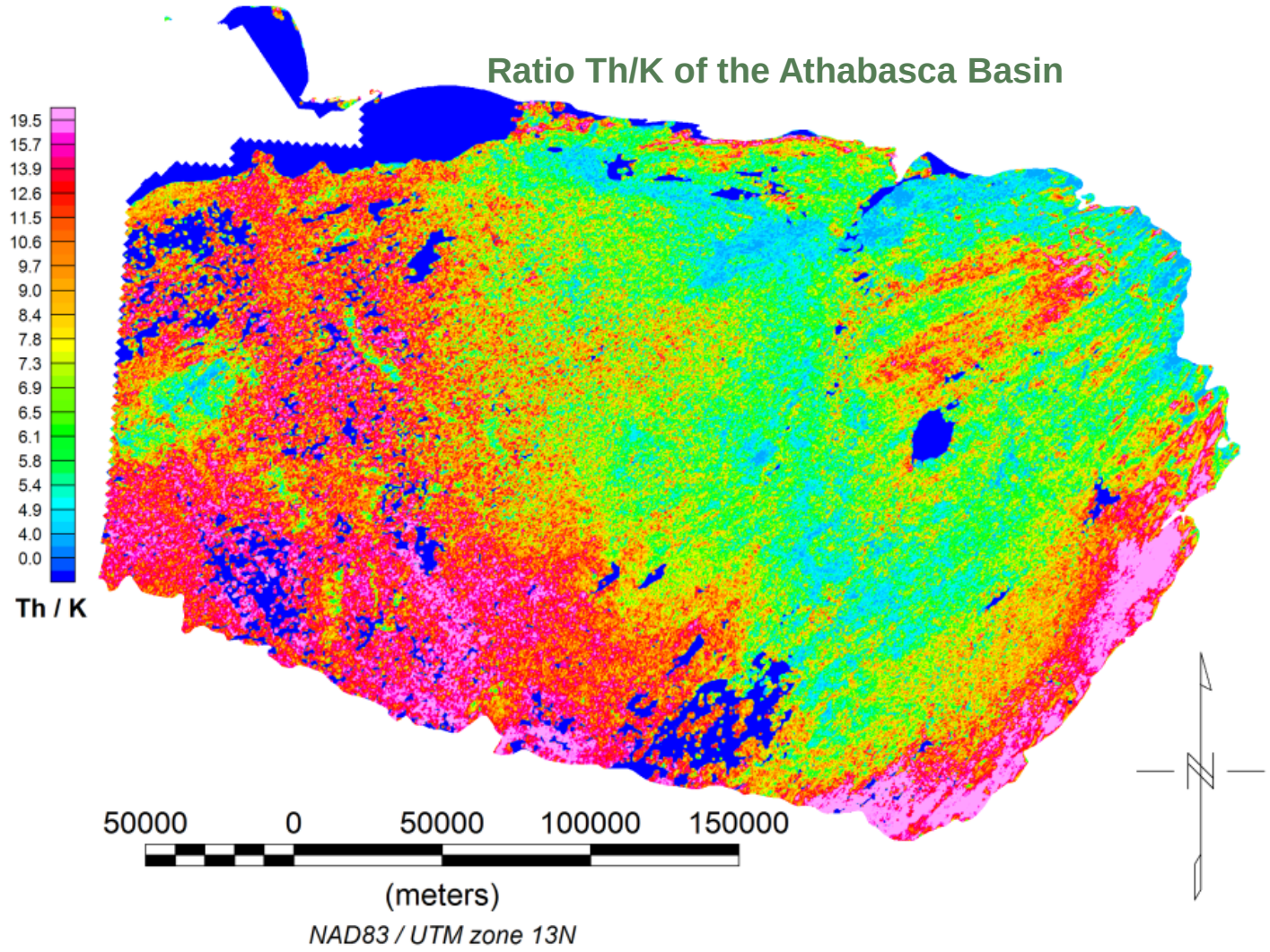


(from Campbell, 2007)

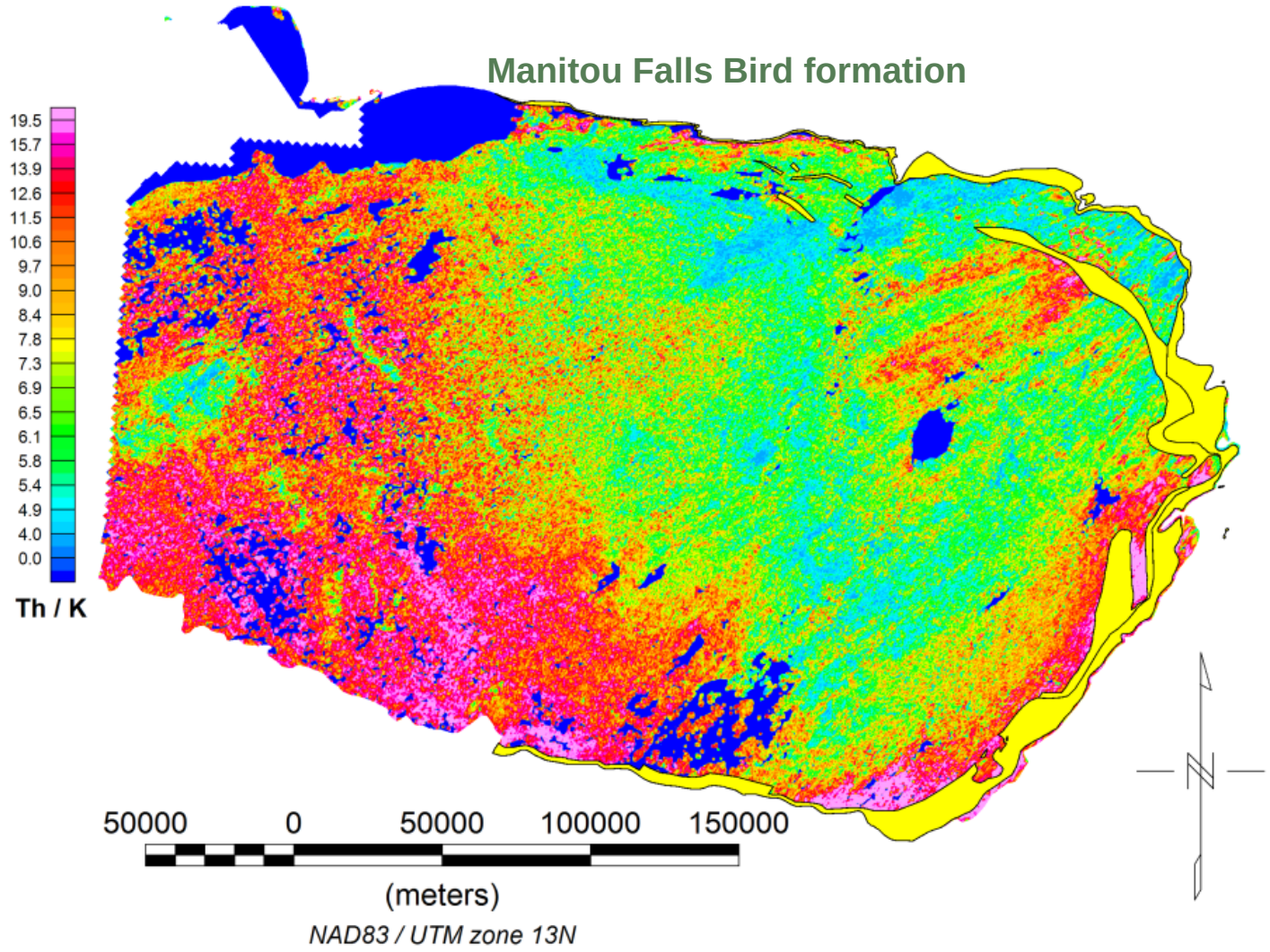
K-U-Th ternary image of the Athabasca Basin



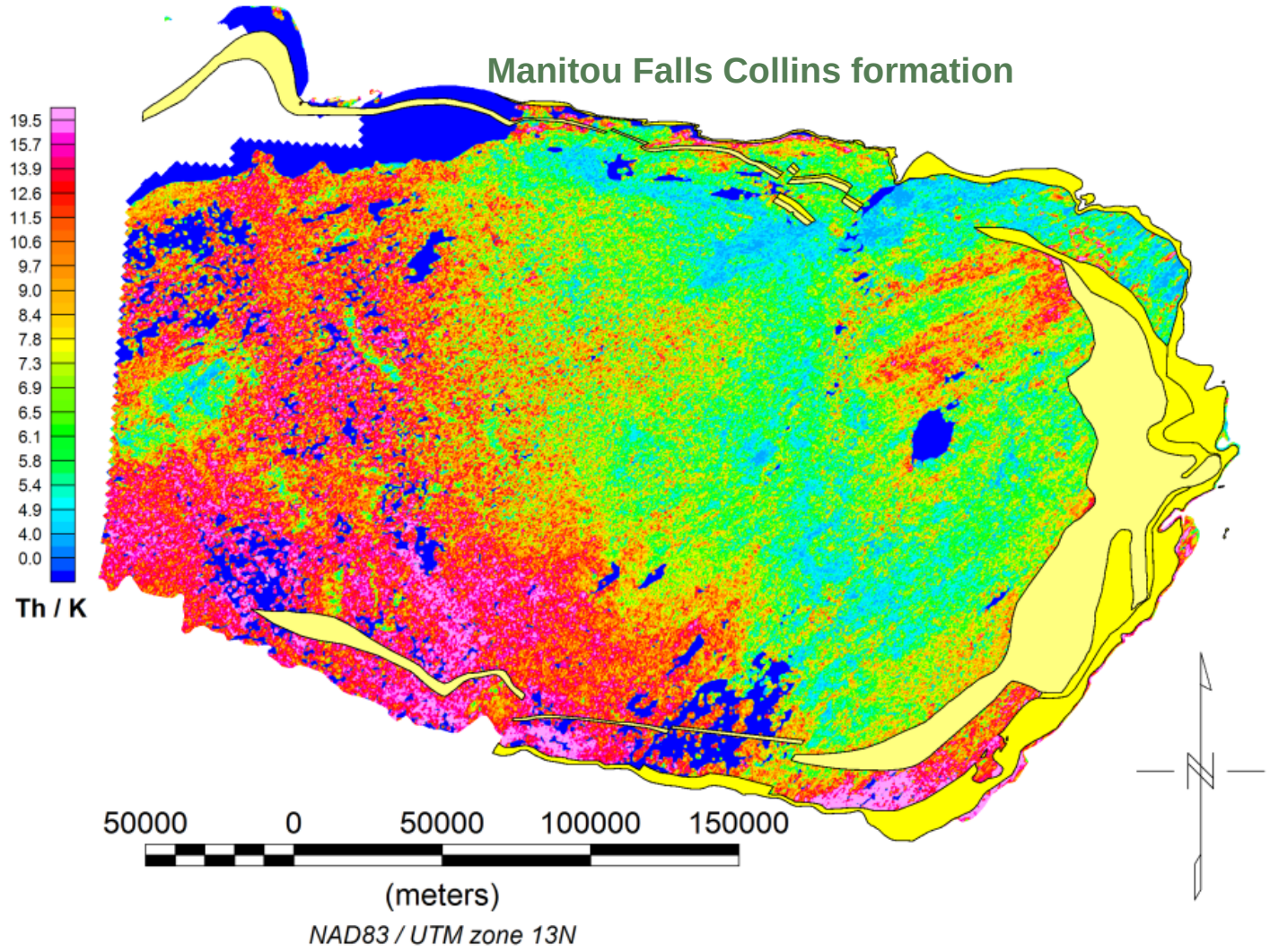
Ratio Th/K of the Athabasca Basin



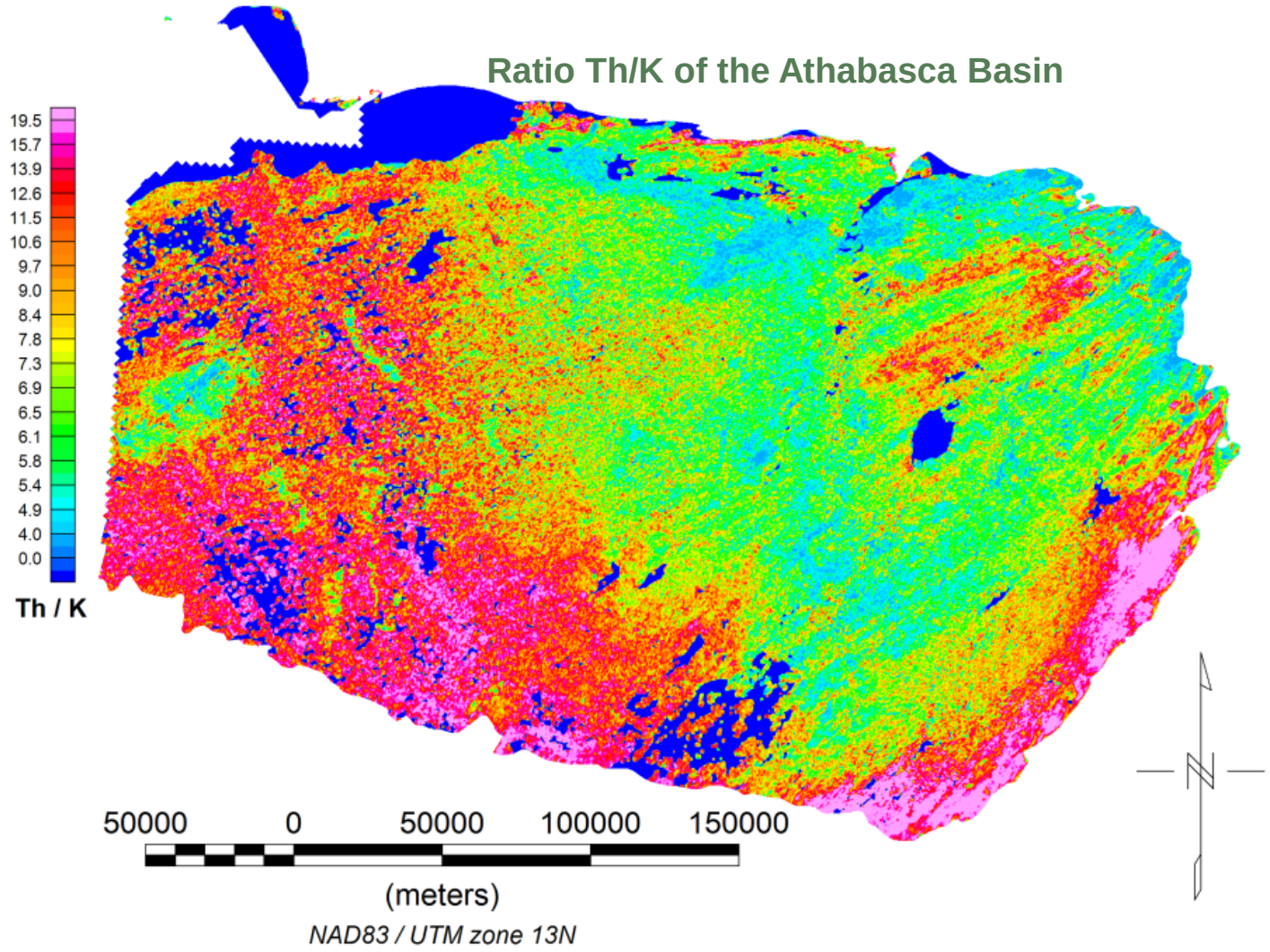
Manitou Falls Bird formation



Manitou Falls Collins formation



Ratio Th/K of the Athabasca Basin

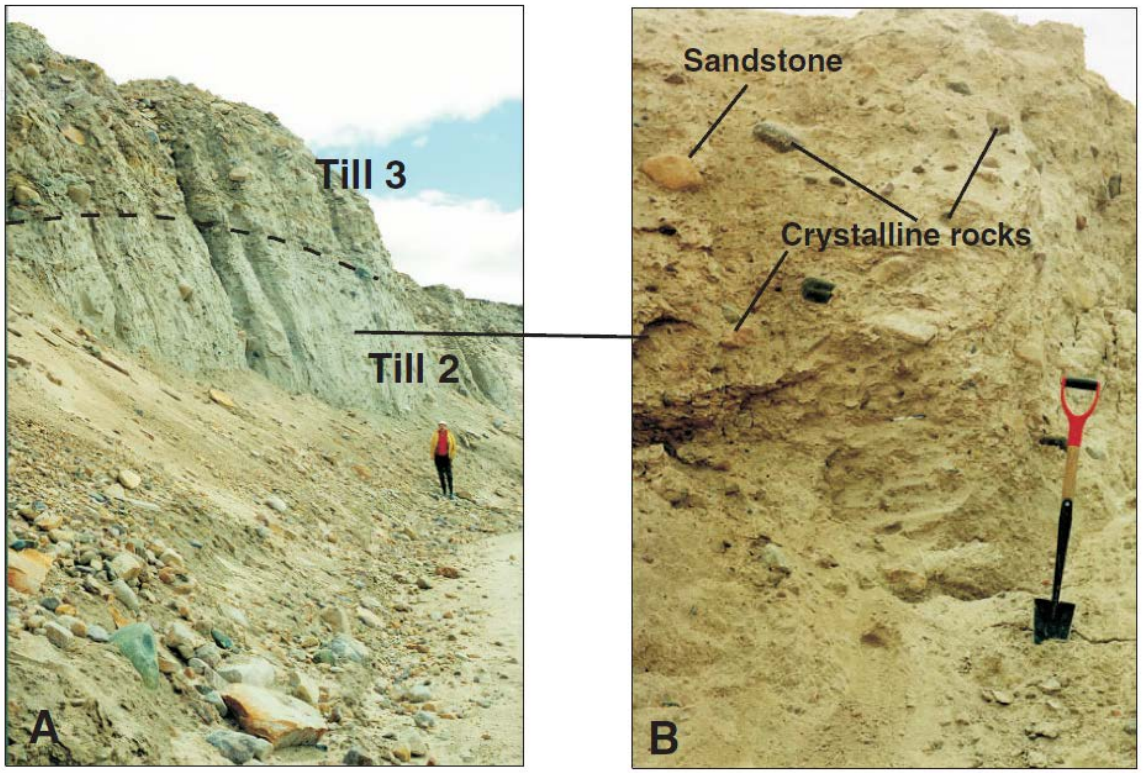


Sandstone-rich and Basement-derived till in the eastern Athabasca Basin

“Basement-derived” till: sandy/silty, contains a significant component of more distally derived, crystalline shield detritus. most extensive till deposit in the region, forming large scale drumlins and ground moraines, deposited by the main late Wisconsinan advance.
Till 2 (Campbell, 2007)

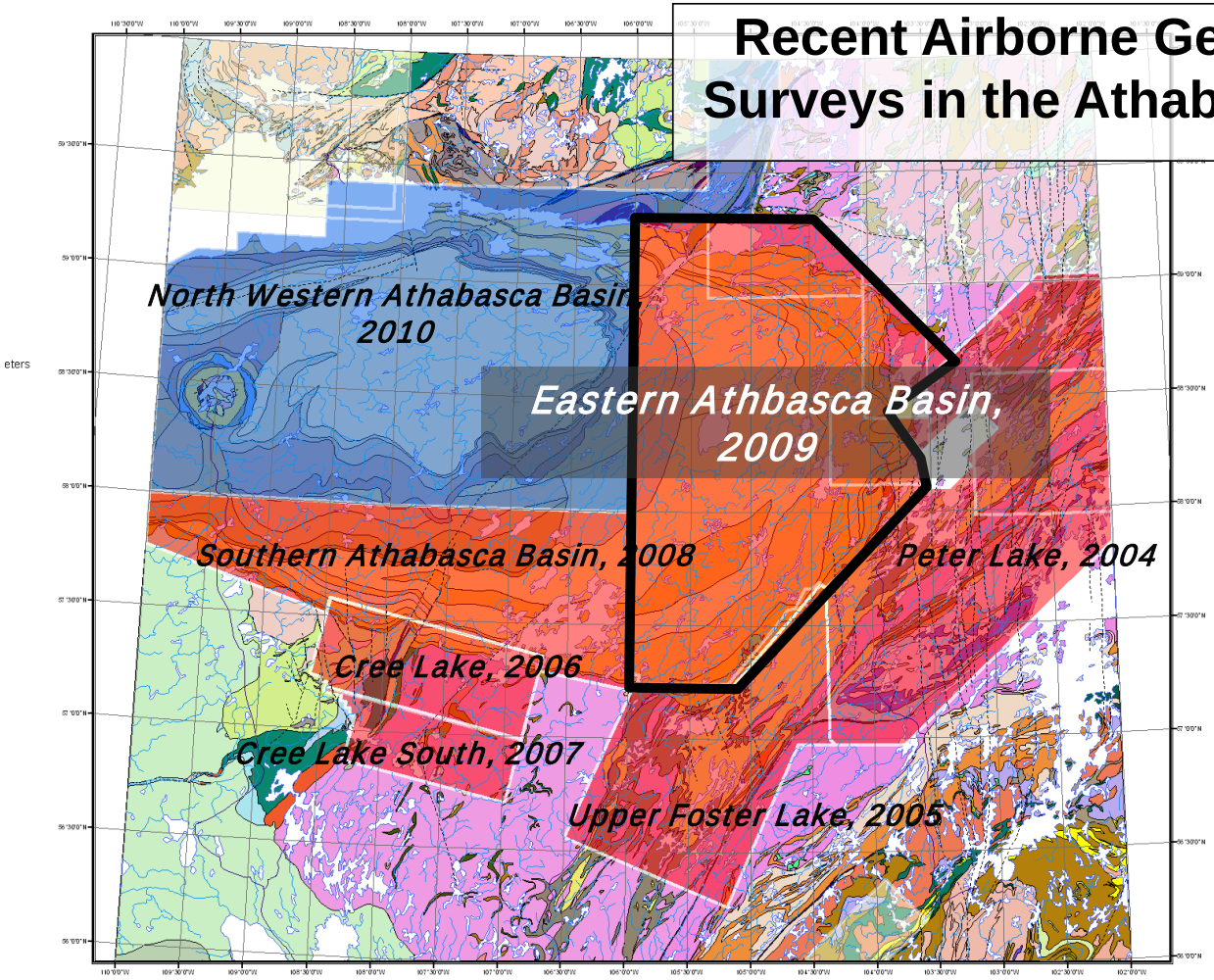
“Sandstone-rich” till: sandy, discontinuously overlies till 2, associated, deposited with/by the late stage re-advance, has a higher component of locally derived material than Till 2.
Till 3 (Campbell, 2007)

Sandstone-derived and Basement-derived till in the eastern Athabasca Basin



(Campbell, 2007)

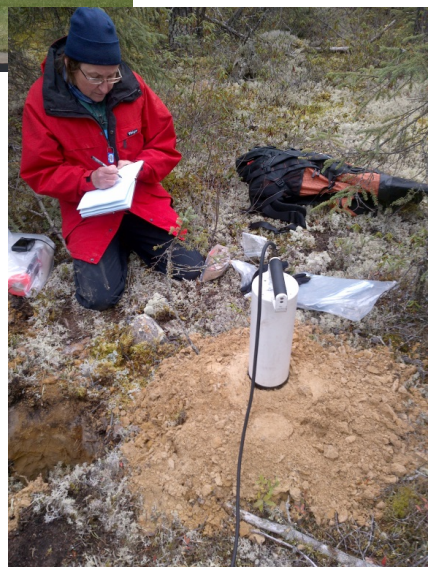
Recent Airborne Geophysical Surveys in the Athabasca Basin



Follow-up field work – Summer and Fall 2013

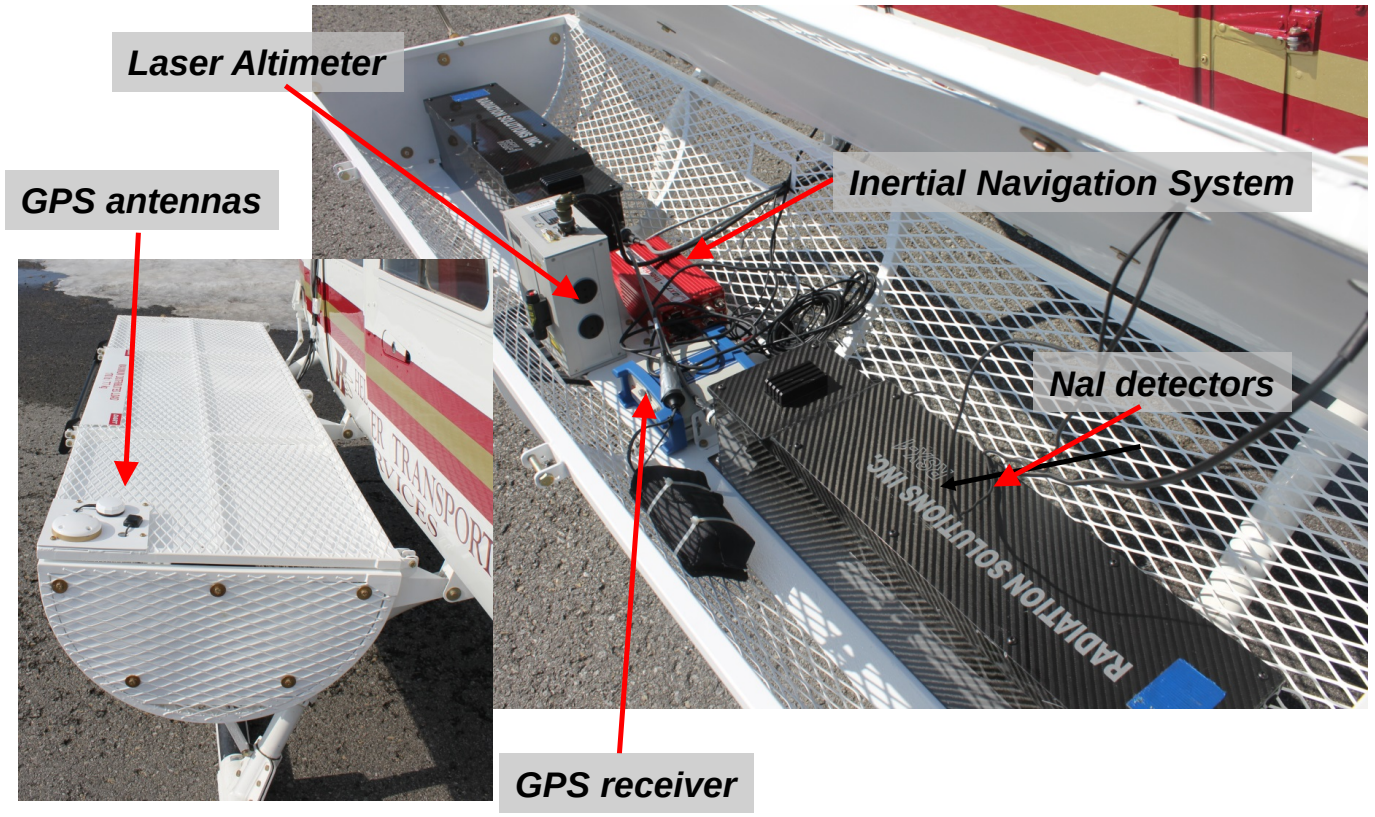






- Targeted airborne spectrometry (25-100 m line spacing)
- Ground spectrometry
- Till sampling and analysis

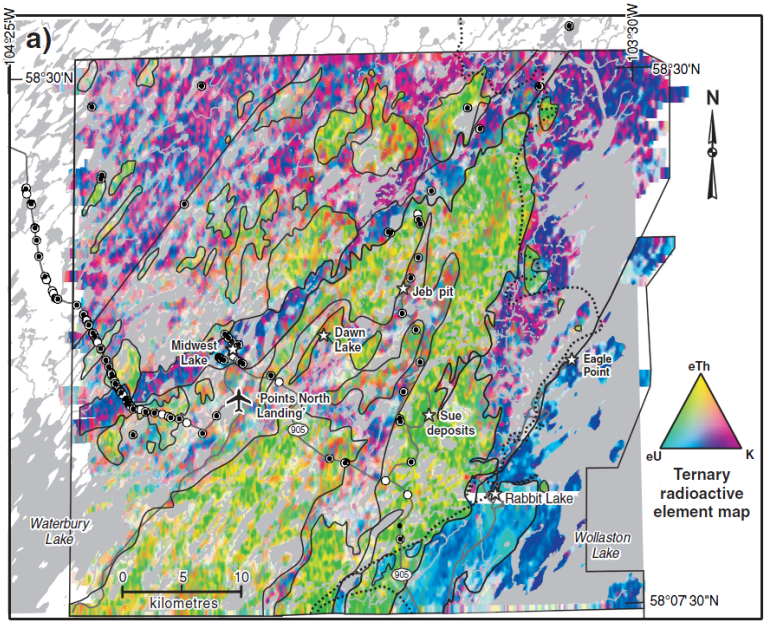
GSC's radiometric survey platform

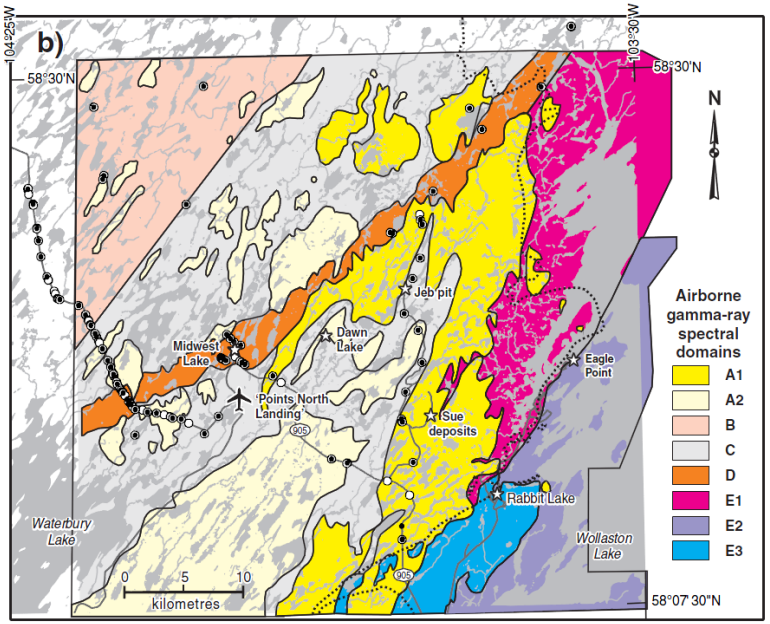


Radiometric Domains

(Campbell, Klassen and Shives, 2007, NEA-IAEA test area, Athabasca Basin)

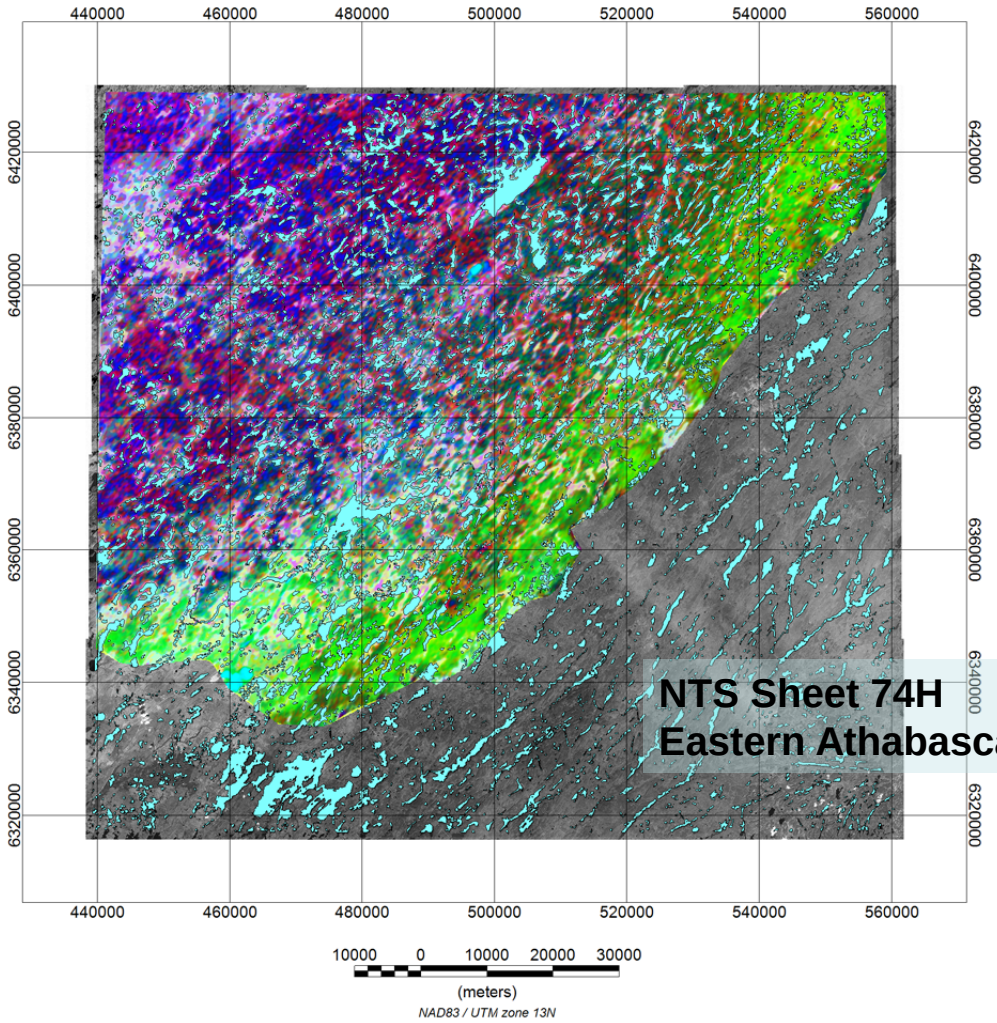
a ***radiometric domain*** is heuristically defined as an area of finite extent that presents a distinctive radiometric signature. It does not imply that concentrations of the three natural radioelements are uniform within a domain, but rather that their spatial distribution has internally consistent qualities that are distinct from those of surrounding areas.



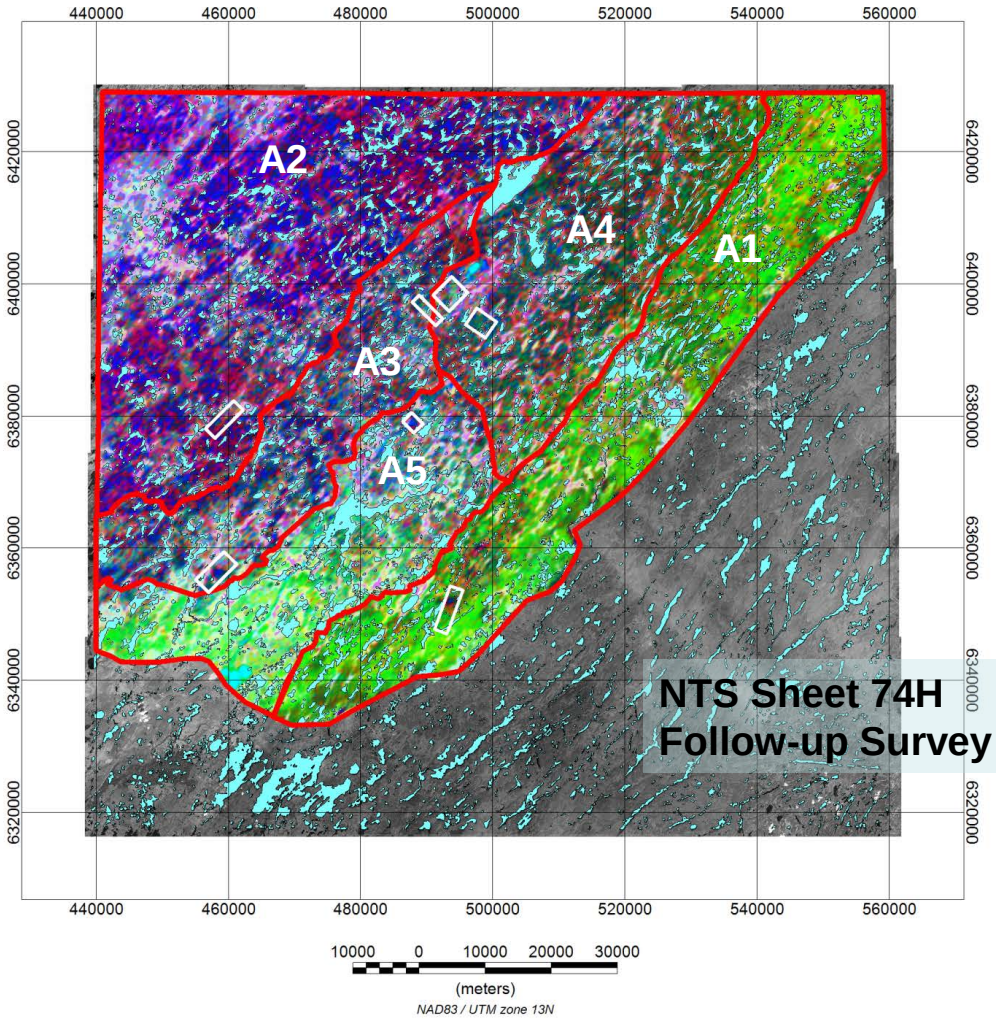


Natural Resources Canada | Ressources naturelles Canada

Canada



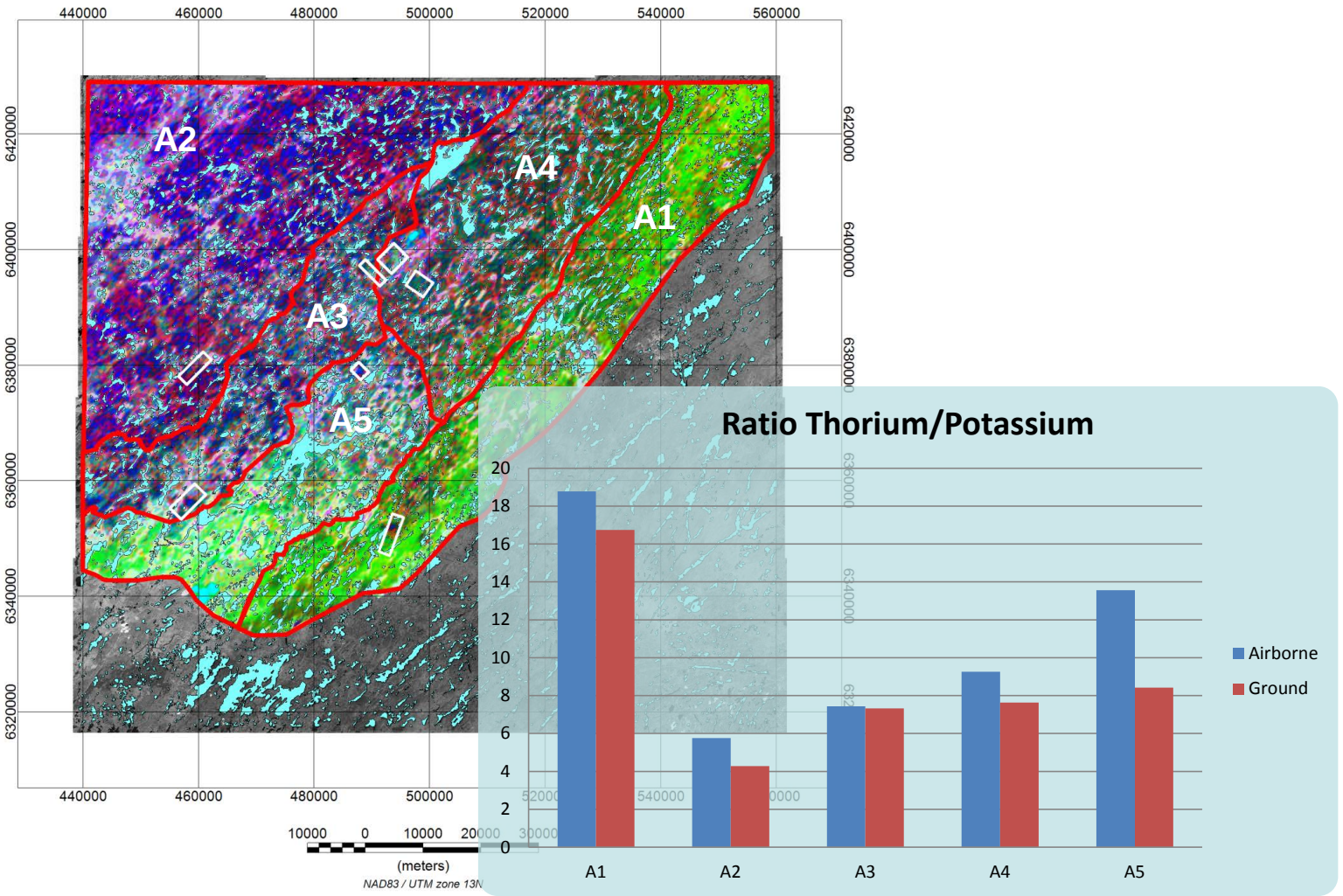
NTS Sheet 74H
Eastern Athabasca Survey



NTS Sheet 74H
Follow-up Survey Areas

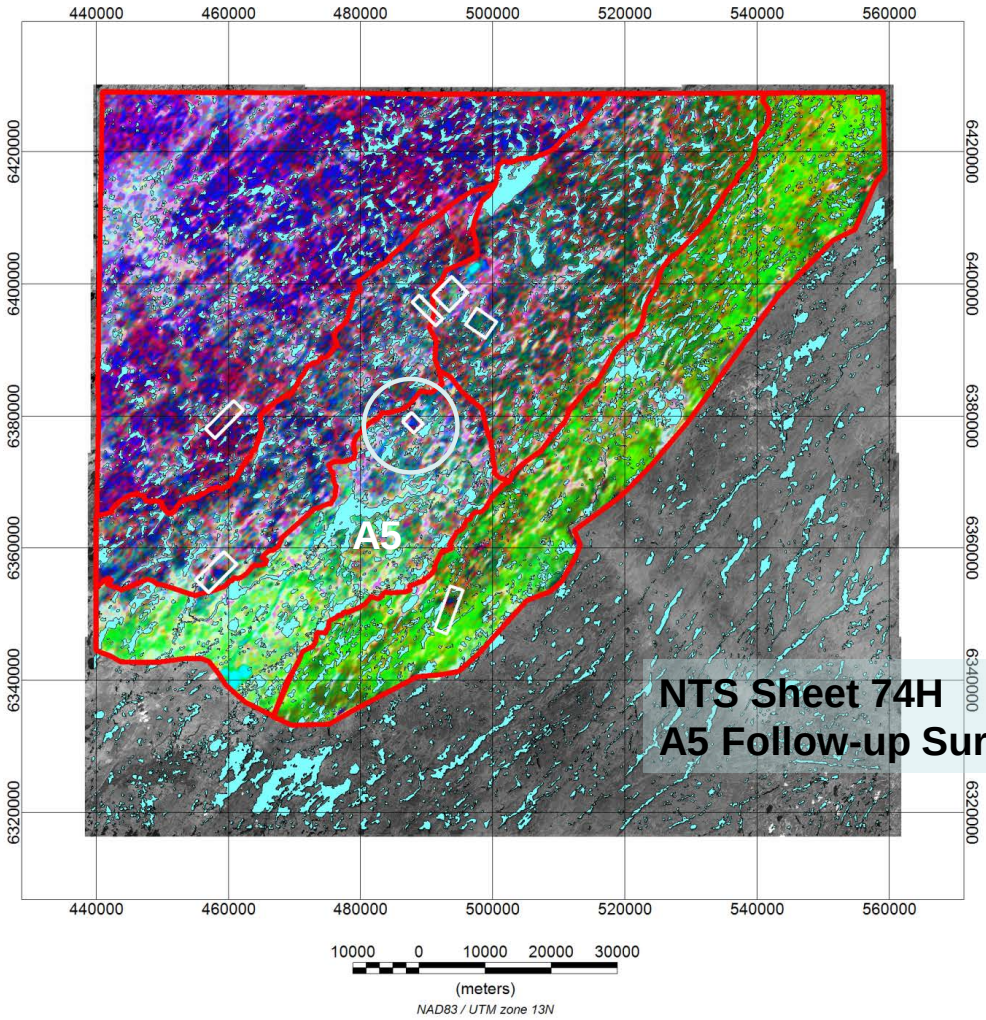
Natural Resources Canada | Ressources naturelles Canada

Canada



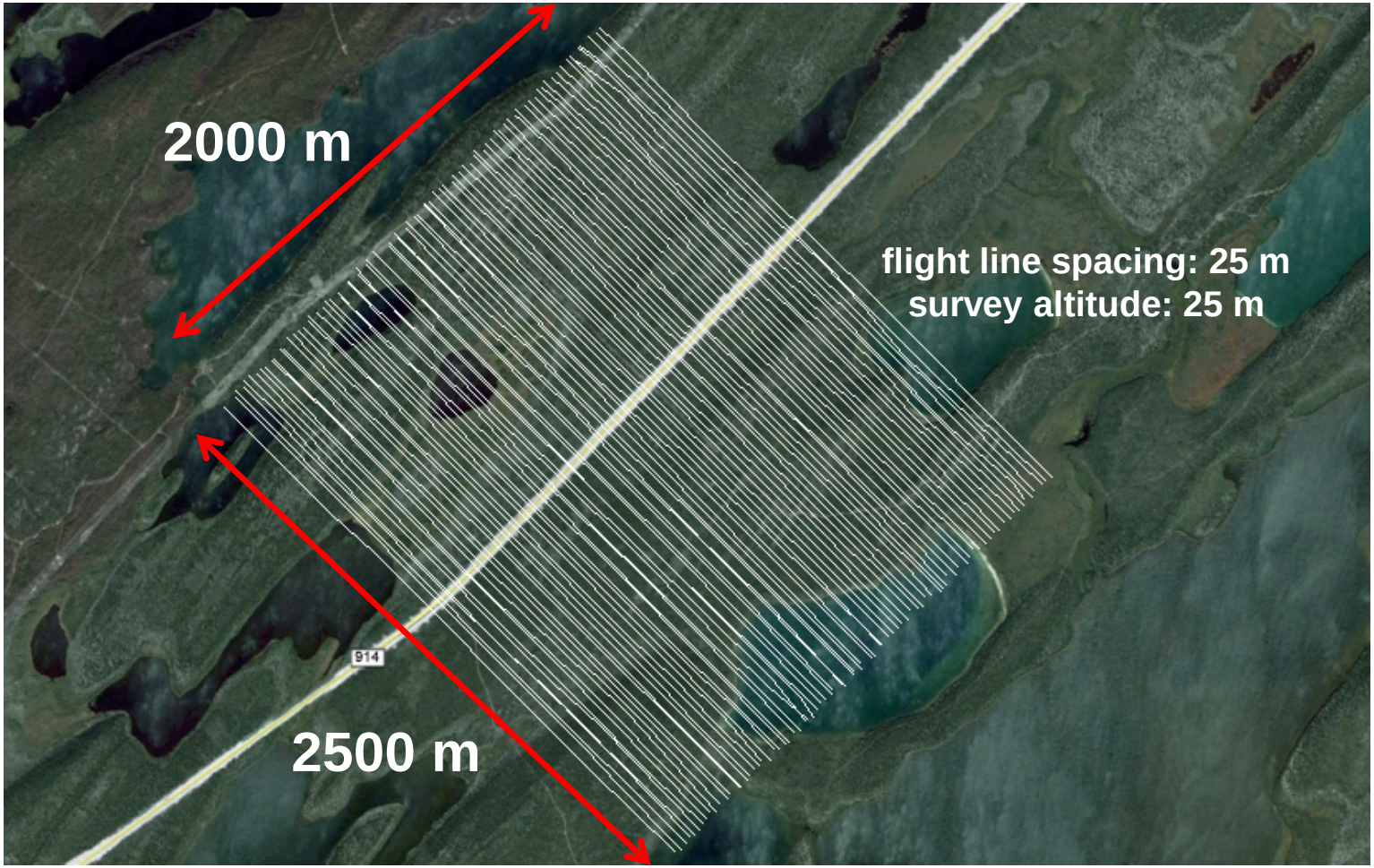
Natural Resources Canada | Ressources naturelles Canada

Canada



NTS Sheet 74H
A5 Follow-up Survey Area

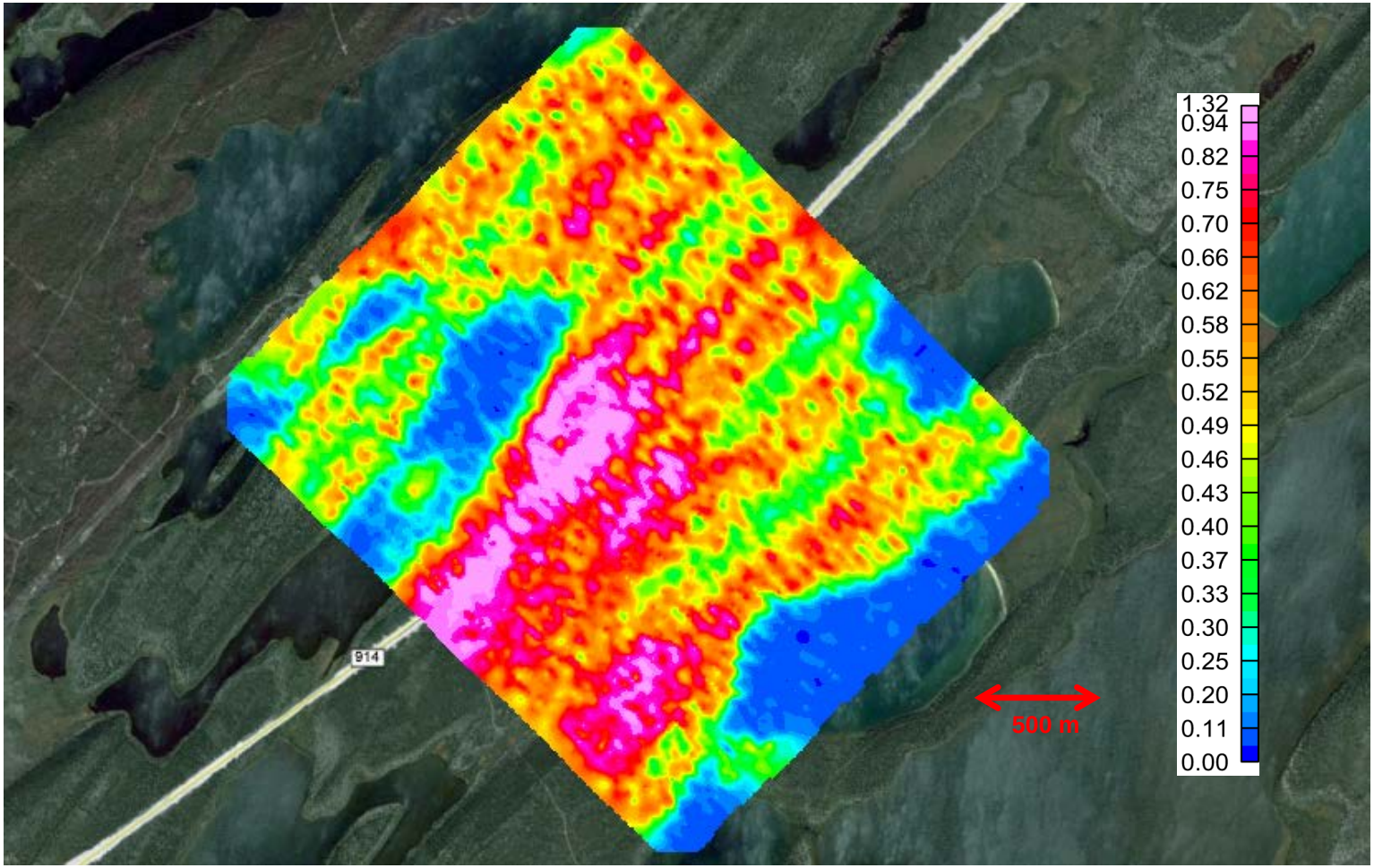
A5 follow-up area – helicopter survey parameters



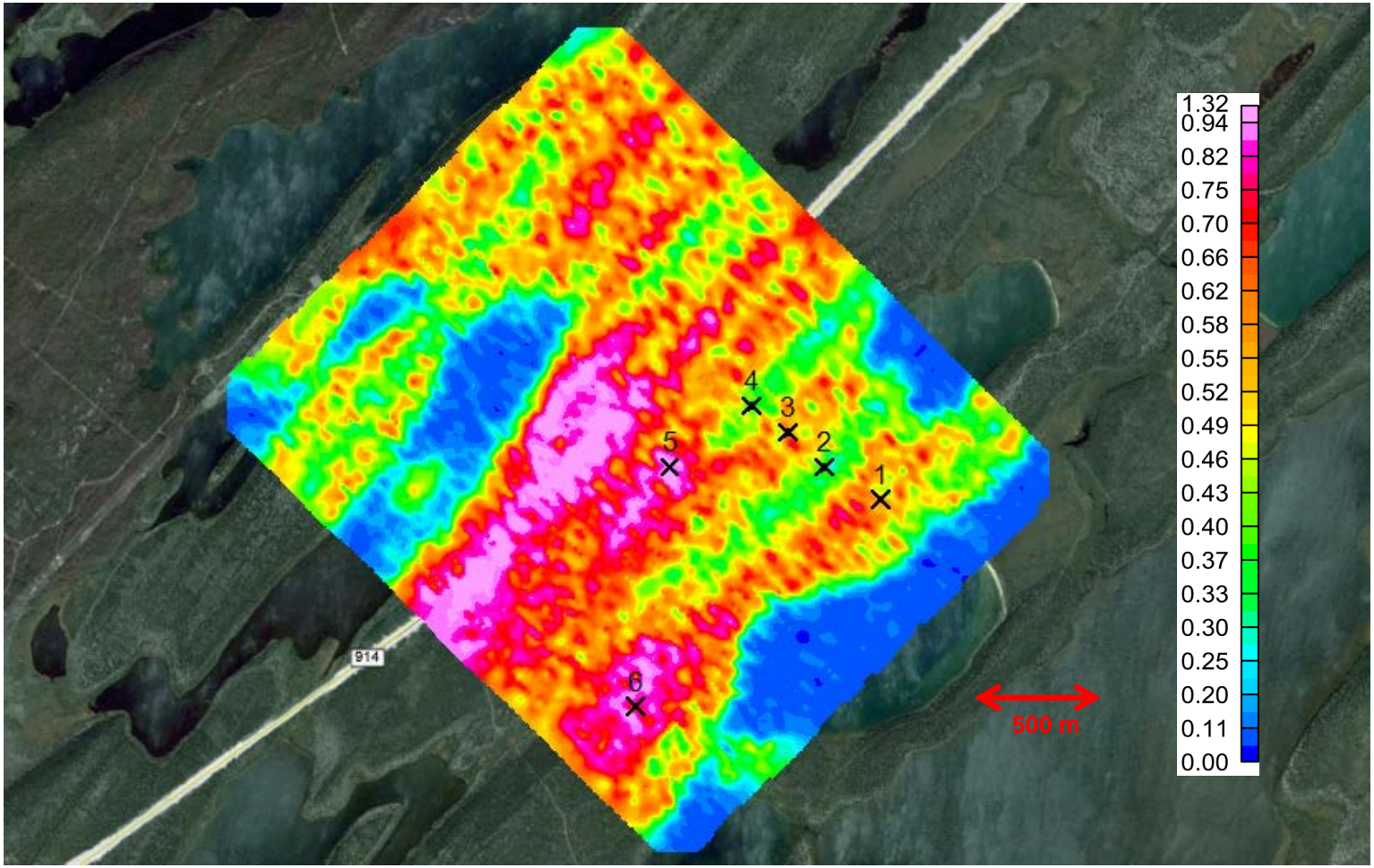
Natural Resources Canada | Ressources naturelles Canada

Canada

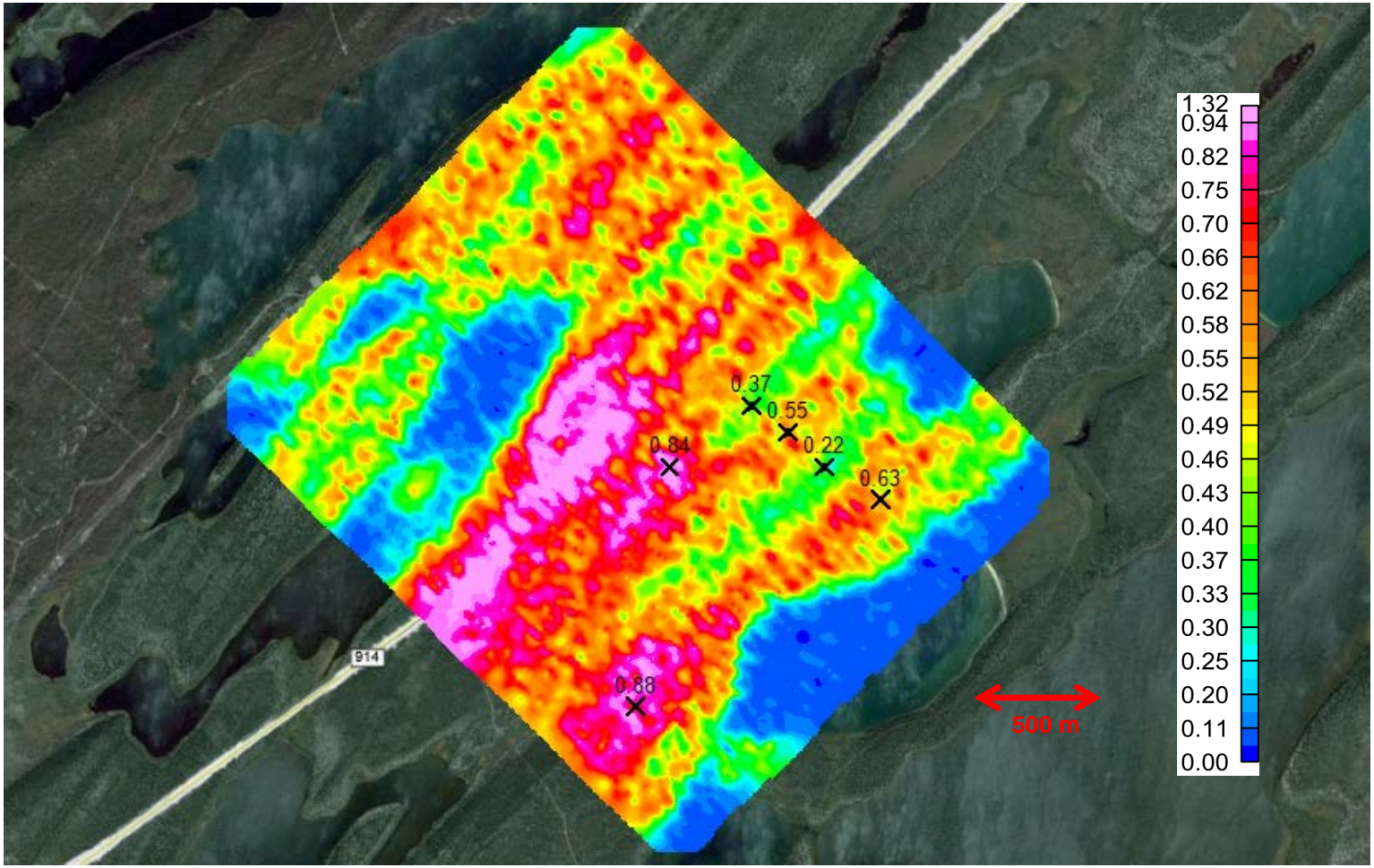
A5 follow-up area – potassium concentration (%) from airborne survey



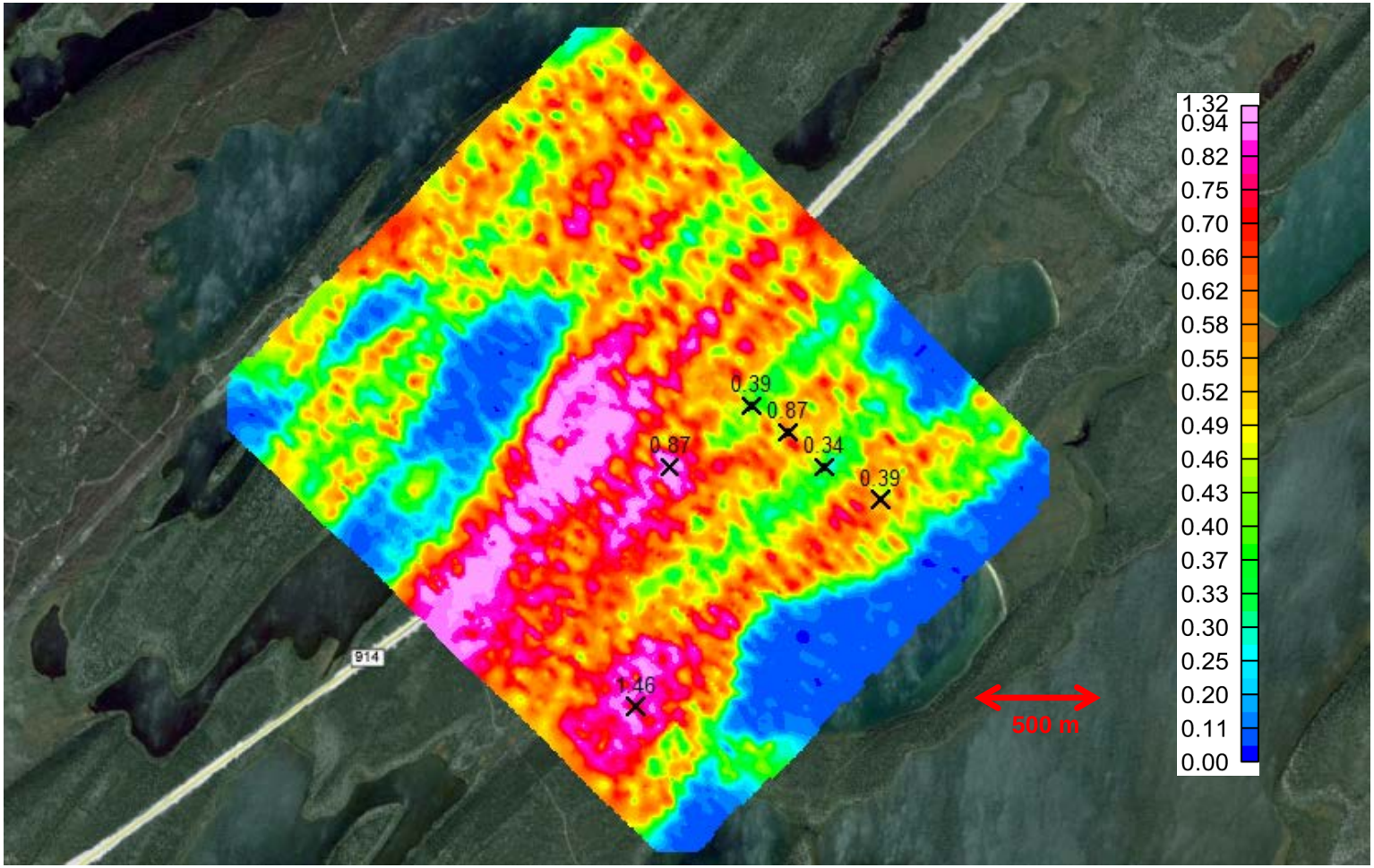
A5 follow-up area – ground sampling stations



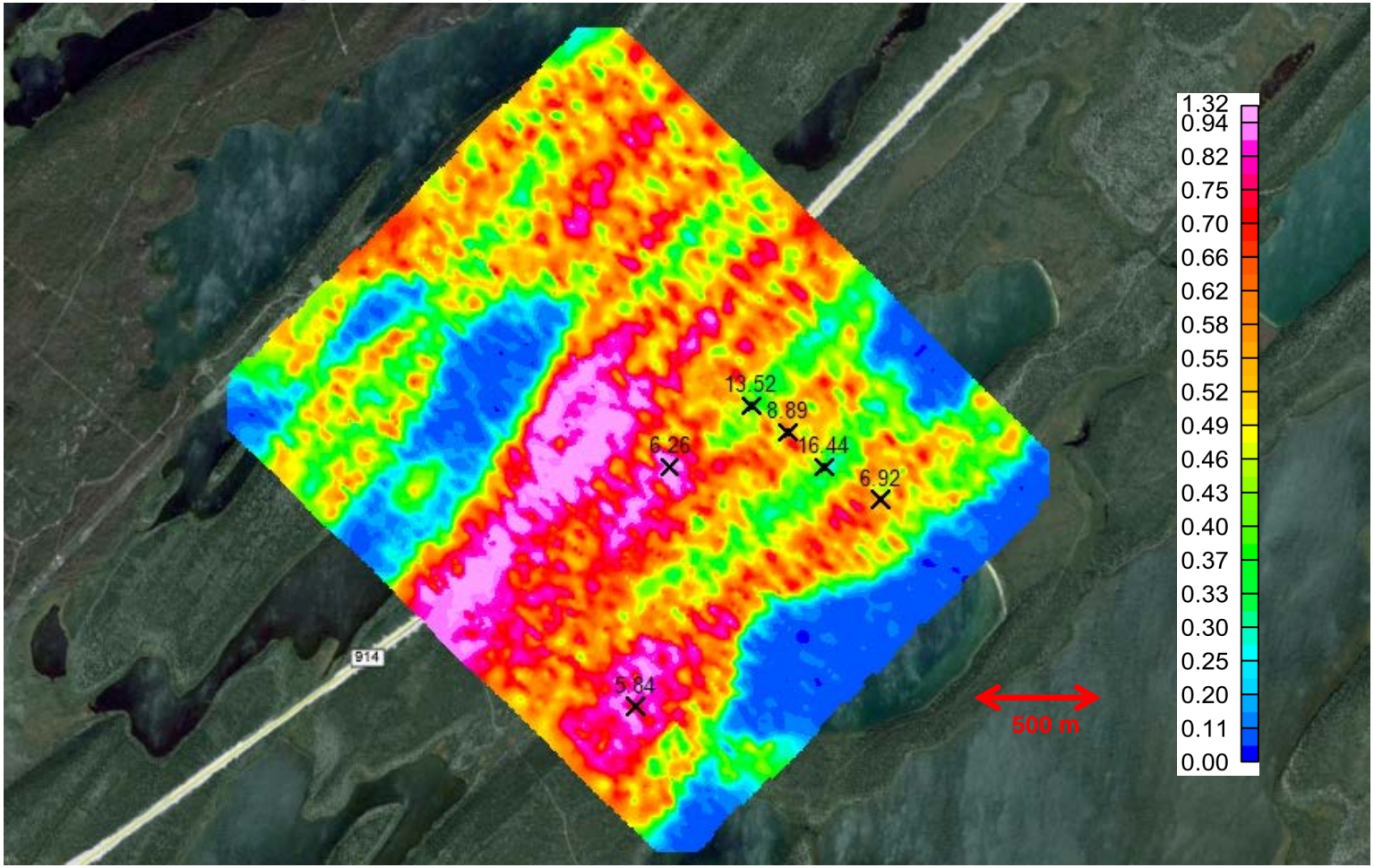
A5 follow-up area – potassium from ground spectrometry



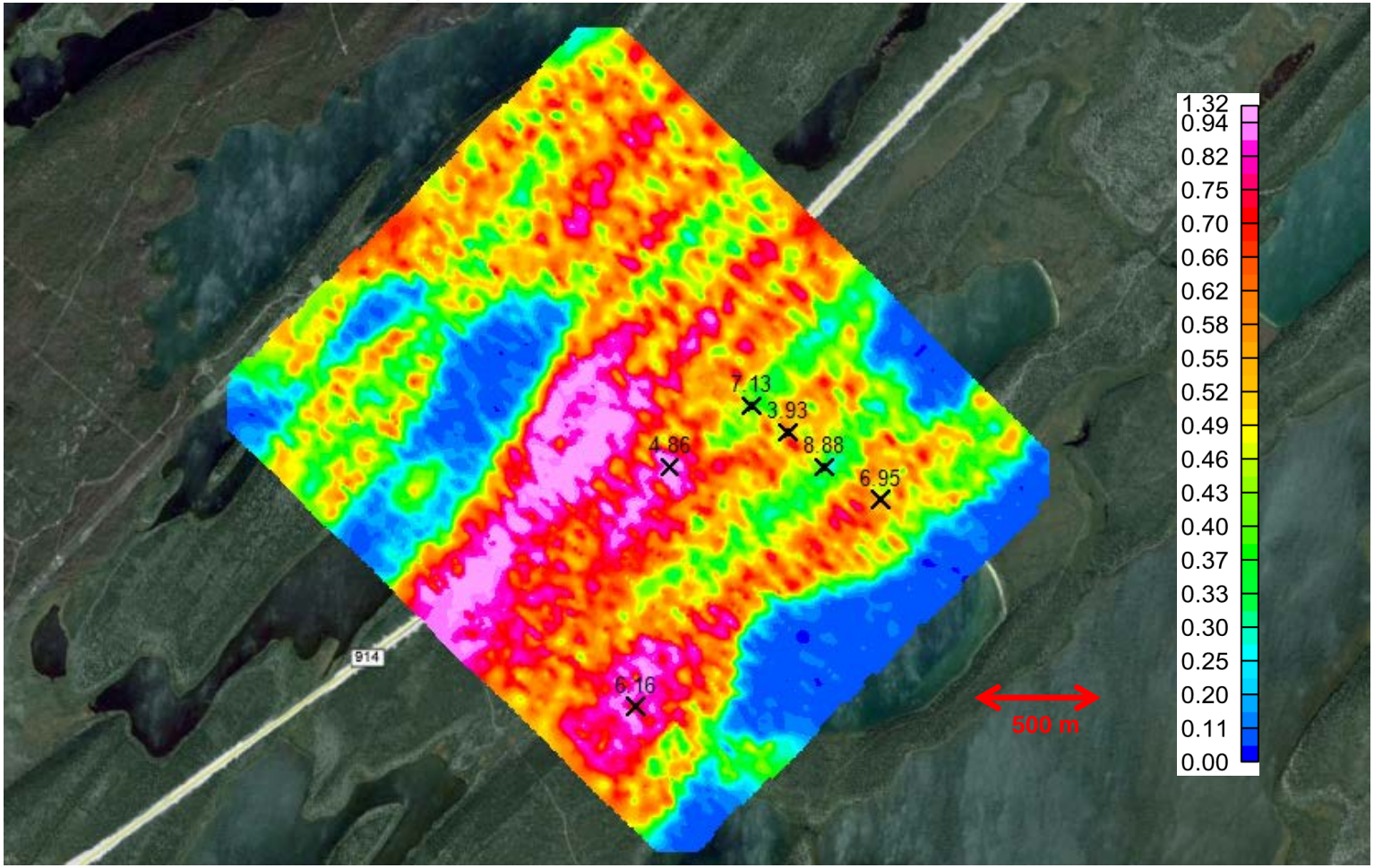
A5 follow-up area – potassium from lab spectrometry of < 2mm fraction



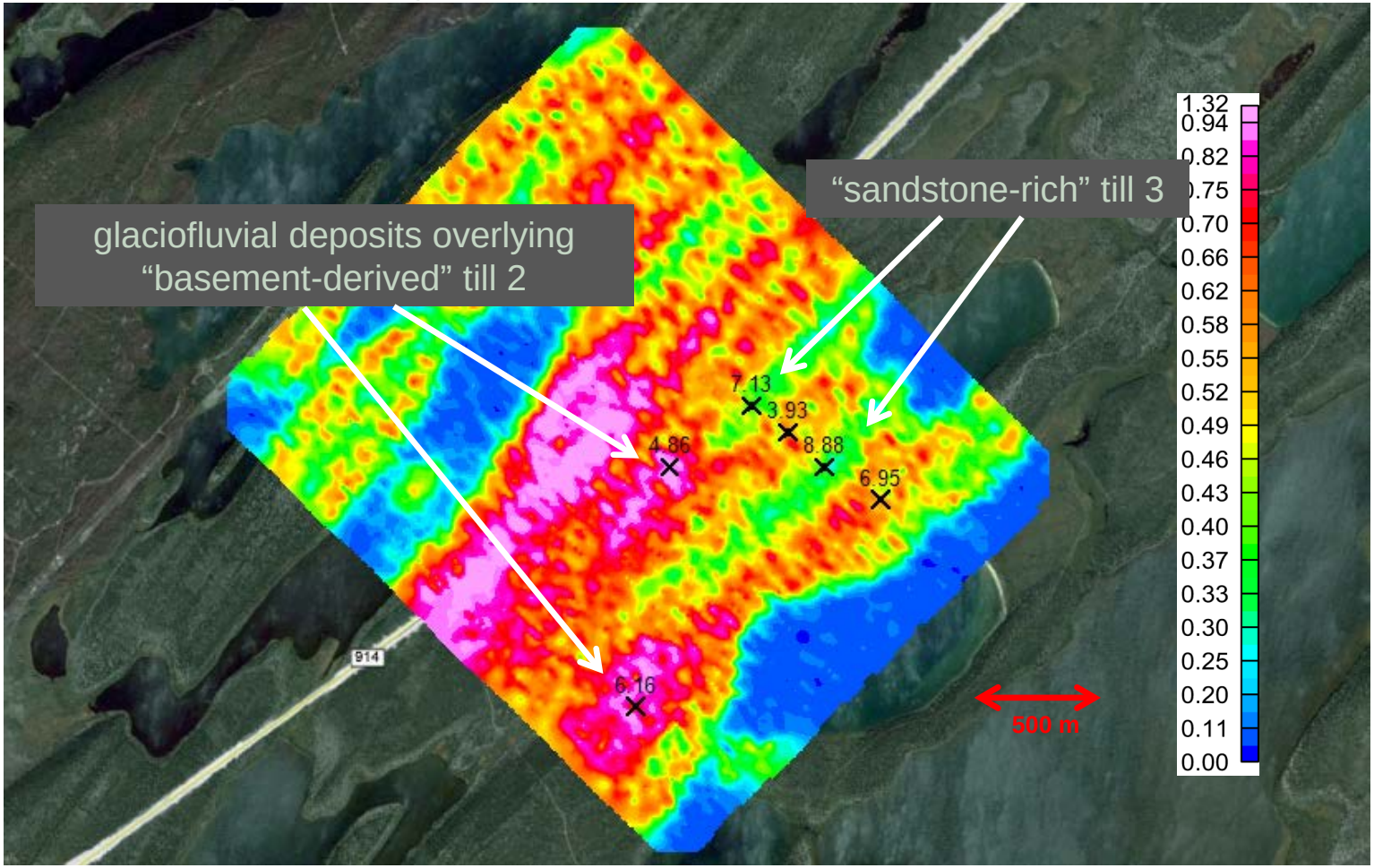
A5 follow-up area – thorium over potassium ratio from ground spectrometry



A5 follow-up area – thorium over potassium ratio from lab spectrometry of < 2mm fraction



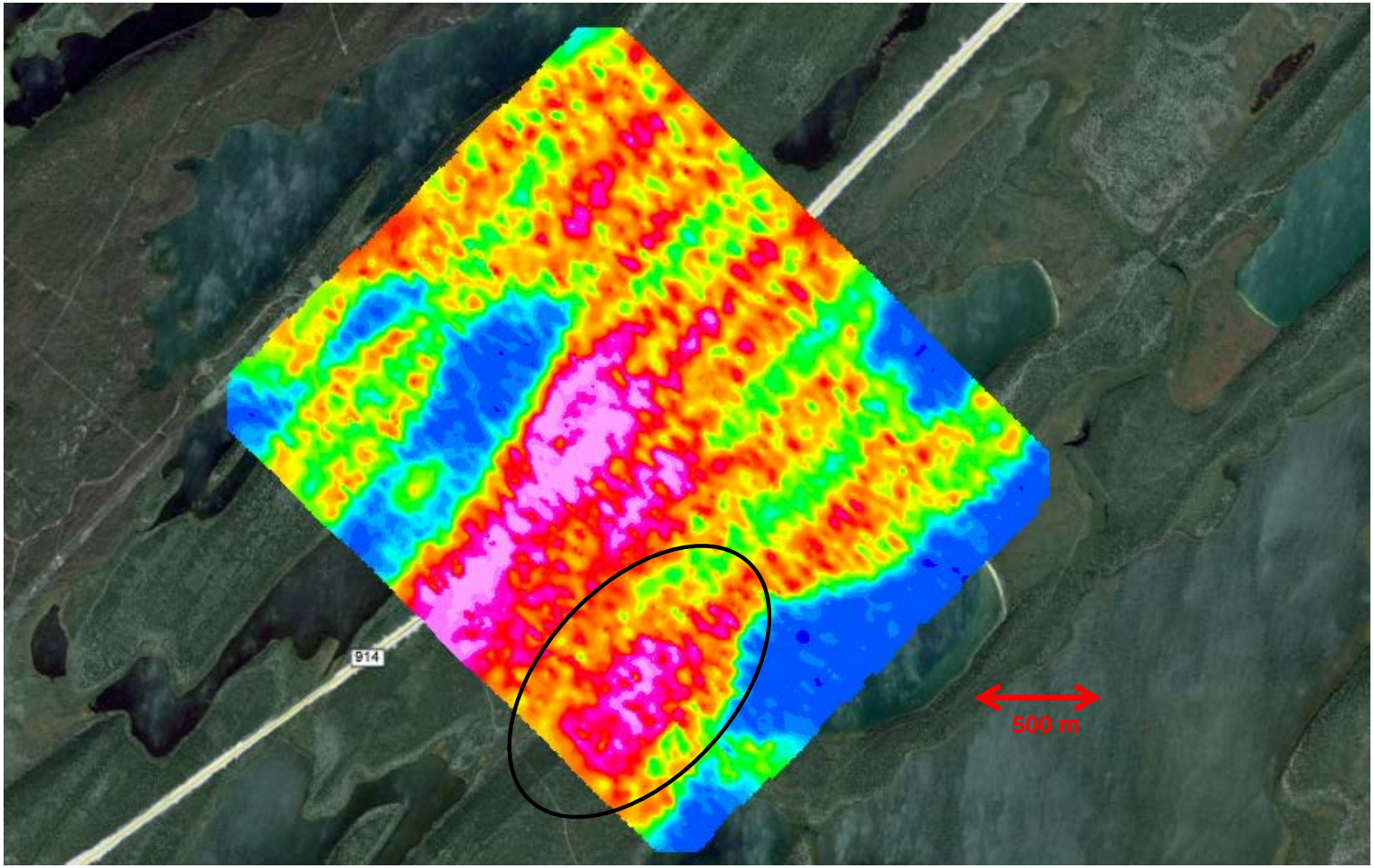
A5 follow-up area – thorium over potassium ratio from lab spectrometry of < 2mm fraction



A5 follow-up area – spectrometry vs landforms



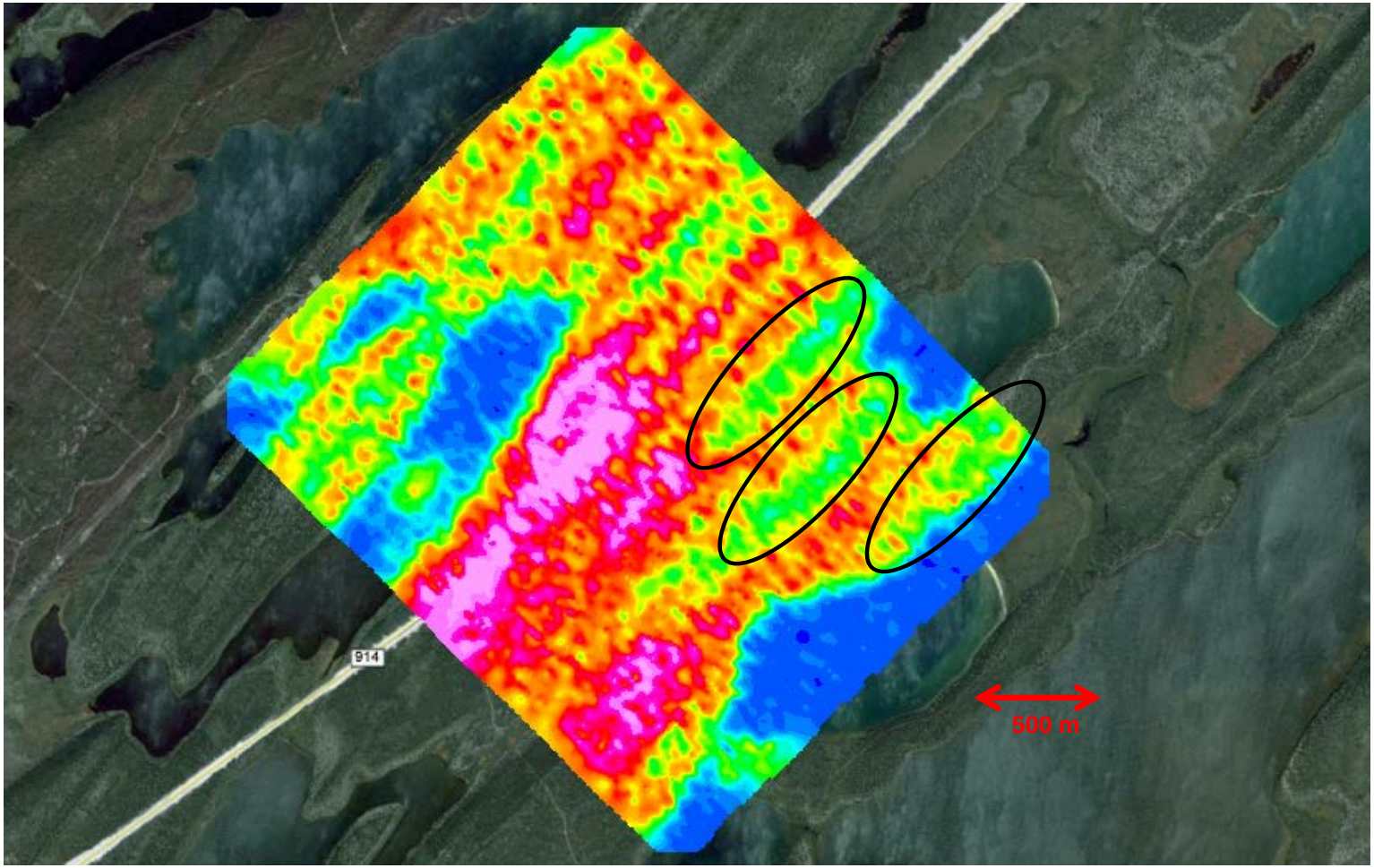
A5 follow-up area – potassium high



A5 follow-up area – potassium high - larger drumlin



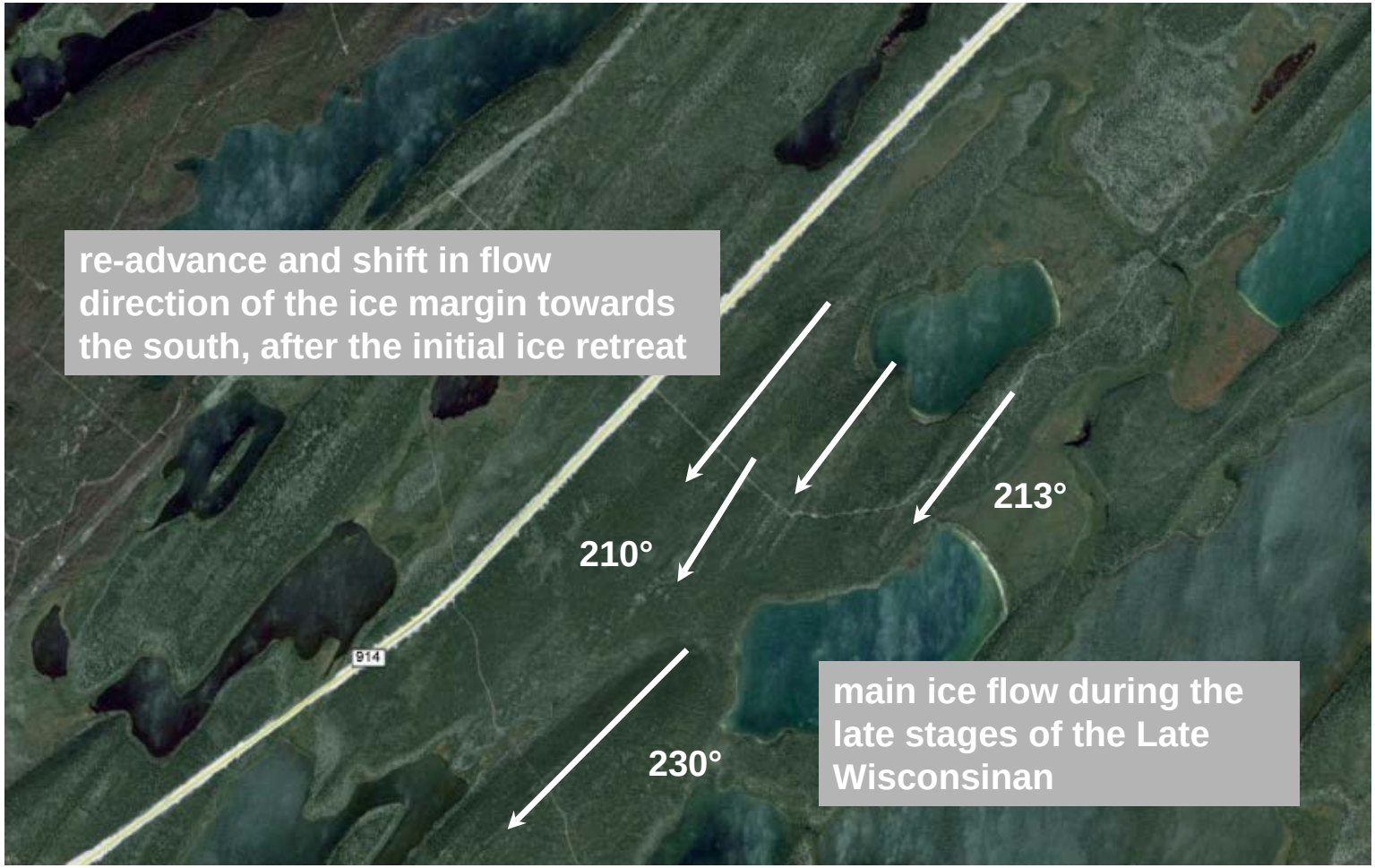
A5 follow-up area – potassium lows



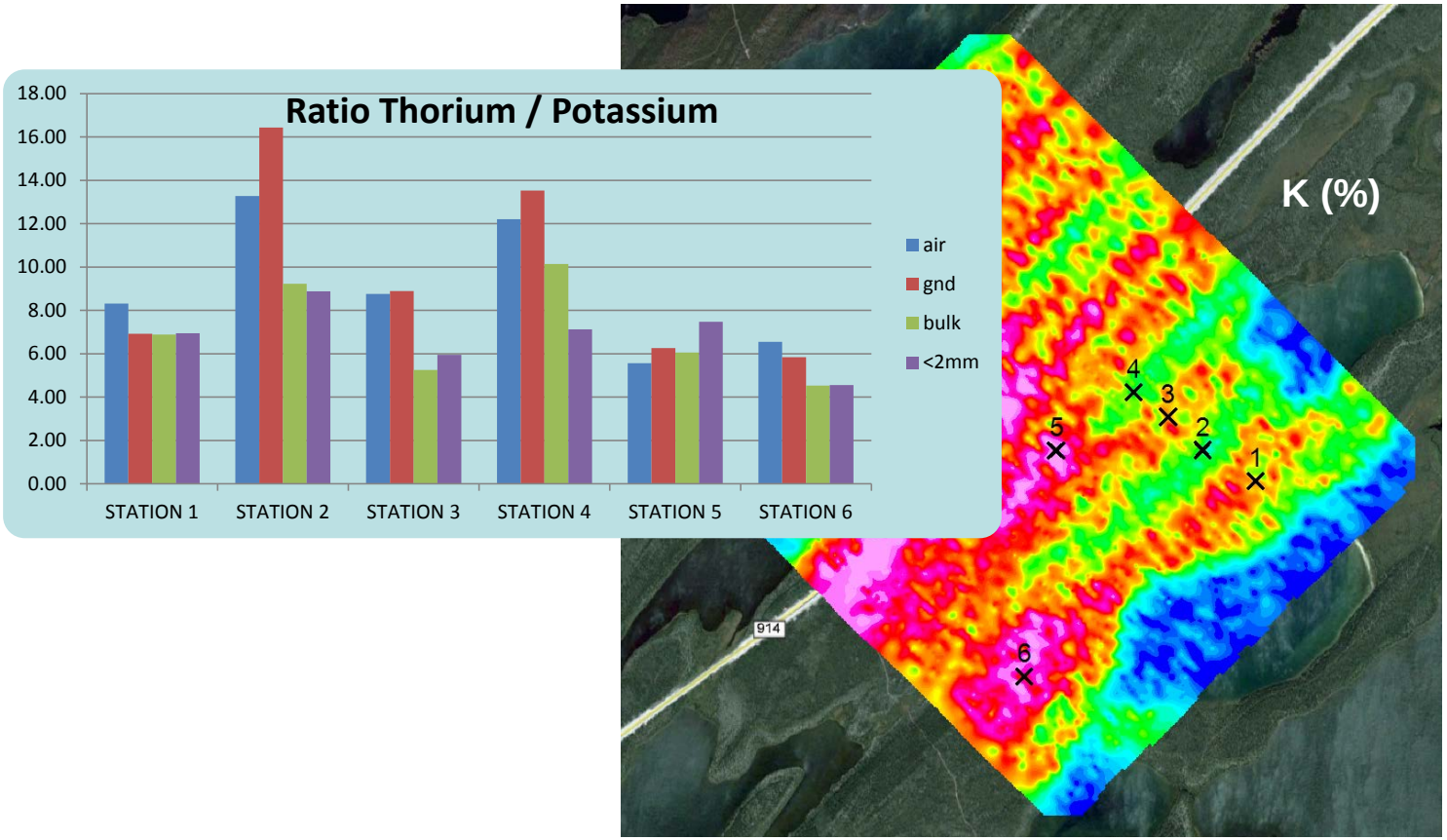
A5 follow-up area – potassium lows - narrower and smaller drumlinoid



A5 follow-up area – landforms provenance

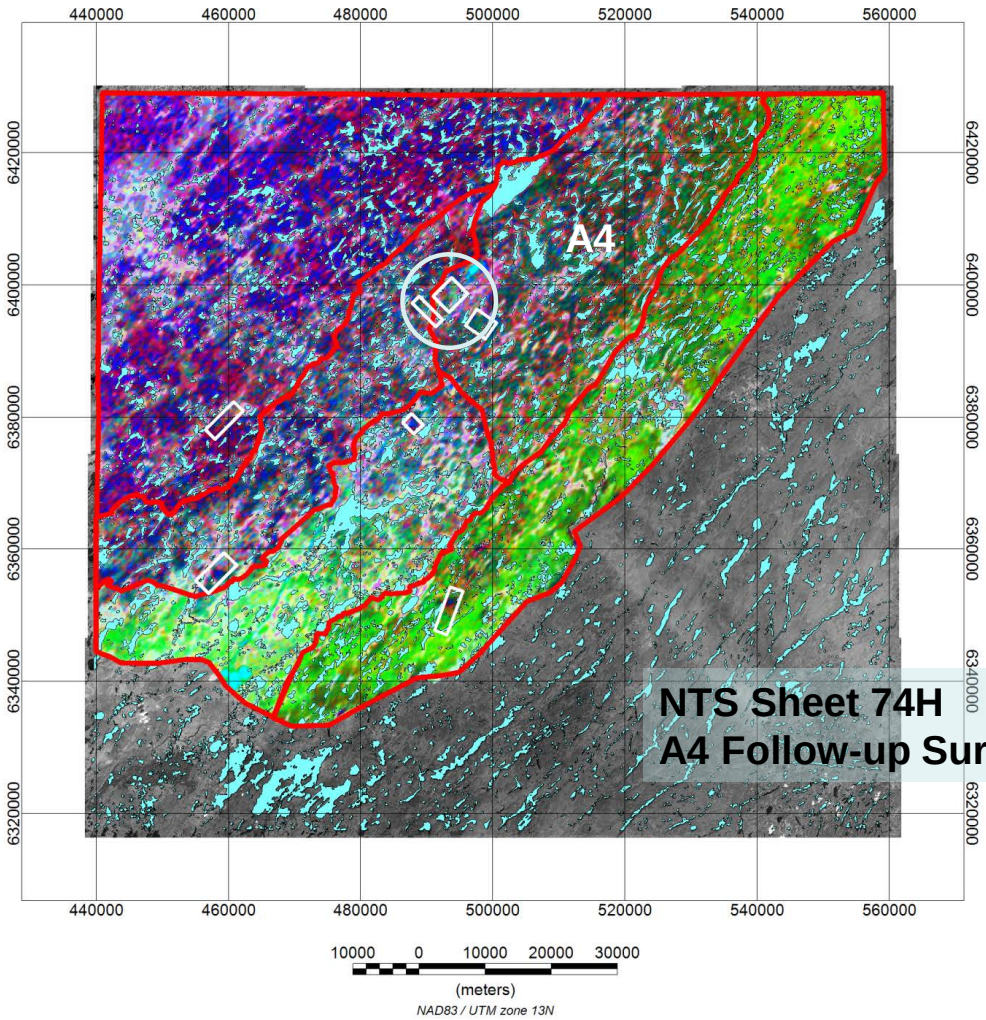


Survey A5 – airborne, ground and lab spectrometry



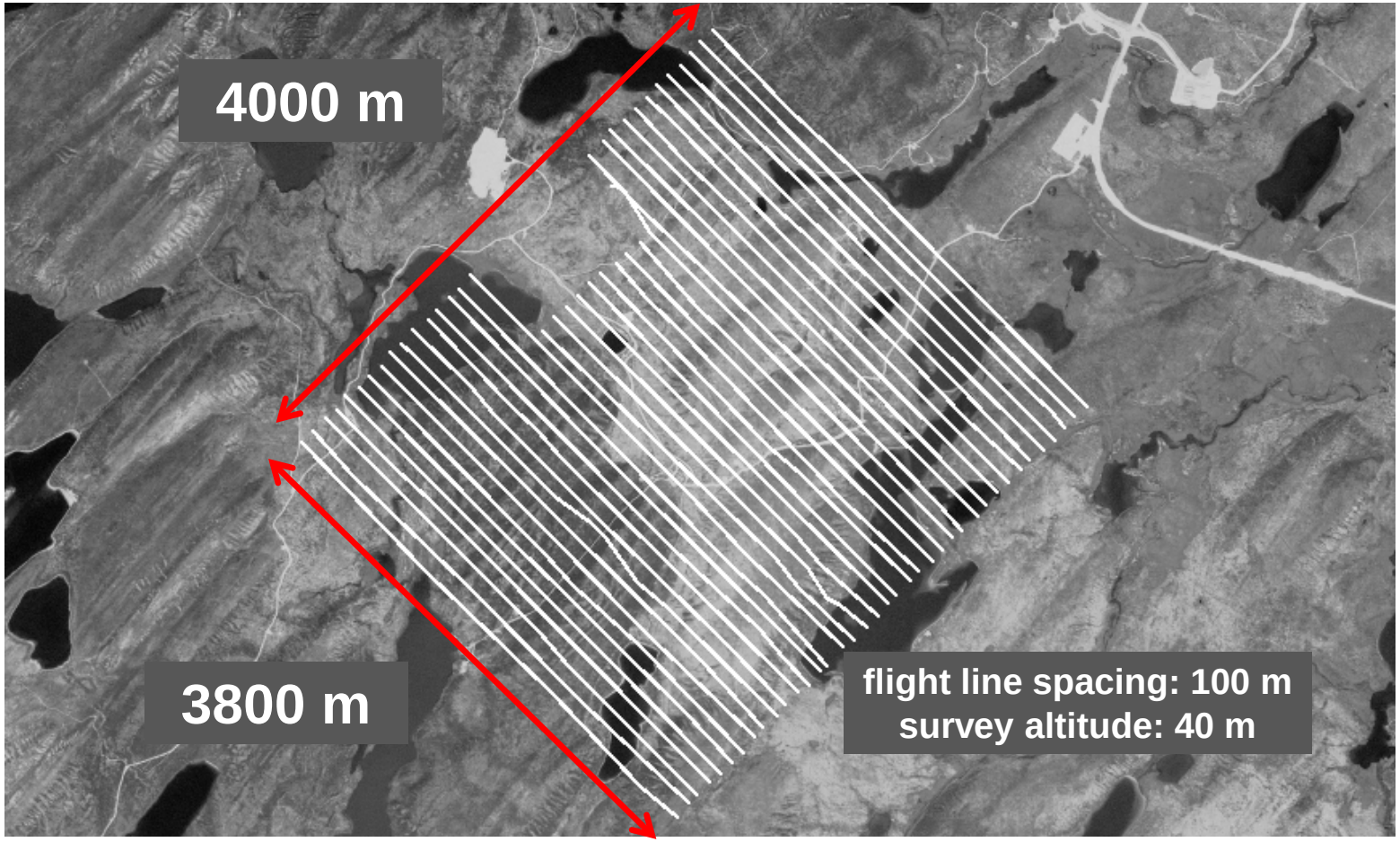
Natural Resources Canada | Ressources naturelles Canada

Canada

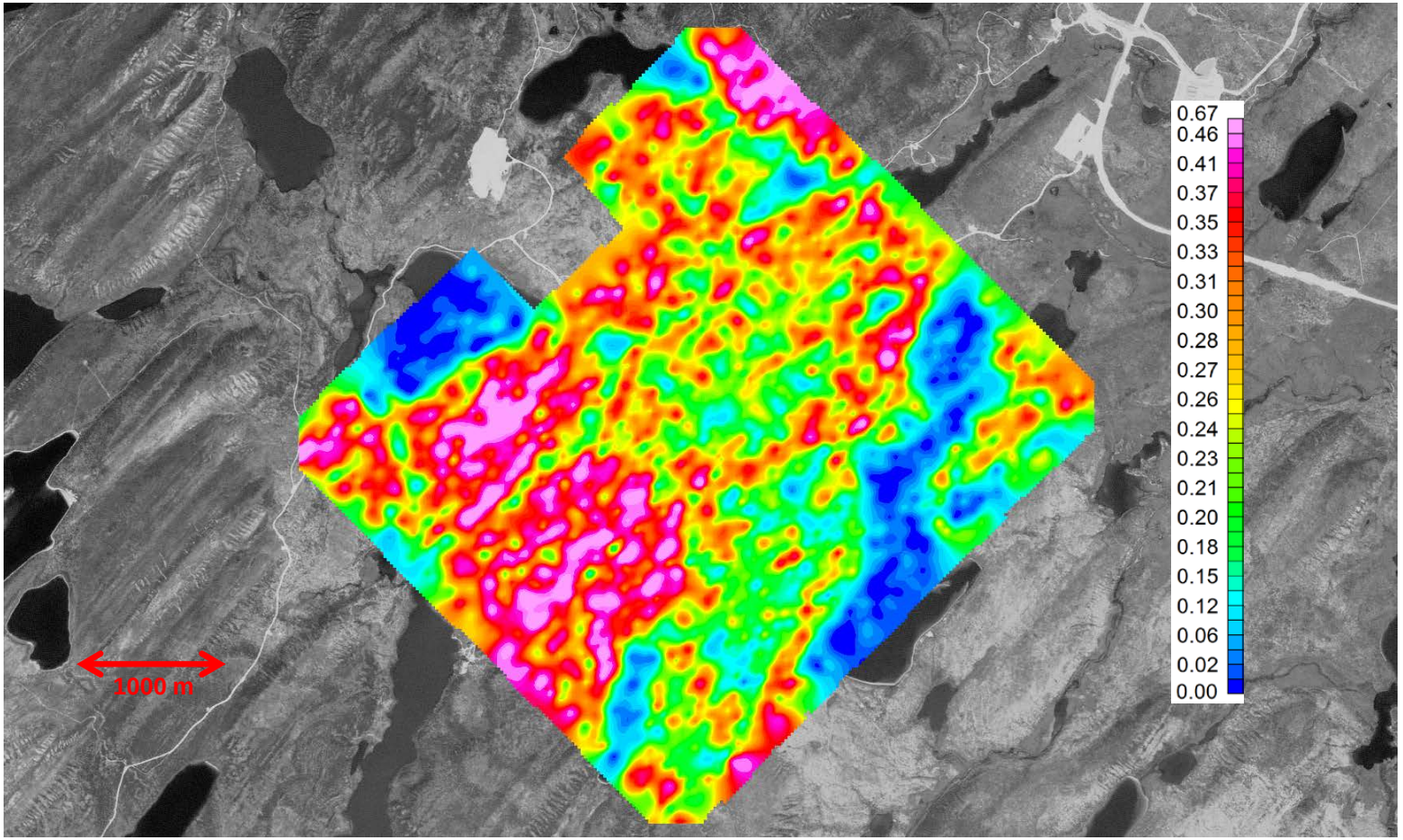


NTS Sheet 74H
A4 Follow-up Survey Area

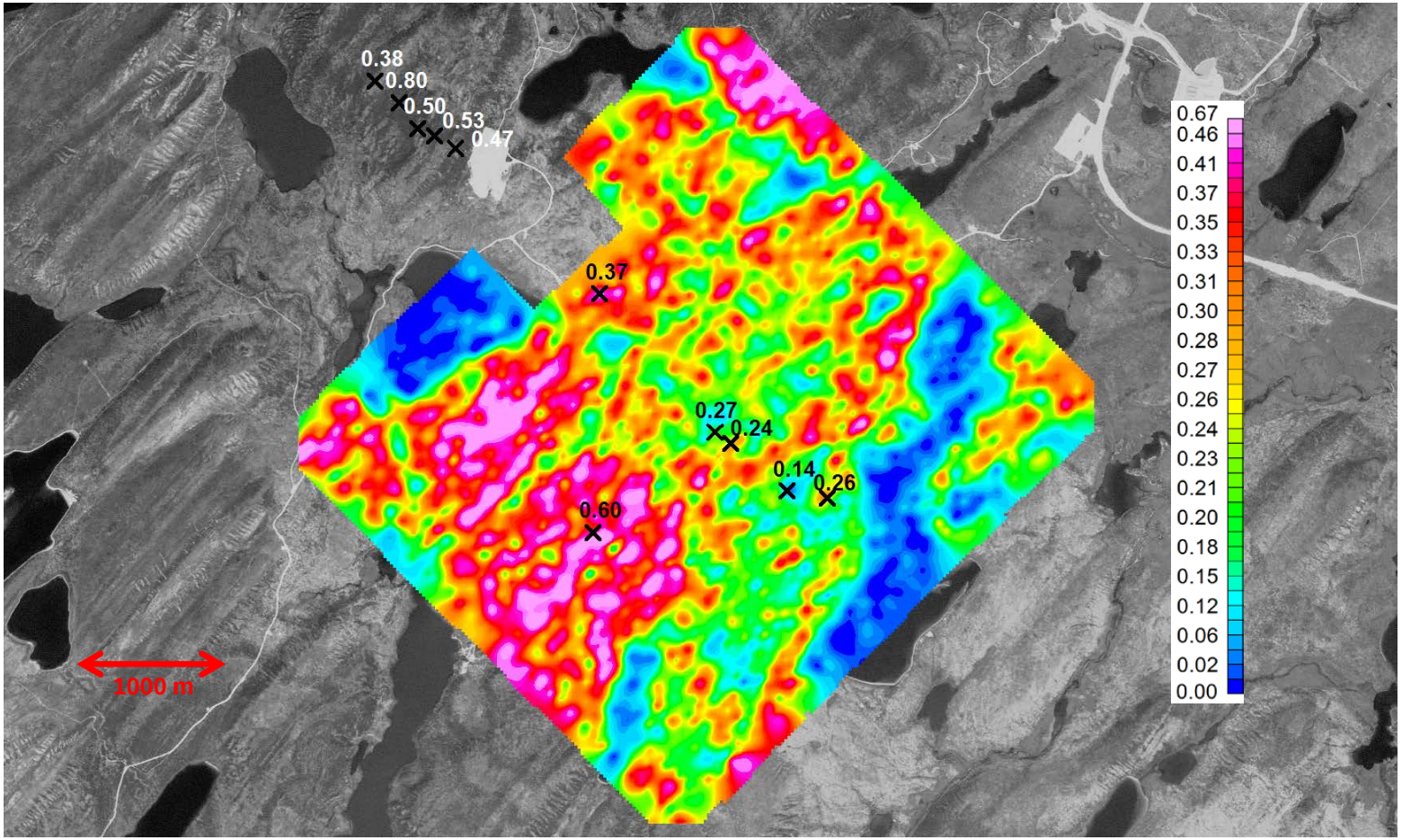
A4 follow-up area – helicopter survey parameters



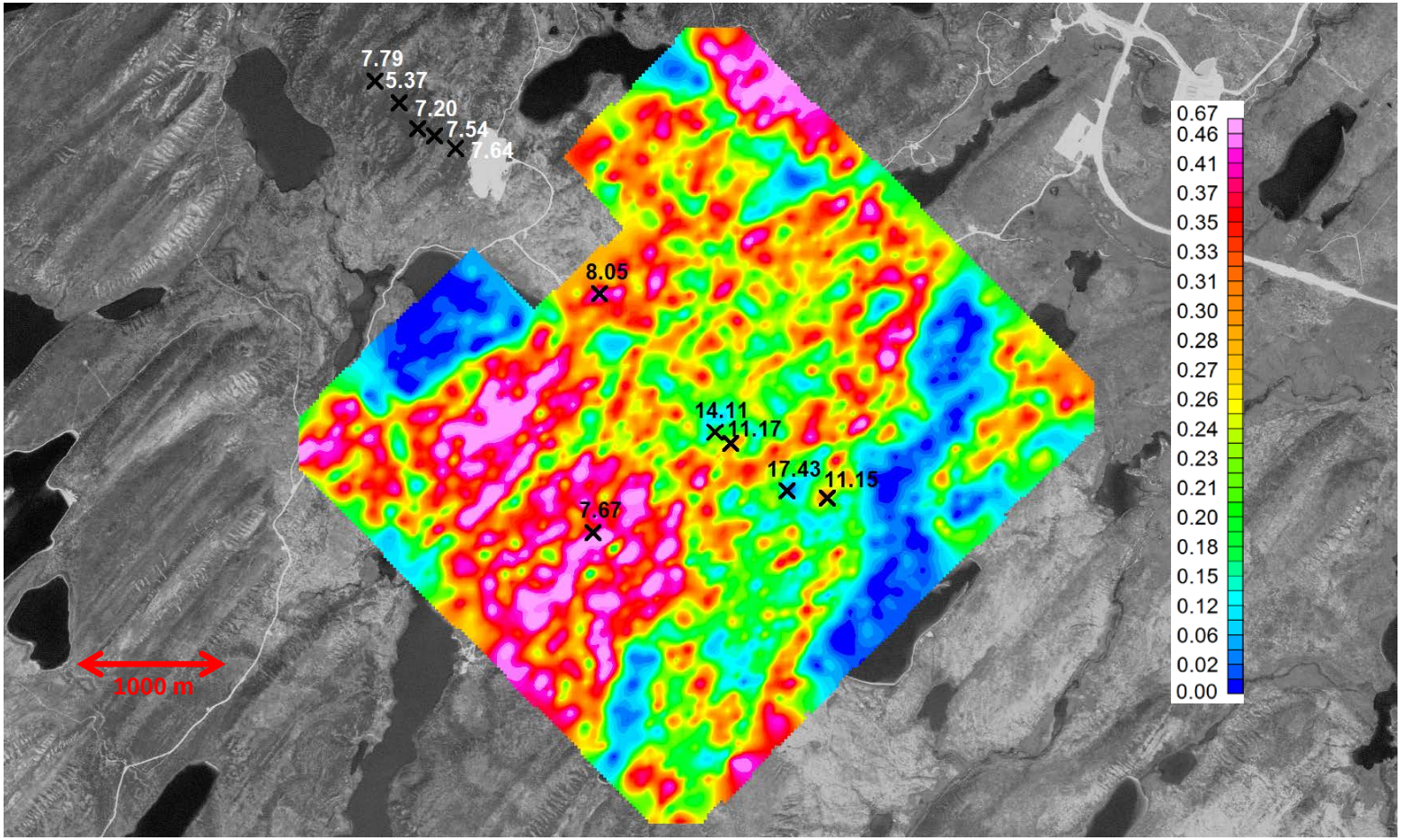
A4 follow-up area – potassium concentration (%) from airborne survey



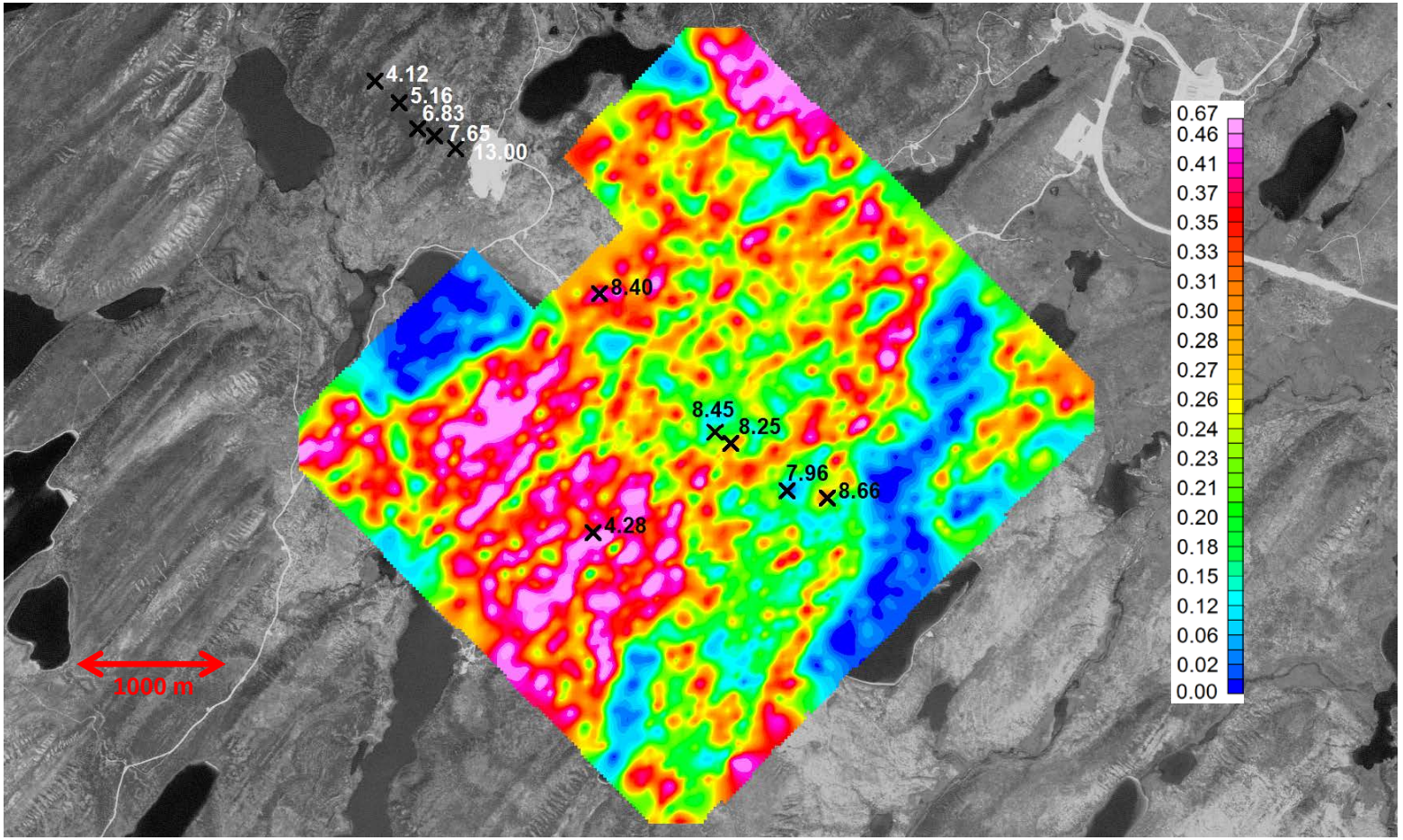
A4 follow-up area – potassium concentration (%) – ground spectrometry



A4 follow-up area – ratio thorium/potassium – ground spectrometry



A4 follow-up area – ratio thorium/potassium – gamma-ray laboratory



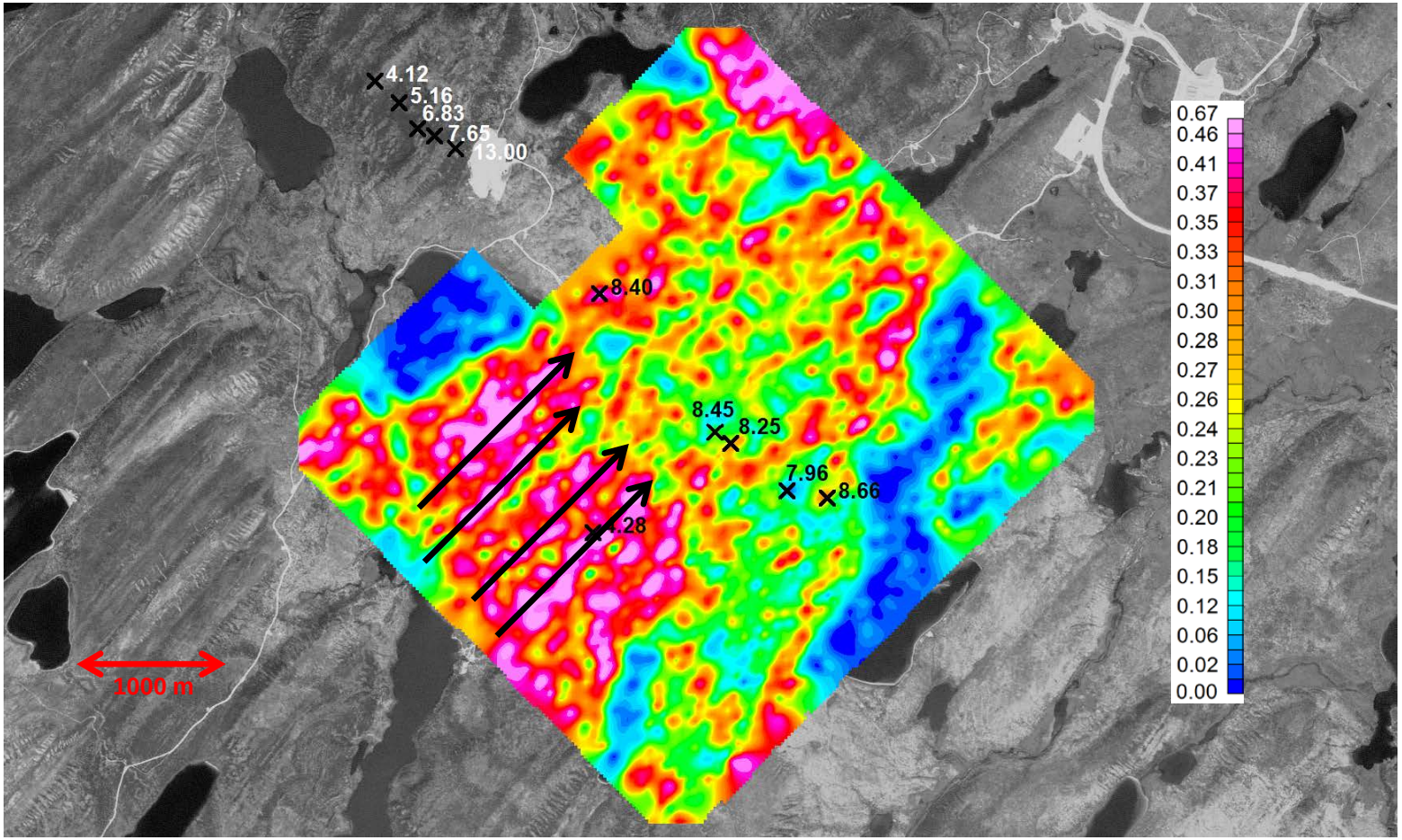
A4 follow-up area – ratio thorium/potassium – gamma-ray laboratory



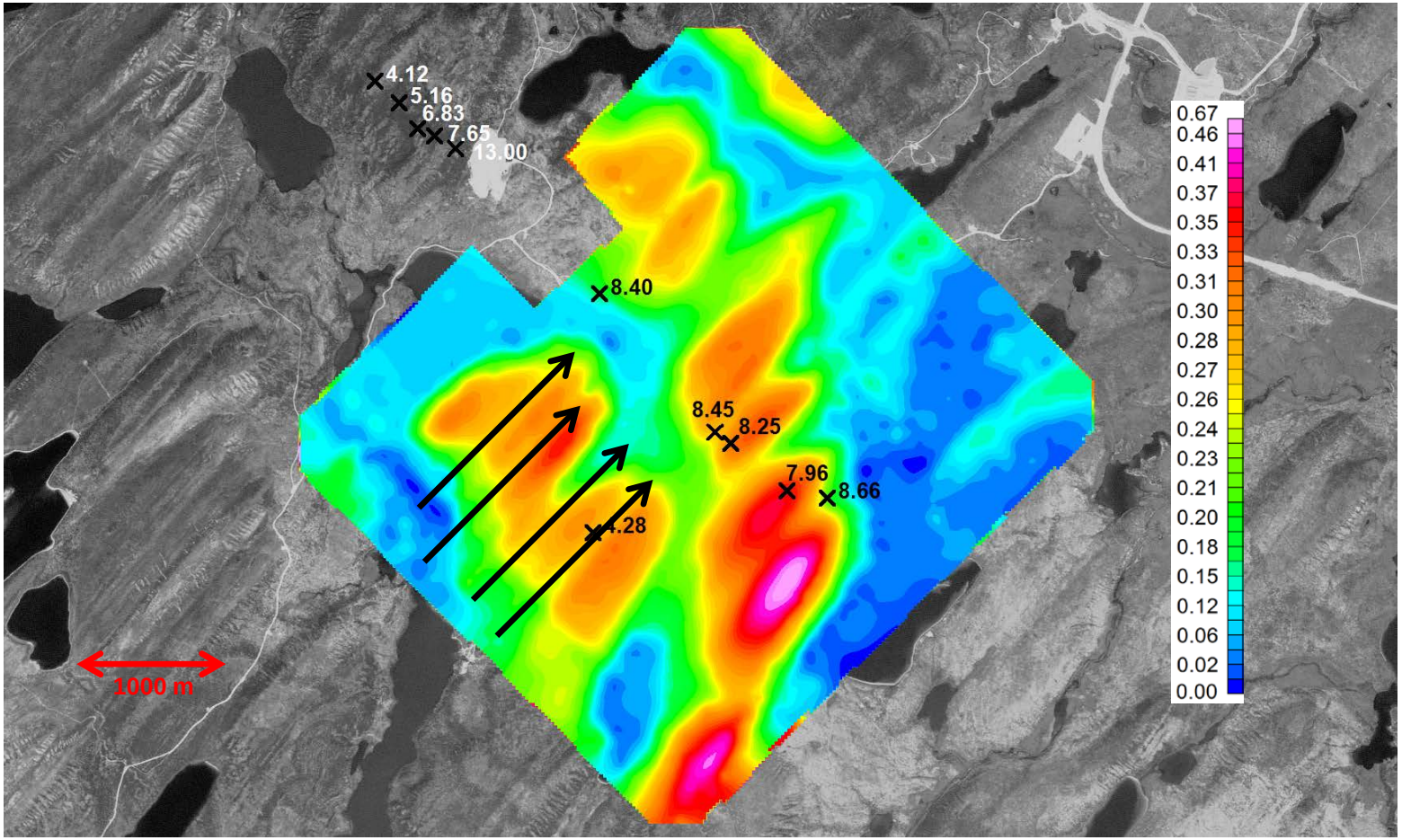
Natural Resources Canada | Ressources naturelles Canada

Canada

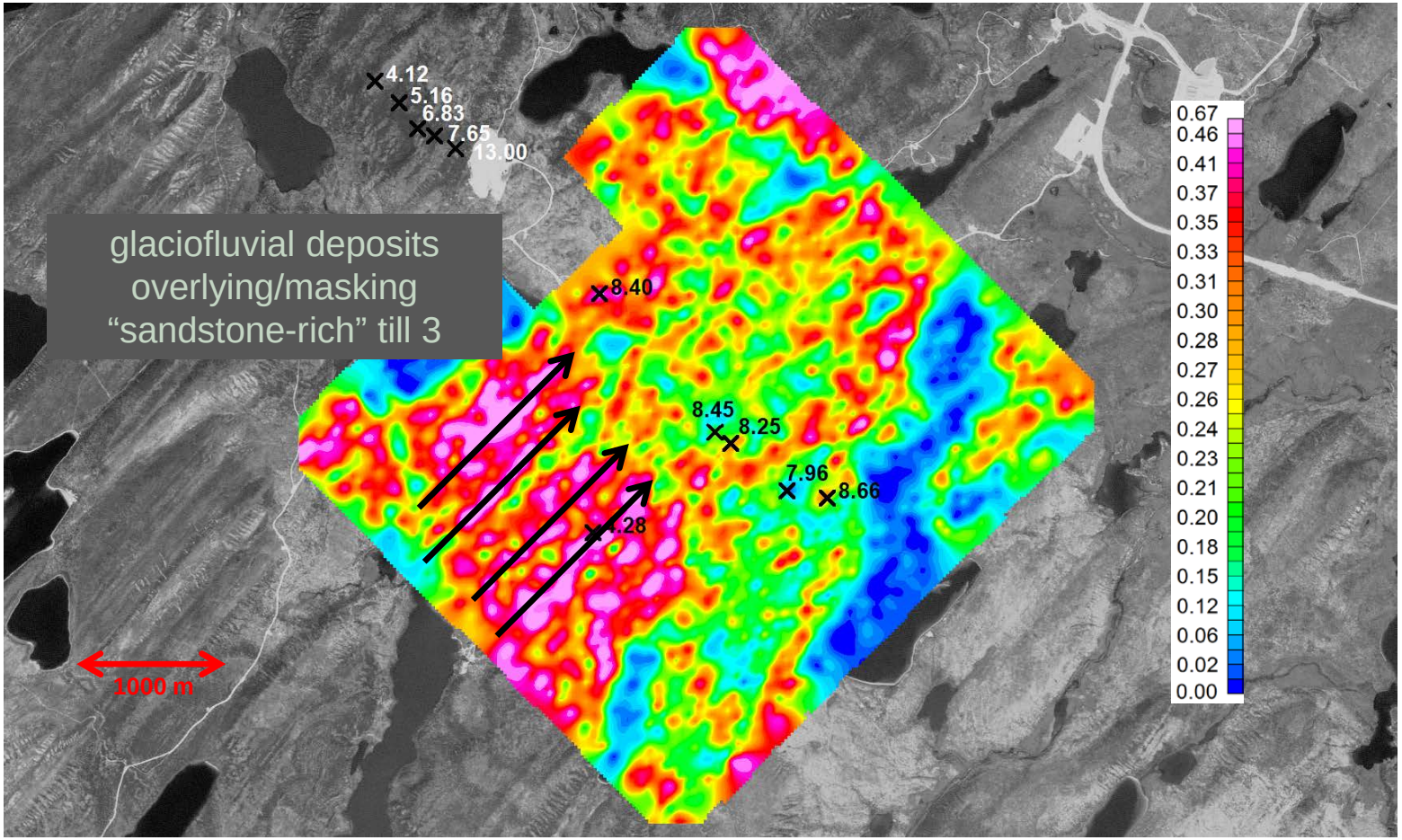
A4 follow-up area – ratio thorium/potassium – gamma-ray laboratory



A4 follow-up area – potassium concentration (%) from airborne survey



A4 follow-up area – ratio thorium/potassium – gamma-ray laboratory



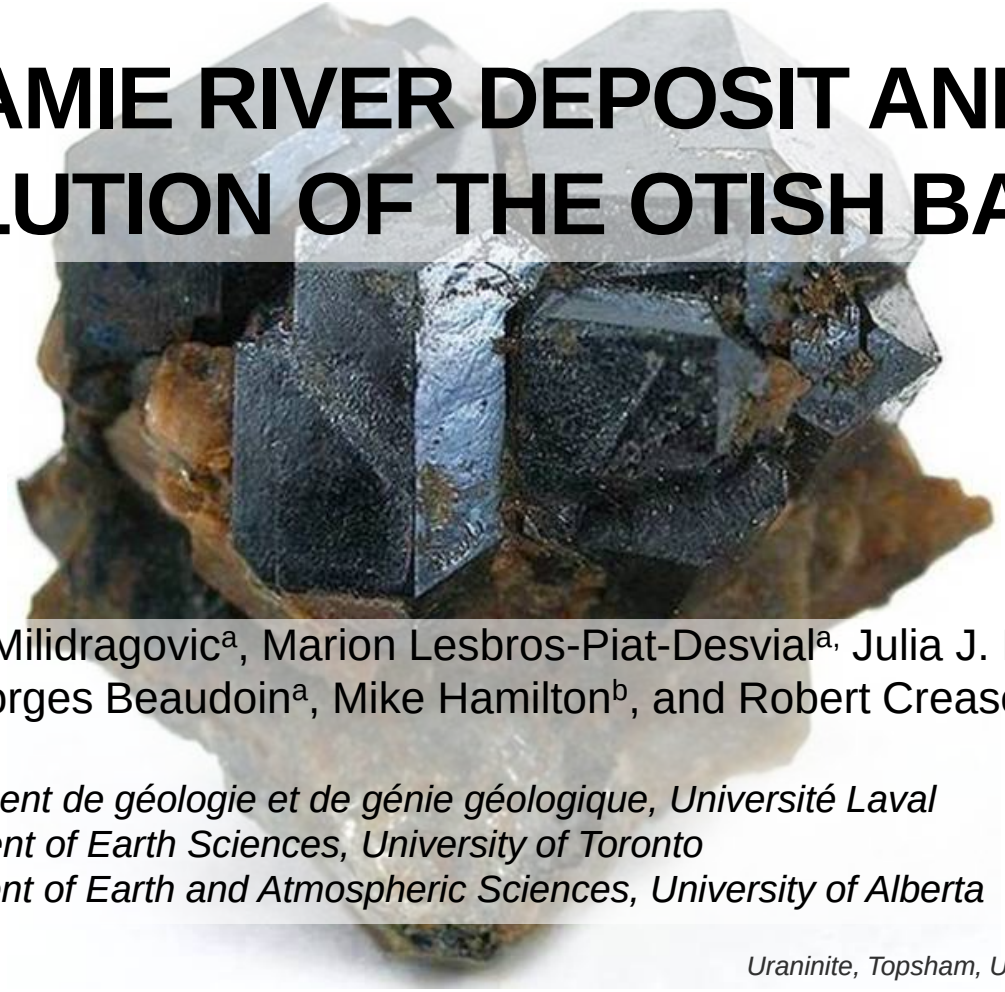
Natural Resources Canada | Ressources naturelles Canada

Canada

Summary

- Airborne gamma-ray spectrometry (AGRS) data is available for the whole Athabasca Basin.
  - should be reviewed, as part of exploration program
  - NRCan's Geoscience Data Repository
- AGRS can discriminate surficial deposits from different provenance.
  - …and specific landforms
- Understanding AGRS, as background
  - Anomalies can be discriminated
  - Sources of anomalies can be traced back
- Data analysis ongoing
  - pebble counts, boulder measurements and geochemistry

CAMIE RIVER DEPOSIT AND EVOLUTION OF THE OTISH BASIN



Dejan Milidragovic[a], Marion Lesbros-Piat-Desvial[a], Julia J. King[a], Georges Beaudoin[a], Mike Hamilton[b], and Robert Creaser[c]

[a] *Département de géologie et de génie géologique, Université Laval*
[b] *Department of Earth Sciences, University of Toronto*
[c] *Department of Earth and Atmospheric Sciences, University of Alberta*

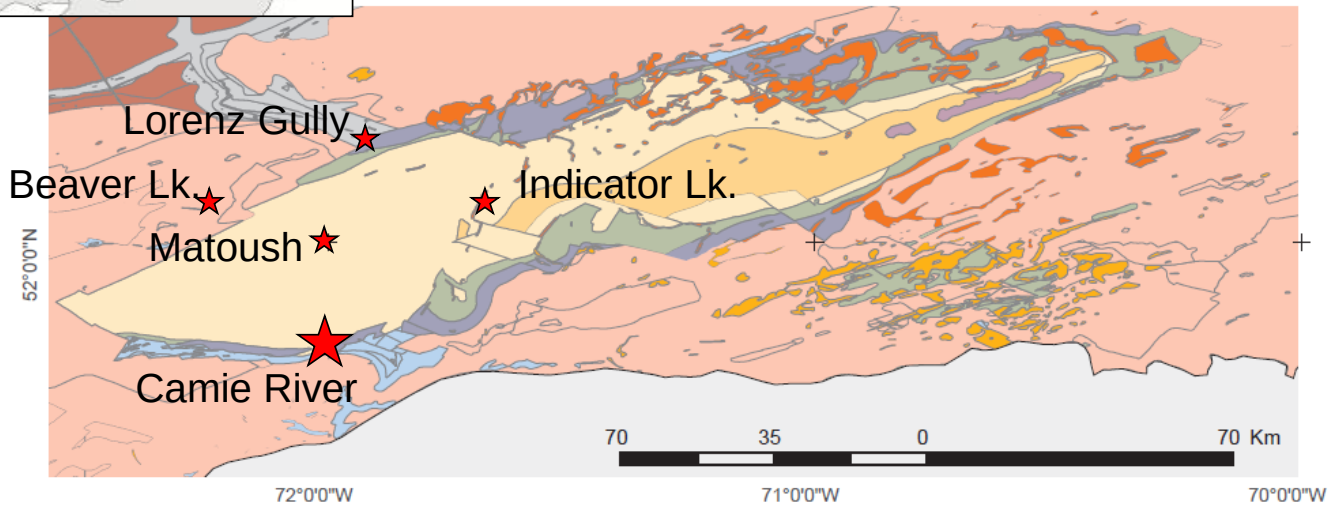
Uraninite, Topsham, USA

TGI-4 workshop, Saskatoon, Dec. 4th, 2014



Over 30 U occurrences, including:

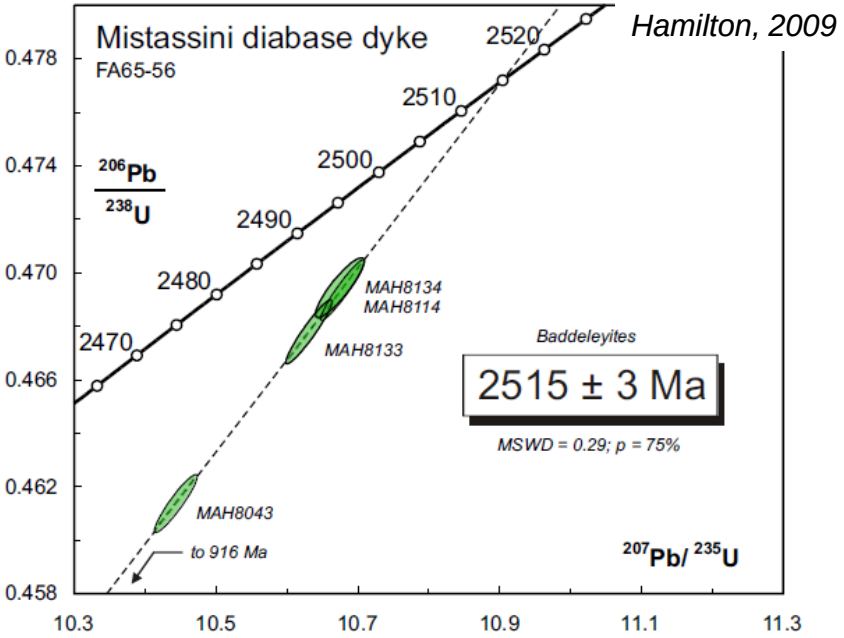
- Matoush (structurally controlled?) indicated resources: 586,000 tonnes @ 0.95 % U_3O_8
- Beaver Lake (breccia hosted) 467,000 lbs @ 0.11% U_3O_8 (not 43-101 compliant)
- Lavoie "L" deposit (indicated) 391,000 t @ 0.45% U_3O_8 (3,910,000 lbs U_3O_8)
- Camie River (unconformity related)
- Otish South
- Lorenz-Gully (structurally controlled)
- Takwa River (stratiform, basement hosted)



Outline

- Geological overview
- The Camie River prospect
- The Otish Gabbro suite
- Revised geological history of Otish Basin
- Implications for uranium mineralization

Intrusion of the Mistassini dykes



2515 Ma

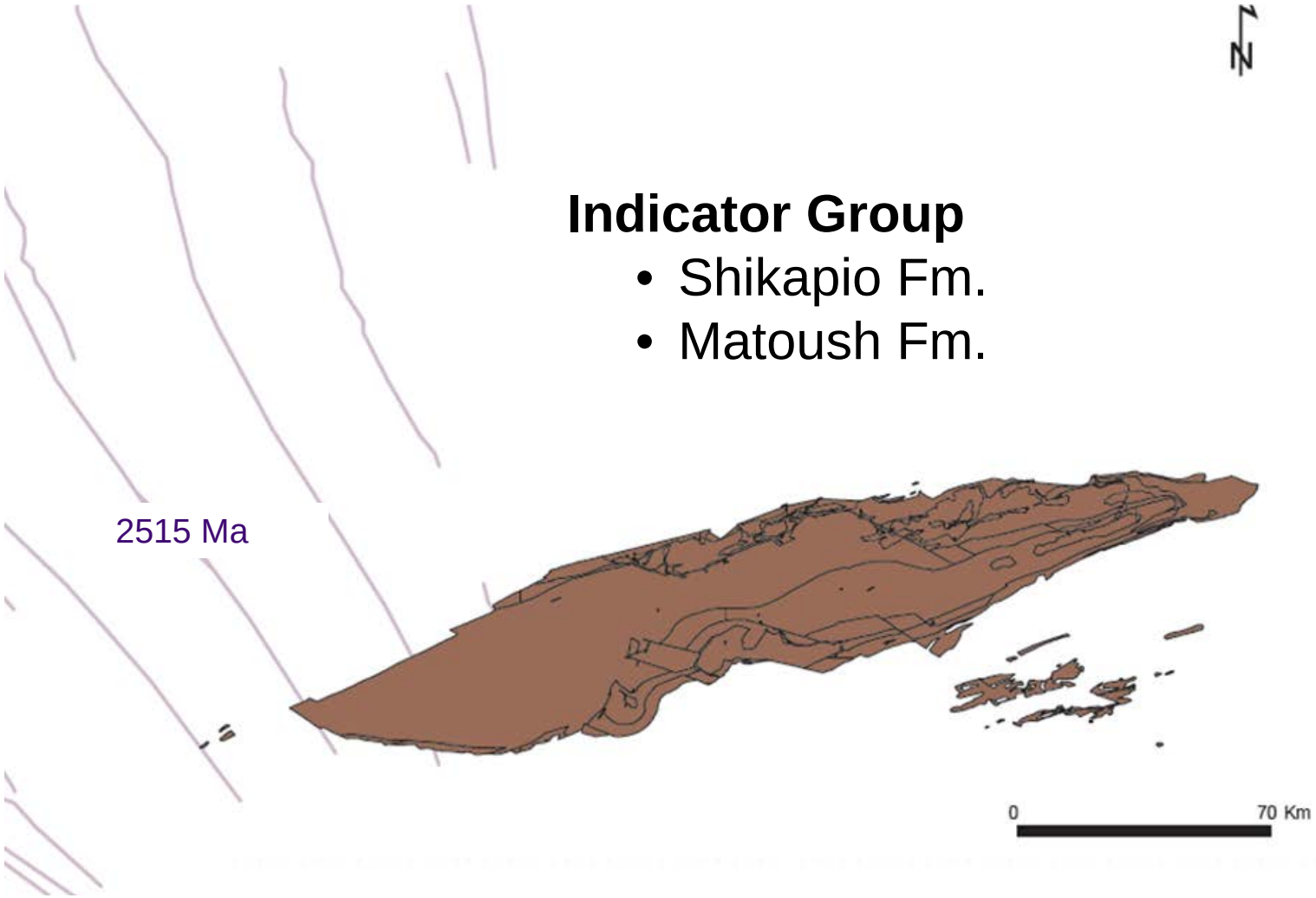
But also **ca. 2500 Ma**
(Heaman, 2004)

0 70 Km

Otish Mountain Supergroup sediments

Indicator Group

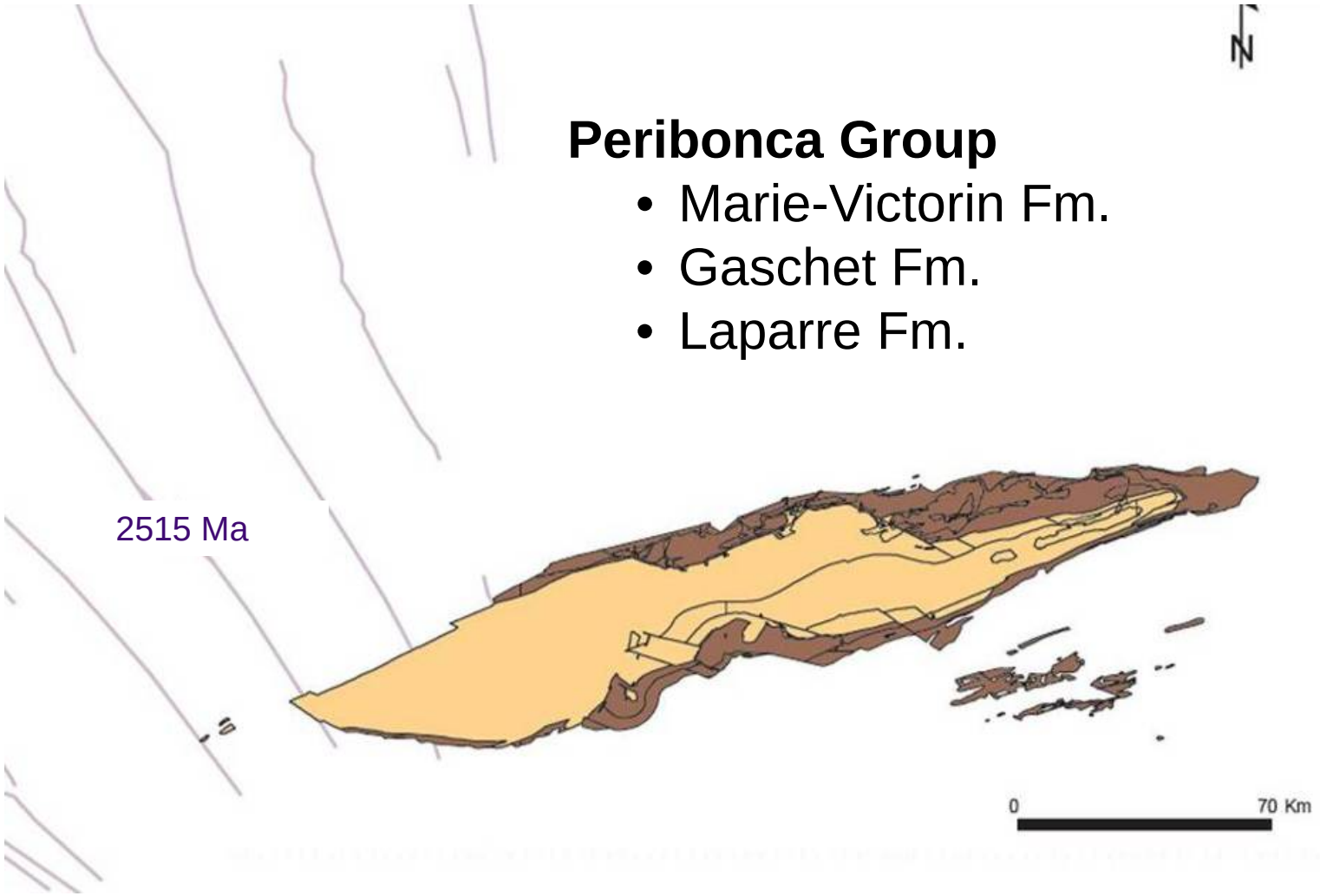
- Shikapio Fm.
- Matoush Fm.



Otish Mountain Supergroup sediments

Peribonca Group

- Marie-Victorin Fm.
- Gaschet Fm.
- Laparre Fm.



Intrusion of the Otish Gabbro dykes and sills

Otish Gabbros

2169.0 ± 1.4 Ma *(U-Pb baddeleyite)*
1730 ± 10 Ma *(Sm-Nd)*
1591 Ma *(K-Ar WR)*
1718 Ma *(K-Ar WR)*
1465 Ma *(K-Ar)*



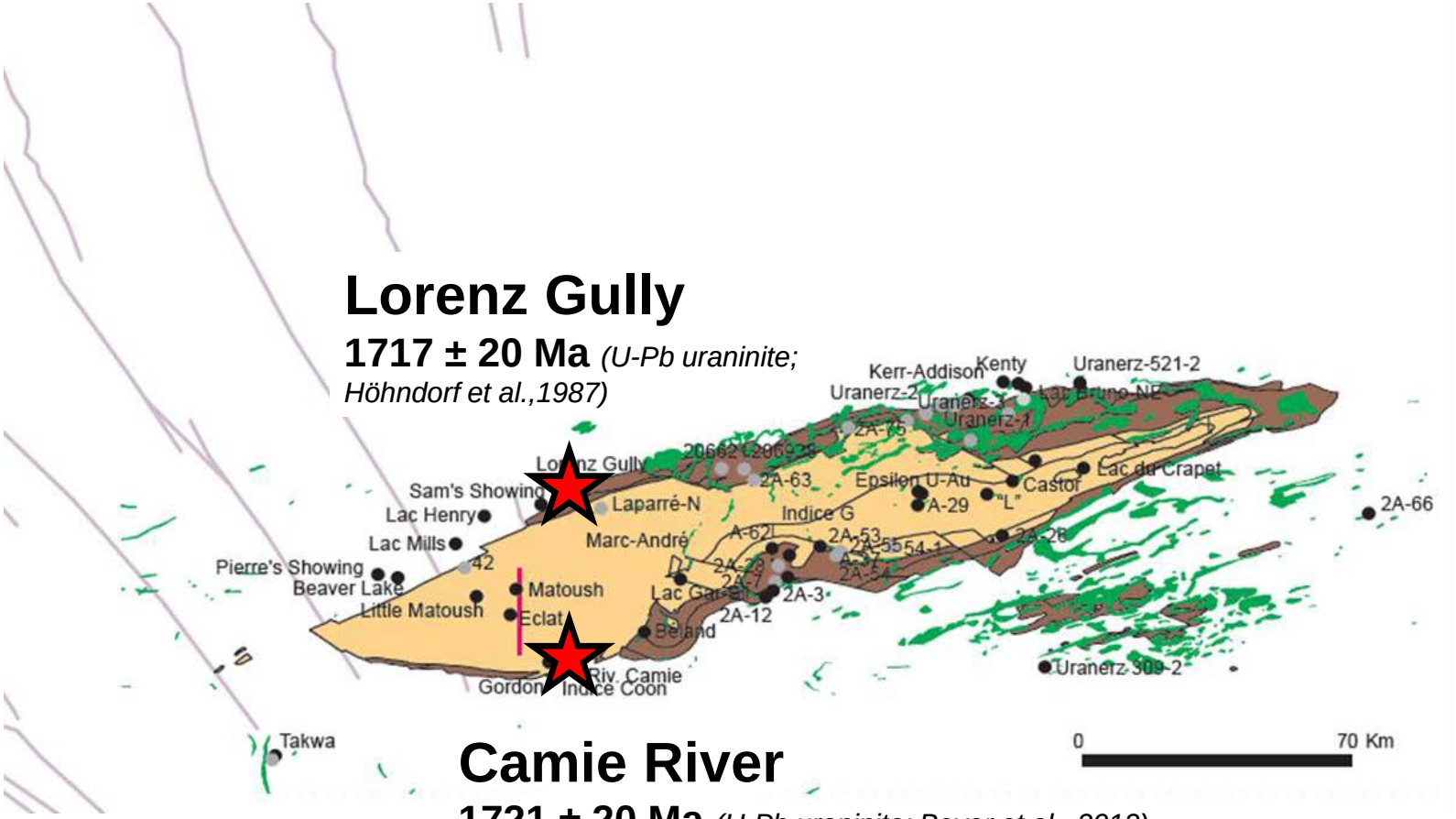


Otish Gabbros constrain the minimum age of the basin!

Uranium Mineralization

Lorenz Gully

1717 ± 20 Ma *(U-Pb uraninite; Höhndorf et al.,1987)*



Camie River

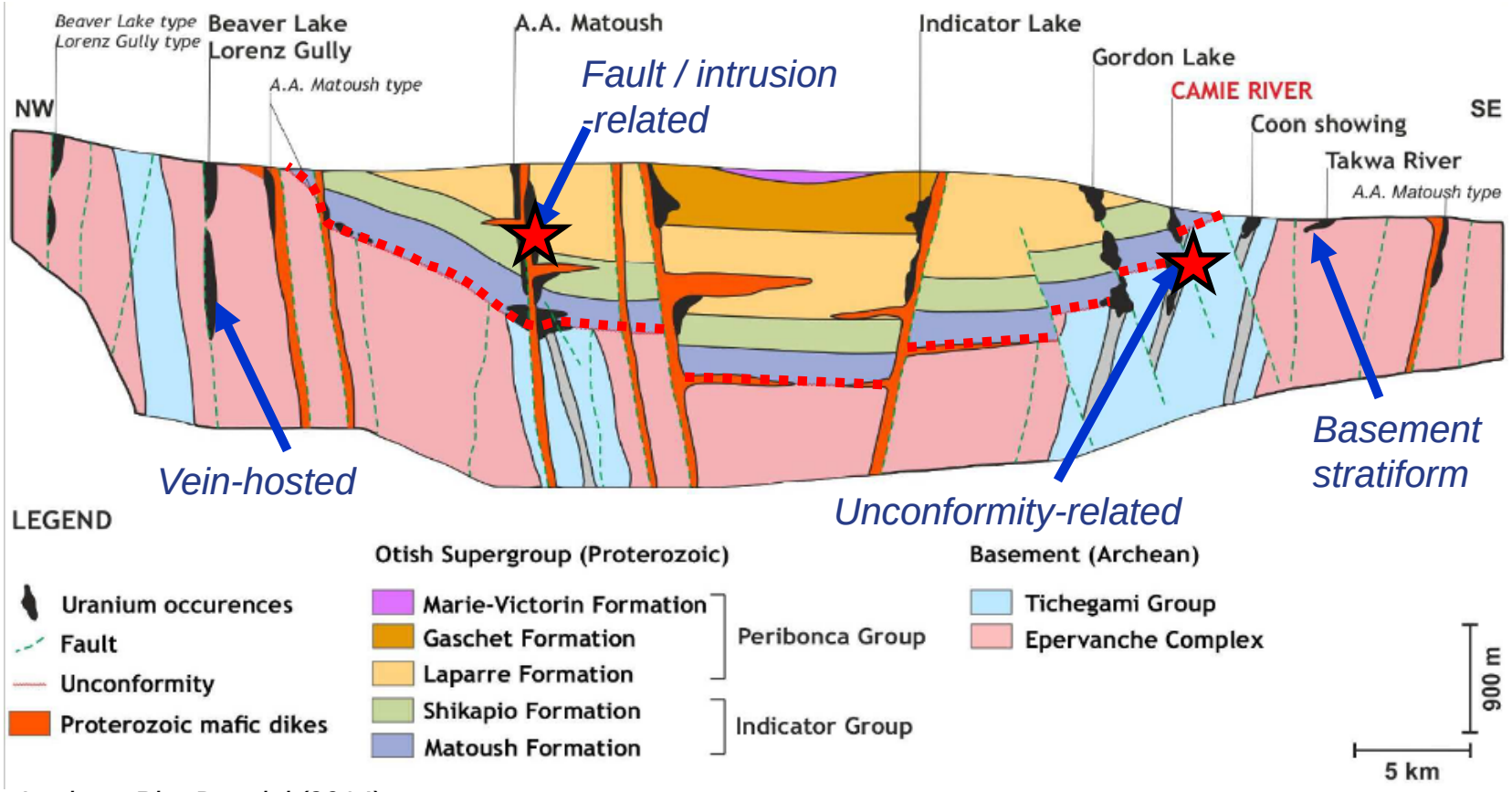
1721 ± 20 Ma *(U-Pb uraninite; Beyer et al., 2012)*

1723 ± 16 Ma *(U-Pb uraninite; Höhndorf et al.,1987)*

Previous age constraints

	Reference	Date	Isotope System	Sample
U-mineral.	Beyer *et al*., 2012	1721 ± 20	U-Pb uraninite	Camie River
	Höhndorf *et al*., 1987	1723 ± 16 Ma	U-Pb uraninite	Camie River
	Höhndorf *et al*., 1987	1717 ± 20 Ma	U-Pb uraninite	Lorenz Gully
OTISH GABBROS	**Hamilton & Buchan, 2007**	**2169.0 ± 1.4 Ma**	**U-Pb baddeleyite**	**Conflans Sill (Otish Gabbro)**
	Fryer, 1972	**1787 ± 55 Ma**	**Rb-Sr**	**Temiscamie Fm. of the Mistassini Gp.**
	Höhndorf *et al*., 1987	**1730 ± 10 Ma**	**Sm-Nd**	**Otish gabbro**
	Stevens *et al*., 1982	**1591 Ma 1718 Ma**	**K-Ar whole rock**	**Dyke from Otish Mountains Dyke N of Lk. Mistassini**
	Wanless *et al*., 1965	**1465 Ma**	**K-Ar age**	**Upper sill near Conflans**

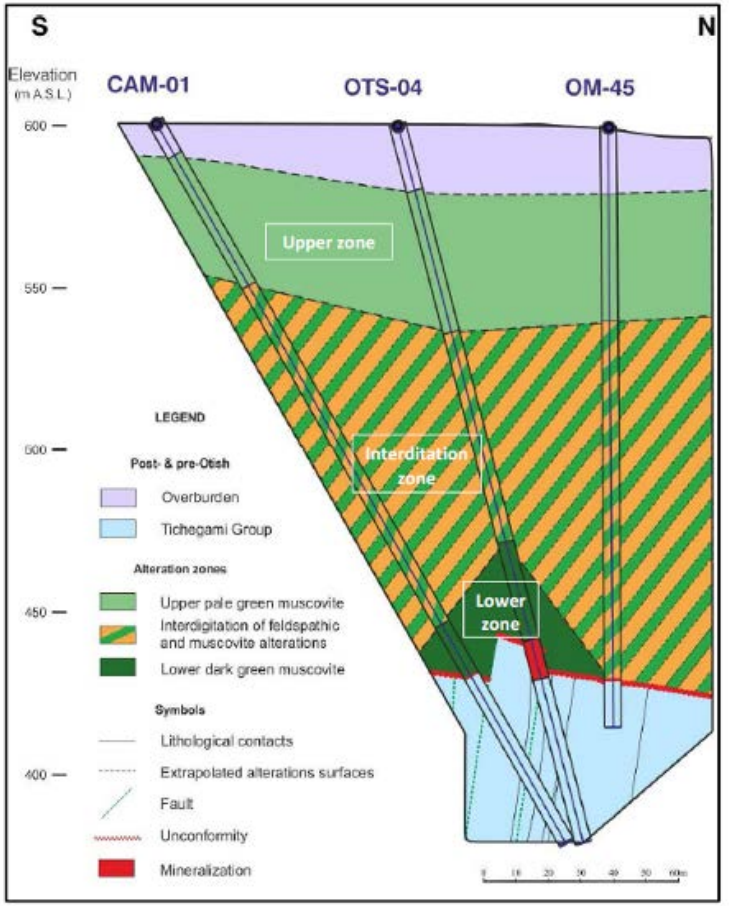
Otish Basin cross-section: U-mineralization



Lesbros-Piat-Desvial (2014)

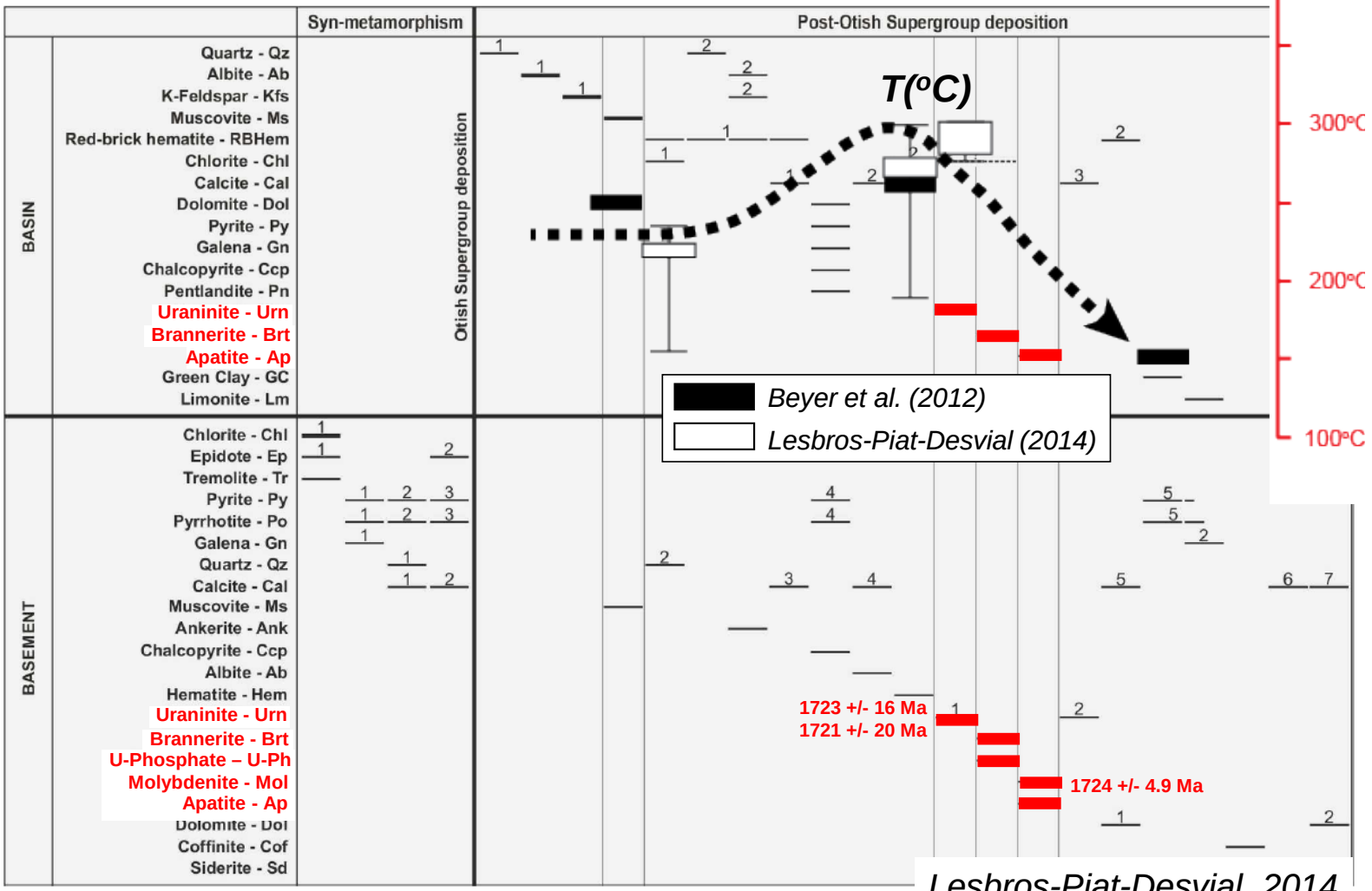
Alteration and U-mineralization at Camie River

- Disseminated and vein uraninite close to the unconformity between:
  - E. Proterozoic fluvatile orange/pink pervasively altered feldspathic and green-muscovite sandstones and conglomerates of the Matoush formation
  - underlying Archean faulted, sulphide-bearing, graphitic schists.
- Feldspathic alteration only identified at Camie River prospect



Lesbros-Piat-Desvial, 2014

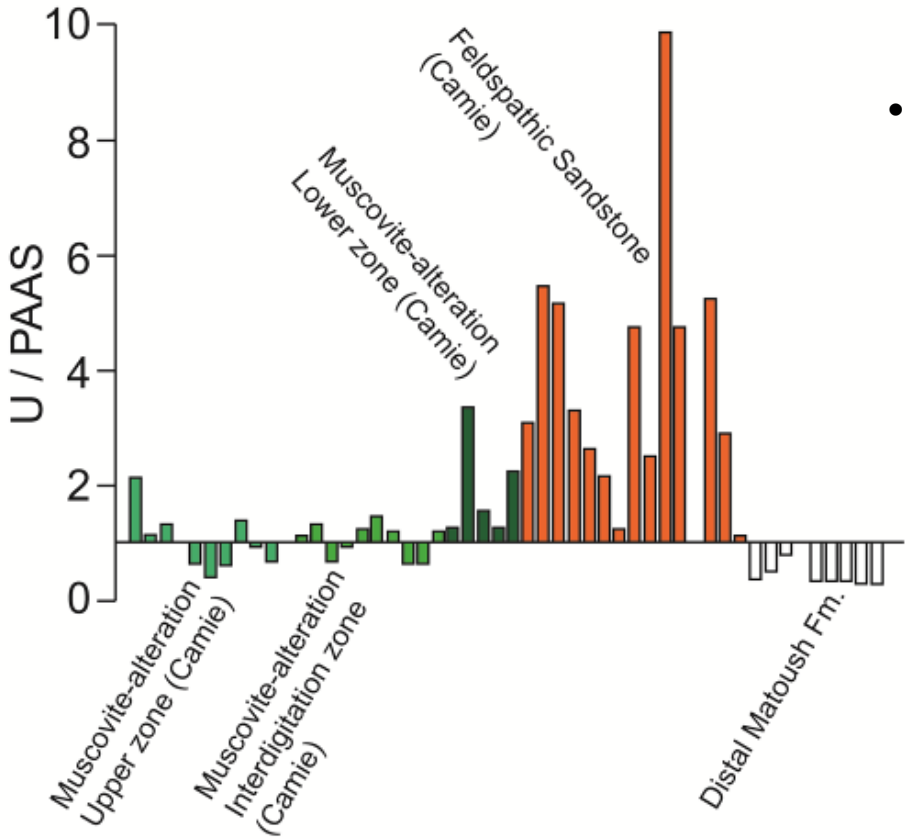
Alteration and U-mineralization at Camie River



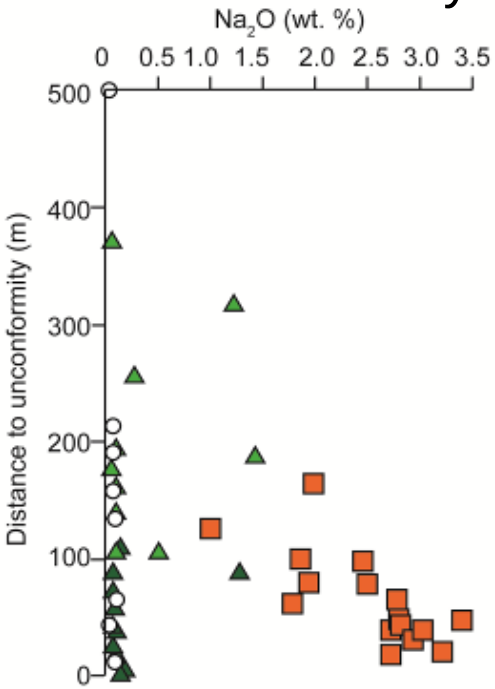
Lesbros-Piat-Desvial, 2014

Alteration and U-mineralization at Camie River

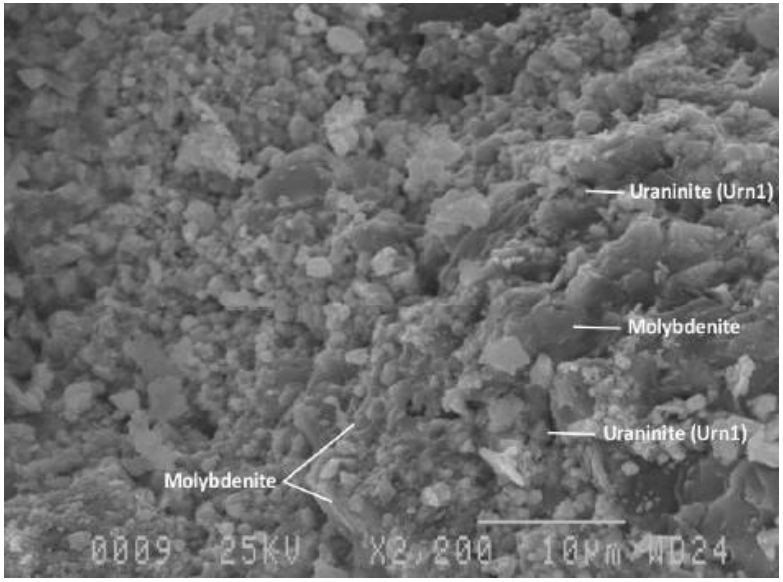
Modified from Lesbros-Piat-Desvial (2014)



- Feldspathic sandstones are strongly enriched in U
- Na_2O in feldspathic sandstones increases toward unconformity



Age of molybdenite (MoS_2) mineralization at the Camie River deposit



SEM Image

Weighted Average:

1724.0 ± 4.9 Ma

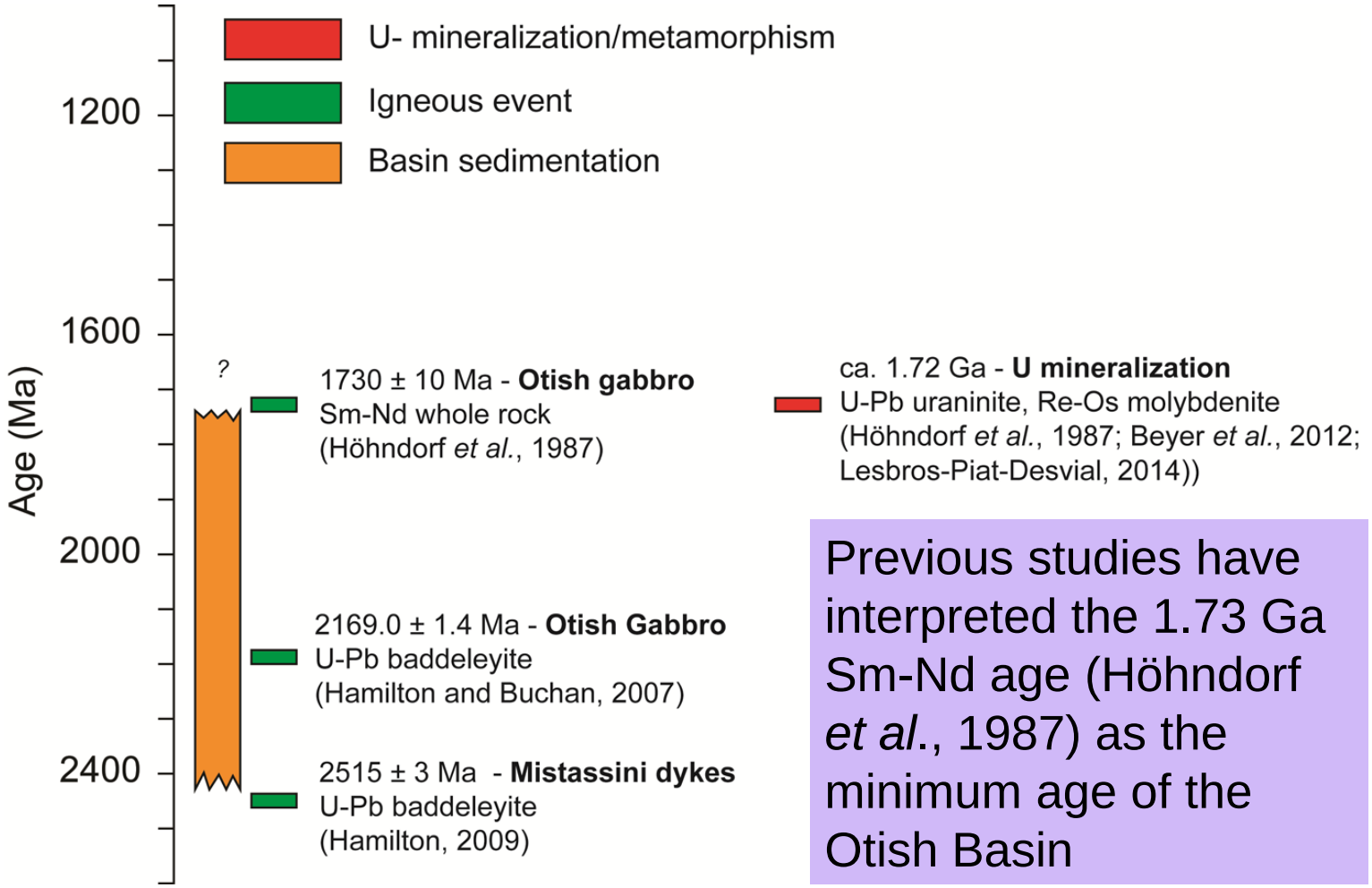
MSWD = 0.050,
probability = 0.82

Sample	*^{187}Re (ppm)*	*±2s*	*^{187}Os (ppb)*	*±2s*	*Age (Ma)*	*±2s*
85780	36.19	0.09	1055	1	***1725***	***7***
85780-2	30.42	0.08	886.1	0.6	***1723***	***7***

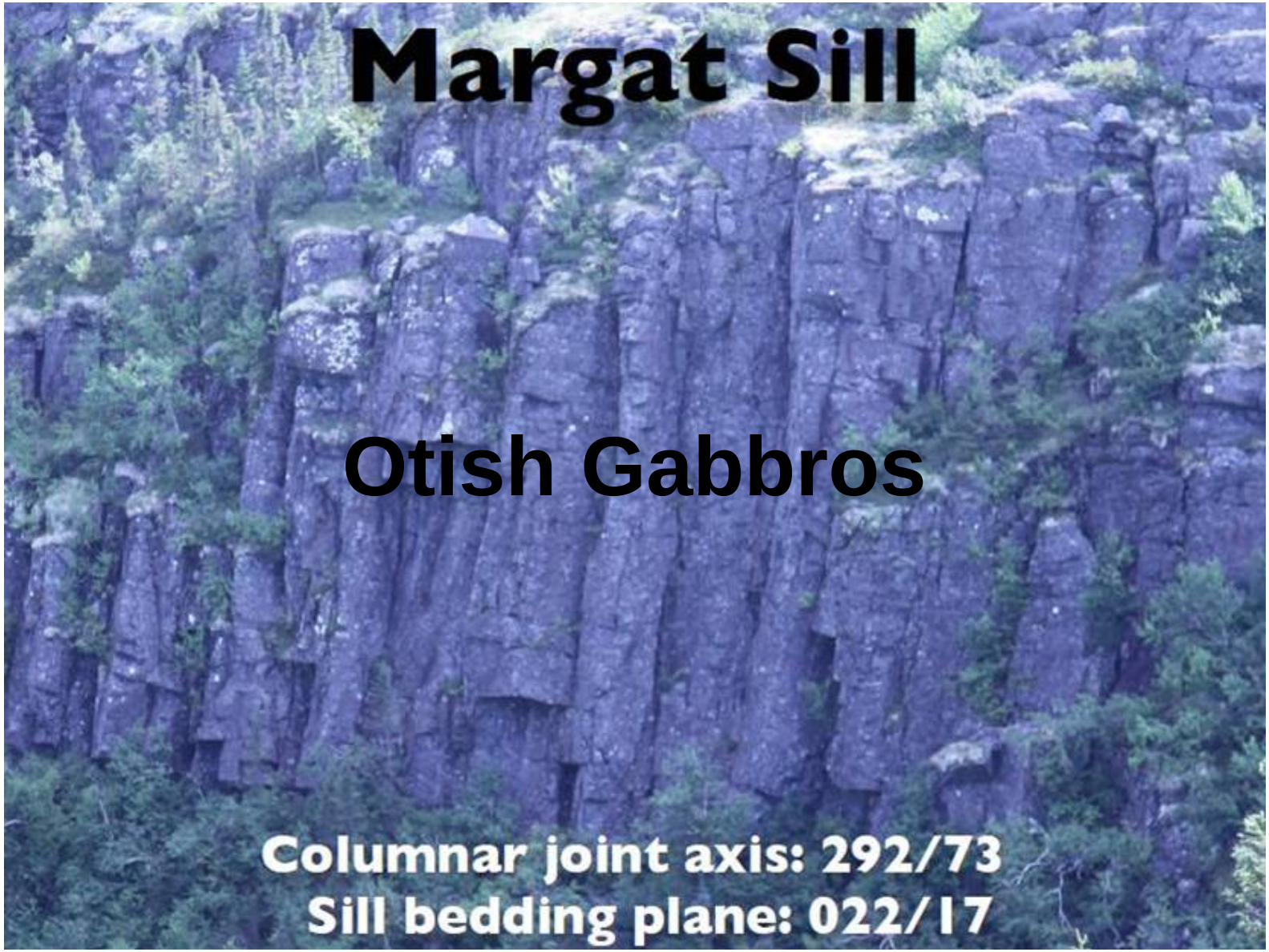
$\lambda^{187}Re = 1.666 \times 10^{-11} y^{-1}$ $^{187}Os = {}^{187}Re\,(e^{\lambda t}-1)$

Lesbros-Piat-Desvial, 2014

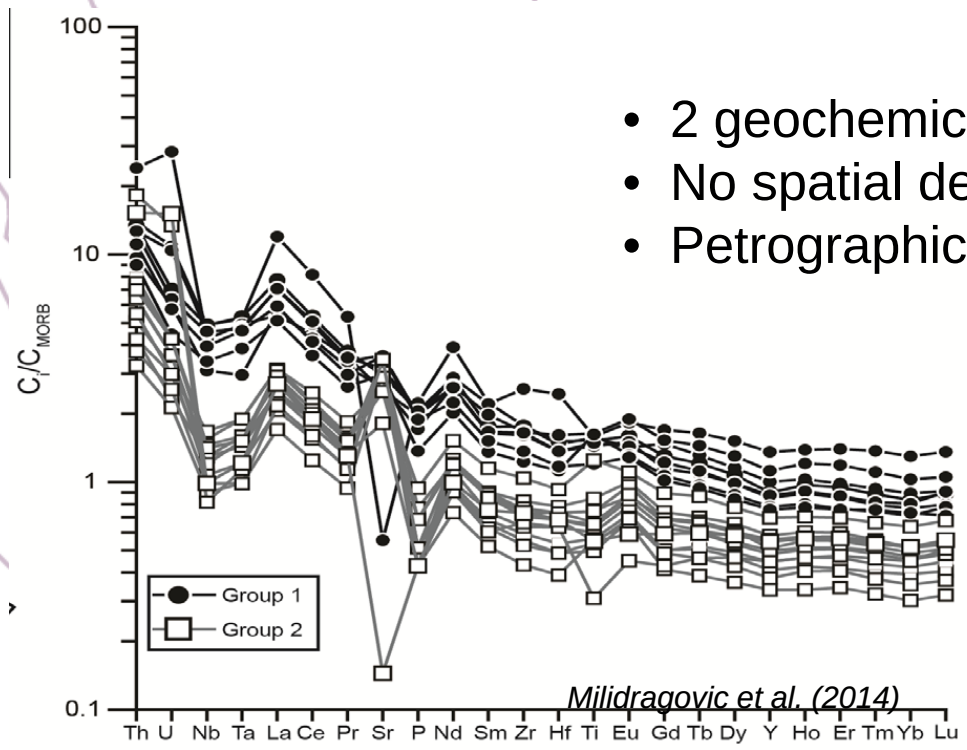
Age of the Otish Basin?



Previous studies have interpreted the 1.73 Ga Sm-Nd age (Höhndorf *et al.*, 1987) as the minimum age of the Otish Basin


Margat Sill
Otish Gabbros
Columnar joint axis: 292/73
Sill bedding plane: 022/17

Two suites of Otish gabbro



Milidragovic et al. (2014)

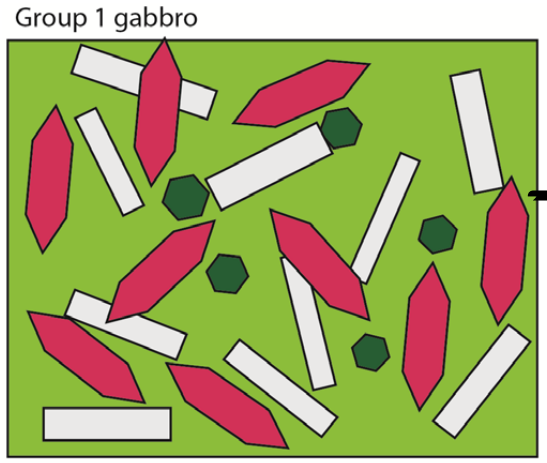
- 2 geochemically defined “suites”
- No spatial dependence
- Petrographically indistinguishable

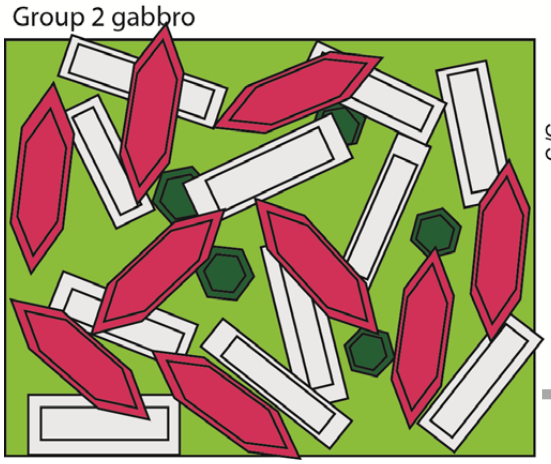


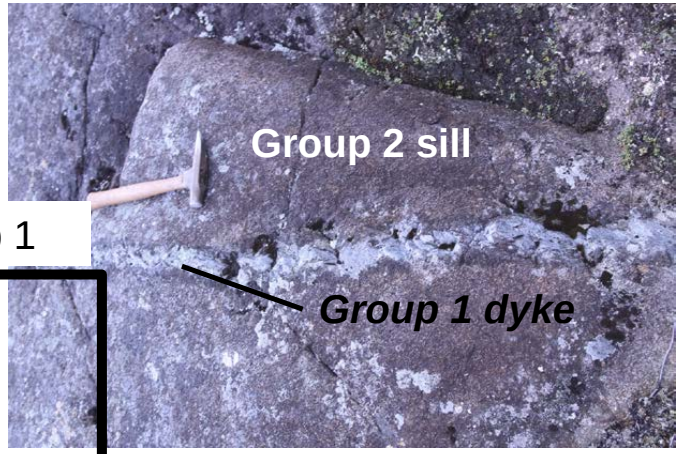




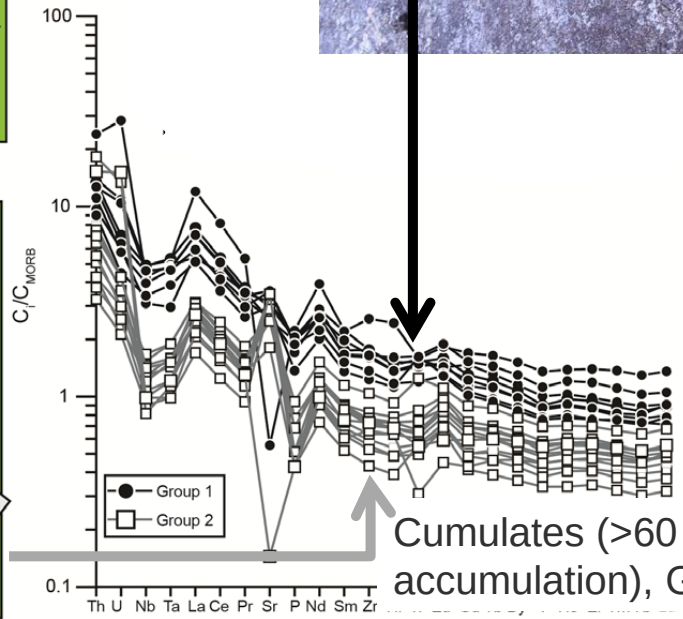
Petrology of Otish Gabbros







Liquids, Group 1



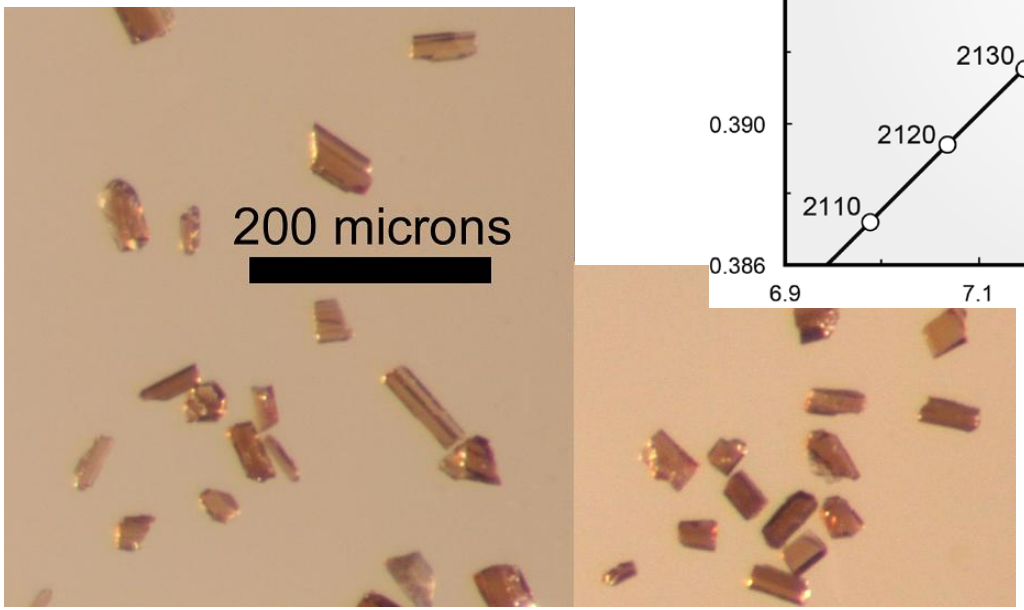
Cumulates (>60 % gabbroic accumulation), Group 2

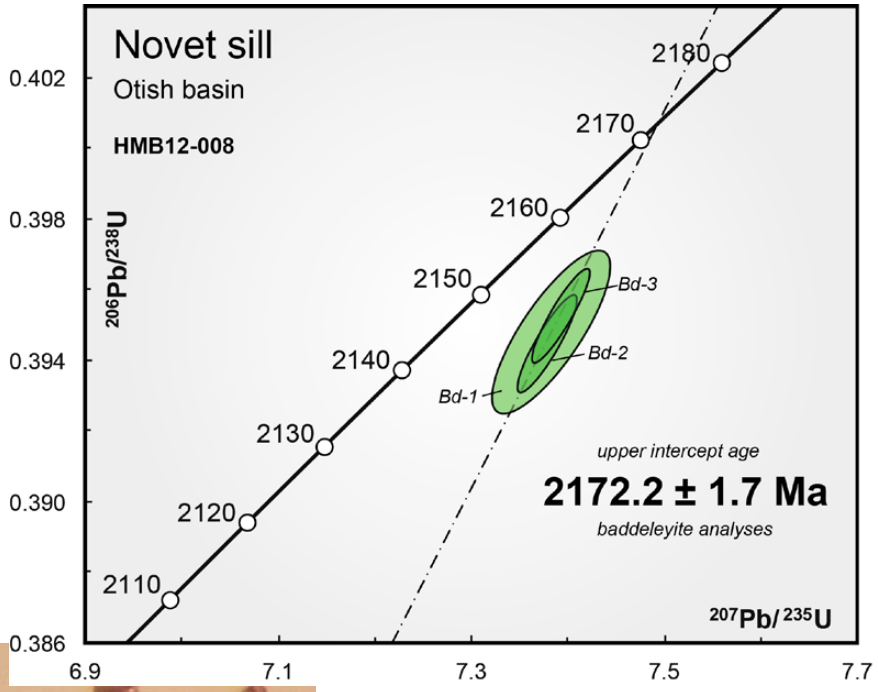
Milidragovic et al., 2014

Age of Otish Gabbros

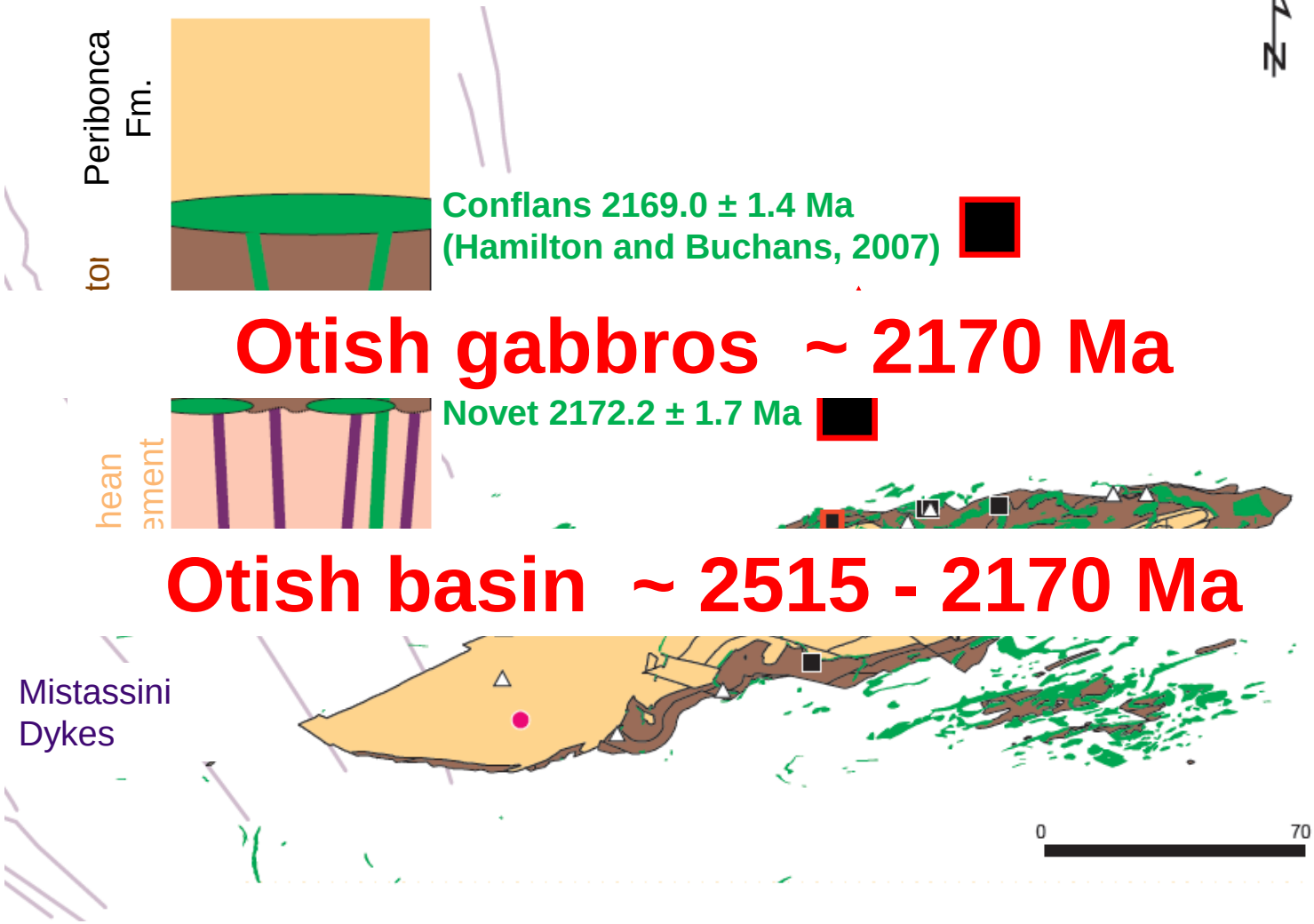
Sample **HMB12-008 (Lower Novet Sill)**

Baddeleyite (ZrO_2)
(fractions Bd-1 to Bd-3)

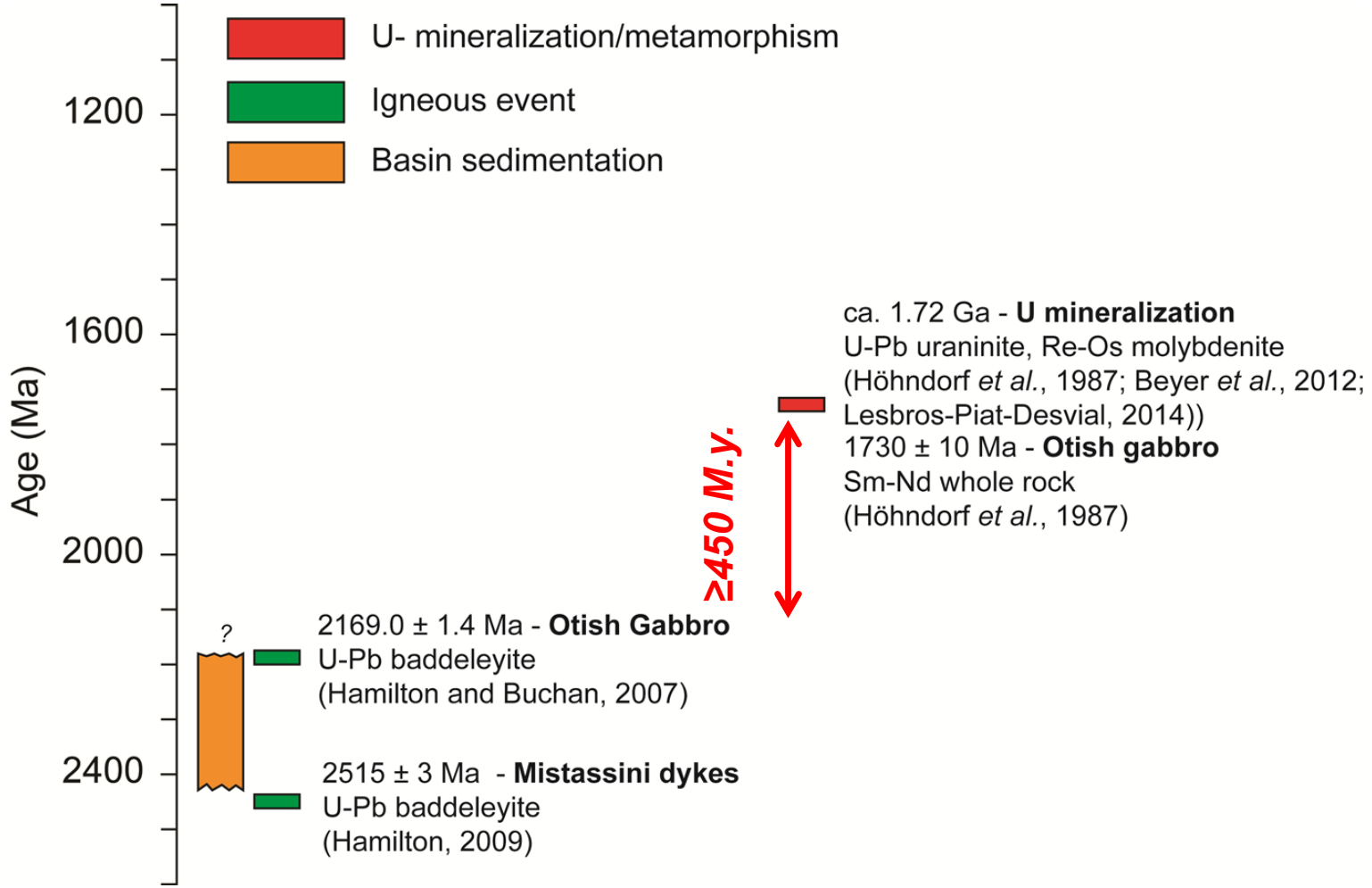




New ages of Otish Gabbro dykes and sills

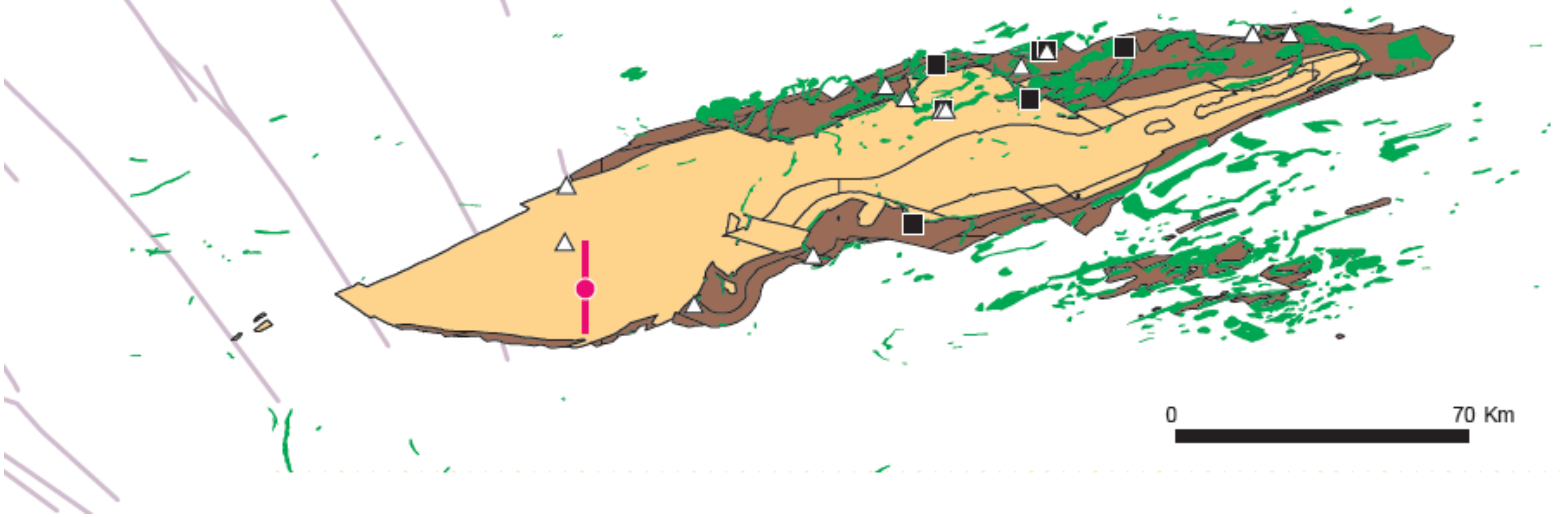


Revised age of the Otish Basin

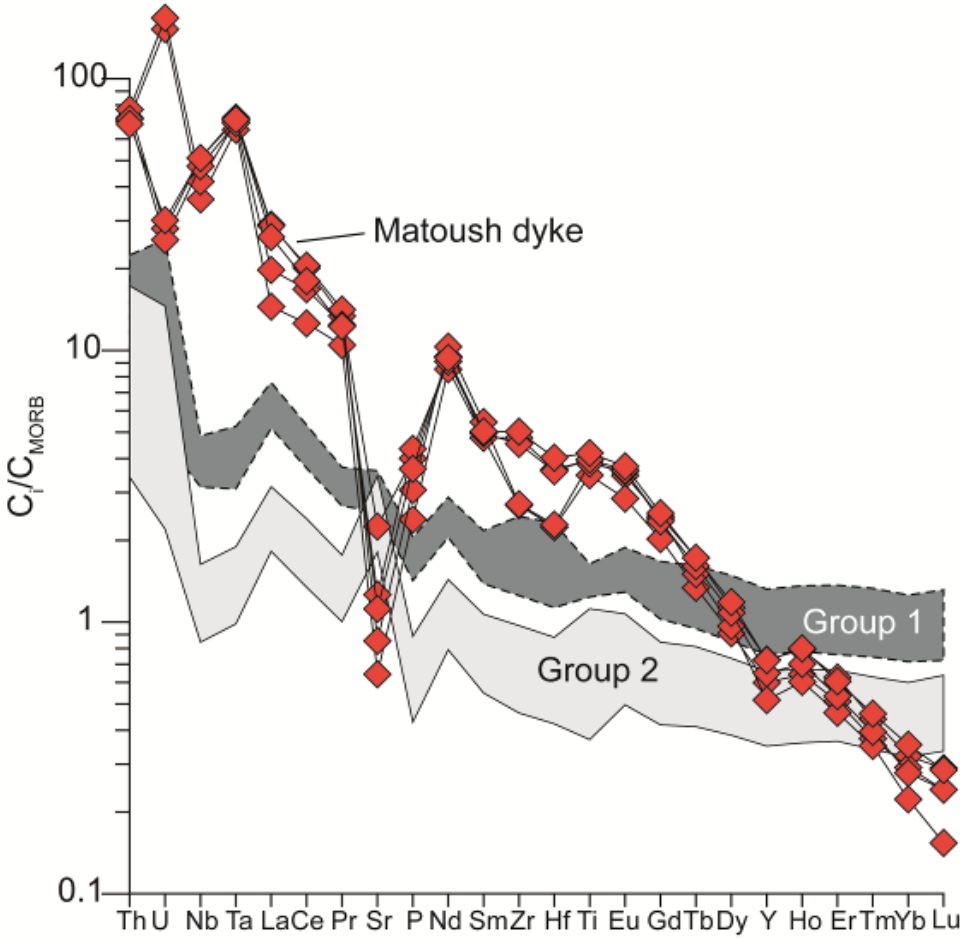


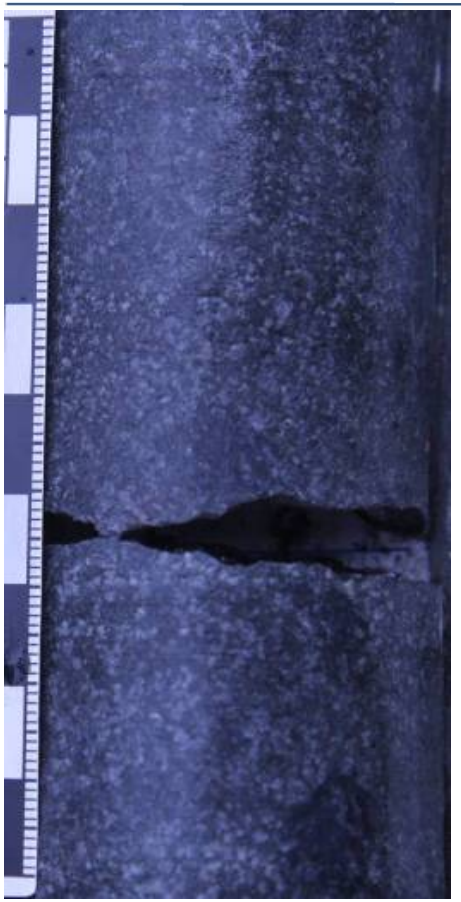
Matoush Dyke

- The timing of the Matoush Dyke is unknown but core logging indicates it is later than the Otish Gabbros

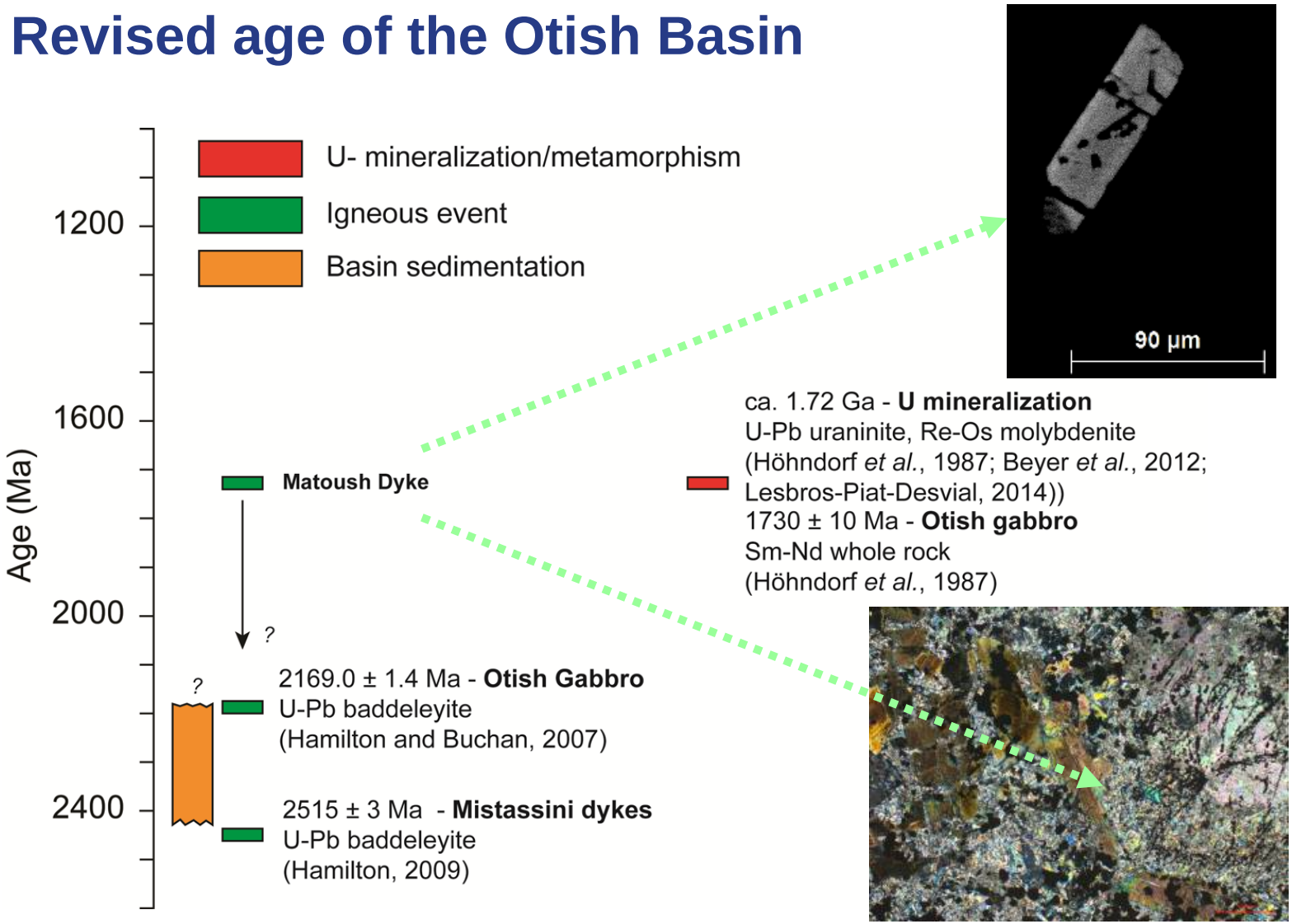


STRATECO RESOURCES

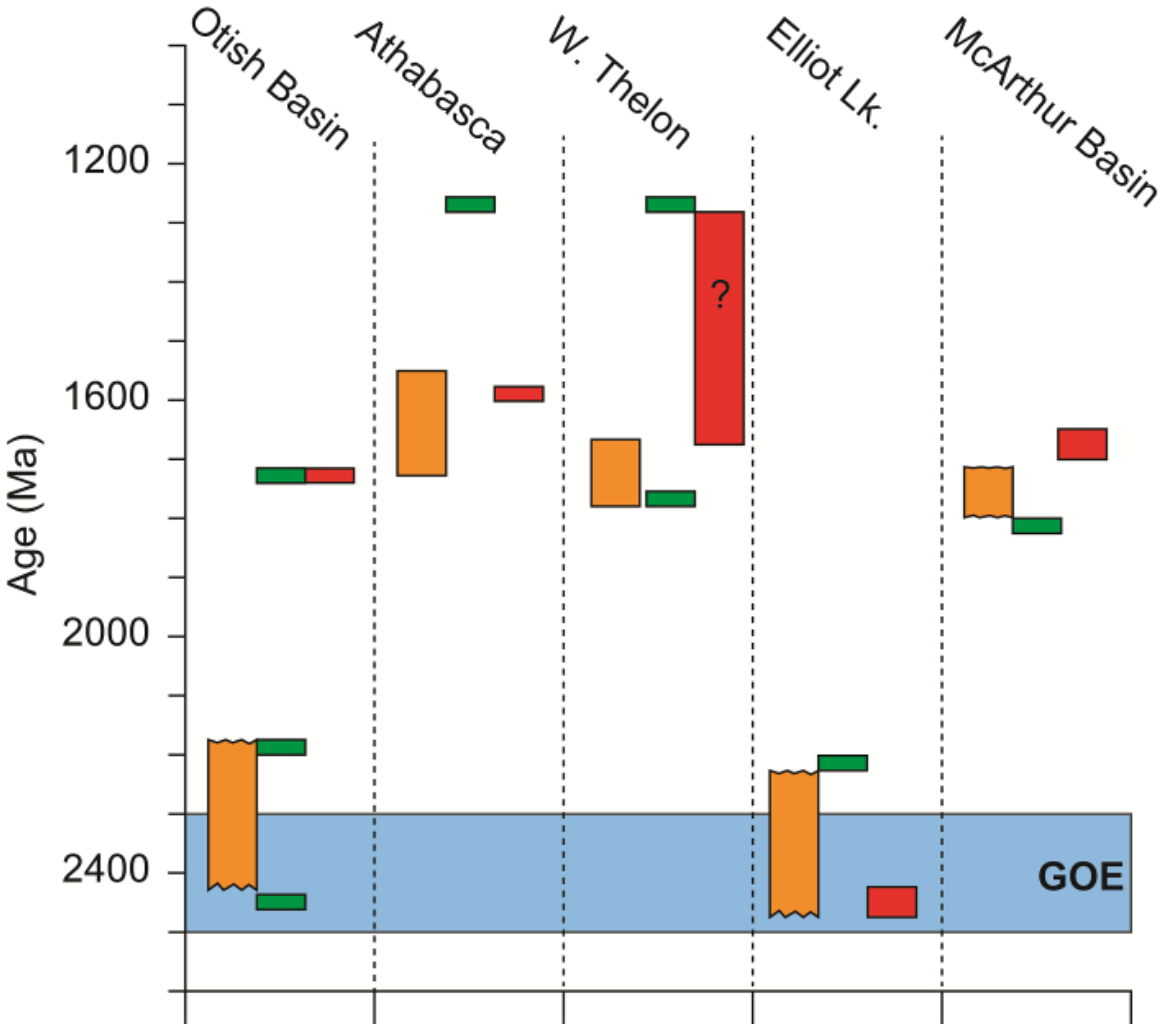




Revised age of the Otish Basin



Otish Basin in the global context



Conclusions

- The Otish Gabbros are a suite derived from a single magmatic event that is 2.17 Ga
- Age of Otish gabbros constrains minimum age of Otish Group sedimentation to 2.17 Ga, which is older than previously thought
- Matoush dyke has no relation to the Otish gabbros but appears to be closely related to mineralization. The age is not yet known
- Re-Os age of molybdenite is identical to uraninite ages and shows that mineralization is much younger than the basin and the intrusion of the Otish gabbros

Thank you!

Ressources naturelles Québec

TGI 4 Ore Systems

Cameco

STRATECO RESOURCES